BIFD EDINBURGH 2024

Bifurcations and Instabilities in Fluid Dynamics

24 to 28 June 2024

University of Strathclyde Glasgow · THE UNIVERSITY of EDINBURGH School of Engineering · Imperial College London

Book of Abstracts

Keynotes
Posters
Talks
Open Colloquia

IMPERIAL · THE UNIVERSITY of EDINBURGH · University of Strathclyde Glasgow

Our Gratitude to

DANTEC DYNAMICS
Gold Sponsor

Springer
Dinner Sponsor

Warm Welcome!

Local Organising Committee

Local Organising Committee

- Prashant Valluri (Engineering, The University of Edinburgh, UK)
- Khellil Sefiane (Engineering, The University of Edinburgh, UK)
- John Christy (Engineering, The University of Edinburgh, UK)
- Daniel Orejon (Engineering, The University of Edinburgh, UK)
- Rachel Schwind (Engineering, The University of Edinburgh, UK)
- Rodrigo Ledesma Aguilar (Engineering, The Unversity of Edinburgh, UK)
- Khushboo Pandey (Engineering, The University of Edinburgh, UK)
- Alexander Morozov (Physics and Astronomy, The University of Edinburgh, UK)
- Omar Matar (Chemical Engineering, Imperial College London, UK)
- Stephen Wilson (Mathematics and Statistics, The University of Strathclyde, UK)
- Alexander Wray (Mathematics and Statistics, The University of Strathclyde, UK)

Conference Secretariat

- Laura Smith (Engineering, The University of Edinburgh, UK)
- Karen Brocklehurst (Engineering, The University of Edinburgh, UK)
- Kimberly Ross (Engineering, The University of Edinburgh, UK)

Conference Main Contact Email

- All Enquiries: Enquiries.BIFD2024@ed.ac.uk

Scientific Committee

- Michael Bestehorn (Brandenburg University of Technology)
- Adrian Daerr (Université Paris Cité)
- Henk Dijkstra (University of Utrecht)
- Alexander Gelfgat (Tel Aviv University)
- Rainer Hollerbach (University of Leeds)
- Christian Ruyer-Quil (Université Savoie Mont Blanc)
- David Smith (University of Birmingham)

BIFD Advisory Committee

- Zvi Pinhas Bar-Yoseph (Technion-Israel Institute of Technology)
- Morten Brøns (Technical University of Denmark)
- Alexander Gelfgat (Tel Aviv University)
- Alex Oron (Technion-Israel Institute of Technology)

Keynotes

Camille Duprat, France

Rama Govindarajan, India

George Karapetsas, Greece

Satish Kumar, USA

Julia Yeomans, UK

Roberto Zenit, USA

Open Colloquia

David Quéré, France

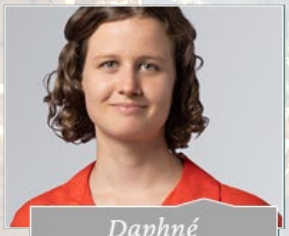

Daphné Lemasquerier, UK

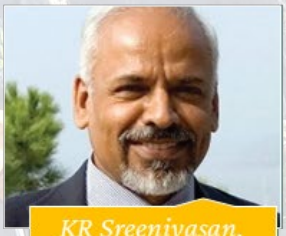

KR Sreenivasan, USA

DAY 1 – Monday, 24 June 2024 Morning sessions			
07:30	Registration, Conference Bag and Badge pick-up (Nucleus Entrance)		
08:30	Tea and Coffee (Alder Hall)		
09:00	Opening & Welcome (Larch Lecture Theatre)		
09:15	**Keynote 1: Prof Rama Govindarajan** ***Chair: Prof Omar Matar*** ***Larch Lecture Theatre***		
	Instabilities & Bifurcations 1 ***Chair: Prof Omar Matar*** ***Larch Lecture Theatre***	***Computational, Theoretical and Experimental Methods*** ***Chair: Prof Alexander Gelfgat*** ***Yew Lecture Theatre***	***Applications & Flow Control*** ***Chair: Prof Bar Yoseph-Pinhas*** ***Elm Lecture Theatre***
10:00	M001: Electrohydrodynamic stability of an oscillating streaming fluid cylinder *by AA Hasan*	M013: Physics informed neural networks for accelerating periodic thermal and fluid engineering simulations *by L Chaplot, A. Sharma*	M025: Stabilising travelling waves from pipe flow turbulence *by D Lucas, T Yasuda*
10:15	M002: Secondary instabilities of hexagonal patterns of Marangoni convection with deformable interface covered by surfactant *by A Mikishev, A Nepomnyashchy*	M014: Seeking for rare events in a backward-facing step flow using real-time particle image velocimetry *by J Pimienta, J-L Aider*	M026: Hele-shaw flow of a nematic liquid crystal *by S Wilson, JRL Cousins, AS Bhadwal, NJ Mottram, CV Brown*
10:30	M003: Compressibility effect on Darcy porous convection *by G Arnone, F Capone*	M015: Spatially-developing disturbance modes in the temporally-periodic burgers equation: a nonlinear analysis *by PV Brandão, A Barletta, M Celli, S Lazzari, E Ghedini*	M027: Optimisation of average quantities in a forced Lorenz system: influence of periodic orbits *by F Jovanovic, TS Eaves*
10:45	M004: Flow in a porous medium considering crossflow and slip *by L Tlau, K Vasuki*	M016: Optimizing external forces for lock-in to the oscillatory flow past a flat plate in a uniform flow *by M Iima*	M028: Active control of trailing vortices by synthetic jets in the axial direction near the wingtip *by C del Pino, L Parras, JH Garcia- Ortiz, J. Aguilar-Cabello, FJ Blanco-Rodriguez, P Gutierrez-Castillo*
11:00	**Coffee Break (Alder Lecture Theatre)**		
11:30	M005: One-dimensional study on instability and dynamics of a surfactant-laden viscoelastic thread *by F Liu, D He*	M017: Numerical properties of the differentially heated cavity with varying aspect ratios *by F Wubs, S Baars, J Thies*	M029: Influence of the theoretical model on an active control of wingtip vortices *by P Gutierrez-Castillo, M Garrido-Martin, T Bölle, FJ Blanco-Rodríguez, C del Pino*
11:45	M006: Effect of a soft-gel coated wall on the evolution of Faraday waves *by D Bhagavatula, G Balram, R Kumar*	M018: The stability of magnetohydrodynamic flows in cylindrical geometries using a velocity-vorticity formulation *by B Knaepen, Y Velizhanina*	M030: Frequency response as a tool for optimizing active control of trailing vortices *by M Garrido-Martin, T Bölle, C del Pino, FJ Blanco-Rodríguez, P Gutierrez-Castillo*
12:00	M007: Instabilities in catalytically active pores *by G Antunes, P Malgaretti, J Harting*	M019: Stability of periodic solutions using Chebyshev polynomials by *LM Witkowski, A Gesla, Y Duguet, P Le Quéré*	M031: Shear migration of ceramic slips *by A Fontanari, M Bellotto, G Artioli*
12:15	M008: Instability of stratified air-water pipe flows *by I. Barmak, Y. Nezihovski, A. Gelfgat, N. Brauner*	M020: A new algorithm and simulation for multiphased strongly fuzzy compressible flows *by B Nyaare, O Ongati, T Aminer*	M032: Aerodynamic forces in wing models with spanwise deformation *by L Parras, P Gutierrez-Castillo, P Solis, C del Pino, FJ Blanco-Rodriguez, E Duran-Venegas*
12:30	**Lunch Break (Alder Lecture Theatre)**		

Keynote 1

A bifurcation and an instability in particulate flow

Rama Govindarajan

International Centre for Theoretical Sciences, Tata Institute for Fundamental Research, Bengaluru, India

Rama Govindarajan is Professor and Dean at the International Centre for Theoretical Sciences, Tata Institute of Fundamental Research, Bengaluru, India. She did her PhD in Aerospace Engineering at the Indian Institute of Science, Bengaluru. Before joining TIFR she worked in the National Aerospace Laboratories and in the Jawaharlal Nehru Centre for Advanced Scientific Research, both in Bengaluru. She is a Fellow of the American Physical Society and of the Indian National Science Academy. She works primarily on particulate and droplet flows, flows with phase change and on instabilities.

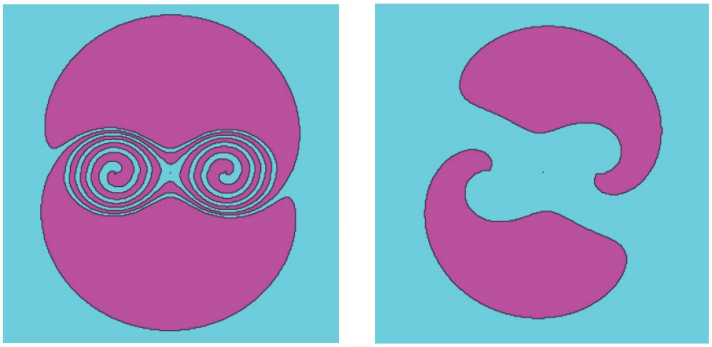

$St = \frac{1}{300\pi}$ $St = \frac{1}{20\pi}$

Abstract

This talk is in two parts. (i) we talk about how heavy inertial particles, which are expected to merely centrifuge out of vortical regions and collect in strain regions in a flow, do something quite different in a rotating system. Particles collect near vortices, and can display fixed points and limit cycles in a period-doubling bifurcation. (ii) Saffman in 1962, assuming a constant viscosity flow, showed how particles in two-way coupling in a laminar shear flow can change its stability. We show how the change in viscosity due to particle concentration can bring down the instability-critical Reynolds number dramatically.

M001

ELECTROHYDRODYNAIMC STABILITY OF ANOSCILLATING STREAMING FLUID CYLINDER

ALFAISAL A. HASAN[1]
[1]*Department of Basic and Applied Sciences, College of Engineering and Technology*
Arab Academy for Science, Technology & Maritime Transport, Aswan,Egypt

Keywords: electrogravitational, stability, oscillating, streaming

Abstract

The electrogravitational instability of an oscillating streaming fluid cylinder surrounded by a self-gravitating tenuous medium pervaded by transverse varying electric field is discussed under the action of selfgravitating, capillary and electro dynamic forces. This has been done for all modes of perturbation. A second order integro-differential equation of Mathieu type has been drived. Several published works are obtained as limiting cases from the prestent general one. The model is stable due to the stabilizing effect of the transverse electric field in all modes of perturbation. The capillary force has a strong destabilizing influence on the selfgravitating instability of the model. The streaming has a strong destabilizing effect in all kinds of perturbation.

References

[1] S. Chandrasekhar and E. Fermi , *Problems of gravitational stability in the presence of a magnetic field*, Astrophysics Journal **118,**1953, pp. 116-141.
[2] S. Chandrasekhar , *Hydrodynamic and Hydromagnetic Stability*, Dover, New York (1981).
[3] S. Sudo, H. Wakuda and D. Asano , *Capillary jet production of magnetic fluid by electromagnetic vibration*, International Journal of Applied Electromagnetic and Mechanics, **33**(1), 2010, pp. 63-69.
[4] A. Hasan , *Electrogravitational stability of oscillating streaming dielectric compound jets ambient with a transverse varying electric field* , Boundary Value Problems, **31**, 2011, pp. 1-14.
[5] A. Hasan , *Capillary electrodynamic stability of self-gravitational fluid cylinder with varying electric field* , Journal of Applied Mechanics Transactions ASME, **79**, 2012, pp. 1-7.
[6] S. Ellingsen , and I. Brevik , *Static and dynamic response of a fluid-fluid interface to electric point and line charge*, Annals of Physics, 327(12), 2012, pp. 2899-2913.
[7] S. Chand , *Effect of rotation on triple-diffusive convection in a magnetized ferrofluid with internal angular momentum saturating a porous medium*, Applied Mathematical sciences **6**(65), 2012, 3245-3258.
[8] S. Chand , *Linear stability of triple-diffusive convection in micropolar ferromagnetic fluid saturating porous medium*, Applied Mathematics and Mechanics 34(3), 2012, 309-326.
[9] C. Yin , F. Ceji and T. Wenchang , *Stability of thermal convection in a fluid-porous system saturated with an oldroyd-B fluid heated from below*, Transport of Porous Media, **99**(2), 2013, pp. 327-347.
[10] M. Ezzat , A. El-Karamany and A. El-Bary , *Electro-magnetic waves in generalized thermo-viscoelasticity for defferent theories*, International Journal of Applied Electromagnetic and Mechanics, **47**(1), 2015, pp. 95-111.
[11] D. Balsara , T. Amano , and J. Kim, *A high-order relativistic two-fluid electrodynamic scheme with consistent reconstruction of electromagnetic fields and a multidimentional Riemann solver for electromagnetism*, Journal of Computational Physics, **318**, 2016, pp169-200.
[12] A. Hasan , *Electrogravitational stability of streaming compound jets*, International Journal of Biomathematics, **9**(3), 2016, pp. 1-13.

M002

SECONDARY INSTABILITIES OF HEXAGONAL PATTERNS OF MARANGONI CONVECTION WITH DEFORMABLE INTERFACE COVERED BY SURFACTANT

Alexander Mikishev[1] & Alexander A. Nepomnyashchy[2]
[1]*Department of Eng. Technology, Sam Houston State University, Huntsville TX, U.S.A.*
[2]*Department of Mathematics, Technion – Israeli Institute of Technology, Haifa, Israel*

Keywords: Marangoni convection, pattern formation, surfactant

Abstract

Gradients of surface tension at the liquid interface created by temperature inhomogeneity and non-uniform distribution of the surfactant are responsible for generation of patterns in vicinity of the instability threshold. The most generic type of these patterns are hexagons. The evolution of hexagons can be described by the system of Ginzburg-Landau-type amplitude equations. Due to asymmetry of the boundary conditions at the top and the bottom of the layer, those equations contain additional non-gradient quadratic terms with spatial derivatives. These terms are especially significant for non-equilateral hexagons based on the resonance of wave vectors with slightly different lengths.

We derive a set of nonlinear equations describing a slow large scale evolution of short-scale hexagonal Marangoni patterns subject to a long-wave deformational Marangoni instability. The set includes equations for two additional variables, a large-scale deformation of the interface and distribution of the surfactant. The interaction of longwave disturbances near the bifurcation point can create a modulational instabilities of periodic patterns. We study the joint action of the liquid deformability and the effect of insoluble surfactant on the regular (equilateral)and deformed (non-equilateral) hexagons and their modulational instability. The governing parameters of the problem are Biot number characterizing the heat transfer resistance of the surface and Galileo number indicating the role of gravity. Stability maps are plotted for different concentrations of insoluble surfactant.

M003

COMPRESSIBILITY EFFECT ON DARCY POROUS CONVECTION

Giuseppe Arnone[1], Florinda Capone[1], Roberta De Luca[1] & Giuliana Massa[1]
[1]*Department of Mathematics and Applications "Renato Caccioppoli", University of Naples "Federico II", Naples, Italy*

Keywords: Porous media · Boussinesq approximation · Extended-quasi-thermal-incompressible fluids · Compressibility effect · Instability analysis

Abstract

Hydrodynamic stability problems have been widely analyzed and in this respect there are several notable results regarding Newtonian and incompressible fluids. It is commonly acknowledged that variations in temperature during non-isothermal processes induce changes in the properties of the fluid, such as density. Analyzing the complete effects of the density variations is so intricate that the use of certain approximations becomes indispensable. In this regard, the majority of studies examining the stability of fundamental steady-state motions in both clear fluids and fluid-saturated porous media, employ a well-established hypothesis known as the Boussinesq or Oberbeck-Boussinesq (OB) approximation, which assumes density to be a constant function in all terms of the equations except in the body force term due to gravity, where the density ρ depends on temperature T, *but not* on the pressure p. However, this assumption is an approximation of the real phenomenon, since perfectly incompressible fluids do not exist in nature. This is the reason why the investigation of compressibility effects in hydrodynamic stability problems is relevant. In particular, a more realistic constitutive equation for the fluid density is the following

$$\rho(p,T) = \rho_0[1 - \alpha(T - T_0) + \beta(p - p_0)], \tag{1}$$

where ρ_0 is the reference density in correspondence of a temperature T_0 and pressure p_0, α is the thermal expansion coefficient and β is the compressibility factor, see [1]. This fluids are called *slightly compressible*.
The main goal of the present talk is to describe the compressibility effect on the onset of convection in porous media, via instability analysis. We address the qualitative analysis of the solutions of the initial boundary value problem modelling slightly compressible convective currents in a Darcy's porous medium, whose well-posedness is proved in [2]. The critical Rayleigh-Darcy number for the onset of convection is determined as a function of a dimensionless parameter $\widehat{\beta}$ (see Figure 1), where $\widehat{\beta}$ is proportional to the compressibility factor β, proving that $\widehat{\beta}$ enhances the onset of convective motions [3].

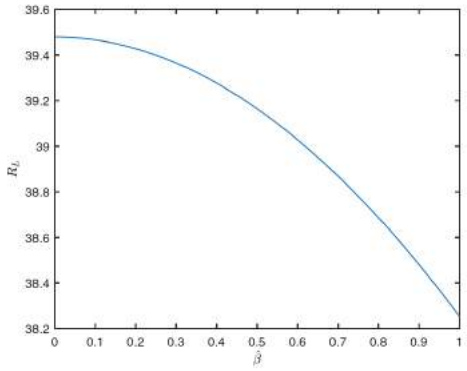

Figure 1. Critical Rayleigh-Darcy number $\mathcal{R}_L$ as function of the compressibility factor $\widehat{\beta}$.

References

[1] H. Gouin, T. Ruggeri, *A consistent thermodynamical model of incompressible media as limit case of quasi-thermal-incompressible materials*,International Journal of Non-Linear Mechanics **47**(6), 688-693 (2012).
[2] G. Arnone, F. Capone, *Existence and uniqueness of slightly compressible Boussinesq's flow in Darcy-Bénard problem*, Preprint ArXiv (2023).
[3] G. Arnone, F. Capone, R. De Luca, G. Massa *Compressibility Effect on Darcy Porous Convection*, Transport in Porous media **147** (2023).

M004

FLOW IN A POROUS MEDIUM CONSIDERING CROSSFLOW AND SLIP

Lalrinpuia Tlau & Vasuki K
Department of Mathematics, National Institute of Technology Puducherry, Karaikal 609609 India

Abstract A hydrodynamic stability analysis is conducted for a fluid flowing in a channel filled with a saturated porous medium considering the effects of crossflow and slip.

We consider a two dimensional flow in a channel filled with a porous medium. The crossflow of fluid is assumed while Navier slip is also considered at the channel walls. We consider the Navier – Stokes equation to model the momentum equation of the flow. The following transformations are used on the momentum equation: $u* = u/U_0,\ v* = v/U_0,\ x* = x/L,\ y* = y/L,\ t* = tU_0/L,\ p* = pL/\mu U_0$. The non – dimensional equation of the flow is thus obtained as shown below [1, 2, 3]:

$$\begin{aligned} Re\left[\frac{\partial u}{\partial t} + u\frac{\partial u}{\partial x} + v\frac{\partial u}{\partial y}\right] &= -\frac{\partial p}{\partial x} + \left[\frac{\partial^2 u}{\partial x^2} + \frac{\partial^2 u}{\partial y^2}\right] - M^2 u \\ Re\left[\frac{\partial v}{\partial t} + u\frac{\partial v}{\partial x} + v\frac{\partial v}{\partial y}\right] &= -\frac{\partial p}{\partial y} + \left[\frac{\partial^2 v}{\partial x^2} + \frac{\partial^2 v}{\partial y^2}\right] - M^2 v \end{aligned} \tag{1}$$

where $M = \Phi L^2/\kappa$ is the porous medium parameter, $Re = \rho U_0 L/\mu$ is the Reynolds number. The boundary condition which encapsulates the crossflow and slip are defined as [1, 2, 4]: $u(-1) = \beta\frac{\partial u}{\partial y},\ u(1) = -\beta\frac{\partial u}{\partial y},\ v(-1) = V_0,\ v(1) = V_0$. We then perturb Eqn. 1 using the following equations: $u = U_b(y) + \tilde{u}(x, y, t),\ v = V_0 + \tilde{v}(x, y, t),\ p = p(x, y) + \tilde{p}(x, y, t)$ and also the stream functions $\tilde{u} = \phi'(y)\exp(i\alpha(x - ct)),\ \tilde{v} = -i\alpha\phi'(y)\exp(i\alpha(x - ct))$. After simplification, we obtain the following equation:

$$i\alpha Re[(\phi'' - \alpha^2\phi)(U_b - c) - U_b''\phi] + r_e[\phi'''' - \alpha^2\phi'] = \phi'''' - \phi''(2\alpha^2 + M^2) + \phi(\alpha^4 + \alpha^2 M^2) \tag{2}$$

while the boundary conditions are simplified to: $\phi' \pm \beta\phi'' = 0,\ \phi = 0$ at $y = \pm 1$. The Orr–Sommerfeld equation is easily obtained from Eqn. 2 by taking $M = 0,\ r_e = 0$. $r_e = ReV_0$ is the crossflow Reynolds number. Eqn. 2 is an eigenvalue problem and is solved using the spectral collocation method. We conduct a thorough analysis of the effect of flow parameters on the stability of the flow. One such result can be seen in Fig. 1. The slip parameter β is seen to increase the critical Reynolds number. The conclusion from this is that increasing slip leads to stabilizing the flow[4, 5].

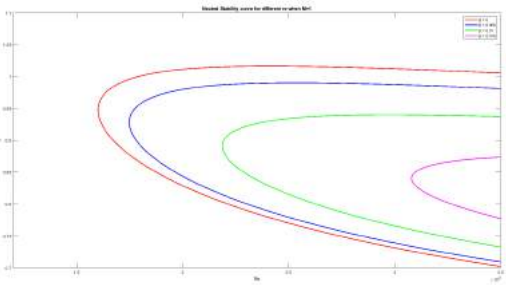

Figure 1. Neutral stability curve for different values of β.

References

[1] B. Straughan, A. J. Harfash, *Instability in Poiseuille flow in a porous medium with slip boundary conditions*, Microfluid Nanofluid **15**, 109–115 (2013).
[2] M. B. M. Khan, M. Sani, S. Ghosh, H. Behera, *Poiseuille – Rayleigh – Benard instability of a channel flow with uniform cross-flow and thermal slip*, Phys. Fluids .**33**, 053612 (2021).
[3] D. A. Nield, *The stability of flow in a channel or duct occupied by a porous medium*, Int. J. Heat Mass Trf., **46**, 4351 – 4354 (2003)
[4] S. Ceccacci, S. A. W. Calabretto, C. Thomas, J. P. Denier, *The linear stability of slip channel flows*, Phys. Fluids. **34**, 074103 (2022)
[5] C. Chai, B. Song, *Stability of slip channel flow revisited*, Phys. Fluids. **31**, 084105 (2019)

M005

ONE-DIMENSIONAL STUDY ON INSTABILITY AND DYNAMICS OF A SURFACTANT-LADEN VISCOELASTIC THREAD

Fang Li[1] & Dongdong He[2]
[1]*Department of Modern Mechanics, University of Science and Technology of China, Hefei, Anhui, PR China*
[2]*School of Science and Engineering, The Chinese University of Hong Kong, Shenzhen, Guangdong, PR China*

Keywords: nonlinear instability, viscoelasticity, slender-body theory, non-Newtonian flows

Abstract

The effect of an insoluble surfactant monolayer on the instability and dynamics of a non-Newtonian viscoelastic liquid thread initially perturbed by a small harmonic disturbance is studied numerically. Based on the slender body theory, a one-dimensional (1-D) model is built, in which the viscoelasticity of the liquid is decribed by the Oldroyd-B or FENE-P constitutive equation and the surface rheological properties of the surfactant are taken into account. The 1-D linear instability result shows that the temporal growth rate of the disturbance can be decreased by increasing the initial surfactant concentration, the Marangoni number, the surface Péclet number, the dilatational Boussinesq number or the shear Boussinesq number. The 1-D nonlinear numerical simulation shows that the formation of the beads-on-a-string structure on the viscoelastic thread can be greatly delayed by the surfactant. The surface Péclet number plays an important role in the nonlinear evolution of the viscoelastic thread: at large values of the surface Péclet number, the surfactant decreases the size of the secondary droplet or even remove it completely from the bead-on-a-string structure, and moreover, the surfactant stretches the primary droplet in the axial direction and leads to its deformation from a spherical to a prolate shape; at moderate values of the surface Péclet number, the surfactant may result in the formation of secondary droplet. At large values of the shear and dilatational Boussinesq numbers, the thinning of the viscoelastic thread can be greatly delayed by the surface viscous stresses and the filament in the beads-on-string structure follows the $1/3De$ exponential law no more. For a FENE-P viscoelastic thread, the surfactant can delay the pinch-off of the thread to a great extent, but it affects little the decrease in the minimum thread radius prior to pinch-off when the surface Péclet number is large.

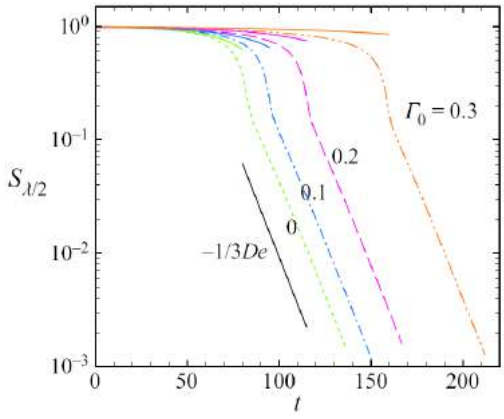

Figure 1. Effect of the initial surfactant concentration Γ_0 on the temporal evolution of the thread radius S at the midpoint of the Oldroyd-B viscoelastic thread.

M006

EFFECT OF A SOFT-GEL COATED WALL ON THE EVOLUTION OF FARADAY WAVES

G. Balram, R. Kumar & B. Dinesh
Department of Chemical Engineering and Technology, Indian Institute of Technology BHU, IIT-BHU, Varanasi, U.P., India

Abstract The natural frequency of a fluid layer overlying on a rigid wall depends on the density of the fluid, surface tension at the free surface and the waveform that evolves at the free surface. However, the presence of a soft-gel layer underneath the fluid layer is expected to alter the natural frequency of the fluid layer. In this work, a linear stability analysis is carried out to show that the natural frequency of the fluid layer is altered by the elasticity of the compliant soft-gel layer. As a consequence of a shift in the natural frequency, there is also a shift in the instability regions when the fluid layer lying on the soft-gel is subjected to Faraday forcing. This indicates that the soft-gel layer either has a stabilizing effect or a destabilizing effect because the presence of a deformable soft-gel layer either raises or lowers the Faraday threshold to induce an instability.

This work focuses on the effect of a soft-gel layer on the evolution of Faraday waves at the free surface of a fluid layer. The fluid is considered to be Newtonian and the soft-gel layer is simulated using a viscoelastic model [1, 2]. Note that the viscoelastic soft-gel layer consists of elastic and viscous stresses. Another crucial aspect of this model is that it also incorporates the inertia in the soft-gel layer. Note that the elastic stresses and the inertia of the soft-gel layer play a key role in the evolution of the Faraday waves at the free surface of the fluid layer. This system is subjected to a parametric forcing $A\omega^2 cos(2\omega t)$, where A is the critical amplitude for the onset of Faraday waves and ω is the forcing frequency [3]. At the fluid soft-gel interface, we impose continuity of velocities, tangential and normal force balance conditions. In addition, it is through these conditions the soft-gel interacts with the fluid. A linear stability analysis is carried out coupled with the Floquet analysis to determine the critical amplitude i.e., A required for the onset of an instability for a given input frequency, ω.

We now discuss the results obtained from the linear stability analysis, where for a given wavenumber the critical dimensionless amplitude (acceleration) required for the onset of the Faraday instability is determined. The soft-gel has a twofold effect on the evolution of the Faraday waves at the free surface of the fluid layer. First, observe from figure 1a that for a range of wavenumbers, the critical dimensionless acceleration required for the onset of instability in the presence of a soft-gel layer (given by the black dots) is higher than that of a rigid wall (given by the red dots). However, in figure 1b the dimensionless amplitude in the presence of the soft-gel layer reduces when compared to that of the case where the bottom wall is rigid. It is noteworthy that figure 1b is obtained by increasing the elastic nature of the soft-gel layer as compared to figure 1a. In figure 1a the increment in the dimensionless acceleration is due to the stabilising effect of the elastic stresses of the soft-gel layer, while the decrement in the dimensionless acceleration in figure 1b is due to the effect of inertia in the soft-gel layer. This inertia coupled with the inertia in the fluid layer drives the Faraday instability at the free surface.

(a) (b)

Figure 1. (a) Dimensionless acceleration versus wavenumber for a rigid soft-gel layer. The red dots represent the critical curve where the bottom wall is rigid. The black dots represent the case where the bottom wall consists of a soft-gel layer. (b) Dimensionless acceleration versus wavenumber for a highly elastic soft-gel layer.

References

[1] Dinesh B., and Pushpavanam S., Linear stability of layered two-phase flows through parallel soft-gel-coated walls, *PHYSICAL REVIEW E*, **56**, 4145-4155, 2017.
[2] Dinesh B., and Narayanan R., Branching behavior of the Rayleigh-Taylor instability in linear viscoelastic fluids. *J. Fluid Mech*, **915**, 2021.
[3] Dinesh B., Livesay J., Ignatius I., B., and Narayanan R., Pattern formation in Faraday instability –experimental validation of theoretical models, *The Royal Society, Philosophical Transactions A*, **381**, 1-20, 2023.

M007

INSTABILITIES IN CATALYTICALLY ACTIVE PORES

Gonçalo Cruz Antunes[1], Paolo Malgaretti[1] & Jens Harting[1,2]
[1] *Helmholtz-Institut Erlangen-Nürnberg für Erneuerbare Energien (IEK–11), Forschungszentrum Jülich, Cauer Str. 1, 91058 Erlangen, Germany*
[2] *Department Chemie- und Bioingenieurwesen und Department Physik, Friedrich-Alexander-Universität Erlangen-Nürnberg, Fürther Straße 248, 90429 Nürnberg, Germany*

Abstract We report on the instabilities displayed by catalytically active pores exhibiting spatially-inhomogeneous chemical reactions (diffusioosmotic flows). These instabilities appear from the competition between advective and diffusive transport of the chemical species in solution.

Much attention is currently being given to the problem of manipulating fluids at the microscale, with successful applications to fields such as 3D fabrication and biomedical research [1]. Often micropumps are a fundamental component of these microfluidic systems. An intriguing technique to manipulate fluid flows in a pore is diffusioosmosis [2]. Fluid flow is obtained upon imposing an inhomogeneous concentration of some solute, which generates flow in a boundary layer around the pore walls. These inhomogeneities may be achieved via an inhomogenous catalytic coating of the pore walls.
We show that a corrugated catalytic pore can act as a micropump even when it is fore-aft symmetric [3, 4]. This phenomenology is possible due to a spontaneous symmetry breaking (pitchfork bifurcation) which occurs when advection rather than diffusion is the dominant mechanism of solute transport. We investigate this phenomenology by Lattice Boltzmann simulations, as well as a semi-analytical approach based on lubrication theory.
Introducing asymmetries to the pore (via the shape or the catalytic coating) leads to an imperfect bifurcation and to discontinuous jumps in the flow rate [4]. Furthermore, relaxing the condition of Stokes flow leads to unsteady flow via a Hopf bifurcation. The result are persistent oscillations in the flow rate with a tunable frequency [3].

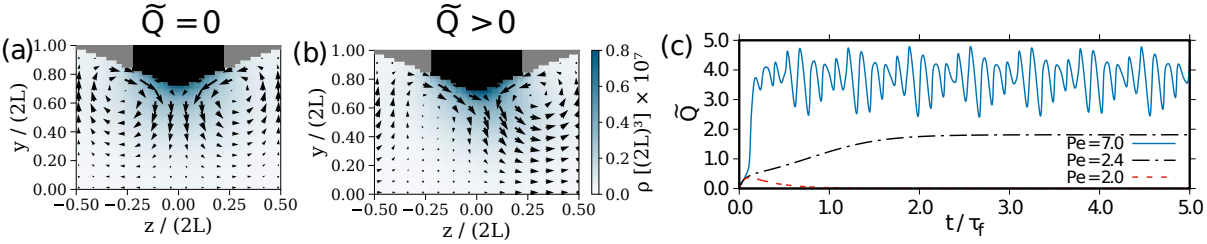

Figure 1. a) Snapshot of a fore-aft symmetric steady state. Black surfaces are covered in catalyst, gray surfaces are chemically inert. Blue represents concentration of solute; b) Spontaneous symmetry breaking leads to steady pumping; c) Normalized flow rate as a function of normalized time for three values of the Péclet number

References

[1] G. M. Whitesides, *The origins and the future of microfluidics*, Nature 442, pages 368–373 (2006)
[2] J. L. Anderson, *Colloid transport by interfacial forces*, Ann. Rev. Fluid Mech., 1989. 21:61-99
[3] G. C. Antunes, P. Malgaretti, J. Harting, and S. Dietrich, *Pumping and Mixing in Active Pores*, Phys. Rev. Lett. 129, 188003 (2022).
[4] G. C. Antunes, P. Malgaretti, and J. Harting, *Turning catalytically active pores into active pumps*, J. Chem. Phys. 159, 134903 (2023)

M008

INSTABILITY OF STRATIFIED AIR-WATER PIPE FLOWS

Ilya Barmak[1,2], Yakov Nezihovski[1], Alexander Gelfgat[1] & Neima Brauner[1]
[1] *School of Mechanical Engineering, Tel Aviv University, Tel Aviv, Israel*
[2] *Soreq NRC, Yavne, Israel*

Keywords:Stability ; two-phase stratified flows ; circular pipe ; bipolar coordinates

Abstract

In this work, we investigate instability of two-phase stratified air-water flows in horizontal circular pipes. The stability problem was formulated and solved for all possible infinitesimal three-dimensional disturbances, and taking into account possible deformation of the air-water interface. No simplifications are made on the pipe geometry and on the velocity field as well as on the interface deformations. We treat the stability problem by two independent approaches, either formulated in the bipolar coordinate system or in the Cartesian one, combined with the immersed boundary technique to account for the circular shape of the pipe wall. In the bipolar coordinates the pipe wall and the fluid-fluid interface of constant curvature coincide with the coordinate lines, thus allowing one to avoid special treatment of the boundaries. Moreover, solving the problem in bipolar coordinates allows us to reproduce numerically the analytical solution of Goldstein et al. [1] for the base flow. The numerical results obtained by the two approaches are in a good agreement and in most cases coincide to within the third decimal place. More details can be found in [2].

The numerical results on stability of air-water stratified flows in horizontal pipes are presented as stability diagrams and compare well with the existing experimental results (e.g., Fig. 1a, pipe diameter of $D = 0.05$m) and with new experimental data obtained in our lab in a different pipe diameter ($D = 0.014$m). The latter are obtained by two independent experimental methods based on a laser beam deflection when it passes through the air-water interface [3] and an ultrasound wave reflected from the interface. The calculated neutral curves are accompanied by the corresponding dimensionless wave numbers and wave speeds of the critical perturbations (Fig. 1b), as well as by the spatial patterns of the velocity components of the critical disturbances, whereby five modes of the critical perturbation are revealed. Long waves ($\alpha = 0.001$ in Fig. 1b) turn out to be the critical disturbance along a part of the stability boundary, which is also then affected by the surface tension, due to the effect of the lateral confinement effect introduced by the pipe walls.

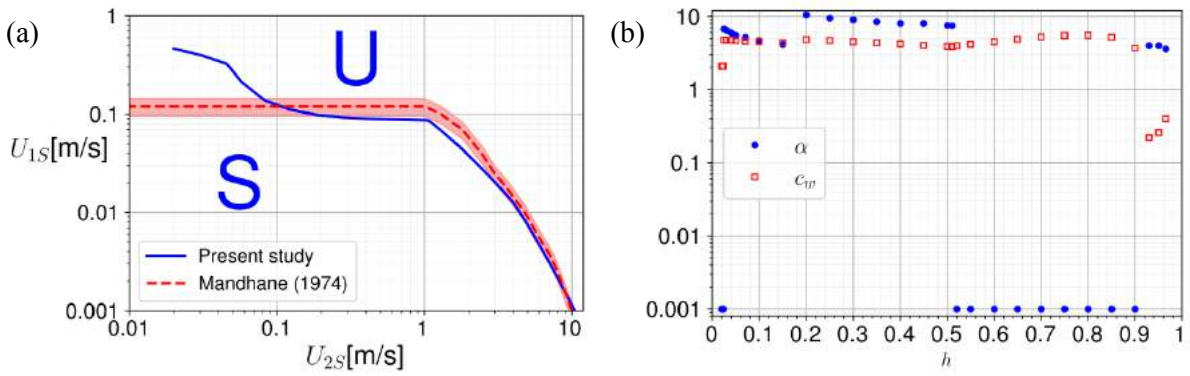

Figure 1. (a) Stability map for a horizontal air-water flow in a pipe of diameter 0.05m. Comparison with the experimental data of [4]. (b) Critical wavenumber (α, blue circles) and critical wave speed scaled by the average velocity in the water layer (c_w, red squares) vs. the holdup along the stability boundary.

References

[1] A. Goldstein, A. Ullmann, N. Brauner. *Characteristics of stratified laminar flows in inclined pipes*. Int. J. Multiphase Flow 75, 267-287 (2015).
[2] I. Barmak, A. Gelfgat, N. Brauner. *A numerical framework for linear stability analysis of two-phase stratified pipe flows,* Theor. Comp. Fluid Dyn. 37, 559-587 (2023).
[3] Y. Nezihovski, A. Gelfgat, A. Ullmann, N. Brauner. *Experimental measurements versus linear stability analysis for primary instability of stratified two-phase flows in a square rectangular duct.* Int. J. Multiphase Flows 153, 104061 (2022).
[4] J. Mandhane, G. Gregory, K. Aziz. *A flow pattern map for gas-liquid flow in horizontal pipes*. Int. J. Multiphase Flow 1,537-553 (1974).

M013

PHYSICS INFORMED NEURAL NETWORKS FOR ACCELERATING PERIODIC THERMAL AND FLUID ENGINEERING SIMULATIONS

Lakshya Chaplot[1], Atul Sharma[1]
[1]*Department of Mechanical Engineering, Indian Institute of Technology Bombay, Mumbai, India*

Keywords: Physics informed neural networks, optimisation, periodic flows and heat diffusion

Abstract
Simulating transient thermal and fluid flows that evolve into periodic states is an indispensable component of CFD in various engineering applications. Most of the computational effort is expended on simulating the initial, non-periodic transient state, which, while necessary, provides limited engineering insights. Traditional finite volume method (FVM) solvers, employing time-stepping techniques, offer no alternative but to initiate simulations from the initial condition, which entails solving through the entire transient phase to reach the desired periodic state. This work introduces a novel approach utilising Physics-Informed Neural Networks (PINNs) to simulate periodic Partial Differential Equations (PDEs). Unlike conventional methods, this solver (introduced by [1]) focuses on the time window beyond the initial transient state, optimizing PINN parameters specifically for this period and the entire spatial domain. The potential implications of this research extend to significantly enhancing the computational efficiency of solving transient PDEs, particularly in TFE applications.
The 2D heat diffusion equation for temperature $T(x, y, t)$ is chosen to demonstrate the research idea–

$$\frac{\partial T}{\partial t} = \nabla^2 T + 25e^{-t/5} \; \forall \; x, y \in [0,1], t \in [0, 35]$$

The initial condition (IC) : $T(x, y, 0) = 0$ and boundary condition (BC) : $T(0, y, t) = T(1, y, t) = T(x, 0, t) = 0$; $T(x, 1, t) = 1 - 2\sin(t)$ are used to introduce periodicity in the system. As the PINN-based algorithm is essentially an optimisation problem, the overall loss function (objective function) is as follows as per [2]–

$$\min_{\boldsymbol{w}} \max_{\lambda_{BC}, \lambda_{IC}, \lambda_r} \{\lambda_{BC} \cdot Loss_{BC} + \; \lambda_{IC} \cdot Loss_{IC} + \; \lambda_r \cdot Loss_{PDE}\}$$

The various loss terms mentioned above are sampled at different spatio-temporal points with the PDE residual as –

- $Loss_{PDE} = \frac{1}{N_r} \Sigma_k^{N_r} \left(\frac{\partial T_{NN}(x_k, y_k, t_k)}{\partial t} - \nabla^2 T_{NN}(x_k, y_k, t_k) - 25e^{-t_k/5} \right)^2$, with $N_r = 2000$ collocation points sampled in a small time window of $t_k \in [25,35] s$.

The time taken by FVM to fully simulate for $t \in [0, 35] s$ is $\mathbf{21.5 \pm 0.7}$ ***mins*** whereas the time taken by PINN solver for $t \in [25, 35] s$ is $\mathbf{5.6 \pm 0.5}$ ***mins***. The centerpoint temperature variation is shown in Figure-1 below.

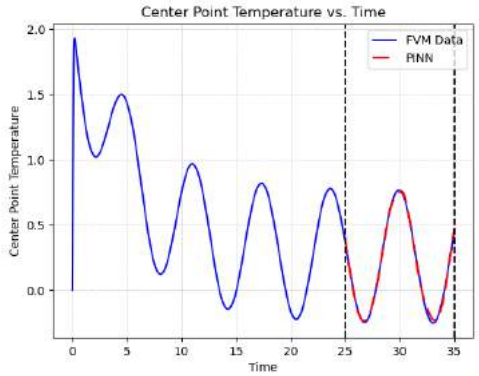

Figure 1. Comparison of PINN solver against FVM solver for transient temperature at domain centerpoint *(x, y) = (0.5, 0.5)*

The PINN-based solver displayed superior performance compared to traditional FVM, efficiently capturing essential periodic behaviours while skipping the initial transient phase with appreciable accuracy.

References

[1] M. Raissi, P. Perdikaris, and G. E. Karniadakis, "Physics-informed neural networks: A deep learning framework for solving forward and inverse problems involving nonlinear partial differential equations," J Comput Phys, vol. 378, pp. 686–707, Feb. 2019, doi: 10.1016/J.JCP.2018.10.045.
[2] S. Li and X. Feng, "Dynamic Weight Strategy of Physics-Informed Neural Networks for the 2D Navier–Stokes Equations," Entropy 2022, Vol. 24, Page 1254, vol. 24, no. 9, p. 1254, Sep. 2022, doi: 10.3390/E24091254.

M014

SEEKING FOR RARE EVENTS IN A BACKWARD-FACING STEP FLOW USING REAL-TIME PARTICLE IMAGE VELOCIMETRY

Juan Pimienta[1,2] & Jean-Luc Aider[1]
[1]*Laboratoire PMMH - UMR7636 CNRS - ESPCI Paris - PSL - Sorbonne Université, 7-9 quai Saint Bernard, 75005 Paris, France*
[2]*Photon Lines, 34 rue de la Croix de Fer, 78100, Saint-Germain-en-Laye, France*

Abstract In this study we show that it is possible to use an innovative real-time optical flow particle image velocimetry setup to monitor as long as needed (hours) the flow downstream a backward-facing step (BFS) to find rare events of high turbulent kinetic energy.

Rare events in fluid flows can be described as a phenomena with a very low probability of occurrence. They are of interest in various cases as they represent peculiar states of the flow. It can be bursts of high energy in a turbulent flow [1], acoustic bursts in a jet [2], emergence of turbulent spots in subcritical flows [3]. In this study, we used a continuous real-time optical flow particle image velocimetry (RT-OFPIV) to monitor the flow past a BFS over a very long time (hours). In this case, the RT-OFPIV allows the instantaneous computation of various quantities, derived from the instantaneous PIV fields, that can be used as "visual sensors" to detect rare events. Using specific detection criteria, like a large burst of kinetic energy computed in a large PIV field, it is then possible to trigger the recording of 1000 PIV fields of the corresponding time-sequence. Using this protocol, we found evidence of rare events that separate themselves from the regular distribution of the velocity data, both in terms of their occurrence and deviation from the mean value. Figure 1 presents the recording of two instantaneous quantities computed in real-time from 2D velocity fields measured in a horizontal plane at the middle of the step height for $Re_h = 800$. One of the sensor is a local velocity probe defined in the PIV field (blue curve). The other is a global measurement of the turbulent kinetic energy. One can see that it is possible to find a rare event corresponding to large streamwise velocity. Once this point is identified, it triggers the recording of a series of snapshots that can then be analyzed. In the present example, POD calculations were performed. POD modes of the spanwise velocity component give evidence of the nucleation of a turbulent spot quadrupole around the reattachment zone of the shear layer. This result opens the path to experiments dedicated to the physics of rare events in shear flows.

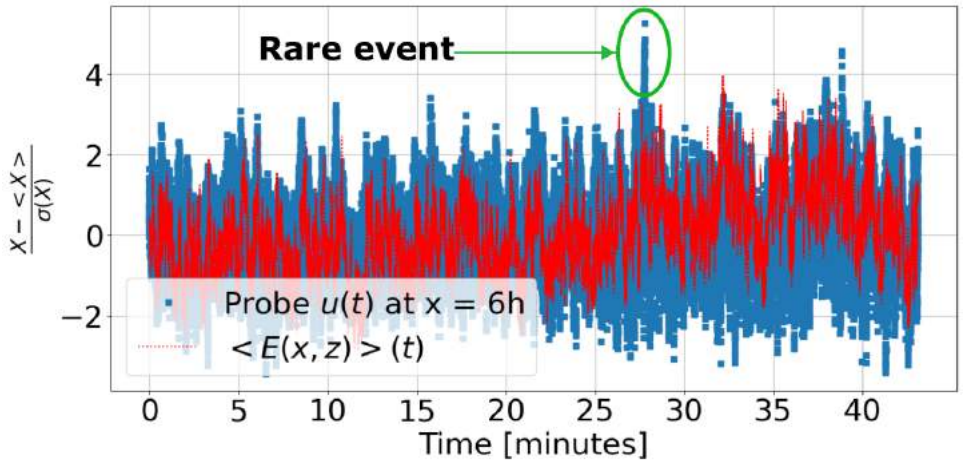

Figure 1. Time series during 43 minutes of two quantities computed in real-time from the instantaneous 2D velocity fields: a square velocity probe of (15 pix^2) located at $x = 6h$ downstream a BFS (blue curve), and the kinetic energy spatially averaged over the image (red curve). A rare event corresponding to a nearly 6σ deviation is shown. This is a single event over 43 min recordings at 40 fps, which corresponds to 103 200 measurements.

References

[1] Moffatt H. K., *Extreme events in turbulent flow*, Journal of Fluid Mechanics, vol. **914**, p. F1, 2021.
[2] Schmidt O. T., Schmid P. J., *A conditional space–time POD formalism for intermittent and rare events: example of acoustic bursts in turbulent jets*, Journal of Fluid Mechanics **867**, R2 (2019).
[3] Lemoult G., Aider J.-L., Wesfreid J. E., *Turbulent spots in a channel: large-scale flow and self-sustainability*, Journal of Fluid Mechanics **731**, R1 (2013).

M015

SPATIALLY-DEVELOPING DISTURBANCE MODES IN THE TEMPORALLY-PERIODIC BURGERS EQUATION: A NONLINEAR ANALYSIS

Pedro Vayssière Brandão[1], Antonio Barletta[1], Michele Celli[1], Stefano Lazzari[2] & Emanuele Ghedini[1]
[1]*Department of Industrial Engineering, Alma Mater Studiorum Università di Bologna, Viale Risorgimento 2, 40136 Bologna, Italy*
[1]*Department of Architecture and Design, University of Genoa, Stradone S. Agostino 37, 16123 Genoa, Italy*

Abstract Spatial instabilities; Numerical simulations; Nonlinear dynamics; Burgers equation.

Traditionally, linear stability analysis deals with the temporal behaviour of infinitesimal disturbances that are superposed to an equilibrium state of some dynamical system. In this sense, if some of these infinitesimal disturbances grow in time, for large times, the problem is said to be unstable, otherwise it is said to be stable. In fluid dynamics studies, the instabilities that can emerge are usually classified as being of convective or absolute nature. A distinction between these types of instability can be made by looking at the long-time behaviour of an infinitesimal wavepacket introduced in a fixed region of space. If the wavepacket amplitude decays, the base flow is said to be stable. Otherwise, if its amplitude grows in time as it is convected away by a base flow, the base flow is said to be convectively unstable. Finally, if the wavepacket amplitude grows in time at its introduction point, the base flow is said to be absolutely unstable. A good review of these concepts can be found in the paper by Huerre & Monkewitz [1], as well as in the books by Drazin & Reid [2] and Barletta [3].

Based on these ideas, to be observed in a laboratory-reference frame, convectively unstable disturbances must be excited continuously in a fixed spatial location. Otherwise, since the disturbances in this regime grow as they are convected away by the base flow, they can eventually leave the domain before been noted by an observer. Then, if the excitation source emits a continuous time periodic signal at an unstable frequency, travelling unstable disturbances that grow as they are convected downstream can be observed. In this case, a growth in space can be observed from the excitation source. Usually, in order to investigate spatially-growing disturbances in the sense mentioned before, initial value problems are considered. This fact restricts the analysis because of the persistence of the initial condition that must be respected, which select a priori some of the instability modes that can exist downstream and upstream from the excitation point. This kind of problem, also known as signaling problem, was first investigated by Gaster [5].

Recently, Barletta [4] has formally investigated spatially developing disturbance modes in the Prats problem, by considering a spatial stability analysis. In his analysis, he considered periodicity in time and investigated the spatial dynamics of the Fourier time-periodic disturbance modes. As expected, he found four modes, instead of the single one found in the classical temporal stability analysis. Since his analysis considers, from the beginning, time periodicity, there is no initial condition to be respected and the four modes are allowed to exist. The direction of propagation of these modes is simply determined by the phase velocity of the plane disturbance waves. He found that, in this sense, spatial instabilities can arise even in temporally stable flow conditions. In order to go further on the investigations started by him, in the present work we propose to study the spatial instabilities on the Burgers equation, by means of nonlinear numerical simulations. The Burgers equation is a partial differential equation formulated as a toy model for developing turbulence. The one-dimensional Burgers equation subject to a linear force can be expressed as

$$\frac{\partial W}{\partial t} + W\frac{\partial W}{\partial x} = \frac{\partial^2 W}{\partial x^2} + R\,(W - W_0), \tag{1}$$

where $R > 0$ is the driving linear force parameter and $W = W_0$ is a possible basic stationary solution of the equation.

We demonstrate here the emergence of disturbances from $x = 0$, even in temporally stable parametric conditions, in both upstream and downstream directions. In order to do so, we consider the method of lines. We discretized the time derivative by using a fourth-order central difference scheme, and imposed a periodicity of $T = 2\pi/\omega$, where ω is the oscillation frequency. The spatial solution in x is found by means of the solver *NDSolve* built-in in the Mathematica software.

References

[1] P. Huerre, P. Monkewitz *Absolute and convective instabilities in free shear layers*, Journal of Fluid Mechanics **159**, 151–168 (1990).
[2] P. Drazin, W. H. Reid, *Hydrodynamic Stability*, Cambridge University Press (2004).
[3] A. Barletta, *Routes to Absolute Instability in Porous Media*, Springer (2019).
[4] A. Barletta, *Time-evolving to space-evolving Rayleigh–Bénard instability of a horizontal porous medium flow*, Physics of Fluids **33** (12), 124106 (2021).
[5] M. Gaster *On the generation of spatially growing waves in a boundary layer*, Journal of Fluid Mechanics **22** (3), 433–441 (1965).

M016

OPTIMIZING EXTERNAL FORCES FOR LOCK-IN TO THE OSCILLATORY FLOW PAST A FLAT PLATE IN A UNIFORM FLOW

Makoto Iima[1]
[1]*Graduate School of Integrated Sciences for Life, Hiroshima University, Higashihiroshima, Japan*

Abstract Key words: Phase reduction, vortex shedding, Kármán's vortex street, synchronization.

Vortex shedding from bluff bodies is ubiquitously observed in nature. The Kármán's vortex street is a classic example. Understanding and controlling vortex shedding is critical for solving engineering challenges and addressing theoretical questions, including determining optimal forms of external forcing. This study focuses on phase control of the vortex shedding as a rhythmic process.

Many rhythmic phenomena manifest across scientific domains, including engineering (mechanical vibrations), chemistry (Belousov-Zhabotinsky reactions), and physiology (circadian rhythms). They are related to the limit cycle in non-linear systems. Phase reduction theory provides a framework to analyze essential dynamics around the limit cycle. For fluid mechanics, the Kármán's vortex street and wake behind a wing in a uniform flow constituting periodic flows can also be analyzed by the phase reduction theory. This theory enables analyzing the synchronization and the entrainment of the system.

Applying the theory, we can describe the dynamics of the phase of the oscillating flow, $\phi(\in [0, 2\pi))$, by the following equation:

$$\frac{d\phi}{dt} = \omega. \tag{1}$$

We remark that the phase can be defined as a function of the position in the phase space, $\boldsymbol{X}$, as $\phi(\boldsymbol{X}, t)$. The phase sensitivity function, $\boldsymbol{Z}$, defined as $\boldsymbol{Z} = \left.\dfrac{\partial \phi}{\partial \boldsymbol{X}}\right|_{\phi=\phi(\boldsymbol{X},t)}$, is a fundamental function of the phase reduction theory. It describes how much the phase shifts due to the state change by weak perturbations, $\boldsymbol{X} \to \boldsymbol{X} + \Delta\boldsymbol{X}$ through the relationship $\phi(\boldsymbol{X} + \Delta\boldsymbol{X}) \simeq \phi(\boldsymbol{X}) + \Delta\boldsymbol{X} \cdot \boldsymbol{Z}(\phi)$ up to the first order.

When periodic flows are considered, the limit cycle constitutes the spatio-temporal flow pattern, where the state in the phase space represents a snapshot of the pattern. Given all the components of $\boldsymbol{Z}$ are provided, we can design the spatial distribution of a temporally periodic external force to satisfy various objectives, such as minimum energy or maximum lock-in range. The author has developed a technique to calculate $\boldsymbol{Z}$ that applies to general systems including fluids [1, 2] .

We first discuss the spatio-temporal properties of the phase sensitivity function's physical space representation, which provides insight into designing optimal external forcing waveforms for the lock-in. Based on these results, we examine the optimal position of a uniform periodic external force applied within a rectangular region. Such simple localized function is useful for practical flow control. The optimal position depends on the external force component and main forcing frequency. We further analyze the lock-in ranges of a couple of optimal positions and frequencies using the Arnold tongue. The results are compared with globally optimal forcing waveforms based on the phase reduction theory, which achieve maximum lock-in range and the minimum energy, against the simple rectangular forcing [3] .

References

[1] M. Iima, *Jacobian-free algorithm to calculate the phase sensitivity function in the phase reduction theory and its applications to Kármán's vortex street*, Phys. Rev. E **99**, 062203 (2019).
[2] M. Iima, *Phase reduction technique on a target region*, Phys. Rev. E **103**, 053303 (2021).
[3] M. Iima, *Optimal external forces of the lock-in phenomena for the flow past inclined plate in a uniform flow*, under review, arXiv:2311.00977.

M017

NUMERICAL PROPERTIES OF THE DIFFERENTIALLY HEATED CAVITY WITH VARYING ASPECT RATIOS

Fred Wubs[1], Ties Leenstra[1], Sven Baars[2] and Jonas Thies[3]
[1]*Bernoulli Institute, University of Groningen, The Netherlands*
[2]*IMAU, Utrecht University, The Netherlands*
[3] *DIAM, Technical University Delft, The Netherlands*

Abstract Study of the numerical solvability of the 2D differentially heated cavity problem with varying aspect ratios. Questions to be answered are: how does this initial behavior influence (i) the convergence of the solvers, and (ii) the determination of the first bifurcation. Moreover, what is the physical origin of the deterioration? And finally: what can be done to enhance the convergence?
Keywords: Differentially heated cavity, nonnormality, aspect ratio dependency, numerical solvability, finite volume discretization, stability

The numerical bifurcation analysis of the differentially heated cavity (DHC) with insulated upper and and lower boundary is reported to be difficult [1]. When experimenting for a textbook [2] we found that this is aggravated for small aspect ratios of the domain, i.e. its height to width ratio. We encountered convergence problems for Pr=0.71(air), Pr=10 (water), and Pr=1000 when trying to find the critical Rayleigh number, i.e. the number for which the steady solution looses stability, when the aspect ratio is decreased below 8. The smallest critical Rayleigh numbers occur for all of these Prandtl numbers between aspect ratios 8 and 10 and are of the order 10^8, 10^9 and 10^8 respectively. For both, smaller and larger aspect ratios, the critical Rayleigh number will be higher (see [3] for a map of flow regimes). This calls for a study of the numerical properties of the DHC which we perform for the 2D case.
The python package TransiFlow [4] allows us to investigate this phenomenon in detail. We find that clustering of eigenvalues near the origin and nonnormality of the Jacobian near critical points appear to play an important role.

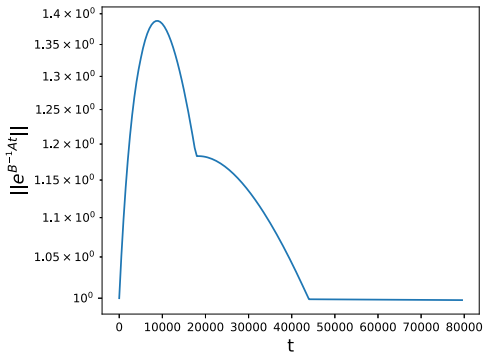

In the figure on the left, the nonnormality is illustrated by showing the maximum possible value of the square root of the energy increase with respect to the initial energy as a function of time. (In fact it results from a low-rank approximation of the problem obtained from the eigenvalue problem solver JaDaPy [5, 6]). This result is for aspect ratio 0.02, Rayleigh number 3×10^9, and $Pr = 1\,000$. One observes a mild increase of the energy, but it takes 40 000 time units before it is finally slowly decaying (showing that the steady solution is stable). Note that for a Jacobian which is normal, the energy will monotonically decrease from the start.

For various aspect ratios results are available in the literature, e.g. [7], to which we compare our results.

References

[1] A. Y. Gelfgat. Time-dependent modeling of oscillatory instability of three-dimensional natural convection of air in a laterally heated cubic box. *Theoretical Computational Fluid Dynamics*, 31(4):447–469, 2017.
[2] Fred W. Wubs and Henk A. Dijkstra. *Bifurcation Analysis of Fluid Flows*. Cambridge University Press, 2023.
[3] D. R. Chenoweth and S. Paolucci. Natural convection in an enclosed vertical air layer with large horizontal temperature differences. *Journal of Fluid Mechanics*, 169:173–210, 1986.
[4] S.Baars, F.W. Wubs, and H.A. Dijkstra. Transiflow, 2023. https://github.com/BIMAU/transiflow.
[5] S.Baars and H.A. Dijkstra. JaDaPy, 2023. https://github.com/BIMAU/jadapy.
[6] Diederik R. Fokkema, Gerard L. G. Sleijpen, and Henk A. Van der Vorst. Jacobi-Davidson style QR and QZ algorithms for the reduction of matrix pencils. *SIAM Journal on Scientific Computing*, 20(1):94–125, 1998.
[7] Alexander Yu. Gelfgat. Stability of convective flows in cavities: solution of benchmark problems by a low-order finite volume method. *International Journal for Numerical Methods in Fluids*, 53(3):485–506, 2007.

M018

THE STABILITY OF MAGNETOHYDRODYNAMIC FLOWS IN CYLINDRICAL GEOMETRIES USING A VELOCITY-VORTICITY FORMULATION

Bernard Knaepen[1] & Yelyzaveta Velizhanina[1]
[1] *Université Libre de Bruxelles, Faculté des Sciences, Physique des Systèmes Dynamiques, CP231, 1050 Brussels, Belgium.*

Abstract A line describing the work (Key words).

We present a novel formulation of the linearized stability equations for magnetohydrodynamic flows in cylindrical geometries, using a closure inspired by the formulation used by Burridge et al. [1] for the hydrodynamic pipe flow. The equations presented are valid for axisymmetric steady state solutions of the form:

$$\boldsymbol{U}(r) = U_z(r)\mathbf{1}_z + U_\theta(r)\mathbf{1}_\theta, \quad \boldsymbol{B}(r) = B_z(r)\mathbf{1}_z + B_\theta(r)\mathbf{1}_\theta, \tag{1}$$

where $\boldsymbol{U}$ and $\boldsymbol{B}$ represent, respectively, the mean velocity field and mean magnetic field, while r, θ, z denote the coordinates of a cylindrical coordinate system. We make no assumption on the magnetic Reynolds number Rm nor on the particular forms of U_z, U_θ, B_z and B_θ. Among others, the potential base flows that can be considered include Poiseuille or Taylor-Couette flows, while admissible configurations for the magnetic field include uniform axial magnetic fields or screw-pinch magnetic fields. As expected, the total order of the linearized system is equal to ten, and it is composed of one fourth-order equation for the radial component of velocity and three second-order equations for the radial components of vorticity, magnetic field and electric current. The resulting generalized eigenvalue problem has a similar structure to that of the traditional Orr-Sommerfeld problem, but with the addition of the contribution from the electromagnetic field. When the magnetic field is absent, the equations differ from the system presented in Burridge et al. [1] only through the mean flow terms as these authors only considered Poiseuille pipe flow. We also discuss the formulation of the electromagnetic boundary conditions and the reduction of the system in the limit of small magnetic Reynolds numbers (also known as the quasi-static limit).

In the pipe flow geometry, the system of equations contains a regular singularity. We show how to modify the equations to guarantee that their solutions are analytical around the origin. This is done by extending the procedure described by Malik et al. [2] for the hydrodynamic pipe flow to include electromagnetic variables. The procedure relies on a change of variables that satisfies the ansatz described by Priymak et al. [3] and uses regularity conditions at $r = 0$ as boundary conditions. This method of addressing the singularity is straightforward to implement using traditional spectral collocation methods and is also flexible as it does not require different basis functions when different boundary conditions are imposed at the pipe's wall. This property is particularly important for MHD flows, as their stability is generally analyzed with different sets of boundary conditions depending on the conductivity of the containing walls.

To illustrate the efficiency and accuracy of our formulation, we benchmark it in the Taylor-Couette and pipe flow geometries for various base flow configurations, using a spectral collocation discretization. As the equations are generic for any of the base flow configurations shown in eq. (1), only the flow parameters have to be modified and the same system can be used to achieve very accurate results. We also demonstrate that in the pipe flow geometry, the formulation enforcing regularity of the solution is better conditioned and results in significantly improved eigenvalue spectra.

References

[1] D. M. Burridge, P. G. Drazin, *Comments on "Stability of Pipe Poiseuille Flow"*, Phys. Fluids **12**, 264–265 (1969).
[2] M. Malik, M. Skote *A linear system for pipe flow stability analysis allowing for boundary condition modifications*, Comput. Fluids **192**, 104267 (2019).
[3] V. G. Priymak, T. Miyazaki, T *Accurate Navier–Stokes Investigation of Transitional and Turbulent Flows in a Circular Pipe*, J. of Comput. Phys. **186**(1), 178–197 (2003).

M019

STABILITY OF PERIODIC SOLUTIONS USING CHEBYSHEV POLYNOMIALS

L. Martin Witkowski[1], A. Gesla[2], Y. Duguet[3] & P. Le Quéré[3]
[1]*Universite Claude Bernard Lyon 1, CNRS, Ecole Centrale de Lyon, INSA Lyon, LMFA, UMR5509, 69622 Villeurbanne, France*
[2]*Sorbonne Université, F-75005 Paris, France*
[3]*LISN-CNRS, Université Paris-Saclay, F-91400 Orsay, France*

Abstract

Being able to compute periodic orbit (PO) stable or unstable (UPO) is of great interest for the fluid mechanics bifurcation community. It allows to establish complete bifurcation diagrams and thus helps understanding the underlying physics of the flow.

In order to determine the stability and bifurcation of periodic orbits, it is necessary first to compute the periodic orbit very precisely and then the Floquet multipliers. A classical approach to find a PO is to use time integration with a shooting method and to converge the initial conditions with Newton's method. The stability of the PO is then determined by computing the eigenvalues of the Monodromy matrix, from which the Floquet multipliers can be deduced.

Instead of using time integration, the periodic orbit of the system can be expressed as a Fourier expansion. This is the well-established Harmonic Balance Method (HBM), which has only recently begun to be used in the fluid mechanics community [1, 2]. The HBM is extremely attractive because of its spectral convergence in time. However, when it comes to computing stability, it suffers from the problem of selecting physically meaningful multipliers [3].

In the present work, a new method for finding the stability of periodic solutions of a dynamical system is proposed. We express the periodic orbit as a sum of Chebyshev polynomials. This expansion does not have the drawback of the HBM because the stability of the orbit can be extracted naturally. There is no need to choose significant multipliers. The new method presented preserves spectral convergence in time.

The results are first presented on Lorenz and Langford systems with only three degrees of freedom. We show that the technique can be easily extended to larger systems. This will be illustrated by calculating the stability of PO for a differentially heated cavity.

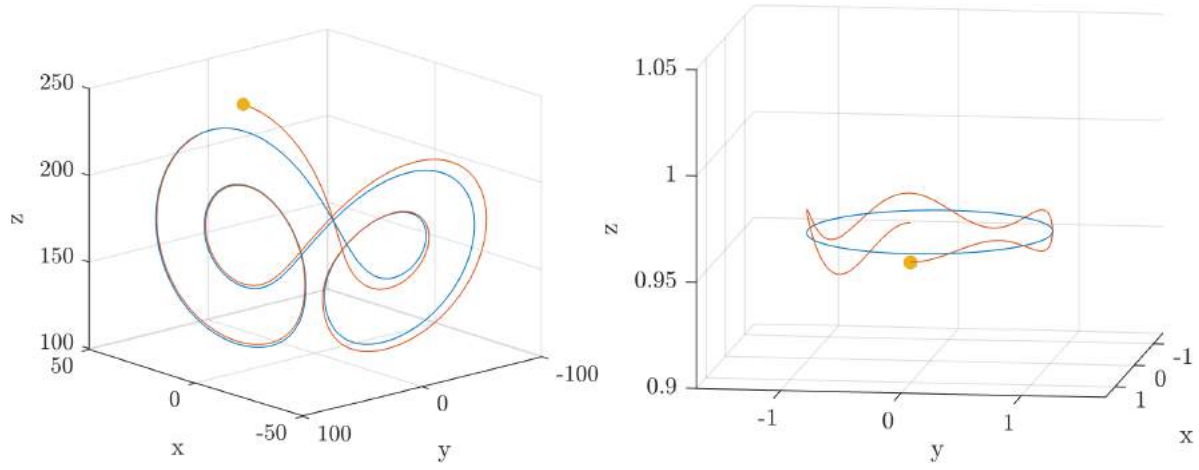

Figure 1. Left: stable orbit (blue) of the Lorenz system $\rho = 160$, $\sigma = 10$, $b = 8/3$ and trajectory (red) deduced from the eigenvector corresponding to the Floquet multiplier 0.247. Right: unstable orbit (blue) of the Langford system $\lambda = 2.02$ and trajectory (red) deduced from the eigenvector corresponding to the Floquet multiplier $-3.612 + 0.458i$. Both trajectories start at the yellow point.

References

[1] Y. Bengana, L. S. Tuckerman, *Frequency prediction from exact or self-consistent mean flows*, Phys. Rev. Fluids **6**, 063901 (2021).
[2] J. Sierra-Ausin, V. Citro, F. Giannetti, and D. Fabre, *Efficient computation of time-periodic compressible flows with spectral techniques*, Comp. Meth. Appl. Mech. Eng. **393**, 114736 (2022).
[3] L. Guillot, A. Lazarus, O. Thomas, C. Vergez, B. Cochelin, *A purely frequency based Floquet-Hill formulation for the efficient stability computation of periodic solutions of ordinary differential systems*, J. Comp. Phys. **416**, 109477 (2020)

M020

A NEW ALGORITHM AND SIMULATION FOR MULTIPHASED STRONGLY FUZZY COMPRESSIBLE FLOWS

Nyaare Benard [1*], Omolo Ongati[2] & Aminer Titus[3]
[1]*Department of Pure and Applied Mathematics, Jaramogi Oginga Odinga University of Science and Technology*
[2,3]*African Institute for Mathematical Sciences, Cape Town, South Africa*

Key words: Compressible flow,Algorithm, Simulation, Model, Fuzziness.

Abstract
In this work we develop a technical theory with a lot of rigor on compressible flows by considering fuzziness. We develop an algorithm to show that multi-phased compressible flows are strongly fuzzy. We consider a ten-equation model phased with a strongly fuzzy component and fuzzy equilibrium. Finally we illustrate the strong fuzziness of the compressible flows using numerical simulations for a depressured nanotube containing Carbon (IV) oxide vapour in 3D approximation.

References

[1] P. Downar-Zapolski, Z. Bilicki, L. Bolle, and J. Franco, *The Non-equilibrium Relaxation Model for One-dimensional Flashing Liquid Flow*, International journal of multiphase flow, **22**, 473–483 (1996).
[2] M. Pelanti and K. Shyue, *A Mixture-energyconsistent Six-equation Two-phase Numerical Model for Fluids with Interfaces, Cavitation and Evaporation Waves*, Journal of Computational Physics, **259**, 331–357, (2014).
[3] A. Zein, M. Hantke, and G. Warnecke, *Modeling phase transition for compressible two-phase flows applied to metastable liquids*, J. Comput. Phys., **229**, 2964–2998, (2010).

M025

STABILISING TRAVELLING WAVES FROM PIPE FLOW TURBULENCE.

Dan Lucas[1] & Tatsuya Yasuda[1,2]
[1] *Department of Mathematics and Statistics, University of St Andrews, Scotland.*
[2] *Advanced Knowledge Laboratory Inc., Tokyo.*

Abstract Time-delayed feedback control is used to stabilise exact coherent structures in pipe flow up to $Re = 3000$.

Time-delayed feedback control (TDFC) is a method known to stabilise unstable periodic orbits and fixed points in low-dimensional dynamical systems [1]. The method introduces a control term $G(t)\,(x(t) - x(t-T))$ into a dynamical system $\dot{x} = f(x)$ where G is some gain function/matrix and T the delayed period. The goal is to stabilise a solution with period T. The attractive feature of this method is that, if successful, the control term vanishes identically since $x(t) = x(t-T)$, and the stabilised state is a solution of the uncontrolled system. In this sense the method is *non-invasive*. This makes this control method a good candidate for improving our ability to compute "exact coherent structures" [4] embedded in fluid turbulence.

It has recently been shown that the method, when formulated in concert with the system symmetries and with an adaptive approach to obtain phase-speeds, can stabilise travelling waves from two-dimensional turbulence [2]. Here we will demonstrate that the method is also effective at stabilising travelling waves from turbulence in a periodic pipe. The main novelty here is in the application of a "multiple time-delayed feedback" (MTDF) approach, where several control terms are required to attenuate a broad range of unstable eigenfrequencies. We implement a gradient descent method to dynamically adjust the gain functions $G_i(t)$ in order to reduce the need for tuning a high dimensional parameter space. In this way we can stabilise nonlinear travelling waves up to moderately high Reynolds numbers, without using any of their properties to initiate the control.

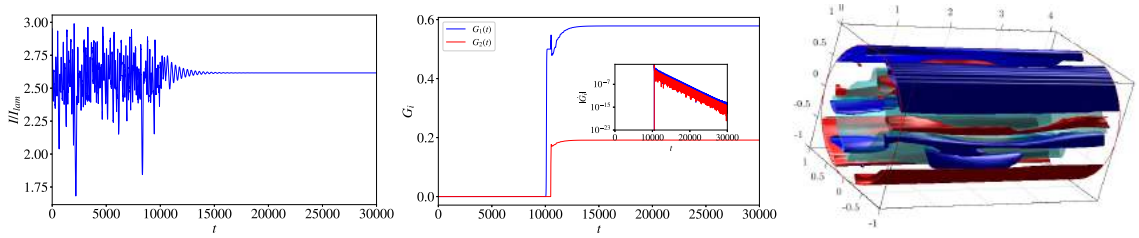

Figure 1. Plots showing the successful stabilisation of the upper branch travelling wave solution [3] at $Re = 3000$ in the $L = 2.5D$ pipe, MTDF is initiated at $t = 10000$. Left: normalised energy input rate, showing turbulent fluctuations before MTDF is applied and then tending towards the constant value of the travelling wave. Centre: gains of the two TDFC terms applied showing their adaptation to stabilising values. Right: final snapshot of the flow, red and blue isosurfaces denote $\omega_z = 0.15$ and -0.15, respectively, where $\omega_z = (\nabla \times \boldsymbol{u})_z$ is the streamwise fluctuating vorticity.

References

[1] K. Pyragas, *Continuous control of chaos by self-controlling feedback*,Physics Letters A **170**, 421–428 (1992).
[2] D. Lucas and T. Yasuda, *Stabilization of exact coherent structures in two- dimensional turbulence using time-delayed feedback*, Phys. Rev. Fluids **7**, 014401 (2022).
[3] Willis, A. P., Cvitanović, P. & Avila, M. *Revealing the state space of turbulent pipe flow by symmetry reduction*, J. Fluid Mech. **721**, 514–540 (2013)
[4] Chandler, G. J. & Kerswell, R. R. *Invariant recurrent solutions embedded in a turbulent two dimensional Kolmogorov flow*, J. Fluid Mech. **722**, 554–595 (2013)

M026

HELE-SHAW FLOW OF A NEMATIC LIQUID CRYSTAL

Stephen K. Wilson[1], Joseph R. L. Cousins[1,2], Akhshay S. Bhadwal[3], Nigel J. Mottram[2] & Carl V. Brown[3]
[1]*Department of Mathematics and Statistics, University of Strathclyde, Livingstone Tower, 26 Richmond Street, Glasgow G1 1XH, UK*
[2]*School of Mathematics and Statistics, University of Glasgow, University Place, Glasgow G12 8QQ, UK*
[3]*SOFT Group, School of Science and Technology, Nottingham Trent University, Clifton Lane, Nottingham NG11 8NS, UK*

Keywords: liquid crystals, lubrication theory, microfluidics

Motivated by the variety of applications in which nematic Hele-Shaw flow occurs, a theoretical model for Hele-Shaw flow of a nematic liquid crystal is formulated and analysed. We derive the thin-film Ericksen–Leslie equations that govern nematic Hele-Shaw flow, and consider two important limiting cases in which we can make significant analytical progress. Firstly, we consider the leading-order problem in the limiting case in which elasticity effects dominate viscous effects, and find that the nematic liquid crystal anchoring on the plates leads to a fixed director field and an anisotropic patterned viscosity that can be used to guide the flow of the nematic. Secondly, we consider the leading-order problem in the opposite limiting case in which viscous effects dominate elasticity effects, and find that the flow is identical to that of an isotropic fluid and the behaviour of the director is determined by the flow. The insight which can be gained by using this approach is illustrated by formulating and analysing a simple model for the squeezing stage of the One Drop Filling method, an important method for the manufacture of Liquid Crystal Displays (see Figure 1) [1].
The flow of a nematic in a Hele-Shaw cell with an electrically-controlled viscous obstruction is investigated both theoretically and experimentally. The viscous obstruction is created by temporarily electrically altering the viscosity of a nematic liquid crystal in a region of the cell across which an electric field is applied. The theoretical model is validated experimentally for the case of a circular cylindrical obstruction, demonstrating user-controlled flow manipulation by varying the applied voltage. This new approach provides a customisable framework for manipulating the flow within heterogeneous single-phase microfluidic devices without relying on time-consuming and/or permanent device-altering methods [2].

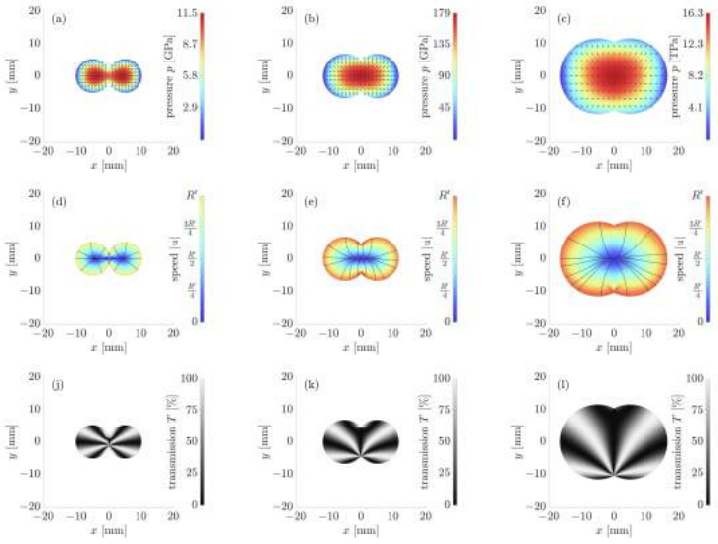

Figure 1. Top row - the pressure (coloured background) and the director field (black rods); Middle row - flow speed (coloured background) and streamlines (solid black lines); Bottom row - the optical transmission: in the limit of small Ericksen number for two coalescing droplets in a Hele-Shaw cell at three different times.

References

[1] J. R. L. Cousins, N. J. Mottram, S. K. Wilson, *Hele-Shaw flow of a nematic liquid crystal*, submitted for publication and arXiv 2401.13061 (2024).
[2] J. R. L. Cousins, A. S. Bhadwal, N. J. Mottram, C. V. Brown, S. K. Wilson, *Flow manipulation in a Hele-Shaw cell with an electrically-controlled viscous obstruction*, submitted for publication (2023).

M027

Optimisation of average quantities in a forced Lorenz system: influence of periodic orbits

Filip A. Jovanovic* and Tom S. Eaves

School of Science and Engineering, University of Dundee, Dundee DD1 4HN, UK

Abstract

Surface drag (skin friction) gives rise to significant levels of energy loss throughout a wide range of transport systems. One approach which proved effective in drag reduction was to oscillate the surfaces of the flow transversely to the flow direction; where through simulations and experiments it was demonstrated that this approach can achieve a drag reduction of up to 25% (Quadrio, 2011) at moderate Reynolds numbers. It is clear that this reduction occurs as a result of structural changes within the flow in the near-wall region. However, what specifically occurs to the structures and the way in which they evolve throughout the periodic forcing remains unknown. Through previous research (see e.g. Kawahara *et al.* (2012)) it is known that the chaotic dynamics of such fluid systems evolve around coherent structures such as equilibrium points and periodic orbits where periodic orbits are often described as the "skeleton" of these dynamics. One approach to understanding how periodic forcing impacts averages of turbulent motion is to focus on how it does so for simple chaotic systems as a preliminary step, such as the Lorenz system of equations (Lorenz, 1963). In this talk, we demonstrate how periodic forcing impacts averages in this system and relate the changes that occur with structural changes to the Lorenz system's unstable periodic orbits. These orbits are known to act as the only components needed for the computation of averages in the Lorenz system (Eckhardt & Ott, 1994), and this talk will demonstrate to what extent this still holds for a periodically forced version of this system. We will demonstrate how oscillatory forcing effects the averages of the chaotic attractor, its dynamics, and their relation to its new unstable periodic orbits. Additionally, we go on to explore optimal forcing methods within Lorenz. The talk will outline a methodology with which to analyse a wider range of chaotic systems that stem from our new understanding of Lorenz, with the aim of designing optimised strategies for drag reduction.

References

Eckhardt, B. & Ott, G. 1994 Periodic orbit analysis of the Lorenz attractor. *Z. Phys. B* **93**, 259–266.

Kawahara, G., Uhlmann, M. & van Veen, L. 2012 The significance of simple invariant solutions in turbulent flows. *Annu. Rev. Fluid Mech.* **44**, 203–225.

Lorenz, E. N. 1963 Deterministic nonperiodic flow. *J. Atmos. Sci.* **20** (2), 130–141.

Quadrio, M. 2011 Drag reduction in turbulent boundary layers by in-plane wall motion. *Philos. T. R. Soc. A* **369** (1940), 1428–1442.

*Email address for correspondence: f.jovanovic@dundee.ac.uk

M028

ACTIVE CONTROL OF TRAILING VORTICES BY SYNTHETIC JETS IN THE AXIAL DIRECTION NEAR THE WINGTIP

Carlos del Pino[1], Luis Parras[1], José Hermenegildo García-Ortiz[2], Jorge Aguilar-Cabello[1], Francisco José Blanco-Rodríguez[3] & Paloma Gutiérrez-Castillo[1]

[1]*Fluid Mechanics, University of Málaga, Institute for Mechatronics Engineering & Cyber-Physical Systems (IMECH.UMA), Málaga, Spain*

[2]*Department of Mechanical Engineering and Industrial Design, School of Engineering, University of Cádiz, Cádiz, Spain*

[3]*Fluid Mechanics, School of Industrial Engineering, University of Seville, Seville, Spain*

Abstract We applied an oscillating synthetic jet in the axial direction to a wingtip vortex and observed a decrease in its strength (active control, synthetic jets, wingtip vortex).

We have designed, manufactured and set up an experimental device to be tested in a towing tank using a NACA0012 wing model at chord-based Reynolds numbers Re_c=40×10^3 [1]. We used this device to create an axial injection jet with zero net mass flux since we have based our design on previous work on stability analyses concerning frequency response [2, 3]. Reducing the vortex strength is the primary objective of the active control. To demonstrate the achievement of this goal, we used different frequency/amplitude pairs, resulting in different jet waveform velocities near the wingtip. We conducted experiments to determine which pairs produced the most significant vorticity reduction. The maximum reduction achieved was 15% of the peak vorticity $max(\Omega)$ in the far-field $z/c \sim 35$, see Fig. 1. Thus, the experimental device has successfully achieved vortex attenuation, indicating effective active control. These results make this device a promising technological candidate for various wing models, including larger ones in future applications. The experimental device is currently pending patent.

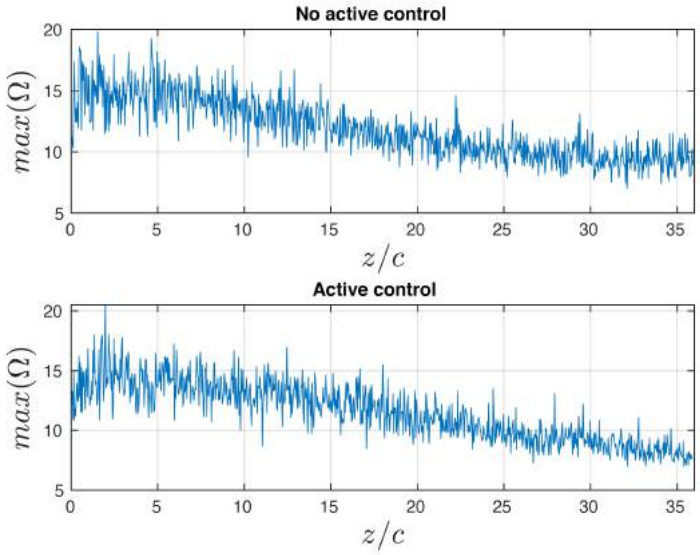

Figure 1. Vorticity peak against axial distance z/c in the reference experiment (top) and using active control (bottom).

References

[1] P. Gutierrez-Castillo, M. Garrido-Martin, T. Bölle, J.H. García-Ortiz, J. Aguilar-Cabello, and C. del Pino, Phys. Fluids **34**, 107116 (2022).
[2] F.J. Blanco-Rodríguez, L. Parras and C. del Pino, Fluid Dyn. Res. **48**, 061417 (2016).
[3] C. del Pino, F. J. Blanco–Rodríguez, M. Garrido-Martin, and L. Parras, 2nd Spanish Fluid Mechanics Conference (2023).

M029

INFLUENCE OF THE THEORETICAL MODEL ON AN ACTIVE CONTROL OF WINGTIP VORTICES

Paloma Gutierrez-Castillo[1], Manuel Garrido-Martin[1], Tobias Bölle[2], Francisco J. Blanco-Rodríguez[3], Carlos del Pino[1]

[1] *Universidad de Málaga, Institute for Mechatronics Engineering and Cyber-Physical Systems (IMECH.UMA), Campus de Teatinos, s/n, 29071 Málaga, Spain*

[2] *Deutsches Zentrum für Luft- und Raumfahrt, Institut für Physik der Atmosphäre, Oberpfaffenhofen, Germany*

[3] *Fluid Mechanics, School of Industrial Engineering, University of Seville, Seville, Spain*

Abstract The Frequency Response of Lamb-Oseen and Batchelor vortex models have been analyzed for a Single Point Injection (vortex, frequency response, optimal response, linear stability, active injection).

The natural dissipation of wingtip vortices primarily results from the intrinsic long-wave and short-wave instabilities [1]. The objective of active control devices is to diminish the strength of vortices by intentionally triggering these instabilities prematurely and/or amplifying the growth rate of the vortex core through the injection of added mass and turbulence. Active control methods employing single-pulse fluidic actuation or forced transverse gusts present promising solutions for reducing vortex strength. Adopting zero net mass flux (ZNMF) devices, such as synthetic jets, has gained widespread attention in the global fluid dynamics community, with particular interest in flow control research.

In this work, we analyze the influence of election of the theoretical model that represents the vortex in the frequency response associated with a Single Point Injection (SPI) by varying the forcing frequency ω_f, the axial wavenumber k and the distance to the center core d_f. The chosen model influences the gain and vortex structure; see Figure 1 for an example of parametric analysis. Furthermore, an optimal response analysis [2] was conducted to understand the regions in the plane (ω_f, k) that are not represented in a linear stability analysis [3] finding areas where non-normal terms have a crucial impact.

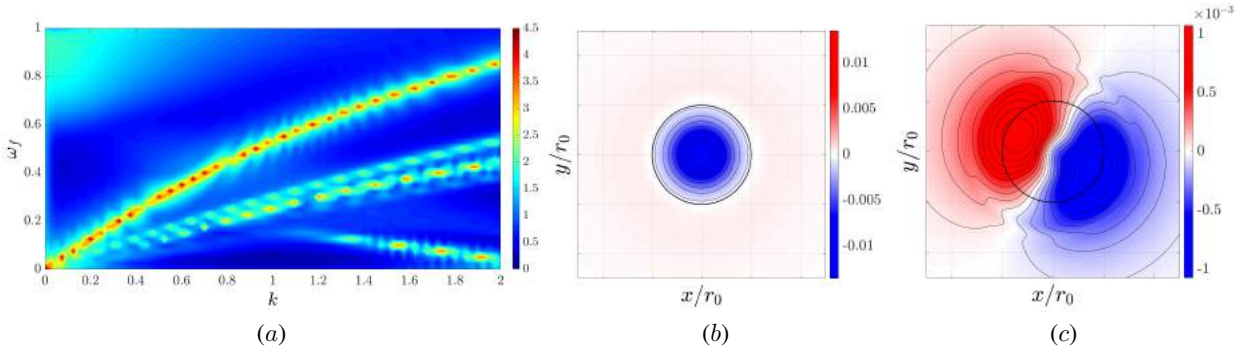

Figure 1. (a) Frequency Response energy gain map (in logarithmic scale) for the Lamb-Oseen vortex model with $Re = 7940$, and contour plots of the axial velocity for and example of (b) $m = 0$ and (c) $m = 1$.

References

[1] T. Leweke, H. U. Quaranta, H. Bolnot, F. J. Blanco-Rodríguez, S. Le Dizès, *Long- and short-wave instabilities in helical vortices*, Journal of Physics: Conference Series **524**, 012154 (2014).

[2] F. J. Blanco-Rodríguez, J. O. Rodríguez-García, L. Parras, C. del Pino, *Optimal response of Batchelor vortex*, Physics of Fluids **29**, 064108 (2017).

[3] D. Fabre, D. Sipp, L. Jacquin, *Kelvin waves and the singular modes of the Lamb-Oseen vortex*, Journal of Fluid Mechanics **526**, 67–76 (2006).

M030

FREQUENCY RESPONSE AS A TOOL FOR OPTIMIZING ACTIVE CONTROL OF TRAILING VORTICES

Manuel Garrido-Martin[1], Tobias Bölle[2], Carlos del Pino[1], Francisco J. Blanco-Rodríguez[3], Paloma Gutierrez-Castillo[1]

[1]*Universidad de Málaga, Institute for Mechatronics Engineering and Cyber-Physical Systems (IMECH.UMA), Campus de Teatinos, s/n, 29071 Málaga, Spain*

[2] *Deutsches Zentrum für Luft- und Raumfahrt, Institut für Physik der Atmosphäre, Oberpfaffenhofen, Germany*

[3]*Fluid Mechanics, School of Industrial Engineering, University of Seville, Seville, Spain*

Abstract A Frequency Response analysis of a Lamb-Oseen vortex with different axial Single Point Injections to determine the optimal location for experimental active control is performed. (wingtip vortex, frequency response, active flow control).

A primary concern in aeronautics revolves around the formation of wingtip vortices, an undesired consequence of finite-span lifting wings. These persistent and highly rotating axial flows remain for a long time over airport runways during landing and takeoff operations, constituting a potential hazard on flight safety and dictating operational restrictions in air traffic management. Efficient control of the wake behind the wing is crucial, not only to minimize the time interval between operations at airports but also to enhance the safe maneuvering of trailing UAVs in flight formation. A potential approach to mitigate trailing vortices involves employing an effective vorticity reduction method utilizing an active control device based on pulsating spanwise blowing of a jet [1].

This study investigates the effect of the variation of the active control application distance, d_f, on the frequency response of a Lamb-Oseen vortex [2]. The theoretical base flow pertains to the experimental configuration of a wing model with a NACA0012 airfoil at an angle of attack of α=9° and a chord-based Reynolds number of $Re_c = 1.7 \times 10^5$ [3]. The harmonic injection was implemented numerically using a Single Point Injection (SPI) jet configuration in the streamwise direction. A parameter analysis has been carried out on the axial wavenumber k, the forcing frequency ω_f and the radial distance, d_f, of the SPI axial forcing. As it is shown in Figure 1, the impact of the active control application distance is evident not only in terms of the energy gain but also in the alteration of the main vortex structure [4]. This analysis is crucial to maximize the effect of the injection for flow control in future applications.

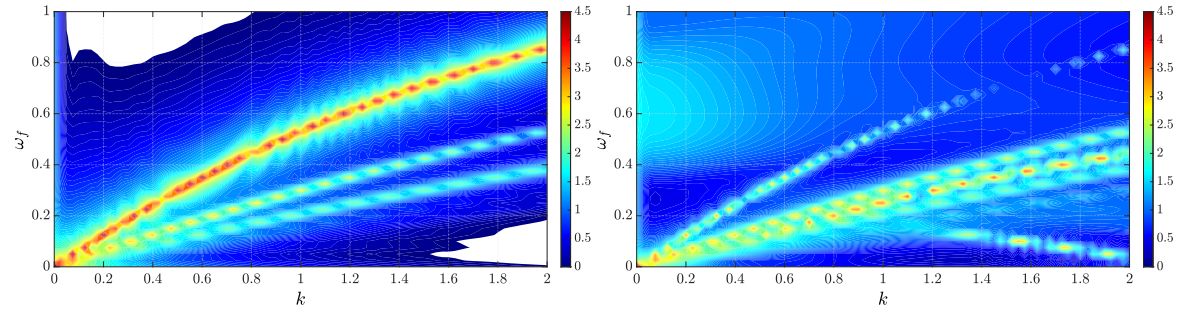

Figure 1. Frequency Response energy gain maps (in logarithmic scale) for the Lamb-Oseen vortex model with $Re = 7940$, considering a SPI forcing located at (a) $d_f = 0$ (vortex center) and (b) $d_f = 1$ (vortex core radius). The blank regions in (a) correspond with energy gain lower than unity.

References

[1] J. H. García–Ortiz, F. J. Blanco–Rodríguez, L. Parras, C. del Pino, *Experimental observations of the effects of spanwise blowing on the wingtip vortex evolution at low Reynolds numbers*, European Journal of Mechanics – B/Fluids **80**, 133–145 (2020).

[2] F. J. Blanco–Rodríguez, L. Parras, C. del Pino, *Frequency response of Lamb-Oseen vortex*, Fluid Dynamics Research **48**, 061417 (2016).

[3] T. Bölle, V. Brion, M. Couliou, P. Molton, *Experiment on jet–vortex interaction for variable mutual spacing*, Physics of Fluids **35**, 015117 (2023).

[4] D. Fabre, D. Sipp, L. Jacquin, *Kelvin waves and the singular modes of the Lamb-Oseen vortex*, Journal of Fluid Mechanics **551**, 235–274 (2006).

M031

SHEAR MIGRATION OF CERAMIC SLIPS

Alessandro Fontanari[1], Maurizio Bellotto[2], Gilberto Artioli[1]
[1]*Department of Geosciences, University of Padua, Padua, Italy*
[2]*Opigeo Srl, Grisignano di Zocco, Vicenza, Italy*

Keywords: Granular suspension, Shear induced migration, Ceramic Slip, CFD

Abstract

Ceramic industries heavily rely on clays as their primary raw material for manufacturing diverse products such as structural clay items, whitewares, refractories, and insulating ceramics. The forming-firing process, commonly employed in these industries, involves the injection of a "slip", a clay slurry with water and various additives, into a porous mould. The water is absorbed by the mold leaving a solid (green) body that undergoes several heat treatments up to 1000°C to improve the mechanical properties and surface finishing. The very high volumetric solid fraction of the ceramic slip (ϕ=0.63) along with a broad particle size distribution allow to classify these ceramic slips as dense granular suspensions. These suspensions are particularly unstable to dynamic segregation when they are subjected to a shear flow and particle segregation is usually observed. The presence of a compositional gradient within the piece, during the drying phase, could result in a differential shrinkage rate for different zones and therefore in the development of internal stresses that contribute to the formation of fractures. Homogenisation of the suspensions could be obtained with properly designed passive mixing elements installed on the pumping line The project endeavours to investigate the rheological behavior of ceramic slips under flow by combining rheological measurements with computational fluid dynamics (CFD) flow simulations, aiming to mitigate shear migration phenomena. Understanding the complex interplay of rheological properties, particle dynamics, and mixing mechanisms is crucial for optimizing the manufacturing process and enhancing product quality in ceramic industries. By integrating experimental observations with computational models, the project seeks to develop strategies to minimize particle segregation and ensure uniformity in composition and structure throughout the ceramic products. This interdisciplinary approach not only addresses fundamental scientific questions related to suspension behavior but also offers practical solutions for industrial applications, contributing to advancements in both materials science and manufacturing technology.

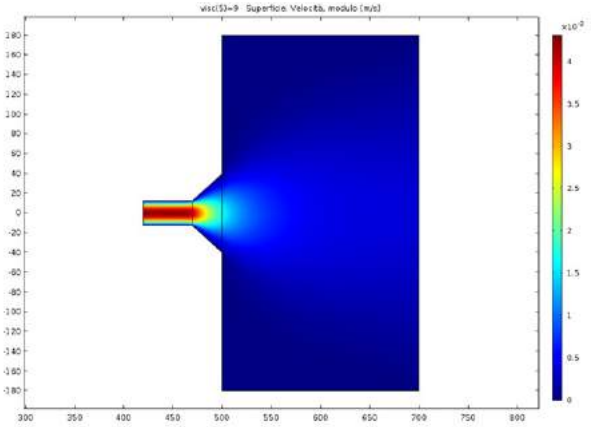

Figure 1. Velocity profile of a ceramic slips injected in the plaster mold

References

[1] Coussot, P., *Rheometry of Pastes, Suspensions, and Granular Materials: Applications in Industry and Environment*: Hoboken, New Jersey, John Wiley & Sons (2005)
[2] Dondi, M., Raimondo, M.R., Zanelli, C., *Clays and bodies for ceramic tiles: Reappraisal and technological classification*, Applied Clay Science **96**, 91-109 (2014)
[3] Guazzelli, É., & Pouliquen, O., *Rheology of dense granular suspensions*. Journal of Fluid Mechanics **852**, 1 (2018)
[4] COMSOL Multiphysics® v. 6.2. www.comsol.com. COMSOL AB, Stockholm, Sweden.

M032

AERODYNAMIC FORCES IN WING MODELS WITH SPANWISE DEFORMATION

Luis Parras[1], Paloma Gutierrez-Castillo[1], Pedro Solis[1], Carlos del Pino[1], Francisco J. Blanco-Rodríguez[2] & Eduardo Duran-Venegas[1]

[1]*Escuela de Ingenierías Industriales, Universidad de Málaga, Málaga, Spain.*
[2]*Área de Mecánica de Fluidos, Departamento de Ingeniería Aeroespacial y Mecánica de Fluidos, Universidad de Sevilla, Sevilla, Spain.*

Abstract In this work, we perform a numerical study of the change in aerodynamic forces due to wing (spanwise) deformation in flight. The results presented are for a NACA0012 wing model of a fixed semi-aspect ratio, sAR, and different chord-based Reynolds numbers, Re, in the range of application of UAVs [1]. Our results show that numerical simulations with turbulence models do not accurately simulate these aerodynamic forces with those compared to experimental results obtained from the wind tunnel, whereas *LES* simulations provide a more approximated value to the experiments. We compare the numerical results with Prandtl's lifting line theory and theoretical results obtained with vortex panel method, showing that the difference obtained with RANS methods is mainly related to the impossibility of simulations with turbulence models to describe the detached flows.

One of the main advances in aeronautics in recent decades has been the reduction of fuel consumption in order to comply with European energy saving regulations [2]. Technological solutions to this problem in aircraft include the development of more efficient turbojets and weight reduction. The latter involves lighter materials and increased length across the wingspan, resulting in slimmer and lighter wings. As a result, this new design concept produces tip deflections of around 4-10% under flight conditions. We have designed and manufactured NACA0012 wing models of different aspect ratios with no deformation and imposed deformation across the wingspan [3]. We obtained the aerodynamic coefficients in a wind tunnel. On the other hand, we performed RANS and LES numerical simulations for $sAR = 4$ wings. Interestingly, RANS simulations do not accurately predict the aerodynamic coefficients for wings with spanwise deformation at high angles of attack (α >7°), as shown in Figure 1. Comparison of the numerical and experimental results with Prandtl's lifting line theory and the vortex panel method indicates that the main difficulty encountered by the RANS simulations is the prediction of the detached flow in the wing with spanwise deformation.

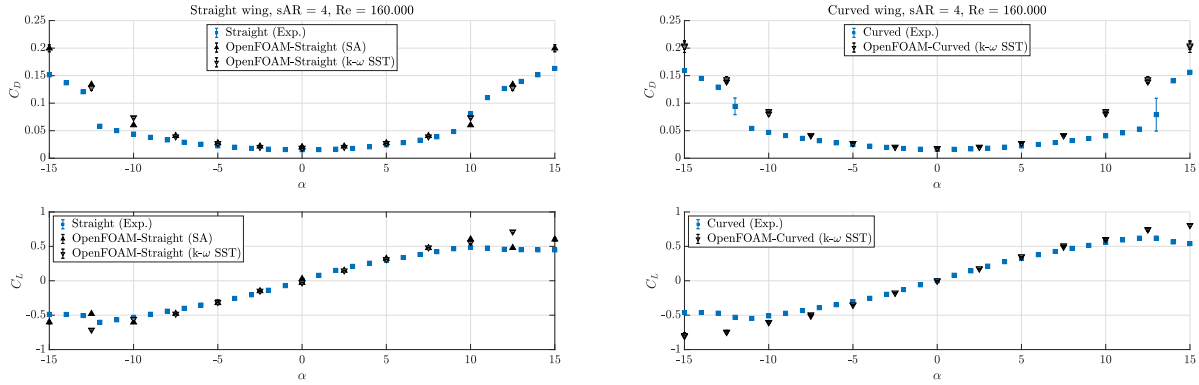

(a) (b)

Figure 1: Experimental aerodynamic characteristics: drag (top) and lift (bottom) coefficients and RANS simulations obtained for a NACA 0012 airfoil for a $sAR = 4$ and $Re = 1.6 \times 10^5$: (a) Non-deformed and (b) deformed NACA0012 wing model (4.5% tip deflection).

References

[1] H. Frost, *Low-Speed Aerodynamic Characteristics of NACA 0012 Aerofoil Section, including the Effects of Upper-Surface Roughness Simulating, Report of the Aeronautical Research Council, 3726 (1970).*

[2] J. Soone, ReFuelEU Aviation initiative: Sustainable aviation fuels and the 'fit for 55' package. BRIEFING, EU Legislation in Progress, PE 698.900 (2022).

[3] J. A. Farnsworth, S. Corbett, J. Seidel and T. E. McLaughlin, Aeroelastic Response of a Finite Span NACA 0018 Wing Part 1: Experimental Measurements, AIAA 2015-0249. 53rd AIAA Aerospace Sciences Meeting.

DAY 1 – Monday, 24 June 2024 Afternoon Sessions			
13:30	**Keynote 2: Prof Roberto Zenit** ***Chair: Prof Stephen Wilson*** ***Larch Lecture Theatre***		
	Instabilities & Bifurcations 2 ***Chair: Prof Lennon Ó Náraigh*** ***Larch Lecture Theatre***	***Geophysical & Astrophysical Flows*** ***Chair: Prof Daphne Lemasquerier*** ***Yew Lecture Theatre***	***Flames & Reacting Flows*** ***Chair: Dr Antonio Attili*** ***Elm Lecture Theatre***
14:15	M009: Effects of heavy and light particles on Rayleigh-Bénard instability *by S. Raza, SC Hirata, E Calzavarini*	M021: Local instabilities of rotating baroclinic flows with radial heating *by O Kirillov, I Mutabazi*	M033: Correlating gas-phase kinetics simulations to liquid monopropellant burning rates at high pressures - the role of phase change and surface temperature *by R Schwind*
14:30	M010: A minimal wave-mean flow model for Rossby wave instability in shear flows *by E Heifetz, E Gengel*	M022: From a vortex gas to a vortex crystal in instability-driven two- dimensional turbulence *by E Knobloch, A van Kan, B Favier, K Julien*	M034: Flickering and shedding of droplet diffusion flames under acoustic excitation *by K Pandey, S Basu, B Krishan, V Gautham*
14:45	M011: Natural convection-induced instability around a Janus particle *by ET Özdemir, F Viola, L Biancofiore*	M023: Numerical investigation on flow field and potential of scouring around reef cubes® in marine environment by *A Bordbar, V Kelefouras, S Hickling, H Short, E De Villiers, J Knir, YC Lee*	M035: Evaluation of the turbulent transport in boundary layers with flame-wall interactions *by B Peterson, X Wei, A Padhiary*
15:00	M012: A local rom for Rayleigh-Bénard bifurcation problems *by J Cortés, H. Herrero, F. Pla*	M024: React, shear and compact: Competing instability mechanisms in the partially molten upper mantle *by DR Jones, H Zhang, RF Katz*	M036: Thermodiffusive and wake instabilities in lean hydrogen flames *by J King, R Feng, SJ Lind*
15:15	**Coffee Break (Alder Lecture Theatre)**		
	Poster Presentations Session (TP - Talk + Poster; P - Poster only) ***Chair: Dr Alex Wray*** ***Larch Lecture Theatre***		
15:45	TP205: Shear layer instability forms asymmetrical turbulent flow distribution in periodic porous media *by V Srikanth. AV Kuznetsov*		
16:00	TP206: Flow behaviour in channels with a meniscus interface replacing part of a solid wall *by E Bold. E Oesterschulze*		
16:15	TP207: Dynamics of pancake-like geophysical vortices: from waves to (bulk) turbulence? *By J Vidal, Y. C de Verdière*		
16:30	TP208: Curve patterns in the spectrogram of ultrasonically driven bubbles under increasing excitation amplitude *by Y Zhang, H Metzger, P Prentice, A Cammarano*		
16:45	TP209: Sloshing instability driven by a bubble plume *by M Vacher, T Boirot, S Perrard, S Ramananarivo*		
17:00	TP210: Thermodiffusive flame instabilities in methane/hydrogen blends *by S Al Kassar, A Attili*		
17:15	TP211: Evaporating sessile droplets: solutal Marangoni effects overwhelm thermal Marangoni flow *by D Rocha, PL Lederer, C Seyfert, A Marin, D Lohse, C Diddens*		
17:30	P212: Application of immersed finite-element method for modelling non-Newtonian fluid around rigid bodies *by F Gaspar Jr, N Mangiavacchi, S McGuinty, GR Anjos*		
17:33	P213: Droplet to thin film dielectrowetting *by C Williams, G McHale, G Wells, R Ledesma-Aguilar, J Terry*		
17:36	P214: Enhanced control of double emulsion formation in microchannels using surface-active agents *by C Tang, L Chagot, P Angeli*		
17:39	P215: Investigating soiling patterns of rotating tire using CFD *by F Gueniat, A Jambholkar, H Penumadu*		
17:42	P216: Turbulent energy spectrum in the DIA approximation *by E Kohler, M Fuchs*		
17:45	P217: Theoretical analysis of flow through a cross-slot *by X Ji, HJ Wilson*		
17:48	**Poster Viewing (Alder Lecture Theatre)**		
18:00	**Welcome Cocktail Reception + Entertainment (Nucleus First Floor)**		

Keynote 2

Hydrodynamic instabilities as tools in artistic painting

Roberto Zenit

School of Engineering, Brown University, Providence, USA

Roberto Zenit received his Ph.D. from the Mechanical Engineering Department at Caltech in 1998. After a postdoctoral period at Cornell University, he moved to Mexico City in 2000 to become a faculty member at the Universidad Nacional Autónoma de México (UNAM), eventually becoming a Full Professor of Mechanical Engineering and a researcher at the Instituto de Investigaciones en Materiales, both at UNAM. He is now the Royce Family Professor of Teaching Excellence in Engineering at Brown University. He is a fellow of the APS, a member of the Mexican Academy of Sciences and the Academy of Engineering of Mexico. His area of expertise is fluid mechanics; he has worked in a wide variety of subjects including multiphase and granular flows, biological flows, rheology, and more recently, the physics of artistic painting.

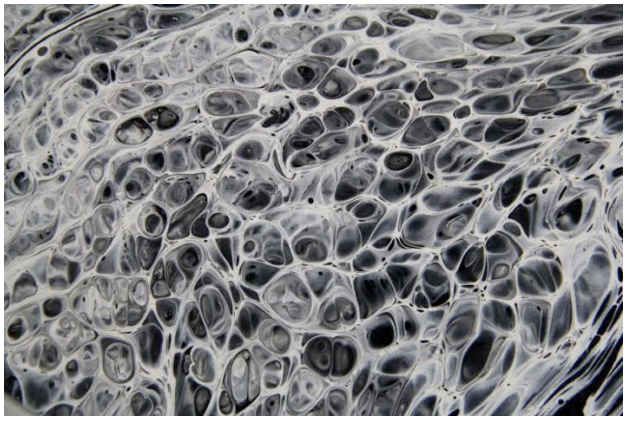

Abstract

Fluid mechanics is a subject that is relevant to every aspect of human activity. Art is not an exception. Artists, mostly painters but not exclusively, learn how to manipulate the material properties and the flow of liquids to produce textures, shapes and forms to create their objects of aesthetic value. As opposed to what is desired in industrial painting, where uniform and fast coatings are needed, artistic painting uses color gradients and non-uniform paint layers. In this talk, a survey of a few modern painting techniques will be discussed. Interestingly, in most cases, the appearance of non-uniformities is governed by hydrodynamic instabilities. Understanding how these instabilities emerge, and how can they be controlled, can be powerful tool understand art and to explore new avenues of artistic creation. Conducting research in this area is inspiring and engaging.

M009

EFFECTS OF HEAVY AND LIGHT PARTICLES ON RAYLEIGH-BÉNARD INSTABILITY

Saad Raza, Silvia C. Hirata & Enrico Calzavarini
Université de Lille, Unité de Mécanique de Lille - J. Boussinesq, UML ULR 7512, F 59000 Lille, France

Abstract In this study we explore the dynamics of particulate matter on the onset Rayleigh-Bénard (RB) convection. Heavy particles are injected from the top with the cold wall temperature, while light particles are injected from the bottom with the hot wall temperature. For the particulate phase we take into account the viscous (Stokes drag) and inertial hydrodynamics forces (pressure gradient and added mass) on the particles as well as the buoyancy force. Furthermore, the particles are also thermally coupled to the fluid as they have a proper thermal diffusivity and specific heat capacity. The particle properties are parametrized by the added-mass adjusted density-ratio β (which varies in the range $[0, 3]$ [1]), particle diameter Φ, particle injection temperature Θ_p^*, and fluid/particle heat capacity ratio E. The two-fluid model is used to investigate the thermal and mechanical interplay between particles and fluid flow.

We present an analysis of the effects of both heavy ($\beta < 1$) and light ($\beta > 1$) particles on the linear stability of the Rayleigh-Bénard system, extending the previous findings limited to the case of heavy particles by Prakhar & Prosperetti [2]. The case $\beta = 1$ corresponds to neutrally buoyant particles, in this condition the model behaviour is close to the classical single-phase RB system, Fig.1. This figure shows that both heavy and light particles stabilize the system with respect to the single-phase RB threshold. It is found that the system undergoes a pitchfork bifurcation giving rise to stationary convection patterns for all conditions in the particle parameter space. An energy budget analysis is also performed in order to gain further insight on the physical mechanisms leading to flow destabilization. The research underscores the complexity of the problem and suggests avenues for future exploration and innovation in alternative modeling approaches.

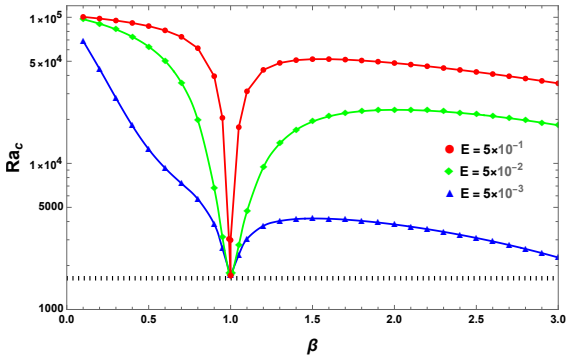

Figure 1. (a) Critical Rayleigh number as a function of the modified density ratio β (where $\beta = 0$ and $\beta = 3$ correspond respectively to the limits of very heavy and very light particles). Results obtained for fixed particle diameter $\Phi = 0.01$ and $\Theta_p^* = 0$ ($\beta < 1$), $\Theta_p^* = 1$ ($\beta > 1$). The horizontal dashed line corresponds to the single-phase Rayleigh-Bénard threshold $Ra_c = 1708$.

References

[1] V. Patocka, E. Calzavarini, *Settling of inertial particles in turbulent Rayleigh-Bénard convection*, Physical Review Fluids.**5**, 114304 (2020).
[2] S. Prakhar, A. Prosperetti, *Linear theory of particulate Rayleigh-BÃ©nard instability*, Physical review fluids **6**, 083901 (2021).

M010

A MINIMAL WAVE-MEAN FLOW MODEL FOR ROSSBY WAVE INSTABILITY IN SHEAR FLOWS

Eyal Heifetz[1] & Erik Gengel[1]
[1]*Department of Geophysics, Porter School of the Environment and Earth Sciences, Tel Aviv University, Tel Aviv, Israel*

Abstract Shear flow instability, Wave-mean flow interaction, wave action at a distance, nonlinear Hamiltonian dynamical system.

Here we extend the work by Heifetz and Guha [1] on the minimal nonlinear dynamical system, describing a prototype of two-dimensional shear instability in terms of action at a distance between two counter-propagating Rossby waves. In this work [2] we add to the model the effect of mutual interaction between the waves and the mean flow, where growth of the waves reduces the mean shear and vice versa. We show that the canonical action-angle Hamiltonian structure of the non-linear dynamical system is preserved when the wave-mean flow interaction is included.
In the linearized stage, modal instability of small amplitudes is obtained when the waves are phase-locked in a way that their counterpropagation rate balances the shear imposed by the mean flow. Therefore, when reaching finite amplitudes, thus consequently reducing the mean shear, the waves' counterpropagation rate overcomes the mean shear and phases unlock. This leads to a transient dynamics by which the wave-wave interaction affects the waves' amplitudes and relative phase, as well as the magnitude of the mean shear. The change in the latter affects the waves' relative phase and consequently the waves' growth. We find that this extended mechanism gives rise to a Hamiltonian dynamics in which the waves settle into libration while their amplitudes remain finite. We close by discussing how the given dynamics relates to familiar models of Kuramoto-type phase oscillators.

References

[1] E. Heifetz, A. Guha, *Normal form of synchronization and resonance between vorticity waves in shear flow instability*, Phys. Rev. E **100**, 043105 (2019).
[2] E. Heifetz, E. Gengel, *Minimal nonlinear dynamical system for the interaction between vorticity waves and shear flows*, Phys. Rev. E **105**, 065109 (2022).

M011

NATURAL CONVECTION-INDUCED INSTABILITY AROUND A JANUS PARTICLE

E. T. Özdemir[1], F. Viola[2] & L. Biancofiore[1,3]
[1]*Department of Mechanical Engineering, Bilkent University, Ankara, Turkey*
[2]*Gran Sasso Science Institute,Viale F. Crispi, 7, 67100, L'Aquila, Italy*
[3]*Department of Industrial and Information Engineering and Economics, University of L'Aquila, Italy*

Abstract We analyze the instability generated by buoyancy around a heated Janus particle. (Janus particle, Instability, Buoyancy).

Janus particles (JPs) are microparticles, whose surfaces have two or more distinct physical or chemical properties, which this feature makes them useful objects in many fields of science and technology [1]. An example of JP is a silica particle, which is half-coated with gold and then shows thermal properties if radiated by a laser [2]. This kind of JP is used in microfluidics, nanotechnology, nanomedicine, drug delivery, and optical applications [3]. Natural convection due to temperature gradients acts around the JP and creates complex flow patterns.

This work explores (i) first a thorough examination of the base flow around a heated JP and (ii) afterwards its three-dimensional axisymmetric instability. For the analysis, three different scenarios are examined in the study: (I) the fully heated particles, (II) the top heated particles, and (III) the bottom heated particles. Different thermal gradients are introduced into the system in each situation, affecting differently the hydrodynamic behaviour. The Rayleigh Number (Ra), which is the ratio between buoyant forces and viscous forces, is the main parameter in our analysis. In the study, the base flow analysis is computed using the FreeFem++ software [4]. The base flow cases are investigated and iterated by the Newton-Ralpson method. The ARPACK library is used for the linear stability analysis.

In Fig. 1a, we show the relationship between Ra and the maximum value of the vertical component of the velocity of the base flow (U_z). It is shown that the flow pattern around the fully heated particle has a greater velocity magnitude than the bottom and the top heated particle. This shows how a lift force, which increases with Ra is created due to viscous and pressure forces generated by buoyancy around the JP by natural convection. In addition, the bottom and the top heated particle's $U_{z,max}$ are considerably close to each other. Concerning the linear stability analysis, the connection between the growth rate (σ) for the azimuthal wavenumber $m = 0$ and Ra is investigated. In Fig. 1b. It is illustrated that the fully heated particle is the most unstable case, while the bottom heated case is the least prone to instability. Particularly, the critical Rayleigh number for the bottom heated case is more than one order of magnitude higher than the other two cases.

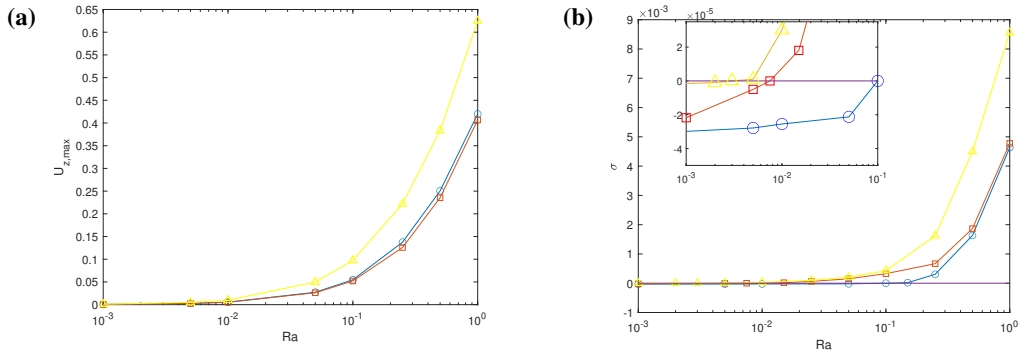

Figure 1: (a) $U_{z,max}$ vs Ra relationship for the fully heated, the top heated and bottom heated particle. (b) The growth rate for $m = 0$ vs Ra for three different heated cases. The critical Ra values are 0.006, 0.0075 and 0.12 for the fully heated, the top heated and the bottom heated case, respectively. The inset in (b) magnifies the behaviour of the growth rate for small Ra.

.

References

[1] A. Walther, A. Müller. *Janus particles*, Soft Matter **4**, 663 (2008).
[2] Ciriza et al. *Optically Driven Janus Microengine with Full Orbital Motion Control*, ACS Photonics **10**, 3223-3232 (2023).
[3] Mousavi et al. *Clustering of Janus Particles in an Optical Potential Driven by Hydrodynamic Fluxes*, Soft Matter **15**, 5748–5759 (2019).
[4] F. Hecht. *C++ Tools to construct our user-level language*, ESAIM: Mathematical Modelling and Numerical Analysis **36**, 809–836 (2002).

M012

A LOCAL ROM FOR RAYLEIGH-BÉNARD BIFURCATION PROBLEMS

Jesús Cortés[1], Henar Herrero[1] & Francisco Pla[1]
[1]*Department of Mathematics, Universidad de Castilla-La Mancha, Castilla-La Mancha, Spain*

Abstract Localized reduced-order methods; Reduced Basis; Bifurcation problems; k-means clustering; Proper Orthogonal Decomposition; Rayleigh Bénard instability

This work presents a local reduced-order method for computing bifurcation diagrams in 2D Rayleigh-Bénard convection problems. The proposed method is based on Proper Orthogonal Decomposition [2], and employs a reduced-order study of the regularity of solutions to detect new solution branches within the bifurcation diagram [1]. The locality of the method is achieved through k-means clustering, as proposed by [3]. However, instead of performing the selection of local problems in the parameter space, a criterion based on the solution space is employed. All the hyperparameters of the reduced method, such as the number of clusters or the number of POD modes, are calculated by deterministic criteria, avoiding ad hoc decisions. The method is applied to a single-parameter problem and a two-parameter problem, showing its ability to rapidly compute bifurcation diagrams with small errors. Compared to a standard reduced-order model that process each branch of the bifurcation diagram separately, the local approach produces more accurate results in less computational time.

References

[1] E. L. Allgower and K. Georg. *Numerical Continuation Methods.* Springer Berlin, Heidelberg, 2012.
[2] A. Quarteroni, A. Manzoni, and F. Negri. *Reduced Basis Methods for Partial Differential Equations: An Introduction.* Springer Cham, Switzerland, Aug. 2016.
[3] M. Hess, A. Alla, A. Quaini, G. Rozza, and M. Gunzburger. *A localized reduced-order modeling approach for PDEs with bifurcating solutions.* Comput. Methods Appl. Mech. Eng., 2019.

M021

LOCAL INSTABILITIES OF ROTATING BAROCLINIC FLOWS WITH RADIAL HEATING

Oleg N. Kirillov[1] & Innocent Mutabazi[2]
[1]*Northumbria University, Newcastle upon Tyne, NE1 8ST, UK*
[2]*Laboratoire Ondes et Milieux Complexes, UMR-6294 CNRS, Universite du Normandie Le Havre, 53 Rue de Prony, 76058 Le Havre Cedex, France*

Abstract We develop an analytical theory of instabilities of rotating baroclinic flows based on the local geometrical optics approach.

Swirling flows in both bounded and unbounded geometry originate in many industrial and natural contexts, such as cooling systems for rotating machinery e.g. cyclone cooling of gas turbines, drilling in HT/HP (high temperature/high pressure) wells in petroleum and gas industry, journal bearing lubrication, purification of industrial waste water, production of wire, cables, and optical fibres as well as in geophysics (tropical cyclones) and astrophysics (stellar interiors). The most popular mathematical models of swirling flows include isothermal spiral Couette (SCF) and spiral Poiseuiile (SPF) flows addressed both numerically and experimentally in [1, 3, 6, 7]. Lüdwieg [1] derived an analytical Rayleigh-like stability criterion for the inviscid SCF in the narrow-gap approximation that was later confirmed via modal linear stability analysis by Leibovich and Stewartson [4] and by the local geometrical optics approach by Eckhoff and Storesletten [2] and Lifshitz and Hameiri [5]. Leblanc and Le Duc [9] analytically connected the modal and local geometrical optics approaches in the limit of high wavenumbers. Treatments of *non-isothermal* swirling flows remain relatively rare in the literature, with an exception provided, e.g., by the numerical study by Cotrell and McFadden of the SPF with the radial temperature gradient and without Archimedean buoyancy [8]. However, the realistic modeling of almost all applications mentioned above requires taking temperature gradients into account. Rotating (azimuthal) flows with radial temperature gradient are well understood and studied using analytical, numerical and experimental methods [10, 12]. In this context the Goldreich-Schubert-Fricke (GSF) instability [14, 15] and non-equal diffusivities of momentum and heat play the major part. In the present work we aim at uncovering the complex interplay between the Lüdwieg-Eckhoff-Leibovich-Stewartson (LELS), GSF, and shear instabilities by considering a helical base flow of an incompressible viscous and thermally conducting fluid in a differentially rotating vertical cylindrical annulus with radial temperature gradient and natural gravity (a rotating baroclinic flow, RBF) by means of the geometrical optics stability analysis [11, 13]. A new explicit generalized Rayleigh criterion that mixes the LELS criterion for instability of isothermal helical flows and the GSF criterion for the instability of azimuthal flows with radial temperature gradient, is derived. In particular, it is shown analytically that the neutral stability surface in the space of the Taylor and Grashof numbers and the angular velocity ratio of the cylinders possesses a fold that describes destabilization of the Rayleigh-stable flows - an effect previously found numerically in isothermal SCF and SPF flows [6, 7].

References

[1] H. Lüdwieg, *Experimentelle Nachprufung des stabilitatstheorien fur reibungsfreie Stromungen mit schraubenlinienformigen stromlinien*, Z. Flugwiss. **12**, 304–309 (1964).
[2] K. S. Eckhoff, L. Storesletten, *A note on the stability of steady inviscid helical gas flows*, J. Fluid Mech. **89**, 401–411 (1978).
[3] D. Takeuchi, D. Jankowski, *A numerical and experimental investigation of the stability of spiral Poiseuille flow*, J. Fluid Mech. **102**, 101–126 (1981).
[4] S. Leibovich, K. Stewartson, *A sufficient condition for the instability of columnar vortices*, J. Fluid Mech. **126**, 335–356 (1983).
[5] A. Lifshitz and E. Hameiri, *Localized instabilities of vortex rings with swirl*, Comm. Pure Appl. Math. **46**, 1379-1408 (1993).
[6] A. Meseguer, F. Marques, *On the competition between centrifugal and shear instability in spiral Couette flow*, J. Fluid Mech. **402**, 33–56 (2000).
[7] A. Meseguer, F. Marques, *On the competition between centrifugal and shear instability in spiral Poiseuille flow*, J. Fluid Mech. **455**, 129–148 (2002).
[8] D.L. Cotrell, G.B. McFadden, *Linear stability of spiral Poiseuille flow with a radial temperature gradient: Centrifugal buoyancy effects*, Physics of Fluids **17**, 114102 (2005).
[9] S. Leblanc and A. Le Duc, *The unstable spectrum of swirling gas flows*, J. Fluid Mech. **537**, 433–442 (2005).
[10] H. N. Yoshikawa, M. Nagata, I. Mutabazi, *Instability of the vertical annular flow with a radial heating and rotating inner cylinder*, Phys. Fluids **25**, 114104 (2013).
[11] O. N. Kirillov, *Singular diffusionless limits of double-diffusive instabilities in magnetohydrodynamics*, Proc. R. Soc. A, **473**(2205), 20170344 (2017).
[12] O. N. Kirillov, I. Mutabazi, *Short wavelength local instabilities of a circular Couette flow with radial temperature gradient*, J. Fluid Mech., **818**, 319–343 (2017).
[13] J. Labarbe, O.N. Kirillov, *Diffusive instabilities of baroclinic lenticular vortices*, Phys. Fluids, **33**(10), 104108 (2021).
[14] E. Chang, P. Garaud, *Modelling coexisting GSF and shear instabilities in rotating stars*, MNRAS **506**, 4914–4932 (2021).
[15] R. W. Dymott, A. J. Barker, C. A. Jones, S. M. Tobias, *Linear and non-linear properties of the Goldreich–Schubert–Fricke instability in stellar interiors with arbitrary local radial and latitudinal differential rotation*, MNRAS **524**(2), 2857–2882 (2023).

M022

FROM A VORTEX GAS TO A VORTEX CRYSTAL IN INSTABILITY-DRIVEN TWO-DIMENSIONAL TURBULENCE

Edgar Knobloch[1*], Adrian van Kan[1], Benjamin Favier[2] & Keith Julien[3]
[1]*Department of Physics, University of California at Berkeley, Berkeley, California 94720, USA*
[2]*Aix Marseille Univ., CNRS, Centrale Marseille, IRPHE, Marseille, France*
[3]*Department of Applied Mathematics, University of Colorado, Boulder, CO 80309, USA*

Abstract We study structure formation in two-dimensional turbulence driven by an external force, interpolating between linear instability and random stirring, subject to nonlinear damping. Using extensive direct numerical simulations, we uncover a rich state space with different stationary solutions featuring large-scale vortices and/or smaller shielded vortices (SVs), including a SV gas state. The SV gas is continued in the forcing parameter, revealing a sharp transition towards a crystal state as the forcing strength decreases. Our study highlights the role of the forcing in 2D turbulence, revealing nontrivial SV states in this system, including a melting SV crystal.

Two-dimensional (2D) and quasi-2D turbulent flows typically display an upscale energy cascade, in contrast with their three-dimensional (3D) counterpart where energy cascades downscale. Sustaining a fluid flow against dissipation requires a driving force. Highly idealized, flow state-independent forcing functions such as random stirring injecting a constant power are often used. However, many real fluid flows result from instabilities that depend on the flow state and lead to an energy injection rate that increases with the amplitude of the forcing-scale modes, producing flows starkly different from random stirring. In flows driven by a scale-localized negative viscosity, the resulting instability can grow without bound, overcoming nonlinear advection, an effect suppressed in the presence of nonlinear damping.

We study 2D turbulence driven by a hybrid force interpolating between a scale-localized instability and random stirring at the same scales, injecting a constant power [1], focusing on late-time behavior [2]. We solve the 2D Navier-Stokes equation for the incompressible velocity $\mathbf{u} = (u, v)$ on the torus $[0, 2\pi]^2$ with nonlinear damping, hyperviscosity and a hybrid forcing $\mathbf{f}_\gamma$,

$$\partial_t \mathbf{u} + \mathbf{u} \cdot \nabla \mathbf{u} = -\nabla p - \nu_n (-\nabla^2)^n \mathbf{u} - \beta |\mathbf{u}|^m \mathbf{u} + \mathbf{f}_\gamma, \qquad \nabla \cdot \mathbf{u} = 0, \tag{1}$$

where the integers n and m set the order of hyperdiffusion and damping, respectively, with $n, m \geq 1$, and

$$\mathbf{f}_\gamma = \gamma \mathcal{L}[\mathbf{u}] + (1 - \gamma)\mathbf{f}_\epsilon. \tag{2}$$

Here, the forcing control parameter $\gamma \in [0, 1]$, and $\mathcal{L}[\mathbf{u}]$ is a linear operator with Fourier transform $\widehat{\mathcal{L}[\mathbf{u}]}(\mathbf{k}) = \nu_* k^2 \hat{\mathbf{u}}(\mathbf{k})$ with $\nu_* > 0$ for wavenumbers $\mathbf{k}$ with $k = |\mathbf{k}| \in [k_1, k_2]$, and $\widehat{\mathcal{L}[\mathbf{u}]}(\mathbf{k}) = 0$ otherwise. The largest forcing scale is denoted by $\ell_1 \equiv 2\pi/k_1$ and the maximum instability growth rate by $\sigma = \nu_* k_2^2$. The second term in (2) involves a zero-mean white-in-time random force $\mathbf{f}_\epsilon(\mathbf{x}, t)$ acting on wavenumbers near k_2, injecting kinetic energy at a rate ϵ. We adopt $k_1 = 33, k_2 = 40, \nu_* = 0.002, \epsilon = 1, n = 4$ and $\nu_4 = 10^{-14}$, with $m = 2$ and $\beta = 10^{-4}$ [2].

We perform long DNS at $\gamma \approx 1$ from rest. Shielded vortices (SVs) rapidly emerge, with only vortices of one sign surviving a spontaneous symmetry breaking process. Subsequently, the number of SVs increases through slow nucleation of additional SVs until a threshold number density of SVs is reached (140 vortices in the domain of area $4\pi^2$), after which an explosive growth phase sets in, leading to a dense SV gas state. The dense SV gas state persists to lower γ (Fig. 1a), but a stable hexagonal SV crystal forms at low γ (Fig. 1b). We use the diffusion coefficient D of the SVs as an order parameter characterizing these two states: we track SVs, computing the mean square displacement (MSD) vs. time at different γ (Fig. 1c). The MSD increases linearly in time indicating Brownian dynamics. Measuring the slope D at different γ reveals a continuous transition at $\gamma = \gamma_c \approx 0.13$ from a crystal (no diffusion) to a gas with $D \propto (\gamma - \gamma_c)^2$.

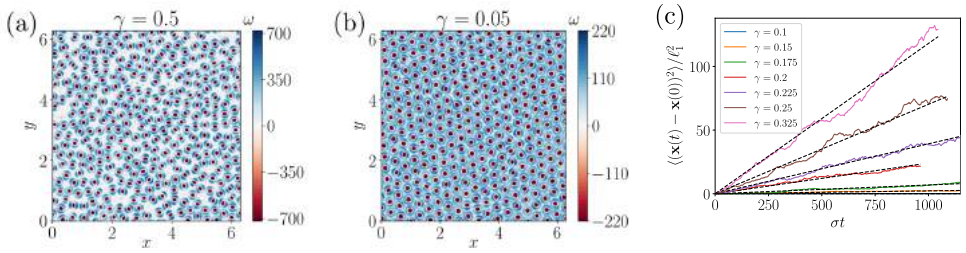

Figure 1. Snapshots of the vorticity field in the dense, statistically stationary state at $\gamma = 0.5$ (a) and $\gamma = 0.05$ (b). Panel (c) shows the mean squared displacement of vortices from their position at $t = 0$ for different γ, which grows linearly with time as vortices diffuse.

References

[1] A van Kan, B Favier, K Julien, E Knobloch "Spontaneous suppression of inverse energy cascade in instability-driven 2-D turbulence." J. Fluid Mech. 952, R4 (2022)
[2] A van Kan, B Favier, K Julien, E Knobloch "From a vortex gas to a vortex crystal in instability-driven two-dimensional turbulence." arXiv:2308.08789 (2023)

M023

NUMERICAL INVESTIGATION ON FLOW FIELD AND POTENTIAL OF SCOURING AROUND REEF CUBES® IN MARINE ENVIRONMENT

Amir Bordbar[1], Vasilios Kelefouras[1], Sam Hickling[2], Harrison Short[2], Eugene De Villiers[3], Jakub Knir[3] & Yeaw Chu Lee[1]

[1]*School of Engineering, Computing and Mathematics, University of Plymouth, Plymouth, U.K.*
[2]*ARC Marine, Torquay, U.K.*
[3]*Engys Ltd., London, U.K.*

Keywords: Artificial Reefs, Marine Restoration, Computational Fluid Dynamics, Shear Stress, Scour, Reef Cubes

Abstract

Artificial reefs are structures designed to enhance marine habitat for ocean-dwelling organisms within coastal infrastructure. In this study, the characteristics and performance of artificial reefs, namely, reef cubes deployed in Torbay, United Kingdom, were investigated. The model utilized incompressible Unsteady Reynolds-Averaged Navier-Stokes (URANS), coupled with the k-ω SST turbulence closure. Different sizes, surface roughness levels, and orientation angles to the incident flow were considered. The study included the modelling of flow field, formation of vorticities, and bifurcations in the creation of upwelling and wake regions, all of which directly affect the performance of artificial reefs. Findings gathered from the study determined how current designs influence flow hydrodynamics, facilitate marine habitat growth and provide shelter for marine life. Furthermore, shear stress analysis for both the reef cube structure and surrounding seabed was carried out. The surface shear stress associated with flow bifurcation on the structure was related to the potential deposition and attachment of invertebrate larvae and seaweed spores on reef surfaces. Simultaneously, bed shear stress also played a primary role in the potential development of local scour. This affected long-term stability of the structures, thus having a direct impact on transforming local habitat features. The accuracy and reliability of the model were ensured by validation against relevant experimental data from literature and qualitative experimental observations. The results demonstrated that the orientation angle of the reef cube to the incident flow direction significantly influenced performance and possibility of scouring in its vicinity. Size variations of the deployed cubes had significant effects on the volume of upwelling and wake regions. The simulation findings revealed that the surface roughness of the cube significantly influenced the shear stress magnitude on reef surfaces, while its impact on bed shear stress and the flow field around the structure was negligible.

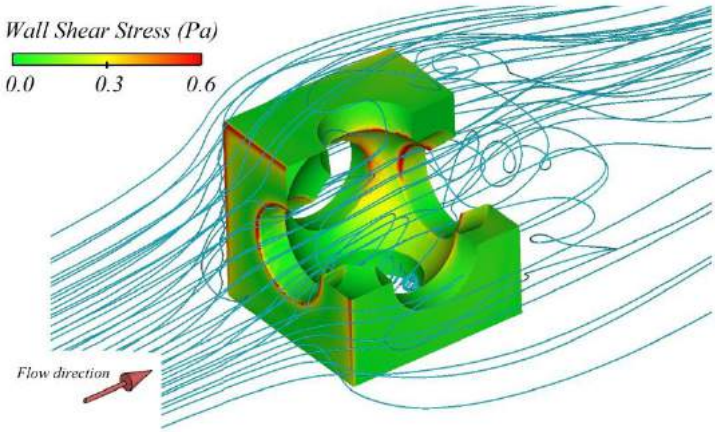

Figure 1. Shear stress on reef surface and bifurcated flow field around it using streamlines.

M024

React, shear and compact: competing instability mechanisms in the partially molten upper mantle

David W. Rees Jones[1], Hanwen Zhang[2] & Richard F. Katz[2]
[1]*School of Mathematics and Statistics, University of St Andrews, St Andrews, U.K.*
[2]*Department of Earth Sciences, University of Oxford, Oxford, U.K.*

Keywords: Geophysical fluid dynamics; multiphase flow; reactive instabilities; magma dynamics

Abstract

Flows in a porous medium can undergo a variety of dynamical and thermochemical instabilities. This presentation is mainly motivated by the partially molten upper mantle. Various lines of evidence point to focused, channelized magma flow through this system. Here, we discuss the two main candidate instability mechanisms: (1) a chemical reaction-infiltration instability [Ref. 2]; (2) a shear-driven instability that relies on the sensitivity of the rheological properties to porosity. We present a combined linear analysis [Ref. 3] of the two instabilities and show that the combination of these mechanisms favours the development of porosity channels that have a tabular geometry, consistent with geological observations. We discuss whether these instabilities are likely to overcome the stabilizing influence of compaction [Refs. 2 & 4] and survey other processes likely to modulate these instabilities.

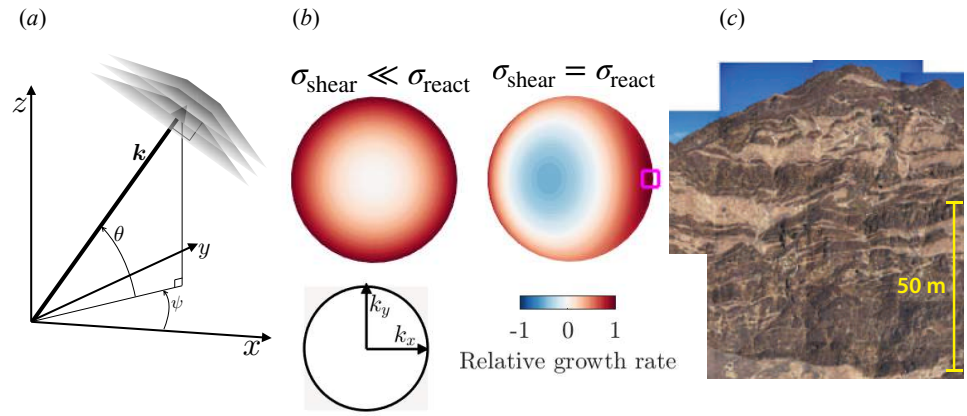

Figure 1. (*a*) Tabular instability with wavenumber ***k***. (*b*) The growth rate of reactive instabilities is horizontally isotropic whereas the presence of some shear leads to a preferred horizontal direction. (*c*) An exhumed section of an ancient mid-ocean ridge. Flow is believed to have been localized in the lighter coloured bands, which have a tabular morphology. [Panels (*a,b*) is adapted from Ref. 3 and panel (*c*) is adapted from Ref. 1.]

References:

[1] Braun and Kelemen, 2002, Geochem. Geophys. Geosyst., 3, 11, doi:10.1029/2001GC000289
[2] D. W. Rees Jones & R. F. Katz, 2018, J. Fluid Mech., 852, 5–36, doi:10.1017/jfm.2018.524
[3] D. W. Rees Jones, H. Zhang and R. F. Katz, 2021, Geophys. J. Int., 226(1), 582–609, doi:10.1093/gji/ggab112
[4] R. F. Katz; D. W. Rees Jones; J. F. Rudge; T. Keller, 2022, Annu. Rev. Earth Planet. Sci., 50:507-540, doi:10.1146/annurev-earth-032320-083704

M033

Correlating Gas-Phase Kinetics Simulations to Liquid Monopropellant Burning Rates at High Pressures - The Role of Phase Change and Surface Temperature

Rachel A. Schwind
Institute for Multiscale Thermofluids, University of Edinburgh, Edinburgh, Scotland, UK

Keywords: liquid propellants, flame oscillations, phase change, high-pressure

Abstract
Green, liquid monopropellants, such as nitromethane (CH_3NO_2) and iso-propyl nitrate ($C_3H_7NO_3$), are strong candidates for leading the transition to low toxicity and high specific impulse propellants in air-independent applications as they do not require external oxidizers, which allows for a single component fuel compartment, and increased control in variable power applications. However, there has been limited exploration of fundamental behaviours these compounds at application relevant conditions, which can range from 50 to 200 bar. Due to this research gap, there is a limited understanding of the phase behaviour of these compounds at elevated pressures, especially approaching the transcritical region, where subcritical burning behaviour is observed at supercritical conditions for some propellants[1] and flame oscillations in others[2]. While recent efforts by Schwind and colleagues have quantified the intrinsic burning rates of nitromethane [3] and iso-propyl nitrate[4], the ability to capture the inherent pressure dependence of the reactivity through kinetic model correlations had not been demonstrated. This work presents updated modelling efforts to correlate kinetic simulations of the laminar flame speed of the pure gas-phase monopropellant to the complex liquid fuel burning rates evaluated in prior studies. This correlation development is crucial to allowing interrogation of the fundamental reaction kinetics in these complex, high-pressure, multi-phase environments. Additionally, this allows us to elucidate key drivers of the pressure dependent and flame oscillatory behaviour, with insights into the chemical contributions as well as the phase dependencies. Further this work demonstrates the strong influence of the liquid surface temperature on the pressure dependent reactivity, with results supporting the hypothesis that the liquid surface temperature at the phase change point decreases as the pressure increases for the first time. Additional analysis explores the influence of the flame stand-off length to understand the potential drivers of oscillatory flame behaviour observed in studies of liquid iso-propyl nitrate [2,4].

References

[1] G. Derk, E. Boyer, G.A Risha, R.A. Yetter. R. Dobbins, M.D. Smooke, “Experimental and numerical investigation of high-pressure nitromethane combustion,” *Proc. Combust. Inst.,* 38 (2021) 3325-3332.
[2] A. Ambekar, S. Sreedhara, A. Chowdhury, Burn rate charaterization of iso-propyl nirtate—A neglected monopropellant, *Combust. Flame* 162 (2015) 836–845.
[3] R.A. Schwind, J.B. Sinrud, C.C. Fuller, C.F. Goldsmith, R.A. Walker, “Linear Burning Rates of Liquid Nitromethane in a Continuous Flow Liquid Strand Burner.” *Proc. Combust. Inst*., 39 (2023) 5083-5090
[4] R.A. Schwind, C.F. Goldsmith, “Experimental study of linear burning rates of liquid isopropyl nitrate.” *Combust. Flame* 257 (2023) 112591

M034

Flickering and shedding of droplet diffusion flames under acoustic excitation

Khushboo Pandey[1], Saptarshi Basu[2], Bal Krishan[2] & Gautham V[2]
[1]*Institute for Multiscale Thermofluids, School of Engineering, University of Edinburgh*
[2]*Department of Mechanical Engineering, Indian Institute of Science, Bangalore, India*

Keywords: Droplet combustion, diffusion flames, Acoustics, Vorticity, Circulation

Abstract

The flicker and flare of buoyant diffusion flames present a captivating challenge within combustion research. The fluctuation in the low-frequency band of such flames, irrespective of nozzle diameter and fuel type [1], remains an intriguing phenomenon. This distinct oscillation of diffusion flames is primarily driven by gravitational buoyancy, as proposed by Buckmaster and Peters [2], who attributed flame perturbations to convective instability, a modified Kelvin-Helmholtz instability, in the flow of buoyant hot gases. Understanding the evolution of vortical structures around these flames and their interaction with flame morphology is crucial for various fire research endeavors, including studying flame spread, shedding, and air entrainment. Experimental investigations by Cetegen and Ahmed [3] on pool fires emphasized that the global flame flicker originated from locally unstable regions near the fuel exit. The vortical shedding frequencies in such flames are proportional to $\sqrt{g/l_0}$, where g represents acceleration due to gravity, and l_0 denotes the characteristic length scale [3–5]. However, this scaling fails to accommodate scenarios where the characteristic length is dynamic, as seen in droplet combustion, where the droplet diameter continuously reduces.

We explore the instabilities of droplet diffusion flames under ambient conditions and in the presence of an external acoustic pressure field. Our findings reveal that the transient occurrence of flickering frequencies in droplet diffusion flames dictates a dynamic self-tuning of oscillation modes over their lifespan. Additionally, we illustrate that the flame response encompasses a blend of multiple frequencies intricately linked to various convective length scales. Furthermore, we discuss the selective coupling of flames with external acoustic fields by comparing their respective spectral responses and energy distributions. Furthermore, to elucidate the mechanism behind acoustic-flame interaction, we introduce the notion of critical circulation buildup and delineate how acoustics contribute to velocity disturbances, ultimately leading to flame roll-up.

Figure 1. Droplet flame response under acoustic excitation [6]

References

[1] L.D. Chen, J.P. Seaba, W.M. Roquemore, L.P. Goss, Proc. Combust. Inst 22 (1989), 677–684.
[2] J. Buckmaster, N. Peters, Proc. Combust. Inst 21(1988), 1829–1836.
[3] B.M. Cetegen, T.A. Ahmed, Combust. Flame 93(1993), 157–184.
[4] D. Moreno-Boza, W. Coenen, A. Sevilla, J. Carpio, A.L. Sánchez, A. Liñán, J Fluid Mech 798(2016), 997–1014.
[5] X. Xia, P. Zhang, J Fluid Mech 855 (2018), 1156–1169.
[6] K. Pandey, S.Basu, B. Krishan, V. Gautham, Proc. Combust. Inst 38 (2021), 3141-3149.

M035

EVALUATION OF THE TURBULENT TRANSPORT IN BOUNDARY LAYERS WITH FLAME-WALL INTERACTIONS

Xiangyu Wei[1], Abhijit Padhiary[1] & Brian Peterson[1]
[1]*Institute of Multiscale Thermofluids, University of Edinburgh, Edinburgh, UK*

Keywords: turbulent boundary layers, energy transfer, flame-wall interaction, laser diagnostics.

Abstract

Flame-wall interaction (FWI) is an inherent phenomenon within most propulsion and power systems, where a flame is bounded by solid surfaces. FWI governs fuel efficiency, pollutant formation, and underpins the cooling processes required for surface durability. As modern combustors are reduced in size and made to operate at higher power densities for improved efficiency, a larger percentage of flame processes will occur near surfaces. As such, FWI is becoming a more prominent topic for next generation propulsion and power systems.

FWI is a couple phenomenon involving a flame as a source of heat, a wall as a heat sink, and a gas flow as a medium to facilitate heat and mass transport. In technically relevant environments, the medium between the flame and wall is a turbulent boundary layer, which introduces a dynamic coupling between the flame, flow, and wall. This dynamic coupling significantly modifies the mass and energy transport at the gas/wall interface.

An experimental understanding of turbulent transport during FWI requires sophisticated diagnostics that can spatially and simultaneously resolve flow field, gas-phase temperature, wall temperature and flame distribution. Typically, laser diagnostics are capable to measure these quantities at spatial scales down to the 10's of micron scale. However, of the required variables, spatially resolved gas-phase temperature measurements during FWI is one of the more difficult quantities to measure experimentally.

In this work, we apply a suite of advanced laser diagnostics to study the flow and temperature transport within a turbulent boundary layer during FWI. Measurements are conducted within a dedicated side-wall quenching (SWQ) burner facility [1], where V-flame impinges onto a vertical stainless-steel wall. Hybrid femtosecond / picosecond (fs/ps) rotational coherent anti-Stokes Raman spectroscopy (referred to as HRCARS) is applied to measure 1D gas temperature normal to the vertical wall. HRCARS is combined simultaneously with particle image velocimetry (PIV; velocity field), laser induced fluorescence; flame distribution) and phosphor thermometry (PT; wall temperature). The combination of the diagnostics allow us to study the effect of the coupling of the flame, flow, and wall. This work will compare the energy and flow transport between laminar and turbulent flow conditions in the boundary layer, and the affect it has on the flame and heat transfer behaviour to the wall.

References

[1] F. Zentgraf, *On the evolution of turbulent boundary layers during flame-wall interaction investigated by highly resolved laser diagnostics,* Combust. Flame **261**, 113276 (2024).

M036

THERMODIFFUSIVE AND WAKE INSTABILITIES IN LEAN HYDROGEN FLAMES

Jack R. C. King[1], Ruofeng Feng[1] & Steven J. Lind[2]
[1]*School of Engineering, University of Manchester, Manchester, UK*
[2]*School of Engineering, Cardiff University, Cardiff, UK*

Abstract Numerical and theoretical investigations of instabilities in lean hydrogen bluff body flames (Combustion, thermodiffusive instability, wake instability).

As we transition to a low carbon future, hydrogen based combustion systems will play a major role. Whilst there has been much research on the dynamics of hydrocarbon combustion, the behaviour of hydrogen flames is less well understood. Theoretical analysis of combustion instabilities has been limited to simple geometries and single-step reaction mechanisms. However, flame dynamics are known to be influenced by geometric confinement, whilst detailed chemical mechanisms are necessary to reproduce the dynamics of thermodiffusive instabilities which occur for lean hydrogen flames [1]. For the canonical problem of a flame anchored to a bluff body (in this case, a cylinder), combustion markedly changes the wake dynamics, as flow dilation across the flame influences hydrodynamic stability of the wake, whilst thermoacoustic instabilities can also occur [2, 3]. Open questions remain, and the behaviour of ultra-lean hydrogen flames in this setting has not previously been investigated in detail.

Here we present high-fidelity mesh-free numerical simulations of lean hydrogen flames anchored to a bluff body. We highlight how bluff body size and shape, flow rates, and stoichiometry influence the onset of hydrodynamic wake instabilities. Furthermore, we show that for lean hydrogen flames in this setting, an additional thermodiffusive instability can occur for a range of flow rates, stoichiometries, and combustor sizes, leading to a previously unobserved oscillatory behaviour. This instability is independent of the acoustic and hydrodynamic instabilities, and is characterised by relatively long time-scales, a highly regular periodicity, increased oxygen consumption, and flame speeds an order of magnitude above the expected laminar flame speed.

The stabilisation of hydrogen-based combustion devices is a key issue, these results have implications for flashback, autoignition and component lifetimes on future combustor designs.

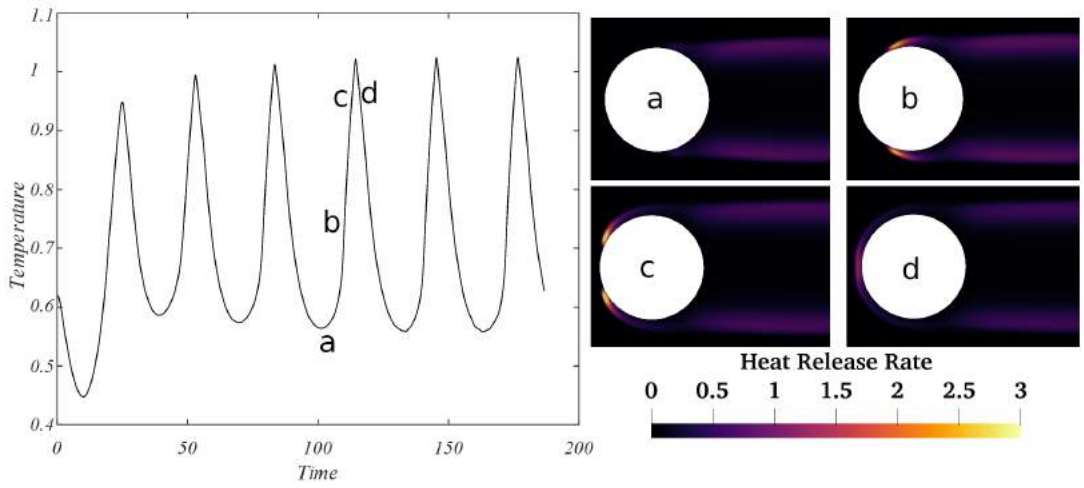

Figure 1. A new periodic thermodiffusive instability for a bluff body flame: Time evolution of mean bluff body temperature for an equivalence ratio of $\phi = 0.32$, Reynolds number $Re_D = 1110$, and bluff body scale $D/\delta_L = 2$. The snapshots on the right show the heat release rate at different times during the thermodiffusive flashback. All quantities are non-dimensional.

References

[1] T. L. Howarth & A. J. Aspden, *An empirical characteristic scaling model for freely-propagating lean premixed hydrogen flames*, Combustion & Flame **237**, 111805 (2022).
[2] Y. J. Kim, B. J. Lee & H. G. Im *Hydrodynamic and chemical scaling for blow-off dynamics of lean premixed flames stabilized on a meso-scale bluff-body*, Proceedings of the Combustion Institute **37(2)**, 1831-1841 (2019).
[3] J. R. C. King *A mesh-free framework for high-order direct numerical simulations of combustion in complex geometries*, Computational Methods in Applied Mechanics & Engineering **421**, 116762 (2024).

TP205

Shear layer instability forms asymmetrical turbulent flow distribution in periodic porous media

Vishal Srikanth[1] & Andrey V Kuznetsov[1]
[1] *Department of Mechanical and Aerospace Engineering, North Carolina State University, Raleigh, NC 27695, USA*

Keywords: Large Eddy Simulation, Symmetry-breaking, Turbulent convection

Abstract

In this paper, we report a novel symmetry-breaking phenomenon that occurs in turbulent convective flow in periodic porous media in the intermediate porosity flow regime for values of porosities in between 0.8 and 0.9. Large eddy simulation is used to numerically simulate the momentum and thermal transport inside the porous medium at the microscale level. The phenomenon is observed to occur for periodically repeating porous media consisting of an in-line arrangement of circular cylinder solid obstacles, such as typically found in heat exchangers. The transition from symmetric to asymmetric flow occurs in between the Reynolds numbers of 37 (laminar) and 100 (turbulent), and asymmetric flow patterns are reported for Reynolds numbers up to 1,000. A Hopf bifurcation resulting in unsteady oscillatory laminar flow marks the origin of a secondary flow instability arising from the interaction of the shear layers around the solid obstacle. In turbulent flow, stochastic phase difference in the vortex wake oscillations caused by the secondary flow instability results in asymmetrical velocity and temperature distributions in the pore space (figure 1). Consequently, high and low velocity flow channels are formed in the pore space that leads to the asymmetrical velocity and pressure distributions. At the macroscale level, symmetry-breaking results in a residual transverse drag force components acting on the solid obstacle surfaces. The vortex wake oscillations caused by the secondary flow instability promote attached flow on the solid obstacle surface, which improves the surface averaged heat flux from the solid obstacle surface.

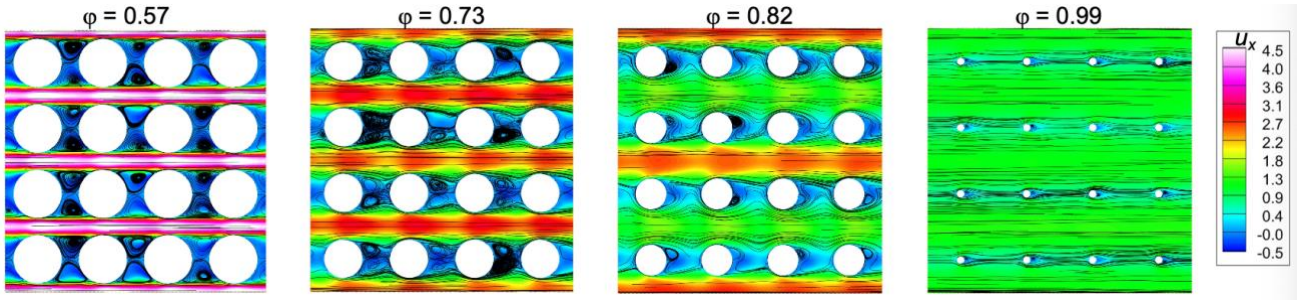

Figure 1. Asymmetrical x- velocity distribution is observed in the intermediate porosity flow regime (φ = 0.82) leading to the formation of alternating high and low velocity channels in the pore space.

TP206

Flow behaviour in channels with a meniscus interface replacing part of a solid wall

E. Bold[1], E.Oesterschulze[1]
[1] RPTU Kaiserslautern-Landau, Physics and Technology of Nanostructures, 67663 Kaiserslautern, Germany
Keywords: meniscus interface, superhydrophobic surfaces

Superhydrophobic surfaces (SHS) combine a large contact angle with low contact-angle hysteresis, similar to those found in nature on lotus leaves or rose petals [1]. In laminar flow, SHS reduces the drag by creating a shear-free air/water interface. An air/water interface is created by nanostructuring the surface to form nanobubbles, or by microstructuring to create ridges [2,3]. However, shear forces close to the walls may cause the partial or complete removal of nanobubbles. Furthermore, water may fill the grooves due to condensation or the collapse of the Cassie state. As a result, the intended drag reduction effect is reduced or even eliminated.

This study aims to introduce a stable meniscus interface as part of the wall of a rectangular channel to investigate the impact of the free gas/fluid interface on the flow in the channel. First theoretical results in case of circular shaped channels with meniscus interface are given by Zimmermann et al. [4]. Perforation of the wall was obtained by structuring silicon wafers using laser lithography followed by dry DRIE etching to create rectangular slits approximately 200µm wide and 2.5mm long. These were installed as one wall of a rectangular channel, with the long side of the slit oriented in the direction of flow. During flow in the channel a complexly shaped meniscus spans the open slit, establishing a Cassie state (Fig. left). The two local radii of curvature of the meniscus depend on the flow rate. The stability of the meniscus was enhanced by placing the sample in MTCS (Methyltrichlorosilane) to create a superhydrophobic nanostructured surface. We performed optical coherent tomography (OCT) microscopy to image the local meniscus profiles as a function of the flow rate (Fig. right). We have simultaneously recorded the pressure drop along the meniscus in the direction of flow and will discuss this flow behaviour in detail.

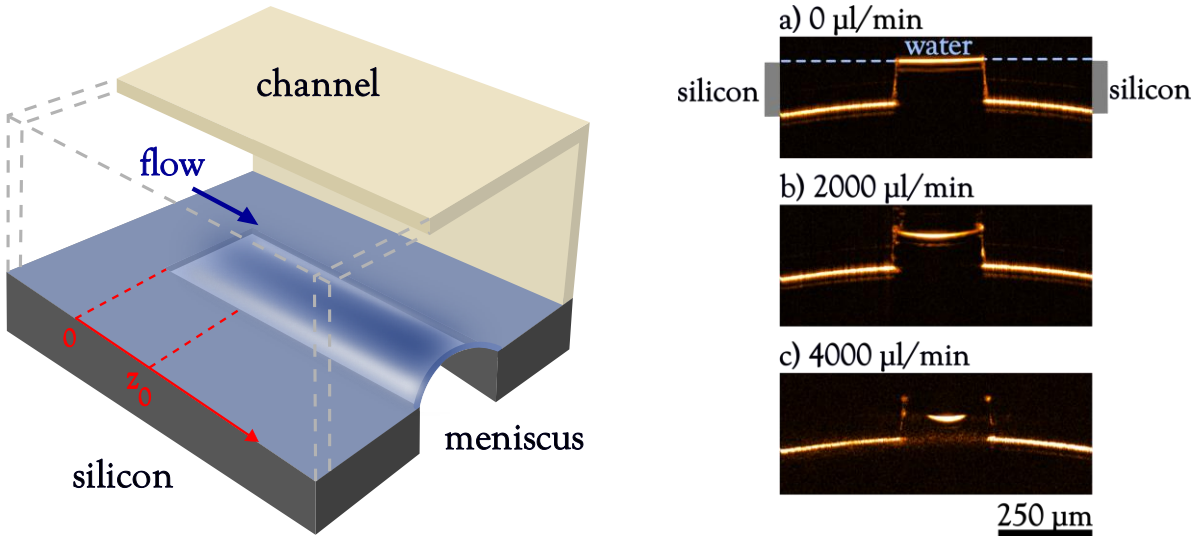

Figure left: Scheme of a rectangular shaped channel with the lower wall partly replaced by a gas/fluid interface. Figure right: OCT images of the meniscus profile of the water/gas interface at z_0=1mm for different flow rates (a) 0, b) 2000, and c) 4000 µl/min). The curvature of profiles is due to the optical aberrations of the objective in use.

References

[1] Lee C, Choi C-H, Kim C-J. (2008). Structured surfaces for giant liquid slip. Phys. Rev. Lett. 101:064501
[2] Vega-Sánchez, Christopher; Peppou-Chapman, Sam; Zhu, Liwen; Neto, Chiara (2022): Nanobubbles explain the large slip observed on lubricant-infused surfaces. In: Nat Commun 13 (1), S. 351. DOI: 10.1038/s41467-022-28016-1.
[3] Rothstein, Jonathan P. (2010): Slip on Superhydrophobic Surfaces. In: Annu. Rev. Fluid Mech. 42 (1), S. 89–109. DOI: 10.1146/annurev-fluid-121108-145558.
[4] S. Zimmermann

TP207

DYNAMICS OF PANCAKE-LIKE GEOPHYSICAL VORTICES: FROM WAVES TO (BULK) TURBULENCE?

Jérémie Vidal[1] & Y. Colin de Verdière[2]
[1] *Université Grenoble Alpes, CNRS, ISTerre, 38000 Grenoble, France*
[2] *Université Grenoble Alpes, CNRS, Institut Fourier, 38000 Grenoble, France*

Abstract Interdisciplinary work (Geophysics-Mathematics) on waves and instabilities in rotating stratified vortices

Rotating stratified flows often exhibit (almost) isolated pancake-like vortices [1], whose lifetime may depend on small-scale turbulence. Here, we present a reduced model to describe the bulk dynamics of such vortices (e.g. Mediterranean eddies or Jupiter's vortices, see figure 1). We consider a fluid enclosed within a rotating triaxial ellipsoid, which is stratified in density with a constant Brunt-Väisälä frequency (using the Boussinesq approximation). We first investigate the linear wave motions in such a model, which are governed by a mixed hyperbolic-elliptic equation for the velocity. As in the rotating non-stratified case [3], we prove that the wave spectrum is pure point in ellipsoids (i.e. only consists of eigenvalues) with polynomial eigenvectors [4]. By combining microlocal analysis and numerical computations (obtained with a bespoke Galerkin method), we also uncover the existence of low-frequency waves below the usual cutoff frequency of inertia-gravity waves [4, 5]. Finally, we explore whether triadic instabilities (e.g. the elliptical instability [6] or the triadic resonant instability [7]) could sustain small-scale bulk turbulence in such stratified vortices.

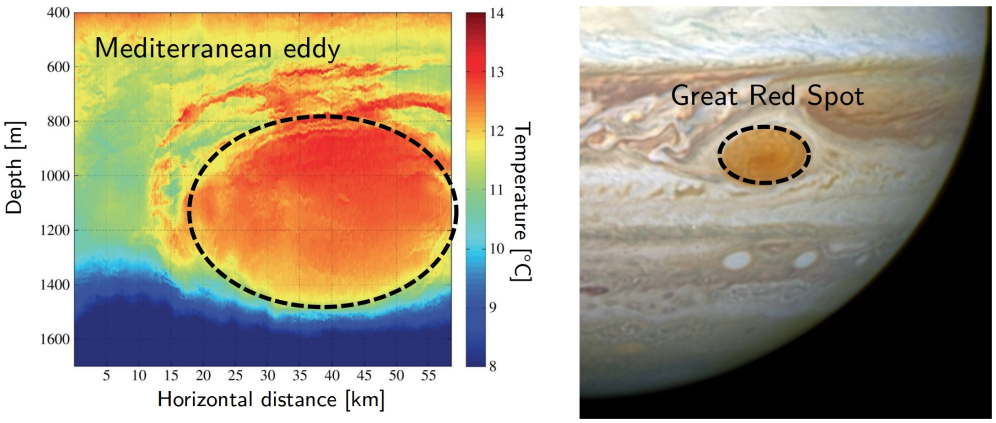

Figure 1. *Left*: Cross-section of the temperature anomaly (acoustic tomography) in a Mediterranean eddy offshore in the Eastern Atlantic. Adapted from [2]. *Right*: Picture of Jupiter's Great Red Spot (GRS) taken on 21 April 2014 with Hubble. Credits: NASA, ESA and A. Simon (Goddard Space Flight Center).

Acknowledgements. JV received funding from the European Research Council (ERC) under the European Union's Horizon 2020 research and innovation programme (grant agreement No 847433, THEIA project).

References

[1] D. Lemasquerier, G. Facchini, B. Favier, M. Le Bars, *Remote determination of the shape of Jupiter's vortices from laboratory experiments*, Nat. Phys., **16** (6), 695–700 (2020)
[2] J. C. McWilliams, *Submesoscale currents in the ocean*, Proc. R. Soc. A, **472** (2189), 20160117 (2016)
[3] Y. Colin de Verdière, J. Vidal, *The spectrum of the Poincaré operator in an ellipsoid*, Preprint, arxiv:2305.01369 (2023)
[4] J. Vidal, Y. Colin de Verdière, *Inertia-gravity waves in geophysical vortices*, Proc. R. Soc. A, arxiv:2402.10749 (2024)
[5] Y. Colin de Verdière, J. Vidal, *On gravito-inertial surface waves*, Preprint, hal:04461197 (2024)
[6] R. R. Kerswell, *Elliptical instability*, Annu. Rev. Fluid Mech., **34** (1), 83–113 (2002)
[7] S. Boury, P. Maurer, S. Joubaud, T. Peacock, P. Odier, *Triadic resonant instability in confined and unconfined axisymmetric geometries*, J. Fluid Mech., **957**, A20 (2023)

TP208

CURVE PATTERNS IN THE SPECTROGRAM OF ULTRASONICALLY DRIVEN BUBBLES UNDER INCREASING EXCITATION AMPLITUDE

Yikai Zhang[1], Hilde Metzger[1], Paul Prentice[1] & Andrea Cammarano[1]
[1]*James Watt School of Engineering, University of Glasgow, Glasgow, UK*

Keywords: Cavitation, Therapeutic ultrasound, Subharmonics, Nonlinear dynamics

Abstract

Subharmonic emissions from acoustic bubbles are important to research due to their potential to harm healthy tissues during ultrasonic therapy [1]. Consequently, there is a keen interest in utilizing bubble equations to predict the behaviour of bubbles. The occurrence of subharmonic bubble emissions is attributed to the period-doubling bifurcation of bubble oscillation. While recent research utilizing these equations has extensively examined the period-doubling bifurcation of acoustic bubbles under steady states, with one constant excitation amplitude employed for each simulation, scant attention has been directed towards understanding the bifurcation structure of an acoustic bubble subjected to a ramping excitation amplitude.

Johansen's theoretical work affirms the Keller-Miksis equation's efficacy in simulating subharmonic emissions [1]. Following his work, we constructed a model for a single bubble system by numerically solving the Keller-Miksis equation using MATLAB to investigate the bifurcation structure of the bubble under a ramping excitation amplitude. And the spectral features of acoustic emissions are presented in spectrograms, figure 1.

As shown in figure 1, the bubble undergoes a sequence of period-doubling, transitioning through frequencies of f_0, $f_0/2$, $f_0/3$, $f_0/2$, $f_0/3$, $f_0/4$, and ultimately returning to f_0. After the occurrence of $f_0/3$, the mediating phase adheres to curve patterns. This implies that the variation in the period of bubble oscillation, under a ramping excitation amplitude, is a continuous process. Figure 1 further illustrates that this process correlates with an increase in the noise floor. Subsequently, we compare this curve pattern with a backbone curve of a Duffin oscillator as both signify a continuous variation of oscillation period. The comparison is based on the free decay curve method from A. Cammarano's research which explained the backbone curve of nonlinear systems [2]. With this method, we can demonstrate that all Rayleigh-Plesset-like equations exhibit a comparable curve pattern.

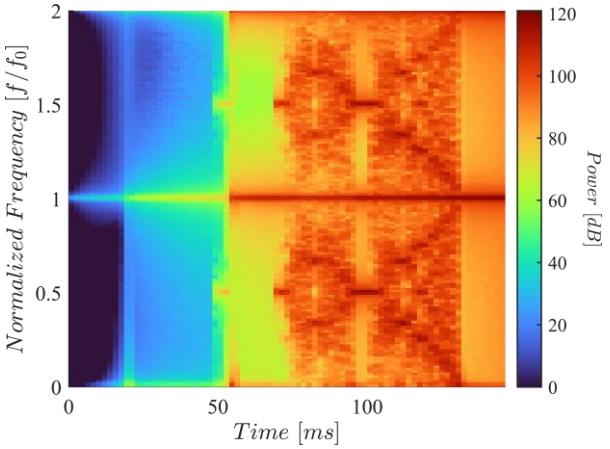

Figure 1. Curve pattern in the spectrogram of an acoustic bubble with a equilibrium radius of 40 μm under a 27 kHz ultrasound ramping from 0 to 0.25 MPa.

References

[1] Johansen, K., Song, J. H., & Prentice, P. *Validity of the Keller-Miksis equation for "non-stable" cavitation and the acoustic emissions generated*. 1–4 (2017).
[2] Cammarano, A., Green, P., Hill, T. L., & Neild, S. A. *Nonlinear system identification through backbone curves and Bayesian inference*. 255–262 (2016).

TP209

SLOSHING INSTABILITY DRIVEN BY BUBBLE PLUME

Marc Vacher[1,2,3], Thomas Boirot[1], Stéphane Perrard[2] & Sophie Ramananarivo[1]
[1]*Laboratoire d'Hydrodynamique, Ecole Polytechnique, Palaiseau, France*
[2]*Physique et Mécanique des Milieux Hétérogène, ESPCI, Paris, France*
[3]*Saint-Gobain Recherche, Saint-Gobain, Aubervilliers, France*

Abstract Coupled-oscillators model is used to describe a new sloshing instability driven by bubble plume.

Some glass furnaces have their molten glass bath stirred by flames in the volume. This heating method may have consequences on the stability of the bath. To study these instabilities, we adopt an experimental approach using a cold replica. A sparger is immersed in a water tank and injects air vertically at a constant air flow rate. An air plume is then created : air bubbles rise up towards the water surface. Above a certain flow rate, a sloshing mode grows at the water surface, due to a complex interaction with the air plume, as previously observed in a similar geometry by Aoki *et al.* [1].

In this study, we aim at identifying when and why the surface destabilises. Our main control parameters are the air flow rate and the tank aspect ratio, $R = \frac{h_0}{L}$, where h_0 is the static water height and L the tank width. To measure the bubble trajectories and the free surface position, we use shadowgraphy techniques.

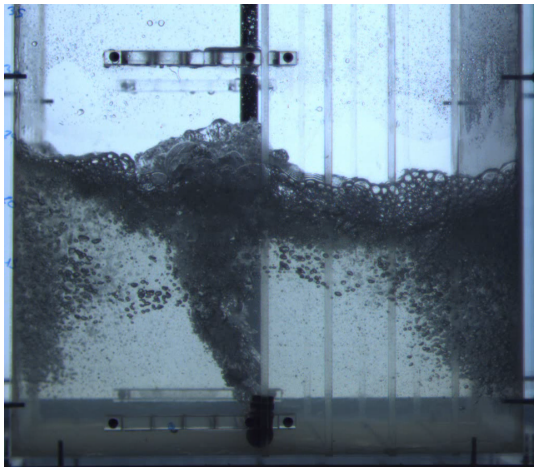

Figure 1. Front view of the tank with plume oscillation and sloshing

We characterise the instability by measuring the critical air flow rate as a function of tank aspect ratio, and the oscillating frequency. To identify the instability mechanism, we performed a spectral analysis in time of both the jet and the surface. We show that the sloshing frequency is incompatible with low frequency oscillations of bubble wakes, which occurs in mixing bubble columns used in chemical engineering for example [2]. We eventually propose a phenomenological model of coupled oscillators to explain what motors this instability.

References

[1] R. Aoki, S. Fujioka, K. Terasaka, *Experimental Study and Prediction by Computational Fluid Dynamics on Self-induced Sloshing Due to Bubble Flow in a Rectangular Vessel*, Journal of Chemical Engineering of Japan, **54-2**, 51–57 (2021).
[2] L. Liu, H. Yan, T. Ziegenhein, H. Hessenkemper, Q. Li, D. Lucas *A systematic experimental study and dimensionless analysis of bubble plume oscillations in rectangular bubble columns*, Chemical Engineering Journal, **372**, 352–372 (2019).

TP210

THERMODIFFUSIVE FLAME INSTABILITIES IN METHANE/HYDROGEN BLENDS

Sofiane Al Kassar[1] & Antonio Attili[1]
[1]*School of Engineering, Institute for Multiscale Thermofluids, University of Edinburgh, United Kingdom*

Abstract Keywords: Thermodiffusive instabilities; Methane/hydrogen blends; Dispersion relations; Flame speed; Decarbonization

The implementation of hydrogen-based solutions to decarbonize many important sectors of energy production and storage will follow a progressive transition from natural gas (methane, CH_4) to hydrogen (H_2). In this context, it is essential to understand how increasing shares of H_2 in CH_4/H_2 blends impact the dynamics, stability, and safety of flames. The H_2 molecule features very specific and unique characteristics, including high reactivity and diffusivity compared to hydrocarbons. The high diffusivity of H_2 is responsible for triggering and sustaining thermodiffusive instabilities, which have a massive impact on the dynamics, speed, and structure of laminar and turbulent flames [1–7].
While theoretical models exist and can predict the onset of the instabilities [7], they are not necessarily accurate quantitatively [3], in particular in predicting the effect of variations of pressure, equivalence ratio, temperature, fuel composition. The impact of thermodiffusive instabilities is analyzed in a series of laminar premixed flames of hydrogen/methane blends at ambient ($p = 1$ atm and $T_u = 298$ K) and gas-turbine ($p = 20$ atm and $T_u = 700$ K) conditions. Both the linear (weakly perturbed) and non-linear (strongly wrinkled) phases of the instability are considered in the study. In the linear phase, the property of the instability is summarized in the dispersion relation (shown in Fig 1), which summarises the growth rate of perturbations for different wavelengths. It is found that increasing the share of hydrogen has strong effects on the dispersion relations, in particular when the amount of hydrogen is increased from zero to 20% in mass. In the non-linear regime, the thermodiffusive instabilities become abruptly dominant for the flame structure and flame speed for shares of hydrogen above 20% in mass; for larger shares of hydrogen, in the range $25 - 100\%$, the flame speed and structure change less in response to further increases of hydrogen. Finally, it is observed that the threshold of about 20% in mass of hydrogen at which thermodiffusive effects become significant corresponds to a reduction of CO_2 of about 30%, highlighting that thermodiffusive effects will certainly need to be considered when methane is replaced by hydrogen to decarbonizing heating, propulsion, and electricity production.

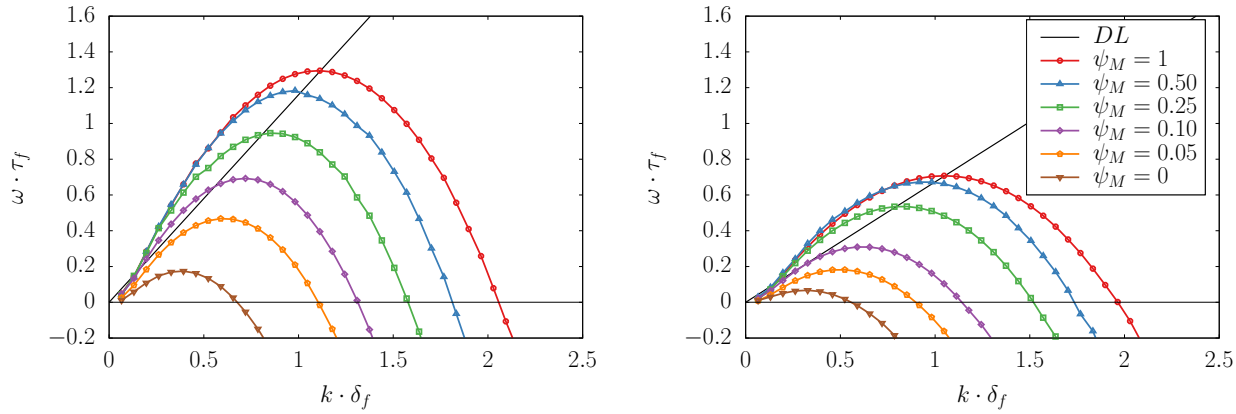

Figure 1. Dispersion relations at ambient conditions, $p = 1$ atm and $T_u = 298$ K (left) and gas-turbine conditions, $p = 20$ atm and $T_u = 700$ K (right), for different H_2/CH_4 blend ratios $\psi_M = Y_{H_2}/(Y_{H_2} + Y_{CH_4})$. The axes are normalized with the flame thickness δ_f and the flame time $\tau_f = \delta_f / s_L$. The black lines indicate the theoretical growth rate in the Darrieus-Landau instability.

References

[1] S. Al Kassar, L. Berger, P.E. Lapenna, F. Creta, P. Pitsch, and A. Attili. *arXiv:2306.10901*, 2023.
[2] L. Berger, K. Kleinheinz, A. Attili, and H. Pitsch. *Proc. Combust. Inst.*, 37(2):1879–1886, 2019.
[3] L. Berger, A. Attili, and H. Pitsch. *Combust. Flame*, 240:111935, 2022.
[4] L. Berger, A. Attili, and H. Pitsch. *Combust. Flame*, 240:111936, 2022.
[5] T.L. Howarth and A.J. Aspden. *Combust. Flame*, 237:111805, 2022.
[6] TL Howarth, EF Hunt, and AJ Aspden. *Combust. Flame*, 253:112811, 2023.
[7] M. Matalon. *Annu. Rev. Fluid Mech.*, 39:163–191, 2007.

TP211

EVAPORATING SESSILE DROPLETS: SOLUTAL MARANGONI EFFECTS OVERWHELM THERMAL MARANGONI FLOW

Duarte Rocha[1], P. L. Lederer[2], C. Seyfert[1], A. Marin[1], D. Lohse[1,3] & C. Diddens[1]
[1]*Physics of Fluids Department, Max-Planck Center Twente for Complex Fluid Dynamics and J. M. Burgers Centre for Fluid Dynamics, University of Twente, Drienerlolaan 5, 7522NB Enschede, The Netherlands*
[2]*Department of Applied Mathematics, University of Twente, Hallenweg 19, 7522NH Enschede, The Netherlands*
[3]*Max-Planck Institute for Dynamics and Self-Organization, Am Faßberg 17, 37077 Göttingen, Germany*

Abstract Thermal Marangoni; Evaporating droplets; Axial Symmetry Breaking.

When a water droplet is deposited on a thermally conductive substrate, latent heat release induces evaporating cooling, resulting in a temperature minimum at the apex. Consequently, density and surface tension gradients emerge within the droplet and at its droplet-gas interface, giving rise to liquid flowing from the apex towards the contact line and vice versa, respectively. In small droplets with diameter below the capillary length, thermal Marangoni effects are expected to dominate over thermal buoyancy (or thermal Rayleigh) effects. However, contrary to theoretical predictions, experiments show a dominant circulation from the apex toward the contact line, indicating a prevailing thermal Rayleigh convection. Furthermore, under different conditions, experiments showed an unexpected asymmetric flow that persisted for several minutes. We hypothesize that a tiny amount of contaminants, commonly encountered in experiments with water/air interfaces, act as surfactants in counteracting the thermal surface tension gradients at the interface and thereby promoting the dominance of Rayleigh convection. Finite element numerical simulations demonstrate that, under the experimental conditions, a mere 0.6% reduction in the initial surface tension caused by surfactants leads to a reversal in the flow direction compared to the theoretical prediction without surfactants. Additionally, we investigate the stability of the stationary solutions obtained under azimuthal perturbation at a specific mode, revealing that the presence of surfactants also affects the axial symmetry of the flow.

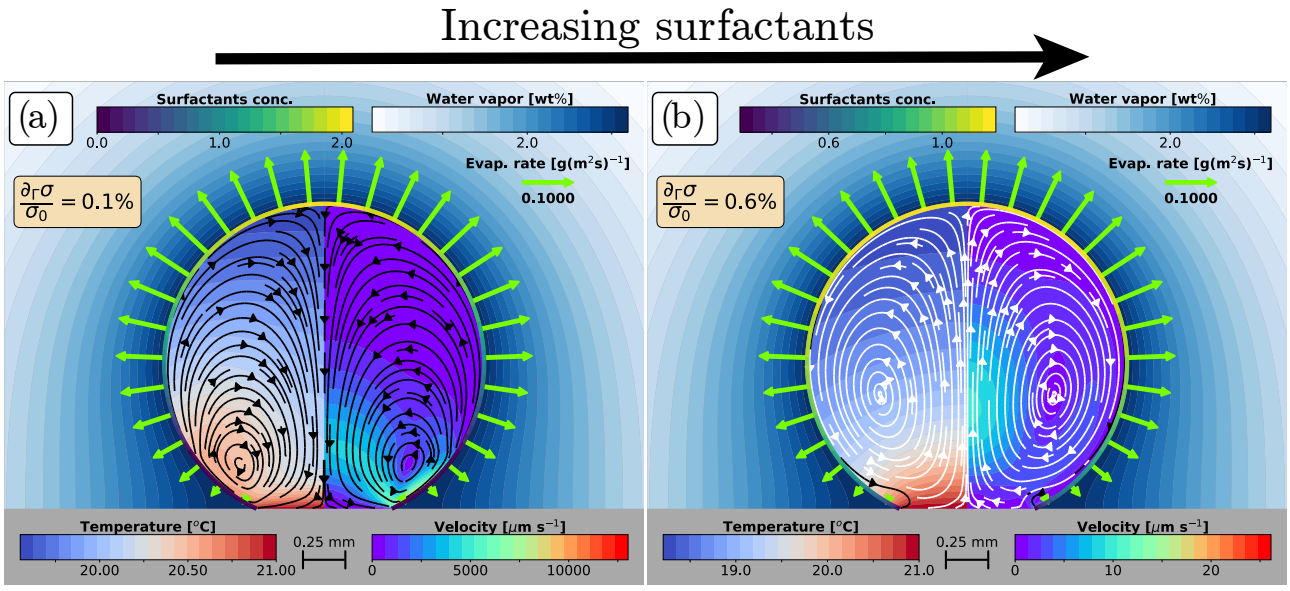

Figure 1. Flow direction changing from anti-clockwise (thermocapillary-dominated) to clockwise (buoyancy-dominated) with increasing amount of surfactants in droplet. Initial surface tension is reduced by 0.1% (a) and 0.6% (b). In the latter, the flow direction is completely reversed as compared to no- or low-surfactants case.

P212

APPLICATION OF IMMERSED FINITE ELEMENT METHOD FOR MODELING NON-NEWTONIAN FLUID AROUND RIGID BODIES

Fabio Gaspar Jr[1], Norberto Mangiavacchi[2], Sean McGuinty[3]& Gustavo R. Anjos[1]
[1]*Department of Mechanical Engineering, Federal University of Rio de Janeiro, Rio de Janeiro, Brazil*
[2] *Department of Mechanical Engineering, Federal Fluminense University, Niteroi, Brazil*
[3] *Division of Biomedical Engineering, University of Glasgow, Glasgow, U.K.*

Keywords: non-Newtonian flow, Arbitrary Eulerian-Lagrangian, Interaction multiphase flow, Bifurcations flow.

Abstract

The study of blood flow is extremely crucial due to its significant importance in the medical and healthcare field. A major concern in this domain is thrombosis, which involves the formation of blood clots within vessels, causing ischemia, the absence of blood (O2) irrigation in a particular region, and leading to serious complications such as pulmonary embolism, stroke, or heart attack. Given this, understanding how blood flow occurs in this phenomenon is extremely important. The present work employs a combination of an Immersed Finite Element Method (iFEM) with the consideration of blood as an incompressible, non-Newtonian fluid, while the clot is treated as a solid part overlaid on the fluid domain. The current test cases demonstrate promising results, especially considering the simplicity of the proposed formulation for simulating fluid-solid multiphase flows.

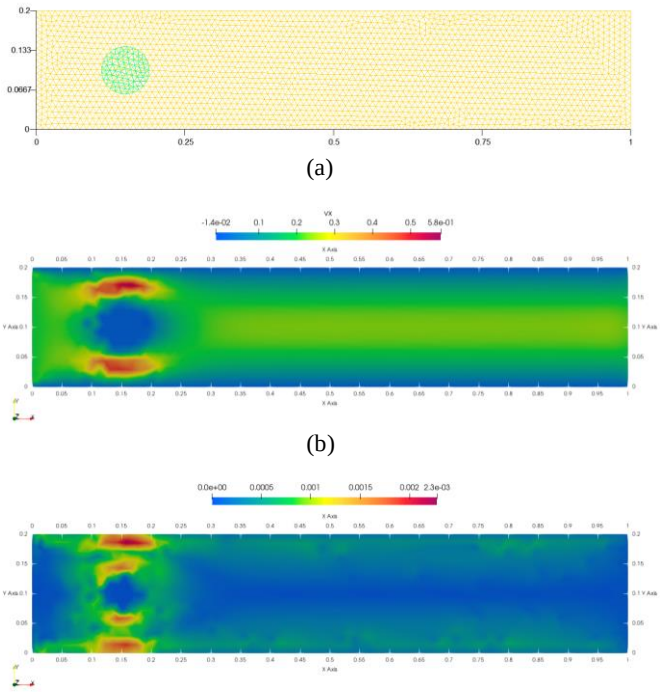

Figure 1. (a) Unstructured Finite Element meshes for the solid domain [Ω_s] in green color and the fluid domain [Ω] in orange color, (b) axial velocity (x-direction) and (c) fluid shear rate at the steady-state with a Power-Law non-Newtonian fluid model for the iFEM model.

References

[1] Glowinski, R., Pan, T.W., Hesla, T.I., Joseph, D.D. and Périaux, J. A fictitious domain approach to the direct numerical simu lation of incompressible viscous flow past moving rigid bodies: application to particulate flow, Journal of computational physics, 169(2), 363-426 (1995).
[2] Lee, T.-R., Chang, Y.-S., Choi, J.-B., Kim, D. W., Liu, W. K. and Kim, Y.-J, 2008, Immersed finite element method for rigid body motions in the incompressible Navier–Stokes flow, Computer Methods in Applied Mechanics and Engineering, 197 (25-28), 2305-2316 (2008).

P213

DROPLET TO THIN FILM DIELECTROWETTING

Callum Williams[1], Glen McHale[1], Gary Wells[1], Rodrigo Ledesma-Aguilar[1], & Jonathan Terry[2]
[1]*Institute for Multiscale Thermofluids, School of Engineering, University of Edinburgh, The King's Buildings, Mayfield Road, Edinburgh EH9 3FB, United Kingdom*
[2]*Institute for Integrated Micro and Nano Systems, School of Engineering, University of Edinburgh, The Kings Buildings, Mayfield Road, Edinburgh EH9 3FB, United Kingdom*

Keywords: Dielectrowetting, Microfluidics, Droplet, Thin-Film, Hysteresis

Abstract

There has been a recent growth in interest in microfluidic research with the development of lab-on-a-chip devices. These are small circuits capable of automatically performing laboratory functions such as mixing, dispensing, and transportation of small volumes of liquid. Currently these devices have limitations, requiring large external components to function and being restricted to one task. The aim of this work is to investigate the use of dielectrowetting to potentially create new microfluidic functions. In order to study the statics and dynamics of dielectrowetting, we focussed on replicating results in the literature by Edwards et al [1,2] using dielectrowetting to reversibly and repeatably manipulate a droplet to a thin film. We used circular patterned interdigitated aluminium electrodes to generate a decaying electric field penetrating into a dielectric droplet, and capped the surface with a thin dielectric Parylene C layer. For an increasing voltage we monitored the decrease in contact angle of the droplet, until it reached a thin film. Taking quasi-static measurements at intervals of increasing voltage we categorised the relationship between the contact angle of the droplet and the applied voltage, which correlated well with literature values [1]. We then extended and applied this methodology to different electrode patterns, controlling the wetting of the droplet into different shapes. As in literature, our results show that droplet to thin film manipulation using dielectrowetting is possible. Following these foundations, we are investigating dielectrowetting on low pinning liquid-like surfaces to reduce contact angle hysteresis and increase the mobility of the contact line. This suggests that the velocity of retraction during dewetting will increase, which gives the potential to act as a foundation for new microfluidic functions.

References

[1] A.M.J. Edwards, C.V. Brown, M.I. Newton, G. McHale, *Dielectrowetting: The Past, Present and Future*, Current Opinion in Colloid & Interface Science. **36**, 28–36 (2018).
[2] A.M.J. Edwards, R. Ledesma-Aguilar, M.I. Newton, C.V. Brown, G. McHale. *Not spreading in reverse: The dewetting of a liquid film into a single drop*, Science Advances. **2**, 9 (2016).

P214

ENHANCED CONTROL OF DOUBLE EMULSION FORMATION IN MICROCHANNELS USING SURFACE-ACTIVE AGENTS

Chen Tang, Loïc Chagot, Panagiota Angeli
ThAMeS Multiphase, Department of Chemical Engineering, University College London, London, UK

Keywords: microfluidics, double emulsion, encapsulation, surface active agents

Abstract

Double emulsions play an import role in many applications, such as pharmaceutics, food production and cosmetics [1-3]. In double emulsions, droplets of one liquid are encapsulated by another immiscible liquid; one of the most used double emulsions is the water-in-oil-in-water one (W/O/W) [4]. Microfluidic systems, which provide a very good control of flow patterns, are the perfect tool to generate these complex emulsions [5]. However, the stability of the double emulsions is limited, and the drops can easily coalesce. The addition of surface-active agents can significantly promote the stability of double emulsions.

This study presents an experimental investigation of the influence of surfactants on the formation of a drop-in-drop pattern (Fig. 1). The experiments were conducted within a glass double flow-focusing microchannel. Glycerol was mixed with water to match the refractive index of the silicone oil, facilitating optimal optical access for high-speed imaging measurements. Two widely used surfactants, SDS and TX100, were added in the outer aqueous phase at different concentrations $C = 0.5\,CMC, 0.8\,CMC$ *and* CMC, where CMC is the critical micelle concentration. For each concentration of surfactants, a 3D flow pattern map was generated to draw the boundaries of the drop-in-drop regime under varying interfacial tension and flow rate conditions. The encapsulation rate and stability of the drop-in-drop regime were then investigated for a range of capillary number ratios. Furthermore, this study highlights the impact of surface-active agents and flow rates on the double emulsion thickness, which is defined as the difference between the outer and the inner droplet sizes.

This experimental approach will enable a deeper understanding of the mechanisms underlying double emulsion formation and will suggest strategies for desired outcomes in various applications.

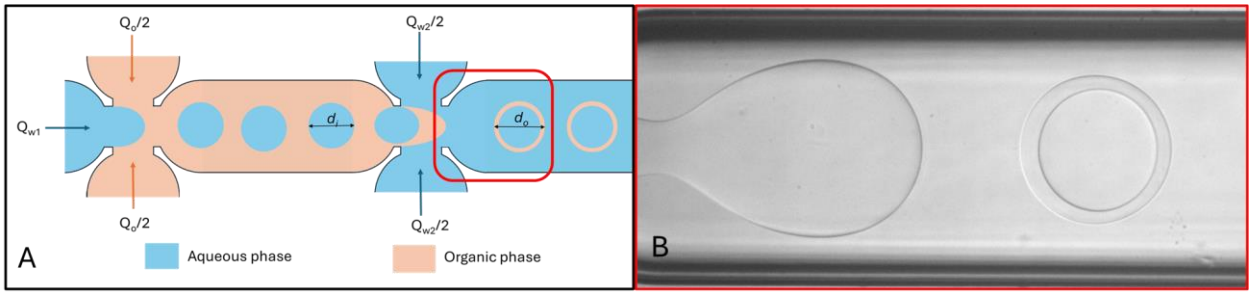

Figure 1. Drop encapsulation in a double flow-focusing microchannel. A) Illustration of drop encapsulation; B) Image of double emulsion in surfactant-free fluid system

References

[1] Langer, R., *Drug delivery and targeting.* Nature **392,** 5-10 (1998).
[2] Gallarate, M., et al., *On the stability of ascorbic acid in emulsified systems for topical and cosmetic use.* INTERNATIONAL JOURNAL OF PHARMACEUTICS **188,** 233-241 (1999).
[3] Muschiolik, G. and E. Dickinson, *Double Emulsions Relevant to Food Systems: Preparation, Stability, and Applications.* Comprehensive reviews in food science and food safety **16**, 532-555 (2017).
[4] Leister, N. and H.P. Karbstein, *Evaluating the stability of double emulsions— A review of the measurement techniques for the systematic investigation of instability mechanisms.* Colloids and interfaces **4**, 8 (2020).
[5] Battat, S., D.A. Weitz, and G.M. Whitesides, *An outlook on microfluidics: the promise and the challenge.* Lab on a chip **22**, 53-536 (2022).

P215

INVESTIGATING SOILING PATTERNS Of ROTATING TIRE USING CFD ANALYSIS

Aditya Jambholkar, Harsha Penumadu & Florimond Gueniat
College of Engineering, Birmingham City University, UK

Keywords: wheel spray dynamics, OpenFOAM CFD, vehicle soiling

Abstract

Inclement weather presents challenges for vehicle visibility and sensor reliability in both conventional and autonomous automobiles [1]. A primary contributor to reduced visibility and sensor soiling in wet conditions is water spray generated by the rotational motion of tires [2]. This spray adheres to windshields and sensor housings, distorting signals and obscuring visual data. Mitigating tire spray will be an important step in improving all-weather performance and safety for both human-operated and self-driving vehicles.

Spray dispersion is inhernenlty multiphysics and depends on the tire geometry. This work aims at investigating the impact of the tire designs on the tire spray properties. Computational fluid dynamics (CFD) is carried out, in order to model and simulate the spray. Various tire tread designs are designed in CAD (Fig. 1) and simulated making wet contact with the road surface using OpenFOAM software. The CFD simulations examine spray propagation as tires rotate at 22.2m/s equivalent linear velocity through a water layer. It corresponds to a Reynolds number of $R_e \approx 950 \times 10^3$. The simulations are validated against existing works of Kabanovs *et al.* [2]. By evaluating flow patterns, particle distributions, velocities, and water fractions in the resulting sprays, this work will assess how tread designs influence spray. A Pareto analysis will allow to identify tread patterns that minimize spray. Overall, this multiphysics approach will reveal new insights into the fluid dynamics underlying tire spray formation.

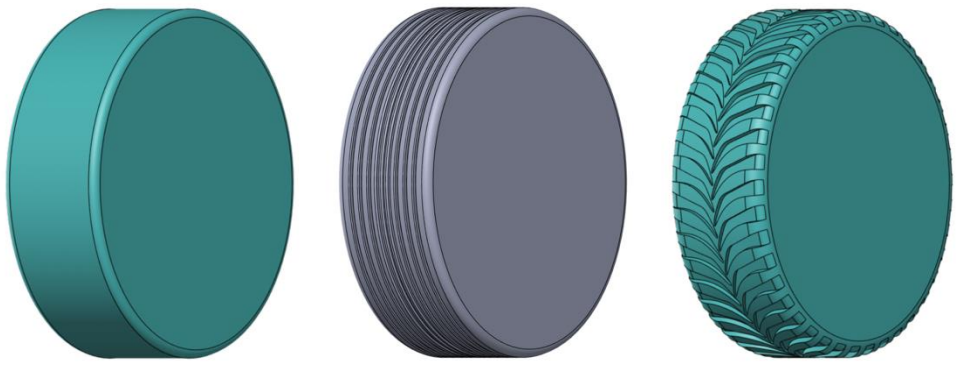

Figure 1. Illustration of the investigated geometries: a) Slick Tire, b) Linear Tire Thread, c) Chevron Tire Thread.

References

[1] Rivero, J. R. V., Gerbich, T., Buschardt, B., & Chen, J. (2021). The effect of spray water on an automotive LIDAR sensor: A real-time simulation study. *IEEE Transactions on Intelligent Vehicles*, 7(1), 57-72.
[2] Schilling, F., Kuthada, T., Gaylard, A., Wiedemann, J., & Wagner, A. (2020). Advances in experimental vehicle soiling tests. *SAE International Journal of Advances and Current Practices in Mobility*, 2(2020-01-0681), 2596-2603.
[3] Kabanovs, A., Garmory, A., Passmore, M., et al. (2019). Investigation into the dynamics of wheel spray released from a rotating tyre of a simplified vehicle model. *Journal of Wind Engineering and Industrial Aerodynamics*, 184: 228–246.

P216

TURBULENT ENERGY SPECTRUM IN THE DIA APPROXIMATION

Elias Kohler[1], Matthias Fuchs[1]
[1]*Department of Physics, University of Konstanz, Germany*

Keywords: Stationary homogeneous and isotropic turbulence, energy spectrum, Direct Interaction Approximation (DIA)

Abstract

Turbulent flows are an everyday phenomenon and a clear understanding of them is of enormous importance for technical applications. In 1959, H. Kraichnan proposed a statistical closure approach (DIA) to derive a parameter free theory for the (lowest) velocity moments [1]. We have numerically solved this system of DIA equations for stationary, homogeneous, and isotropic turbulence, in which case the problem is reduced to two coupled integro-differential equations. To achieve stationary turbulence, we stir the fluid with an external force, characterized by the spectrum $F(k) \propto (k\kappa_c^{-1})^2 \exp(-k\kappa_c^{-1})$. Through this external force, we generate large vortices with the characteristic length κ_c^{-1}. The energy spectrum $E(k)$ of the turbulence results directly from the numerical solution, which is shown in the figure below for three Taylor-Reynolds numbers Re_λ. Kraichnan predicted that the energy spectrum in the inertial range, between k_E and k_D, follows a power-law of the form $E(k) \propto k^{-3/2}$ for large Re_λ. This prediction agrees almost perfectly with the numerical solution, where the deviation $\gamma(k)$ from the power law is shown in the subplot and is defined by $E(k) = Ak^{-(3/2+\gamma(k))}$. With the numerical solution of the energy spectrum $E(k)$, the energy-containing range ($k < k_E$) and the dissipation range ($k > k_D$) can now be investigated in more detail. Furthermore, the transition between laminar and turbulent flow can also be analyzed.

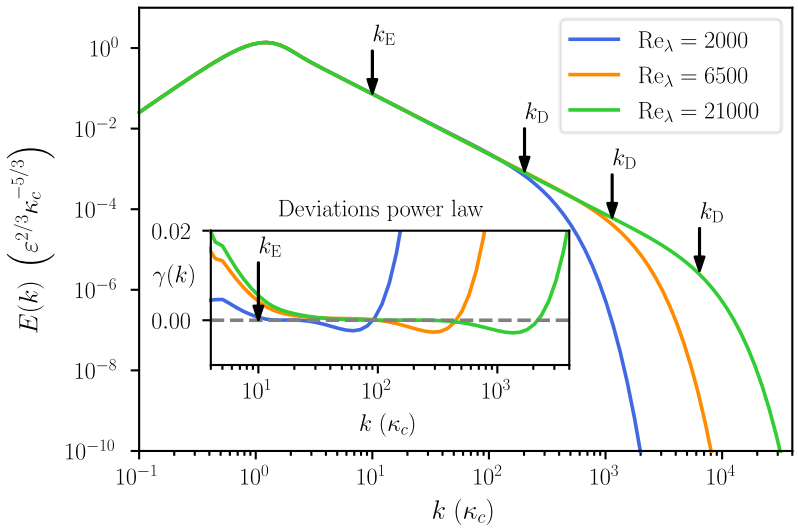

Figure 1. In the main plot, the energy spectrum is shown for three different Taylor Reynolds numbers Re_λ. In the subplot, the deviations $\gamma(k)$ from the power law are illustrated. Furthermore, κ_c^{-1} denotes the characteristic length of the generated vortices, and ε represents the dissipation rate.

References

[1] R.H. Kraichnan, *The structure of isotropic turbulence at very high Reynolds numbers*, J. Fluid Mech. **5**, 497 (1959).

P217

THEORETICAL ANALYSIS OF FLOW THROUGH A CROSS-SLOT

Xintong Ji[1] & Helen J. Wilson[1]
[1]*Department of Mathematics, University College London, London, United Kingdom*

Abstract Fluid instability; bifurcation phenomena; microfluidic flow; viscous flow.

A cross-slot (or cross-channel) is a flow geometry with four 'arms'. The inflow comes from two opposite (horizontal as default) 'arms' and the outflow goes away from the other two opposite (vertical as default) 'arms'. A slow flow through this geometry produces a pattern with reflectional symmetry and produces a good approximation to a pure planar extension near the stagnation point at the centre.

For viscoelastic flow through the cross-slot, there is substantial evidence of a symmetry-breaking event as the flow rate is increased. A body of experimental evidence follows from the original work of [1] and numerical evidence (e.g. [2]) to show an initial bifurcation to a steady asymmetric flow that results from purely elastic effects (generating) and inertial effects (stabilising); however, as yet we have no analytical insight into this complex fluid behaviour.

In this work we begin by studying Stokes flow in the cross-slot geometry, in order to provide a theoretical foundation on which to base an analysis of viscoelastic flow. We use two techniques in parallel. The first is a transform method, in which the flow is calculated as a sum of spectral contributions. The second is to use a conformal mapping to transform the cross-slot geometry (relatively complex geometry) into a unit disk (relatively simple geometry). In either case, the viscous/base flow solution with all physical quantities of interest (including velocity, stream function and so on) can be calculated. We will build on this solution to address the effects of viscoelasticity and finally the linear stability which must underlie the bifurcation phenomenon.

References

[1] P. E. Arratia, C. C. Thomas, J. Diorio, and J. P. Gollub, *Elastic instabilities of polymer solutions in cross-channel flow*, Physical Review Letters **96(14)**, 144502 (2006).
[2] R. J. Poole, M. A. Alves, and P. J. Oliveira. *Purely elastic flow asymmetries*, Physical Review Letters **99(16)**, 164503 (2007).

DAY 2 - Tuesday, 25 June 2024 Morning Sessions			
09:00	**Keynote 3: Prof Satish Kumar** ***Chair: Prof Glen McHale*** ***Larch Lecture Theatre***		
	Instabilities & Bifurcations 3 ***Chair: Dr Alex Wray*** ***Larch Lecture Theatre***	***Phase-Change 1*** ***Chair: Dr Dani Orejon*** ***Yew Lecture Theatre***	***Multiphase & Interfacial Flows 1*** ***Chair: Dr Rachel Schwind*** ***Elm Lecture Theatre***
09:45	Tu037: Coupled instability fostered mesoscale sunflowers in porous medium *by V Vanarse, D Bandyopadhyay*	Tu056: Does the Van der Waals force play a part in evaporation? *by E Benilov*	Tu075: Optimum viscosity ratio for enhanced instability and mixing in layered channel flows *by P Banga, SN Maharana, M Mishra*
10:00	Tu038: Bifurcations and flow topology in a model branching flow with an aneurysmal perturbation *by A Chatterjee, J Sesterhenn*	Tu057: Flow stability in shallow droplets subject to localized heating of the bottom plate *by KE Pang, C Cuvillier, Y Kita, L Ó Náraigh*	Tu076: Influence of capillary instability on the stratified liquid-liquid flow pattern transition *by P Miranda, JE Arrollo-Caballero, OMH Rodriguez*
10:15	Tu039: Instability and bifurcation of poiseuille flow in fluid overlying porous domain *by P Bera, A Aleria*	Tu058: Experimental study of thermocapillarity–induced deformation of evaporating films on structured copper surfaces *by R Behle, P Stephan, T Gambaryan-Roisman*	Tu077: A multidimensional examination of phase separation in single-component fluids *by S Das, M Mussel*
10:30	Tu040: Monotone energy stability of plane Couette and Poiseuille flows: critical Reynolds numbers and Squire's theorem for nonlinear stability *by G Mulone*	Tu059: Evaporation-induced translation of multiple binary droplets *by D Debnath, A Malachtari, G Karapetsas, D Orejon, K Sefiane, A Amirfazli, P Valluri*	Tu078: Partial encapsulation in binary droplet collisions of miscible liquids *by É Ruiz-Gutiérrez, K Dalgarno, N Chakraborty*
10:45	Tu041: Marangoni instability in a surfactant solution above the cmc point *by A Nepomnyashchy*	Tu060: Evaporative behavior of liquid-liquid phase separated alcohol droplets *by JA Lazo, R-H Chen*	Tu079: Mitigation of generated air-entrainment from free surface vortices at pump suction using combined multipoint intakes and air separator system *by RK Mondal, D Debnath, P Kumar*
11:00	**Coffee Break (Alder Lecture Theatre)**		
11:30	Tu042: Experimental study on the stability of core-annular flow using particle image velocimetry (PIV) and planar laser induced fluorescence (PLIF) techniques *by JEA Caballero, PJM Lugo, OMH Rodriguez*	Tu061: Stability analysis of dryout inception for boiling CO2 *by G Cantini, G Arnone, F Capone, J Gianfrani, M Carnevale*	Tu080: The role of Marangoni effect on the non-isothermal falling fluid film instability *by AY Özel, C Ruyer-Quil, L Biancofiore*
11:45	Tu043: Analytical model for long-time Rayleigh-Taylor bubble evolution *by Z Xiao, C Liu, Y Zhang*	Tu062: The impact of evaporation regime on the stability of volatile liquid films *by O Mohamed, L Biancofiore*	Tu081: Mass transport in a horizontally vibrated fluid layer *by M Bestehorn, ID Borcia, R Borcia, S Richter, F-T. Schoen, U Harlander*
12:00	Tu044: Stability of Hartmann flows in inclined layers *by P Falsaperla, G Mulone*	Tu063: Droplet evaporation and the stick-slip modes trifurcation *by D Orejon, KM Al Balushi, G Duursma, P Valluri, K Sefiane*	Tu082: Suppression of magnetohydrodynamic interfacial wave instabilities by means of parametric anti-resonance by *GM Horstmann, J Kuhn, F Dohnal*
12:15	Tu045: The Jacobian analytical method (JAM) *by MA Herrada*	Tu064: Field-induced capillary condensation: surface diffusion or spontaneous nucleation? *by A Afzalifar, RHA Ras*	Tu083: Numerical simulations of surfactant-covered Faraday Waves: role of Marangoni stresses in pattern formation *by D Panda, L Kahouadji, L Tuckerman, S Shin, J Chergui, D Juric, OK Matar*
12:30	**Lunch Break (Alder Lecture Theatre)**		

Keynote 3

Nonuniformities in multilayer, multicomponent liquid-film coatings

Satish Kumar

Department of Chemical Engineering and Materials Science, University of Minnesota, Minneapolis, USA

Satish Kumar is a Distinguished McKnight University Professor at the University of Minnesota where he is on the faculty of the Department of Chemical Engineering and Materials Science. Prof. Kumar received his undergraduate degree from Minnesota (1993), and his master's (1994) and doctoral degrees (1998) from Stanford University, all in chemical engineering. Following postdoctoral work at École Normale Supérieure (Paris) and the University of Michigan, he joined the faculty at Minnesota in 2001. Prof. Kumar currently serves as Faculty Director of the Industrial Partnership for Research in Interfacial and Materials Engineering (IPRIME), a university-industry consortium. He is both a Fellow and an Outstanding Referee of the American Physical Society, is Co-Editor-in-Chief of the Journal of Engineering Mathematics, and serves on the editorial board of the Journal of Non-Newtonian Fluid Mechanics. He has served as a member of the Executive Committee of the American Physical Society Division of Fluid Dynamics, and is a former president of the International Society of Coating Science and Technology. Prof. Kumar's research involves integration of transport phenomena, colloid and interface science, rheology, applied and computational mathematics, and experiments to address fundamental issues motivated by problems in materials processing. These fundamental investigations, which are described in over 150 journal articles and 27 PhD theses, are frequently inspired by industrial applications such as coating and printing processes, polymer processing, nanofluidics/microfluidics, and energy.

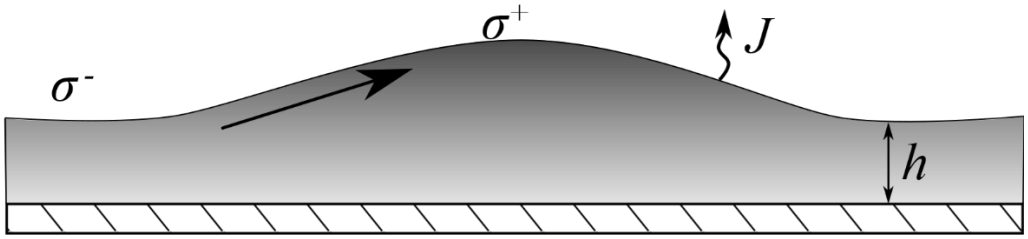

Abstract

Depositing and obtaining a liquid film of uniform thickness is a problem integral to numerous applications in the multibillion-dollar coatings industry. Film thickness is determined by the interplay of capillary leveling, Marangoni flows, evaporation, and various other phenomena. Applications often demand multilayer films where each layer has distinct properties, and this gives rise to additional challenges due to the presence of multiple components. This talk will provide an overview of these challenges and describe recent advances in our fundamental understanding of the physical mechanisms underlying film-thickness nonuniformities in multilayer, multicomponent liquid-film coatings.

Tu037

Coupled Instability Fostered Mesoscale Sunflowers in Porous Medium

Vinod Vanarse[1], Tapas Kumar Mandal[1,2,3], & Dipankar Bandyopadhyay[1,2,3]
[1]*Department of Chemical Engineering, Indian Institute of Technology Guwahati, Assam, India*
[2]*Centre for Nanotechnology, Indian Institute of Technology Guwahati, Assam, India*
[3]*School of Health Sciences and Technology, Indian Institute of Technology Guwahati, Assam, India*

Keywords: viscous fingers, interfacial instability, linear stability analysis, porous medium

Abstract

Figure 1. The schematic shows the micrographs of artificially formed mesoscale sunflowers. Color pictures show the similarity between artificial and natural flowers.

Interfacial instability occurs as a high-viscosity fluid displaces a lower-viscosity leading to finger-like pressure gradient-driven structures in a porous medium [1], known as viscous fingers [2]. This study explores the prominent features of an unconfined and coupled instability modes mediated system leading to viscous finger formation results in mesoscale sunflower, unlike the confined Hele-Shaw cell [3], through the general linear stability analysis (GLSA) approach substantiated with experiments. Experiments revealed that dispensing a water drop on the thin film of a solution (polymer-solvent) forms a thin and porous polymer layer at the water-polymer interface. A denser water drop on the rarer polymer solution film manifests the Rayleigh-Taylor instability – RTI and the dynamic formation of the porous layer at the water-solvent interface nurtures the Saffman-Taylor instability – STI. The polymer concentration (C) in the solution plays an important role in deciding the morphological evolution, length - L_F, and average number of fingers - N_{avg} in the interfacial instability-induced finger sunflower (Figure 1). The simple theoretical model based on the GLSA establishes the platform to predict the onset of the instability in the system. Furthermore, the reduction in interfacial tension promotes system instability for random perturbations, which is correlated to the polymer concentration in the solution. An increase in the density difference (ρ_D) destabilizes the system, whereas by offering high resistance to the instability, the viscosity ratio (μ_r) brings the system towards stability. These estimates are accredited to the concentration gradients at the interface. The model can predict the time and length scales, which follow experimental findings. Moreover, the inverse relationship of polymer concentration, $C \sim We^{-0.3}$ and $C \sim Re^{-0.7}$ emphasize its role in the overall dynamics of the sunflower formation.

References

[1] Homsy GM. Viscous fingering in porous media. Ann. Rev. Fluid Mech. 19, 271–311 (2003).
[2] Saffman P. G., Taylor G. I. The penetration of a fluid into a porous medium or Hele-Shaw cell containing a more viscous liquid. Proc R Soc Lond A Math Phys Sci **245**, 312–29 (1958).
[3] HELE-SHAW HS. Flow of Water. Nature **58**, 520–520 (1898).

Tu038

BIFURCATIONS AND FLOW TOPOLOGY IN A MODEL BRANCHING FLOW WITH AN ANEURYSMAL PERTURBATION

Ajay Chatterjee[1], Jörn Sesterhenn[2]
[1]*School of Engineering, Santa Clara University, Santa Clara, California, USA*
[2]*Department of Applied Mechanics & Fluid Mechanics, University of Bayreuth, 95440 Bayreuth, Germany*

Abstract We study laminar flow and stability of a Newtonian and a shear thinning fluid in a branching channel with a shallow local perturbation of the impinging surface.
Key words: Branching flow, Model aneurysm, Laminar, Shear thinning, Pitchfork, Vortex breakdown, Flapping instability.

We consider low Reynolds number laminar flow in a model geometry which consists of a branching channel with a local perturbation of the impinging surface at the stagnation zone. The perturbation is a bulge which mimics a saccular aneurysm type deformation and the geometry also models low speed flow into a rectangular cavity. The surface perturbation is shallow with a depth less than the width of the branching channels. Due to the symmetric location of the surface perturbation the base flow is steady and symmetric in the two planes parallel to the inlet flow direction. The first bifurcation is a pitchfork which destroys symmetry of the flow along the spanwise direction. For a Newtonian fluid linear theory predicts that instability occurs at a relatively low Reynolds number around 100 based on the flow rate and the width of the inlet channel. The value for a shear thinning fluid is similar when a volume averaged viscosity is used to compute the Reynolds number, $\overline{Re} = \frac{Re}{V}\int_V \frac{1}{\mu}\, dV$, where the non-Newtonian viscosity has been normalized to the Newtonian value, and the shear thinning model is the well known Carreau viscosity relation. Computation of the leading instability mode indicates that the perturbed flow field is localized in the high shear region of the base flow where countercurrent flow occurs due to the surface perturbation. Both Newtonian and shear thinning fluids exhibit similar behavior at the first bifurcation, indicating a shear instability of the symmetric base flow in both cases. The symmetry breaking flow engendered by the pitchfork bifurcation leads to highly asymmetrical shear stress distributions along the walls of the surface perturbation, suggesting implications in a physiological context as well as for scalar transport across its boundaries.

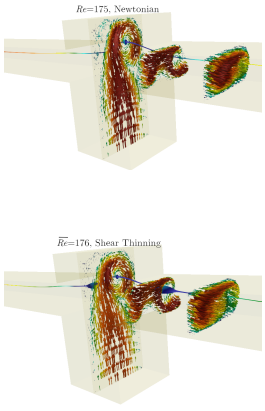

The presence of the perturbation generates swirl and helical flow, but the symmetry breaking bifurcation effectively suppresses this characteristic on one half of the asymmetry plane. As the Reynolds number is increased the steady asymmetric flow displays increasing complexity for the shear thinning fluid. At a Reynolds number not much larger than the critical value corresponding to the pitchfork bifurcation, the shear thinning fluid displays flow topology suggestive of vortex breakdown. This feature is not observed in the steady asymmetric Newtonian flow, and it is theorized to occur in the shear thinning flow as a result of differences in the shapes of the velocity profiles between the two rheologies. We present some initial results to characterize these flow features. A secondary bifurcation occurs at a higher Reynolds number around 200, this being a Hopf bifurcation of the asymmetric steady flow, and it leads to weak flapping like motion in the spanwise plane. Therefore, this secondary nonstationary instability results in a flow which is quite distinct from the time dependent flow due to the classic flapping instability of the two dimensional plane impinging jet (Chatterjee & Fabris, 2017). In the present geometry the left-right symmetry in the plane of the two exit branches is preserved. All of these stability and flow characteristics are fundamentally related to the presence of the local surface perturbation in the neighborhood of the stagnation zone, and they represent richer flow topology and dynamics than the corresponding two dimensional plane impinging flow in the presence of a local cavity (Boucher & Climent, 2012).

References

[1] Chatterjee, A., Fabris, D., Planar non-Newtonian confined laminar impinging jets: Hysteresis, linear stability, and periodic flow, *Phys. Fluids*, **29** 103103 (2017).
[2] Boucher, G., Climent, E., Unsteady behavior of a confined jet in a cavity at moderate Reynolds numbers, *Fluid Dyn. Res.* **44**, 025505 (2012).

Tu039

INSTABILITY AND BIFURCATION OF POISEUILLE FLOW IN FLUID OVERLYING POROUS DOMAIN

P. Bera[1] & A. Aleria [1]
[1]*Department of Mathematics, Indian Institute of Technology Roorkee, India*

Abstract The present study examines the weakly nonlinear stability analysis of Poiseuille flow in a porous domain underlying a fluid domain. The nonlinear interactions are investigated by imposition of finite amplitude perturbations to the classical models of isothermal [2] and non-isothermal [3] Poiseuille flow. The nonlinear stability reveals the existence of both subcritical and supercritical bifurcations for isothermal Poiseuille flow in such superposed fluid-porous systems. Interestingly, on the other hand, only supercritical bifurcation exists for the non-isothermal Poiseuille flow.

The system under consideration consists of a horizontal fluid domain of depth, d, that overlies a porous domain of depth, d_m, with the domains separated by a permeable interface. Such systems find extensive application in many geological and industrial set-ups. To name a few: contaminant flow beneath the Earth's surface [5], cooling of electronic components [8], subglacial lakes [4], etc. The present system is governed by Navier-Stokes equation and the Darcy's law in fluid and porous domain, respectively. An externally applied pressure gradient introduces the Poiseuille flow in the system. For thermal convection situation, the system is heated from below and buoyancy is introduced by preservation of constant temperatures at the top plate of fluid domain and bottom plate of porous domain. The governing equations for linear stability analysis of isothermal and non-isothermal Poiseuille flow are adopted from the works of Chang *et al.* [2] and Chang [3], respectively. The weakly nonlinear analysis is consummated on the same lines as performed by Stewartson *et al.* [7] and Sharma *et al.* [6]. The cubic Landau equation is derived and its real part (a_{1r}) is utilized to identify the different types of bifurcation: the subcritical and supercritical bifurcation. The weakly nonlinear results of isothermal Poiseuille flow are excerpts from the recent work of Anjali *et al.* [1].

The linear stability analysis of Chang *et al.* [2] and Chang [3] is reiterated and the weakly non-linear stability analysis of Poiseuille flow for both isothermal and non-isothermal cases is performed in the present study, the latter for the non-isothermal case being the novel contribution of this work. For the isothermal Poiseuille flow, both subcritical and supercritical bifurcation have been observed, whereas, for the non-isothermal Poiseuille flow, only supercritical bifurcation is witnessed. This indicates that higher order analysis/ DNS is required for the isothermal case in order to find the exact lower critical value of Reynolds number for transition to turbulence. However, for the non-isothermal case, the linear stability theory suffices to provide the global stability for Poiseuille flow in fluid overlying porous domain.

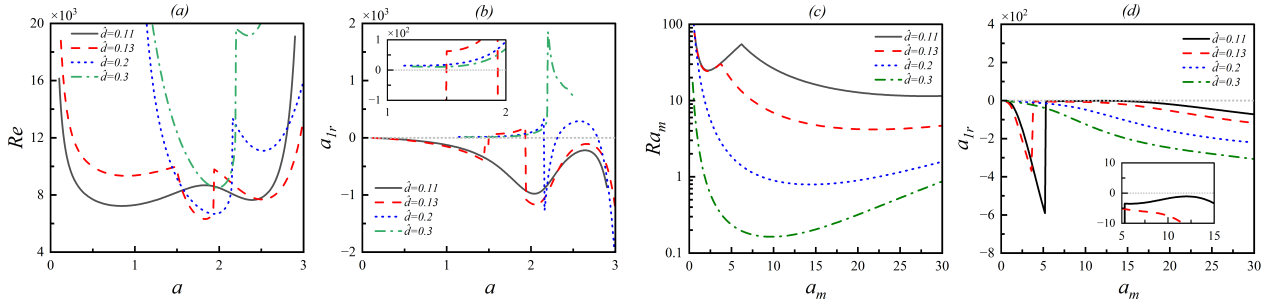

Figure 1: (a,c) Neutral stability curves obtained by linear stability theory, (b,d) Variation of a_{1r} obtained by weakly nonlinear stability analysis for different values of $\hat{d}$ and $\delta = 0.001$ in (a,b) isothermal and (b,d) non-isothermal Poiseuille flow.

References

[1] ANJALI, KHAN, A. AND BERA, P. Finite amplitude analysis of Poiseuille flow in fluid overlying porous domain, Accepted in *SIAM J. App. Math.*.
[2] CHANG, M. H., CHEN, F. AND STRAUGHAN, B. Instability of Poiseuille flow in a fluid overlying a porous layer, *J. Fluid Mech.* **564** (2006) 287–303.
[3] CHANG, M. H. 2006 Thermal convection in superposed fluid and porous layers subjected to plane Poiseuille flow. *Phys. Fluids* **18**, 035104.
[4] COUSTON, L.-A. Turbulent convection in subglacial lakes. *J. Fluid Mech.* **915** (2021) A31.
[5] EWING, R. E. AND WEEKES, S. L. 1998 Numerical Methods for Contaminant Transport in Porous Media. *Comput. Maths* **202**, 75–95.
[6] SHARMA, A. K., KHANDELWAL, M. K. AND BERA, P. Finite amplitude analysis of non-isothermal parallel flow in a vertical channel filled with a highly permeable porous medium, *J. Fluid Mech.* **857** (2018) 469–507.
[7] STEWARTSON, K. AND STUART, J. T. A non-linear instability theory for a wave system in plane Poiseuille flow, *J. Fluid Mech.* **48** (1971) 529–545.
[8] YOSHIKAWA, Y., AKITOMO, K. & AWAJI, T. 2001 Formation process of intermediate water in baroclinic current under cooling. *J. Geophys. Res.* **106**, 1033–1051.

Tu040

MONOTONE ENERGY STABILITY OF PLANE COUETTE AND POISEUILLE FLOWS: CRITICAL REYNOLDS NUMBERS AND SQUIRE'S THEOREM FOR NONLINEAR STABILITY

Giuseppe Mulone[1]
[1]*Department of Mathematics and Computer Science, Catania University, Italy*

Abstract Couette flow, Poiseuille flow, monotone energy stability, Squire's theorem

Critical Reynolds numbers of stability of Couette and Poiseuille laminar flows between parallel planes are different in the linear case, nonlinear case, and experiments. The plane Couette flow is linearly stable for any Reynolds number, the plane Poiseuille flow is unstable for spanwise perturbations if the Reynolds numbers are greater than 5772. Furthermore, in the linear case a transformation and a Squire's theorem hold: "for the study of the stability of flow between parallel walls it is sufficient to confine attention to disturbances of two-dimensional *spanwise* type".

In the case of the nonlinear Navier-Stokes equations, the search for critical values of monotone energy stability has given contrasting results (Orr 1907, Joseph 1966, Joseph and Carmi 1969) for both Couette and Poiseuille motions. Orr obtains critical values on spanwise perturbations and Joseph obtains lower critical values on streamwise perturbations. None of authors gives a rigorous demonstration of their results.

We prove that the correct results are those of Orr, and a Squire's theorem holds also for nonlinear monotone energy stability of parallel shear flows that include Couette and Poiseuille flows between parallel walls. Moreover, streamwise perturbations are nonlinear monotone stabilizing for any Reynolds number.

References

[1] W. M'F. Orr, *The stability or instability of the steady motions of a perfect liquid and of a viscous liquid,* Proc. Roy. Irish Acad. A **27**, 9–68 and 69–138 (1907).
[2] H. B. Squire, *On the stability of three-dimensional disturbances of viscous flow between parallel walls*, Proc. Roy. Soc. A **142**, 621 (1933).
[3] D. D. Joseph, *Eigenvalue bounds for the Orr-Sommerfeld equation*, J. Fluid Mech. **33** part 3, 617–621 (1966).
[4] P. Falsaperla, A. Giacobbe, G. Mulone, *Nonlinear stability results for plane Couette and Poiseuille flows*, Physical Review E **100**, 013113 (2019). https://doi.org/10.1103/PhysRevE.100.013113
[5] P. Falsaperla, G. Mulone, C. Perrone, *Energy stability of plane Couette and Poiseuille flows: a conjecture*, European J. Mech./B Fluids **93**, 93–100 (2022) https://doi.org/10.1016/j.euromechflu.2022.01.006
[6] G. Mulone, *Nonlinear monotone energy stability of plane shear flows: Joseph or Orr critical thresholds?*, SIAM J. Appl. Math. **84**, 60–74 (2024) https://doi.org/10.1137/22M1535826
[7] G. Mulone, *Squire's theorem for nonlinear monotone energy stability*, submitted (2024), http://ssrn.com/abstract=4705305

Tu041

MARANGONI INSTABILITY IN A SURFACTANT SOLUTION ABOVE THE CMC POINT

Alexander Nepomnyashchy
Department of Mathematics, Technion - Israel Institute of Technology, Haifa, Israel

Abstract The influence of the micelle formation on the Marangoni instability in a layer of surfactant solution is investigated.

The influence of micelles on the Marangoni instability in a layer of a surfactant solution is a controversial issue. On one side, the experiments show that the surface tension of a solution is almost independent on the total amount of dissolved surfactant above the CMC point. One could think that the Marangoni convection is suppressed. On another side, the surface tension is determined by the *surface* concentration of the adsorbed surfactant that depends on the bulk concentration of *single* surfactant molecules near the surface, because micelles are not adsorbed. One could assume that the appearance of micelles does not influence the Marangoni instability.

In the present talk, we use a simplified model of Marangoni instability in a surfactant solution containing micelles. We disregard the polydispersity of micelle sizes and describe the aggregation process by kinetic equations for bulk concentrations of surfactant monomers and micelles. In the framework of that model, we consider a layer of a surfactant solution heated or cooled from below. Due to the Soret effect for monomers and the thermophoresis of micelles, a spatial nonuniformity of both concentrations is generated. The surface tension is assumed to depend on the temperature and the concentration of the adsorbed surfactant. Monotonic and oscillatory instability thresholds are calculated. It is shown that both "naïve" suggestions concerning the influence of micelles on the Marangoni instability written in the first paragraph of the abstract are not correct.

Tu042

EXPERIMENTAL STUDY ON THE STABILITY OF CORE-ANNULAR FLOW USING PARTICLE IMAGE VELOCIMETRY (PIV) AND PLANAR LASER INDUCED FLUORESCENCE (PLIF) TECHNIQUES.

J. E. Arrollo-Caballero, P. J. Miranda-Lugo & O. M. H. Rodriguez
University of São Paulo (USP), São Carlos School of Engineering (EESC), Mechanical Engineering Department, Industrial Multiphase Flow Laboratory (LEMI), Av. Trab. São Carlense, 400 - Parque Arnold Schimidt, São Carlos - SP, 13566-590, Brazil.

Abstract keywords: Core-annular flow, Interfacial wave, Oil-water flow, PIV, PLIF, Stability, Velocity profile.

The interaction of non-miscible liquids is common in industries such as oil, food and chemistry. When these fluids flow simultaneously through a pipeline, different spatial configurations or flow patterns can be observed. Prominent among these patterns is core-annular flow, in which the more viscous fluid travels in the core region of the pipe, while the less viscous fluid forms a ring that keeps the latter from touching the pipe wall. This flow pattern has beneficial applications, such as reducing pressure losses in pipelines in oil transportation or production activities. Although it has been widely studied, it is still not fully understood from the hydrodynamic stability point of view, especially when dealing with low viscosity oils. Therefore, this research aims to study the interface shape and core-annular flow dynamics in a 9.7mm ID horizontal pipe by synchronizing two optical techniques. The experimental campaign was carried out in a new facility designed for the study of liquid-liquid two-phase flows, focusing on the identification and classification of interfacial waves using the planar laser induced fluorescence (PLIF) technique, Figure 1. In addition, velocity profiles and turbulence statistics were explored using the particle image velocimetry (PIV) technique. Results related to turbulence statistics in axial and radial directions are presented, and a connection with the interfacial behavior of the waves is established. A direct relationship was identified between increasing inlet velocities and an aspect ratio, expressed as a dimensionless parameter related to the wavelength and amplitude of the wave, defined as the aspect ratio (λ/α). A decrease in aspect ratio is observed, indicating an increase in amplitude relative to wavelength. This behavior is linked to the increase in velocity and may have implications for flow stability. With these data, a general transition criterion based on the linear stability theory proposed by Rodriguez and Bannwart (2008) was applied. Its main contribution lies in the simplicity of the one-dimensional approach. On the one hand, the stability of the waves is examined assuming the existence of a stationary core-annular flow. On the other hand, different interfacial waves are imposed and their effect on stability is also studied. This general criterion encompasses the Kelvin-Helmholtz criterion as a particular case and allows the influence of various properties, such as densities, viscosities, interfacial tension, shape factors and neutral stability wave number, to be analyzed. It suggests that waves should provide additional "rigidity" to the core because of the curvature and the magnitude of the interfacial tension, thus demonstrating the crucial factor that interfacial tension plays in ensuring stability.

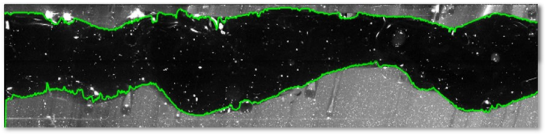

$$0 \le \frac{\phi_\mu}{-\phi_V + \phi_{\sigma_1} + \phi_g - \phi_{\sigma_2}} \le 1 \qquad (1)$$

Figure 1. Example of interface identification // **Equation 1.** Represents the general stability criterion, in which the viscous term, ϕ_μ, can favor or disfavor stability, the inertial term, ϕ_V, is destabilizing, the gravitational term, ϕ_g, is stabilizing, the first interfacial tension term, ϕ_{σ_1}, is stabilizing and the second interfacial tension term, ϕ_{σ_2} is destabilizing in the core-annular flow pattern.

References

[1] Marcelo S. de Castro and Cleber C. Pereira and Jorge N. dos Santos and Oscar M.H. Rodriguez, *Geometrical and kinematic properties of interfacial waves in stratified oil-water flow in inclined pipe*, Experimental Thermal and Fluid Science.**37**, pp. 171-178 (2012).

[2] Roberto Ibarra and Omar K. Matar and Christos N. Markides, *flow structures,inclined flows,laser-induced fluorescence,liquid-liquid flows,oil-water pipe flow,particle image velocimetry*, International Journal of Multiphase Flow.**135**, 03019322 (2021).

[3] O. M.H. Rodriguez and A. C. Bannwart, *Experimental study on interfacial waves in vertical core flow*, Journal of Petroleum Science and Engineering.**54**, 09204105 (2006).

[4] Rodriguez, O.M. and Bannwart, A.C., *Stability analysis of core-annular flow and neutral stability wave number.*, AIChE Journal **54**, No. 1, pp. 20–31 (2008).

[5] Ivan Zadrazil and Omar K. Matar and Christos N. Markides, *An experimental characterization of downwards gas-liquid annular flow by laser-induced fluorescence: Flow regimes and film statistics*, International Journal of Multiphase Flow. **60**, pp.87-102 (2014).

[6] Ivan Zadrazil and Omar K. Matar and Christos N. Markides, *An experimental characterization of liquid films in downwards co-current gas-liquid annular flow by particle image and tracking velocimetry*, International Journal of Multiphase Flow.**67**, pp.42-53 (2014).

Tu043

ANALYTICAL MODEL FOR LONG-TIME RAYLEIGH-TAYLOR BUBBLE EVOLUTION

Changwen Liu[1], Yousheng Zhang[2] & Zuoli Xiao[1]
[1]*State Key Laboratory for Turbulence and Complex Systems, College of Engineering, Peking University, Beijing 100871, China*
[2]*Institute of Applied Physics and Computational Mathematics, Beijing 100094, China*

Abstract Rayleigh-Taylor instability (RTI), which is named after Lord Rayleigh [1] and G. I. Taylor [2], happens when a heavy fluid is accelerated or supported by a light fluid layer. One of the most significant problems in such instability is the growth rate of the interface, which plays an important role in both scientific research (e.g., supernova explosion) and engineering application (e.g., inertial confinement fusion). Since Taylor's pioneering work in 1950, many efforts have been made to theoretically predict the nonlinear bubble evolution of single-mode RTI, but it still remains as an unsolved and challenging problem. This paper reports an analytical model for the long-time evolution of bubble velocity, curvature and vorticity including not only the classical linear, nonlinear and quasi-steady (QS) stages, but also the later re-acceleration and secondary velocity saturation (VS) regimes. The model is established by considering the vorticity accumulation around the bubble in a bilaterally rotational flow system based on the classical potential-flow theory [3]. Specifically, a dual-source model is introduced in the present potential-flow theory to address the long-standing difficulty highlighted by the initial-value sensitivity and strong nonlinearity. The present model is in very good agreement with numerical simulations for all density ratios and dimensions. It is found that, in the classical RTI stages, the neighboring vorticity at bubble front is negligibly small, and the vorticity-induced velocity can be ignored. In such situation, the initially perturbed interface reaches the QS stage due to the standard balance between buoyancy and drag forces. However, with the accumulation of vorticity around the bubble, the vorticity-induced velocity gradually becomes important, which breaks the standard balance and causes the acceleration of bubble into a new interface balance owing to the coupled effect of vorticity and gravity. Furthermore, the generation and breakdown of vortices in the flow field prompt the single-mode RTI to enter the chaotic stage.

Key words: Rayleigh-Taylor instability, Layzer potential theory, nonlinear coupling mechanism, vorticity accumulation.

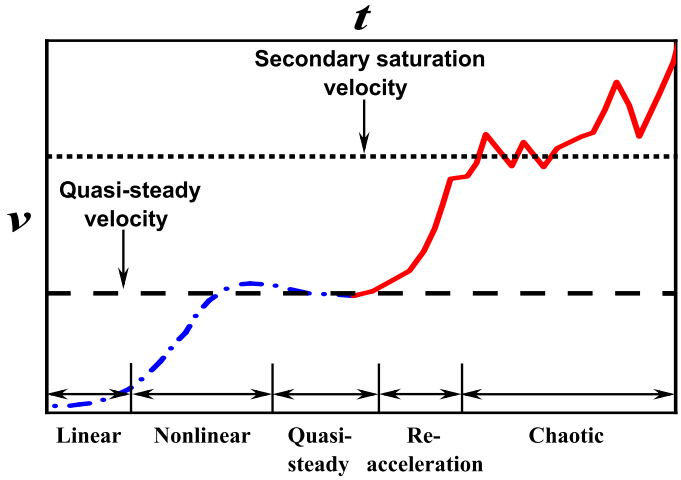

Figure 1. Schematic of different development stages of RTI based on the numerical results from Wei and Livescu [4] and Ramaprabhu *et al.* [5]. The blue dash-dotted line represents the classical single-mode RTI stages. The red solid line characterizes the later stages without *a prior* analytical model. The horizontal black dashed line and black dotted line denote the asymptotic values of quasi-steady velocity and secondary saturation velocity, respectively.

References

[1] Rayleigh L, *Investigation of the equilibrium of an incompressible heavy fluid of variable density*, Proc. R. Soc. London **14** (1), 170 (1883).
[2] Taylor GI, *The instability of liquid surfaces when accelerated in a direction perpendicular to their planes, I*, Proc. R. Soc. London Ser. A **201** (1065), 192 (1950).
[3] Layzer D, *On the instability of superposed fluids in a gravitational field*, Astrophys. J. **122**, 1 (1955).
[4] Wei T, Livescu D, *Late-time quadratic growth in single-mode Rayleigh-Taylor instability*, Phys. Rev. E **86**, 046405 (2012).
[5] Ramaprabhu P, Dimonte G, Woodward P, Fryer C, Rockefeller G, Muthuraman K, Lin P, Jayaraj J, *The late-time dynamics of the single-mode Rayleigh-Taylor instability*, Phys. Fluids **24**, 074107 (2012).

Tu044

STABILITY OF HARTMANN FLOWS IN INCLINED LAYERS

Paolo Falsaperla[1], Giuseppe Mulone[1]
[1]*Department of Mathematics and Computer Science, University of Catania, Catania, Italy*

Abstract Hartmann flow, Nonlinear stability, Inclined layer.

We study the stability of an electrically conducting fluid [1] flowing down an inclined layer, subject to an external magnetic field and to different boundary conditions. We consider both a linear (perturbative) analysis, and a nonlinear (Lyapunov) approach. This work generalizes previous results on similar flows [2, 3].

References

[1] J. Hartmann, *Hg-dynamics I: Theory of the laminar flow of an electrically conductive liquid in a homogeneous magnetic field*, K. Dan. Vidensk. Selsk. Mat. Fys. Medd. **15** (6), 1-28 (1937).
[2] P. Falsaperla, G. Mulone, C. Perrone, *Stability of Hartmann shear flows in an open inclined channel*, Nonlinear Analysis: Real World Applications **64**, 103446 (2022).
[3] P. Falsaperla, A. Giacobbe, G. Mulone, *Linear and nonlinear stability of magnetohydrodynamic Couette and Hartmann shear flows*, International Journal of Non-Linear Mechanics **123**, 103490 (2020).

Tu045

THE JACOBIAN ANALYTICAL METHOD (*JAM)*

Miguel A. Herrada
E.S.I., Universidad de Sevilla, Camino de los Descubrimientos s/n 41092, Spain

Abstract keywords:bubble dynamics, solid-fluid interaction, bifurcations.
We propose a generalization of the numerical method of Herrada and Montanero [1] for solving complex non-linear problems.[2] In order to show the ability of the method to describe bifurcations and instabilities in fluids, two examples are presented. The first is the study of the global stability analysis of bubbles in a vertical capillary with an external flow.[3] This problem presents a wide variety of bubble dynamics when a downward external flow is applied that opposes the buoyancy-driven bubble ascent. Three overlapping solution branches were found to exist over a finite range of the capillary number of the downward external flow in cases where the Reynolds number is small and the Bond number is larger than the critical value for which the bubble can spontaneously rise (see Figure 1 (a)).

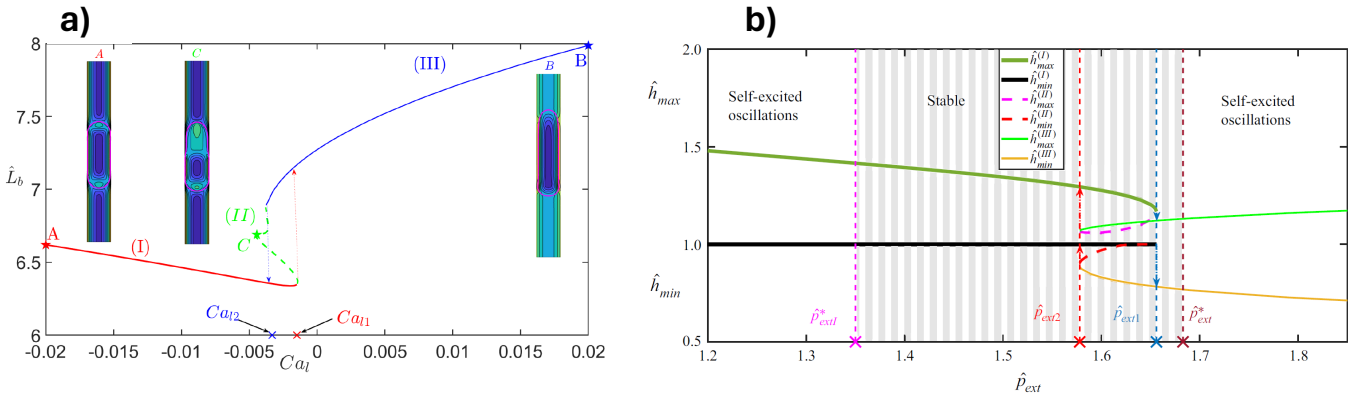

Figure 1. a) Nonlinear axisymmetric steady solutions of the model for bubbles in a vertical capillary with an external flow. b) Nonlinear 2D steady solutions of the model for the channel flow problem.

The second example is the study of a Newtonian fluid flow through a two-dimensional channel in which part of the rigid channel is replaced by a hyperelastic solid.[4] As in the case of bubbles, in this problem there are also three branches of stationary solutions when the Reynolds number is sufficiently high, (see Figure 1 (b)). For both problems, the method not only allows to study these bifurcations but also to determine the global stability of the different branches of the stationary solutions found.

References

[1] M.A. Herrada, JM Montanero. *A numerical method to study the dynamics of capillary fluid systems*, Journal of Computational Physics **230**, 1939-1955 (2016)
[2] Examples of JAM codes can be found at https://github.com/miguelherrada/JAM.
[3] M. Herrada, Y. Yu, H. Stone. Global stability analysis of bubbles rising in a vertical capillary with an external flow. Journal of Fluid Mechanics,**958**, A45. (2023)
[4] M. Herrada, S. Blanco-Trejo, J. Eggers, P. Stewart . *Global stability analysis of flexible channel flow with a hyperelastic wall.* Journal of Fluid Mechanics, **934**, A28. (2022)

Tu056

DOES THE VAN DER WAALS FORCE PLAY A PART IN EVAPORATION?

Eugene Benilov[1]
[1]*Department of Mathematics and Statistics, University of Limerick, Limerick, Ireland*

Keywords:evaporation

Abstract

It is argued that the van der Waals force exerted by the liquid and vapor/air on the molecules escaping from one phase into the other affects strongly the characteristics of evaporation. This is shown using two distinct descriptions of the van der Waals force: the Vlasov and diffuse-interface models [1,2], each of which is applied to two distinct settings: a liquid evaporating into its vapor and that evaporating into air (in all cases, the vapor-to-liquid density ratio is small). For the former setting, the results are consistent with the Hertz–Knudsen Law (HKL), but the evaporation/condensation probability is very small (in the classical HKL, it is supposed to be order one). For the latter setting, the dependence of the evaporation rate on the difference between the saturated vapor pressure and its actual value is shown to be nonlinear (whereas the classical HKL predicts a linear dependence). The difference between the two settings indicates that the van der Waals force exerted by the air affects strongly evaporation (contrary to the general belief that the ambient gas is unimportant).

References

[1] E. S. Benilov, *The multicomponent diffuse-interface model and its application to water/air interfaces.* J. Fluid Mech. **954**, A41 (2023).
[2] E. S. Benilov, *Does Maxwell's hypothesis of air saturation near the surface of evaporating liquid hold at all spatial scales?* J. Fluid Mech. **971**, A20 (2023).

Tu057

FLOW STABILITY IN SHALLOW DROPLETS SUBJECT TO LOCALIZED HEATING OF THE BOTTOM PLATE

Khang Ee Pang[1], Charles Cuvillier[2], Yutaku Kita[3,4] & Lennon Ó Náraigh[1]
[1]*School of Mathematics and Statistics, University College Dublin, Dublin, Ireland*
[2]*MA Applied Mathematics Department, ENSTA Paris, Paris, France*
[3]*Department of Engineering, King's College London, London, United Kingdom*
[4]*International Institute for Carbon-Neutral Energy Research, Kyushu University, Fukuoka, Japan*

Abstract We investigate theoretically the stability of thermo-capillary convection within a droplet in the lubrication theory when subject to localized heating from below. (Keywords: Marangoni flow, lubrication theory, stability analysis).

When the surface tension of a droplet or a film varies inhomogeneously, surface-tension gradient occur, which induces a flow inside the fluid. Thermo-capillary flows induced by localized heating have been observed experimentally in millimeter-sized water droplets [1,2]. In particular, these experiments reveal that when such droplets are heated from below by a localized heat source targeted at the droplet center, a twin vortex pair perpendicular to the substrate is observed. The aim of this work is to obtain some theoretical understanding to explain the onset of such vortices. A schematic description of the vortex pair is shown in Figure 1.

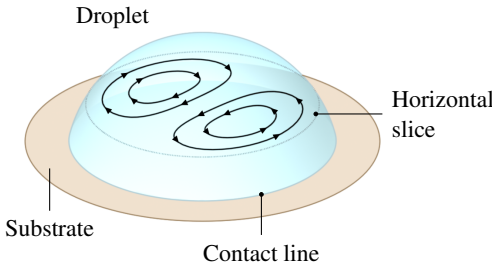

Figure 1. Schematic description of the experimentally observed flow in a locally heated sessile droplet.

Lubrication theory is a standard tool in analysing thermo-capillary flows in thin films and droplets – provided the latter possesses a sufficiently small equilibrium contact angle [2]. The resulting (non-dimensionalized) thin-film equation is given by

$$\partial_t h + \nabla \cdot \left[\tfrac{1}{2}h^2\nabla\gamma - \tfrac{1}{3}h^3\nabla\left(-\nabla^2 h + \phi\right)\right] = 0, \tag{1}$$

where ϕ is the potential of any external conservative forces and the surface tension γ is modelled as a linear function of the temperature at the droplet's interface.

We solve various forms of Eq. (1) numerically to investigate mechanisms by which the axisymmetry of the time-independent base state may be lost. We use a shooting method to compute the axisymmetric base state and an eigenvalue analysis to study the linear stability of the axisymmetric base state with respect to small perturbations. The linear stability analysis reveals that the axisymmetric base state is stable in all the cases we tested. In other words, the onset of the twin vortex pair *cannot* be explained by hydrodynamic instability in the lubrication theory. The stability of the base state is verified using a separate transient simulation in three dimensions with the base state solution as the initial condition. As such, we also investigate other mechanisms for the onset of such vorticies – namely a small perturbation of the heating location away from the droplet center, which reveals that such a setup could produce a twin vortex pair in the droplet. Furthermore, the vortices persist when the contact line is pinned. These findings are consistent with experimental studies of locally heated sessile droplets.

References

[1] Kita Y., Askounis A., Kohno M., Takata Y., Kim J., and Sefiane K.: Induction of Marangoni convection in pure water drops. *Appl. Phys. Lett.* **109**(17):171602, 2016.
[2] Askounis A., Kita Y., Kohno M., Takata Y., Koutsos V., and Sefiane K.: Influence of Local Heating on Marangoni Flows and Evaporation Kinetics of Pure Water Drops. *Langmuir* **33**(23):5666-5674, 2017.
[3] Oron A., Davis S.H., and Bankoff S.G.: Long-scale evolution of thin liquid films. *Rev. Mod. Phys.* **69**(3):931–980, 1997.
[4] Ehrhard P., and Davis S.H.: Non-isothermal spreading of liquid drops on horizontal plates. *J. Fluid Mech.* **229**:365–388, 1991.

Tu058

Experimental study of thermocapillarity–induced deformation of evaporating films on structured copper surfaces

Robin Behle, Peter Stephan & Tatiana Gambaryan-Roisman
Institute for Technical Thermodynamics, Technical University of Darmstadt, Darmstadt, Germany

Keywords: Thin films, Marangoni convection, long-wave theory, thermocapillarity, evaporation

Abstract

Thin liquid films play a crucial role in energy and chemical technology as they facilitate heat dissipation through evaporation. These films play an important role in cooling systems used in terrestrial and extraterrestrial environments that require high heat transfer rates. The determining factor that influences the behavior of thin films on heated surfaces is the Marangoni effect, which arises from variations in surface tension. This phenomenon not only enhances convective heat transport but also carries the risk of liquid film rupture, leading to the formation of dry patches and decreased heat transfer efficiency. Theoretical and numerical studies indicate that using surfaces with topography can induce Marangoni stresses, allowing for better control of the flow pattern, liquid topology and heat transfer.
In the present study, we experimentally investigated the thermocapillarity-induced deformation and rupture of a thin liquid film on a topographically structured surface. The setup includes a copper substrate with sinusoidal grooves, placed in a temperature-controlled test cell. The wavelength of the topography is much larger than its amplitude. In each experimental run, a thin liquid film of the fluorinated fluid HFE-7100 is deposited on the substrate, and its evolution and deformation is measured using a chromatic confocal line sensor. The data analysis includes the evaluation of the characteristics of the long-wave Marangoni-driven film deformation and the determination of the evaporation rate by measuring the pressure evolution in the cell.
Two series of experiments were carried out: one in a closed isothermal cell with variable air pressure and initial vapor concentration and another in an open cell with a heated substrate. In the first series, the temperature difference between the substrate and the liquid-gas interface arises due to the evaporative cooling of the interface. In the second series, the liquid-gas interface is cooled additionally by the ambient air. In both series of experiment, a controlled film deformation occurred due to thermocapillary stresses caused by the non-uniform temperature at the liquid-gas interface. The film flow resulted in localized thinning over crests and thickening over valleys of grooves, which is consistent with the predictions of the long-wave theory [1]. Fig. 1 illustrates the deformation profiles of the liquid film in the open cell at different temperature differences between the substrate and the ambient gas. It shows that the surface deformation increases with rising temperature difference.

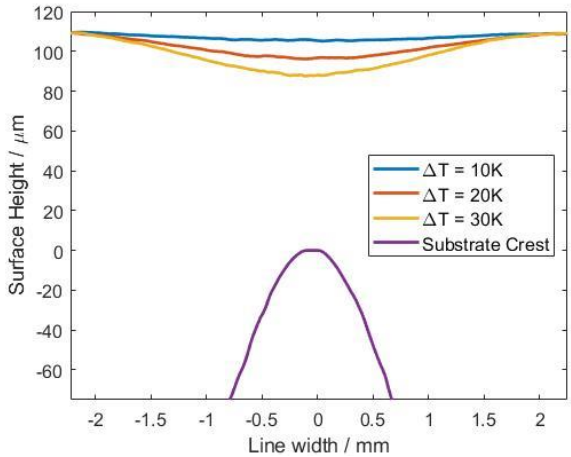

Figure 1. Liquid surface deformation over substrate crest. Illustrated deformation at temperature differences ΔT=10K,20K,30K between substrate and cell.

This work was supported by the German Aerospace Center (DLR) in the framework of the "Verständnis und Beeinflussung von Marangoni-Strömungen und Transportprozessen unter μ-g Bedingungen: "Marangoni in Films II"" project, grant no. 50WM2353.

References

[1] A. Bender, P. Stephan and T. Gambaryan-Roisman, *Numerical investigation of the evolution and breakup of an evaporating liquid film on a structured wall,* Int. J. Heat Fluid Flow 70, 104-113 (2018)

Tu059

Evaporation-induced translation of Multiple Binary Droplets

Debarshi Debnath[1], Anna Malachtari[2], George Karapetsas[2], Daniel Orejon[1], Khellil Sefiane[1], Alidad Amirfazli[3] and Prashant Valluri[1]

[1]*Institute for Multiscale Thermofluids, School of Engineering, University of Edinburgh, Edinburgh EH9 3FB, UK.*
[2]*Department of Chemical Engineering, Aristotle University of Thessaloniki, Thessaloniki.*
[3]*Department of Mechanical Engineering, York University, Toronto.*

Keywords: *Evaporation, sessile droplets, Binary mixture*

Abstract

Evaporation of multiple sessile droplets is a complex physical scenario due to their dynamic interaction through the vapour phase[1]. In situations when such evaporating droplets comprise a binary mixture, their interaction becomes more complex due to the inclusion of solutal Marangoni[2]. The physical understanding of such instances is extremely important for many crucial applications ranging from inkjet printing and spray cooling[3] to disease diagnosis and DNA chip manufacturing[4]. We propose a lubrication theory-based finite element model for two evaporating sessile drops comprising a binary mixture on a heated surface. We consider a diffusion-limited evaporation regime for thin droplets in the presence of a pre-cursor film. We consider that the liquid components are ideally mixed and that both components are volatile. The net surface tension is taken as a linear function of both temperature and concentration. Further, we also solve for the vapour concentration for both the volatile components in the presence of air in 2D using the standard diffusion equation. Our solutions for two adjacent droplets comprising the same binary mixture compositions demonstrate attraction, coalescence, and repulsion between the droplets as a function of thermal and solutal Marangoni. One such instant of attraction between two binary drops (water-morpholine mixture) is demonstrated in Fig. 1, as obtained from the model. In addition, we also performed experiments with water-morpholine drops to physically demonstrate the predictions from our model as shown in Fig. 2.

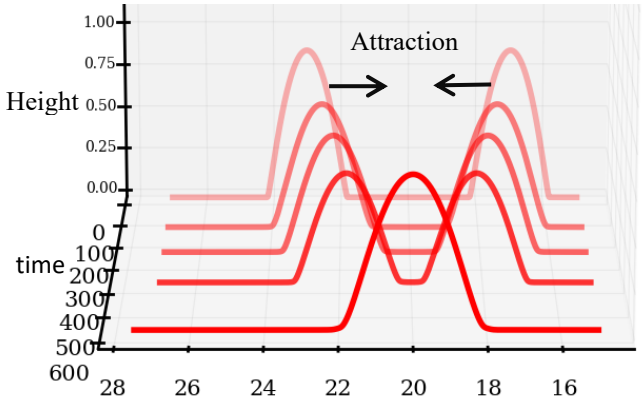

Fig. (1) Attraction of two binary drops (50% Water -Morpholine mixture) observed from the model.

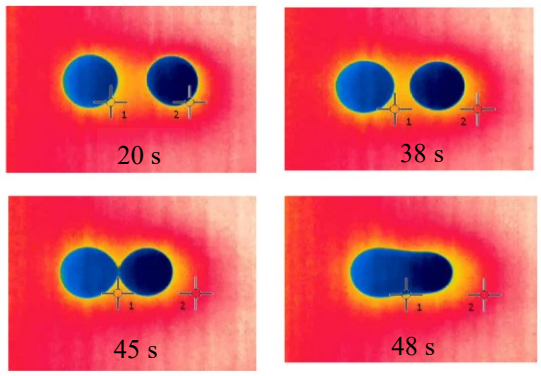

Fig. (2) Experimental observation for Attraction of two binary drops (50% Water -Morpholine mixture).

References :

[1]Wray, A. W., Duffy, B. R., & Wilson, S. K. (2020). Competitive evaporation of multiple sessile droplets. *Journal of Fluid Mechanics*, *884*, A45.

[2]Williams, A. G. L., Karapetsas, G., Mamalis, D., Sefiane, K., Matar, O. K., & Valluri, P. (2021). Spreading and retraction dynamics of sessile evaporating droplets comprising volatile binary mixtures. *Journal of Fluid Mechanics*, *907*, A22.

[3]Brutin, D., Sobac, B., Loquet, B., & Sampol, J. (2011). Pattern formation in drying drops of blood. *Journal of fluid mechanics*, *667*, 85-95.

[4]Kim, J. (2007). Spray cooling heat transfer: The state of the art. *International Journal of Heat and Fluid Flow*, *28*(4), 753-767.

EVAPORATIVE BEHAVIOR OF LIQUID-LIQUID PHASE SEPARATED ALCOHOL DROPLETS

Jorge Ahumada Lazo[1], Ruey-Hung Chen[2]
[1]*Department of Mechanical Engineering, City College of New York, New York, U.S.A.*
[2]*Department of Mechanical Engineering, University of Maryland Baltimore County, Baltimore, U.S.A.*

Keywords: Alcohol droplet; Electrodynamic balance; Liquid-liquid phase separation; Hygroscopy; Evaporation behavior

Abstract

The evaporation dynamics of single charged droplets of short-chain alcohols, suspended in the air by means of an electrodynamic balance are investigated as reported in [1]. The droplets evaporate into an uncontrolled environment, with relative humidity (RH) varying between 13% and 63%. Condensation of water from the ambient air onto the evaporating droplet results from evaporative cooling and droplet evaporation becomes that of a multi-component system [2, 3]. Photographs reveal a liquid-liquid phase separation inside the droplet, as shown in Fig. 1. Small nucleating sites appear, which later grow and merge until a single pocket of phase separation is formed. Two modes of phase separation were identified: enclosed-phase (at low RH, < 40% for ethanol) and Janus drop (RH > 40%). Each mode of separation exhibited a distinct evaporation behavior (observed in plots of d^2 in Fig. 1). In enclosed-phase separation, the evaporation rate constant (K) gradually decreases until evaporation stops completely (as marked by the red frame in Fig. 1). Janus drops have a period of water-dominated evaporation ($K_{water} < K_{ethanol}$) prior to the cease of evaporation. The cease of evaporation is explained by a combination of the charge-dipole effect described in [4] and a reduced surface activity of the droplet due to Raoult's law. These results were consistent with varying values of RH and were observed in five different alcohols. Similar observations on liquid-liquid phase separation and its de-mixing dynamics have been recently reported in [5] for levitated droplets of triethylene glycol and ammonium sulfate.

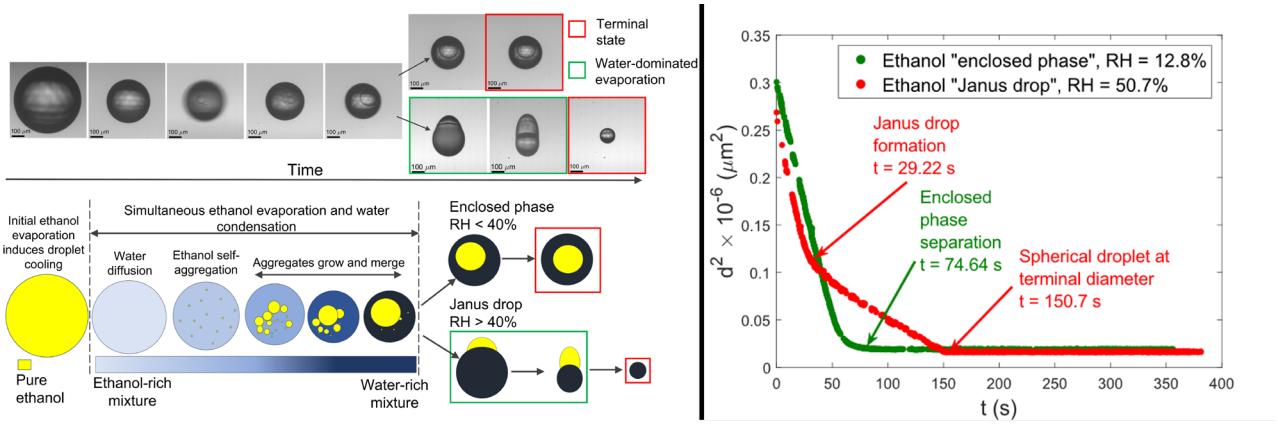

Figure 1. Photographic images of water condensation and phase separation in an evaporating droplet of ethanol, with their corresponding schematic illustration. The separated phase of ethanol either remains enclosed within a water-rich phase or migrates to the surface of the droplet forming a Janus drop (enclosed by green frames). Plots of d^2 show the evaporation behavior of both modes of separation.

References

[1] J.A. Ahumada Lazo, R.-H. Chen, *Evaporation of charged alcohol droplets suspended by electrodynamic balance*, Intl. J. of Heat and Mass Transf. **209**, 124118 (2023).
[2] Y. Kita, Y. Okauchi, Y. Fukatani, D. Orejon, M. Kohno, Y. Takata, K. Sefiane, *Quantifying vapor transfer into evaporating ethanol drops in a humid atmosphere,* Phys.Chem. Chem. Phys **20**, 19430 (2018).
[3] F.K.A. Gregson, M. Ordoubadi, R.E.H. Miles, A.E. Haddrell, D. Barona, D. Lewis, T. Church, R. Vehring, J.P. Reid, *Studies of competing evaporation rates of multiple volatile components from a single binary-component aerosol droplet*, Phys. Chem. Chem. Phys. **21,** 9709 (2019).
[4] J.K. Nielsen, C. Maus, D. Rzesanke, T. Leisner, *Charge induced stability of water droplets in subsaturated environment*, Atmos. Chem. Phys. **11**, 2031 (2011).
[5] J.M. Choczynski, B. Shokoor, J. Salazar, A. Zuend, J.F. Davies, *Probing the evaporation dynamics of semi-volatile organic compounds to reveal the thermodynamics of liquid-liquid phase separated aerosol*, Chemical Sci. DOI:10.1039/D3SC05164A (2024).

Tu061

STABILITY ANALYSIS OF DRYOUT INCEPTION FOR BOILING CO_2

Giulio Cantini[1,2], Giuseppe Arnone[3], Florinda Capone[3], Jacopo Gianfrani[4]& Mauro Carnevale[1,2]
[1]*Department of Mechanical Engineering, University of Bath, Bath, United Kingdom*
[2]*CERN, Geneva, Switzerland*
[3]*Dipartimento di Matematica e Applicazioni 'R.Caccioppoli', Universit'a degli Studi di Napoli Federico II*
[4]*Coventry University, Priory Street, Coventry, United Kingdom*

Keywords: Dryout, Boiling flow, Annular flow, Stability analysis, Small diameter evaporators

Abstract
Precision in forecasting dryout conditions is vital for optimizing the design of evaporators in cooling systems, particularly those with small-diameter evaporators used for Silicon detector cooling. In situations where there is a specified heat flux at the wall, the occurrence of dryout conditions can result in a sudden decline in the Heat Transfer Coefficient (HTC). The use of saturated CO_2 in such scenarios introduces uncertainties, particularly in relation to dryout prediction, thereby impacting the overall design process.
The vapor quality at dryout (x_{dry}) for saturated CO_2 varies based on mass flux and displays two distinct behaviors, each of them identifying a specific regime:

- **Regime** δ^+: x_{dry} increases with rising mass flux G, $\frac{\partial x_{dry}}{\partial G} > 0$.
- **Regime** δ^-: x_{dry} decreases with increasing mass flux G, $\frac{\partial x_{dry}}{\partial G} < 0$.

In contrast with δ^- regime, a gap in the current open literature has been identified in describing physical mechanism withstanding δ^+ regime. δ^+ regime can be observed typically for low heat flux and low saturation temperature. Under such conditions, in contrast to δ^- regime, the surface tension forces are no longer negligible compared to shear stress and buoyancy and the liquid-vapour interface in annular flow is assumed as smooth. The analysis of such a behaviour is so treated as a stability eigenvalue problem. Assuming a two-phase, two-dimensional annular flow with a smooth interface (Figure 1a), a model is constructed by solving two coupled Orr-Sommerfeld equations, one for each phase. This involves addressing 8 boundary conditions: 2 at the pipe axis, 2 at the wall, and 4 at the interface. A dimensional analysis of the equations is performed, obtaining qualitative trends based on the dimensionless parameters of the set of equations and boundary conditions. Based on such analysis a correlation is defined and applied to In-house experimental data and extended to available literature data (Figure 1b).

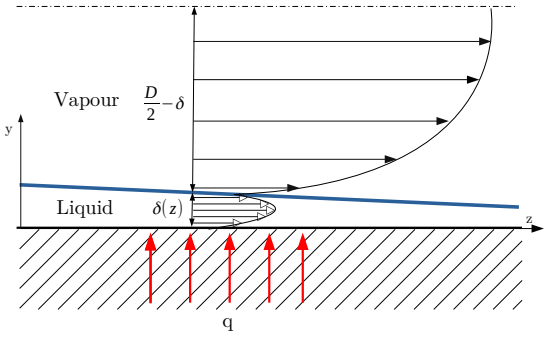

(a) Schematic of annular flow with phase change

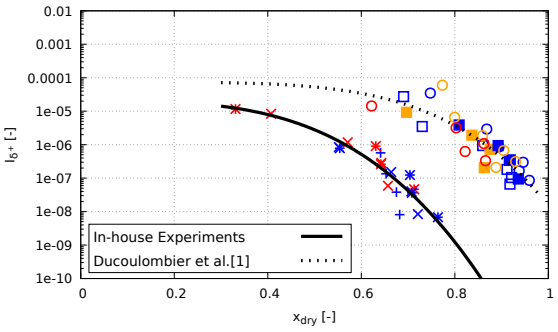

(b) Experimental data comparison with dimensionless parameter obtained from the model

Figure 1

References

[1] Ducoulombier, M and Colasson, S and Bonjour, J and Haberschill, P *Carbon dioxide flow boiling in a single microchannel–Part II: Heat transfer* Experimental Thermal and Fluid Science, **35**, 4, 597-611, (2011)

Tu062

THE IMPACT OF EVAPORATION REGIME ON THE STABILITY OF VOLATILE LIQUID FILMS.

Omair A. A. Mohamed[1] & Luca Biancofiore[1,2]
[1]*Department of Mechanical Engineering, Bilkent University, Ankara, Türkiye,*
[2]*Department of Industrial Engineering, Information and Economics, University of L'Aquila, L'Aquila, Italy.*

Abstract Stability analysis of an evaporating liquid film in different evaporation regimes.

Evaporating liquid films play a crucial role in various industries, including distillation, combustion, cooling processes, and chemical synthesis. In many cases, the performance of these systems depends directly on the evolution of the liquid film's interface, and therefore, gaining a better understanding of this evolution can result in substantial benefits.

Therefore, we consider a thin volatile liquid film flowing over a hot solid surface, where we focus on the role of the evaporation regime on the stability of the film. On the other hand, we utilize a modified version of Sultan *et al.*'s [1] general evaporation model and, thus, include in our analysis a variety of evaporation states ranging from (i) transfer-rate-limited evaporation where vapor diffusion is completely absent, to (ii) diffusion-limited evaporation which is completely dominated by vapor diffusion effects. Notably, the transfer-rate limit of this evaporation model corresponds to a one-sided system after some appropriate rescaling. In our formulation we (i) combine a Benney-type lubrication equation for the liquid film with a modified version of Sultan *et al.*'s evaporation model, and (ii) apply linear stability theory to derive a dispersion relationship relating the wavenumber and the angular frequency, which is used to examine the stability of the film.

Our investigation uncovers the important effect the evaporation regime has on the stability of the film. We show that the when vapor diffusion is considered, the thermocapillary instability results from a combination of two distinct phenomena: (i) the conduction of heat from the wall across the bulk of the film and (ii) the latent cooling at the liquid interface. The distinct contributions of these two components to perturbation growth are combined into a single thermocapillary term in the transfer-rate-limited case, representing the exclusive dependence of both the temperature gradient through the film and the vapor flux at the interface on film height. On the contrary, in the diffusion-limited case, the thermocapillary instability is represented by two separate terms since the temperature gradient relies on the film height while the vapor flux now depends on the vapor density gradient.

Moreover, when molecular dynamics play the larger role in driving the evaporation process, heat conduction across the bulk and the latent cooling at the interface compete against each other yielding a relatively weaker instability. However, in the case where vapor diffusion has the greater influence, the two phenomena are positively reinforcing, resulting in a significantly stronger instability. Notably, we find that when evaporation is dominated by the vapor diffusion process, the latent cooling at the interface can cause a thermocapillary instability that would be absent under conditions where the evaporation process is transfer-rate-limited. Finally, we find that this particular form of the thermocapillary instability competes against vapor recoil, as opposed to the thermocapillary instability driven by purely heat conduction across the bulk of the liquid film, which is on the contrary reinforced by vapor recoil.

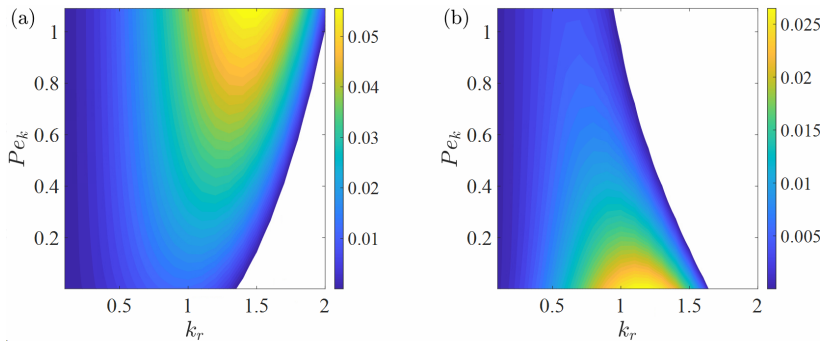

Figure 1. Contour plots of the temporal growth rate ω_i in the (Pe_k, k) parameter space for two different values of the vapor recoil parameter V_r, where Pe_k is a kinetic Péclet number determining the evaporation regime, and k is the dimensionless wave number. (a) V_r=0.5. (b) V_r=1.5. White regions correspond to stable flow. Notice the suppression of the thermocapillary instability at $Pe_k \approx 1$ in figure (b), due to the increased stabilizing action of vapor recoil.

References

[1] E. Sultan, A. Boudaoud, and M. B. Amar, "Evaporation of a thin film: diffusion of the vapour and Marangoni instabilities," *J. Fluid. Mech.*, vol. 543, pp. 183–202, 2005.

Tu063

DROPLET EVAPORATION AND THE STICK-SLIP MODES TRIFURCATION

Khaloud Moosa Al Balushi[1,2], Gail Duursma[2], Prashant Valluri[2], Khellil Sefiane[2] & Daniel Orejon[2,3]
[1]*College of Engineering and Technology, The University of Technology and Applied Sciences, Suhar 311, Oman*
[2]*School of Engineering, Institute for Multiscale Thermofluids, The University of Edinburgh, Edinburgh EH9 3FD, Scotland, UK*
[3]*International Institute for Carbon-Neutral Energy Research (WPI-I2CNER), Kyushu University, 744 Motooka, Nishi-ku, Fukuoka 819-0395, Japan*

Keywords: Droplet Evaporation, Contact Line Dynamics, Mixed mode, Stick-Slip, Structured Surfaces

Abstract

It was almost 3 decades ago when the stick-slip motion of the contact line was theoretically postulated by Martin Shanahan aiming to provide the reasons and mechanisms behind the observed contact angle hysteresis on hydrophobic solid surfaces [1]. Since then, several research works have been able to impose such stick-slip motion of the contact line following the instability or out of equilibrium configuration as a consequence of evaporation in nanoparticle-laden fluids [2] and/or structured surfaces [3]. On one hand, the presence of particles droplet evaporation can lead to stick-slip behaviour as the particles deposit at the contact line hindering its receding motion until the droplet gains enough energy for the jump to ensue, which can be a rather stochastic process [2]. On the other hand, in the presence of structures a more deterministic stick-slip behaviour can be imposed, which is governed by the initial wetting behaviour [4] and by the size and spacing of the structures [3]. Besides the classic evaporation modes earlier observed on structured surfaces such as the constant contact radius (CCR) and the stick-slip modes, this latter occurring within a specific range of contact angles, in this work we report on two further modes coined as the decreasing contact angle mixed stick-slip (↓MSS) and increasing contact angle mixed stick-slip mode (↑MSS) modes, as shown in Figure 1. The ↓MSS mainly takes place in the last stages of droplet evaporation, similar to the mixed mode taking place on smooth counterparts where both contact angle and contact radius decrease in time. However, the presence of structures additionally forces the contact line to *jump*, i.e., undergo a stick-slip behaviour with the associated decrease in the contact angle. Moreover, for binary mixtures with different volatilities on structured surfaces, as the most volatile and lower surface tension component evaporates preferentially, causing increase in surface tension as the most volatile and lower surface tension fluid evaporates, the ↑MSS ensues as the surface tension of the droplet increases. Hence two novel mixed stick-slip evaporation regimes added to the traditional stick-slip mode proposes the potential for trifurcation following the instability arising from pinning and evaporation function of the surface and the fluid, which allow for the accurate control of the contact line dynamics.

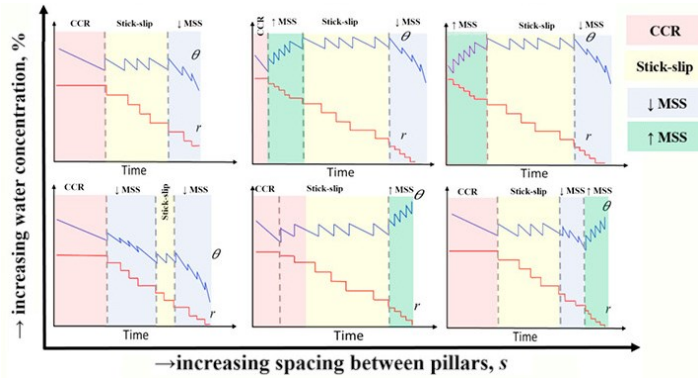

Figure 1. Schematics of the different droplet evaporation behaviour in terms of contact angle and base radius versus normalised time for binary mixtures on hydrophobic microstructured surfaces as: constant contact radius (CCR), stick-slip, decreasing contact angle mixed stick-slip (↓MSS) and increasing contact angle mixed stick-slip mode (↑MSS) modes [3].

References

[1] M.E.R. Shanahan, *Simple Theory of "Stick-Slip" Wetting Hysteresis*, Langmuir **11**, 1041-1043 (1995).
[2] D. Orejon, K. Sefiane, M.E.R. Shanahn, *Stick–Slip of Evaporating Droplets: Substrate Hydrophobicity and Nanoparticle Concentration*, Langmuir **27**, 12834-12843 (2011).
[3] K.M. Al Balushi, G. Duursma, P. Valluri, K. Sefiane, D. Orejon, *Binary Mixture Droplet Evaporation on Microstructured Decorated Surfaces and the Mixed Stick–Slip Modes*, Langmuir **39**, 8323-8338 (2023).
[4] K.M. Al Balushi, K. Sefiane, D. Orejon, *Binary mixture droplet wetting on micro-structure decorated surfaces*, Journal of Colloids and Interface Science **612**, 792-805 (2022).

Field-Induced Capillary Condensation: Surface Diffusion or Spontaneous Nucleation?

Ali Afzalifar[1] & Robin H. A. Ras[1,2]
[1]*Department of Applied Physics, Aalto University School of Science, Aalto University, Espoo, Finland*
[2]*Center of Excellence in Life-Inspired Hybrid Materials (LIBER), Aalto University, Espoo, Finland*

Keywords: External electric field; Capillary condensation; Surface diffusion; Water adsorption

Abstract

The effect of the electric field on nucleation was hotly debated in late 20th century. This effect is of intrinsic interest to the research communities of physical chemists and aerosol scientists who made the main contributions to the understanding of this effect. With recourse to the thermodynamic aspect of classical nucleation theory, one can show that the internal or external electric field reduces the Gibbs free-energy barrier to nucleation, subject to the condition that the electric permittivity of the new phase is larger than that of the old phase. [1] Therefore, the relative permittivity of liquid water with respect to its vapor suggests that, in the case of water condensation, droplet nucleation on ions or charged particles is enhanced. A large body of empirical evidence supports the existence of such enhancement; for instance, enhanced formation of aerosols and raindrops on particles charged by cosmic radiation [2] and experimental studies on ion-induced nucleation of supersaturated vapor of different substances [3]. However, in the case of the external electric field, existing studies are relatively scarce, and the experimental outcomes are sometimes contradictory.

Our work theoretically and experimentally investigates the effects of an external electric field (up to 10^9 V/m) capillary condensation of water in nano- and sub-nanoscopic confinement. Here we report the quantitative observation on the effect of external electric field nucleation and growth of liquid water meniscus in confinements between two electrodes with a distance in range of <1-100 nm. We discuss the thermodynamics and kinetics of meniscus formation separately to highlight the importance of adsorbed water layer on the substrate in the course of water liquid meniscus formation. We show that the diffusion of water molecules towards the meniscus is strongly enhanced by means of the electric field between tip and substrate. And, the water films (on the two electrode surfaces) deform under the effect of the electric filed and bulge out towards one another forming the water meniscus. In fact, the enhanced surface diffusion along with the deformation of water films constitute the driving force for the meniscus formation as opposed to the current consensus in literature that the meniscus formation is owing to reduction of the free energy barrier to the nucleation by means of the electric field.

References

[1] D. Kashchiev, "Nucleation," Elsevier, **2000**.
[2] A. Hirsikko, T. Nieminen, S. Gagné, K. Lehtipalo, H. E. Manninen, M. Ehn, M. Hõrrak and U. Kerminen, "Atmospheric ions and nucleation: a review of observations," *Atmospheric Chemistry and Physics,* **2011**, 11(2), 767-798.
[3] A. Laaksonen, V. Talanquer and D. W. Oxtoby, "Nucleation: Measurements, theory, and atmospheric applications," *Annual Review of Physical Chemistry*, **1995**, 46(1), 489-524.

Tu075

OPTIMUM VISCOSITY RATIO FOR ENHANCED INSTABILITY AND MIXING IN LAYERED CHANNEL FLOWS

Priyanka Banga[1], Surya Narayan Maharana[2] & Manoranjan Mishra[1]
[1]*Department of Mathematics, Indian Institute of Technology Ropar,*
[2]*Nonlinear Physical Chemistry Unit,Université libre de Bruxelles, 1050*

Abstract When two miscible fluids with different viscosities in a layered manner are sheared, it leads to interfacial instabilities. This scenario of varying viscosity within a flow is quite common in the petroleum industry, especially in pipeline transportation. The viscosity gradient between two fluids causes a favorable difference in velocity, allowing the less viscous fluid to flow faster and pull filaments of the more viscous fluid, resulting in the formation of Kelvin-Helmholtz instability or ligament wave-like structures. Understanding these instabilities is paramount for optimizing fluid transport and mixing in diverse industries, given their significant impact on the efficiency of transportation and mixing processes. In the case of a two-layer viscosity-stratified channel flow, previous studies [1], [2] have indicated that the growth of these instabilities is directly related to the increasing viscosity ratio between the upper and lower layers of fluid. However, instead of being a straightforward, monotonic progression, we have found that the viscosity difference between the fluids and instability growth actually follows a non-monotonic pattern [3]. Figure 1 illustrates concentration plots at a specific time where the red represents the more viscous fluid, the blue represents the less viscous one, and the logarithm of the viscosity ratio is denoted as m . These concentration plots clearly show that the flow becomes more unstable for intermediate values of m. In our study, we have also identified the existence of an optimal viscosity ratio that corresponds to the maximum instability and, consequently, the highest level of mixing in the flow. In the presentation, I will explain the instability growth mechanism and present various phase diagrams that characterize flow stability.

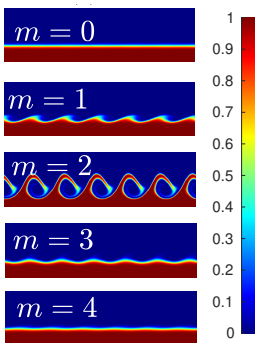

Figure 1. Nonlinear simulation results depicting spatial variations in concentration at $t = 10$ for different m.

References

[1] P. Ern, and F. Charru, and P. Luchini, *Stability analysis of a shear flow with strongly stratified viscosity*, J. Fluid Mech. **496**, 295-312 (2003).
[2] K.C. Sahu, and R. Govindarajan, *Linear stability analysis and direct numerical simulation of two-layer channel flow.*, J. Fluid Mech. **798**, 889–909 (2016).
[3] P.Banga, and S.N. Maharana, and M. Mishra, *Unraveling instabilities and mixing behavior in two-layered flows: A quest for the optimum viscosity ratio*, Phys. Fluids **35**, 082116 (2023).

Tu076

INFLUENCE OF CAPILLARY INSTABILITY ON THE STRATIFIED LIQUID-LIQUID FLOW PATTERN TRANSITION

P. J. Miranda-Lugo, Jorge E. Arrollo-Caballero & O. M. H. Rodriguez
University of São Paulo (USP), São Carlos School of Engineering (EESC), Mechanical Engineering Department, Industrial Multiphase Flow Laboratory (LEMI), Av. Trab. São Carlense, 400 - Parque Arnold Schimidt, São Carlos - SP, 13566-590, Brazil.

Abstract Keywords: Capillary instability, Flow-pattern transition, Interface curvature, Oil-water flow, PIV-PLIF, Secondary flow.

The literature contains different theories explaining the stratified flow transition. One theory attributes such a transition to instabilities resulting from the temporal amplification of a disturbance wave at the interface between the phases [1]. Rodriguez and Castro [2] suggested that for high-viscosity ratio stratified flow, the observed interface's cross-section curvature is related to capillary instability, which effect is stronger at high water volumetric fractions. In such conditions, eddy structures associated with secondary flows may contribute to forming a concave interface at the flow's cross-section. However, to the best of the authors' knowledge, no experimental study quantifies those effects that can lead to the stratified flow transition. In this work, the effects of the destabilizing interfacial-tension term related to the interface's cross-section curvature and the secondary flow on the instability of a stratified oil-water pipe flow are studied using Planar Laser-Induced Fluorescence (PLIF) synchronized with 2D Particle Image Velocimetry (2D-PIV). Unlike most studies [2, 3, 4, 5, 6], mineral oil and water with low viscosity ratio of 1.44 are used. Velocity profiles, turbulence statistics, and geometrical parameters of the interfacial wave are measured at the longitudinal diametrical vertical plane, Fig. 1 (left). The interface's cross-section curvature is determined by a scanning algorithm that identifies the oil-water interface and fits a circle to it through the least-squares method. The variation of the fitted circles' radii at the interface's cross-section (R_2) as a function of oil and water superficial velocities for stable and unstable stratified flow conditions is presented in Fig. 1 (right). The results indicate that R_2 decreases as the water superficial velocity (J_w) increases while keeping the oil superficial velocity (J_o) constant. In other words, the interface's cross-section curvature ($1/R_2$) increases as the water holdup and turbulence increase, which was observed to have connection to increase of stratified flow instability and transition. Such preliminary result suggests that capillary instability may be strong enough to promote the transition from stratified to slug flow.

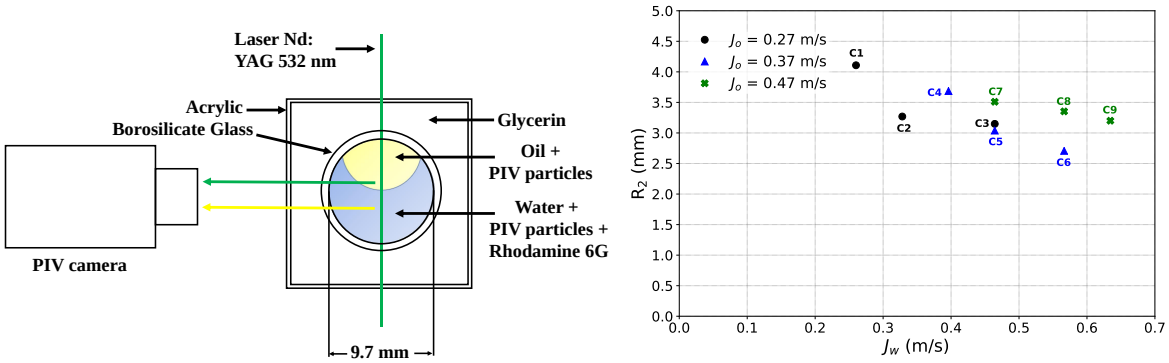

Figure 1. (Left) 2-D PIV-PLIF setup to study the stability of oil-water stratified flow and the interface shape in the longitudinal diametrical vertical plane, and (right) variation of the fitted circles' radii at the interface's cross-section (R_2) with the water superficial velocity (J_w) for different oil superficial velocities (J_o). The conditions C1, C2, C4, C5, C7, C8 represent stable stratified flows, while C3, C6 and C9 indicate unstable stratified flows.

References

[1] Wallis, G. B., One-dimensional two-phase flow, (1969).
[2] Rodriguez, O. M. and Castro, M. S., Interfacial-tension-force model for the wavy-stratified liquid–liquid flow pattern transition. International Journal of Multiphase Flow, **58**, 114–126 (2014).
[3] Barmak, I., Gelfgat, A., Vitoshkin, H., Ullmann, A., and Brauner, N., Stability of stratified two-phase flows in horizontal channels. Physics of Fluids, **28(4)**, 044101 (2016).
[4] Ibarra, R., Zadrazil, I., Matar, O. K., and Markides, C. N., Dynamics of liquid-liquid flows in horizontal pipes using simultaneous two-line planar laser-induced fluorescence and particle velocimetry. International Journal of Multiphase Flow, **101**, 47–63 (2018).
[5] Rodriguez, O.M. and Bannwart, A.C., Stability analysis of core-annular flow and neutral stability wave number., AIChE Journal, **54(1)**, 20–31 (2008).
[6] Castro, M.S., Pereira, C.C., Santos, J.N., Rodriguez, O.M.H., Geometrical and kinematic properties of interfacial waves in stratified oil water flow in inclined pipe. Exp. Therm. Fluid Sci. **37**, 171–178 (2012).

Tu077

A MULTIDIMENSIONAL EXAMINATION OF PHASE SEPARATION IN SINGLE-COMPONENT FLUIDS

Sandip Das[1] & Matan Mussel[1]

[1]*Department of Physics and Center for Biophysics and Quantitative Biology, University of Haifa, 199 Aba Khoushy Avenue, Haifa 3103301, Israel*

Abstract A thermodynamic instability in a homogeneous fluid can lead to spontaneous formation of distinct domains within the fluid. This process involves not only the spatial redistribution of fluid density but also transient exchanges of pressure, temperature, and energy. However, classical theoretical frameworks, such as the Ginzburg-Landau and Cahn-Hilliard models, lack incorporation of these essential thermodynamic aspects. To investigate the dynamics of multiple physical fields during phase separation, we numerically solve a two-dimensional van der Waals fluid model. Thermodynamic consistency is demonstrated by verifying the coexistence curve. While the equilibrium pressure remains similar across the unstable region of the isotherm, we demonstrate that the energy in the system depends on the initial density. Although the majority of energy is stored as heat at typical values of the heat capacity, high-density domains contain less specific energy compared to their low-density counterparts due to interparticle attraction. Consequently, the transition of low-density domains into high-density through the process of coalescence releases excess energy, which redistributes in the form of longitudinal waves and heat. We also highlight the role of parameters, such as heat capacity and thermal conductivity, in less intuitive phenomena, including elevated temperature fluctuations and memory preservation.

Keywords: Phase separation, Van der Waals fluid, Spinodal decomposition, Longitudinal waves

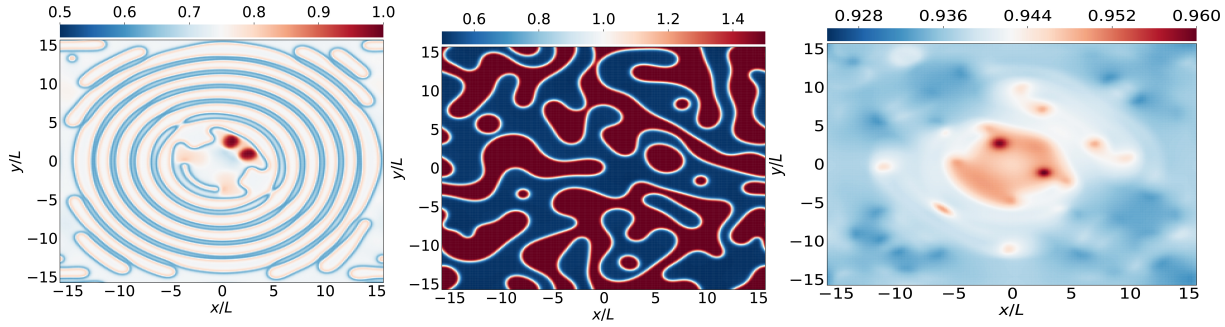

Figure 1. Snapshots capturing the $2D$ pressure, density, and temperature fields, respectively.

Tu078

PARTIAL ENCAPSULATION IN BINARY DROPLET COLLISIONS OF MISCIBLE LIQUIDS

Élfego Ruiz-Gutiérrez[1], Kenny Dalgarno[1] & Nilanjan Chakraborty[1]
[1]*Newcastle University, School of Engineering, Claremont Road, Newcastle upon Tyne, NE1 7RU, UK*

Abstract Partial encapsulation, binary droplet collision, convex hull, mixing, additive manufacturing, VoF method.

The study of binary droplet collisions is an active research topic that has gathered interest due to its complexity and industrial applications such as bioprinting. In this process, one liquid might encapsulate the other in different extents; see Fig. 1a. For immiscible liquids, the equilibrium configuration depends on the surface tensions and relative volumes of the liquid phases [1]. For miscible liquids, encapsulation for an equilibrium state does not exist as the system eventually becomes a homogeneous mixture. However, encapsulation can still be observed during the mixing process. In this work, we propose a way of quantifying partial encapsulation (see Fig. 1b). This is done by constructing the convex hull from the contact surface between the two liquids, that is, the smallest convex set that contains the contact surface [2]. We identify complete encapsulation when the convex hull contains one of the liquids and no encapsulation when the convex hull does not span out any volume. Therefore, we quantify partial encapsulation, $\mathcal{E} := v_i/V_i$, as the ratio of the volume that a liquid is captured by the convex hull, v_i and its total volume, V_i. Direct numerical simulations in the framework of the Volume-of-Fluid method are used to analyse the effects that the fluid properties, such as viscosity and surface tension, have on the extent of encapsulation.

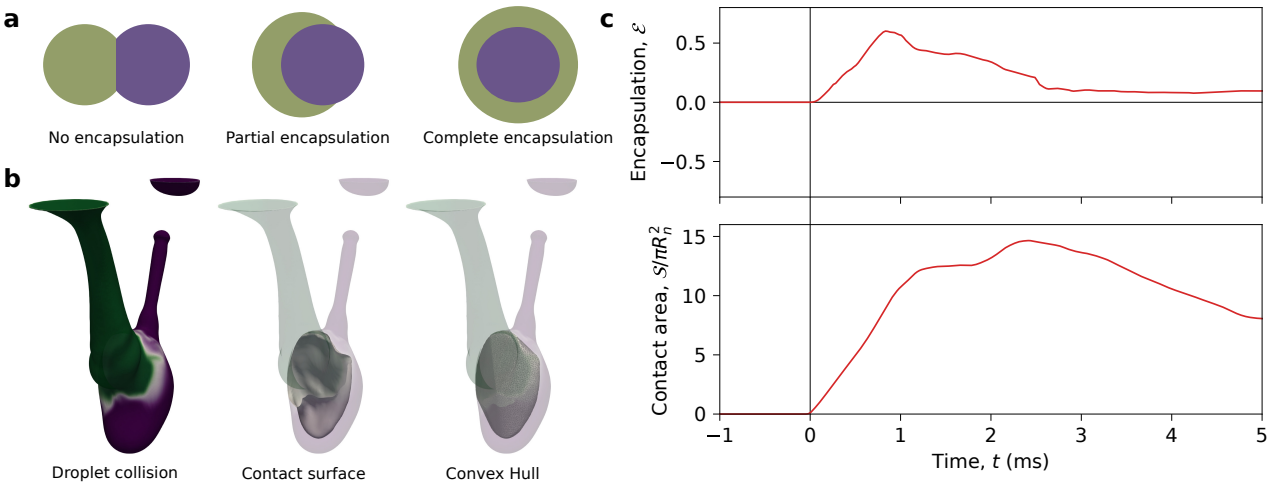

Figure 1. Encapsulation in binary droplet collision of miscible liquids. (**a**) Schematic representation of different states of encapsulation. (**b**) Snapshot at $0.5\,\mathrm{ms}$ after the contact between the two droplets. The first image shows the concentration of each liquid in colour-code of the liquid-gas interface, i.e., the green coloured liquid has a kinematic viscosity of $\nu_1 = 3.16 \times 10^{-6}\,\mathrm{m^2\,s^{-1}}$ and a surface tension of $\gamma_{01} = 62.6\,\mathrm{mN\,m^{-1}}$ and the purple liquid, $\nu_2 = 1 \times 10^{-6}\,\mathrm{m^2\,s^{-1}}$ and $\gamma_{02} = 72\,\mathrm{mN\,s^{-1}}$. The transition between the two liquids is the contact surface, show as the grey isosurface in the following snapshot. The convex hull, constructed from the points of the contact surface, is shown in the last snapshot. The partial volume of each liquid enclosed by the convex hull is used to quantify encapsulation. (**c**) The evolution of the encapsulation as a function of time and the evolution of the contact surface area is shown below. The time $t = 0\,\mathrm{ms}$ is set when the first contact between the two liquids occurs.

References

[1] C. Planchette, E. Lorenceau, G. Brenn; *Liquid encapsulation by binary collisions of immiscible liquid drops*, Colloids Surf. A Physicochem. Eng. Asp. **1**, 89–94 (2010)
[2] S. R. Lay, *Convex sets and their applications*, Courier Corporation, 2007

Tu079

Mitigation of generated air-entrainment from free surface vortices at pump suction using combined multipoint intakes and air separator system

Rahul Kumar Mondal[1], Debarshi Debnath[2] & Parmod Kumar[1]
[1] *School of Mechanical and Materials Engineering, Indian Institute of Technology Mandi, Kamand-175075, Himachal Pradesh, India*
[2]*School Of Engineering, The University Of Edinburgh, Scotland, United Kingdom*

Keywords: free vortex, air-entrainement, interfacial flows, multipoint intakes, air-separator system.

Abstract
This research paper proposes a way to prevent the entrainment of air into the pump associated with the free vortex. The generation of free vortices is always a serious concern for industrial and engineering applications e.g. sodium-cooled fast reactors (SFRs) in the nuclear industry and the thermal crisis caused by a rapid drop in the local heat transfer coefficient where safety is always the priority. Mondal and Kumar (2021) have developed an air separator system that is sufficiently capable of removing the entrained air associated with free vortices before reaching the pump suction. Mondal and Kumar (2022) have discussed the comprehensive investigation of vortex profiles inside the tank and corresponding entrainment patterns within the flow pipeline for a wide range of parametric conditions. Thakur et al. 2023, have numerically investigated stage 2 of vortex formation and focused on reducing its effects through the implementation and evaluation of multiple intakes. Stage 2 vortex is a long-elongated interface that resembles an inverted cone. In the present study, we are proposing a strategy for mitigating the undesired occurrence of pump intake vortex by combining multiple intakes and an air separator system. This combination provides pure liquid at the pump suction in the presence of both low and high-water submergence of the reservoir. The multiple intake concept is taken from parallel pipe connection where the rate of flow in the main pipe is equal to the sum of the rate of flow through its branch pipes. Decreased pressure inside water and increased local downward velocity are the main reasons for free surface vortex generation above drainpipe inlet. Froude number is one key factor for characterizing the strength of vortex formation where Froude number $\left(Fr = \frac{Inertia\ force}{Gravitational\ force} = \frac{V}{\sqrt{gH}}\right)$. Number of intakes increase cross-section area and decreases local downward velocity for same flow rate (Q = AV = $A_1V_1 + A_2V_2 + A_3V_3$ ....) equivalent to a single intake flow rate (Q = AV).
The study successfully demonstrates that the use of multiple intakes, while maintaining a constant flow rate, significantly reduces the velocity and Froude number, and subsequently decreases the strength of vortex formation. Figure 1 shows the schematic diagram of the experimental setup. Quantification of air is analyzed through air flow sensor and pressure drop within air separator gives the information of air entrance. Ansys fluent software is used to simulating the real-scale experiment. Simulation results will help in exploring the physics of reducing vortex strength using multiple intakes.

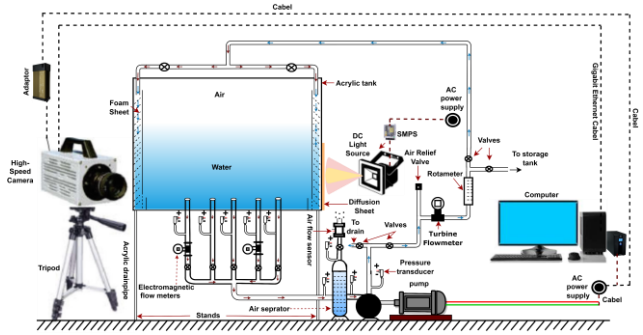

Figure 1. Schematic diagram of the experimental setup *x*.

References

[1] Kumar, P., and **Mondal, R.K**., System and method for separating air from air-liquid mixture, *Patent Application Number: 202111009994* & Patent Grant Number: 490294 (2021).
[2] **Mondal, R.K.**, and Kumar, P., Experimental study of entrained air-core structures induced by a pump intake vortex, Physics of Fluids, 34(5) (2022).
[3] Thakur, K., **Mondal, R. K.,** and Kumar, P., Numerical investigation of pump intake vortex suppression using multiple intakes, Proceedings of the 10th International and 50th National Conference on Fluid Mechanics and Fluid Power (FMFP), December 20-22, 2023, IIT Jodhpur, India.

Tu080

THE ROLE OF MARANGONI EFFECT ON THE NON-ISOTHERMAL FALLING FLUID FILM INSTABILITY

Ayhan Yiğit Özel[1], Christian Ruyer-Quil[2] & Luca Biancofiore[1,3]
[1] *Department of Mechanical Engineering Bilkent University 06800 Bilkent, Ankara, Turkey*
[2] *LOCIE, UMR 5271, CNRS, Universite Savoie Mont Blanc, Le Bourget-du-Lac, France*
[3] *Department of Industrial and Information Engineering and Economics, Università dell'Aquila, L'Aquila, Italy*

Abstract We analyze the nonlinear evolution due to the Marangoni effect of non-isothermal falling fluid films periodically forced at the inlet. (Marangoni effect, instability, nonlinear waves)

The Marangoni effect, resulting from surface tension variations induced by temperature changes along an inclined/vertical plane [1], imparts a peculiar dynamic to fluid film flows, forming roll waves. When an inclined plane non-isothermally heated from below is used, gravity and thermocapillarity will drive the fluid flow and cause a strong nonlinear wave evolution along the fluid film [1]. Moreover, if some forcing is applied at the inlet, the effect of thermocapillarity can be strengthened and, thus, intensify fluid flow instability. This phenomenon, in turn, can enhance the formation of the nonlinear waves within the fluid film flow.

For the analysis of nonlinear evolution of falling film flows, the non-isothermal falling film model proposed by Cellier and Ruyer-Quil is used [2]. This model enables adjustments to the Biot number Bi, which characterizes the ratio of surface convection to internal conduction, and the Peclet number Pe, which expresses the ratio of diffusive to advective transport, to attain desired values for the simulations. Moreover, the plane inclination angle θ, the Reynolds number Re, and the Weber number We, which expresses the ratio of inertial forces to surface tension forces, are all subject to modifications to tailor the flow model to specific conditions.

In Fig. 1, we show how the evolution of nonlinear waves changes for various Marangoni numbers Ma, which compares the relative effects of thermocapillarity and viscosity in fluid flows. By comparing the $Ma = 0$ case with the experimental results obtained by Liu and Gollub [3], we show that the equations used are in good agreement with the base case in which the thermocapillarity is disregarded (see Fig. 1a). The slight difference is rooted from the use of the non-isothermal falling film model that includes the Biot and Peclet numbers that are absent in the compared equations [2]. As the Marangoni number is increased up to 10, the maximum fluid film thickness reached for the waves heightens, increasing by 10% (see Fig. 1b). Furthermore, the enhanced nonlinear wave formation is evident as $Ma > 5$. Finally, we investigate the nonlinear evolution of the fluid film for large Peclet numbers.

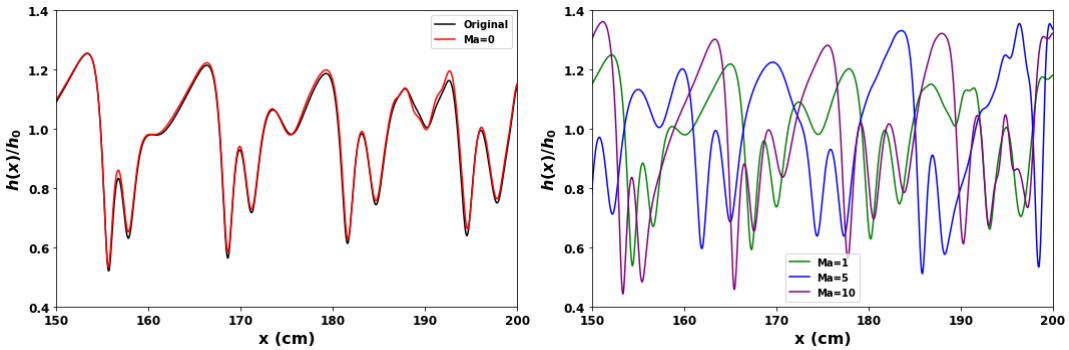

Figure 1. The evolution of nonlinear waves that are periodically forced at a frequency $f = 4.5Hz$ for $\theta = 6.4$, $Re = 29$, and $We = 35$. (a) Comparison of the $Ma = 0$ case with the original case [3]. (b) Comparison of the nonlinear wave evolution trend for varying Marangoni number. The simulations are conducted with $Bi = 0.1$ and $Pe = 0.01$.

References

[1] S. Kalliadasis, C. Ruyer-Quil, B. Scheid, M.G. Velarde, *Falling Liquid Films*, Applied Mathematical Sciences **176**, 9–13 (2012).
[2] N. Cellier, C. Ruyer-Quil, *A new family of reduced models for non-isothermal falling films*, International Journal of Heat and Mass Transfer
[3] J. Liu, J. P. Gollub , *Solitary wave dynamics of film flows*, Physics of Fluids **6**, 1702—1712 (1994).

Tu081

MASS TRANSPORT IN A HORIZONTALLY VIBRATED FLUID LAYER

Michael Bestehorn[1], Ion D. Borcia[1], Rodica Borcia[1], Sebastian Richter[1],
Franz-Theo Schön[2], Uwe Harlander[2]
[1]*Department of Theoretical Physics,* [2]*Department of Aerodynamics and Fluid Mechanics*
BTU Cottbus-Senftenberg, Cottbus, Germany

Abstract Integrated boundary layer model, shallow water waves, numerical solutions

An integrated boundary layer model is derived to describe the formation of surface waves in a long channel with periodic boundary conditions. The channel including an immersed mirror symmetric obstacle on its ground oscillates anharmonically in lateral direction with a sawtooth-like shape

$$a(t) = a_0(\sin(\omega t) + \alpha \sin(2\omega t)) \; .$$

We show that depending on the behavior of the lateral excitation with respect to time reversal characterized by the parameter α an averaged mean flow either to the right or to the left side may occur. The existence of the average flow is also confirmed by our experiments performed in an annular channel [1]. If the fluid layer is very thin we observe in addition a Faraday unstable surface for certain excitation frequencies and amplitudes [2]. It is interesting to see that the lateral mass flux only exists if inertia terms in the thin film equation are present.

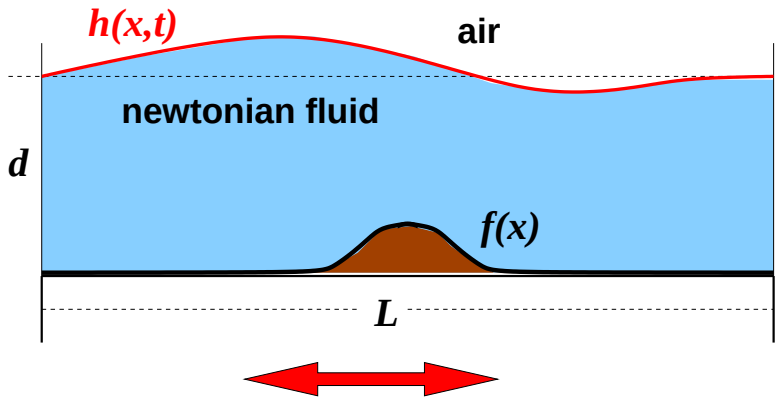

Figure 1. Horizontally vibrated layer with mean depth d and variable ground $f(x)$.

References

[1] I.D. Borcia et al., *Wave propagation in a circular channel: sloshing and resonance*, EPJST **232**, 461 (2023).
[2] M. Bestehorn, *Laterally extended thin liquid films with inertia under external vibrations*, Phys. Fluids **25**, 114106 (2013).

Tu082

SUPPRESSION OF MAGNETOHYDRODYNAMIC INTERFACIAL WAVE INSTABILITIES BY MEANS OF PARAMETRIC ANTI-RESONANCE

Gerrit Maik Horstmann[1], Julia Kuhn[1] & Fadi Dohnal[2]
[1]*Institute of Fluid Dynamics, Helmholtz-Zentrum Dresden-Rossendorf, Bautzner Landstrasse 400, D-01328 Dresden, Germany*
[2]*Research Center for Microtechnology, Vorarlberg University of Applied Sciences, CAMPUS V, Hochschulstraße 1, 6850 Dornbirn, Austria*

Abstract Magnetohydrodynamics, Wave Dynamics, Parametric Anti-Resonance.

Aluminum electrolysis consumes about 3 percent of the electricity generated worldwide. Magnetic field-induced interface instabilities, including in particular the metal pad roll (MPR) instability considered here, are one of the limiting factors in aluminum reduction cells that impede a further increase in energy efficiency. Aluminum reduction cells consist of two stably stratified liquid layers, a cryolite bath with dissolved alumina is floating on top of molten aluminum. Alumina can only be electrochemically reduced on exposure to strong electrolysis currents, which inevitably cause Lorentz forces in interaction with both self-induced and external magnetic fields. The Lorentz force resulting from the vertical component of the magnetic field is known to trigger the MPR instability [1], which manifests itself by growing rotating wave motions in the cryolite-alumina interface. More precisely, the Lorentz force energetically couples a pair of two transverse wave modes, which can mutually reinforce each other into a superimposed circular wave motion, provided that the natural frequencies of the wave pair become sufficiently close. Just as in reduction cells, the MPR instability can further arise in liquid metal batteries, which are physically similar, but consist of two instead of three liquid layers, which form two freely movable interfaces that can be set in coupled wave motions [2]. In both technologies, the MPR waves pose the risk of provoking short circuits, which is why the MPR instability must be suppressed during operation.
Most of the methods that have been implemented up to date for preventing these types of magnetic field-induced wave instabilities are invasive and impair the efficiency. Quite recently, however, a novel non-invasive stabilization technique was presented by [3, 4] that relies on a clever modulation of the electrolysis current, namely adding an alternating current (AC) component to the direct electrolysis current. It was demonstrated by means of both a simplified pendulum model and realistic cell simulations that for some heuristically chosen AC frequencies and amplitudes the MPR instability can be efficiently suppressed, but the suppression mechanism along with the underlying physics could not be explained yet. In an attempt to explore the involved physics and to identify the mechanism of action behind the stabilization, we examined the stability of the pendulum model extensively using Floquet analysis. We found that the suppression mechanism is a form of so-called parametric anti-resonance, an effect that has been known for only 25 years [5, 6] despite the relative simplicity of the governing equations. For small AC contributions, stability boundaries of anti-resonance can be described analytically, which now makes it possible to identify optimal stability points in the cells. We show that electrolysis cells can be stabilized much more effectively than initially anticipated by the inventors, potentially allowing aluminum production at lower cost, with less energy, and a smaller carbon footprint.

References

[1] J.-F. Gerbeau, C. Le Bris, T. Lelièvre, *Mathematical methods for the magnetohydrodynamics of liquid metals*, Numerical Mathematics and Scientific Computation, Oxford University Press (2006).
[2] G. M. Horstmann, N. Weber, T. Weier, *Coupling and stability of interfacial waves in liquid metal batteries*, J. Fluid Mech. **845**, 1–35 (2018).
[3] I. Mohammad, M. Dupuis, P. D. Funkenbusch, D. H. Kelley *Oscillating Currents Stabilize Aluminum Cells for Efficient, Low Carbon Production*, JOM **74**, 1908–1915 (2022).
[4] I. Mohammad, D. H. Kelley, *Stabilizing a Low-Dimensional Model of Magnetohydrodynamic Instabilities in Aluminum Electrolysis Cells* In: Eskin, D. (eds) Light Metals 2022, The Minerals, Metals & Materials Series, Springer, Cham (2022).
[5] A. Tondl, *To the problem of quenching self-excited vibrations*, Acta Tech CSAV **43**, 109–116 (1998).
[6] F. Dohnal, F. Verhulst, *Averaging in vibration suppression by parametric stiffness excitation*, Nonlinear Dyn. **54**, 231–248 (2008).

Tu083

NUMERICAL SIMULATIONS OF SURFACTANT-COVERED FARADAY WAVES: ROLE OF MARANGONI STRESSES IN PATTERN FORMATION

Debashis Panda[1], Lyes Kahouadji[1], Laurette Tuckerman[2], Seungwon Shin[3], Jalel Chergui[4], Damir Juric[4,5], & Omar K Matar[1]

[1]*Department of Chemical Engineering, Imperial College London, SW7 2AZ, London, United Kingdom,*
[2]*PMMH, CNRS, ESPCI, Université PSL, Sorbonne Université, Université de Paris, 75005 Paris, France*
[3]*Department of Mechanical and System Design Engineering, Hongik University, Seoul 04066, South Korea*
[4]*LISN, CNRS, Université Paris Saclay, 91400 Orsay, France*
[5]*Department of Applied Mathematics and Theoretical Physics, University of Cambridge, Cambridge CB3 0WA, UK*

Abstract

Exotic patterns in Faraday waves interest the fluid dynamicists to study the bifurcations when the stable interface transitions to various patterns. In the past three decades, patterns like squares, triangles, hexagons, stripes and superlattices have been studied extensively. However, the pattern formation becomes intricate in complex fluids like surfactant-laden interface. In the past, theoretical studies like linear stability, long-wave approximation, and two-dimensional numerical methods are carried out to study surfactant-laden Faraday waves. Recently, surfactant-laden square patterns were observed but not critically discussed. In this work, we carry out a three-dimensional direct numerical simulation of surfactant-covered Faraday waves in a laterally periodic minimal domain. We explore three patterns, i.e., squares, triangles, and hexagons and the elasticity parameter β_s is varied to observe the different pattern formation.

An example of the square pattern is shown below in figure 1. It is evident that the surfactants are concentrated at the crests than the troughs due to (i) the surface compression and dialation at the crest and the trough respectively, and (ii) the high Péclet number, that advects the surfactant from the trough to the crest. It creates a surface backflow from the crest to the trough, called the Marangoni stresses; it redistributes the surfactant at the crest, resulting in lower concentration at higher β_s (compare the Γ in the red circle at $t = T/4$ and $5T/4$ for $\beta_s = 0.1$ and 0.3). Upon increasing the β_s, we find parallel beaded-striped patterns as shown in figure 1 for $\beta_s = 0.5$. We call the patterns beaded as a concentrated Γ regions (see the orange circle) is found on the parallel stripes.

We, then, illustrate a qualitative damping parameter $B = t_i/t_m$ (similar to the viscous damping parameter [1]), that defines the ratio of vibratory inertial (t_i) and Marangoni (t_m) timescales. At $B < 1$ ($\beta_s = 0.1, 0.3$), we find the squares and at $B > 1$ ($\beta_s = 0.5$), we found the beaded-stripes. We extend this idea to the triangles and hexagons to study the effects of surfactants and Marangoni stresses on the the boundary between different pattern formations.

Keywords: Faraday waves, Surfactants, Pattern formation

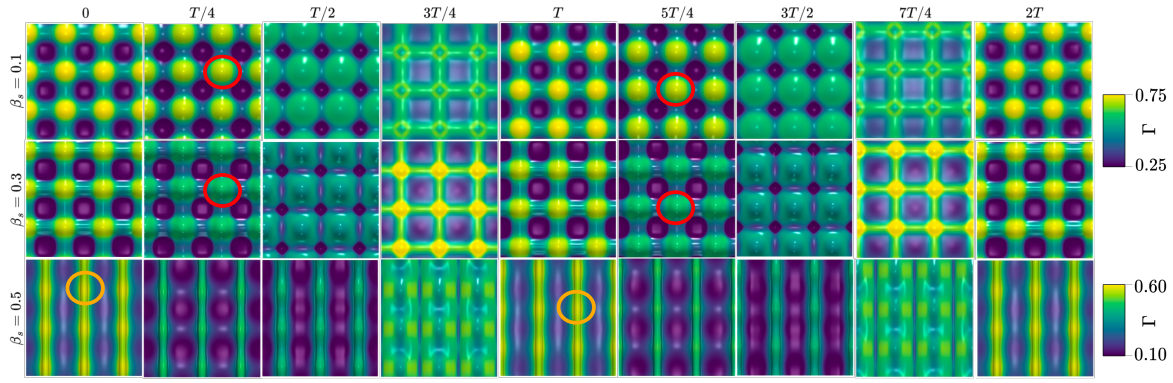

Figure 1. Pattern formation in surfactant-covered interfaces ($\Gamma_0 = 0.5$) at their respective $F = 1.1F_c^D$ for $\beta_s = 0.1$, 0.3, and 0.5. Square patterns are observed for $\beta_s = 0.1$, 0.3, and parallel stripe patterns for $\beta_s = 0.5$. Here, F is the forcing amplitude and F_c^D is the threshold forcing amplitude for the instability.

References

[1] Chen, P. and Vinals, J.: Amplitude equation and pattern selection in Faraday waves. Physical Review E (1999), 60(1), p.559.

DAY 2 – Tuesday, 25 June 2024 Afternoon Sessions			
13:30	**Keynote 4: Prof Camille Duprat** ***Chair: Dr Dani Orejon*** ***Larch Lecture Theatre***		
	Instabilties & Bifurcations 4 ***Chair: Dr Pedro Sáenz*** ***Larch Lecture Theatre***	***Phase-Change & Multiphase Flows 2*** ***Chair: Dr John Christy*** ***Yew Lecture Theatre***	***Waves & Interfacial Flows 2*** ***Chair: Prof Satish Kumar*** ***Elm Lecture Theatre***
14:15	Tu046: Marangoni convection and instability in a wall film: Three-dimensional CFD simulation *by A Khazayialiabad, T. Gambaryan-Roisman*	Tu065: Condensation and evaporation of a sessile droplet on asymmetric wavy surfaces *by L Bisquert, É Ruiz-Gutiérrez, M Pradas, R Ledesma-Aguilar*	Tu084: What leads to stokes drift? *By A Guha, A Gupta*
14:30	Tu047: Shape stability of an encapsulated microbubble in a non-5ewtonian liquid *by I Kaykanat, AK Uguz*	Tu066: Scaling effects of substrate wettability and bubble population density on pool boiling *by G Minozzi, A Lavino, E Smith, T Karayiannis, K Sefiane, OK Matar, D Scott, T Krueger, P Valluri*	Tu085: Dynamic liquid-liquid interfaces of aqueous phase-separating systems *by HC Shum*
14:45	Tu048: Roses are red, violets are blue, and streaming may seed flowers too *by B Vincent, A Kumar, D Henry, S Miralles, V Botton, A Pothérat*	Tu067: Stability of evaporating drops comprising binary mixtures *by K Thomson, G Karapetsas, Y Kita, OK Matar, K Sefiane, D Orejon, P Valluri*	Tu086: Driven shock in 3D: Euler equation versus molecular dynamics, and Navier-Stokes equation *by A Kumar, R Rajesh*
15:00	Tu049: Heat transfer transition during the melting process of subcooled PCMs *by M Li, L Zhu*	Tu068: Stabilizing an adverse density difference across an interface using phase change *by R Narayanan, LE Johns*	Tu087: Faraday waves in thin containers: A Floquet analysis *by F Viola, A Bongarzone, B Jouron, F Gallaire*
15:15	**Coffee Break (Alder Lecture Theatre)**		
15:45	Tu050: Neimark-Sacker bifurcation in viscoelastic time-modulated Taylor-Couette flow *by M Riahi, M HayaniChoujaa, S Aniss*	Tu069: Effect of different wind velocity on phase transformation of absolute ethanol in capillary tube *by L Bin, Y Ji*	Tu088: Electrokinetic dynamics and resonance when electrical double layers entangle with surface acoustic waves *by O Manor, O Dubrovsky, S Aremanda*
16:00	Tu051: Reduced order models for supercritical and subcritical transition to rotating convection with rigid boundaries *by S Sarkar, S Mandal, P Pal*	Tu070: Effect of the shape of point-heated water drops on the flow instability *by Y Kita*	Tu089: Horseshoe vortex around a micro pillar governed by spontaneous meniscus formation *by I Ueno, K Ozawa, H Nakamura, K Shimamura, GF Dietze, HN Yoshikawa, F Zoueshtiagh, K Kurose*
16:15	Tu052: Stability and flow laws in open foams, a porosity study *by Y Jobic, M. Médale, F. Topin*	Tu071: ACoolTPS – advanced cooling of high power microsystems using two-phase flows systems in complex geometries *by GR Anjos, DBV Santos, P Valluri*	Tu090: Periodic excitation of waves in a water filled annular channel with a submerged hill *by ID Borcia, F-T Schön, U Harlander, R Borcia, M Bestehorn, S Richter*
16:30	Tu053: Matchmaking shake: a parametric instability coupling longitudinal and transverse waves on rivulets *by A Daerr, G. Le Lay*	Tu072: Flow instability and dry out profile in flow boiling of binary mixtures in microchannel under low mass flux *by A Widyatama, D Orejon, K Sefiane*	Tu091: Perturbation theory for metal pad roll instability in rectangular reduction cells *by P Hegde, GM Hortsmann*
16:45	Tu054: Simultaneous bifurcations from D3 and D4 symmetric states in vertical natural convection *by Z Zheng, LS Tuckerman, T M Schneider*	Tu073: Bounds on the spreading radius in droplet impact: the inviscid case *by LÓ Náraigh, A Amirfazli, M Bustamante, Y Hu*	Tu092: Analyzing the survivability and investigating hydrodynamic nonlinearities in submersible buoy shaped point absorber wave energy converter *by VM Brathikan, S Kalanithi, V Janarthanan*
17:00	Tu055: Instability in Taylor-Couette flow past a deformable cylinder at low Reynolds number *by A Khan, PP Chokshi*	Tu074: Experimental study on the electrohydrodynamic instability between three immiscible liquids flowing in a microchannel by E Nur Soysal, AK Uguz, S Altundemir	Tu093: Integrating machine learning with CFD for accurate prediction of 5usselt number in wall jet impingement *by H Agarwal, A Lagwankar, L Chaplot, A Chandy*

Keynote 4

Capturing drops with fibers: aerodynamics and capillary effects

Camille Duprat

LadHyX, École Polytechnique, Palaiseau, France

Camille Duprat is Professor of Mechanics at École polytechnique, which she joined as assistant professor in 2013 after a PhD at Sorbonne Université and post-doctoral stays at Princeton University, USA and ESPCI, Paris. Her research focusses on fluid structure interactions at small scale, in particular in situations where fluid-fluid interfaces are important or in systems where viscous forces dominates. She is particularly interested in fiber-flow interactions, for example the transport of flexible fibers in viscous flows, or wetting and elastocapillarity in textiles.

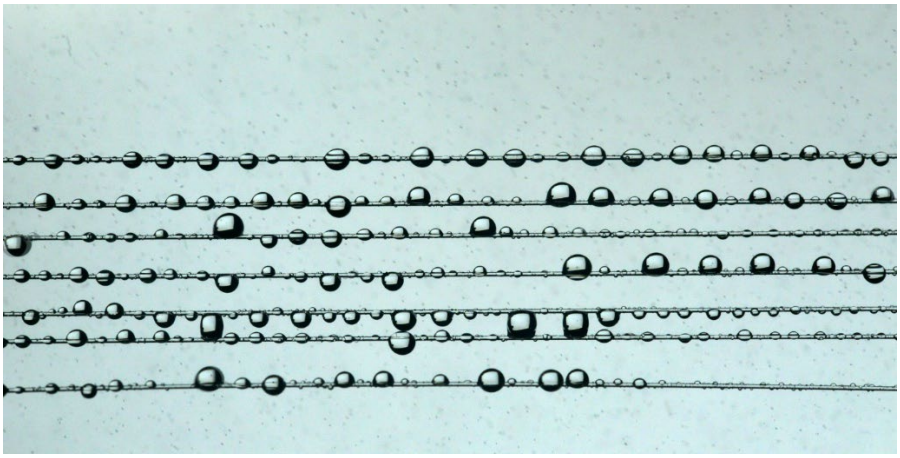

Abstract

We consider fibrous meshes placed in a flow of fog. This system, often encountered in aerosol filtration, exhibits a wealth of phenomena coupling aerodynamics and capillarity. In particular, we characterize experimentally and theoretically the flow through and around the porous mesh, the corresponding aerodynamic forces as well as the deposition of the mist droplets on the fibres, that all strongly depend on the mesh porosity and fine structure (i.e. the fibres' arrangements). These droplets accumulate on the wire to form large drops exposed to a crossflow. For a range of Reynolds numbers, the wake of these drops is asymmetric, the drops spontaneously move along the fiber and interact aerodynamically with both with their downstream and upstream neighbors. Under a strong acceleration of the wind, the drops further interact with their unsteady wake and may eventually break up to be re-entrained by the flow.

Tu046

Marangoni Convection and Instability in a Wall Film: Three-Dimensional CFD Simulation

Amirhossein Khazayialiabad, Tatiana Gambaryan-Roisman
Institute for Technical Thermodynamics, Technische Universität Darmstadt, Darmstadt, Germany
khazayialiabad@ttd.tu-darmstadt.de

Keywords: Film evaporation; Marangoni convection; Arbitrary lgrangian Eulerian

Abstract

Marangoni convection and instability in wall films arise from surface tension gradients. The temperature-induced Marangoni effect, or thermocapillarity, can be influenced by introducing wall topography, a local wall heating, or a local variation of wall thermal properties [1]. The Marangoni convection induced by the wall topography or a local heating, as well as the Marangoni instability, can exhibit characteristics on both short and long length scales. The short-scale Marangoni convection, as well as the short-wave instability, is characterized by development of convection cells. In the long-wave mode, the liquid-gas interface deforms, with temperature perturbations prompting thermocapillary stresses that initiate outward liquid motion from hot spots, resulting in a reduction of local film thickness [2].

The majority of numerical studies of Marangoni convection in liquid films have been performed using long-wave theory, suitable for situations with long wavelengths of surface perturbation. While effective for capturing overall behavior, this theory is unable to describe the short-wave phenomena. The long-wave theory is not applicable to processes, in which localized heat transfer effects are vital [3].

We apply the Finite Element Method using the Arbitrary Lagrangian Eulerian (ALE) approach for the full-scale three-dimensional simulation of Marangoni convection in evaporating confined liquid film. The numerical model incorporates evaporative cooling, heat conduction and convection, along with the advective-diffusive transport of vapor in the atmosphere of the non-condensible gas. The interplay between the induced Marangoni convection and Marangoni instability is demonstrated.

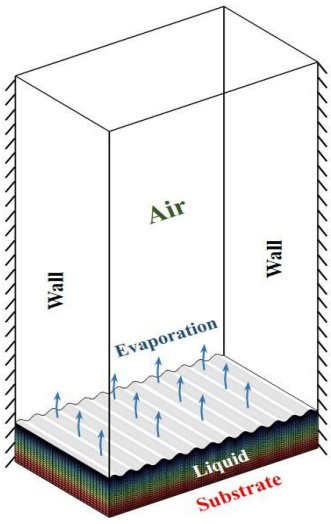

Figure 1. Schematic of the evaporating confined film

References

[1] T. Gambaryan-Roisman, *Modulation of Marangoni convection in liquid films*, Adv. Colloid Interface Sci. **222**, 319–331 (2015).
[2] S. H. Davis, *Thermocapillary instabilities*, Annu Rev. Fluid Mech. **19**, 403-435 (1987)
[3] A. A. Golovin, A. A. Nepomnyashchy, L. M. Pismen, *Interaction between short-scale Marangoni convection and long-scale deformational instability*, Phys Fluids **6**, 34-48 (1994).

Acknowledgments

This project has received funding from the European Union's Horizon 2020 research and innovation programme under the Marie Skłodowska-Curie grant agreement No 955612 (NanoPaInt).

Tu047

SHAPE STABILITY OF AN ENCAPSULATED MICROBUBBLE IN A NON-NEWTONIAN LIQUID

Ilke Kaykanat[1] & Kerem Uguz[1]
[1]*Department of Chemical Engineering, Bogazici University, Istanbul, Turkey*

Keywords: Non-spherical bubble oscillations, Spherical harmonics, Power-law liquid

Abstract

Therapeutic ultrasound-mediated microbubbles are used to improve the targeted delivery of drugs and genes by temporarily increasing cell membrane permeability in specific tissues [1,2]. This approach is applicable in cancer treatment, where microbubbles enhance the transport of chemotherapy drugs to tumors, enhancing treatment effectiveness while minimizing side effects. This study focuses on the onset of the shape stability of encapsulated microbubbles under the effect of an acoustic field. Microbubbles are encapsulated in a lipid or protein shell to increase their lifetime in blood. power-law and Kelvin-Voigt constitutive laws are employed for blood and bubble shell, respectively. The bubble is in an unbounded liquid (blood) and encapsulated with a shell, as shown in FIG.1. The spherical interface of the microbubble is perturbed with a harmonic non-spherical perturbation. After reaching a steady periodic state of spherical oscillations, Floquet theory is employed to determine system eigenvalues. Effects of the power-law index, consistency index, and acoustic pressure amplitude are investigated. Phase diagrams are generated for different pressure amplitudes of the acoustic field and initial bubble radius to explore stable and unstable regions. Stable bubbles in the blood live longer than unstable bubbles, extending the treatment time. The results reveal that larger pressure amplitudes and initial radius values lead to bubble instability. A higher power-law index causes the damping of the oscillations for both spherical and non-spherical oscillations. At a low consistency index, the damping effect of the power-law index decreases. Unlike Newtonian liquids, the viscosity of power-law liquids is affected by the frequency of the acoustic field.

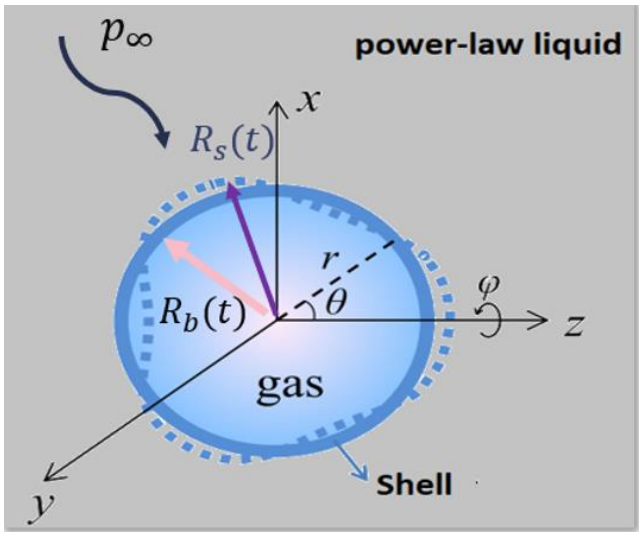

Figure 1. Non-spherical bubble geometry in spherical coordinates. The solid and dashed lines show the spherical and non-spherical oscillations.

References

[1] M. Wang, Y. Zhang, C. Cai, J. Tu, X. Guo and D. Zhang, *Sonoporation-induced cell membrane permeabilization and cytoskeleton disassembly at varied acoustic and microbubble-cell parameters*. Scientific Reports, **8(1),** 3885 (2018).
[2] S. I., Kaykanat, S. I., and A. K., Uguz, *The role of acoustofluidics and microbubble dynamics for therapeutic applications and drug delivery*, Biomicrofluidics, **17(2)**, 2023.

Tu048

ROSES ARE RED, VIOLETS ARE BLUE, AND STREAMING MAY SEED FLOWERS TOO

Bjarne Vincent[1,2], Abhishek Kumar[2], Sophie Miralles[1], Daniel Henry[1], Valéry Botton[1] & Alban Pothérat[2]
[1]*INSA Lyon, CNRS, Ecole Centrale de Lyon, Universite Claude Bernard Lyon 1, Laboratoire de Mécanique des Fluides et d'Acoustique, UMR5509, 69621, Villeurbanne France*
[2]*Centre for Fluid and Complex Systems, Coventry University, Coventry CV1 5FB, UK*

Abstract Stability analysis of an acoustic streaming jet (ultrasounds, acoustofluidics).

As it propagates within a fluid, a sound wave is attenuated due to viscous and thermal effects. This, in turn, drives a nearly steady flow called *acoustic streaming* [1]. Thanks to its weakly-intrusive nature, acoustic streaming represents an attractive solution for industrial systems, such as solidification processes of melted metals and semiconductors. We are particularly interested in controlling the flows that may occur in the melts using jets driven by beam-shaped fields of progressive ultrasounds. For an efficient use of acoustic streaming in this context, it is necessary to first gain a deep understanding of the stability of the streaming jet itself.

We initiated a numerical study of the stability of an acoustic streaming jet flowing in a closed cylindrical cavity. The latter is entirely filled with a newtonian fluid and is fitted with a plane circular transducer at one end, which continuously emits a beam of ultrasonic waves propagating towards the opposite sound-absorbing wall. The attenuation of that beam yields a body force driving the flow, with a magnitude defined by the acoustic Grashof number Gr_{ac}. Besides of seeking the instability onset in terms of a critical Gr_{ac}, we consider different jet confinements, which are obtained by modifying the size of the cavity with respect to the size of the beam. In each case, the streaming jet is axisymmetric, and features a strong acceleration close to the transducer followed by a smooth velocity decay further away from the source. The jet finally impinges the wall facing the transducer, creating vortices near that wall.

Besides of having a stabilising effect, we found that confining the streaming flow significantly affects the nature of the leading unstable perturbations: whilst these are non-oscillatory for the largest aspect ratios, narrowing the cavity causes the destabilising mode to become oscillatory. Furthermore, we show that different bifurcation criticalities are achieved simply by changing the cavity size. Nevertheless, the mechanism responsible for the flow destabilisation is the extra shear caused by the jet impingement at the end wall, whatever the aspect ratio of the cavity. On the impinged surface, the unstable friction perturbations display floral patterns we called *sonic bloom* (figure 1). The change of unstable mode shape as the cavity size is varied can be explained using critical point analysis.

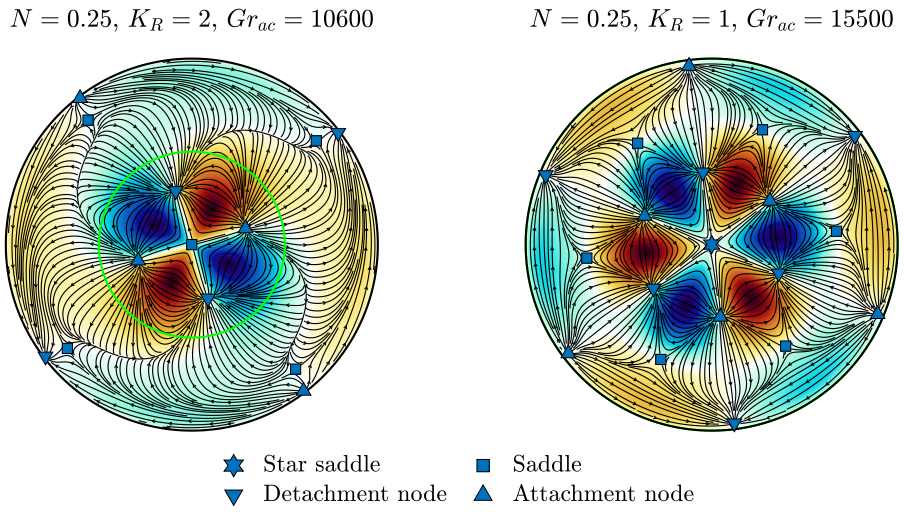

Figure 1. Skin friction lines exerted by the leading unstable perturbation on the downstream wall for two cavity sizes. The background colour is related to the azimuthal friction (red is positive, blue is negative). Critical points, i.e., points of zero friction perturbation, are also reported (blue symbols). The ratio between the sound attenuation distance and cavity length is defined by N, and K_R is the ratio between the cavity and beam (green circle) diameters. Both modes are oscillatory.

References

[1] J. Lighthill, *Acoustic streaming*, J. Sound Vib. **61**(3), 391–418 (1978).

Tu049

lailai_zhu@nus.edu.sg

HEAT TRANSFER TRANSITION DURING THE MELTING PROCESS OF SUBCOOLED PCMS

Li Min, Zhu Lailai*
Department of Mechanical Engineering, National University of Singapore, 117575, Singapore

Abstract Phase change materal, Linear stability analysis, Melting curve
Phase Change Materials (PCMs) are highly sought after for the effective utilization of thermal energy from renewable resources, owing to their high energy storage density and zero-carbon emissions. However, a major limitation of almost all PCMs is their low thermal conductivity. This leads to a poor energy charging rate, an issue that remains largely unresolved due to complex melting dynamics. In this study, we present theoretical insights into the melting process of subcooled PCMs within a laterally heated rectangular cavity. Utilizing linear stability analysis, we identify a critical liquid fraction that serves as a criterion to differentiate between conduction- and convection-dominated melting regimes. Building upon this, we develop a mathematical model to describe the temporal evolution of the liquid fraction. These results align well with reported experimental measurements and our two-dimensional simulation data, providing valuable insights for enhancing the energy charging rate in PCMs.

Tu050

NEIMARK-SACKER BIFURCATION IN VISCOELASTIC TIME-MODULATED TAYLOR-COUETTE FLOW

Mehdi Riahi[1,2], Mohamed Hayani Choujaa[2] & Saïd Aniss[2]
[1] *Department of Mechanics, Royal Air School, Marrakech, Morocco*
[2]*Laboratory of Mechanics, B.P 5366, Mâarif, Faculty of Sciences Aïn Chock, University Hassan II Casablanca, Morocco.*

Abstract Modulated Taylor-Couette flow; upper convected Maxwell model; spectral method; Floquet theory; codimension-two bifurcation point; inertio-elastic parametric resonance.

Time-periodically forced systems can lose their stability via three generic ways: a synchronous bifurcation corresponding to a single real eigenvalue of the Floquet multiplier (based on Poincaré map) crossing the unit circle through $+1$, a period doubling bifurcation where a single negative real critical Floquet multipliers crosses the unit circle at -1 or a Neimark-Sacker bifurcation where a pair of complex-conjugate Floquet multipliers cross the unit circle. In the latter case, we are dealing with a quasi-periodic state often characterized by two incommensurate frequencies.
Time modulated Taylor-Couette flow is one of the generic examples that can exhibit such bifurcations at the onset of the instability. However, for a Newtonian fluid in a Taylor-Couette flow generated by oscillating the inner cylinder in the azimuthal direction with a stationary outer cylinder, Avila et al.[1] showed that this system loses its stability only via synchronous bifurcations. Neither subharmonic nor quasi-periodic solutions were observed. In this paper, the focus is on this family of flows, especially when the inner and outer cylinders co-oscillate and the fluid obeys the upper convected Maxwell model. The linear stability of the basic state is considered when the elastic and inertial mechanisms are of the same order of magnitude corresponding to an elasticity number $E = 1$ defined as a ratio between the elastic effects, measured by the Weseinberg number, and the inertial ones, measured by the Reynolds number. It is shown that the presence of the first normal stress difference in the destabilization mechanism leads to the apparition of new quasi-periodic flows and significantly alters the flow reversal of the system by completely suppressing the non-reversing instability mode observed in the Newtonian case [1, 2, 3].
In Figure (1) the time series of the radial velocity at a fixed point of the geometrical space related to the quasi-periodic state and its corresponding power spectra are shown over 58 oscillation periods. As it can be seen, we are dealing with a quasi-periodic state oscillating with four fundamental frequencies written as linear combinations of ω_s and ω_f denoting respectively the Neimark-Sacker and forcing frequencies. This multiplicity of oscillation frequencies could be attributed to the presence of the subsequent bifurcations that occur very close to the primary instability.

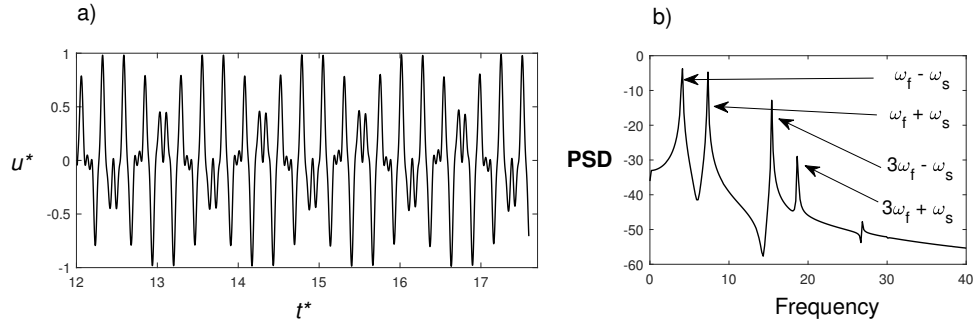

Figure 1. a) Time series of the radial velocity $u^*(t^*)$ for the quasiperiodic instability mode at the mid-point $(x, \theta, z) = (1/2, 0, 0)$ over 58 oscillation period and b) the corresponding power spectra at the first critical onset of instability : $Ta_c = 20.4198$, $q_c = 9.7$ and $\gamma = 4.225778$. Her, the dimensionless quantities Ta_c, q_c and γ represent respectively the critical Taylor number, the critical axial wave number and the frequency number. The radial, azimuthal and axial coordinates are denoted by x, θ and z respectively.

References

[1] M. Avila , M. J. Belisle , J. M. Lopez , F. Marques & W. S. Saric, *Mode competition in modulated Taylor-Couette flow*, J. Fluid Mech. 601, 381-406 (2008).
[2] A. J. Youd, A. P. Willis & C. F. Barenghi, *Reversing and non-reversing modulated Taylor-Couette flow*, J. Fluid Mech. 487, 367-376, (2003).
[3] M. Riahi , S. Aniss, and M. Ouazzani Touhami, *Families of reversing and non-reversing Taylor vortex flows between two cooscillating cylinders with different amplitudes*, Phys. Fluids 31, 014101 (2019).

Tu051

REDUCED ORDER MODELS FOR SUPERCRITICAL AND SUBCRITICAL TRANSITION TO ROTATING CONVECTION WITH RIGID BOUNDARIES

Snehashish Sarkar[1], Sutapa Mandal[1] & Pinaki Pal[1]
[1]*Department of Mathematics, National Institute of Technology Durgapur, West Bengal, India*

Abstract Rotating Rayleigh-Bénard convection, low dimensional model, bifurcation analysis.

We present an one dimensional (1D) model to study the supercritical and subcritical transitions to stationary convection in rotating Rayleigh-Bénard convection in the presence rigid boundary conditions. The 1D model is derived using the adiabatic elimination process from a five dimensional model obtained by applying Galerkin technique. The 1D model explains the origin of supercritical and subcritical stationary cellular flow patterns at the onset of convection for relatively lower rotation rate (Ta) (Figure 1). On the other hand, the five dimensional model explains the origin of oscillatory convection for higher rotation rate. Both the models qualitatively mimics the previously reported experimental [1] and numerical [2] simulation results.

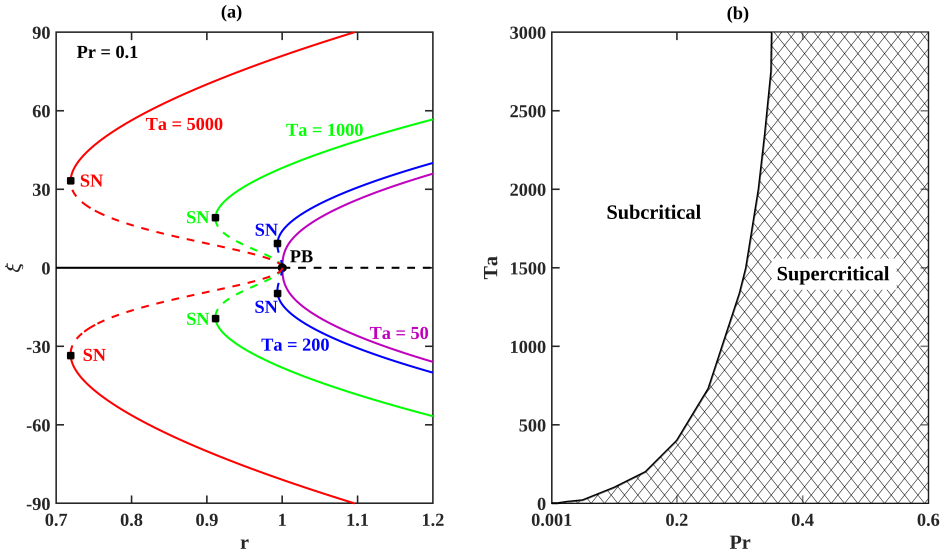

Figure 1. Figure (a) shows the bifurcation diagram for most energetic mode ξ with fixed Prandtl number $(\mathrm{Pr}) = 0.1$ and for four Taylor number (Ta). Pitchfork and saddle-node bifurcation points are marked by PB and SN respectively. Figure (b) shows the two-parameter diagram demarcating supercritical and subcritical flow regimes on the Pr-Ta plane.

References

[1] H. T. Rossby, *A study of Bénard convection with and without rotation*, Journal of Fluid Mechanics **36**, 309–335 (1969).
[2] S. Mandal, M. Ghosh, P. Maity, A. Banerjee, and P. Pal, *Supercritical and subcritical rotating convection in a horizontally periodic box with no-slip walls at the top and bottom*, Physics of Fluids **34**, 10 (2022).

Tu052

STABILITY AND FLOW LAWS IN OPEN FOAMS, A POROSITY STUDY

Yann Jobic[1], Marc Médale[1] & Frédéric Topin[1]
[1]*Aix Marseille Univ, CNRS, IUSTI, Marseille, France*

Abstract This work aims to enhance industrial heat exchangers thanks to numerical computations. Spatially and temporally resolved Incompressible NS equations have been computed at pore scale to identify the macroscopic coefficients involved in Darcy and Forchheimer laws. This approach enables us to determine the transition regions from Darcy to Fochheimer regimes for various porosities in tri-periodic Kelvin cells. Moreover, we have also identified Hopf and steady-state bifurcations that occur in the transition region from moderate to strong inertial regimes.

Fluid flow predictions in porous media is critical in many industrial applications [1]. The final goal of this work is to model and optimize heat exchangers involving porous media at small costs (e.g. pressure drop). Those porous media can be geometrically too complex or computationally too expensive to perform parametric studies that involve individually each parameters (e.g., strut shape, pore elongation, etc). Therefore we have considered a simplified model consisting in a tri-periodic Kelvin cell for which direct numerical simulations are performed at the pore scale. The geometry is discretized with a conforming finite element mesh on which the INS Equations are computed either with a steady-state solver or an unsteady one.

To reach the desired goal, we have developed three complementary numerical tools. The first one uses a steady-state continuation algorithm, based on the Asymptotic Numerical Method (ANM). It computes the INSE solution decomposed in high order power series. It enables to determine critical points along the continuation parameter path (here the pressure drop) where there is a steady-state bifurcation. The type of this bifurcation (simple or multiple) is independently checked by computing the size of the kernel's algebraic system. The second tool performs linear stability analysis of the previously computed steady-state solutions. The linearization of the system is done by a first order perturbation method, followed by a decomposition in normal modes. The linear stability analysis results in a generalized eigenvalue problem solved by PETSc/SLEPc/MUMPS libraries [2], which enables us to determine the Hopf bifurcation(unsteady and periodic solution).

Using the above numerical methods, we have computed the bifurcation diagram in a periodic Kelvin cell made up of triangular struts (c.f. Fig. 1a). Moreover, we have linked both (dynamical and state-state) bifurcation types to the macroscopic flow regimes (Darcy, transition, Forchheimer). We have shown that no bifurcation occurs in the smooth transition from Darcy to non Darcy flows, and that steady-state and dynamic bifurcations occur at the vicinity of the transition to Forchheimer flows [3]. Furthermore, we have also performed time integration in the dynamical regime beyond the Hopf bifurcation and shown that the pressure drop in the dynamical regime is lower that in the steady-state one at the same Reynolds number (c.f. Fig. 1b).

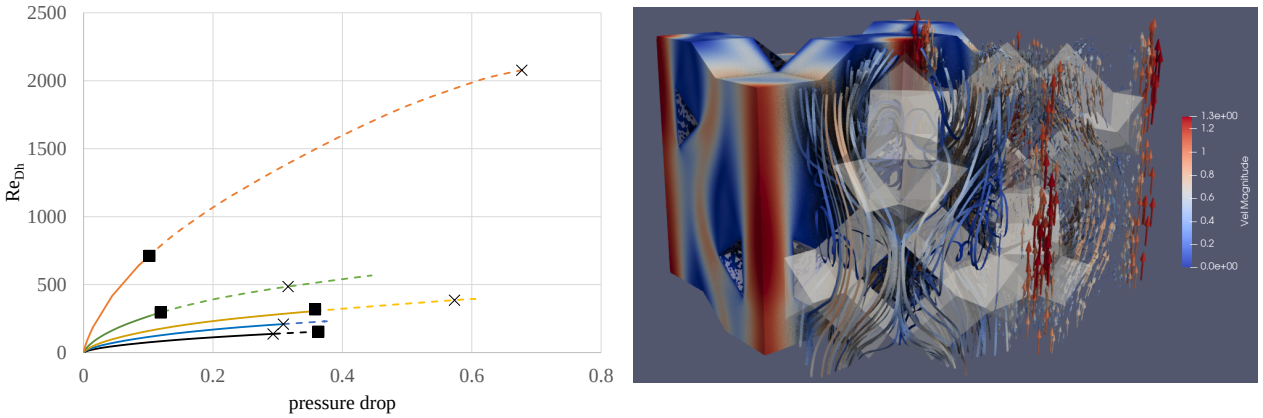

Figure 1: Computations in tri-periodic Kelvin cell with triangular struts of porosity 86.4%. Left: bifurcation diagram. Right: Fluid flow patterns in the Hopf dynamical regime at Reynolds number Re=320.

References

[1] Pauthenet, M., Davit, Y., Quintard, M., Bottaro, A.: Inertial sensitivity of porous microstructures. Transp. in Porous Media 125, 211–238, 2018.
[2] Balay, S. et al. : PETSc users manual. Technical Report ANL-95/11 - Revision 3.20, Argonne National Laboratory, 2023.
[3] Y. Jobic, M. Médale, F. Topin, Flow stability and regime transitions on periodic open foams, Inter. J. of Multiphase Flow, Vol 172, 104717, 2024.

Tu053

MATCHMAKING SHAKE: A PARAMETRIC INSTABILITY COUPLING LONGITUDINAL AND TRANSVERSE WAVES ON RIVULETS

Grégoire Le Lay[1], Adrian Daerr[1]
[1]*Matière et Systèmes Complexes UMR CNRS 7057, Université Paris Cité, 75231 Paris, France*

Abstract Horizontal movements imposed on a vertically flowing liquid rivulet in a Hele-Shaw cell causes linearly damped transverse and longitudinal waves to mutually amplify. (parametric instability, capillary flow, contact line dynamics)

Two-phase flows in confined geometries have attracted a lot of interest since the work of Bretherton on bubble motion in a capillary tube [1] and the work of Saffman and Taylor on interface dynamics in a Hele-Shaw cell. [2]. The high viscous dissipation in moving menisci, caused by enhanced shear, strongly affects slug flows in pipes as well as in rivulet flow in a Hele-Shaw cell [3].

Here we consider a liquid filament, or rivulet, flowing . We subject the rivulet to homogeneous acoustic forcing, and describe a previously unreported instability where the path followed by the rivulet becomes sinuous, while simultaneously the streamwise mass distribution becomes inhomogeneous. We show that both features, although damped under normal conditions, grow by amplifying one another through a coupling created by the the acoustic forcing. For a perturbation wavelength precisely given by the fluid advection distance during a period, the coupling becomes coherent and phase-locked, leading to reciprocal amplification.

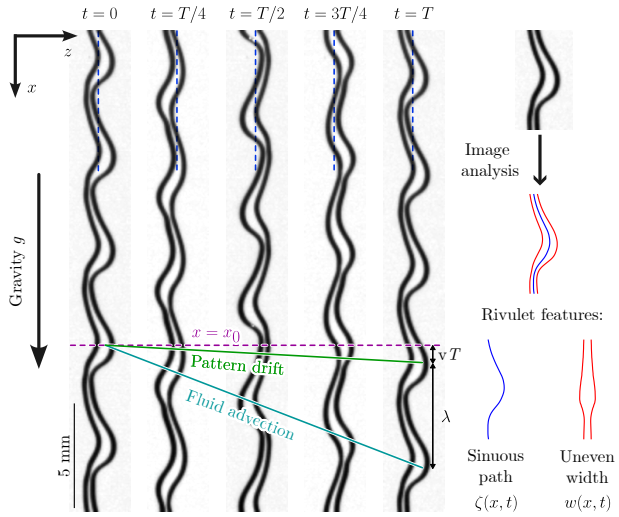

Figure 1. Snapshots of the rivulet over one forcing period T. The menisci delimiting the rivulet appear dark in this back-lit view. The phase velocity v_{drift} of the sinuous deformations $\zeta(x,t)$ is smaller than that at which the liquid bulges (modulations of the width $w(x,t)$) flow downstream. The pattern reproduces exactly after one period T, up to a translation.

References

[1] F. P. Bretherton, J. Fluid Mech. **10** (1961), 166
[2] P. G. Saffman, and G. I. Taylor, Proc. Roy. Soc. London A. Math. Phys. Sc. **245** (1958), 312
[3] A. Daerr, J. Eggers, L. Limat and N. Valade, Phys. Rev. Lett. **106** (2011), 184501

Tu054

SIMULTANEOUS BIFURCATIONS FROM D_3 AND D_4 SYMMETRIC STATES IN VERTICAL NATURAL CONVECTION

Zheng Zheng[1], Laurette S. Tuckerman[2] & Tobias M. Schneider[1]
[1]*Emergent Complexity in Physical Systems Laboratory (ECPS), École Polytechnique Fédérale de Lausanne, CH 1015 Lausanne, Switzerland*
[2]*Physique et Mécanique des Milieux Hétérogènes (PMMH), CNRS, ESPCI Paris, PSL University, Sorbonne Université, Université de Paris, 75005 Paris, France*

Keywords: thermal convection, bifurcation theory, symmetry.

Convection in a vertical channel subjected to a horizontal temperature gradient is numerically investigated. Previous numerical simulations by Gao et al. [1] reveal a variety of behaviors – steady, time-periodic and chaotic. We extend their work by constructing stable and unstable branches of the equilibria and periodic orbits of the underlying Oberbeck–Boussinesq equations by parametric continuation.
In a narrow domain of aspect ratio ten, the phenomenology is dominated by the competition between three and four co-rotating rolls. This seemingly simple interaction turns out to be mediated by a variety of bifurcation scenarios, which are in turn dictated by the symmetries of the primary branches. D_4 symmetry requires that several intermediate branches bifurcate simultaneously from the four-roll branch, while D_3 symmetry requires that their intersection with the three-roll branch be transcritical (figure 1). We observe other manifestations of the competition between three and four rolls, in which the symmetry in time or in the transverse direction is broken, leading to limit cycles or wavy rolls, respectively.
Our work highlights the interest of combining numerical simulations, bifurcation theory, and group theory, in order to understand the transitions between and origin of flow patterns.

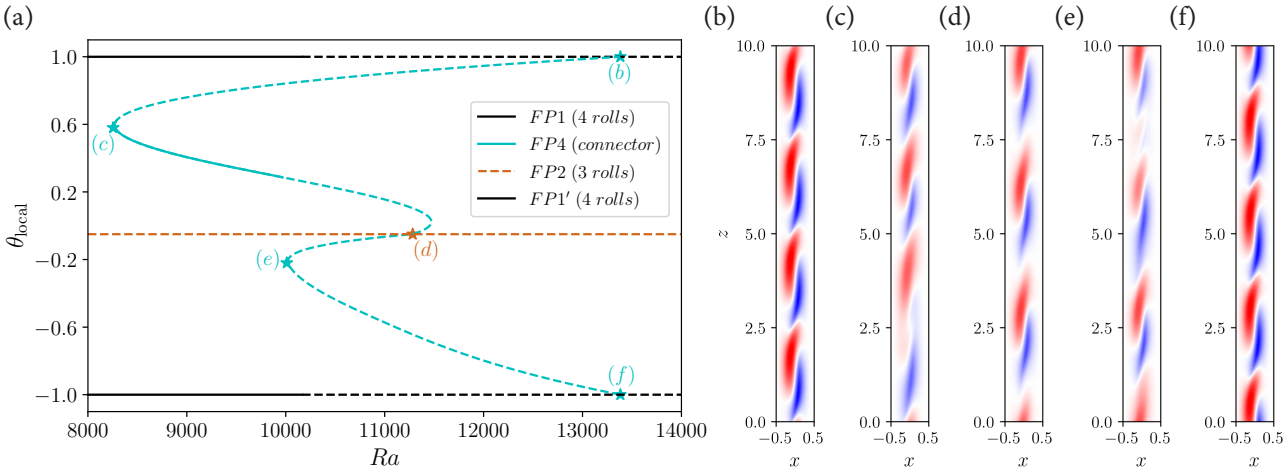

Figure 1. Convection in a vertical channel. The rigid vertical wall at $x = -0.5$ is maintained at a higher temperature than the wall at $x = 0.5$. Periodic boundary conditions are imposed at the horizontal domain boundaries at $z = 0$ and $z = 10$. (a) Bifurcation diagram focusing on mixed-mode or connector branch FP4 using $\theta_{\text{local}} \equiv \theta(x = 0, y = 0.5, z = 4.375)$. ($\theta_{\text{local}}$ is normalized and its variation for pure three- and four-roll branches omitted for clarity.) Solid and dashed curves signify stable and unstable states respectively. (b-f) Equilibria visualized on the x-z plane at $y = 0.5$. The domain contains three or four rolls, all rotating in the clockwise direction, with red indicating warm fluid rising along the warmer wall and blue indicating colder fluid descending along the colder wall. The two ends, (b) and (f), of the connector branch FP4 are created at the same Rayleigh number via subcritical pitchfork bifurcations from four-roll branches FP1 and FP1′ that vary by a half-roll phase-shift in z. Two different manifestations of the Eckhaus instability from four to three rolls are observed, (b)→(c)→(d) along which two rolls merge and (f)→(e)→(d), along which one roll disappears. At (d), the two pathways meet the three-roll branch FP2 in a transcritical bifurcation.

References

[1] Z. Gao, A. Sergent, B. Podvin, S. Xin, P. Le Quéré, L.S. Tuckerman, *Transition to chaos of natural convection between two infinite differentially heated vertical plates*, Phys. Rev. E **88**, 023010 (2013).

Tu055

INSTABILITY IN TAYLOR-COUETTE FLOW PAST A DEFORMABLE CYLINDER AT LOW REYNOLDS NUMBER

Arshan Khan & Paresh P. Chokshi
Department of Chemical Engineering, IIT Delhi, New Delhi, India

Keywords: Flow instability,, Taylor-Couette Flow, Interfacial instability, deformation

Abstract

This study investigates the stability of a Taylor-Couette flow past a flexible cylinder using linear stability theory. The flow arises from the rotation of a rigid inner cylinder, while the outer cylinder held stationary consists of a deformable elastic solid continuum modelled using a nonlinear neo-Hookean elastic solid model. It has been reported in the literature that a plane Couette flow overlying a neo-Hookean solid plate [1,2] becomes unstable even in the absence of inertia, with the two-dimensional mode being the least stable, referred to as the viscous mode. In the present investigation of Taylor-Couette flow with a deformable outer cylinder under the creeping flow limit, the effect of streamline curvature on the viscous mode instability arising out of fluid-structure interaction is examined. It is found that the three-dimensional non-axisymmetric disturbances are the least stable modes, while the two-dimensional unstable disturbance waves are stationary. This instability is attributed to the work done by the mean flow at the interface, resulting in energy transfer from the mean flow to the travelling disturbances. Notably, we observed the existence of short-wave instability, which arises due to a non-zero first normal stress difference. Our analysis examined the effect of several parameters, such as fluid layer thickness, solid layer thickness, and interfacial surface tension on the critical value of the shear rate for the onset of instability. Increasing the fluid layer thickness and decreasing the thickness of the deformable cylindrical solid led to an increase in the critical shear rate, indicating that the solid layer thickness destabilizes the flow. Moreover, the least stable azimuthal wavenumber was observed to increase with an increasing fluid layer thickness. In the absence of interfacial tension, a transition from finite-wave instability to shortwave instability occurs for a thinner solid layer with respect to the fluid layer thickness. The presence of interfacial tension tends to attenuate the short-wave instability. Overall, comparing with the planar Couette flow, the streamline curvature is found to delay the onset of instability (see figure 1).

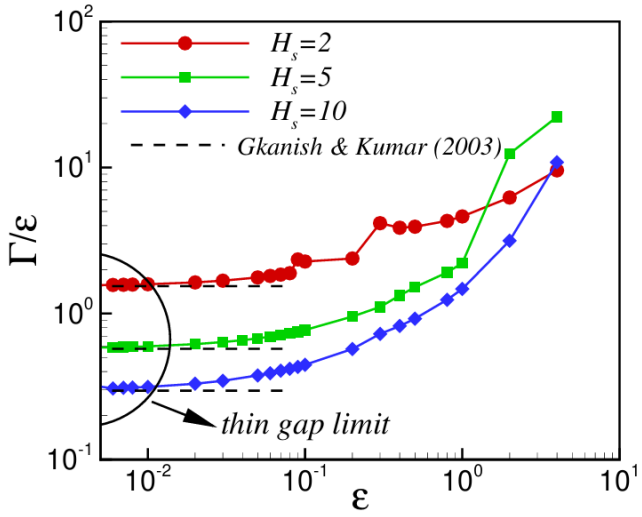

Figure 1. Validation of critical shear rate (Γ) with Ref.[1] and impact of streamlined curvature on the instability boundary. H_s=H/ϵ where H and ϵ represent the thickness of the neo-Hookean solid layer and the Newtonian fluid layer, respectively.

References

[1] V. Gkanis, S. Kumar, *Instability of creeping Couette flow past a neo- Hookean solid*, Phys. Fluids **15**, 2864–2471 (2003).
[2] R. Patne, D. Giribabu, V. Shankar, *Consistent formulations for stability of fluid flow through deformable channels and tubes*. J. Fluid Mech. **827**, 31–66 (2017).

Tu065

CONDENSATION AND EVAPORATION OF A SESSILE DROPLET ON ASYMMETRIC WAVY SURFACES

Lucile Bisquert[1], Élfego Ruiz-Gutiérrez[2], Marc Pradas[3], Rodrigo Ledesma-Aguilar[1]
[1]*Institute for Multiscale Thermofluids, School of Engineering, University of Edinburgh, The King's Buildings, Mayfield Road, Edinburgh EH9 3FB, United Kingdom*
[2] *School of Engineering, Newcastle University, Claremont Road, Newcastle upon Tyne NE1 7RU, United Kingdom*
[3] *School of Mathematics and Statistics, The Open University, Milton Keynes, MK7 6AA, United Kingdom*

Keywords: Droplets, condensation, evaporation, Lattice Boltzmann, patterned surfaces, bifurcations.

Abstract

The condensation and evaporation of droplets on solid surfaces play an essential role in nature and in applications. Examples include desert beetles gathering water in sand dunes [1] and industrial applications such as heat transfer and water harvesting. It is possible to guide the behaviour and morphology of sessile droplets by introducing topographical [2] or chemical patterns [3] on a solid surface. The aim of this work is to study drop-wise condensation and evaporation through computational modelling. We focus on studying the stability of a droplet that undergoes slow variations in volume on patterned solid surfaces. We use the coupled Cahn-Hilliard and Navier-Stokes equations, solved using the Lattice-Boltzmann method, to capture this effect under isothermal conditions. Previously, the evaporation of a droplet on a smooth wavy surface has been studied, revealing a new effect called snap evaporation [2]. On symmetric surface patterns, this effect consists of a spontaneous and sharp change of the droplet base radius due to a saddle-node bifurcation. Intuition would suggest that a similar effect would be observed when the droplet undergoes condensation. However, our simulations show that a condensing droplet presents asymmetric snap behaviour. Using a stability analysis, we found that, for droplets undergoing condensation, pitchfork bifurcations are dominant, leading to asymmetric snap events. We also study the effect of an asymmetric surface pattern, and show that, for both condensation and evaporation, the droplet undergoes directional snaps imposed by the solid. This work highlights the importance of the surface involved in the process of a slow variation of the droplet volume, providing insight for the development of surface driven droplet manipulation systems.

References

[1] K.-C Park, P. Kim, A. Grinthal, N. He, D. Fox, J. C. Weaver and J. Aizenberg, Condensation on slippery asymmetric bumps, Nature 531, 78–82 (2016).
[2] G. G.Wells, E. Ruiz-Gutierrez, Y. L. Lirzin, A. Nourry, B. V. Orme, M. Pradas, and R. Ledesma-Aguilar, Snap evaporation of droplets on smooth topographies, Nat. Commun. 9, 1380 (2018).
[3] M. Ewetola, R. Ledesma-Aguilar, and M. Pradas, Control of droplet evaporation on smooth chemical patterns, Phys. Rev. Fluids 6, 033904 (2021)

Tu066

SCALING EFFECTS OF SUBSTRATE WETTABILITY AND BUBBLE POPULATION DENSITY ON POOL BOILING

Giada Minozzi[1], Alessio D. Lavino [2], Edward R. Smith [3], Tassos Karayiannis [3], Khellil Sefiane [1], Omar K. Matar [2], David Scott [1], Timm Krüger [1] & Prashant Valluri [1]

[1]*The University of Edinburgh, School of Engineering, Edinburgh EH9 3JL, UK*

[2]*Imperial College London, Department of Chemical Engineering, London SW7 2AZ, UK*

[3]*Brunel University London, Department of Aerospace and Mechanical Engineering, London UB8 3PH, UK*

Abstract Nucleate boiling, Diffuse Interface method, DNS, wettability.

Phase-change phenomena, in particular boiling, are common in many industrial applications, including the power generation plants and thermal management of micro-devices. These devices are distinguished by the high heat power density and high dissipation rate which requires a high-level thermal management, such as in space applications under microgravity and on ground applications such as radar management. Therefore, phase-change phenomena such as boiling holds promise as an efficient cooling system to ensure their reliability. Boiling performance is a function of structure and the wettability of the underlying substrate. Moreover, boiling surfaces have multiple nucleating sites. Here we investigate the effects of going from small-scale i.e. $O(1)$ nucleation sites to large-scale i.e. $O(1000)$ nucleation sites We perform direct numerical simulations using our in-house TPLS solver [1] which exploits the diffuse-interface method [2] to track the evolution of liquid-vapour interface. This method removes the stress singularity at three-phase contact line, thereby allowing imposition of a contact angle boundary condition to prescribe surface wettability [3]. This approach helps us understand the role of surface wettability on nucleate boiling heat transfer coefficient (NBHTC), bubble growth and departure. We analyse the effect of wettability on the heat transfer coefficient which is a measure of energy efficiency and of the interaction between neighbouring nucleated bubbles, as shown in Fig. 1. We evaluate this for different contact angles in multiple bubble systems to account for various industrial surfaces. We validate our simulations with our in-house nucleate boiling experiments using FC72 on silicon surfaces. We show that hydrophilic substrates enhance the NBHTC and also evaluate the residual volumes after bubble departures. To discern the relation between nucleation and wettability and formaiton of micro-layer, we use an improved hybrid-pseudopotential lattice Boltzmann method [4, 5].

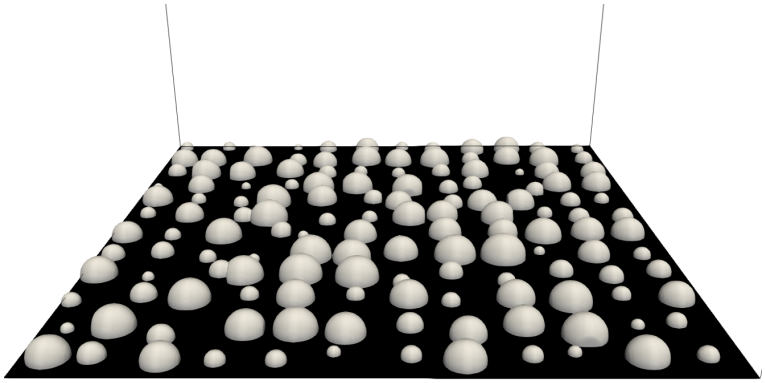

Figure 1. 3D simulation in multiple bubble system with random generation of bubble seeds.

References

[1] L. Ó Náraigh, P. Valluri, D. Scott, T. Collis, I. Bethune and P. Spelt, *TPLS: high resolution direct numerical simulation (DNS) of two-phase flows. Available at:* `https://sourceforge.net/projects/tpls/`, (2013).

[2] P. J. Saenz, K. Sefiane, J. Kim, O. K. Matar, and P. Valluri, *Evaporation of sessile drops: a three-dimensional approach*, Journal of Fluid Mechanics Vol. **772**, (2015).

[3] H. Ding, P. Spelt, *Wetting condition in diffuse interface simulations of contact line motion*, Physical Review E **75**, (2007).

[4] Q Li, Y Yu, and Z. X Wen, *How does boiling occur in lattice Boltzmann simulations?*, Physics of Fluid Vol. **32**, (2020).

[5] T. Krüger, H. Kusumaatmaja, A. Kuzmin, O. Shardt, G. Silva, E. M. Viggen, *The Lattice Boltzmann Method*, Springer Cham, (2016).

Tu067

Stability of evaporating drops comprising binary mixtures

Katie Thomson[1], George Karapetsas[2], Yutaku Kita[3], Omar Katar[4], Khellil Sefiane[1], Dani Orejon[1] & Prashant Valluri[1]
[1]*Institute for Multiscale Thermofluids, School of Engineering, University of Edinburgh, UK*
[2]*Department of Chemical Engineering, Aristotle University of Thessaloniki, Greece*
[3]*Department of Engineering, King's College London, UK*
[4]*Department of Chemical Engineering, Imperial College London, UK*

Keywords:

Abstract
The evaporation and spreading dynamics of a binary mixture sessile drop are complex due to the interplay of thermal and solutal Marangoni stresses alongside the hydrodynamic transport, evaporation, mass diffusion and capillary stress of the drop. We investigate the stability of volatile bicomponent sessile drops with high wettability comrpising ethanol-water deposited onto heated substrates (Figure 1). Our quasi-steady linear stability analysis of volatile bicomponent sessile drops demonstrates that evaporation is highly unstable with several competing modes. Whilst the analysis qualitatively agrees with the experiments, presence of multiple competing modes indicates that the quasi-steady analysis may not be fully representative and suitable for volatile bi-component sessile droplet systems. To understand the roles of these modes better, we perform a transient growth analysis of this system. Here, we apply small disturbances to the binary system base state governing equations and boundary conditions, giving perturbed stability equations that evolve with time. The lubrication approximation is used to derive our one-sided model, and the stress singularity at the contact line is avoided by including a thin precursor film. Perturbations are introduced into the system at an early time instance. These are solved alongside the base state to find the linear stability growth characteristics, in order to compare to the dispersion curves obtained from the quasi-steady state stability analysis. Similar to the findings from our quasi-steady state analysis, our results show droplet interfacial instabilities occur predominantly at the contact line. Results from our numerical stability analysis demonstrate qualitative agreement with experiments performed on volatile ethanol-water droplets on heated substrates.

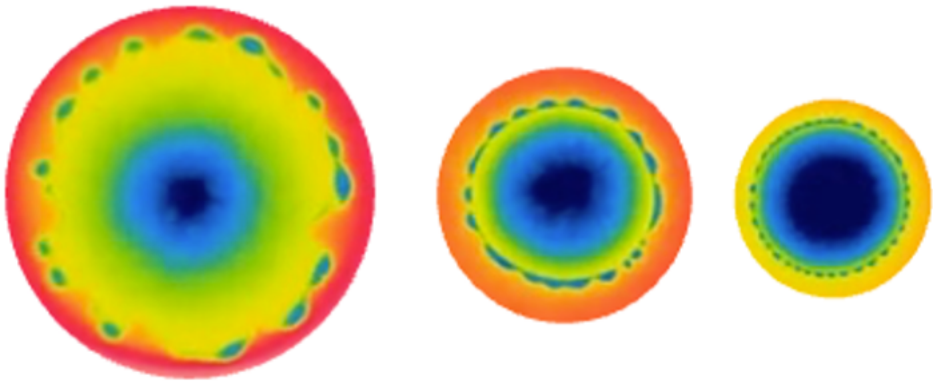

Figure 1. Experimental results for an evaporating droplet comprising a volatile binary mixture of 25, 50 and 75 wt % ethanol, respectively, and water.

Tu068

STABILIZING AN ADVERSE DENSITY DIFFERENCE ACROSS AN INTERFACE USING PHASE CHANGE

L.E. Johns[1] & R. Narayanan[1]
[1]*Department of Chemical Engineering, University of Florida, Gainesville, FL 32611, USA*

Key words : Phase Chaange, Rayleigh Taylor

Abstract
We show how to stabilize an adverse density arrangement for two phases in equilibrium in a porous solid, the heavy phase lying above the light phase in a gravitational field by heating from below with a phase change. We derive a formula for how steep the temperature gradient must be to do this. The input temperature gradient has two effects on the stability of our system. Its effect on the heat convection is destabilizing, its effect on the heat conduction at the surface is stabilizing. By directing our attention to the case of zero growth rate, we obtain the critical value of the input temperature gradient as it depends on the permeability of the porous solid, the density difference across the surface, the distance between the planes bounding our system, and the physical properties.

Our problem makes connections to the Bénard problem where it has two, one, or no critical points, and to the Rayleigh-Taylor problem where it has no critical points if surface tension were ignored.

Effect of Different Wind Velocity on Phase Transformation of Absolute Ethanol in Capillary Tube

Yuqi Ji[1], Bin Liu[1,2,3*],

[1] *Tianjin Key Laboratory of Refrigeration Technology, Tianjin University of Commerce, Tianjin 300134, China*

[2] *International Centre in Fundamental and Engineering Thermophysics, Tianjin University of Commerce, Tianjin 300134, China*

[3]*Key Lab of Agricultural Products Low Carbon Cold Chain of Ministry of Agriculture and Rural Affairs, Tianjin University of Commerce, Tianjin 300134, China*

Keywords:Evaporation, Wind speed, Meniscus, Infrared camera, Marangoni number

Abstract

Evaporation is one of the most common phenomena in nature. When the natural conditions change, the evaporation process will be significantly affected. In this paper, the evaporation process of absolute ethanol in a 1 mm inner diameter capillary tube under different wind speeds were studied experimentally. And we explore the morphology and temperature distribution of the meniscus. We use infrared camera to measure the temperature distribution of meniscus when the capillary is placed horizontally and vertically. The interesting finding is that when the capillary is placed horizontally, the slip phenomenon at the meniscus interface increases with the increase in wind speed. Therefore, at low wind speed (wind speed is lower than 0.8m/s), the intensity of the Marangoni vortex in the upstream is higher than that in the downstream, which is opposite to that at high wind speed (wind speed is higher than 0.8m/s). When the capillary is placed vertically, the shape of the meniscus does not change with the increase in wind speed. At this time, the change trend of the Marangoni number is consistent with that of the Marangoni number when the capillary is placed horizontally, but the change rate is slower. We prove the relationship between the vapor pressure difference in the capillary tube and the wind speed and Marangoni number under different wind speed conditions(0~1.5m/s). Among them, the coincidence degree is better when the wind speed is 0.2,0.3,0.4and 1.4m/s, but the accuracy is lower for other cases.

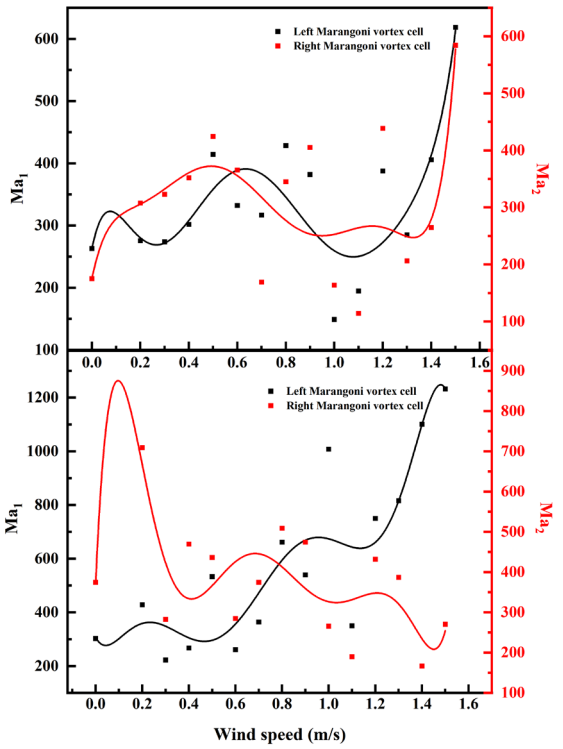

Figure 1. Placed horizontally under the capillary inside the Marangoni vortex strength.

References

[1] Buffone C. How external buoyancy controls the Marangoni convection for a volatile meniscus inside a pore[J]. International Journal of Thermal Sciences, 2019, 138: 605-611.

Tu070

EFFECT OF THE SHAPE OF POINT-HEATED WATER DROPS ON THE FLOW STABILITY

Yutaku Kita
Department of Engineering, King's College London, London, UK

Abstract The present contribution reports thermal imaging of point-heated water sessile drops revealing distinctive flow instabilities that depend on the contact angle. (Keywords: Drops, Themocapillary Instabilities, Evaporation, Contact Angle).

A millimetre-sized drop of pure water placed on a substrate in isothermal or uniformly heated conditions generally shows a gentle flow pattern mostly induced by the evaporation pronounced at the contact line. When the drop is heated locally, however, thermocapillary-induced (Marangoni) recirculating flows with oscillatory behaviour may be observed [1, 2, 3]. In the present work, we investigated experimentally the influence of drop shape e.g., contact angle on the flows induced by localised heating. Coating a thin copper substrate with different materials allowed us to obtain the contact angles varying from 70° to 150°, approximately. Localised heating was provided by a laser that heated the substrate directly below the centre of edge of the drop. Thermal activities of the drop during heating were followed with an infrared thermography from the top. Our experiments showed distinct thermal patterns on the drop interface depending on the contact angle. In particular, the thermal activity was relatively weak for a lower contact angle. If the contact angle was ca. 100°, by contrast, a pair of vigorous vortices emerged with their oscillatory behaviour. Another type of instabilities was observed for the superhydrophobic case (i.e., contact angle of 150°), where the drop itself oscillated with more complex flow structures. From the experimental observations, we propose the aspect ratio of drops has a significant impact on the flow stability for a given volume. However, we believe that it is also dependent on the volume, which we aim to explore in the near future.

References

[1] Y, Kita, A. Askounis, M. Kohno, Y. Takata, J. Kim, K. Sefiane, *Induction of Marangoni convection in pure water drops*, Applied Physics Letters **109**, 171602 (2016).
[2] A. Askounis, Y. Kita, M. Kohno, Y. Takata, V. Koutsos, K. Sefiane, *Influence of local heating on Marangoni flows and evaporation kinetics of pure water drops*, Langmuir **33**, 5666–5674 (2017).
[3] K. E. Pang, C. Cuvillier, Y. Kita, L. Ó Náraigh, *Flow stability in shallow droplets subject to localized heating of the bottom plate*, Physical Review Fluids **9**, 014003 (2024).

Tu071

ACOOLTPS – ADVANCED COOLING OF HIGH POWER MICROSYSTEMS USING TWO-PHASE FLOWS SYSTEMS IN COMPLEX GEOMETRIES

Gustavo R. Anjos[1], Daniel Barbedo[1], Prashant Valluri[2]
[1]*Universidade Federal do Rio de Janeiro, Coppe, Department of Mechanical Engineering, Rio de Janeiro, Brazil*
[2]*Institute for Multiscale Thermofluids, Chemical Engineering School of Engineering, University of Edinburgh, U.K.*

Abstract moving mesh, surface tension, finite element method, Laplace-Beltrami operator.

The present work aims at developing a new flexible computational framework based on modern programming language to simulate macro and microscale two-phase flows with dynamic boundaries in complex geometries sponsored by The Royal Society - Advanced Newton Fund. Such a technique is extremely useful for periodic and very large domains which requires exhaustive computational resources, consequently, reducing the required numerical domain. In this presentation the one-fluid interface tracking Finite Element (FE) method is used to solve the equations governing the motion of two immiscible incompressible fluids in the Arbitrary Lagrangian-Eulerian framework (ALE). The equations are written in axisymmetric coordinates; however, the proposed moving boundary technique can be extended to 3-dimensional flows and any other methods using the ALE framework such as the finite volume method (see [Anjos(2020), Anjos(2021)a, Anjos(2021)b, barbedo2024] for further details).

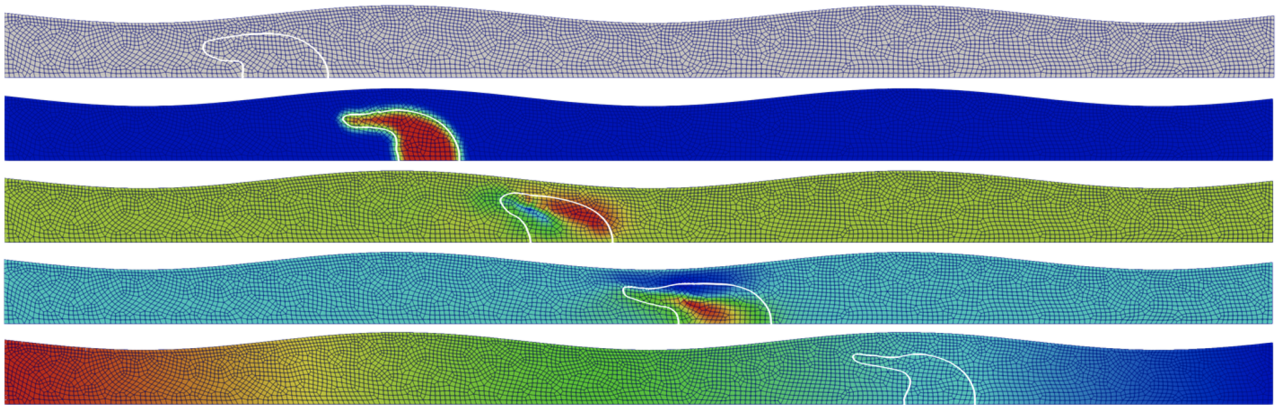

Figure 1. Snapshots of the current numerical simulation of two-phase flows using unstructured quadrilateral mesh showing 1) the fluid mesh in time t=2.2, 2) the smoothed Heaviside function in time t=5.08, 3) the vertical velocity in time $t = 8.8$, 4) the horizontal velocity in time t=12.92 and 5) the pressure field in time $t = 17.56$.

References

[Anjos(2020)] Anjos, G.R., N. Mangiavacchi, J.R. Thome, An ALE-FE method for two-phase flows with dynamic boundaries, Computer Methods in Applied Mechanics and Engineering, Vol 362 (2020)

[Anjos(2021)a] Anjos, G.R. Moving Mesh Methods for Two-Phase Flow Systems - Assessment, Comparison and Analysis, Computers and Fluids, (2021).

[Anjos(2021)b] Anjos G.R. Numerical Investigation of Two-Phase Flows in Corrugated Channel with Single and Multiples Drops. Fluids. 2021; 6(1):13. https://doi.org/10.3390/fluids6010013

[barbedo2024] Daniel B. V. Santos, Gustavo P. Oliveira, Norberto Mangiavacchi, Prashant Valluri, Gustavo R. Anjos, Numerical Investigation of Gas Bubble Interaction in a Circular Cross-Section Channel in Shear Flow, Fluids 2024, 9(2), 32; https://doi.org/10.3390/fluids9020032

Tu072

- **FLOW INSTABILITY AND DRY OUT PROFILE IN FLOW BOILING OF BINARY MIXTURES IN MICROCHANNEL UNDER LOW MASS FLUX**

Arif Widyatama[1,2], Daniel Orejon[1] & Khellil Sefiane[1]
[1] *Institute for Multiscale Thermofluids, School of Engineering, University of Edinburgh, James Clerk Maxwell Building, The King's Buildings, Edinburgh EH9 3FD, UK*
[2]*Department of Mechanical & Industrial Engineering, Faculty of Engineering, Gadjah Mada University, Jalan Grafika No.2, Yogyakarta, 55281, Indonesia*

Keywords:
Flow boiling, flow instability, binary mixtures

Abstract

Understanding the occurrence of flow boiling instability and its influence on heat transfer performance is crucial in designing microscale heat transfer devices. Particularly in the low mass flux, severe hydrodynamic fluctuations followed by temperature changes can be observed [1]. The present work aims to investigate the flow instability and dry-out characteristics during the flow boiling in a microchannel under low mass flux conditions. The experiment was conducted in a single rectangular channel (a hydraulic diameter of 606 and an aspect ratio of 20). Three different types of fluid were used as working fluid: pure water, 5% v/v ethanol/water and 5% v/v butanol/water. The flow was set on G = 15 kg m^{-2} $s^{-1,}$ and various heat fluxes were applied from 14.6 kW m^{-2} to 27.4 kW m^{-2}. First, the characteristics of flow instability were captured through flow visualisation and pressure fluctuation. Next, the dry-out regions were plotted based on the wall temperature profile and the time series evolution was recorded. It is concluded that the small addition of alcohol to the pure water can influence the flow boiling characteristics. In detail, the 5% v/v butanol/water cases produce the lowest flow fluctuation. Furthermore, the 5% v/v butanol/water cases show the smallest dry-out region.

References

[1] T. A. Kingston, J. A. Weibel, and S. V. Garimella, *High-frequency thermal-fluidic characterization of dynamic microchannel flow boiling instabilities: Part 2 – Impact of operating conditions on instability type and severity*, Int. J. Multiph. Flow **106**, 189–201 (2018).

Tu073

BOUNDS ON THE SPREADING RADIUS IN DROPLET IMPACT: THE INVISCID CASE

Alidad Amirfazli[1], Miguel Bustamante[2], Lennon Ó Náraigh[2], & Yating Hu[1]
[1]*Department of Mechanical Engineering, York University, Toronto, Ontario M3J 1P3, Canada*
[2]*School of Mathematics and Statistics, University College Dublin, Belfield, Dublin 4, Ireland*

Abstract Droplet-Impact Modelling, Applied Analysis of Differential Equations
We consider the classical problem of droplet impact and droplet spread on a smooth surface in the case of an ideal inviscid fluid. We revisit the rim-lamella model of Roisman et al. [1] . This model comprises a system of ordinary differential equations (ODEs); we present a rigorous theoretical analysis of these ODEs, and derive upper and lower bounds for the maximum spreading radius. Both bounds possess a We1/2 scaling behaviour, and by a sandwich result, the spreading radius itself also possesses this scaling. We demonstrate rigorously that the rim-lamella model is self-consistent: once a rim forms, its height will invariably exceed that of the lamella. We introduce a rational procedure to obtain initial conditions for the rim-lamella model. Our approach to solving the rim-lamella model gives predictions for the maximum droplet spread that are in close agreement with existing experimental studies and direct numerical simulations.

References

[1] Roisman, I.V., Rioboo, R. and Tropea, C., *Normal impact of a liquid drop on a dry surface: model for spreading and receding*, Proceedings of the Royal Society of London. Series A: Mathematical, Physical and Engineering Sciences, **458**, 1411–1430 (2002).

Tu074

EXPERIMENTAL STUDY ON THE ELECTROHYDRODYNAMIC INSTABILITY BETWEEN THREE IMMISCIBLE LIQUIDS FLOWING IN A MICROCHANNEL

Eda Nur Soysal[1], Sercan Altundemir[1], Abdullah Kerem Uguz[1]

[1]*Department of Chemical Engineering, Bogazici University, Istanbul, Turkey*

Keywords: Microfluidics, Electrohydrodynamic instability, Micro Droplet

Abstract

The science of microfluidics is a discipline that has provided many benefits over the past few years in biological and chemical industries due to the use of small amounts of samples, reduced cost, and faster analysis. Droplet microfluidics provide even more advantages. Applying an electric field as an external force is a preferred active method to generate mono-dispersed micro droplets in a microchannel. It is proved numerically that due to electrohydrodynamic instability between two immiscible liquids flowing in a microchannel, once the electric field is strong enough, the flat interface may deform, hitting the microchannel walls and forming droplets [1, 2]. Experimental studies have demonstrated that the formation of droplets of the second immiscible liquid was not feasible regardless of the type or direction of the applied electric field [3-5]. Eribol et al. [6] proved numerically for three immiscible liquids flowing in a microchannel under the effect of a DC electric field applied perpendicular to the flat interfaces. Furthermore, for three-phase flow, the total flow rate affects the droplet size even though the viscosity and the thicknesses of fluids are the same, contrary to two-phase flow under the effect of the electric field. The total flow rate can be easily manipulated in an experiment. The purpose of this study is to investigate the electrohydrodynamic instability of the interfaces between three immiscible liquids flowing in a microchannel under a DC electric field and verify the results demonstrated in [6]. The critical voltage, i.e., the voltage at which the interfaces start to deflect, the development of the instability, and the formation of droplets will be investigated as a function of the volumetric flow rates, the total flow rate, and the viscosities of the liquids.

References

[1] Ozan SC, Uguz AK (2017) Nonlinear evolution of the interface between immiscible fluids in a micro channel subjected to an electric field. Eur Phys J Spec Top 226:1207.
[2] A. Kerem Uguz, N. Aubry (2008) Quantifying the linear stability of a flowing electrified two-fluid layer in a channel for fast electric times for normal and parallel electric fields. Physics of Fluids 1 September; 20 (9): 092103.
[3] Eribol, P., Uguz, A. (2015). Experimental investigation of electrohydrodynamic instabilities in micro channels. Eur. Phys. J. Spec. Top. 224, 425–434.
[4] O. Ozen, N. Aubry, D.T. Papageorgiou, and P.G. Petropoulos (2006), Monodisperse drop formation in square microchannels, Phys. Rev. Lett. 96, 144501.
[5] Altundemir S, Eribol P, Uguz A (2018) Droplet formation and its mechanism in a microchannel in the presence of an electric field. Fluid Dyn Res 50:051404.
[6] Eribol P., Kaykanat S., Ozan S. C., Uğuz, K., (2022), Electrohydrodynamic instability between three immiscible fluids in a microchannel: lubrication analysis. Microfluidics and Nanofluidics. 26.

Tu084

WHAT LEADS TO STOKES DRIFT?

Anirban Guha[1], & Akanksha Gupta[2]
[1]*School of Science & Engineering, University of Dundee, UK*
[2]*Scripps Institution of Oceanography, University of California San Diego, USA.*

Abstract Stokes drift, Lagrangian drift, water waves.

In a generic way, Stokes drift is defined as the difference between wave-averaged velocity following a particle (i.e. Lagrangian) and that in a fixed reference frame (i.e. Eulerian). The current physical understanding of Stokes drift is as follows [1]: "*A fluid particle, which oscillates backwards and forwards due to the linear wave motion, spends more time in the forward-moving region underneath the crest than in the backwards-moving region underneath the trough and undergoes its forward motion at a greater height, where the velocities are larger.*" However, these qualitative arguments have not been backed by mathematical statements. The goal of this work is to provide mathematical estimates so as to answer the fundamental question – "what leads to Stokes drift"? Although overwhelmingly understood for water waves, Stokes drift is a generic mechanism that stems from kinematics and occurs in any non-transverse wave in fluids. To showcase its generality, we undertake a comparative study of the pathline equation of sound (1D) and intermediate-depth water (2D) waves. Although we obtain a closed-form solution $\mathbf{x}(t)$ for the specific case of linear sound waves, a more generic and meaningful approach involves the application of asymptotic methods and expressing variables in terms of the Lagrangian phase θ. We show that the latter reduces the 2D pathline equation of water waves to 1D. Using asymptotic methods, we solve the respective pathline equation for sound and water waves, and for each case, we obtain a parametric representation of particle position $\mathbf{x}(\theta)$ and elapsed time $t(\theta)$. Such a parametric description has allowed us to obtain second-order-accurate expressions for the time duration, horizontal displacement, and average horizontal velocity of a particle in the crest and trough phases. All these quantities are of higher magnitude in the crest phase in comparison to the trough, leading to a forward drift, i.e. Stokes drift. We also explore particle trajectory due to second-order Stokes waves and compare it with linear waves. While finite amplitude waves modify the estimates obtained from linear waves, the understanding acquired from linear waves is generally found to be valid.

References

[1] Van den Bremer, T. S. and Breivik, Ø, *Stokes Drift*, Philos. Trans. R. Soc. A **376**, 20170104 (2017).

Tu085

DYNAMIC LIQUID-LIQUID INTERFACES OF AQUEOUS PHASE-SEPARATING SYSTEMS

Ho Cheung Shum[1,2]
[1] *Department of Mechanical Engineering, The University of Hong Kong, Pokfulam Road, Hong Kong*
[2] *Advanced Biomedical Instrumentation Centre, Hong Kong Science Park, Shatin, New Territories, Hong Kong*

Keywords:Aqueous phase separation, aqueous liquid-liquid interfaces

Abstract

Aqueous phase separation has been increasingly recognized as an important process in cell biology. By regulating and redistributing macromolecules in water, immiscible aqueous solution phases can be formed. The resultant interfaces between immiscible aqueous phases have a few unique properties, such as ultralow interfacial tension, re-mixing upon dilution, osmotic flows across interfaces and accessibility to water-soluble molecules. These together with the microscaled precision in manipulating fluids facilitate understanding of hydrodynamic behaviors of fluids and interfacial phenomena associated with ultralow interfaces. The ease in inducing phase separation also enables investigation of hydrodynamic flows coupled with phase separation dynamics. In this talk, I will introduce aqueous two-phase systems, where phase behaviors can be controlled. Remarkable two-phase behaviors, such as droplet [1] and jet [2] breakup, as well as Marangoni flows [3] and colloidal assemblies [4-5], can be observed. The interfaces can also be used for assembling macromolecules in highly versatile manners, resulting in fluidic and materials structures with unique features [6-7]. In summary, aqueous phase separation and aqueous two-phase flows can lead to fascinating dynamics, offering model systems to other more complex phase-separating multiphase flows.

References

[1] Hau Yung Lo, Yuan Liu, Sze Yi Mak, Zhuo Xu, Youchuang Chao, Kaye Jiale Li, Ho Cheung Shum and Lei Xu, Diffusion-dominated Pinch-off of Ultralow Surface Tension Fluids. *Physical Review Letters*, **123:** 134501 (2019).
[2] Jingxuan Tian, Neil Ribe, Xiaoxiao Wu and Ho Cheung Shum, Steady and Unsteady Buckling of Viscous Capillary Jets and Liquid Bridges. *Physical Review Letters*, **125**: 104502 (2020).
[3] Yang Xiao, Neil M Ribe, Yage Zhang, Yi Pan, Yang Cao and Ho Cheung Shum, Generation of Fermat's spiral patterns by solutal Marangoni-driven coiling in an aqueous two-phase system. *Nature Communications*, **13**: 7206 (2022).
[4] Chang Li, Yafeng Yu, Huizeng Li, Jingxuan Tian, Wei Guo, Yanting Shen, Huanqing Cui, Yi Pan, Yanlin Song and Ho Cheung Shum, One-Pot Self-Assembly of Dual-Color Domes Using Mono-Sized Silica Nanoparticles. *Nano Letters*, **22**: 5236 (2022).
[5] Chang Li, Yafeng Yu, Huizeng Li, Haisong Lin, Huanqing Cui, Yi Pan, Ruotong Zhang, Yanlin Song and Ho Cheung Shum. Heterogeneous Self-Assembly of a Single Type of Nanoparticle Modulated by Skin Formation. *ACS Nano*, **17**: 11645 **(**2023).
[6] Youchuang Chao, Sze Yi Mak, Shakurur Rahman, Shipei Zhu and Ho Cheung Shum, All-Aqueous Emulsions: Generation of High-Order All-Aqueous Emulsion Drops by Osmosis-Driven Phase Separation. *Small*, **14**: 7 (2018).
[7] Yuan Liu , Jack Hau Yung Lo , Janine K Nunes , Howard A Stone, and Ho Cheung Shum, High-throughput measurement of elastic moduli of microfibers by rope coiling. *PNAS*, accepted (2024).

Tu086

DRIVEN SHOCK IN THREE DIMENSIONS : EULER EQUATION VERSUS MOLECULAR DYNAMICS, AND NAVIER-STOKES EQUATION

Amit Kumar[1,2], R. Rajesh[1,2]
[1]*The Institute of Mathematical Sciences, C.I.T. Campus, Taramani, Chennai 600113, India*
[2]*Homi Bhabha National Institute, Training School Complex, Anushakti Nagar, Mumbai 400094, India*

Abstract Isotropic and continuous localised perturbations in a stationary gas, created by an external point source, cause a spherically symmetric shock wave with the energy $E(t)$ increasing in time t as $E(t) \sim t^{\delta}$, where $\delta \geq 0$. The analytical solution of the Euler equation providing the spatio-temporal behavior of the shock wave, is a classic problem in gas dynamics. The exact solution shows that the asymptotic behavior of non-dimensionalised thermodynamic quantities, near the shock center, obey power law behavior in rescaled distance with the exponents independent of δ [1] . However, using Event Driven Molecular Dynamics Simulations, we find that the exact solution does not match with EDMD results, anywhere, mainly in terms of the power law exponents near the shock center. We show that this mismatch is due to ignoring the contribution of heat conduction and viscosity terms, and the mismatch between theory and numerics can be resolved by taking into account the Navier-Stokes equation. We showed that the direct numerical solution of Navier-Stokes equation captures these observed power law exponents in the EDMD simulations indicating the significance of viscosity and heat conduction in shock problems.

References

[1] V. I. Dokuchaev, *Self-similar spherical shock solution with sustained energy injection*, Astronomy & Astrophysics **395**, 1023–1029 (2002).

Tu087

FARADAY WAVES IN THIN CONTAINERS: A FLOQUET ANALYSIS

Alessandro Bongarzone [1], Baptiste Jouron[1], Francesco Viola[2] & François Gallaire[3]
[1]*Laboratory of Fluid Mechanics and Instabilities, École Polytechnique Fédérale de Lausanne, Switzerland.*
[2]*Gran Sasso Science Institute, Viale F. Crispi 7, 67100 L'Aquila, Italy*

Abstract Faraday waves, dynamic contact angle, Womersley flow, Floquet analysis

Recent experiments in Hele-Shaw cells have expanded our understanding of Faraday waves [1] revealing a novel form of highly localized standing waves termed oscillons, characterized by their steep and solitary-like nature [2]. However, existing theoretical analyses of Faraday waves in Hele-Shaw cells rely on the Darcy approximation and assume a parabolic flow profile in the narrow direction, which is known to be inaccurate when convective or unsteady inertial effects are important. In this work, we introduce a gap-averaged Floquet theory that incorporates inertial effects induced by the unsteady terms in the Navier-Stokes equations [3], a scenario that corresponds to a pulsatile flow where the fluid motion reduces to a two-dimensional oscillating Poiseuille flow, similarly to the Womersley flow in arteries. Upon gap-averaging the linearised Navier-Stokes equation, this results in a modified damping coefficient dependent of the ratio between the Stokes boundary layer thickness and the cell's gap, and whose complex value depends on the frequency of the wave response specific to each unstable parametric region. Initially, we revisit the standard case of horizontally infinite rectangular Hele-Shaw cells by also accounting for a dynamic contact angle model. A comparison with existing experiments shows the predictive improvement brought by the present theory and points out how the standard gap-averaged model often underestimates the Faraday threshold. The analysis is then extended to the less conventional case of thin annuli. A series of dedicated experiments for this configuration highlights how Darcy's thin-gap approximation overlooks a frequency detuning that is essential to correctly predict the locations of the Faraday tongues in the frequency-amplitude parameter plane. These findings are systematically explained and captured by the present model [4]. Additionally, a detailed examination of experimentally observed meniscus and contact angle dynamics highlights the importance of the out-of-plane curvature, which is generally neglected in the literature. This evidence justifies the use of a dynamical contact angle model to account for the extra contact line dissipation, closing the gap with experimental measurements.

Figure 1. Snapshot of the wave pattern experimentally observed within a thin annular container for a subharmonic Faraday tongues associated with the azimuthal wavenumber $m = 5$.

References

[1] M. Faraday, *On the forms and states assumed by fluids in contact with vibrating elastic surfaces.*, Phil. Trans. R. Soc. Lond. **121**, 319-340 (1831).
[2] J. Rajchenbach, A. Leroux and D. Clamond, *New standing solitary waves in water*, Phys. Rev. Lett. **107**2, 024502 (2011).
[3] F. Viola, F. Gallaire, and B. Dollet, *Sloshing in a Hele-shaw cell: experiments and theory*, J. Fluid. Mech. **831**, R1 (2017).
[4] A. Bongarzone, B. Jouron, F. Viola and F. Gallaire, *A revised gap-averaged Floquet analysis of Faraday waves in Hele-Shaw cells*, J. Fluid. Mech. **977**, A45 (2023).

Tu088

ELECTROKINETIC DYNAMICS AND RESONANCE WHEN ELECTRICAL DOUBLE LAYERS ENTANGLE WITH SURFACE ACOUSTIC WAVES

Ofer Manor, Oles Dubrovsky & Sudeepthi Aremanda
Department of Chemical Engineering, Technion - Israel Institute of Technology, Haifa, Israel

Abstract Electrokinetics, electrical double layer, surface acoustic wave, boundary layer flow, acoustic flow

We capture ion dynamics in electrical double layers (EDLs) using an evanescent mechanical wave (or a spatiotemporal periodic boundary layer flow) in an electrolyte solution, which is generated by a MHz-frequency surface acoustic wave (SAW), a mechanical Rayleigh wave in a neighboring solid; the interaction is a reminiscent of field effects.

EDLs of ions are a surface phenomenon. They appear at the interface between charged surfaces and electrolyte solutions and are one of the most fundamental and abundant mechanisms on earth. They give rise to the complexity of biology and to life as well as to countless industrial processes and products from water desalination to shampoo, toothpaste, and super-capacitors. Measuring steady and quasi-steady EDL properties are commonplace. However, the EDL Debye length, measured in nanometers, and the intrinsic ion relaxation time through the EDL's Debye length, measured in nanoseconds, have made measurements of ion dynamics inside isolated transient EDLs elusive.

A previous theory [1] suggests that surface acoustic waves generate an evanescent wave that vibrates ions in EDLs to result in the emission of electrical fields. At MHz to GHz SAW frequency, the evanescent wave appears at similar length and time scales to the ones of ion motion in EDLs; existing at the same space and time, they become entangled. Ions in the EDL diffusive layer vibrate at the exciting SAW frequency and its harmonics and support a same frequency leakage of AC (alternating) electrical field off the EDL that we measure. Moreover, a SAW excitation frequency comparable to the inverse of an ion relaxation time supports electro-mechanical ion resonance. The latter maximizes ion vibration and the magnitude of the electrical field leakage, rendering ion-specific relaxation times measurable, giving the intrinsic rate of EDL charge and discharge by specific ions, and showing that a dynamic EDL is much more than a capacitor. [2]

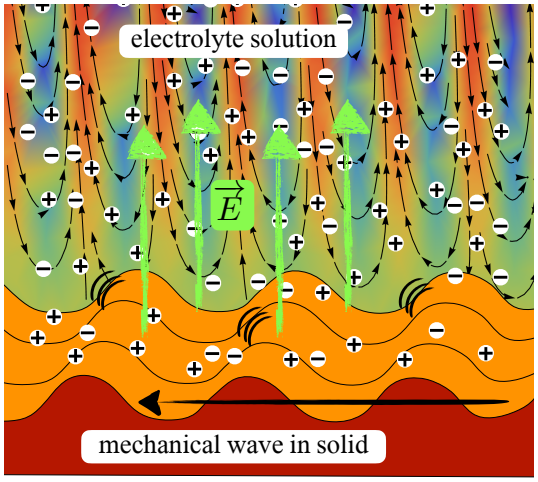

Figure 1. Positive (+) and negative (–) ions vibrate in an electrical double layer (EDL), which emanates from a solid substrate that supports a MHz-frequency traveling surface acoustic wave (SAW). The SAW dynamically perturbs ion positions, resulting in the leakage of an electrical field off the near-equilibrium EDL, where red and blue indicate fast and slow advective ion motion within the evanescent SAW viscous penetration length in the solution [3].

References

[1] O. Dubrovski and O. Manor, *Revisiting the electroacoustic phenomenon in the presence of surface acoustic waves*, Langmuir, **37**, 14679–14687 (2021)
[2] S. Aremanda and O. Manor, *Measurements of Ion Dynamics and Electro-Mechanical Resonance in an Electrical Double Layer near a Surface Acoustic Wave*, J. Phys. Chem. C, **127**, 20911–20918 (2023)
[3] O. Manor, L.Y. Yeo, and J.R. Friend, *The appearance of boundary layers and drift flows due to high-frequency surface waves*, J. Fluid Mech., **707**, 482–495 (2012)

Tu089

HORSESHOE VORTEX AROUND A MICRO PILLAR GOVERNED BY SPONTANEOUS MENISCUS FORMATION

Kogen Ozawa[1], Hayate Nakamura[1], Kenta Shimamura[1], Georg F. Dietze[2], Harunori N. Yoshikawa[3], Farzam Zoushtiagh[4], Kizuku Kurose[5] & Ichiro Ueno[6]

[1] *Division of Mechanical & Aerospace Engineering, School of Science &Technology, Tokyo University of Science, Chiba, Japan*

[2] *FAST, CNRS, Université Paris-Saclay, Orsay, France*

[3] *Institut de Physique de Nice, CNRS, Université Côte d'Azur, CNRS, Nice, France*

[4] *IEMN, CNRS, Univ. Lille, Lille, France*

[5] *Faculty of Engineering, Division of Systems Research, Yokohama National University, Kanagawa, Japan*

[6] *Department of Mechanical & Aerospace Engineering, Faculty of Science & Technology, Tokyo University of Science, Chiba, Japan*

Keywords: Horseshoe vortex, capillary-driven, meniscus

Abstract Horseshoe vortices are widely considered to emerge around large-scale obstacles, such as bridge pillars, due to an inertia-driven adverse pressure gradient forming on the upstream-side of the obstacle [1, 2]. That is, the necessary condition to induce the horseshoe vortex had been considered in terms of the Reynolds number $\mathrm{Re} = UL/\nu \gg 1$, where U and L are the characteristic velocity and length, respectively, and ν is the kinematic viscosity. A similar flow structure can emanate in thin-film Stokes flow around micro-obstacles of $\mathcal{O}(10\,\mu\mathrm{m})$ [3], such as used in textured surfaces to improve wettability under the capillary-dominant conditions of the Reynolds number $\mathrm{Re} = \mathcal{O}(10^{-3}) \ll 1$ and of the capillary number $\mathrm{Ca} = \mathcal{O}(10^{-5}) \ll 1$ [4, 5]. The flow structure within the liquid meniscus forming at the foot of the micro-pillar evinces a horseshoe vortex wrapping around the obstacle (Fig. 1 (i)), notwithstanding that the Reynolds number in the system is extremely low. Here, the adverse pressure gradient driving flow reversal near the bounding wall is caused by capillarity instead of inertia in the meniscus formation process (Fig. 1 (ii)). The horseshoe vortex is entangled with other v

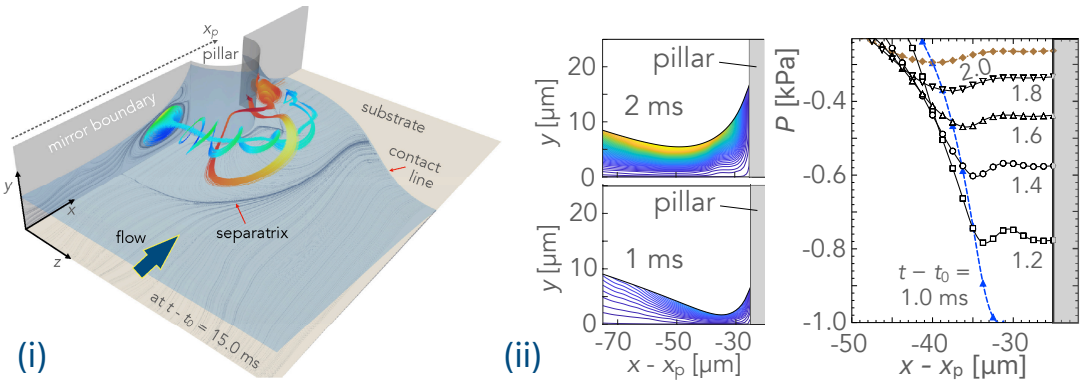

Figure 1. (i) Horseshoe vortex (HSV) forming around a cylindrical micro-pillar (diameter $d_\mathrm{p} = 50\,\mu\mathrm{m}$ and a static contact angle $\theta_\mathrm{p} = 20^\circ$) engulfed by a liquid film spreading on a smooth substrate ($\theta_\mathrm{s} = 5^\circ$), and (ii) Meniscus formation (left) and corresponding pressure distribution on substrate (right) in upstream side of micropillar.

References

[1] C.J. Baker, *The laminar horseshoe vortex*, J. Fluid Mech. **95**, 347–367 (1979).

[2] G. Launay, E. Mignot, N. Riviere, R. Perkins, *An experimental investigation of the laminar horseshoe vortex around an emerging obstacle*, J. Fluid Mech. **830**, 257–299 (2017).

[3] K. Ozawa, H. Nakamura, K. Shimamura, G.F. Dietze, H.N. Yoshikawa, F. Zoueshtiagh, K. Kurose, L. Mu, I. Ueno, *Capillary-driven horseshoe vortex forming around a micro-pillar*, J. Colloid & Interface Science **642**, 227–234, 2023.

[4] L. Mu, D. Kondo, M. Inoue, T. Kaneko, H.N. Yoshikawa, F. Zoueshtiagh, I. Ueno, *Sharp acceleration of a macroscopic contact line induced by a particle*, J. Fluid Mech. **830**, R1 (2017).

[5] H. Nakamura, T. Ogawa, M. Inoue, T. Hori, L. Mu, H.N. Yoshikawa, F. Zoueshtiagh, G. Dietze, T. Tsukahara, I. Ueno, *Pumping effect of heterogeneous meniscus formed around spherical particle*, J. Colloid & Interface Science **562**, 133–141 (2020).

Tu090

PERIODIC EXCITATION OF WAVES IN A WATER FILLED ANNULAR CHANNEL WITH A SUBMERGED HILL

Ion Dan Borcia[1] , Franz-Theo Schön[2], Uwe Harlander[2], Rodica Borcia[1],
Michael Bestehorn[1] & Sebastian Richter[1]

[1] *Institut für Physik, Brandenburgische Technische Universität Cottbus–Senftenberg, Germany*
[2] *Dept. Aerodynamics and Fluid Mechanics, Brandenburgische Technische Universität Cottbus–Senftenberg, Germany*

Abstract Keywords: water waves, sloshing, submerged hill.

A large annular channel is filled with water [1]. The channel is placed on a rotating table that oscillates harmonically in azimuthal direction. In place of a barrier [2], a submerged hill is placed on the channel bottom, acting as wave maker. Two cases are investigated. For a symmetric hill the waves become also symmetric after few oscillations; in contrast, if the hill is asymmetric, the resulting waves will be stronger in one direction. We found that wave pattern and amplitude are strongly dependent on the excitation frequency (see Figure 1). We present resonance curves of the mean square of the water surface deflection. The curves show maxima for multiples of the fundamental resonance frequency $fr = c_0/(2L)$ where c_0 is the shallow water wave velocity. The value of the ratio between hill height and undisturbed water level $\delta_{hill} = h_{hill}/h_0$ influences the relative height of the even modes due to wave transmission and the odd modes due to reflection.

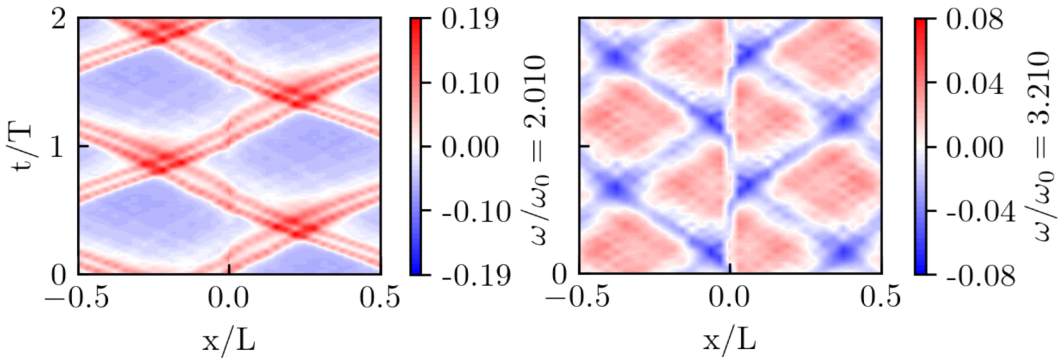

Figure 1. Space-time plots from experiment for two excitation frequencies, harmonic excitation and symmetric submerged hill.

References

[1] I.D. Borcia, R. Borcia, Rodica, W. Xu, M. Bestehorn, S. Richter, U. Harlander, *Undular bores in a large circular channel*, European Journal of Mechanics - B/Fluids **79**, 67–73 (2020).

[2] I.D. Borcia, S. Richter, R. Borcia, F.-T. Schön, U. Harlander, M. Bestehorn, *Wave propagation in a circular channel: sloshing and resonance*, The European Physical Journal Special Topics **232**, 461–468 (2023).

Tu091

PERTURBATION THEORY FOR METAL PAD ROLL INSTABILITY IN RECTANGULAR REDUCTION CELLS

Pranav Hegde[1] & Gerrit Maik Hortsmann[1]
[1]*Institute of Fluid Mechanics, Helmholtz-Zentrum Dresden-Rossendorf, Bautzner Landstr. 400, 01328 Dresden, Germany*

Abstract Metal Pad Roll Instability, Magnetohydrodynamics, Wave Dynamics .

Magnetic field-induced interfacial wave instabilities can occur as an undesired attribute in aluminum reduction cells (ARCs) [1], which must be controlled for maintaining a stable electrolytic process, and are also a limiting factor for the scale-up of liquid metal batteries (LMBs) [2]. Both technologies are physically related and can be described as stably stratified two- or three-layer systems consisting of molten salts and liquid metals. Also, both systems carry strong cell currents, which inevitably cause Lorentz forces in interaction with accompanying or external magnetic fields. These Lorentz forces can destabilize the freely moving interfaces between the layers and cause interfacial wave motions close to gravity waves. Particularly important in this regard is the so-called metal pad roll (MPR) instability, which arises from the interaction of horizontal compensating currents with vertical external magnetic fields and manifests itself by usually rotating wave motions in the interface as shown in Figure 1, which grow exponentially under unstable conditions.

Recently, a new perturbation approach for predicting MPR stability onsets and growth rates in cylindrical reduction cells [1] and cylindrical LMBs [3] was developed, which, in contrast to previous studies, avoids the shallow-water approximation, contains the capillary wave limit and takes viscous and magnetic damping into account. The theory was successfully applied for benchmarking different multiphase magnetohydrodynamic solvers and allowed for the precise delineation of linear stability and wave regimes. However, the cylinder geometry is artificial in the context of ARCs and can rather be understood as an academic example. This is precisely our starting point and we apply the same perturbational technique to rectangular cells better representing industrial ARCs. The MPR instability is far more intricate in rectangular geometries as stability onsets are largely determined by the lateral aspect ratio and several pairs of different transverse wave modes can be destabilized.

In this talk we will present explicit analytical expressions for stability onsets, MPR growth rates as well as viscous and magnetic damping rates for arbitrary wave pairs that can be destabilized. Compared to previous models, this makes our description much more accessible and directly applicable. We validate our model with numerical simulations carried out with OpenFOAM and also compare our predictions with former wave models by [4] and [5] in the shallow-water limit. However, the main value of our model resides in its applicability outside the shallow-water regime, because both existing [6] (but so far overlooked) and planned MPR experiments were/will be mostly conducted in non-shallow regimes. The theory can therefore serve as a quantitative benchmark for future MPR model experiments.

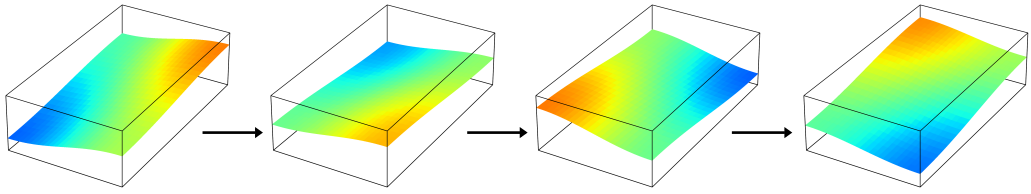

Figure 1. Illustration of a rotating metal pad in a rectangular cell.

References

[1] W. Herreman, C. Nore, J.-L. Guermond, L. Cappanera, N. Weber and G. M. Horstmann, *Perturbation theory for metal pad roll instability in cylindrical reduction cells*, J. Fluid Mech., **878**, pp. 598–646, Nov. 2019, doi: 10.1017/jfm.2019.642.

[2] G. M. Horstmann, N. Weber and T. Weier, *Coupling and stability of interfacial waves in liquid metal batteries*, J. Fluid Mech., **845**, pp. 1–35, Jun. 2018, doi: 10.1017/jfm.2018.223.

[3] W. Herreman, L. Wierzchalek, G. M. Horstmann, L. Cappanera and C. Nore, *Stability theory for metal pad roll in cylindrical liquid metal batteries*, J. Fluid Mech., **962**, A6, Mar. 2023, doi: 10.1017/jfm.2023.238

[4] P. A. Davidson and R. I. Lindsay, *Stability of interfacial waves in aluminium reduction cells*, J. Fluid Mech., **362**, pp. 273–295, May 1998, doi: 10.1017/S0022112098001025.

[5] G. Politis and J. Priede, *Fractality of metal pad instability threshold in rectangular cells*, J. Fluid Mech., **915**, p. A101, May 2021, doi: 10.1017/jfm.2021.100.

[6] I. D. Borisov, S. A. Poslavskii and J. I. Rudnev, *Experimental study of wave processes in a two-layer system of immiscible current-carrying liquids*, Prikladnaja Gidromehanika, **12** (1), p. 3-10, 2010

Tu092

Analyzing the survivability and investigating hydrodynamic nonlinearities in submersible buoy shaped point absorber wave energy converter

Brathikan VM[1], Kalanithi S[2], Janarthanan V[2]
[1]*Department of Renewable Energy, University of Edinburgh,UK.*
[2]*Department of Mechanical Engineering, Kumaraguru College of Technology, Coimbatore, India.*

Keywords:
Stability, CFD analysis, Significance of metacentre during various environmental conditions.

Abstract
The ocean has the most abundant energy reservoir in the world because it occupies 70% of the world. Despite being researched for decades, wave energy converters are still uneconomical for implementation due to various reasons, one of which is their robust need for survivability characteristics. The survivability properties of the wave energy convertors are used to protect the device in extreme environmental conditions wherein the device has to undergo these boundaries but can't generate power. Designing a wave energy converter that reduces the need for survivability and robustness will reduce the cost of the converter, which makes wave energy harvesting companies design submersible wec's. This study deals with understanding the reliability of WEC by studying the pressure encountered by the structure submerged in the water. The paper focuses on studying the forces exerted on the surface of a buoy-shaped point absorber-based wave energy convertor in shallow, transitional, and deep water regions of the water body when the structure is semi-submerged and fully submerged for different metacentres of the wec. This will help in understanding the implications of hydrodynamic nonlinearities on the stability of WEC for maximum energy harvest. The results of this time domain analysis will help to further understand the complex interactions between the structures of the WEC through frequency domain analysis.[1], [2]

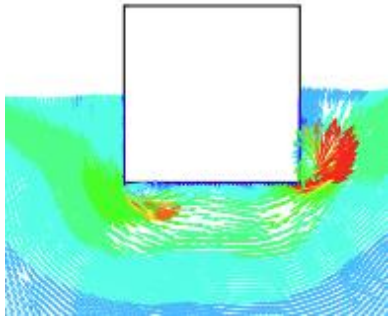

Figure 1. Flow Fields around the Bouy at wave cycle[3]

References

[1] C. V. Amaechi and J. Ye, "An Investigation on the Vortex Effect of a CALM Buoy under Water Waves Using Computational Fluid Dynamics (CFD)," *Inventions*, vol. 7, no. 1, p. 23, Feb. 2022, doi: 10.3390/inventions7010023.

[2] J. Palm, C. Eskilsson, G. M. Paredes, and L. Bergdahl, "Coupled mooring analysis for floating wave energy converters using CFD: Formulation and validation," *International Journal of Marine Energy*, vol. 16, pp. 83–99, Dec. 2016, doi: 10.1016/j.ijome.2016.05.003.

[3] X. Zhang, Q. Zeng, and Z. Liu, "Hydrodynamic Performance of Rectangular Heaving Buoys for an Integrated Floating Breakwater," *J Mar Sci Eng*, vol. 7, no. 8, p. 239, Jul. 2019, doi: 10.3390/jmse7080239.

Tu093

INTEGRATING MACHINE LEARNING WITH CFD FOR ACCURATE PREDICTION OF NUSSELT NUMBER IN WALL JET IMPINGEMENT

Harshita Agarwal[1], Atharva Lagwankar[1], Lakshya Chaplot[1], Abhilash Chandy[1]
[1]*Department of Mechanical Engineering, Indian Institute of Technology Bombay, Mumbai, India*

Keywords: compressible flow, Nusselt number, machine learning, regression, wall jet impingement

Abstract

Jet impingement is a widely employed technique in heat transfer applications for its efficiency, both in free and confined configurations, particularly in contexts requiring high heat flux [1]. This method is prevalent across diverse domains, including gas turbine engine cooling, metalworking mills operations, fabric and paper manufacturing processes, and electronic component cooling. [2] explored the effect of jet pulsation on wall jet flow and Nusselt number (Nu), but practical constraints limited the range of experimental iterations. The study kept Reynolds number (Re) and nozzle-to-plate separation (L/D), a constant, varying only the pulsating frequency. Another study analyzed the effect of nozzle profile on Nu in a subsonic turbulent air jet, producing correlations for parameters like Mach number (Ma), Re, and L/D, within the impingement region, with approximately 10% margin of error [3]. However, the absence of specific correlations for compressible wall jet flows requires using existing correlations for incompressible wall jet flows, despite resulting in deviations of up to 15% from experimental data [3]. These correlations are defined by piecewise functions for impingement, transition, and wall jet regions. Prior CFD investigations focused on impinging wall jets [4, 5]. However, they mainly used either steady turbulent ([4]) or incompressible models [5], limiting their applicability and relevance to industrial contexts.

This study aims to develop a CFD model capable of accurately simulating compressible air impingement on a stationary wall. Validation will cover stagnation Nu, centerline velocity, and wall shear stress, to ensure the model's robustness in capturing turbulent characteristics. Parameters like L/D, nozzle inlet Re, nozzle inlet Ma, and pulsation frequency (represented by the Strouhal number (St)); will be systematically varied to study their impact on heat transfer. Additionally, the study will compile data from multiple CFD simulations to train a machine learning-based regression model, mapping Nu to input parameters (Re, Ma, St, L/D), offering a unified and more accurate means of predicting Nu across the entirety of the wall jet domain. The innovative approach promises expedited design considerations, reducing the computation time required for Nu determination significantly.

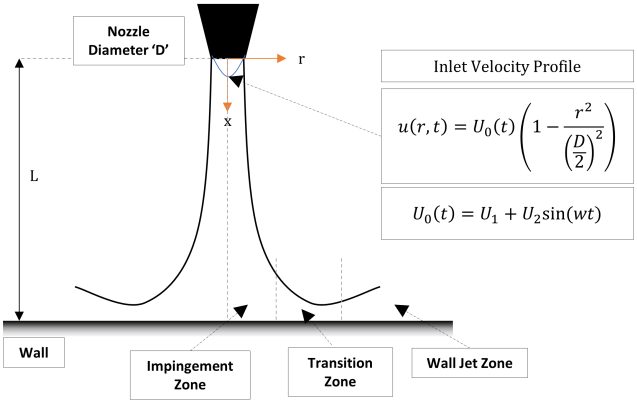

Figure 1. Schematic of the jet

References

[1] M. A. Ebadian and C. X. Lin, "A review of high-heat-flux heat removal technologies," J Heat Transfer, vol. 133, no. 11, Nov. 2011
[2] A. Mishra, H. Yadav, L. Djenidi, and A. Agrawal, "Effect of pulsation on the wall jet flow in the near region of an impinging jet," Exp Fluids, vol. 62, no. 8, pp. 1–19, Aug. 2021
[3] R. Vinze, S. Chandel, M. D. Limaye, and S. V. Prabhu, "Effect of compressibility and nozzle configuration on heat transfer by impinging air jet over a smooth plate," Appl Therm Eng, vol. 101, pp. 293–307, May 2016
[4] M. Shademan, R. Balachandar, and R. M. Barron, "ARTICLE CFD analysis of the effect of nozzle stand-off distance on turbulent impinging jets"
[5] E. Pulat and E. Beyazoglu, "Computational investigation of confined wall inclination effects on impinging jet fluid flow and heat transfer," International Journal of Thermal Sciences, vol. 163, p. 106749, May 2021

DAY 3 – Wednesday, 26 June 2024 Morning Sessions			
09:00	**Keynote 5: Prof George Karapetsas** ***Chair: Dr Khushboo Pandey*** ***Larch Lecture Theatre***		
	Instabilities & Bifurcations 5 ***Chair: Prof Stephen Shaw*** ***Larch Lecture Theatre***	***Jets, Turbulence & Transition*** ***Chair: Prof Alexander Morozov*** ***Yew Lecture Theatre***	***Bubbles, Threads & Films 1*** ***Chair: Prof Camille Duprat*** ***Elm Lecture Theatre***
09:45	W094: Energy harvesting regimes of a three-dimensional flapping flag: a numerical investigation *by B Nagy, S. Olivieri, R. Verzicco, F. Viola*	W110: The effects of wall compliance on the stability of jets and wakes *by R Poole*	W126: Galloping bubbles *by JH Guan, SI Tamim, CW Magoon, P Sáenz,*
10:00	W095: Experimental analysis of Saffman–Taylor instability in Hele-Shaw cell using photoelastic technique *by M Kawaguchi, Y Yokoyama, WKA Worby, RX Suzuki, Y Nagatsu, Y Tagawa*	W111: Stable production of fluid jets with arbitrarily small diameters via tip streaming *by JM Montanero, M Rubio, J Eggers, MA Herrada*	W127: How can a surfactant affect bubble bursting? *By EJ Vega, JM Montanero*
10:15	W096: Suppression of Marangoni-driven dry-out using parametric forcing *by IB Ignatius, B Dinesh, GF Dietze, R Narayanan*	W112: Numerical investigation on the formation of side-jets in light jets *by L Walter, J Fontane, G Nastro, D Donjat, O Léon*	W128: Cavitation microstreaming induced by pendent and sessile bubbles in water under confinement *by V Karma, S Pushpavanam,*
10:30	W097: Elastic instability in microserpentine channel at low Reynolds numbers by *YA Degirmenci, A Senyurek, L Biancofiore, K Nolan*	W113: Transition to turbulence in the stokes boundary layer. Part 1: Minimal seeds *by TS Eaves*	W129: Evolution of the surfactant monolayer in a bubble rising in water with traces of surfactant *by D Fernández-Martínez, JM Montanero, JM López-Herrera, MA Herrada*
10:45	W098: Temporal stability analysis of spiral Couette flow for small radius ratio *by MK Khandelwal*	W114: Transition to turbulence in the stokes boundary layer. Part 2: edge states *by J Sandoval, TS Eaves*	W130: Rayleigh-Plateau instability of surfactant-laden liquid nano-threads *by L Carnevale, P Deuar, Z Che, PE Theodorakis*
11:00	**Coffee Break (Alder Lecture Theatre)**		
	Gold Sponsor: Dantec Dynamics Talk, Alder Lecture Theatre (11:05 to 11:25)		
11:30	W099: Primary instability in the wake of polygonal cylinders *by A Marshall, L Gan, D Sims-Williams*	W115: Internal wave instabilities and transition to turbulence in large aspect ratio domains *by I Sibgatullin, S Elistratov, T Dauxois*	W131: Surfactant-induced Marangoni effects on capillary waves and Worthington jets in bursting bubble applications *by P Pico, L Kahouadji, S Shin, J Chergui, D Juric, OK Matar*
11:45	W100: Translation and oscillation of a gas bubble under asymmetric deformation *by S Shaw*	W116: Fibre buckling in a confined co-flowing jet *by G Clément, SH Caballero, M Oléron, F Box, JD McGraw, M Labousse*	W132: Global stability analysis of hydrodynamic focusing in the presence of a soluble surfactant *by M Rubio MG Cabezas, JM Montanero, MA Herrada*
12:00	W101: Experimental bifurcation analysis of a deformable bubble using control-based continuation *by S Ayoubi, JVN Fontana, A. Juel, AB Thompson*	W117: Lift-up and self-sustaining process (SSP) in a Couette-Poiseuille flow *by T Liu, B Semin, R Godoy-Diana, JE Wesfreid,*	W133: The effect of viscoelasticity in a thin squeezed film *by U Akyüz, H Ahmed, L Lombardi, PL Maffettone, L Biancofiore*
12:15	W102: Mechanochemical waves in an active fluid film *by J Picardo, K Vijay Kumar*	W118: Subcritical transition to elastic turbulence in parallel shear flows: Recent progress *by M Lellep, M Linkmann, A Morozov*	W134: Primary instability of roll waves on thin films of non-Newtonian fluids down a slope *by F Depoilly, S Dagois-Bohy, S Millet, F Rousset, HB Hadid*
12:30	**Lunch Break (Alder Lecture Theatre)**		

Keynote 5

Unravelling the complex dynamics of wetting and phase change

George Karapetsas

Department of Chemical Engineering, Aristotle University of Thessaloniki, Greece

George Karapetsas is an Associate Professor in the Department of Chemical Engineering at the Aristotle University of Thessaloniki (Greece). He obtained his PhD (2008) in Fluid Mechanics from the University of Patras (Greece) and then went to Imperial College London (UK) for postdoctoral research. He moved back to Greece in 2012 and successively joined as a Research Associate at the University of Thessaly, the National Technical University of Athens and the University of Patras. In 2018, he joined the faculty of the Aristotle University of Thessaloniki as an Assistant Professor. His research and teaching interests lie in the area of transport phenomena, fluid mechanics and applied mathematics. He is particularly interested in theoretical modelling and computations with special focus on interfacial and multiphase flows, phase-change, fluids with complex rheology, hydrodynamic stability, surface-tension-driven flows, wetting of complex surfaces, droplet dynamics, and fluid-structure interaction problems.

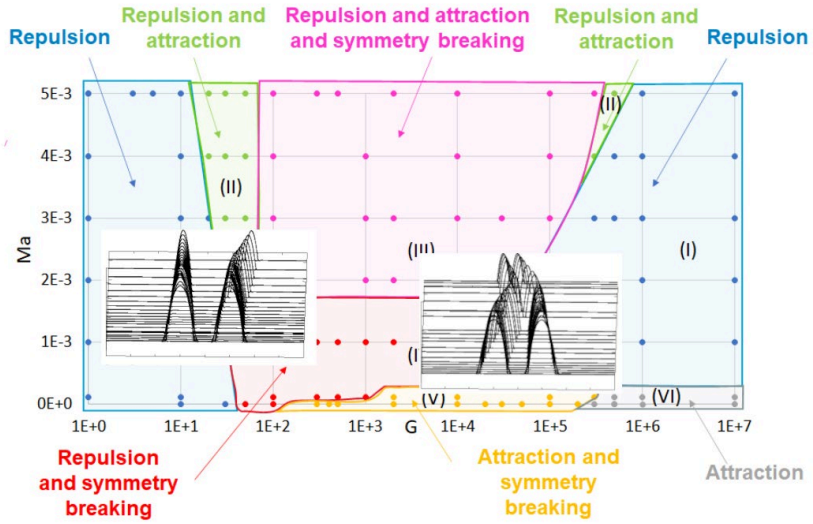

Abstract

Wetting of evaporating and condensing droplets is a common occurrence in nature, with significant implications for various industrial and everyday processes. Examples include painting, printing, oil recovery, pesticide applications, thermal management devices, DNA microarray analysis, and biological functions such as human perspiration. These systems typically involve complex liquids containing contaminants, particles, salts, or mixtures, interacting with micro-structured or soft substrates, and exhibiting a wide range of dynamic behaviors. In this talk, I will discuss our recent efforts to unravel the complexities within these multiphase systems, utilizing a combination of theoretical analysis, numerical simulations, and experiments.

W094

ENERGY HARVESTING REGIMES OF A THREE-DIMENSIONAL FLAPPING FLAG: A NUMERICAL INVESTIGATION

Bálint Nagy[1,2], Stefano Olivieri [3], Roberto Verzicco [1,4,5] & Francesco Viola[1,2]

[1]*Gran Sasso Science Institute, L'Aquila, Italy*
[2] *INFN-LNGS, Via G. Acitelli 22, 67100 Assergi (AQ), Italy*
[3]*Universidad Carlos III de Madrid, Leganés (Madrid), Spain*
[4]*University of Rome Tor Vergata, Rome, Italy*
[5]*University of Twente, Enschede, the Netherlands*

Abstract This seminar will discuss recent developments in the numerical and theoretical modeling of a three-dimensional, finite-span plate fully immersed in a viscous laminar flow.

The flutter of a flexible plate invested by a uniform incoming flow can be used to harvest energy [1], but the efficiency of the corresponding energy device depends on the onset of aeroelastic instabilities. Restricting ourselves to the case of inextensible plates, such instabilities are sensitive to four nondimensional parameters, namely the Reynolds number, the structure-to-fluid mass ratio, the bending rigidity and the aspect ratio of the plate. In the literature, the corresponding high-dimensional parametric space has been only partially explored through a combination of experimental and numerical [1, 6, 2] investigations.

In this work, we wish to explore systematically the onset of aeroelastic instabilities occurring in a three-dimensional viscous flow and explore a wide range of post-critical regimes for potential energy harvesting applications, through direct numerical simulations (DNS). To this aim, an *in-house* numerical code is used to solve the fluid-structure-interaction problem. The incompressible Navier-Stokes equations are discretized through a staggered second order finite difference method and the no-slip condition at the plate surface is enforced using immersed boundary method (IBM). The internal elastic loads of the moving structure are solved using a thin shell approach based on a two-dimensional spring-network model. The whole solver has been GPU-accelerated, thus providing an efficient computational tool to explore the parametric space [6]. In particular, three distinct regimes of response can be identified [2, 5] : (i) fixed-point stability, (ii) limit-cycle flapping, and (iii) chaotic flapping. For each case, we measure the temporal average of the elastic strain energy and the energy conversion ratio [1], which allow us to identify the optimal flow configurations for energy harvesting both in regimes (ii) and (iii). Furthermore, following the work of Connell and Yue [5], the instability onset is rationalized through linear stability analysis, where we propose an estimation for the added mass, accounting for the finite aspect ratio of the plate [3] and the hinged leading edge condition . Lastly, based on our numerical simulations, we calibrate the coefficient of a viscous correction for the added mass, similar to the one introduced by Kozlovsky [4] for a clamped circular plate.

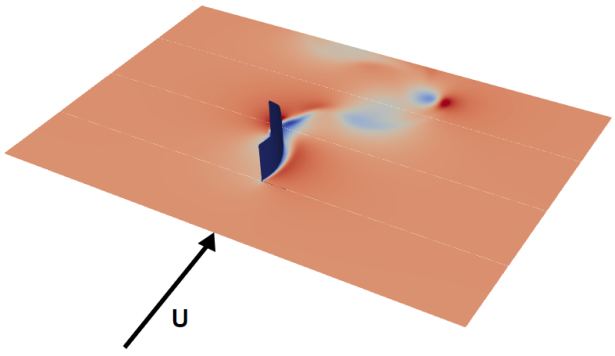

Figure 1. Velocity contours of the streamwise velocity component at $Re = 400$.

References

[1] Michelin, S. & Doaré, O. Energy harvesting efficiency of piezoelectric flags in axial flows. *Journal Of Fluid Mechanics*. **714** pp. 489-504 (2013)
[2] Yu, Y., Liu, Y. & Amandolese, X. A review on fluid-induced flag vibrations. *Applied Mechanics Reviews*. **71**, 010801 (2019)
[3] Lucey, A. & Carpenter, P. The hydroelastic stability of three-dimensional disturbances of a finite compliant wall. *Journal Of Sound And Vibration*. **165**, 527-552 (1993)
[4] Kozlovsky, Y. Vibration of plates in contact with viscous fluid: Extension of Lamb's model. *Journal Of Sound And Vibration*. **326**, 332-339 (2009)
[5] Connell, B. & Yue, D. Flapping dynamics of a flag in a uniform stream. *Journal Of Fluid Mechanics*. **581** pp. 33-67 (2007)
[6] Olivieri, S., Viola, F., Mazzino, A. & Rosti, M. Direct numerical simulation of flapping flags in grid-induced turbulence. *Physics Of Fluids*. **33** (2021)

W095

EXPERIMENTAL ANALYSIS OF SAFFMAN–TAYLOR INSTABILITY IN HELE-SHAW CELL USING PHOTOELASTIC TECHNIQUE

Misa Kawaguchi[1], Yuto Yokoyama[1] William Kai Alexander Worby[2], Ryuta X. Suzuki[3], Yuichiro Nagatsu[4] & Yoshiyuki Tagawa[1,3]

[1]*Dept. of mechanical System Engineering, Tokyo University of Agriculture and Technology, Tokyo, Japan*
[2]*Dept. of Ind. Tech. and Innov., Tokyo University of Agriculture and Technology, Tokyo, Japan*
[3]*Institute of Global Innovation Research, Tokyo University of Agriculture and Technology, Tokyo, Japan*
[4]*Dept. of Appl. Phys. Chem. Eng., Tokyo University of Agriculture and Technology, Tokyo, Japan*

Abstract (Key words) Viscous fingering, Flow birefringence, Hele-Shaw flow

When a less viscous fluid displaces a more viscous one in small area, such as porous media or Hele-Shaw cells (a thin gap between two parallel plates), the interface become a finger-like pattern due to the viscosity difference. This is known as Saffman–Taylor instability or viscous fingering. It has been suggested that the interface shape in the gap direction of a Hele-Shaw cell changes with onset of instability occurring laterally in the Hele-Shaw cell [1] [2]. Although much effort has been devoted to this issue, the connection between the interface shape and the onset of instability has not been fully understand. Integrated photoelasticity [3] have a potential to discuss this issue including three-dimentional information. However, to the best of the our knowledge, there have been no reports on photoelastic measurements for Saffman–Taylor instability. The aim of this study is to visualize the phase retardation distribution around the Saffman–Taylor instability. Experimental setup is shown in Fig. 1(a). The radial Hele-Shaw flow using single fluid and Saffman–Taylor instability in Hele-Shaw cell were measured using high-speed photoelastic camera (CRYSTA PI-5WP, Photron) with frame rate 250 fps. For radil Hele-Shaw flow, the working fluid was cellulose nanocrystal (CNC) suspension with the concentration of 3 wt%. CNC suspension injected to the radial Hele-Shaw cell with a thin gap b (thickness: $b = 0.3$, 0.5 mm) with constant flowrate Q = 10 ml/min using syringe pump (PUMP 11 ELITE, Harvard Apparatus). To validate the experimental measurement, the analytical solution of phase retardation in radial direction was calculated from analytical solution of velocity profile [4]. For Saffman–Taylor instability, the mixture of glycerol (80 %) and CNC suspension (3 %) and water were used as more and less viscous fluid, respectively. Cell gap was b = 0.3 mm and flow rate was set to Q = 5 ml/min. As a result, in the case of radial Hele-Shaw flow, the phase retardation distribution in radial direction was reasonably agreement with the theoretical solution except in the vicinity of the entrance (Fig. 1(b)). In the case of Saffman–Taylor instability, lower region of phase retardation at the finger tip was observed (Fig. 1(c)). When the velocity profile becomes blunted, the sum of velocity gradient in z-direction decreases. Therefore, one possible reason lower region of phase retardation at the fingertip is blunt structures in the cross-section. In summary, photoelastic measurement was performed to investigate the characteristics of phase retardation in Hele-Shaw cell. As a result, the phase retardation in radial Hele-Shaw cell was validated by comparison with theoretical solution. With Saffman–Taylor instability, the lower region of phase retardation was observed at the finger tip. It was suggested that this lower region of phase retardation at the finger tip may be related to the blunted velocity profile. Future work will investigate whether lower region of phase retardation in the fingertip can be explained by changes in the velocity distribution determined from changes in the interface shape.

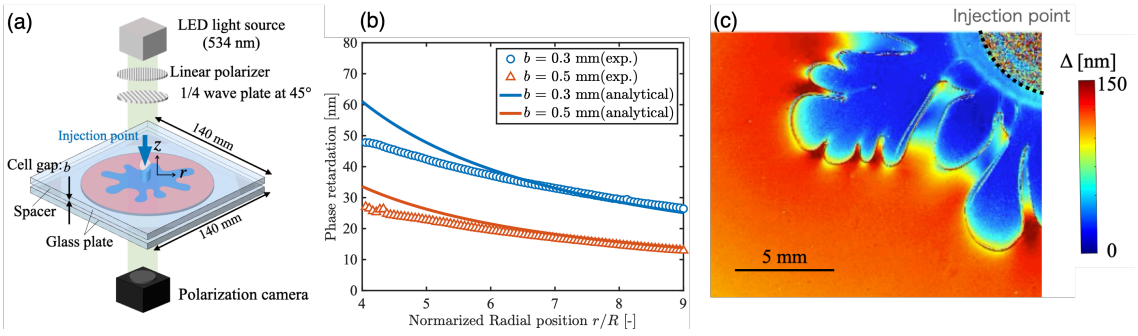

Figure 1. (a)Experimental setup and phase retardation distribution (b) of radial Hele-Shaw flow and (c) around S.–T. instability.

Acknowledgments

This study is supported by JST PRESTO Grant Numbers JPMJPR21O5 and JPMJPR22O5, and JSPS KAKENHI Grant Numbers JP23K13252 and JP20H00223.

References

[1] Yang, Z., Yortsos, Y. C.: *Phys. Fluids*, **9**(2),286–298, 1997.
[2] Bischofberger, I. *et al.*: *Nat. commun.*, **5**(1), 5265, 2014.
[3] Yokoyama, Y. *et al.*: *Opt. Lasers Eng,*, **161**, 107335, 2023.
[4] Goldstein, A. S., DiMilla, P. A.: *AIChE J.*, **44**(2), 465–473, 1998.

W096

SUPPRESSION OF MARANGONI-DRIVEN DRY-OUT USING PARAMETRIC FORCING

I. B. Ignatius[1], B. Dinesh[2], G. F. Dietze[3] & R. Narayanan[1]
[1]*Department of Chemical Engineering, University of Florida, Gainesville, FL 32611, USA*
[2]*Department of Chemical Engineering and Technology, Indian Institute of Technology-BHU, Varanasi, UP 221005, India*
[3]*Université Paris-Saclay, CNRS, FAST, 91405, Orsay, France.*

Key words : Thin films, Marangoni instability, Faraday instability

Abstract

This work focuses on the interface behavior of a thin liquid layer in contact with a passive gas in the absence of gravity, heated from the liquid side, and subjected to vertical oscillations. Typically, in the absence of external forcing, such systems exhibit long-wave Marangoni instability and a subsequent dry-out when the temperature gradient exceeds a critical value. This study aims to understand the effect of parametric forcing on this system through linear stability analysis and computations utilizing a nonlinear reduced-order model developed using the weight residual integral boundary layer (WRIBL) technique.

The results show that at low forcing frequencies, the liquid film becomes stable with a flat surface within a certain range of forcing amplitudes. Outside this range, the flow becomes unstable, leading to the Marangoni instability and dry-out at lower forcing amplitudes, or Faraday instability accompanied by large free surface oscillations at higher forcing amplitudes. Beyond a critical value of the parametric frequency (marked by a star in figure 1), the liquid film cannot be rendered stable with a flat surface. Instead, as the forcing amplitude increases, a long-wavelength Marangoni-dominated flow directly transitions to a short-wavelength resonance-dominated flow. Nonetheless, a saturated interface with an infinitesimal deflection may still be achieved through a nonlinear mechanism at forcing amplitudes close to but below the Faraday threshold. Consequently, dry-out in thin films can be suppressed at both low and high frequencies due to the action of Faraday forcing.

The suppression of dry-outs in thin films is important due to its relevance in coating industries for the manufacture of thin optical films and in additive manufacturing of metals in microgravity environments for human habitation in space.

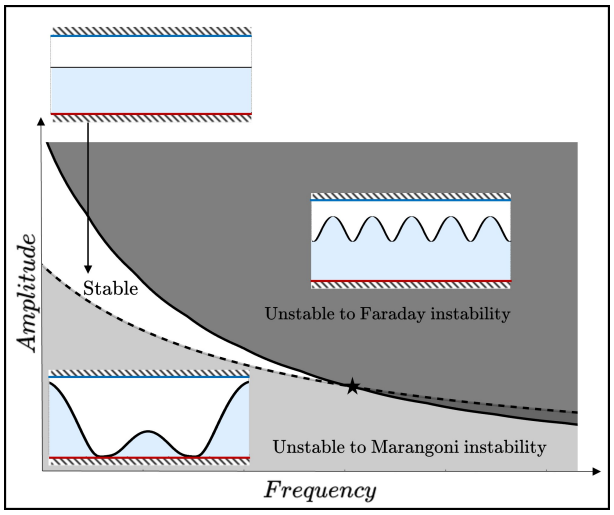

Figure 1. The Amplitude versus Frequency curves demarcating the regions of stability/instability

Acknowlegements
The authors gratefully acknowledge funding from NSF via grant number CBET-2025117 and NASA via grant numbers 80NSSC20M0093 and 80NSSC23K0457.

W097

ELASTIC INSTABILITY IN MICROSERPENTINE CHANNEL AT LOW REYNOLDS NUMBERS

Yusuf Alperen Degirmenci[1], Arda Senyurek[1], Luca Biancofiore[1,2] & Kevin Nolan[3]
[1]*Department of Mechanical Engineering Bilkent University 06800 Bilkent, Ankara, Turkey*
[2] *Department of Industrial and Information Engineering and Economics, University of L'Aquila*
[3]*School of Mechanical and Materials Engineering, University College Dublin, D04 C1P1, Dublin, Ireland*

Abstract We conducted direct numerical simulations of viscoelastic fluids on micro serpentine channels and compared with experimental results showing an elastic instability growing as viscoelastic effects increase. (Visoelasticity, elastic instability, serpentine channel).

In their earlier work, Nolan et al. conducted an experimental study on a serpentine-like microchannel to investigate the inertial and viscoelastic effects [1]. The study concluded that, in simulations with strong viscoelasticity, local significant velocity fluctuations were observed after the turning point (see fig. 1a). It was hypothesized that these elastic instabilities could potentially enhance heat transfer in microelectronics, a formidable task given the predominant laminar flow at low Reynolds numbers.

In this current study, we performed direct numerical simulations (DNS) to thoroughly investigate the previously obtained results. The open-source rheoTool package in OpenFOAM, known for its stability due to the log-confirmation representation (LCR) algorithm [2], was employed. [3]. The simulation setup was set to match the experimental conditions, and the Oldroyd-B viscoelastic model was chosen as the constitutive relationship for the viscoelastic stresses. Also, throughout these simulations, both β, defined as the ratio of solvent viscosity to total viscosity ($\frac{\eta_s}{\eta_0}$), and the Reynolds number were maintained at constant values: $\beta = 0.2$ and Re = 0.5 while varying the Weissenberg number (Wi) which is the relation between the polymer relaxation time and the reference strain rate.

The results demonstrated a qualitative agreement with the experimental findings reported by Nolan et al. [1]. As the Weissenberg number increased, the velocity fluctuations became more pronounced in the whole domain. Also, at a relatively low Weissenberg number (i.e., Wi = 5), the fluctuations became apparent. However, particularly at the starred point (see fig. 1a), the elastic instabilities significantly increased (see fig. 1b). Additionally, the fluctuation magnitude increased up to 10% of the mean velocity in the region of interest for Wi = 20.

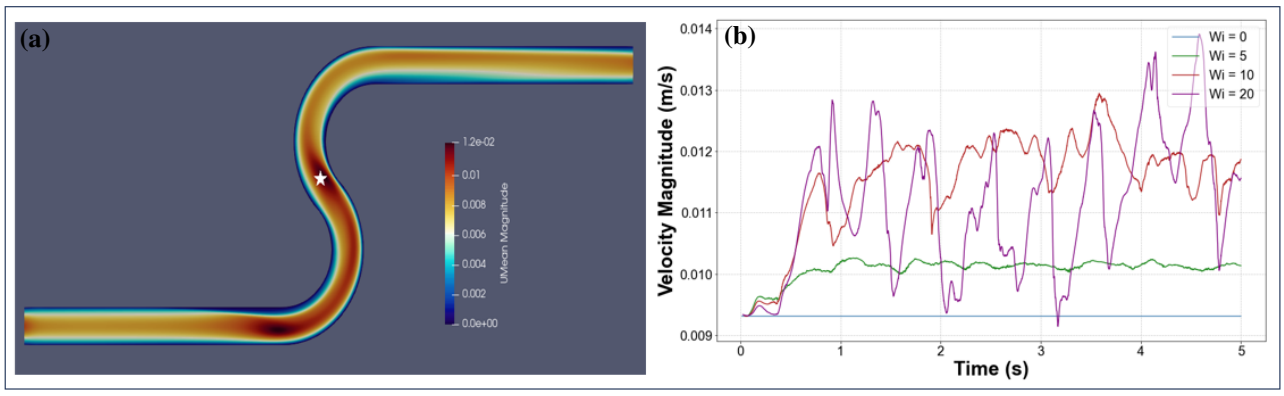

Figure 1: a) Overall mean velocity distribution in the serpentine channel (Wi = 20). b) Velocity magnitudes at the starred point of (a) for different values of Wi.

References

[1] P. Nolan, A. Agarwal, S. Lei and E. Dalton, *Mixing enhancement due to viscoelastic instability in serpentine microchannels at very large Weissenberg numbers*, 2016 15th IEEE Intersociety Conference on Thermal and Thermomechanical Phenomena in Electronic Systems (ITherm), Las Vegas, NV, USA, 2016, pp. 301-306, doi: 10.1109/ITHERM.2016.7517564.

[2] R. Fattal, & R. Kupferman, *Constitutive laws for the matrix-logarithm of the conformation tensor*, *Journal of Non-Newtonian Fluid Mechanics, 123*(2–3), 281–285. https://doi.org/10.1016/j.jnnfm.2004.08.008

[3] Pimenta, F., & Alves, M. A. (2017). Stabilization of an open-source finite-volume solver for viscoelastic fluid flows. *Journal of Non-Newtonian Fluid Mechanics, 239*, 85–104. https://doi.org/10.1016/j.jnnfm.2016.12.002

W098

TEMPORAL STABILITY ANALYSIS OF SPIRAL COUETTE FLOW FOR SMALL RADIUS RATIO

Manish K. Khandelwal
Department of Mathematical Sciences, Indian Institute of Technology (BHU), Varanasi, India

Keywords: Linear Stability Analysis, Spiral Couette Flow, Centrifugal-Shear Instability

Abstract

The fluid flow between two concentric rotating cylinders (known as the Taylor–Couette flow) has attracted attention since Taylor's landmark work [1]. Spiral Couette flow (SCF) is a flow between two independently rotating concentric cylinders with axial sliding, and fluid motion driven by the rotation of one/both cylinder(s) and an inertial sliding of the cylinders relative to one another along the cylinder axis. The SCF has generated much attention due to its extensive use in several relevant practical applications in many fields, such as the purification of industrial wastewater, production of wire and cables, optical fiber fabrication, etc. Many researchers have investigated the hydrodynamic stability analysis of SCF with different radius ratios (a parameter related to the gap between cylinders) (See Ref, [2-5] and the references therein). The wide-gap SCF case is of significant potential interest in many biomedical and biotechnology mixing applications. Therefore, we wish to explore the instability mechanism of SCF for a small radius ratio η =0.1.

We consider an incompressible viscous fluid flow between two concentric rotating cylinders that rotate independently about a common axis at constant angular velocities. The inner cylinder also moves parallel to the common axis with a constant speed U. The inner and outer radii and angular velocities of cylinders are R_i, R_o and Ω_i, Ω_o, respectively. The geometric sketch with the coordinate system is shown in Figure 1. The basic motion, whose stability we wish to analyze, is a combination of rotation of the cylinders (Taylor-Couette component) and moving of the inner cylinder parallel to the axial direction. The governing equations for the considered problem can be seen in reference [2].

In this work, the instability properties of SCF are examined numerically using linear temporal stability theory. We have comprehensively analyzed the growth rate profile, neutral stability curves and linear stability boundaries, and secondary flow analysis for axisymmetric and non-axisymmetric disturbances cases. The competition between shear instability (induced by the axial sliding of the cylinder) and centrifugal instability (induced by the rotation of cylinders) mechanisms are determined in detail. Depending on the rotation parameter as well as the axial velocity of the moving cylinder, the considered flow is least stable for axisymmetric disturbance as well as non-axisymmetric disturbance. The competition of different instability mechanisms gives multiple minima in (Re_i, α)-plane and significant change in the azimuthal wavenumber, where Re_i and α are inner rotation Reynold number and axial wavenumber, respectively. The co-rotation of cylinders shows complex behavior for instability mechanism.

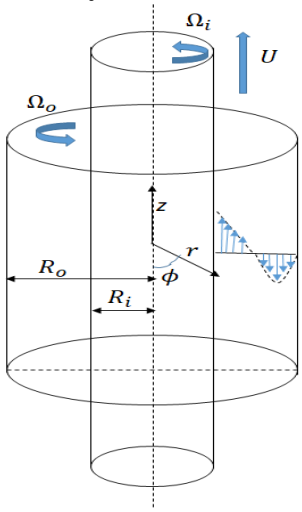

Figure 1. Geometric sketch of physical problem and coordinate system.

References

[1] G. I. Taylor, *Stability of a viscous liquid contained between two rotating cylinders*, Philos. Trans. R. Soc. Lon. A **223** 89-343 (1923).
[2] A. Meseguer, F. Marques, *On the competition between centrifugal and shear instability in spiral Couette flow*, J. Fluid Mech. **402**, 33-56 (2000).
[3] M. E. Ali, A. D. Weidman, *On the stability of cellular spiral Couette flow*, Phys. Fluids A, **5** 1188-1200, (1993).
[4] J. Peng, K. Q. Zhu, *Linear stability of Bingham fluids in spiral Couette flow*, J. Fluid Mech., 512, 21-45, (2004).
[5] A. Y. Weisberg, I. G. Keverkidis A. J. Smits, *Delaying transition in Taylor-Couette flow with axial motion of the inner cylinder*, J. Fluid Mech. **348**, 141-151 (1997).

W099

PRIMARY INSTABILITY IN THE WAKE OF POLYGONAL CYLINDERS

Adam Marshall[1], Lian Gan[1] & David Sims-Williams[1]
[1]*Department of Engineering, Durham University, Durham, U.K.*

Abstract instability, Hopf bifurcation, vortex streets

While most existing flow stability studies around bluff-bodies focused on circular cylinders, polygonal cylinders, owing to their quasi-axisymmetric and discontinuous surface geometry, the wake flow exhibits unique stability characteristics. This study numerically investigates the primary wake flow instability behind polygonal cylinders of side number $N = 5 - 8$, over the entire range of angles of incidence α. In total, six incidence angles are studied for each polygon between corner ($\alpha^* = 0$) and face ($\alpha^* = 1$) orientations with respect to the direction of the incoming flow U, where $\alpha^* = N\alpha/180$, Figure 1 (a). Numerical simulations were performed using the hp/spectral element method using Nektar++ and a O-type structured grid was used. A schematic of the computational domain is presented in Figure 1 (a).

At low Re, the flow is steady, similar to the circular cylinder, above the critical Reynolds number (Re_{cr}), the flow undergoes a Hopf bifurcation [1] to a time-periodic oscillatory wake flow. Re_{cr} can be obtained by using the linear growth rate (σ) in the Stuart-Landau equation [2]. Near Re_{cr}, the Stuart-Landau equation can be linearised to be $\sigma = K(Re - Re_{cr})$, where K is a positive constant. Therefore, Re_{cr} is obtained by finding the Re corresponding to $\sigma = 0$, which is obtained by determining the slope of the linear part of the instantaneous lift coefficient (C_L) amplitude envelopes, Figure 1 (b). Re_{cr} shows a non-monotonic dependence on both N and α^*. This can clearly be seen in Figure 1 (c). When a polygon is in off-principal orientations, thus geometrically asymmetric, the growth rate of the instability shows a spatial dependence. This can be seen by comparing the upper and lower envelopes of C_L in Figure 1 (b). Re_{cr} presented in Figure 1 (c) are computed from the least stable side of envelopes for a given N-α^* condition.

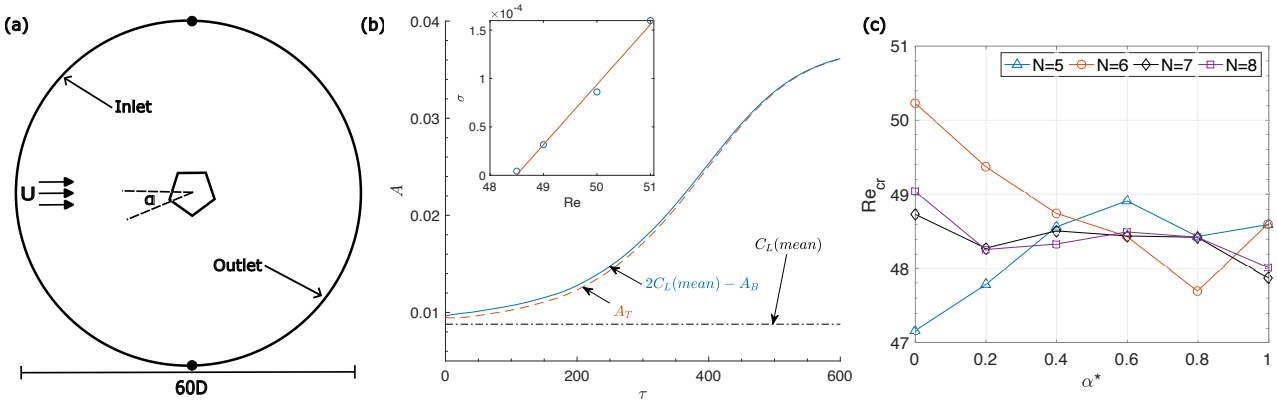

Figure 1. (a) The computational domain and configuration of polygonal cylinders in a O-type structured grid. Not to scale. (b) The upper (A_T) and lower (A_B) envelopes of the C_L amplitude for the $N = 7, \alpha^* = 0.6$ case at $Re = 50$. A_B is flipped about $C_L(mean) = 0.0088$, for better comparison with A_T. $\tau = tU_\infty/D$. Note that in off-principal orientations, $C_L(mean)$ has a non-zero value. The inserted figure illustrates the determination of Re_{cr} from σ and K. (c) Dependence of Re_{cr} of the primary instability on α^* for polygons of side number $N = 5 - 8$.

References

[1] K.R. Sreenivasan, P.J. Strykowski, D.J. Olinger, *Hopf Bifurcation, Landau Equation, and Vortex Shedding Behind Circular Cylinders*, American Society of Mechanical Engineers, Fluids Engineering Division, 1–33 (1987).
[2] D. Park, K.-S. Yang, *Flow instabilities in the wake of a rounded square cylinder*, Journal of Fluid Mechanics **793**, 915–932 (2016).

W100

TRANSLATION AND OSCILLATION OF A GAS BUBBLE UNDER ASYMMETRIC DEFORMATION

Stephen J. Shaw
Department of Applied Mathematics, School of Mathematics and Physics,
Xi'an Jiaotong-Liverpool University,
111 Ren Ai Road, Dushu Lake Higher Education Town,
Suzhou, Jiangsu Province, 215123, P.R. China

The asymmetric shape distortion of a gas bubble in water due to the growth of parametrically induced surface instabilities is considered. Representing the bubble surface deformation by a set of spherical harmonic functions, a set of coupled nonlinear ordinary differential equations are derived for the temporal evolution of the volume oscillations, translation and surface shape modes. The model accounts for both viscous and thermal damping together with compressibility effects. The existence of finite amplitude shape distortion as a consequence of nonlinear shape mode interactions is demonstrated. An assessment of the importance of three dimensional effects on previously determined axisymmetric results is made.

W101

EXPERIMENTAL BIFURCATION ANALYSIS OF A DEFORMABLE BUBBLE USING CONTROL-BASED CONTINUATION

Sammy Ayoubi[1], João V. N. Fontana[1], Anne Juel[2] and Alice B. Thompson[1]
[1] *Department of Mathematics, University of Manchester, Manchester, UK*
[2]*Department of Physics & Astronomy, University of Manchester, Manchester, UK*

Abstract Control-based continuation (CBC) is an experimental method used to explore the bifurcation structure of nonlinear systems. Feedback control and continuation techniques are used to discover and non-invasively stabilize steady states, thus allowing them to be observed. We apply CBC for the first time in experiments for free-surface fluid dynamics, seeking steady states with up to two unstable eigenmodes. The system investigated is a deformable air bubble confined in a Hele-Shaw channel filled with silicone oil, with imposed fluid injection generating a background straining flow. Bubbles placed at the centre of this straining flow can reach steady state shapes with mild or more severe deformation but are always unstable to translation. Real-time feedback control is used to stabilize bubbles in a range of configurations by injecting/withdrawing fluid from the channel, based on observations of bubble position and/or shape. Our CBC strategy enables our experiments to uncover two unstable solution branches, one singly-unstable and one doubly unstable, and to construct a bifurcation diagram mapping bubble deformation to the strength of the straining flow.
Keywords: feedback control, experiments, nonlinear dynamics, bubbles.

We use control-based continuation (CBC) for the first time in experiments for a free-surface fluid dynamical system. We choose the specific problem of steady shapes of a bubble confined within a Hele-Shaw cell with deformation driven by an imposed straining flow (figure 1(a)). As the system is almost two-dimensional and the flow at low Reynolds number, top-view images of the bubble shape, via its radius $r(\theta, t)$, provide the necessary observations for feedback control. Feedback actuation is delivered by injecting fluid through four additional channels, two on each side of the two main injection points.

The feedback amplitudes are chosen as a linear combination of the bubble centroid position X relative to the centre of the channel (to suppress a translational instability) and a measure of the shape deformation: $m(t) = \int_0^{2\pi} r(\theta, t)\cos(2\theta)dt$. We set $A = \alpha X + \beta(m - m_T)$, where m is the observed measure and m_T is a target value. The gains α and β are chosen so that equilibrium bubbles are stable. We seek values of m_T where the system reaches a steady state with $A = 0$ and the control is non-invasive, hence coinciding with steady states with no control.

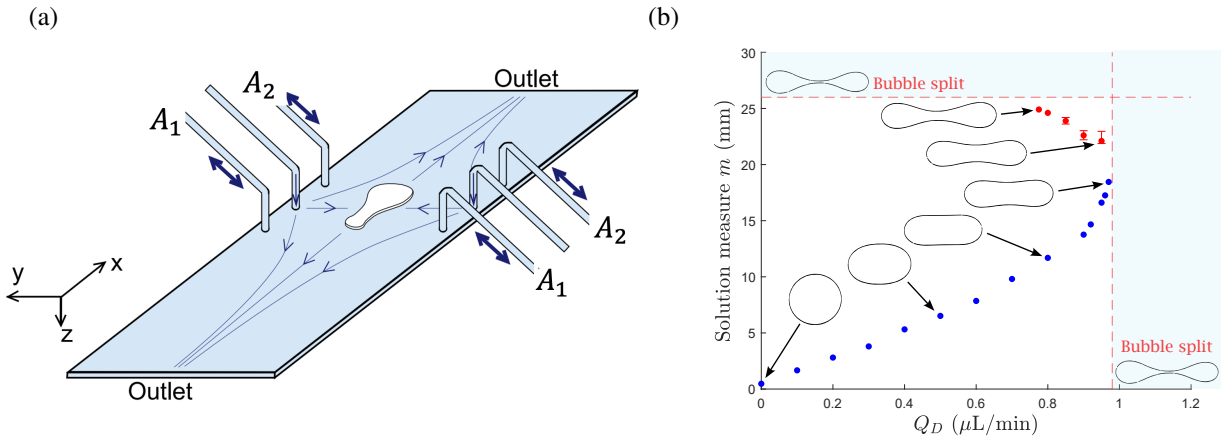

Figure 1. (a) A schematic version of the experimental setup, with two central fluid inlets driving a straining flow and four side channels used to inject/withdraw fluid with amplitudes chosen in real time to deliver feedback control. (b) Bifurcation diagram for non-invasively controlled states in the experiment, with two unstable branches connected by a limit point.

Our experiments allow us to recover two branches for steady states in this system, connected by a limit point (figure 1(b)). The first branch, connected to circular bubbles at zero flow rate, is unstable to translation only. The second branch is unstable to both deformation and translation and can only be revealed using our feedback control and continuation strategy.

W102

MECHANOCHEMICAL WAVES IN AN ACTIVE FLUID FILM

Jason R. Picardo[1] & K. Vijay Kumar[2]
[1]*Department of Chemical Engineering, Indian Institute of Technology Bombay, Mumbai, India*
[2]*International Centre for Theoretical Sciences, TIFR, Bangalore, 560089, India*

Abstract In contrast to traditional reaction-diffusion mechanisms, we show that a single chemical species can give rise to travelling waves, provided the species is a stress-generator that drives fluid flow. Surprisingly, the role of the *nonlinear* bifurcation parameter is played by the rate constant of a *linear* reaction, which triggers the onset of nonlinear waves (active flows, nonlinear travelling waves, reduced-order modelling).

Below the plasma membrane of every eukaryotic cell resides the actomyosin cortex, a thin layer of actin filaments and myosin molecular motors, which behaves like an active fluid film and is the site of fascinating morphogenetic processes at the cell and tissue scale [1, 2]. The fundamental mechanochemical feedback—myosin motors generate contractile forces within the cortex which drive flows that in turn redistribute the myosin—may be described by a simple one dimensional model, consisting of an advection-diffusion-reaction equation for the concentration of a stress regulator (myosin) and the creeping flow Stokes equation [3]. While this model gives rise to stationary patterned states via a linear instability, it has hitherto been thought that it is insufficient to explain the wave-like patterns observed in experiments [3, 4], and that one must introduce additional features, such as a second biochemical species [5] or cortical elasticity [4]. In this work, we show and explain how the inclusion of a simple linear reaction, which models turnover of material in the cortex, can surprisingly trigger the onset of waves via a secondary bifurcation of the stationary pattern (Fig.1*a*). The waves first arise as perfect travelling waves with a constant shape, but when the active stress strength is increased they develop shape oscillations as well (Fig.1*a,c*).

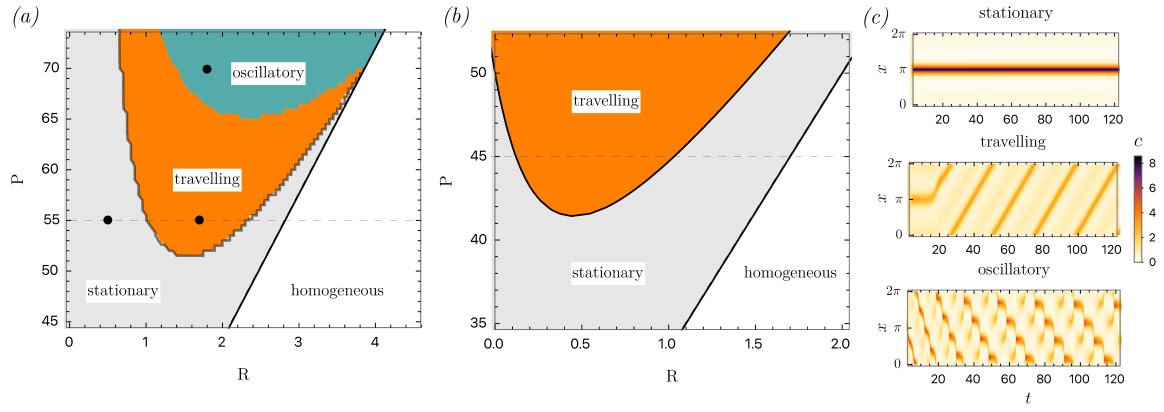

Figure 1. Regime map showing the emergence of travelling and oscillatory waves in the Pe – R parameter plane (non-dimensional measures of the strength of active stresses and the rate of the linear reaction, respectively), as predicted by (a) numerical simulations of the full PDE model in a one-dimensional periodic domain and (b) analytical results of a two-mode reduced-order ODE model. (c) Space-time plots of the concentration field for stationary patterns, travelling waves, and modulated or oscillatory travelling waves.

The waves arise due to an interplay between different spatial modes of the concentration field of the *single* active species. We elucidate this nonlinear inter-mode interaction, and the crucial role of the linear reaction, with the help of a Galerkin-truncated reduced-order model consisting of just two spatial modes. Remarkably, this ODE model is able to reproduce all the key features of the far-from-onset nonlinear travelling waves (Fig.1*b*). These mechano-chemical waves represent a new paradigm of pulsatory pattern formation and are insensitive to changes in the domain: we find these waves in both one and two dimensional domains, with either periodic or no-flux boundaries, and even on a sphere.

References

[1] K. V. Kumar, The actomyosin cortex of cells: a thin film of active matter, *J. Indian Inst. Sci.*, **101**, 97, 2021.
[2] P. Gross, K. V. Kumar, and S. W. Grill, How active mechanics and regulatory biochemistry combine to form patterns in development, *Ann. Rev. Biophys.*, **46**, 337, 2017.
[3] J. Bois, F. Jülicher, and S.W. Grill, Pattern formation in active fluids, *Phys. Rev. Lett.*, **106**, 1, 2011.
[4] D.S. Banerjee, A. Munjal, T. Lecuit, M. Rao, Actomyosin pulsation and flows in an active elastomer with turnover and network remodeling, *Nat. Commun.*, **8**, 1121, 2017.
[5] K. V. Kumar, J. Bois, F. Jülicher, and S.W. Grill, Pulsatory patterns in active fluids, *Phys. Rev. Lett.*, **112**, 208101, 2014.

W110

THE EFFECTS OF WALL COMPLIANCE ON THE STABILITY OF JETS AND WAKES

Ryan Poole
School of Mathematics and Physics, University of Surrey, Guildford, GU2 7XH

Abstract Absolute instability of jets and wakes confined by compliant surfaces. (compliant wall; global stability; jets; wakes).

In this talk, we examine the global stability properties of two-dimensional planar jets and wakes which are confined by two identical 'Kramer-type' compliant boundaries [1, 2, 3, 4]. The basic flow profile is modelled as a three-part piecewise linear flow profile, while the compliant walls are modelled as a spring backed elastic plate. The piecewise linear base flow profile has the advantage that an analytical dispersion relation of the form $\Delta(\omega, \alpha) = 0$ can be derived for both varicose and sinuous modes of the system. Here ω is the angular frequency of the stability waves, where in particular $\mathrm{Im}(\omega)$ describes the wave growth rate, and α is the wavenumber.

We perform a spatio-temporal stability analysis on the system, and hence by following the position of special saddle points (pinch points) of the dispersion relation in the complex wavenumber plane, we identify the absolute and convective instability stability properties of the flow for various system parameters. The compliant walls are shown to modify the shear-induced instabilities, which exist in the rigid wall case explored in [5, 6], as well as introduce new additional instabilities originating from the presence of the wall itself. As system parameters are varied the saddles corresponding to these new wall-induced modes move around the complex wavenumber plane and interact with the shear-induced instabilities, see figure 1. For some system parameters these wall-induced modes become the dominant instability present in the system, and can induce an global instability into flows which are only convectively unstable when confined by rigid walls. They can also extend the region of absolute instability to large confinement parameters, where originally there is only convective instability.

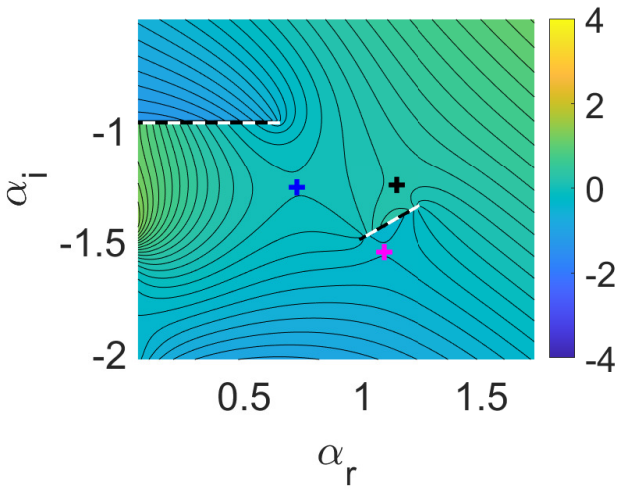

Figure 1. A plot of the complex wavenumber plane showing the saddle point complexity due to two new wall-induced modes (pink and black marks), interacting with the shear induced mode (blue mark).

In order to ascertain whether the observed behaviour of the new wall-induced modes is just a consequence of choosing a piecewise linear velocity profile with discontinuities in velocity at the shear layers, we examine a smoothed version of this flow field for comparison. In this case we cannot derive an analytical form of the dispersion relation and instead we resort to solving the Rayleigh equation directly using a shooting-corrector numerical scheme. We find that the results of the smooth base flow calculations are in qualitative agreement with those of the piecewise linear base flow, hence the observed behaviour is expected in real flows.

The final part of the talk looks at how the global stability properties of this flow are affected by breaking the flow symmetry, either by asymmetrically confining the flow by identical walls, or symmetrically confining the flow by non-identical compliant walls.

References

[1] Max O Kramer. Boundary-layer stabilization by distributed damping. *Journal of the Aerospace Sciences*, 27(1):69–69, 1960.
[2] PW Carpenter and AD Garrad. The hydrodynamic stability of flow over kramer-type compliant surfaces. part 1. tollmien-schlichting instabilities. *J. Fluid Mech.*, 155:465–510, 1985.
[3] Peter W Carpenter, Christopher Davies, and Anthony D Lucey. Hydrodynamics and compliant walls: Does the dolphin have a secret? *Curr. Sci*, pages 758–765, 2000.
[4] Ryan Poole and M. R. Turner. Stability of jets and wakes confined by compliant walls. *Phys. Rev. Fluids*, 8:063901, Jun 2023.
[5] Matthew P Juniper. The effect of confinement on the stability of two-dimensional shear flows. *J. Fluid Mech.*, 565:171, 2006.
[6] Matthew P Juniper. The full impulse response of two-dimensional jet/wake flows and implications for confinement. *J. Fluid Mech.*, 590:163, 2007.

W111

STABLE PRODUCTION OF FLUID JETS WITH ARBITRARILY SMALL DIAMETERS VIA TIP STREAMING

M. Rubio[1], J. M. Montanero[2], J. Eggers[3] & M. A. Herrada[4]
[1]*Depto. de Ingeniería Energética y Fluidomecánica and Instituto de las Tecnologías Avanzadas de la Producción (ITAP), Universidad de Valladolid, E-47003 Valladolid, Spain*
[2]*Departamento de Ingeniería Mecánica, Energética y de los Materiales and Instituto de Computación Científica Avanzada (ICCAEx), Universidad de Extremadura, E-06071 Badajoz, Spain*
[3]*School of Mathematics, University of Bristol, Fry Building, Bristol BS8 1UG, UK*
[4]*Departamento de Ingeniería Aeroespacial y Mecánica de Fluidos, Universidad de Sevilla, E-41092 Sevilla, Spain*

Abstract Tip streaming, microjettng, uniaxial extensional flow, global linear stability.

We study numerically the microjetting mode (Fig. 1-left graph) [1, 2] obtained when a fluid is injected through a tube submerged in a uniaxial extensional flow. The steady solution to the full nonlinear Navier-Stokes equations is calculated. We obtain the linear global modes determining the linear stability of the steady solution. For sufficiently large outer viscosity, the flow remains stable for infinitely small values of the injected flow rate. This implies that jets with vanishing diameters can be produced regardless of the jet viscosity and outer flow strength. For a sufficiently small inner-to-outer viscosity ratio, the microjetting instability is associated only with the flow near the entrance of the jet. The tapering meniscus stretches and adopts a slender quasi-conical shape. Consequently, the cone tip is exposed to an intense outer flow, which stabilizes the flow in the cone-jet transition region. This work presents the first evidence that fluid jets with arbitrarily small diameters can be stably produced via tip streaming. The results are related to those of a droplet in a uniaxial extensional flow with its equator pinned to an infinitely thin ring (Fig. 1-right graph). The pinning of the equator drastically affects the droplet stability and breakup.

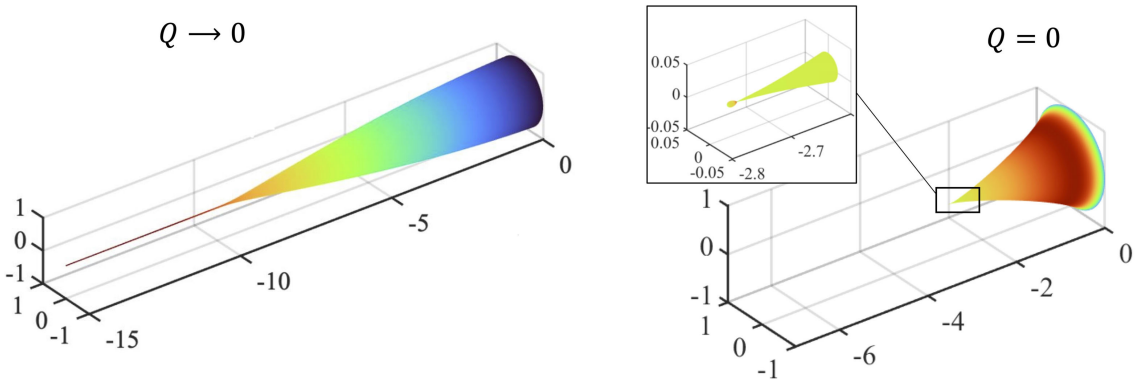

Figure 1. Numerical simulation of the microdripping (upper graph) and microjetting (lower graph) modes produced by a uniaxial extensional flow for $Q = 0$ and $Q > 0$, respectively.

References

[1] J. M. Montanero, and A. M. Gañán-Calvo, *Dripping, jetting and tip streaming*, Rep. Prog. Phys. **83**, 097001 (2020)
[2] M. Rubio, J. M. Montanero, J. Eggers and M. A. Herrada, *Stable production of fluid jets with vanishing diameters via tip streaming*, J. Fluid. Mech., submitted (2024)

W112

NUMERICAL INVESTIGATION ON THE FORMATION OF SIDE-JETS IN LIGHT JETS

Leo Walter[1,2], Jerôme Fontane[1], Gabriele Nastro[1], David Donjat[2] & Olivier Léon[2]
[1]*ISAE-SUPAERO, Université de Toulouse, France*
[2]*ONERA/DMPE, Université de Toulouse, France*

Abstract A linear nonmodal stability analysis is conducted on an unsteady Kelvin–Helmholtz billow developing over a variable-density round jet, through the use of a direct-adjoint optimisation method, in order to ascertain the physical mechanism underlying the emergence of side-jets in light jets.

The variable-density round jet is subject to various types of primary and secondary instabilities which render its spatio-temporal evolution quite unique. Under certain conditions of jet-to-ambient density ratio S, Reynolds number *Re*, and jet aspect ratio α, these instabilities can give rise to side-jets leading to a dramatic spreading of the jet. This phenomenon promotes mixing through an increase of the interface between the jet and the ambient fluid, but the physical mechanisms underlying the emergence of side-jets and their characteristics are yet to be clarified. Indeed, there exist two different hypotheses to explain the formation of side-jets. The first is due to Monkewitz and Pfizenmaier (1991), based on the induction of radial velocity by counter-rotating longitudinal vortices whose intensity increases sufficiently to trigger side-jets when the primary instability becomes absolute (Figure 1a). However, Fontane (2005) showed that side-jets also appear when the primary instability is of convective nature, prompting Lopez-Zazueta, Fontane, and Joly (2016) to suggest another explanation for their formation. In the case of a variable-density binary mixing layer, they have shown the appearance of opposing streaks of longitudinal velocity in the vicinity of the hyperbolic stagnation point on the braid of the Kelvin–Helmholtz billow (Figure 1b). In this region, the baroclinic production of vorticity is intensified by the high strain rate. This instability mechanism suggests an alternative mechanism for side-jets generation, however as of yet it has only been observed in the case of the variable-density binary mixing layer. The present work aims at investigating the physical mechanism at the origin of side-jets in the case of a light round jet in order to clarify the aforementioned open question. We conduct a linear nonmodal stability analysis on the development of an unsteady Kelvin–Helmholtz billow over a light round jet, through the use of a direct-adjoint optimisation method and extend the study of Nastro, Fontane, and Joly (2022) to lower Atwood numbers $At = (S-1)/(S+1)$ corresponding to the physical domain for which side-jets are observed experimentally.

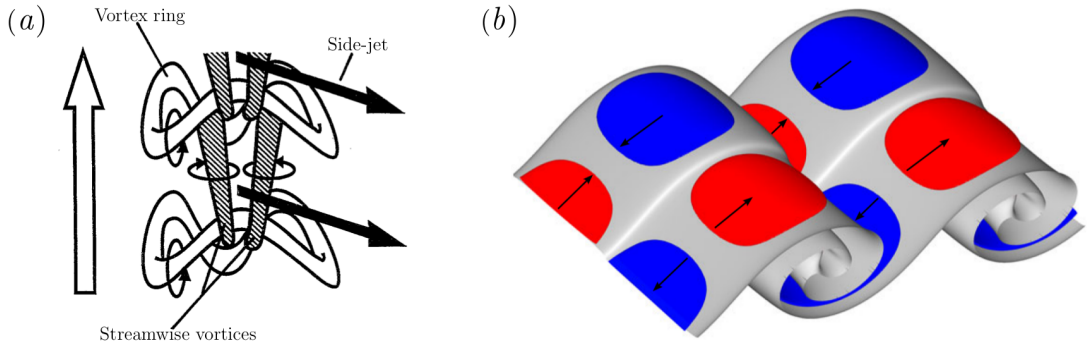

Figure 1. (a) Vortical structures involved in the side-jet generation process according to the proposition of Monkewitz and Pfizenmaier (1991), revised by Brancher, Chomaz, and Huerre (1994). (b) Illustration of the three-dimensionalisation process of variable-density free shear layers. Longitudinal velocity u_x contours of the optimal perturbation for longitudinal wavenumber $k = .6$ and $At = .5$. The red (resp. blue) region corresponds to $u_x > 0.2u_{x,\max}$ (resp. $u_x < 0.2u_{x,\min}$) (Lopez-Zazueta, Fontane, & Joly, 2016).

References

Monkewitz, P. A. & Pfizenmaier, E. (1991). Mixing by side jets in strongly forced and self-excited round jets. *Physics of Fluids A: Fluid Dynamics*, *3*(5), 1356–1361. doi:10.1063/1.858065

Brancher, P., Chomaz, J. M., & Huerre, P. (1994). Direct numerical simulations of round jets: Vortex induction and side jets. *Physics of Fluids*, *6*(5), 1768–1774. doi:10.1063/1.868238

Fontane, J. (2005). *Transition des écoulements cisaillés libres à densité variable* (Doctoral dissertation, Institut National Polytechnique de Toulouse). Retrieved from https://oatao.univ-toulouse.fr/7338/

Lopez-Zazueta, A., Fontane, J., & Joly, L. (2016). Optimal perturbations in time-dependent variable-density Kelvin–Helmholtz billows. *Journal of Fluid Mechanics*, *803*, 466–501. doi:10.1017/jfm.2016.509

Nastro, G., Fontane, J., & Joly, L. (2022). Optimal growth over a time-evolving variable-density jet at Atwood number $|At| = 0.25$. *Journal of Fluid Mechanics*, *936*. doi:10.1017/jfm.2022.45

W113

TRANSITION TO TURBULENCE IN THE STOKES BOUNDARY LAYER. PART 1: MINIMAL SEEDS

Tom S. Eaves[1]
[1]*School of Science and Engineering, University of Dundee, U.K.*

Abstract Minimal seeds for transition to turbulence in the Stokes boundary layer. (transition to turbulence, Stokes boundary layer).

The Stokes boundary layer is the oscillatory flow above a plate, with oscillations driven either by (1) transverse sinusoidal motion of the plate or (2) a sinusoidal applied pressure gradient. Beyond a critical Reynolds number of 2511, the laminar solution of the Stokes boundary layer is susceptible to linear instability (the eigenvalues of the linear problem in case 1 and 2 above are identical [1]). However, this instability is subcritical given that turbulence is observed for Reynolds numbers above approximately 700 despite the flow being linearly stable in this range of Reynolds numbers [2].

In order to examine potential mechanisms which may cause transition to turbulence from the laminar flow in this subcritical range, Biau [3] computed linear optimal perturbations in the Stokes boundary layer using linear transient nonmodal analysis, noting the importance of the Orr mechanism. However, it is well-established (see Kerswell [4] for a review) that linear transient growth results offer limited insight into the inherently finite-amplitude disturbances which are most likely to trigger transition to turbulence. Instead, the 'minimal seed' for turbulence, the smallest amplitude perturbation that causes transition, provides such a nonlinear description. This talk will describe minimal seeds and their dynamics in the Stokes boundary layer, how they differ between cases (1) and (2), and their dependence on Reynolds number.

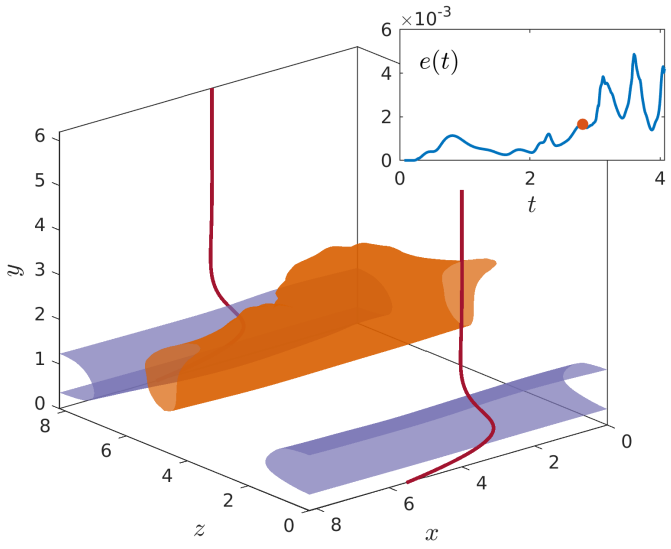

Figure 1. A snapshot of the flow during the minimal seed's transition to turbulence in the wall-driven Stokes boundary layer at Reynolds number 1000 (based upon the boundary layer thickness and the wall speed amplitude). Isosurfaces of positive (blue) and negative (orange) streamwise (x) velocity, the laminar flow profile at this moment in time (red lines), and the energy density against time for the minimal seed's trajectory to turbulence as an inset, in which the red dot indicates the current time. A streamwise streak generated by the lift-up mechanism is about to break down.

This work is supported by an EPSRC New Investigator Award (EP/W021099/1).

References

[1] P. J. Blennerhassett, A. P. Bassom, *The linear stability of flat Stokes layers*, J. Fluid Mech. **464**, 393–410 (2002).
[2] C. Ozdemir, T.-J. Hsu, S. Balachandar, *Direct numerical simulations of transition and turbulence in smooth-walled Stokes boundary layer*, Phys. Fluids **26**, 245108 (2014).
[3] D. Biau, *Transient growth of perturbations in Stokes oscillatory flows*, J. Fluid Mech. **794**, R4 (2016).
[4] R. R. Kerswell, *Nonlinear nonmodal stability theory*, Annu. Rev. Fluid Mech. **50**, 319–345 (2018).

W114

TRANSITION TO TURBULENCE IN THE STOKES BOUNDARY LAYER. PART 2: EDGE STATES

Jorge Sandoval[1] & Tom S. Eaves[1]
[1]*School of Science and Engineering, University of Dundee, U.K.*

Abstract Edge states in the Stokes boundary layer (edge states, Stokes boundary layer).

The Stokes boundary layer is the oscillatory flow above a plate, with oscillations driven either by (1) transverse sinusoidal motion of the plate or (2) a sinusoidal applied pressure gradient. Beyond a critical Reynolds number of 2511, the laminar solution of the Stokes boundary layer is susceptible to linear instability (the eigenvalues of the linear problem in case 1 and 2 above are identical [1]). However, this instability is subcritical given that turbulence is observed for Reynolds numbers above approximately 700 despite the flow being linearly stable in this range of Reynolds numbers [2].
The state space of a subcritical flow consists of two basins of attraction, that of the laminar flow, and that of turbulence. These basins are separated by a saddle point, termed the 'edge state', and its codimension-one stable manifold, termed the 'edge manifold', or simply 'edge'. In simple shear flows in small domains, the edge state is typically an equilibrium or travelling-wave solution of the Navier–Stokes equations [4]. However, for more complex flows (e.g. those at higher Reynolds number), or flows with an inherent oscillatory nature [5], the edge state may be a periodic orbit, relative periodic orbit, or chaotic saddle (e.g. [6]). Regardless of their character, edge states may be found by 'edge tracking' [3], an iterative procedure in which the trajectories of initial conditions either side of the edge are computed and bisected, until finally the edge state itself can be converged using a Newton–Krylov–GMRES scheme and continued in Reynolds number using arclength continuation.
This talk will present edge states in the Stokes boundary layer, comparing them to known edge states in other non-oscillatory flows, indicating how edge states in the wall- and pressure-driven Stokes layer differ, and discussing the effect of Reynolds number.

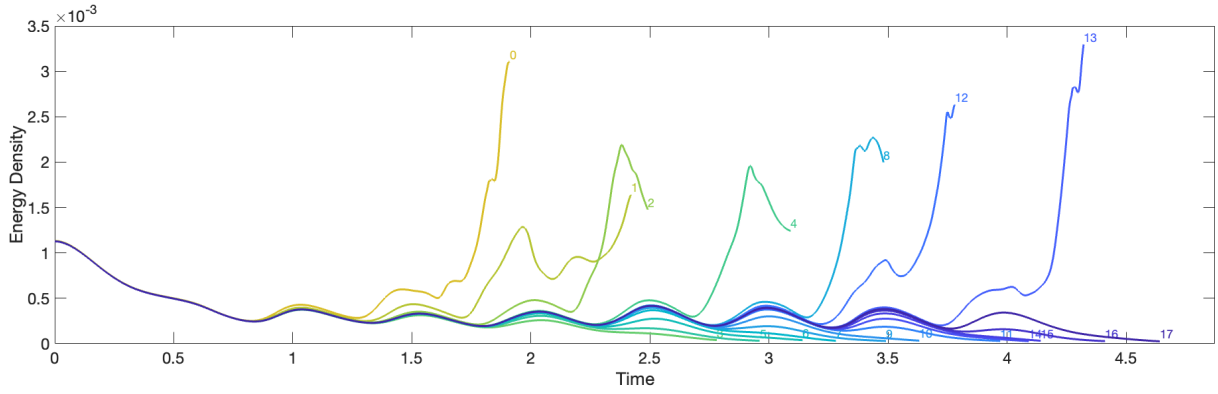

Figure 1. Time evolution of the energy density of successive iterates in the edge tracking algorithm for the wall-driven Stokes boundary layer at Reynolds number 1000 (based upon the boundary layer width and the wall speed amplitude). Iterates are converging towards the periodic edge state.

This work is supported by an EPSRC New Investigator Award (EP/W021099/1).

References

[1] P. J. Blennerhassett, A. P. Bassom, *The linear stability of flat Stokes layers*, J. Fluid Mech. **464**, 393–410 (2002).
[2] C. Ozdemir, T.-J. Hsu, S. Balachandar, *Direct numerical simulations of transition and turbulence in smooth-walled Stokes boundary layer*, Phys. Fluids **26**, 245108 (2014).
[3] J. D. Skufca, J. A. Yorke, B. Eckhardt, *Edge of chaos in a parallel shear flow*, Phys. Rev. Lett. **96**, 174101 (2006).
[4] Y. Duguet, A. P. Willis, R. R. Kerswell, *Transition in pipe flow: the saddle structure on the boundary of turbulence*, J. Fluid Mech. **613**, 255–274 (2008).
[5] A. Pershin, C. Beaume, T. S. Eaves, S. M. Tobias, *Optimizing the control of transiion to turbulence using a Bayesian method*, J. Fluid Mech. **941**, A25 (2022).
[6] T. S. Eaves, C. P. Caulfield, *Disruption of SSP/VWI states by a stable stratification*, J. Fluid Mech. **784**, 548–564 (2015).

W115

INTERNAL WAVE INSTABILITIES AND TRANSITION TO TURBULENCE IN LARGE ASPECT RATIO DOMAINS

Ilias Sibgatullin[1], Stepan Elistratov & Thierry Dauxois[1]
[1]*Laboratoire de Physique (UMR CNRS 5672) ENS de Lyon 46, allée d'Italie LYON, France*

Abstract Internal waves, inertial waves, wave attractors, wave turbulence.

Geophysical turbulence exhibits distinct characteristics compared to conventional turbulence flows, primarily due to the effects of stratification and/or rotations which are different at various scales of flows. We will focus on the small-scale effects where the direct action of buoyancy significantly affects momentum equations and cannot be neglected, as opposed to quasi-hydrostatic modeling at large scales.

Continuous stratification itself profoundly impacts the onset of hydrodynamical instabilities due to a unique dispersion relation. According to this relation, wave beams and wave energy propagate perpendicular to the phase lines. It has also been observed that the dynamics of wave beams (webs of rays) in closed domains differ considerably from conventional ray tracing. In a general case, an attracting trajectory exists for the wave beams, referred to as wave attractors. These trajectories evolve due to the focusing/defocusing of wave packets upon reflection from the walls inclined with respect to gravity or rotation axis [1].

Owing to the high concentration of wave energy along these attracting paths, they are particularly susceptible to instabilities and serve as a source for the propagation of secondary waves. In our previous works, we demonstrated that if the aspect ratio of the motion is of the order of one, the transitions to turbulence can be effectively described using a laboratory toy-box model [2, 3]. In such a laboratory model, turbulence originates from cascades of triadic resonances. This model represents an important case of natural flows. Another case involves large aspect ratio motions, where the horizontal scale is much larger than the vertical, yet buoyancy effects cannot be neglected.

Previously, we described the peculiarities of linear regimes of large aspect ratio wave attractors and their instabilities at multiples of half the forcing frequency. Now we complement this scenario with cascades of triadic resonance instabilities in each half-harmonic frequency interval and show the corresponding changes in spatial spectra.

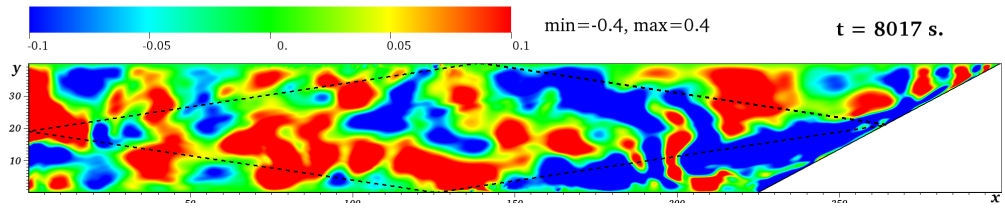

Figure 1. A fully developped internal wave turbulence produces by linear wave attractor shown with the dashed line.

References

[1] L. R. M. Maas, D. Benielli, J. Sommeria, and F.-P. A. Lam. *Observation of an internal wave attractor in a confined, stably stratified fluid.* Nature, **388**:557–561, August 1997.

[2] Christophe Brouzet, Ilias Sibgatullin, Helene Scolan, Evgeny Ermanyuk, and Thierry Dauxois. *Internal wave attractors examined using laboratory experiments and 3d numerical simulations. Journal of Fluid Mechanics, **793**:109–131, 2016.*

*[3] Christophe Brouzet, Evgeny Ermanyuk, Sylvain Joubaud, Ilias Sibgatullin, and Thierry Dauxois. Energy cascade in internal-wave attractors. EPL (Europhysics Letters), **113(4)**:44001, 2016.*

W116

FIBRE BUCKLING IN A CONFINED CO-FLOWING JET

Grégoire Clément[1,2], Samuel Hidalgo Caballero[1,2], Mathieu Oléron[1,2], Finn Box[3], Joshua D. McGraw[1,2] & Matthieu Labousse[1,2]
[1]*Gulliver, CNRS, ESPCI Paris, PSL, Paris, France.*
[2]*Institut Pierre-Gilles de Gennes, Paris , France.*
[3]*Physics of Fluids & Soft Matter, University of Manchester, Manchester, UK*

Keywords: Microfluidics, Buckling Instability, Soft Boundaries

Abstract

The buckling and transport of flexible fibers in viscous flows has been largely studied from a theoretical and experimental point of view [1,2]. It has been shown that compressive forces exerted on a fiber and viscous dissipations in the fluid domain surrounding the fiber play a major role in the triggering of the instability [1,2]. In addition, the effect of confinement has been proven to play a significant role in the buckling of long fibers that align with the flow [3].

In this study we present experimentally the impact of fluid boundaries on the evolution of the buckling instability. We have built a microfluidic chip that allows for extruding an elastic fiber into a stable confined coflowing jet [4]. We observe a plethora of distinct dynamics behaviors ranging from the buckling of the fiber within the jet boundary, to the combine buckling of the jet and the fiber. The study qualitatively present the impact of the liquid-liquid surface tension γ, the elastic modulus of the fiber B and the viscosity of the different phases.

References

[1] B. Chakrabarti *et al.*, *Flexible filaments buckle into helicoidal shapes in strong compressive flows*, Nat. Phys. **16**, 689-694(2020)
[2] F. P. Gosselin *et al.*, *Buckling of a beam extruded into highly viscous fluid*, Phys. Rev. E, **90**, 052718(2014)
[3] J. Cappello *et al.*, *Fiber Buckling in Confined Viscous Flows: An Absolute Instability Described by the Linear Ginzburg-Landau Equation*, Phys. Rev. Lett. **129** 074504(2022)
[4] P. Guillot *et al.*, *Stability of a jet in confined pressure-driven biphasic flows at low Reynolds number in various geometries*, Phys. Rev. E **78** 016307(2008)

W117

LIFT-UP AND SELF-SUSTAINING PROCESS (SSP) IN A COUETTE-POISEUILLE FLOW

Tao Liu, Benoit Semin, Ramiro Godoy-Diana & José Eduardo Wesfreid
PMMH, CNRS, ESPCI, Université PSL, Sorbonne Université, Université Paris Cité, F-75005, Paris, France

Keywords: Transition to turbulence

Abstract

In the transition to turbulence in wall-bounded shear flows, activity is localized in turbulent spots. They contain coherent structures, described by streamwise vortices called rolls and modulations of the streamwise velocity called streaks. Many theoretical and numerical works have shown that the nonlinear interaction between these structures is responsible for the self-sustaining process (SSP) of the turbulence, but experimental studies are scarce. We investigate experimentally the interaction between these coherent structures [1].

We perform the experiments in a plane Couette-Poiseuille channel in which the flow is driven by one moving belt and connected to two reservoirs so that the mean flux is zero (fig. 1A). The direction of the moving belt defines the streamwise direction x, z is the spanwise direction and y the wall-normal direction. The streaks are quantified by the streamwise velocity fluctuations u_x, and the rolls by the spanwise velocity u_z and by the wall-normal velocity u_y.

In a set of experiments, we study the waviness of streaks using vortex generators to induce unstable wavy streaks [2]. The evolution of the streaks becoming wavy from a straight state is characterized using stereoscopic PIV, and processed using a new method we developed. Using spatial Fourier filtering, we define a proxy for the waviness $\langle|\omega_{y,wavy}|\rangle$. Our experimental results show that the wall- normal velocity, which is a proxy for the rolls, is correlated to the increase of the waviness of the streaks, as expected from SSP models (fig. 1B). Moreover, for streaks of low waviness, the value of $|u_y|$ is small and related to the amplitude of the streak $|u_x|$, as expected for linear lift-up.

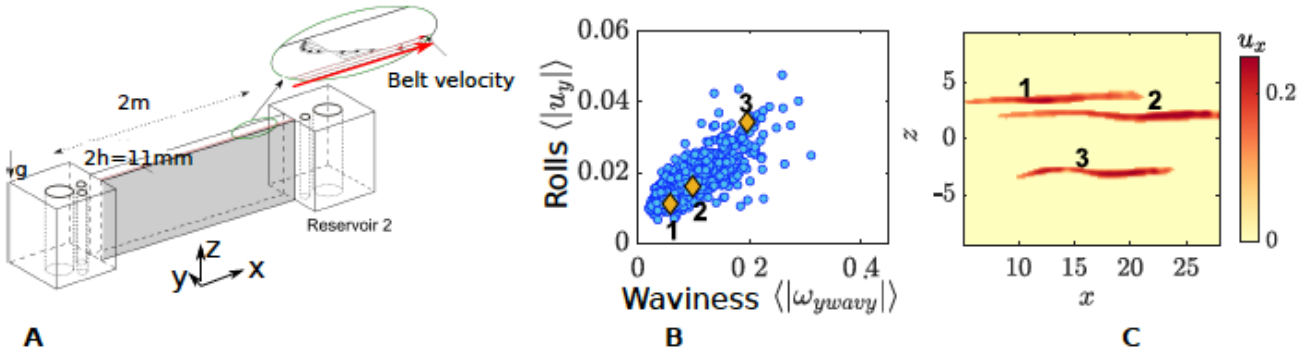

Figure 1. A : schematic view of the experimental set-up. B : link between rolls and waviness, a point corresponds to the average on a streak. C : corresponding streaks for 3 different points.

References

1. T. Liu, B. Semin, L. Klotz, R. Godoy-Diana, J. E. Wesfreid & T. Mullin, *Decay of streaks and rolls in plane Couette-Poiseuille flow,* J. Fluid Mech., **915**, A65 (2021).
2. T. Liu, B. Semin, R. Godoy-Diana & J. E. Wesfreid, *Lift-up and streak waviness drive the self-sustained process in wall-bounded transition to turbulence*, Phys. Rev. Fluids., accepted

W118

SUBCRITICAL TRANSITION TO ELASTIC TURBULENCE IN PARALLEL SHEAR FLOWS: RECENT PROGRESS

Martin Lellep[1], Moritz Linkmann[2], Alexander Morozov[1],
[1]*SUPA, School of Physics and Astronomy, University of Edinburgh, Edinburgh, EH9 3FD, UK*
[2]*School of Mathematics and Maxwell Institute for Mathematical Sciences, University of Edinburgh, Edinburgh, EH9 3FD, UK*

Abstract Non-newtonian fluids, turbulence.

Solutions of long, flexible polymer molecules are complex fluids that simultaneously exhibit fluid-like and solid-like behaviour. When subjected to an external flow, dilute polymer solutions exhibit elastic turbulence - a unique, chaotic flow state absent in Newtonian fluids, like water. Unlike its Newtonian counterpart, elastic turbulence is caused by polymer molecules stretching and aligning in the flow, and can occur at vanishing inertia. While experimental realisations of elastic turbulence are well-documented, there is currently no understanding of its mechanism.

In this talk we will review our recent progress in identifying the mechanism of elastic turbulence in pressure-driven flows through straight channels. Using large-scale direct numerical simulations of such flows [1] we demonstrate that the transition to elastic turbulence is sub-critical, giving rise to spot-like flow structures that, further away from the transition, eventually spread throughout the domain, see the visualisations in fig. 1(a). Phase portraits showing the time evolution of key observables, the total kinetic energy and the polymer extension, suggest that the dynamics are organised by the presence of invariant solutions to the equations of motion, see fig. 1(b). In summary, our numerical results produce circumstantial evidence suggesting that the transition to elastic turbulence proceeds in a similar way as the transition to turbulence in Newtonian parallel shear flows, that is, mediated by exact unstable solutions of the equations of motion.

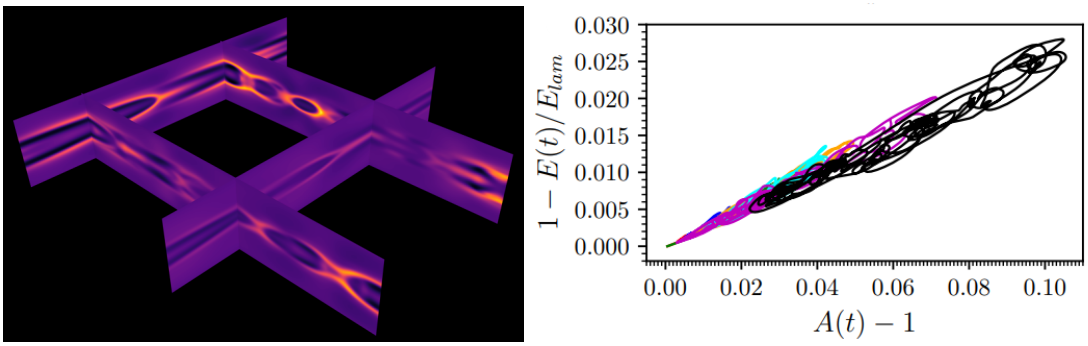

Figure 1. Left: Visualisation of the relative polymer stretch at several positions in the domain for Weissenberg number $Wi = 150$. Right: Phase portrait showing the total kinetic energy against the normalised polymer stretch. The colours indicate different values of the Weissenberg number.

References

[1] Lellep, M. and Linkmann, M. and Morozov, A. Purely elastic turbulence in pressure-driven channel flows. PNAS **15**, e2318851121 (2024)

W126

GALLOPING BUBBLES

Jian H. Guan[1], Saiful I. Tamim[1], Connor W. Magoon[1] & Pedro J. Sáenz[1]
[1]*Department of Mathematics, University of North Carolina, Chapel Hill, U.S.A.*

Abstract We introduce a new spontaneous symmetry-breaking instability that leads to the self-propulsion of vertically vibrated bubbles
(Keywords: bubbles, self-propulsion, symmetry breaking).

Bubbles moving in a liquid are simple in appearance yet display a wealth of intriguing dynamics relevant to innumerable practical applications. Here, we demonstrate that a millimetric bubble may undergo a spontaneous symmetry breaking and start to 'gallop' steadily along the boundaries of a vibrating fluid chamber, self-propelled through a resonant interaction between its vibration modes. We characterize the dynamics of these self-propelled bubbles experimentally in terms of the key system parameters, including bubble volume, viscosity, and vibrational forcing. Our results reveal that the bubble propulsion is intimately related to their resonant shape oscillations, which may be fine-tuned to produce a myriad of dynamics, including rectilinear, circular, and zig-zag motions. We complement our experimental observations with direct numerical simulations to extend the galloping instability to hemispherical bubbles. Our spectral analysis demonstrates that the galloping instability results from the excitation of shape oscillations asymmetric about the vibration axis. We then perform a stability analysis using perturbation theory to rationalize theoretically the symmetry breaking mechanism in terms of resonant shape modes. By computing the inertial reaction of an inviscid external liquid to the bubble deformation, we describe the galloping propulsion mechanism as a case of swimming in potential flow. We conclude by demonstrating how the galloping instability may be harnessed for practical applications, including bubble removal and sorting, on-demand bubble size generation, and surface cleaning tasks.

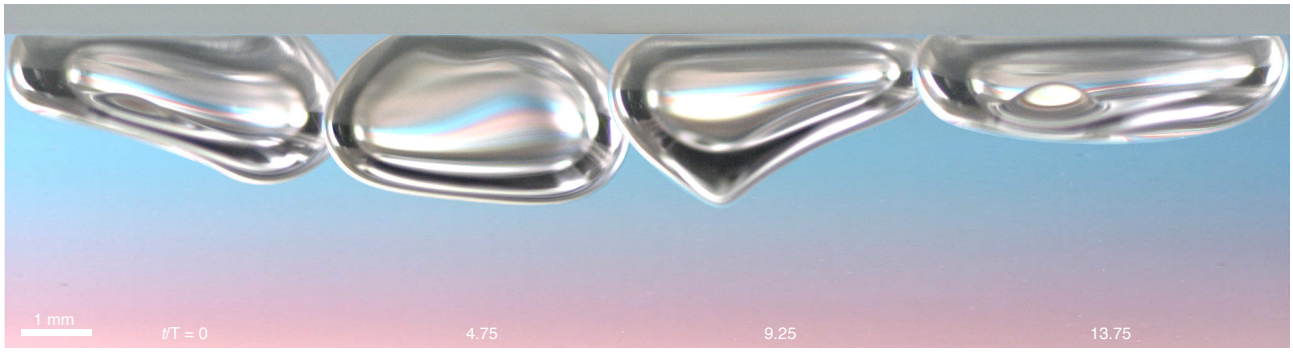

Figure 1. Temporal evolution of a vertically vibrated bubble 'galloping' along a solid boundary.

W127

HOW CAN A SURFACTANT AFFECT BUBBLE BURSTING?

E. J. Vega & J. M. Montanero
Depto. de Ingeniería Mecánica, Energética y de los Materiales and Instituto de Computación Científica Avanzada (ICCAEx), Universidad de Extremadura, E-06006 Badajoz, Spain

Keywords: Bubble bursting, Surfactant, Droplet, Aerosols

Abstract

We study the bursting of a bubble covered with a surfactant experimentally. We conclude that the bubble bursting takes longer than that of a surfactant-free bubble with the same equilibrium surface tension due to the interfacial elasticity. A tiny bubble is formed at the cavity bottom right before the free surface reversal due to the Marangoni stress. This stress also drives the liquid flow that makes the jet escape from the end-pinching mechanism for a certain surfactant concentration interval. A diminutive liquid droplet manages to escape from the jet for a sufficiently large surfactant concentration. This droplet is much smaller than its surfactant-free counterpart but moves at a similar speed. The surfactant molecules are convected toward the jet tip so that the monolayer covering the first-emitted droplet is practically saturated [1].

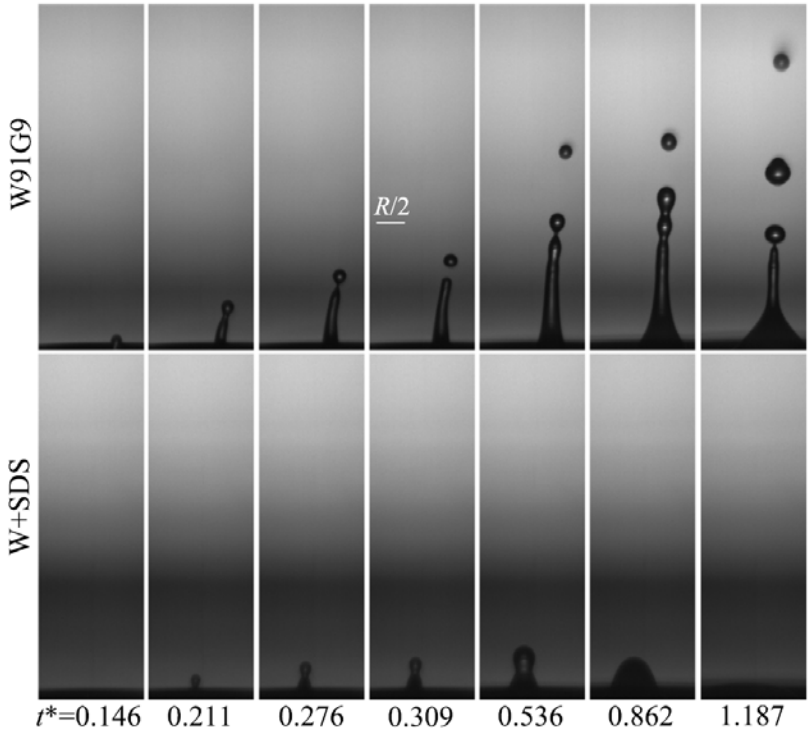

Figure 1. Images of the jet and droplet ejection for a Bond numer B = 0.15 and a Ohnesorge numer Oh = 0.0049. The upper and lower images correspond to a equilibrium surfactant surface density Γ_{eq} = 0 and 0.992, respectively. The images have been scaled with the bubble radius R (which took different values with and without surfactant).

References

[1] E. J. Vega, J. M. Montanero, *Influence of a surfactant on bubble bursting*, Experimental Thermal and Fluid Science **151**, 111097 (2024).

W128

Cavitation Microstreaming Induced by Pendent and Sessile Bubbles in Water Under Confinement

Vivek Karma[1], S Pushpavanam[1]
[1]*Department of Chemical Engineering, Indian Institute of Technology Madras, Chennai, India*

Keywords: Oscillating bubble, cavitation microstreaming, acoustic energy, microPIV, numerical simulation

Abstract

Cavitation microstreaming refers to the non-oscillatory flow induced by an oscillating bubble subjected to an acoustic field. This type of streaming plays a significant role in microfluidic-based cell lysis, where high shear stresses near an oscillating bubble cause the cell wall to rupture without affecting the cell material. The present study investigates the effect of rigid boundaries on cavitation microstreaming induced by an oscillating bubble attached to a glass wall. Two bubble types are considered: sessile and pendent. The bubbles of constant volume were placed in chambers of different heights, which mimicked the proximity to rigid boundaries. The surrounding fluid is seeded with 2μm polystyrene microspheres to visualise the flow. The Energy Minimization Method was used to verify the stationary bubble profile observed experimentally. The study revealed different patterns at smaller bubble-to-wall distances. The disappearance of patterns at lower heights and the appearance of new patterns can be attributed to hindrance to free flow from the enclosing wall.

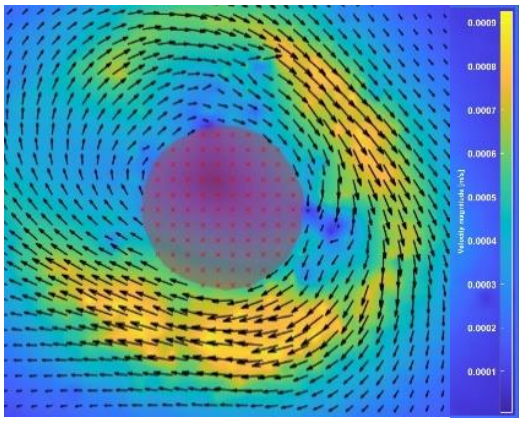

Fig 1. PIV image representing the vector field and velocity magnitude for the circular orbiting pattern.

We also performed microPIV in PIVlab to estimate the Lagrangian velocity field and shear stress in the enclosing wall. The effect of acoustic frequency and amplitude on streaming patterns was studied. It was revealed that the amplitude of acoustic wave only affects the velocity of the surrounding fluid. The experiments were simulated in COMSOL Multiphysics software using a Laminar flow (Level set) module to verify the streaming generated around the bubble. We present a flow regime map plot between chamber height and driving frequency for sessile and pendent-type bubbles. These maps may assist future researchers in identifying suitable patterns for sonoporation, cell-lysis, micro-pumping, and micro-mixing applications.

W129

EVOLUTION OF THE SURFACTANT MONOLAYER IN A BUBBLE RISING IN WATER WITH TRACES OF SURFACTANT

Daniel Fernández-Martínez[1], José M. Montanero[1], José M. López-Herrera[2] & Miguel A. Herrada[2]
[1]*Departamento de Ingeniería Mecánica, Energética y de los Materiales and Instituto de Computación Científica Avanzada (ICCAEx),Universidad de Extremadura, Spain*
[2]*Departamento de Ingeniería Aerospacial y Mecánica de Fluidos, Universidad de Sevilla, Spain.*

Keywords: rising bubble ; path instability; surfactant

Abstract

Bubble dynamics are of great importance in many natural and industrial processes involving heat and mass transfer. The understanding of the single-bubble case provides the basis for studying much more complex systems consisting of many bubbles. In particular, the motion of a single bubble rising due to buoyancy in a liquid bath is a paradigmatic problem, which has been studied for several centuries and continues to be of great interest today. When a single bubble is released in the bottom of a liquid tank, it accelerates and deforms until it reaches a terminal (steady) velocity and shape. Small bubbles rise following a straight path. But when bubbles exceed a critical size, they follow a zig-zag or spiral trajectory (this is known as path instability). The mechanism responsible for this behavior is still under discussion [1,2].

Surfactants are molecules that adsorb onto the interface and reduce the surface tension. When the bubble rise in a liquid containing surfactant, the adsorbed molecules are swept towards the rear part of the bubble producing an uneven surfactant density. The corresponding surface tension gradient produces Marangoni stress that reduce the surface mobility. Even for low concentrations, surfactant reduce the bubble terminal velocity and affect the path instability [3].

In this work we present experimental and numerical results showing the dynamics of a single bubble rising in different surfactant solutions. We focus on the effect of the surfactant properties on the evolution of the monolayer until it reaches the steady state (Fig. 1). The model considers the surfactant transport in the bulk and over the monolayer, and the adsorption/desorption process, coupled with the Navier-Stokes equations.

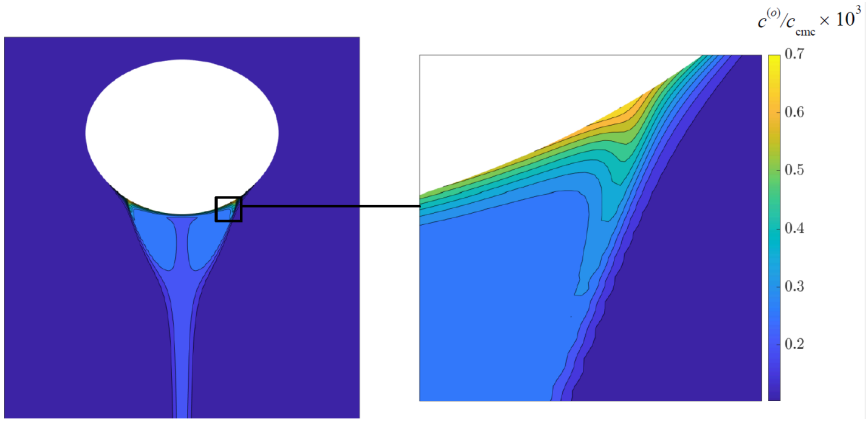

Figure 1. Surfactant concentration around a bubble rising in water with traces of SDS.

References

[1] P. Bonnefis, D. Fabre, and J. Magnaudet, *When, how, and why the path of an air bubble rising in pure water becomes unstable*, Proc. Natl. Acad. Sci. **120**, e2300897120 (2023).
[2] M.A. Herrada and J.G. Eggers, *Leonardo's paradox resolved: path instability of an air bubble rising in water*, Proc. Natl. Acad. Sci. **120**, e2216830120 (2023)
[3] A. Tzounakos, D. G. Karamanev, A. Margaritis, and M. A. Bergougnou, *Effect of the surfactant concentration on the rise of gas bubbles inpower-law non-newtonian liquids*," Ind. Eng. Chem. Res. 43, 5790–5795900 (2004).

W130

RAYLEIGH-PLATEAU INSTABILITY OF SURFACTANT-LADEN LIQUID NANO-THREADS

Luís H. Carnevale[1], Piotr Deuar[1], Zhizhao Che[2] & Panagiotis E. Theodorakis[1]
[1]*Institute of Physics, Polish Academy of Sciences, Warsaw, Poland*
[2]*State Key Laboratory of Engines, Tianjin University, Tianjin, China*

Abstract Surfactant concentration effects on liquid thread breakup at molecular scales analysed from MDPD simulations. (Many-body Dissipative Particle Dynamics, Surfactants, Liquid Thread Breakup).

The formation of droplets from a liquid jet plays a crucial role in various industrial applications such as inkjet printing, nanoprinting, nanoscale manufacturing, chemical processing, and spraying. This process relies on a surface tension-driven instability called the Rayleigh-Plateau instability, and a comprehensive understanding of the thinning dynamics leading to the breakup of the continuous liquid phase is essential for precise droplet control.

Surfactants, molecules that adsorb to the liquid interface and reduce surface tension based on their concentration, offer a means of controlling this process. However, their adsorption is limited up to the critical micelle concentration (CMC), beyond which surfactant molecules saturate the interface and aggregate into micelles in the liquid bulk.

At small length scales, molecuar thermal motion also influences the breakup dynamics ([2]), introducing a thermal fluctuation (TF) thinning regime ([1]). This study employs many-body dissipative particle dynamics (MDPD) simulations to investigate the impact of surfactants on liquid thread breakup driven by thermal fluctuations. Notably, we investigate how the concentration of surfactants affects the the most unstable wavenumber and the thinning neck dynamics, showing a transition from the inertial regime at low concentrations to the TF regime at higher concentrations, as depicted in Figure 1c. The study also discusses a possible transition to a "breakup" regime, initially reported as a power-law in prior research ([3]).

Additionally, the analysis of surfactant distribution along the thread axial direction, as presented in Figure 1a, sheds light on the surfactant transport mechanism, providing insights into the intricate breakup process of surfactant-laden liquid threads driven by thermal fluctuations. This work contributes to a deeper molecular-scale understanding of the phenomenon, advancing knowledge in this field.

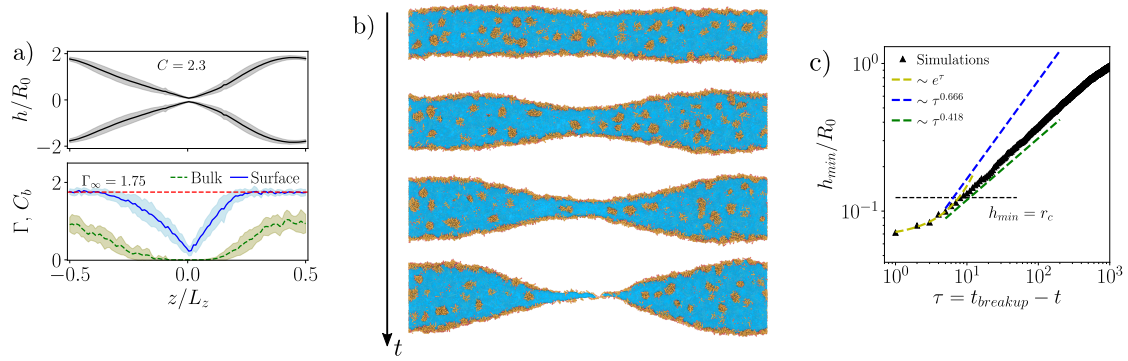

Figure 1. a) Top – Average breakup profile of a liquid thread with a concentration above the CMC showing an almost symmetric double cone. Bottom – Surfactant distribution along the thread axis on the surface (Γ) and in the bulk (C_b). The shaded area represents one standard deviation and the averages were done with 20 simulations. b) Example of a typical simulation above the CMC where the length of the thread is equal to the fastest growing perturbation wavelength. c) Thinning dynamics of the pinching point revealing it to be in the thermal fluctuation regime and a transition to a possible exponential regime when it reaches a MDPD cutoff parameter (r_c).

* *This research has been supported by the National Science Centre, Poland, under Grant No. 2019/34/E/ST3/00232. We gratefully acknowledge Polish high-performance computing infrastructure PLGrid (HPC Centers: ACK Cyfronet AGH) for providing computer facilities and support within computational Grant No. PLG/2022/015747.*

References

[1] J. Eggers, *Dynamics of Liquid Nanojets*, Phys. Rev. Lett. **89**, 084502 (2002).
[2] L. H. Carnevale, P. Deuar, Z. Che, and P. E. Theodorakis, *Liquid thread breakup and the formation of satellite droplets*, Phys. Fluids **35**, 074108 (2023).
[3] J. Zhao, N. Zhou, K. Zhang, S. Chen, Y. Liu, and Y. Wang, *Rupture process of liquid bridges: The effects of thermal fluctuations*, Phys. Rev. E **102**, 023116 (2020).

W131

SURFACTANT-INDUCED MARANGONI EFFECTS ON CAPILLARY WAVES AND WORTHINGTON JETS IN BURSTING BUBBLE APPLICATIONS

Paula Pico[1], Lyes Kahouadji[1], Seungwon Shin[2], Jalel Chergui[3], Damir Juric[3,4], & Omar K Matar[1]
[1]*Department of Chemical Engineering, Imperial College London, SW7 2AZ, London, United Kingdom,*
[2]*Department of Mechanical and System Design Engineering, Hongik University, Seoul 04066, South Korea*
[3]*LISN, CNRS, Université Paris Saclay, 91400 Orsay, France*
[4]*Department of Applied Mathematics and Theoretical Physics, University of Cambridge, Cambridge CB3 0WA, UK*

Abstract
The collapse of an air cavity and the subsequent ejection of a liquid jet exhibit intricate dynamics relevant to various fluid mechanics problems, including bursting bubbles, drop impact, Faraday waves, and interfacial oscillations. This study delves into the stages leading to aerosol formation in the context of bursting bubbles through high-fidelity simulations (see fig.1(a)). These stages entail the propagation of capillary waves across the bubble, their convergence at the bubble's centre, the ascent of a Worthington jet, and its fragmentation via a Rayleigh–Plateau instability to release liquid droplets. These mechanisms hold significant importance in diverse natural occurrences and daily activities, including oceanic spray and effervescent beverages. We focus specifically on the individual and combined effects of surface active material and non-negligible gravitational forces, quantified by the Bond number, $Bo > 0.1$. Despite their relevance in real-life scenarios and their remarkable influence on the bursting phenomena, these aspects have largely been overlooked in the literature, with only a handful of recent studies on the matter [1].
Our results suggest a dramatic alteration of the system's dynamics with the addition of surfactant. Fig. 1(b)-(c) depicts the temporal evolution (scaled by collapse time, $\tilde{t}_{coll}$) of the angular position of the dominant capillary wave, $\tilde{\theta}$. A break from the linear behaviour featured in surfactant-free interfaces [2] is introduced by the presence of surfactant, where $\tilde{\theta} \sim \tilde{t}^2$. This linearity break is accompanied by a wave propagation retardation, manifesting in an approximately 40% decrease in the capillary wave's average velocity. We propose a mechanism to explain this delay in figure 1(d)-(e), whereby the capillary waves create a high surfactant concentration region exposed to 'upwards' ($\tilde{\tau}_{m,z} > 0$) and 'downwards' ($\tilde{\tau}_{m,z} < 0$) Marangoni stresses at the initial stages ($\tilde{t} = 0.1$). As collapse is approached ($\tilde{t} = 0.32$), the saturated region at the bubble's apex eliminates $\tilde{\tau}_{m,z} < 0$, subjecting the interface to strong, uni-directional stresses opposing motion. We also make connections to the jetting behaviour stemming from finite-amplitude interfacial oscillations (figure 1(f)-(j)) reported previously in [3], elucidate the influence of surfactants on its dynamics, and link them to bursting bubbles.

Keywords: Bursting bubbles, capillary-gravity waves, cavity collapse, Marangoni stresses, Worthington jet

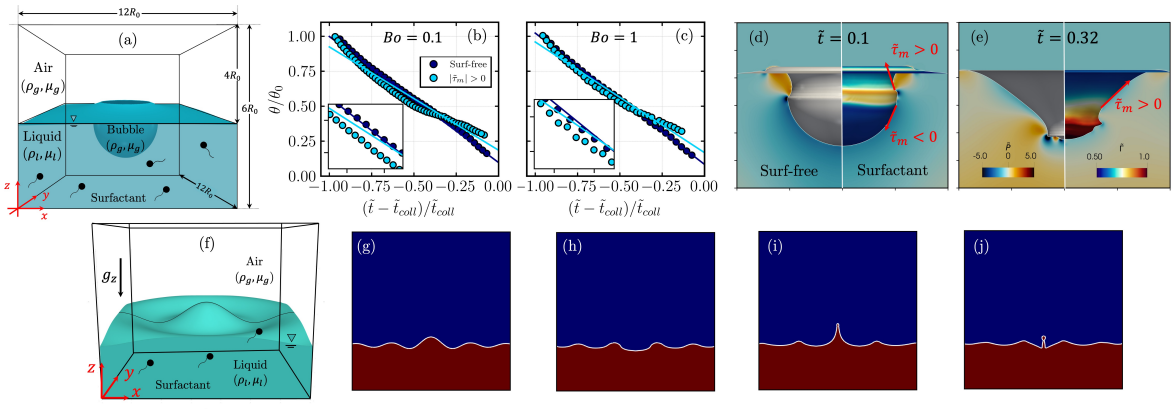

Figure 1. (a) Bursting bubble simulation setup. (b)-(c) Comparison between surfactant-free and surfactant-laden capillary wave's motion. (d)-(e) Role of Marangoni stresses. (f)-(j) Jetting behaviour caused by finite-amplitude interfacial oscillations

References

[1] J. Pierre, M. Poujol & T. Séon: *Influence of surfactant concentration on drop production by bubble bursting*, Phys. Rev. Fluids, **7**:073602 (2022).
[2] J.M. Gordillo & J. Rodríguez-Rodríguez: *Capillary waves control the ejection of bubble bursting jets*, J. Fluid Mech, **867**:556–571 (2019).
[3] P.K.Farsoiya, Y.S.Mayya & R.Dasgupta: *Axisymmetric viscous interfacial oscillations: theory and simulations*,J. Fluid Mech,**826**:797-818 (2017).

W132

GLOBAL STABILITY ANALYSIS OF HYDRODYNAMIC FOCUSING IN THE PRESENCE OF A SOLUBLE SURFACTANT

Manuel Rubio[1], M. Guadalupe Cabezas[2], José M. Montanero[2] & Miguel A. Herrada[3]
[1]*Departamento de Ingeniería Energética y Fluidomecánica and Instituto de las Tecnologías Avanzadas de la Producción (ITAP), Universidad de Valladolid, Spain*
[2]*Departamento de Ingeniería Mecánica, Energética y de los Materiales and Instituto de Computación Científica Avanzada (ICCAEx),Universidad de Extremadura, Spain*
[3]*Departamento de Ingeniería Aerospacial y Mecánica de Fluidos, Universidad de Sevilla, Spain.*

Keywords: flow focusing, surfactant, global stability analysis, tip streaming, microemulsions

Abstract
We numerically analyze the influence of soluble surfactant on the microjetting mode of a liquid-liquid flow focusing configuration. Most of the surfactant adsorption occurs next to the feeding capillary. The focusing effect of the outer current accelerates and compresses the interface increasing the surfactant surface concentration towards the meniscus tip and significantly reducing the surface tension. Marangoni stress alters the tangential stress balance at the interface but does not reduce the interface velocity. For this reason, the base flow with and without surfactant are very similar on the scale of the injection capillary (Fig. 1). However, the addition of surfactant stabilizes the flow and allows the production of thinner jets.
We use global stability analysis at the minimum flow rate [1,2] to unveil the mechanism responsible for stabilization. In our analysis, we can distinguish the effect of the surfactant monolayer through the base flow and the perturbation. Our results show that the stabilization is not produced by the surface tension reduction caused by the surfactant. Instead, it occurs due to the dynamical response of the surfactant monolayer to perturbations. Most of the effect can be associated with the Marangoni stress due to surface tension perturbations which induces a flow that opposes the growth of the perturbation. Additionally, there is a reduction of the adverse capillary pressure due to accumulation of surfactant in the meniscus tip which may also contribute to stabilizing the microjetting mode. Surfactant concentration needs to exceed the critical micellar concentration to observe a noticeable reduction of the minimum flow rate, in agreement with experimental results [3,4]. The minimum flow rate depends on the adsorption constant and the concentration through the product of both. On the contrary, surfactant desorption and diffusion hardly affect the stability limit. The stabilizing effect of the surfactant monolayer increases with the capillary number (the outer flow rate). Interestingly, the magnitude of the surfactant stabilizing effect can increase even when the reduction of the jet surface tension decreases.

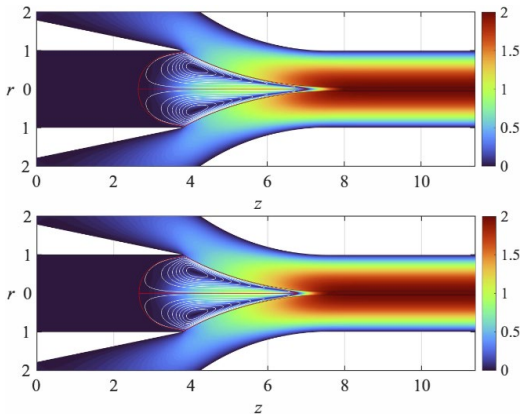

Figure 1. Streamlines for the same capillary number and flow rate, without (a) and with surfactant (1.47 times the critical micellar concentration). The color indicates the velocity magnitude in terms of the mean velocity in the discharge tube.

References

[1] M.A. Herrada, J.M. Montanero, *A numerical method to study the dynamics of capillary fluid systems.* J. Comput. Phys. **306**, 137–147 (2016).
[2] V. Theofilis, *Global linear instability.* Annu. Rev. Fluid Mech. **43**, 319–352 (2011).
[3] T.M. Moyle, L.M. Walker, S.L. Anna, Predicting conditions for microscale surfactant mediated tipstreaming. Phys. Fluids 24, 082110 (2012).
[4] M. López, M.G. Cabezas, J.M. Montanero, M.A. Herrada, M.A. *On the hydrodynamic focusing for producing microemulsions via tip streaming*. J. Fluid Mech. **934**, A47 (2022).

W133

THE EFFECT OF VISCOELASTICITY IN A THIN SQUEEZED FILM

Ulaş Akyüz[1], Humayun Ahmed[1], Lorenzo Lombardi[2], Pier Luca Maffettone[2], Luca Biancofiore[1,3]
[1]*Department of Mechanical Engineering, Bilkent University, Ankara, Turkey,*
[2]*Department of Chemical, Materials and Production Engineering, University of Naples Federico II, Italy,*
[3]*Department of Industrial and Information Engineering and Economics, University of L'Aquila, Italy*

Abstract We analyze both experimentally and numerically the effect of viscoelasticity in a thin squeezed film . (Viscoelasticity, thin film, lubrication theory).

Modeling viscoelasticity is crucial for comprehending the complex rheological behaviors of polymeric materials, under specific conditions, e.g., at high mechanical stress. Viscoelastic materials exhibit a combination of elastic and viscous properties, rendering them highly versatile for numerous applications, including enhancing the load-carrying capacity of lubricants [2]. How viscoelasticity influences a thin film squeezed via the vertical motion of the bounding channel walls, where channel walls approach each other, is particularly intriguing. Understanding the impact of viscoelastic properties on lubrication and wear in this context can be pivotal for optimizing performance and enhancing durability.

This study delves into the comparison between the previously proposed viscoelastic Reynolds (VR) model [1], experimental observations, and a third-order perturbation in the Deborah number (De), i.e., the ratio between the polymer relaxation time λ and the flow residence time, $De = \lambda \frac{V_0}{H_0}$ where V_0 is the squeezing speed, and H_0 is the maximum height of the film. VR has been observed to be effective in modeling viscoelastic lubricants in sliding geometries and helped to show that viscoelasticity can reduce friction and enhance load-bearing capabilities in bearings [1].

We examine (i) the Oldroyd-B and (ii) the modified Phan-Thien-Tanner (MPTT) constitutive relationships implemented in the VR algorithm [1, 3] by comparing them to experimental results, as depicted in Figure 1a. In the experiment, we measure the behavior of a polyvinyl alcohol and borax solution with $\lambda = 0.0324$ s relaxation time. The upper plate, moving at a constant 0.4 mm/s under constant volume squeezing, covered a distance of 0.5 mm, resulting in $De = 0.016$. We recorded the load on the upper plate.

The VR model accurately predicts the variation in the net vertical force at small squeeze depths when compared to experimental data as depicted in Figure 1a. Both constitutive relations demonstrate a qualitative agreement with the experimental data but vary in terms of accuracy. It should be noted that achieving exact quantitative alignment becomes challenging beyond a certain squeeze depth. This disparity arises because the VR model's domain is fixed in the r-direction, whereas the experiment assumes constant volume squeezing. The perturbation approach effectively predicts variations in net vertical force under specific conditions but is lacking at the initial phases of the squeezing.

The effect of viscoelasticity on the load-carrying capacity of the lubricant film versus time is shown in Figure 1b. We observe a net decrease compared to the Newtonian case for the Oldroyd-B model. However, the MPTT model predicts an overshoot that causes the load to increase beyond the Newtonian case at $t = 0.6$ when $De = 0.16$. Furthermore, for all models, we have a zero load, initially at $t = 0$, since we have imposed a stress-free initial condition for our model.

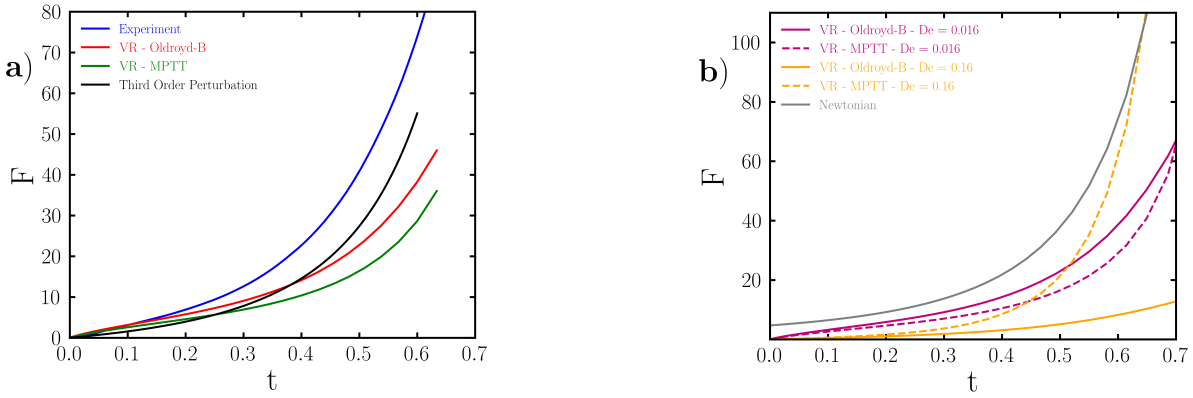

Figure 1: A comparison for the net vertical force versus time, between the VR model (with both Oldroyd-B and MPTT) for $De = 0.016$ and a) experimental data and third-order perturbation b) Newtonian solution with comparison $De = 0.16$. Note that $\beta = 0$ for all the viscoelastic simulations.

References

[1] Ahmed, H., Biancofiore, L., Journal of Non-Newtonian Fluid Mechanics, Volume 292, 2021, 104524.
[2] N. Phan-thien, et al., Journal of Non-Newtonian Fluid Mechanics, Volume 24, Issue 1, 1987, Pages 97-119, ISSN 0377-0257.
[3] Ahmed, H., Biancofiore, L., Journal of Non-Newtonian Fluid Mechanics, Volume 321, 2023, 105123.

W134

PRIMARY INSTABILITY OF ROLL WAVES ON THIN FILMS OF NON-NEWTONIAN FLUIDS DOWN A SLOPE

F. Depoilly[1], S. Dagois-Bohy[1], S. Millet[1], F. Rousset[2] & H. Ben Hadid[1]
[1]*Univ Lyon, Univ Claude Bernard Lyon 1, CNRS, Ecole Centrale de Lyon, INSA Lyon, LMFA, UMR5509, 69622 Villeurbanne France*
[2]*Univ Lyon, INSA Lyon, CNRS, CETHIL, UMR5008, 69621 Villeurbanne, France*

Key words: film flows, non-Newtonian fluids, primary instability, roll waves.

Abstract

Fluids flowing down a slope are common in civil engineering (dams, channels, etc.), industrial processes (heat exchangers, surface coating, etc.), and natural events (mud flows, landslides, etc.). Small disturbances in these flows can turn into large amplitude roll waves (also known as Kapitza waves) if the Reynolds number Re of the flow is above a critical value Re_c. Pioneering works focused on the formation of roll waves on the surface of Newtonian fluids [1, 2]. The authors were able to compute a theoretical value for Re_c, which was confirmed later by experiments [3]. However, in many of the aforementioned contexts, the fluids exhibit a non-Newtonian behaviour. This has led to studying roll waves on non-Newtonian fluids with various rheologies, such as shear-thinning [4, 5], viscoplastic [6, 7] and shear-thickening fluids [8], but also for fluids exhibiting a frictional $\mu(I)$ rheology such as dense granular flows [9].

Each study with a new rheology necessitated the authors to initiate the analysis anew and to derive a new stability condition from the motion equations. They often made different choices of characteristic scales, leading to variations in dimensionless numbers. Analysing the influence of rheology on the flow stability is difficult due to these different choices.

We present a new stability analysis performed for a generic rheological law. The novelty of our approach lies in two aspects. First, we consider a generalised Newtonian fluid with a rheological law of the form $\tau(\dot{\gamma}) = \eta(\dot{\gamma})\dot{\gamma}$, where τ is the shear stress, $\dot{\gamma}$ is the shear rate and η is the viscosity function of the fluid. Second, we choose our typical scales so that the dimensionless numbers depend the less possible on the rheological properties of the fluid. We derive a generalised Orr-Sommerfeld equation for the small disturbances, which is valid for any generalised Newtonian fluid. Through an asymptotic expansion, we obtain analytical expressions for the wave celerity and the stability threshold. These expressions give consistent results with former experimental and numerical works and can be easily extended to any other generalised Newtonian fluids.

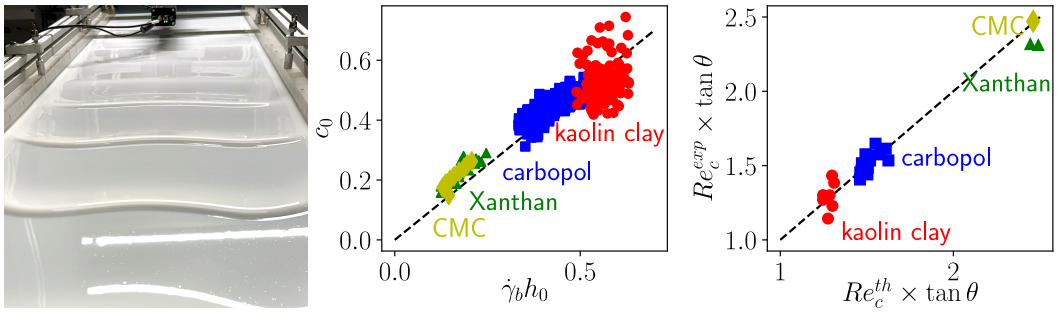

Figure 1. Left: roll waves on the surface of Carbopol. Right: comparison of the wave celerity and critical Reynolds number with experimental results for shear thinning [5] and viscoplastic fluids [7].

References

[1] P.L. Kapitza *Wave flow of thin layers of viscous liquids*, Zhurnal Eksperimentalnoi i Teoreticheskoi Fiziki **18**, (1948)
[2] Benjamin *Wave formation in laminar flow down an inclined plane*, JFM **2**, (1957)
[3] J. Liu, J.D. Paul, J.P. Gollub *Measurements of the primary instabilities of film flows*, JFM **250**, (1993)
[4] C.-O. Ng, C.C. Mei *Roll waves on a shallow layer of mud modelled as a power-law fluid*, JFM **263**, (1994)
[5] A. Allouche *et al. Primary instability of a shear-thinning film flow down an incline: experimental study*, JFM **824**, (2017)
[6] N.J. Balmforth, J.J Liu *Roll waves in mud*, JFM **519**, (2004)
[7] D.M. Noma *et al. Primary instability of a viscoplastic film flow down an incline: experimental study*, JFM **922**, (2021)
[8] B. Darbois Texier *et al. Shear-thickening suspensions down inclines: from Kapitza to Oobleck waves*, JFM **959**, (2023)
[9] Y. Forterre *et al. Kapiza waves as a test for three-dimensional granular flow rheology*, JFM **563**, (2006)

DAY 3 - Wednesday, 26 June 2024 Afternoon Sessions			
	Instabilities & Bifurcations 6 ***Chair: Prof Rama Govindarajan*** ***Larch Lecture Theatre***	***Contact Lines & Surface Interactions*** ***Chair: Prof George Karapetsas*** ***Yew Lecture Theatre***	***Droplets & Films 1*** ***Chair: Dr Yutaku Kita*** ***Elm Lecture Theatre***
13:30	W103: Kelvin-Helmholtz instability in a composite porous fluid system *by M Jadidi, Y Mahmoudi*	W119: Manipulating droplet jumping behaviors on hot microstructured surfaces - From vibration to explosion *by W Huang, L Zhao, J Cheng*	W135: Spreading of micellar films in the evaporation of emulsion droplets *by T Dong, K Kotsi, TK Xu, K Takeshi, M Alexander, I McRobbie, A Striolo, P Angeli*
13:45	W104: Observation of propagating trains of oscillons over Faraday waves *by S Kucher, JE Wesfreid, P Cobelli*	W120: Transforming auxetic metamaterials into superhydrophobic surfaces *by G McHale, A Alderson, GG Wells, R Ledesma-Aguilar, S Armstrong, M Meyari, E Carter, S Mandhani, C Semprebon, KE Evans*	W136: A thin film model for surfactant-mediated electrowetting: Role of bulk and surface charges *by S Goel, DS Pillai*
14:00	W105: Linear stability of aeroacoustic spinning waves trapped into an axisymmetric cavity *by D Özev, A Faure-Beaulieu, N Noiray*	W121: Drag reduction at high Péclet numbers in surfactant-contaminated superhydrophobic channels *by S Tomlinson, F Gibou, P Luzzatto-Fegiz, F Temprano-Coleto, OE Jensen, JR Landel*	W137: Falling liquid films on a “hole-board” *by A Ramamonjy, M Periyapattana-Iyer, L Vincent, M Wattiau, H Duval,*
14:15	W106: The effect of finite compliant panels on the development of linear disturbances in the rotating disk BL *by S Almammary, C Thomas, Z Hussain*	W122: Viscoelastic effects in three-dimensional sliding contacts *by H Ahmed, L Biancofiore*	W138: Instabilities in falling thin liquid films laden with soluble surfactants above CMC *by A Katsiavria, DT Papageorgiou*
14:30	W107: Tuning Marangoni bursting for micro/nano fabrication *by Z Wang, T Nagata, C Inoue*	W123: The liquid-solid Amontons’ laws: Friction coefficients for droplets on solids *by H Barrio-Zhang, G McHale, N Gao, G Wells, R Ledesma-Aguilar*	W139: Molecular simulation of surface-directed phase separation *by SSH Zaidi, PK Jaiswal, M Priya, S Puri*
14:45	W108: Amplifying fluid dynamics: harnessing surface acoustic waves for nano-channel flow enhancement *by S Datta, G Dayao, R Pillai*	W124: Wetting and evaporation of binary mixture droplets on hydrophilic decorated surfaces *by KM Al Balushi, G Duursma, P Valluri, K Sefiane, D Orejon*	W140: Chemically-active droplet swimming near a wall *by S Michelin, N Desai*
15:00	W109: Heterodyn interferometry to unravel capillary interactions in particle laden interfaces *by G Plohl, K Schulte, C Planchette*	W125: Effect of needle and dosing parameters on contact angle hysteresis *by J To, K Sefiane, R Ledesma Aguilar, D Orejon*	W141: Drop behavior on heterogeneous ratchet–structured substrate vibrated harmonically in lateral direction *by R Borcia, ID Borcia, M Bestehorn*
15:15	***Introduction to Next BIFD and Coffee Break (Alder Lecture Theatre)***		
15:30	***Enjoy Edinburgh (Free time)***		
19:00	***Gala Dinner at Dynamic Earth***		

W103

KELVIN-HELMHOLTZ INSTABILITY IN A COMPOSITE POROUS FLUID SYSTEM

Mohammad Jadidi, Yasser Mahmoudi
School of Engineering, The University of Manchester, M13 9PL, Manchester, UK

Keywords: Porous Turbulent flow; Flow leakage; Kelvin-Helmholtz instability; Coherent structure; Pore-scale Large Eddy Simulations.

Abstract
In the present paper, turbulent flow in a composite porous-fluid system including a permeable surface-mounted bluff body immersed in a turbulent channel flow is investigated using pore-scale large eddy simulation (LES). The effect of Reynolds number (Re) on the flow leakage from porous to non-porous regions, Kelvin-Helmholtz (K-H) instabilities, as well as coherent structures over the porous-fluid interface are elaborated by comparing cases with three Reynolds numbers (Re = 3600, 7200, and 14400). Results show that more than 52% of the fluid entering the porous blocks leaks from the first half of the porous region to the non-porous region through the porous-fluid interface. As the Re number increases from 3600 to 14400, the flow leakage decreases by 24%. Flow visualization shows that the Re number affects the size of counter-rotating vortex pairs (CRVPs) and coherent hairpin structures above the porous block. At the Re=3600, the CRVPs are larger, and their centres locate farther away from the porous-fluid interface at Y/D ~ 0.3 (D is the distance between the centres of two consecutive pores), while at the highest Re number (Re=14400), they are 200% smaller, and their centres become closer to the interface at Y/D ~ 0.1. Moreover, turbulence statistics show that by reducing the Re number, turbulence production is delayed downstream; at the Re=14400, it begins from the leading edge of the porous block (X/D=0), while at the Re=3600, turbulence production is postponed and starts nearly at the middle of the porous block (X/D=4.6). Finally, the distribution of pressure gradient for the three Re numbers confirms the occurrence of the K-H instability vortices over the porous-fluid interface. For Re = 3600, the K-H instability vortices show a linear growth rate in the vertical and horizontal directions with the slope of 0.136 and 0.05, respectively. However, by increasing the Re from 3600 to 14400, the growth rate slop in the horizontal direction decreases by nearly 33.8%, while in the vertical direction, it increases by 201%.

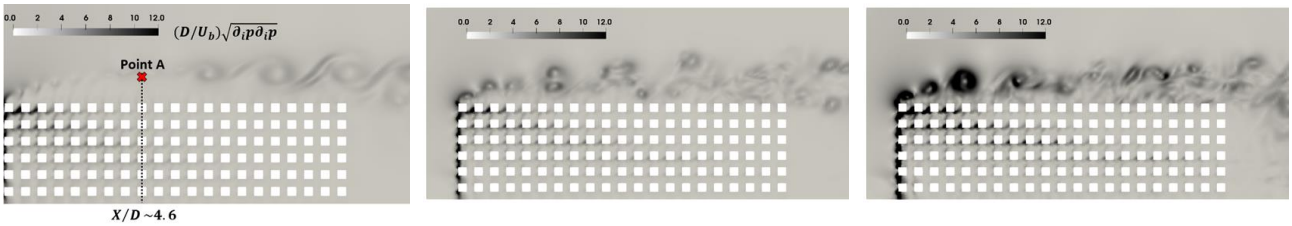

(a) Re=3600 (b) Re=7200 (c) Re=14400

Figure 1. Representation of Kelvin-Helmholtz instabilities identified by non-dimensional magnitude of instantaneous pressure gradient; left: Re=3600, Middle: Re=7200, and Right: Re=14400.

Figure 1 displays K-H instabilities characterized by the magnitude of instantaneous pressure gradient normalized by the inlet velocity (U) and D=0.006m for three Re numbers. At Re=3600 the formation of K-H instabilities in is retarded downstream, starting approximately at “Point A” with X/D~4.6, as marked in Figure 1(a). Before this point, the hairpin vortices (attached eddies) populate the shear layer and elongate downstream in an organized schematic. This point (Point A) coincides with the sudden rise in the TKE production, which will be discussed in detail in the TKE section of the paper. It is worth noting that before “Point A” the infinitesimal values of TKE production demonstrates that there is no turbulence for Re=3600 before x/D~4.6. This means that the hairpin vortices’ formation before X/D~4.6 occurs in a quasi-laminar boundary layer. This observation does not conflict with the findings of Manes et al. [1] since the hairpin vortices can also be generated in the quasi-laminar boundary layer, as reported in Malkiel et al. [2]. Here, the porous pores play a crucial role in triggering disturbances for forming hairpin vortices before X/D~4.6 for Re=3600. Figure 1(b, c) illustrates that for Re=7200 and 14400, the K-H instabilities embark just after the leading edge of the porous block. Thus, the shear layer is dominated by K-H instabilities (shear instability eddies). It will be argued in the following section that the commencement of the K-H instabilities coincides with the enhancement of Reynolds stress and, subsequently TKE production.

References

[1] C. Manes, D. Poggi, and L. Ridolfi, "Turbulent boundary layers over permeable walls: scaling and near-wall structure," Journal of Fluid Mechanics, vol. 687, pp. 141-170, 2011.
[2] M. Raupach, "Conditional statistics of Reynolds stress in rough-wall and smooth-wall turbulent boundary layers," Journal of Fluid Mechanics, vol. 108, pp. 363-382, 1981.

W104

OBSERVATION OF PROPAGATING TRAINS OF OSCILLONS OVER FARADAY WAVES

Samantha Kucher,[1, 2] José Eduardo Wesfreid[2] & Pablo Cobelli[1, 3]
[1]Universidad de Buenos Aires, Facultad de Ciencias Exactas y Naturales,
Departamento de Física, Ciudad Universitaria, 1428 Buenos Aires, Argentina
[2]PMMH-Laboratoire de Physique et Mécanique des Milieux Hétérogènes, UMR CNRS 7636,
ESPCI-Paris, Université PSL, Sorbonne Université, Université Paris Cité, 75005 Paris, France
[3]CONICET - Universidad de Buenos Aires, Instituto de Física Interdisciplinaria
y Aplicada (INFINA), Ciudad Universitaria, 1428 Buenos Aires, Argentina

Keywords: Faraday instability; Localized structures

Abstract

We report the experimental discovery of propagating trains of localized structures - oscillons - on top of Faraday waves in a vertically-vibrated fluid layer confined in a thin annular cell.
These structures emerge spontaneously beyond a threshold driving level and coexist with the underlying periodic pattern, which experiences a slow drift; their height significantly surpassing that of the pattern.
Appearing individually or in groups of trains, they move in the same or opposite directions with velocities largely exceeding Faraday waves drift.
These results on pattern formation in parametrically driven systems raise an open question about the theoretical explanation of this complex behavior.

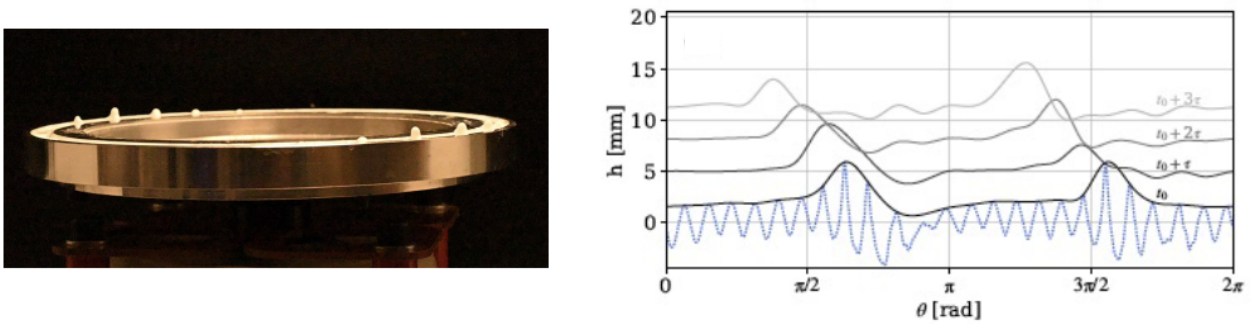

Figure 1. (a) Picture of a train of propagating localized structures as seen in a side view of our experimental setup.
(b) Height profiles of the free-surface as measured by Fourier Transform Profilometry, showing a counter-clockwise propagation of two trains of super-peaks over the spatially-periodic background of Faraday waves,

W105

LINEAR STABILITY OF AEROACOUSTIC SPINNING WAVES TRAPPED INTO AN AXISYMMETRIC CAVITY

Dilara Özev, Abel Faure-Beaulieu & Nicolas Noiray

CAPS Laboratory, Mechanical and Process Engineering Department, ETH Zürich, CH-8092 Zürich, Switzerland

Keywords: Linearized Navier-Stokes Equations (LNSE), whistling, azimuthal aeroacoustic eigenmodes

Abstract

Experimentally observed aeroacoustic instabilities involving spinning waves trapped into an axisymmetric cavity [1] are studied with the compressible Navier-Stokes equations linearized around the mean flow. In [1], the hydrodynamic stability of the shear layer modes involved in the aeroacoustic instability was investigated with the incompressible LNSE. This study showed that the aeroacoustic instability results from the inherent coupling between the linearly stable incompressible hydrodynamic modes and linearly stable acoustic modes of the system. In the present work, the stability of the aeroacoustic system is predicted from the compressible LNSE. This study also follows the experimental and theoretical investigations [2, 3, 4] and the compressible Large Eddy Simulations and incompressible LNSE analysis [5] of the two-dimensional counterpart of the present axisymmetric geometry.

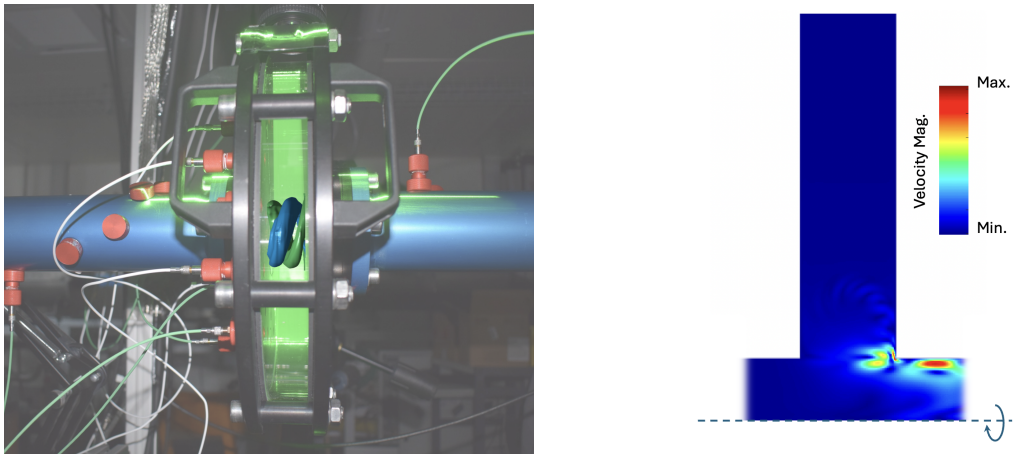

Figure 1. Left: 3D reconstruction of the velocity field from high-speed stereoscopic PIV during loud self-sustained aero-acoustic limit cycle 160 dB at 800 Hz, for a bulk flow velocity in the pipe of 60 m/s [1]. The helical structure of the coherent flow motion results from the advection and amplification of spinning perturbations. The figure shows isosurfaces of the radial component of the velocity field. Right: Velocity magnitude of the first shear layer mode obtained from the compressible LNSE analysis for the two-dimensional geometry.

References

[1] A. Faure-Beaulieu, Y. Xiong, T. Pedergnana and N. Noiray, *Self-sustained azimuthal aeroacoustic modes. Part 1. Symmetry breaking of the mean flow by spinning waves*, Journal of Fluid Mechanics **971**, A21 (2023), doi:10.1017/jfm.2023.352.

[2] C. Bourquard, A. Faure-Beaulieu and N. Noiray, *Whistling of deep cavities subject to turbulent grazing flow: intermittently unstable aeroacoustic feedback*, Journal of Fluid Mechanics **909**, A19 (2021), doi:10.1017/jfm.2020.984.

[3] T. Pedergnana, C. Bourquard, A. Faure-Beaulieu and N. Noiray, *Modeling the nonlinear aeroacoustic response of a harmonically forced side branch aperture under turbulent grazing flow*, Physical Review Fluids **6**, 023903 (2021), doi: 10.1103/PhysRevFluids.6.023903.

[4] A. K. Stoychev, T. Pedergnana and N. Noiray, *Nonlinear acoustics of an aperture under grazing flow*, Royal Society of London. Proceedings A **480**, 2283 (2024), doi:10.1098/rspa.2023.0718.

[5] E. Boujo, M. Bauerheim and N. Noiray, *Saturation of a turbulent mixing layer over a cavity: response to harmonic forcing around mean flows*, Journal of Fluid Mechanics **853**, 386–418 (2018), doi:10.1017/jfm.2018.568.

W106

THE EFFECT OF FINITE COMPLIANT PANELS ON THE DEVELOPMENT OF LINEAR DISTURBANCES IN THE ROTATING DISK BOUNDARY LAYER

Sara Almammary[1,2], Christian Thomas[3], Zahir Hussain[4]
[1]*School of Computing and Mathematical Sciences, University of Leicester, University Road, Leicester LE1 7RH, UK*
[2]*Department of Mathematics, Taif University, Taif, 26571, Kingdom of Saudi Arabia*
[3]*Department of Mathematics and Statistics, Macquarie University, NSW 2109, Australia*
[4]*School of Engineering, University of Leicester, University Road, Leicester LE1 7RH, UK*

Abstract
The rotating disk boundary layer is a classic model for the study of cross-flow instability due to its similarity to flow on a swept wing, and is a helpful simplification of a variety of flows in industrial applications with rotating setups. The study of the transition from laminar to turbulent flow in the boundary layer region has sparked a lot of interest due to its applicability to drag reduction, allowing for reduced energy consumption. Controlling transition can be achieved by active or passive flow control methods. Compliant panels are one type of passive method that can be employed to postpone laminar-turbulent transition. We consider a model in which an annular region of the disk surface is replaced by a compliant panel. The purpose of this research is to examine whether a compliant panel of finite length may be used as a passive drag reduction technique for controlling convective and absolute instabilities over a rotating disk. If so, what is the appropriate length and position of the compliant panel? To address this problem, a velocity–vorticity form of the linearised Navier–Stokes equations (Davies & Carpenter (2001)) is used to study the behaviour of convective and absolute instabilities that develop in the rotating disk boundary layer. The compliant wall is modelled using a plate–spring model. Time-periodic and impulsive forcing are used to excite linear disturbances located at a fixed radius.

References

[1] Davies, C. & Carpenter, P. W. 2001 A novel velocity-vorticity formulation of the Navier–Stokes equations with applications to boundary-layer disturbance evolution. J. Comput. Phys. 172, 119–165
[2] C. Thomas and C. Davies, On the impulse response and global instability development of the infinite rotating-disc boundary layer, J. Fluid Mech. 857, 239 (2018).
[3] C. Davies and C. Thomas, Global stability behaviour for the BEK family of rotating boundary layers, Theor. Comput. Fluid Dyn. 31, 519 (2017).
[4] C. Davies and P. W. Carpenter, Global behaviour corresponding to the absolute instability of the rotating- disc boundary layer, J. Fluid Mech. 486, 287 (2003).

W107

TUNING MARANGONI BURSTING FOR MICRO/NANO FABRICATION

Zhenying Wang[1,2], Tomoya Nagata[1] & Chihiro Inoue[1]
[1]*Department of Aeronautics and Astronautics, Kyushu University, Nishi-Ku, Motooka 744, Fukuoka 819-0395, Japan*
[2] *International Institute for Carbon-Neutral Energy Research (WPI-I[2]CNER), Kyushu University, Nishi-Ku, Motooka 744, Fukuoka 819-0395, Japan*

Keywords:Marangoni bursting, contact line instability, micro/nano crystals, microPIV, laser induced fluorescence (LIF)

Abstract

When putting a binary volatile droplet onto a low-viscosity oil layer, the binary droplet will spread and retract with contact line instability, fragmenting into thousands of small droplets in seconds. This so-called Marangoni bursting phenomenon is known for its beauty and rich physics of fluid dynamics, as demonstrated by several successive studies in recent years [1-5]. A quantitative understanding of the interacting mechanisms are yet reached due to the complexity of the problem.

In this research, we combine laser induce fluorescence (LIF) and micro particle tracing velocimetry (μPIV) based on selective laser wavelengths to simultaneously visualize the spreading of binary droplet and the evolution of flow field inside the oil layer. The approach enables a quantitative explanation to the effects of oil layer thickness and viscosity on droplet spreading and contact line instability.

By taking further use of the contact line instability and fragmentation, we are able to fabricate boundary-free high-quality micro/nano crystals with designated salts dissolved in the binary mixture, where the crystal sizes can be controlled by tuning the solvent concentration, the viscosity of oil base, and the gradient in the oil layer thickness.

The conclusions contribute to an extensive understanding of various Marangoni and instability phenomena at liquid-liquid interfaces, and demonstrates the feasibilty of micro/nano fabrication by taking advantage of the instabilities in fluid dynamics.

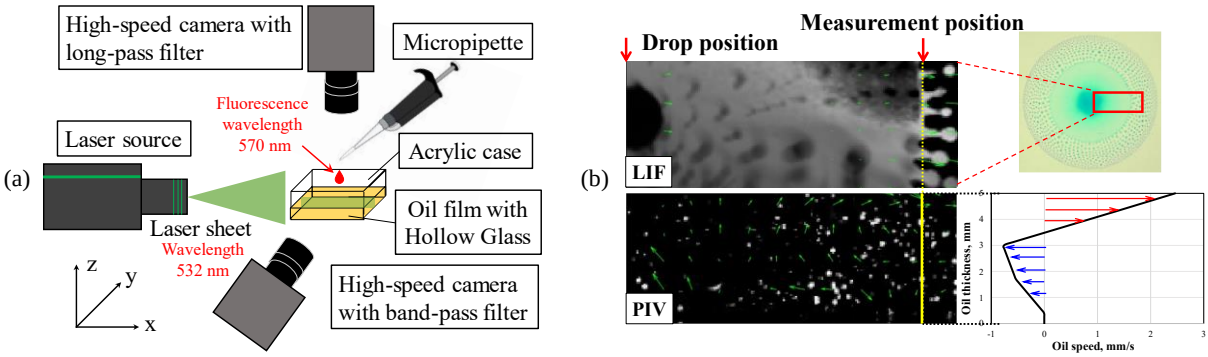

Figure 1. (a) Experimental setup combining laser induce fluorescence (LIF) and micro particle tracing velocimetry (μPIV) enables simultaneous visualization of droplet spreading and development of flow field in the oil base; (b) Demonstration of the Marangoni bursting phnomenon with images and results by LIF and μPIV.

References

[1] Keiser, L., Bense, H., Colinet, P., Bico, J., & Reyssat, E. "Marangoni bursting: evaporation-induced emulsification of binary mixtures on a liquid layer." *Physical Review Letters* 118.7 (2017): 074504.
[2] Durey, G., Kwon, H., Magdelaine, Q., Casiulis, M., Mazet, J., Keiser, L., ... & Reyssat, E. "Marangoni bursting: Evaporation-induced emulsification of a two-component droplet." *Physical Review Fluids* 3.10 (2018): 100501.
[3] Wodlei, F., Sebilleau, J., Magnaudet, J., & Pimienta, V. "Marangoni-driven flower-like patterning of an evaporating drop spreading on a liquid substrate." *Nature Communications* 9.1 (2018): 820.
[4] Seyfert, C., & Marin, A. "Influence of added dye on Marangoni-driven droplet instability." *Physical Review Fluids* 7.4 (2022): 043602.
[5] Kim, H. "Multiple Marangoni flows in a binary mixture sessile droplet." *Physics of Fluids* 34.12 (2022).

W108

AMPLIFYING FLUID DYNAMICS : HARNESSING SURFACE ACOUSTIC WAVES FOR NANO-CHANNEL FLOW ENHANCEMENT

Saikat Datta[1], Gregory Dayao[1] & Rohit Pillai[1]
[1]*School of Engineering, University of Edinburgh, Edinburgh, United Kingdom*

Keywords: Nano-channel, surface acoustic wave, molecular dynamics, flow enhancement, vibration, amplitude, frequency

Abstract

The phenomenon of fluid flow within micro-nano channels is omnipresent in various natural systems, including the circulation within biological nano-porins present in all living organisms, vascular dynamics in fungi, and intestinal peristalsis resulting from wall contractions. Moreover, its application extends to a broad spectrum of engineering and biomedical domains, encompassing nanorobotics, printing technology, quantum computing, optics, chemical process control, hydrogen energetics, molecular medicine, medical drug delivery, and cell biology.

Owing to the elevated surface-to-volume ratio inherent in micro/nanochannels, the dissipation of energy within them is substantially pronounced. Consequently, flow within such channels exhibits considerable inefficiency compared to macroscale counterparts. With surface-to-volume ratios ranging from 10^6 to 10^9, nanochannels demand high pressures to achieve necessary flow rates, leading to deviations from conventional pressure-driven flow observed at macro-scales. For instance, a flow rate of 1 μl/min necessitates pressures as high as 700 GPa; under such conditions, computer microchips would rupture [1]. In addition to the surface-to-volume ratio, fluid-wall interaction influences the flow efficiency, including fluid viscosity, surface wettability, and surface roughness. Conventional methodologies aimed at enhancing flow within micro/nano channels typically involve making the channel walls hydrophobic [2] or altering surface morphology [3] to mitigate friction.

Xie and Cao[4] demonstrated that reducing channel wall friction through the application of travelling surface waves could augment the flow rate within nanochannels. However, their approach entailed the use of exceedingly high frequencies of applied surface waves, typically in the terahertz (THz) range, which could be challenging to attain using contemporary surface acoustic devices. Along the same lines, Marbach et al.[5], employing mathematical formalism, elucidated that nanochannel wall oscillations induced by thermal fluctuations could significantly amplify diffusion and, consequently, enhance flow rates. They further demonstrated that the introduction of active surface oscillations via external stimuli could yield similar enhancements. Nonetheless, a comprehensive understanding of this flow augmentation remains elusive. Hence, we employ Molecular Dynamics simulations to investigate the behaviour of acoustic wave-driven (with frequencies in the GHz order) flow within nanochannels at the molecular scale. In contrast to the prior studies, our observations reveal a decrease in flow rate at low vibration frequencies, followed by an increment beyond a certain threshold frequency. The diminution in flow rate is explained by constraints generated by effective "roughness" from the waviness of the channel wall. Beyond the threshold frequency, our findings indicate a substantial augmentation in local velocity magnitudes across the channel while maintaining a parabolic velocity profile. Furthermore, our study indicates that nanochannels featuring hydrophobic surfaces exhibit higher flow enhancements in response to travelling surface waves. In the SAW-enhanced flow regime, the flow exhibited characteristics of being incompressible and convective. This allows for the flow to be modelled using continuum physics, which is typically unexpected for molecular scale flow inside a nano-confinement. We demonstrated that SAW-enhanced nanochannel flow can be approximated and modelled using a modified Poiseuille flow model. In this model, SAW enhancement is represented by an effective slip and viscosity that vary linearly with SAW frequency. These simplified models can predict SAW-enhanced flow for larger channels beyond the scope of MD simulations due to their high computational cost.

References

[1] E. Tamaki, A. Hibara, H. B. Kim, M. Tokeshi, T. Kitamori, *Pressure-driven flow control system for nanofluidic chemical process*, J. Chromatogr. A, **1137**, 256–62 (2007).
[2] A. Liakopoulos, F. Sofos, T. E. Karakasidis, *Friction factor in nanochannel flows*, Microfluid. Nanofluidics, **20**, 1-7 (2016).
[3] B. Y. Cao, M. Chen, Z. Y. Guo, *Liquid flow in surface-nanostructured channels studied by molecular dynamics simulation*, Phys. Rev. E. **74**, 066311 (2006).
[4] J. F. Xie, B. Y. Cao, *Fast nanofluidics by travelling surface waves*, Microfluid. Nanofluidics. **21**, 1-14 (2017).
[5] S. Marbach, D. S. Dean, L. Bocquet, *Transport and dispersion across wiggling nanopores*. Nat. Phys. **14**, 1108-1113 (2018).

W109

HETERODYN INTERFEROMETRY TO UNRAVEL CAPILLARY INTERACTIONS IN PARTICLE LADEN INTERFACES

Gregor Plohl[1], Kathrin Schulte[2] & Carole Planchette[1]
[1]*Institute of Fluid Mechanics and Heat Transfer, Graz University of Technology, Graz, Austria*
[2]*Institute of Aerospace Thermodynamics, University of Stuttgart, Stuttgart, Germany*

Keywords: particle-laden interfaces, capillary adsorption, contact line, meniscus, interferometry

Abstract
Sub-millimetric particles are found to adsorb quasi-irreversibly at fluid interfaces [1]. This trapping causes a local modification of the energy landscape [2], which in turn gives rise to capillary lateral interactions. These interactions govern the dynamics of particle self-assembling and the cohesion of resulting rafts [3].
More particularly, unavoidable undulations of the contact line and their aging are expected to have critical effects on the mechanical properties of macroscopic assemblies [4-5]. Yet, to date, the experimental exploration of these characteristics mostly relies on optically trapped particles or shock freezing of the liquid(s), and remains therefore limited to quasi-static regimes and isolated particles. In this work, we propose a new approach, based on heterodyne interferometry that enables to resolve interfacial deflections with unequalled combination of temporal and spatial resolutions [6]. Typically, vertical and lateral resolutions of about 20nm and 5µm can be reached at kHz frequencies. The principle relies on the imprint at the fluid interface of a periodic modulation of the light intensity. Digital image analysis can thus be advantageously used to filter low and high frequencies noise. The light modulation is obtained via classical interferometry, for example, with a Mach-Zehnder interferometer, and the interferogram filtration is performed on the frequency domain, for instance, using FFT (Fast Fourier Transformation).
This method is tested on several types of particles covering small (50µm), medium (130µm) and large diameters (330µm); heavy (2500kg/m^3) and light (400kg/m^3) materials; smooth (silanized glass) and rough (nanoparticle coated) surfaces; as well as spherical and non-spherical shapes. Our results show strong deviations from regular multipoles theoretically derived for ideal particles [7]. The application of a rough coating to a medium particle does not significantly modify the magnitude or number of the main extremum but causes the emergence of higher frequency modulations, in agreement with the promotion of higher modes by local pinning [8]. The effect of buoyancy follows expected trend with large particles approaching monopoles. Finally, dynamic observations made during particle self-assembling suggest strong coupling of the deflections caused by individual particles, see figure 1 for illustration. The consequences of this phenomenon on the behaviours of particle assemblies remain to be elucidated.

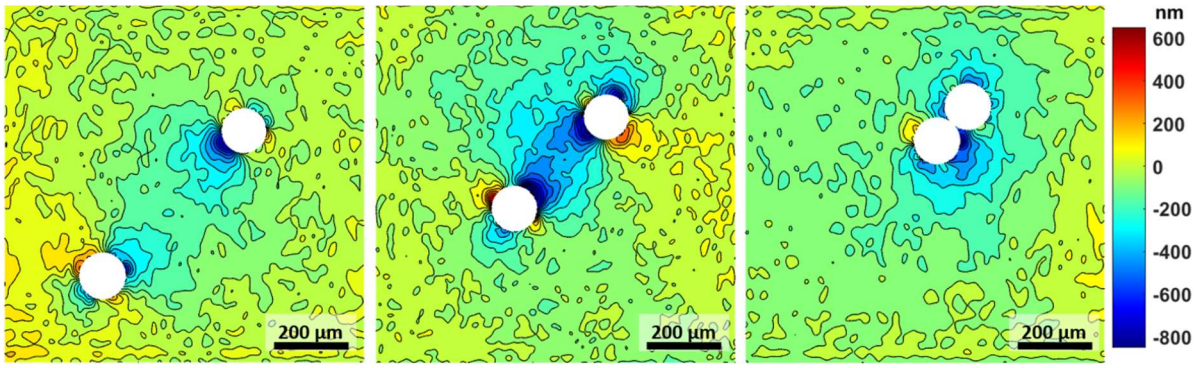

Figure 1 : interfacial deflections around two silanized glass beads and their evolution during pair formation (from left to right). A few seconds lapse between two consecutive images.

References

[1] S. Protiere, *Particle rafts and armored droplets*. Annu. Rev. Fluid Mech. **55**, (2023).
[2] M. Nicolson, *The interaction between floating particles*. In Mathematical Proceedings of the Cambridge Philosophical Society, **45**, (1949).
[3] D. Vella, & L. Mahadevan, *The "cheerios effect"*. Am. journal physics **73**, (2005).
[4] D. M. Kaz, et. al, *Physical ageing of the contact line on colloidal particles at liquid interfaces*. Nat. materials **11**, (2012).
[5] N. Xue, et. al, *Strongly metastable assemblies of particles at liquid interfaces*. Langmuir **30**, (2014).
[6] C. Planchette & G. Plohl, *Method and device for determining deflections of a fluid interface*, European patent application (2023)
[7] K.D. Danov, et al, *Interactions between particles with an undulated contact line at a fluid interface: Capillary multipoles of arbitrary order*. J. Colloid Interface Sci. **287**, (2005).
[8] N. Sharifi-Mood et al, *Capillary interactions on fluid interfaces: Opportunities for directed assembly*. Soft Matter **193**, (2016).

W119

MANIPULATING DROPLET JUMPING BEHAVIOURS ON HOT MICROSTRUCTURED SURFACES: FROM VIBRATION TO EXPLOSION

Wenge Huang, Lei Zhao, and Jiangtao Cheng
Department of Mechanical Engineering, Virginia Tech, Blacksburg, VA 24061, USA

Keywords: Leidenfrost effect, droplet vibration and jumping, Rayleigh–Plesset equation, lotus effect

Abstract Liquid droplet facile detachment and rapid removal from a substrate surface has received increasing attention due to its broad applications in a wide range of fields such as surface self-cleaning, substrate anti-icing, fog harvesting, and thermal management. During the past several decades, many research efforts have been made for droplet purging by designing various functional substrates with complex macro/micro/nanostructures or resorting to costly external stimuli such as electrical, photothermal or magnetic fields. But our understating of the inherent and intricate droplet-substrate interactions remains elusive, impeding simple designs of engineered surfaces for agile droplet manipulations. Here we introduce a simple but effective method to manipulate droplet jumping behaviors on micro-pillared substrates at moderate superheat of about 30 °C by controlling the vapor bubble growth thereon. In particular, we systematically investigated the versatile out-of-plane jumping behaviors, i.e., Cassie state maintaining, Wenzel to Cassie transition, vibration jumping, capillary jumping, explosion jumping, Cassie state hovering and Wenzel state trampolining, of a boiling water droplet on a variety of micropillared substrates at a temperature much lower than the typical Leidenfrost point. By tuning the feature sizes, i.e., micropillar height, of the engineered surfaces, we can accomplish and modulate the different vapor bubble growth modes in a sessile microdroplet. In essence, the enlarged contact area between the droplet and the substrate with relatively taller micropillars leads to enhanced heat transfer, providing the necessitated energy for the rapid commencement of explosive vapor bubble growth. As such, the vapor bubble growth at the droplet base can be transferred from the heat-transfer-controlled slow growth mode to the inertia-controlled rapid growth mode by simply tuning the geometric configuration of the micropillars on the substrate. As opposed to the relatively slow vibration jumping in hundreds of milliseconds on a substrate decorated with relatively short micropillars, the change of vapor bubble growth to the inertia-controlled mode at the droplet base leads to the prompt droplet out-of-plane explosion jumping in milliseconds on the substrate with tall micropillars. The rapid sessile droplet detachment stems from the vapor bubble explosion at the droplet base on the hot substrate, during which the vapor bubble expanding velocity can reach as high as ~4 m/s. The phase map presents a comprehensive view of distinct vapor bubble growth modes and diverse droplet jumping behaviors contingent on the topology of the surface microstructures. Our observations in this study unveil the mechanism of droplet rapid detachment from a hot micro-structured surface and shed lights on engineered surface design avoiding the damage of vapor explosion or alleviating condensate flooding.

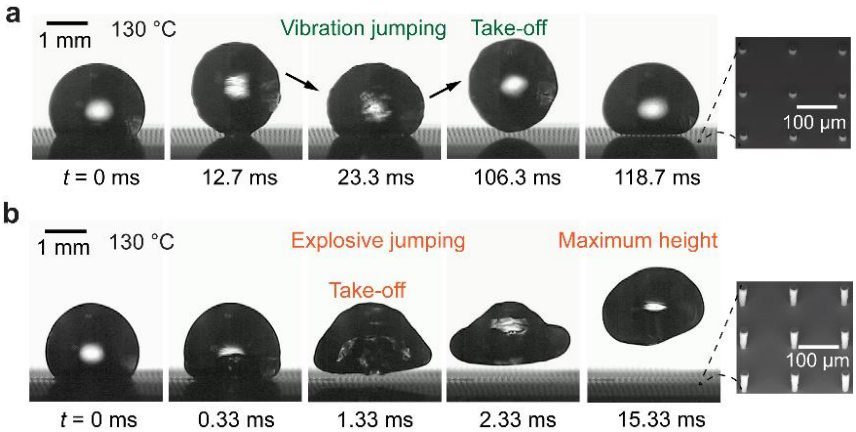

Figure 1: **a** Selected snapshots of a droplet vibration jumping on the micropillared substrate heated at 130 °C. The inset in (a) is the scanning electron micrography (SEM) of micropillared substrate with micropillar diameter D = 20 μm, periodicity L = 120 μm and height H = 20 μm ([D, L, H] = [20, 120, 20]μm). **b** Selected snapshots of a droplet explosive jumping on the micropillared substrate ([D, L, H] = [20, 120, 80]μm) heated at 130 °C.

W120

TRANSFORMING AUXETIC METAMATERIALS INTO SUPERHYDROPHOBIC SURFACES

Glen McHale[1], Andrew Alderson[2], Gary G. Wells[1], Rodrigo Ledesma-Aguilar[1], Steven Armstrong[1], Mahya Meyari[1], Emma Carter[2], Shruti Mandhani[2], Ciro Semprebon[3] & Kenneth E. Evans[4]
[1]*School of Engineering, The University of Edinburgh, Edinburgh, U.K.*
[2]*Materials & Engineering Research Institute, Sheffield Hallam University, Sheffield, U.K.*
[3]*Faculty of Engineering & Environment, Northumbria University, Newcastle upon Tyne, U.K.*
[4]*Department of Engineering, University of Exeter, Exeter, U.K.*

Keywords: Droplet, Superhydrophobicity, Auxetic, Metamaterial

Abstract

It is a common misconception that when a material is stretched it necesarily becomes narrower. However, when an auxetic metamaterial is stretched it has the counterintuitive property that it becomes wider [1,2]. This is because the properties of an auxetic material are determined by its lattice arrangement and not by the materials properties of the individual solid elements. Here we show that, because the expansion of the surface area is entirely due to increased space between the solid elements, a hydrophobic auxetic metamaterial can be transformed under strain into a unique type of superhydrophobic surface [3]. To illustrate these ideas, we present a theory and a physical model for a hydrophobic bow-tie element based auxetic lattice constructed with joints that rotate under strain to create a conventional hexagonal lattice (Figure 1). We show theoretically and experimentally how the wetting and superhydrophobicity of these materials behave under strain for both positive and negative Poisson's ratio. We also suggest that the cuticle water repelling surface of the soil-dwelling springtail *Orchesella cincta* may be a naturally occuring example of a superhydrophobic auxetic metamaterial surface. Finally, we show how a superhydrophobic droplet state on an auxetic metamaterial may transition into a penetrating state with changes in the liquid surface tension [4].

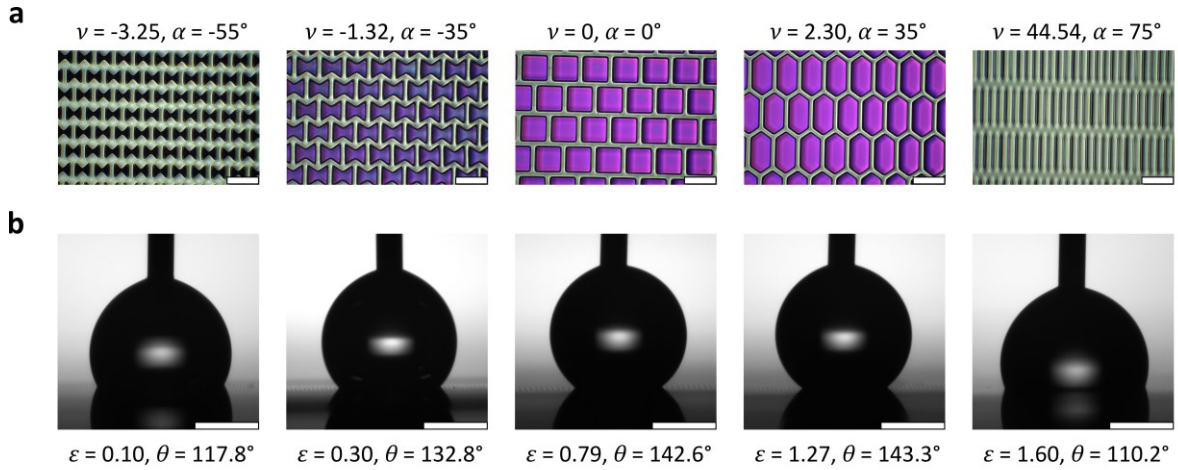

Figure 1. Model of a hydrophobic auxetic surface. a, Top images of low-pinning hydrophobic surfaces representing different strained states of a bow-tie lattice (scale bar 100 μm). b, Side profile images of water droplets in contact with the surfaces (scale bar 500 μm)

References

[1] K. E. Evans, A. Alderson, *Auxetic materials: Functional materials and structures from lateral thinking!*, Advanced Materials **12**, 617-628 (2000)
[2] R. S. Lakes, *Negative-Poisson's-ratio materials: Auxetic solids*, Annual Review of Materials Research **47**, 63-81 (2017).
[3] G. McHale, A. Alderson, S. Armstrong, S. Mandhani, M. Meyari, G.G. Wells, E. Carter, R. Ledesma-Aguilar, C. Semprebon, K.E. Evans, *Transforming auxetic metamaterials into superhydrophobic surfaces*, Small Structures (2024).
[4] S. Armstrong, G. McHale, A. Alderson, S. Mandhani, M. Meyari, G.G. Wells, E. Carter, R. Ledesma-Aguilar, C. Semprebon, *Wetting transitions on superhydrophobic auxetic metamaterials*. Applied Physics Letters **123**, 151601 (2023).

Acknowledgements

The authors were supported by funding from the UK Engineering & Physical Sciences Research Council (EP/T025158/1 and EP/T025190/1). M.M. was supported by the EPSRC CDT in Soft Matter for Formulation and Industrial Innovation, EP/S023631/1.

W121

DRAG REDUCTION AT HIGH PÉCLET NUMBERS IN SURFACTANT-CONTAMINATED SUPERHYDROPHOBIC CHANNELS

Samuel D. Tomlinson[1], Frédéric Gibou[2], Paolo Luzzatto-Fegiz[2], Fernando Temprano-Coleto[3], Oliver E. Jensen[1] & Julien R. Landel[1, 4]

[1]*Department of Mathematics, University of Manchester, Oxford Road, Manchester, M13 9PL, UK*
[2]*Department of Mechanical Engineering, University of California, Santa Barbara, CA 93106, USA*
[3]*Andlinger Center for Energy and the Environment, Princeton University, Princeton, NJ 08544, USA*
[4]*Univ. Lyon, Univ. Claude Bernard Lyon 1, CNRS, École Centrale de Lyon, INSA Lyon, LMFA, UMR5509, 69622 Villeurbanne, France*

Keywords: Marangoni effects, drag reduction, microfluidics

Abstract

Motivated by microfluidic applications and by applications to viscous sublayers, we investigate the drag reduction in a steady laminar pressure-driven channel flow bounded between a streamwise-periodic superhydrophobic surface (SHS) (bottom) and a solid wall (top), where the liquid has been contaminated with soluble surfactant (figure 1a). Such contamination has been shown to be essentially unavoidable in practice [1]. We derive a model in the long-wave and weak-diffusion limit, where the streamwise period ($2\hat{P}$) is long compared to the channel height ($2\hat{H}$) and the Péclet number is large compared to the other surfactant-related parameters. We solve the model numerically to investigate the drag reduction across the parameter space, comparing our results with models derived when the Péclet number is small [2]. We exploit the relative strength of Marangoni effects, advection, diffusion and bulk-surface exchange to derive asymptotic solutions for the surfactant distribution and drag reduction. When Marangoni effects are strong, the interfacial concentration is linear and the liquid-gas interface is mostly no-slip (low drag reduction), and when Marangoni effects are weak, the interfacial concentration forms a stagnant cap and the liquid-gas interface is mostly shear-free (high drag reduction). For strong bulk-surface exchange, the bulk surfactant concentration exhibits boundary-layer profiles (figure 1b), where the drag reduction depends on the boundary-layer thickness and surfactant strength. We compare our asymptotic results with numerical simulations of the full transport problem using parameters characteristic of microchannel applications, offering insight into the role of surfactants in laminar flows bounded by SHSs.

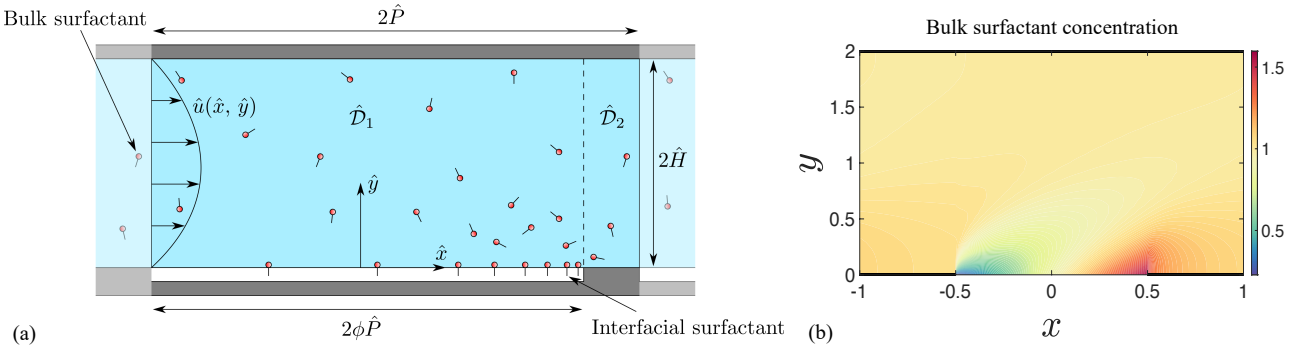

Figure 1. (a) A steady two-dimensional laminar channel flow (illustrated by the arrows) transporting soluble surfactant bounded between a streamwise-periodic SHS (bottom) and a solid wall (top). Surfactants adsorb onto the liquid-gas interface, are advected by the flow and accumulate at the downstream stagnation point, where they change the interfacial stress and generate Marangoni stresses that can increase the drag. (b) Contours of the bulk-concentration boundary layer when Marangoni effects and bulk-surface exchange are strong. The thick black lines represent the solid regions of the SHS and the solid wall.

We acknowledge support from CBET-EPSRC (EPSRC Ref. EP/T030739/1, NSF #2054894), as well as partial support from ARO MURI W911NF-17-1-0306.

References

[1] F. J. Peaudecerf, J. R. Landel, R. E. Goldstein & P. Luzzatto-Fegiz, *Traces of surfactants can severely limit the drag reduction of superhydrophobic surfaces*, Proc. Natl. Acad. Sci. **114**, 7254–7259 (2017).
[2] S. D. Tomlinson, F. Gibou, P. Luzzatto-Fegiz, F. Temprano-Coleto, O. E. Jensen & J. R. Landel, *Laminar drag reduction in surfactant-contaminated superhydrophobic channels*, J. Fluid Mech **963**, A10 (2023).

W122

VISCOELASTIC EFFECTS IN THREE-DIMENSIONAL SLIDING CONTACTS

Humayun Ahmed[1], Luca Biancofiore[1,2]
[1]*Department of Mechanical Engineering, Bilkent University, Ankara, Turkey,*
[2]*Department of Industrial and Information Engineering and Economics, University of L'Aquila, Italy*

Abstract We analyze the effect of viscoelasticity on the load carrying capacity in a three dimensional lubricated contact via reduced-order computational models. (viscoelasticity, thin film lubrication, computational methods).

Polymer-enhanced thin-film lubrication is crucial for minimizing undesirable friction between contacting surfaces. These additives introduce non-Newtonian effects like viscoelasticity and shear thinning when subjected to high-speed motion. A net enhancement of the load carrying capacity is observed owing to the viscoelasticity of the polymer, the strength of which, for a typical lubricated contact spanning length ℓ_x, width ℓ_z and height H_0, is measured via the Deborah number (De), i.e. the ratio between the polymer relaxation time (λ) and the residence time scale ($t_r = \frac{\ell_x}{U^*}$). The use of reduced-order computational models (satisfying the lubrication approximation, i.e., where $H_0 << \ell_x$) such as, the viscoelastic Reynolds approach (VR) (see Ahmed and Biancofiore, JNNFM, 2021 [1]), validated against direct numerical simulations, allows us to (i) estimate the observed increase in the lubricant film's load carrying capacity, and also (ii) provides visualization of the pressure distribution in the contact. In this work, we explore the influence of lubricant viscoelasticity for more realistic three-dimensional channel configurations (e.g, textured surfaces, finite width journal bearings, ball-bearings, synovial joints etc.) via an (i) extension of the VR approach to three dimensions (i.e., where $\ell_z \approx \ell_x$), and (ii) a linearized model in De for the purpose of comparing the results.
Considering the unwrapped eccentric journal bearing, having film height is $h = 1 + e\cos(2\pi x)$, we evaluate the load carrying capacity, $F_\ell = \int_0^1 \int_0^1 p\, dxdz$, where, p is the gauge pressure, versus the channel aspect ratio ($a = \ell_x/\ell_z$). A comparison between the linearized model in De (LIN) and the VR approach, is presented in Fig. 1(a), and the same examination is conducted using several non-linear constitutive relations, given in Fig. 1(b), that account for the (i) finite extension of the polymers, captured via the parameters L and κ, for the finitely extensible non-linear elastic (FENE) and the Phan-Thien-Tanner (PTT) models, respectively, and (ii) shear thinning.

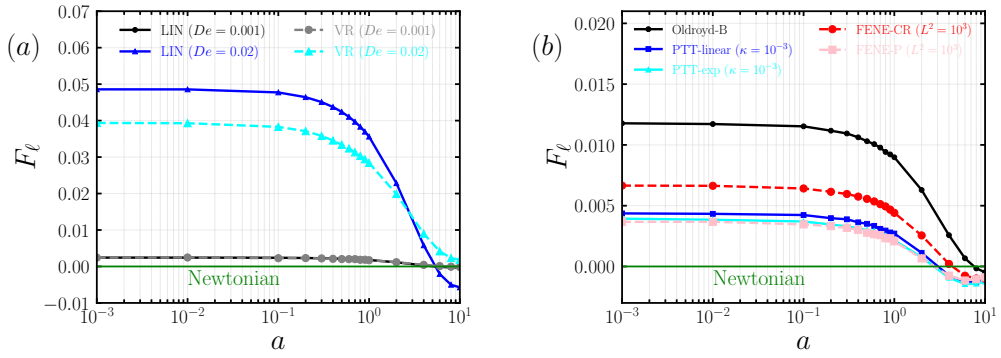

Figure 1: Load versus the channel aspect ratio for the unwrapped journal bearing: a comparison between (a) the linearized model (LIN) and the VR model, and (b) different non-linear constitutive relations ($De = 0.005$, $e = 0.9$, $\epsilon = 0.001$, $\beta = 0.8$). Note that the Newtonian load is identically zero for all a.

We find an enhancement of the load as De increases, which depends strongly on the aspect ratio of the channel, captured by both the LIN and the VR model. As the channel aspect ratio increases (transitioning from an infinitely wide, $a \to 0$, to an infinitely long, $a \to \infty$, channel), we observe a diminishing load. The linear model, even for small De, can overestimate (underestimate) the load for wide (long) channels, which reflects its sensitivity to high channel eccentricity (or undulation). Using non-linear constitutive relations, such as the FENE type, and the PTT (network type) models, we observe similar trends in the load versus a, as shown in Fig. 1(b). A reduction in load is attributed to finite polymer chain extension and decreased effective viscosity due to shear thinning, with the latter having a significant impact on the load-carrying capacity.

References

[1] Ahmed, H., & Biancofiore, L.: Journal of Non-Newtonian Fluid Mechanics, 2021, *292*, p.104524.
[2] Ahmed, H., & Biancofiore, L.: Journal of Non-Newtonian Fluid Mechanics, 2023, *321*, p.105123.
[3] Boyko, E., & Stone, H. A.: Journal of Fluid Mechanics, 2022, *936*, p.A23.
[4] Fattal, R., & Kupferman, R. .: Journal of Non-Newtonian Fluid Mechanics, 2005, *126*(1), pp.23-37.

W123

THE LIQUID-SOLID AMONTONS' LAWS: FRICTION COEFFICIENTS FOR DROPLETS ON SOLIDS

Hernán Barrio-Zhang[1], Glen McHale[1], Nan Gao[2], Gary G. Wells[1] & Rodrigo Ledesma-Aguilar[1]
[1] *Wetting, Interfacial Science & Engineering Lab, University of Edinburgh, Edinburgh, UK*
[2] *Department of Mechanical Engineering, University of Birmingham, Birmingham, UK*

Keywords: Friction, Contact line dynamics, Droplets, contact-angle hysteresis

Abstract

Understanding of the friction between two solids was pioneered by the work of Amontons in 1699, inspired by the work of Leonardo da Vinci. Since then, the pinning and sliding between solids has been understood by empirical laws tying the normal force between the solids with static and kinetic coefficients of friction. Liquids on solid surfaces also experience resistive forces and have been studied from the perspective of moving contact lines. Recently, there have been works that have identified different resistive regimes when the droplet is static and when it is in motion [1], [2]. This has allowed to view liquid-solid friction from the perspective of coefficients of friction. In this work, we show that by considering the surface energy interactions of the liquid-solid-air interfaces, that the frictional force is directly proportional to the normal component of the surface tension force. This allows us to obtain "liquid" coefficients of friction, analogue to Amontons' first and second laws, where the normal component of the force is replaced by the normal surface tension force of a droplet. In order to overcome the static friction, the force needed is linked to the contact angle hysteresis. However, in the kinetic regime, the friction experienced by the liquid is proportional to the advancing and receding dynamic contact angles. Comparisons with Amontons' Laws and Furmidge's equation on resistance to droplet motion allows the derivation of the liquid-solid Amontons' Laws, which describe friction coefficients for several liquid-solid systems in the literature. This work provides insight into liquid-solid friction and provides a framework for the design of engineered surfaces to control droplet motion.

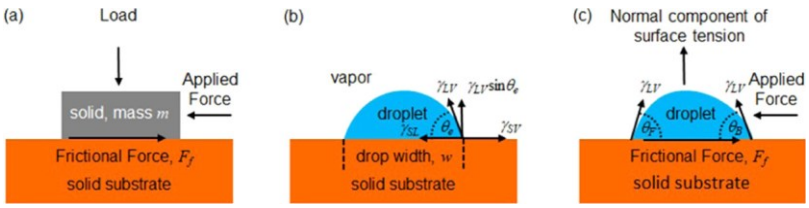

Figure 1: ***Solid-solid and solid-liquid friction analogy*** *: (a) Solid sliding on a solid due to an applied force. (b) Droplet equilibrium without an applied force. (c) Droplet sliding/rolling on a solid due to an applied force.*

References

[1] N. Gao *et al.*, *How drops start sliding over solid surfaces*, Nat Phys, **14**, 191–196 (2018).
[2] H. Barrio-Zhang, E. Ruiz-Gutiérrez, S. Armstrong, G. McHale, G. G. Wells, and R. Ledesma-Aguilar, *Contact-Angle Hysteresis and Contact-Line Friction on Slippery Liquid-like Surfaces*, Langmuir, **36**, 15094–15101 (2020).

Acknowledgements

Hernán Barrio Zhang would like to acknowledge funding from the UK Engineering & Physical Sciences Research Council (EP/V049348/1)

W124

WETTING AND EVAPORATION OF BINARY MIXTURE DROPLETS ON HYDROPHILIC DECORATED SURFACES

Khaloud Moosa Al Balushi[1,2], Gail Duursma[2], Prashant Valluri[2], Khellil Sefiane[2] & Daniel Orejon[2,3]
[1]*College of Engineering and Technology, The University of Technology and Applied Sciences, Suhar 311, Oman*
[2]*School of Engineering, Institute for Multiscale Thermofluids, The University of Edinburgh, Edinburgh EH9 3FD, Scotland, UK*
[3]*International Institute for Carbon-Neutral Energy Research (WPI-I2CNER), Kyushu University, 744 Motooka, Nishi-ku, Fukuoka 819-0395, Japan*

Keywords:Wetting, Contact angle, Structured surfaces, Cassie-Baxter, Wenzel, Hemi-wicking

Abstract

There is a promising future for the development of structurally and chemically decorated surfaces in a variety of applications, including everyday practices as well as industrial and biomedical applications. When structured surfaces are used, their intrinsic hydrophobicity/hydrophilicity strongly affects the wettability and evaporation process of microlitre droplets. In this work, pure water, pure ethanol, and their binary mixtures are used to examine their wettability and evaporation behaviour on 6 intrinsically hydrophilic micro-structured surfaces having the same height to diameter aspect ratio and varying the spacing between pillars. On one hand, since the surface energy of hydrophilic/superhydrophilic surfaces is rather high, these surfaces are easily contaminated by impurities present in the air and/or in other media [1-3]. Similarly, in this research, it is found that the ambient laboratory exposure time following air plasma cleaning strongly influences the wettability of the surfaces studied. Unlike cleaning with organic solvents, which are not able to remove the adsorbed contaminant, air plasma enables the removal of any contaminants that are adsorbed on them and liquids are typically completely spread on them. Hence, surfaces exposed to laboratory environments exhibit less-wetting surface behaviour as the exposure time prolonged, and droplets display a higher contact angle as illustrated in the right-hand side of Figure 1. Moreover, upon deposition, the wettability of droplets on short-spacing surfaces depends highly on the liquid surface tension and spacing between pillars; however, on large-spacing surfaces, droplets behave similarly as on their smooth counterparts independently of the liquid studied. On the other hand, upon deposition and for liquids not in equilibrium with the environment full evaporation process ensues, which is highly dependent on the initial wetting regime adopted. Three different evaporative modes are revealed: the constant contact radius (pinning), stick-slip mode and mixed mode, in the absence of the constant contact angle mode. The duration of each mode has been analysed to clearly show the dependence of the evaporation modes on the different initial wetting regimes governed by the liquid surface tension and the spacing between structures used. Accordingly, choosing the proper spacing of the structure combined with the proper binary mixture concentration, the initial wetting regime, the initial pinning time, and the duration of evaporation modes can be optimized according to the application and objective, making these fundamentals useful in a variety of biological, agricultural and medical fields, among others.

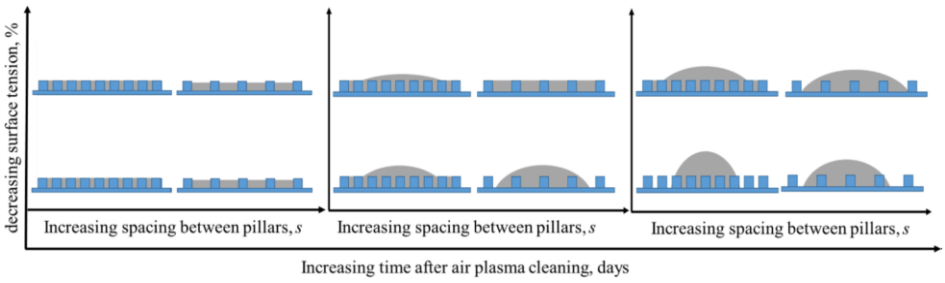

Figure 1. Schematics representation of typical wetting behavior function of the liquid surface tension, micropillar spacing, and exposure time to laboratory environmental conditions after air plasma cleaning.

References

[1] Orejon, D., Oh, J., Preston, D. J., Yan, X., Sett, S., Takata, Y., Miljkovic, N., Sefiane, K., Ambient-mediated wetting on smooth surfaces, *Advances in Colloid and Interface Science* **324**, 103075 (2024).
[2] Thanu, D. P. R., Srinadhu, E. S., Zhao, M., Dole, N. V. & Keswani, M. Fundamentals and applications of plasma cleaning. *Developments in Surface Contamination and Cleaning: Applications of Cleaning Techniques* **11**, 289– 353 (2018).
[3] Xu, F., Li, X., Li, Y. & Sun, J. *Oil-repellent antifogging films with water-enabled functional and structural healing ability*. ACS Appl. Mater. Interfaces **9**, 27955– 27963 (2017).

W125

EFFECT OF NEEDLE AND DOSING PARAMETERS ON CONTACT ANGLE HYSTERESIS

Janice To[1], Khellil Sefiane[1] & Rodrigo Ledesma Aguilar[1], Daniel Orejon[1]
[1]*Institute for Multiscale Thermofluids, School of Engineering, The University of Edinburgh, Edinburgh EH9 3FD, Scotland, UK*

Keywords: contact angle hysteresis, drop shape analysis, surface characterisation, contact line dynamics, needle effect

Abstract

Contact angle hysteresis is one of the most fundamental steps in characterising surface and wetting phenomena, as it provides insight into the interactions between liquids and solid surfaces. One of the many methods is the optical needle method, where a needle inflates and deflates a droplet to measure the resulting contact angle hysteresis. Multiple factors can influence contact angle hysteresis results, and despite being a widely used surface characterisation method, there is no established standard across the board to ensure accurate and repeatable results between studies.

Jin *et al.* looked into replacing the solid needle with a liquid needle produced by a jet of liquid using a pressure dosing system [1]. They found that the static contact angles measured using the liquid needle were comparable to the solid needle, with the added benefit of reducing the duration of the experiment.

This research uses the optical drop-shape analysis method to examine the influence of needle type, size, and dosing parameters on the measurement accuracy of contact angle hysteresis. The study focuses on deionised water droplets on a smooth silicon wafer coated with a hydrophobic self-assembled monolayer, perfluorodecyltrichlorosilane (FDTS), as well as on an uncoated silicon wafer, which is intrinsically hydrophilic. The classical drop shape analysis method assesses the interaction between the droplet and the surface while clearly overlooking the interaction between the needle and the droplet at their triple-phase contact point and its potential impact on droplet shape, consequently affecting the baseline contact angle measurement and, thus, the contact line dynamics.

Independent variables investigated include dosing flowrate, needle size in terms of external and internal diameter, and needle material/coating varying from hydrophilic stainless steel to superhydrophobic Glaco-coated needles. Figure 1 highlights the degree of deviation from the typical spherical cap-shaped droplet due to a needle with varying material and coating but with the same external diameter of 0.50 mm on the same smooth hydrophobic surface. The objective is to determine the individual and combined effects of needle and dosing parameters on contact angle hysteresis measurements. Developing a comprehensive protocol based on the findings can enhance the accuracy and reliability of future experiments.

Additionally, the subsequent phase of the study will compare the results obtained from the optical needle method to those acquired using a needleless approach via a microgoniometer. This ongoing fundamental investigation holds promise for establishing a refined methodology for precise contact angle hysteresis measurements, enabling researchers to obtain more accurate and repeatable data characterisation in various surface-wetting studies.

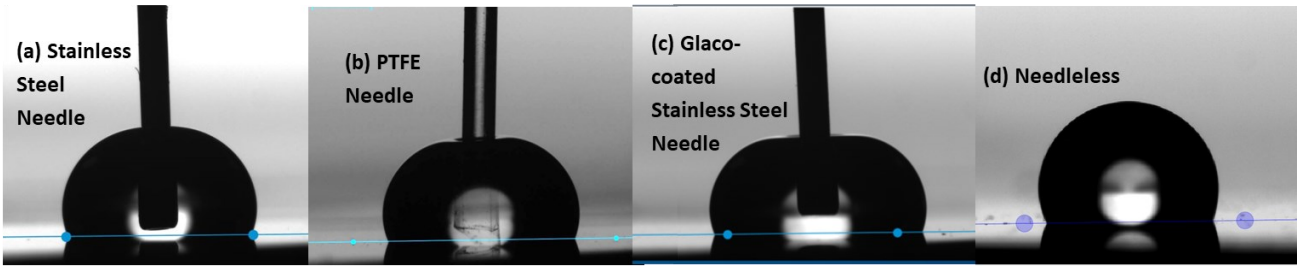

Figure 1. A series of images with (a) hydrophilic stainless steel, (b) hydrophobic PTFE, (c) superhydrophobic Glaco-coated stainless steel 0.50 mm needle inside a droplet, showcasing the degree of deviation during droplet growth or advancing motion of the contact line from the typically observed (d) spherical cap-shaped droplet where the needle is absent.

[1] M. Jin, R. Sanedrin, D. Frese, C. Scheithauer, and T. Willers, "Replacing the solid needle by a liquid one when measuring static and advancing contact angles," *Colloid and Polymer Science,* vol. 294, no. 4, pp. 657-665, 2016-04-01 2016, doi: 10.1007/s00396-015-3823-1.

W135

Spreading of Micellar Films in the Evaporation of Emulsion Droplets

Teng Dong[1], Kristo Kotsi[1], Teke Xu[1], Kobayashi Takeshi[1], Moriarty Alexander[1],
Ian McRobbie[2], Alberto Striolo[2], Panagiota Angeli[1]

[1]Department of Chemical Engineering, University College London, London WC1E 7JE, UK.

[2]Innospec Ltd. Oil Sites Road, Ellesmere Port, Cheshire, CH65 4EY, UK.

[3]School of Sustainable Chemical, Biological and Materials Engineering, The University of Oklahoma, Norman, OK 73019, United States

Keywords: ***Droplet, Film spreading, Disjoining Pressure, Evaporation***

Abstract

In industrial processes such as spray cooling, agrochemical applications and inkjet printing, the evaporation of emulsion droplets presents unique challenges. Unlike the evaporation of colloidal droplets with dispersed particles, the evaporation of emulsion droplets is complicated. It involves processes like bulk convection, coalescence of dispersed droplets, and the spreading of continuous liquids [1]. This study focuses on experimentally investigating the evaporation of emulsion drops with water as the continuous phase and oil dispersed in it on microscope glass surfaces that have a contact angle with water equal to 30°. The emulsion comprises 10% w/w silicone oil, 88% w/w deionized water, and 2% w/w Span 80, mixed in a Pulse 150 homogenizer. The majority of dispersed oil droplets are below 1 μm in size, and the evaporation process of submillimetre drops is observed under a microscope.

Upon deposition, uneven evaporation induces strong convection in the drop. Dispersed oil droplets are carried by convection to the edge of the large drop, where they coalesce, forming a continuous silicone oil film that spreads well beyond the initial drop size. Using a blue light at a 475nm wavelength and light interference, the film thickness is measured. The results reveal a novel two-layer spreading phenomenon during evaporation, as depicted in Figure 1(a). As the film thins to the nanometer scale, disjoining pressure is believed to govern the spreading. The high concentration of Span 80 in the oil leads to micellar assemblies, which generate oscillatory forces in the disjoining pressure that contribute to the two-layer spreading.

The increase of the film radius is measured during the spreading. It was found the spreading for both the bottom layer and the second layer only follows Tanner's law [2] ($r \sim t^{1/10}$) in the early stages, while it becomes much faster later and follows $r \sim t^{1/2}$ or $r \sim t^{1/3}$. By introducing the disjoining pressure and the slip condition into the lubrication model for the spreading, we derived a new spreading law for both layers of the film that agrees well with the experimental measurements.

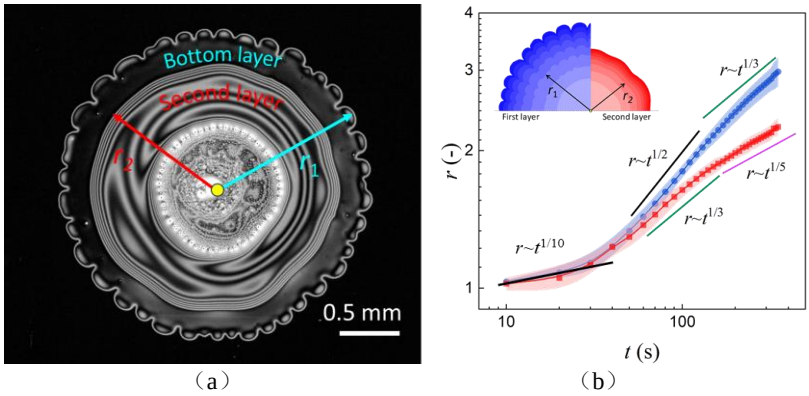

Figure 1. Two-layer spreading of the oil film during the evaporation of emulsion drop that contains 10% silicone oil (a) and the corresponding spreading dynamics of the bottom and the second layer.

References

[1] M. Bittermann, A. Deblais, S. L´epinay, D. Bonn, and N. Shahidzadeh, Deposits from evaporating emulsion) drops, Scientific reports 10, 14863 (2020).

[2] L. Tanner, The spreading of silicone oil drops on horizontal surfaces, Journal of Physics D: Applied Physics 12, 1473 (1979).

W136

A THIN FILM MODEL FOR SURFACTANT-MEDIATED ELECTROWETTING: ROLE OF BULK AND SURFACE CHARGES

Shreyank Goel[1], & Dipin S. Pillai[1]
[1]*Department of Chemical Engineering, IIT Kanpur, Kanpur, India*

Keywords: Electrowetting, WRIBL, Debye Length, Marangoni Number

Abstract

Miniaturization is a necessity in today's world. Size reduction through the advent of microfluidics has facilitated the integration and intensification of multiple processes over a single microfluidic chip. In droplet-based microfluidics, the incorporation of an external electric field provides control over the mixing, transport, and manipulation of droplets. The electrowetting behavior of a charge-carrying, surfactant-loaded sessile droplet is important for applications like point-of-care diagnostics. In biomedical assays, droplets with charged molecules like dissolved ions, proteins, and DNA are often used. In addition, the majority of biological samples examined during point-of-care diagnostics are biofluids with dissolved salt and surfactants, e.g. respiratory droplets comprising protein (mucin), salt (NaCl), and surfactant (dipalmitoylphosphatidylcholine) in addition to water, which is anticipated to have a significant impact on electrowetting. In this work, we develop two reduced-order models for electrowetting of a sessile droplet under a closed co-planar configuration. The weighted residual integral boundary layer (WRIBL) method is used to obtain evolution equations that describe how the liquid-air interface and the depth-integrated flow rate change over time and space. The solutions to the evolution equations are obtained numerically using the spectral collocation method.

In the first part [1], we investigate the role of domain charges, characterized by the Debye length, on droplet wetting. Under low relaxation time scales, both droplet deformation and wetting alteration under an AC field are shown to be equivalent to that under a root-mean-square (RMS) DC field. We show that a charge-carrying electrolytic sessile droplet can exhibit a larger deformation in comparison to the two asymptotic limits of a perfect-conductor and perfect-dielectric droplet, corresponding respectively to very low and high Debye lengths. The effect of several other parameters such as the inherent equilibrium wettability, permittivity ratio, and electric field strength are also investigated.

In the second model [2], an insoluble surfactant-laden leaky dielectric droplet is considered. We show that the competition between the charge relaxation and forcing timescales governs the charge buildup at the interface, and consequently determines the equivalence between periodic and steady forcing. The presence of surfactants and the associated Marangoni flow is shown to delay the interfacial charge buildup. While the mean droplet deformation under AC forcing remains the same as that under DC forcing, the amplitude of droplet oscillation is shown to be significantly damped by the surfactants.

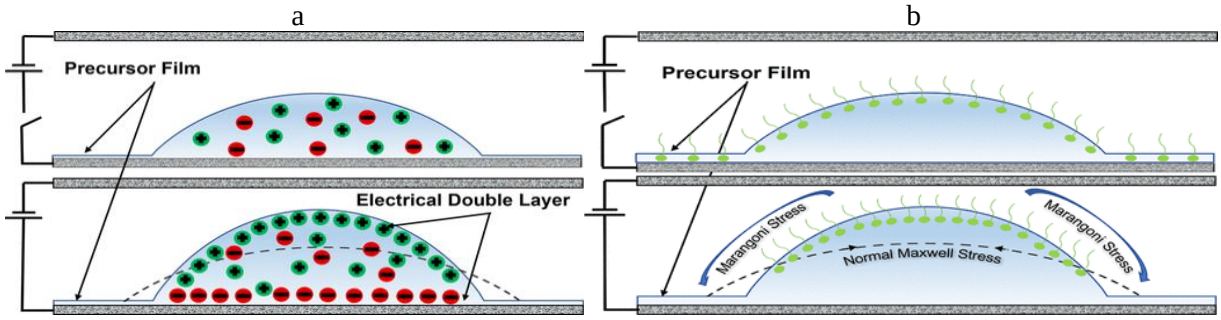

Figure 1. **a)** Schematic of an electrolytic sessile droplet under a parallel-plate electrode configuration gets deformed when subjected to periodic electrostatic forcing. The deformation depends the formation of electrical double layer characterised by inver Debye length. **b)** Schematic of a surfactant-laden sessile droplet under a parallel plate electrode configuration. The normal Maxwell stress caused by the electric field is conteracted by the Marangoni stress resulting from surface tension gradient.

References

[1] Goel, Shreyank, and Dipin S. Pillai, *Electrokinetic Thin-Film Model for Electrowetting: The Role of Bulk Charges*. Langmuir 39.37, 13076-13089 (2023).
[2] Goel, Shreyank, and Dipin S. Pillai, *Reduced-Order Model for Surfactant-Laden Electrified Sessile Droplets*. Langmuir 39.37, 15177-15188 (2023).

W137

Falling liquid films on a "hole-board"

Aina Ramamonjy[1], Manasa Periyapattana-Iyer[1], Lionel Vincent[1], Mikael Wattiau[2] & Hervé Duval[1]
[1]*LGPM, CentraleSupélec, Université Paris-Saclay, Gif-sur-Yvette, France,*
[2]*Air Liquide Paris Innovation Campus, Les-Loges-en-Josas, France.*

Keywords: liquid curtain, liquid nappe, rivulet, scaling law, Kapitza waves, resonance

Abstract

Many technological systems implement falling liquid films to intensify mass and heat transfers. This strategy is used mainly in absorption or distillation processes, in cooling towers, or in cooling systems for electric mobility. Thin liquid films usually flow over complex surfaces, characterized by the presence and repetition of geometrical features or topographies, such as corrugations, slits, or perforations. Since the pioneering work of Nusselt and Kapitza, liquid film flows have been the subject of extensive literature. The reference configuration is the vertical/inclined flat plate with a fully covering film. Much less work has been done on the interactions between liquid films and surface features. Most of these studies concern falling liquid films on undulated substrates. There are very few works on perforations and their impact on liquid film flow. The present study focuses on a falling liquid film flowing over a perforation.

We considered a simplified configuration where a vertical flat sheet with a single circular perforation is supplied with liquid on its front side only. The film free surface could be forced periodically by a loudspeaker placed at the inlet to properly examine the long-wave behavior. The liquid flow patterns developing on the front and on the back of the plate (rivulet leaking from the perforation) were observed and recorded using a CMOS high-speed camera. The instantaneous pointwise thickness of the liquid film was measured using confocal chromatic imaging. The test plates were cut from 1 mm-thick aluminum sheets. The perforation diameter ranged between 2 and 16 mm. The present experiments were carried out with propan-2-ol (Kapitza number, $\mathrm{Ka} = 348$, and highly favorable wetting). The film Reynolds number (Re) was varied between 5 and 80.

We characterized the different flow patterns occurring on a singly perforated plate as a function of Re. At low Re-values, the liquid film flow is mainly deflected by the perforation, and the liquid does not fill it. Above a critical Re-value, referred to as the curtain Reynolds number (Re_{cr}), the liquid fills the perforation entirely and forms a liquid curtain. The curtain exhibits stationary varicose capillary waves. The curtain transition is hysteretic: when Re is decreased from Re_{cr}, the liquid curtain may persist within the perforation for Re-values well below Re_{cr}. We established a criterion for the curtain formation from the macroscopic momentum balance on the rim that surrounds the perforation before the transition to curtain. We also showed that the wavelength of the varicose waves is selected such that the velocity of the waves both satisfies Taylor's dispersion relation and matches the curtain local speed.
Then, we focused on the curtain mode and measured the volume flow rate transferred through the perforation from the front side (supplied) to the back side of the plate. The fluid leaks from the bottom edge of the perforation and forms a single straight rivulet on the back of the plate. In the Re-range we investigated, the overflow number (ratio of the transferred flow rate per unit diameter of perforation to the supply flow rate per unit width) increases with Re and may exceed 0.5, i.e., the value corresponding to an equal partition between the front and the back of the perforation. This increasing behavior can be explained by the exact mechanism responsible for the so-called teapot effect. The rivulet leaking from the perforation evolves self-similarly, it widens (resp. flattens) as the 0.25 (resp. -0.075) power of the traveled distance from the perforation. The scaling exponents are very close to the theoretical exponents (3/13 and -1/13, respectively) established by Shetty & Cerro [1] and Duffy & Moffatt [2] for a rivulet spreading in the capillary-dominant regime.
Last, we examined the behavior of the waves traveling on the surface of the falling film when the film free surface is periodically forced at the inlet. Vertical liquid films are unconditionally unstable with respect to long waves. However, we observed that for specific frequencies, the waves are more amplified over the perforation than away from it This amplification is related to the excitation and the resonance of sinuous waves traveling on the liquid curtain that closes the perforation. The resonance satisfies the *integer-minus-one-third* criterion recently found by Della Pia et al. [3] for liquid sheets flowing in unconfined environments.

References

[1] S.A. Shetty, R.L. Cerro, *Spreading of liquid point sources over inclined solid surface*s, Ind Eng Chem Res. **34**, 4078–4086 (1995).
[2] B.R. Duffy, H.K. Moffatt, *A similarity solution for viscous source flow on a vertical plane*, Eur J Appl Math. **8**, 37–47 (1997).
[3] A. Della Pia, M. Chiatto, L. de Luca, *Global eigenmodes of thin liquid sheets by means of Volume-of-Fluid simulations*, Physics of Fluids **32**, 082112 (2020).

W138

Instabilities in falling thin liquid films laden with soluble surfactants above CMC

Anna Katsiavria[1] & Demetrios T. Papageorgiou[1]
[1]*Department of Mathematics, Imperial College London, London, UK*

Keywords:Linear stability analysis, thin falling film, soluble surfactant, micelles

Abstract

The linear stability of a thin falling liquid film which is laden with soluble surfactant above the critical concentration for the formation of micelles (CMC) and flows down an inclined plane is addressed in two dimensions. In the case of a clean liquid the critical Reynolds number is well-known to be a function of the inclination angle[1]. It is also known that the presence of surfactants significantly affects the behaviour of the system through surface concentration gradients, which in turn induce Marangoni forces and attribute an elasticity to the interface, thus stabilising the film and increasing the critical Reynolds number. Insoluble and soluble surfactants below CMC have already been considered in the literature by addressing the equations for momentum and mass transfer coupled at the interface. In the latter case, the number of parameters involved increases, and the effects of surfactant solubility and sorption kinetics are non-trivial[2,3]. The presence of micelles further complicates the system dynamics mainly through the kinetics of monomer aggregation and micelle dissociation which are coupled to the sorption phenomena. Analytical and numerical techniques are employed to explore the effects of this coupling on the critical Reynolds number.

References

[1] Smith MK. The mechanism for the long-wave instability in thin liquid films. Journal of Fluid Mechanics. 1990;217:469-485.
[2] Karapetsas G, Bontozoglou V. The role of surfactants on the mechanism of the long-wave instability in liquid film flows. Journal of Fluid Mechanics. 2014;741:139-155. doi:10.1017/jfm.2013.670
[3] Karapetsas G, Bontozoglou V. The primary instability of falling films in the presence of soluble surfactants. Journal of Fluid Mechanics. 2013;729:123-150. doi:10.1017/jfm.2013.291

W139

MOLECULAR SIMULATION OF SURFACE-DIRECTED PHASE SEPARATION

Syed Shuja Hasan Zaidi[1], Prabhat K. Jaiswal[1], Madhu Priya[2] & Sanjay Puri[3]
[1]*Department of Physics, Indian Institute of Technology Jodhpur, Jodhpur, Rajasthan - 342030, India*
[2]*Department of Physics, Birla Institute of Technology Mesra, Ranchi, Jharkhand - 835215, India*
[3]*School of Physical Sciences, Jawaharlal Nehru University, New Delhi, Delhi - 110067, India*

Keywords: Phase separation of fluid mixtures, Wetting kinetics, Surface-directed spinodal decomposition

Abstract

We present molecular dynamics simulation results of surface-directed phase separation in unstable binary mixtures at flat wetting surfaces [1]. Our primary focus is to study the early-stage wetting kinetics for various surface potentials. First, we consider the long-ranged power-law potential. In this case, the wetting-layer thickness $R_1(t)$ at very early times exhibits a potential-dependent power-law growth. It then crosses over to a fast-mode regime with the growth exponent ~ 3/2 (see Figure 1) as observed by Wiltzius and Cumming [2]. In contrast, for the short-ranged surface potential, a logarithmic behavior in $R_1(t)$ is observed at initial times which further displays the similar rapid growth. The results for the effect of an amorphous surface on the wetting kinetics will also be presented.

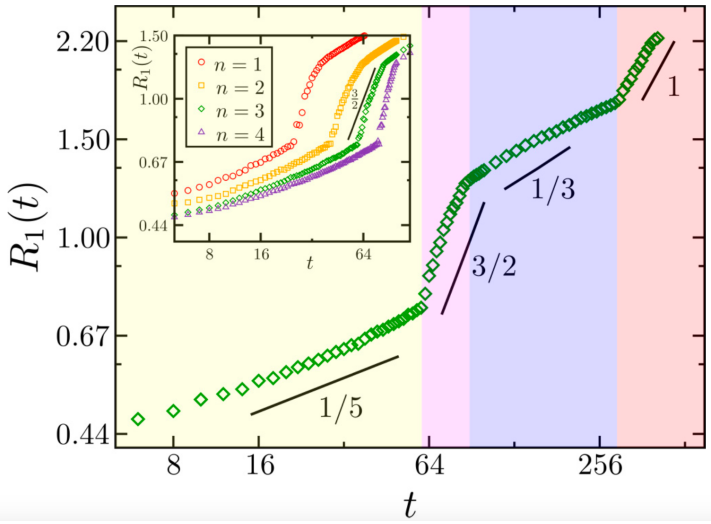

Figure 1. The time dependence of $R_1(t)$ on a log-log scale for the complete wetting morphology.

References

[1] S. S. H. Zaidi, P. K. Jaiswal, M. Priya, and S. Puri, Phys. Rev. E **106**, L052801 (2022).

[2] P. Wiltzius and A. Cumming, Phys. Rev. Lett. **66**, 3000 (1991).

W140

CHEMICALLY-ACTIVE DROPLET SWIMMING NEAR A WALL

Sébastien Michelin[1] & Nikhil Desai[1,2]
[1]*LadHyX, CNRS – Ecole Polytechnique, Institut Polytechnique de Paris, Palaiseau, France*
[2]*Department of Applied Mathematics and Theoretical Physics, Universisty of Cambridge, Cambridge, U.K.*

Abstract Instead of reducing or suppressing it, confinement can actually promote propulsion of chemically-active droplets.
Chemically-active droplets are intriguingly simple systems that can swim at micron scale as a result of their physico-chemical activity. In particular, self-solubilising droplets can self-propel spontaneously in surfactant-laden solutions as a result of the non-linear transport of surfactant molecules and micellar compounds by the interfacial flows induced at their surface by gradients of such species. Many recent experiments have reported the intriguing individual behaviour of these droplets and the onset of propulsion is now relatively well understood conceptually and modelled [1]. Yet, almost all modeling considerations of such fascinating systems focus exclusively on the case of an isolated self-propelled droplet in an unbounded and quiescent fluid. These assumptions are in fact particularly restrictive as they ignore an intrinsic feature of the experimental systems [4], namely the immediate vicinity of one or more confining boundaries, as a result of the relative buoyancy of the droplet. This is not anecdotal, since the instability and propulsion could well be hindered or suppressed as a result of the the strong and dissipative lubrication stresses within the thin fluid layers separating the droplets from the inactive substrate.
In this work, we resolve this major shortcoming and analyse for the first time the stability and onset of propulsion of isotropic active droplets close to a rigid boundary, using the canonical fully-coupled hydro-chemical model of active droplets for arbitrary distance to the wall. We demonstrate how confinement, far from preventing propulsion, can actually promote and enhance it, and explain the underlying physical mechanisms [2, 3].

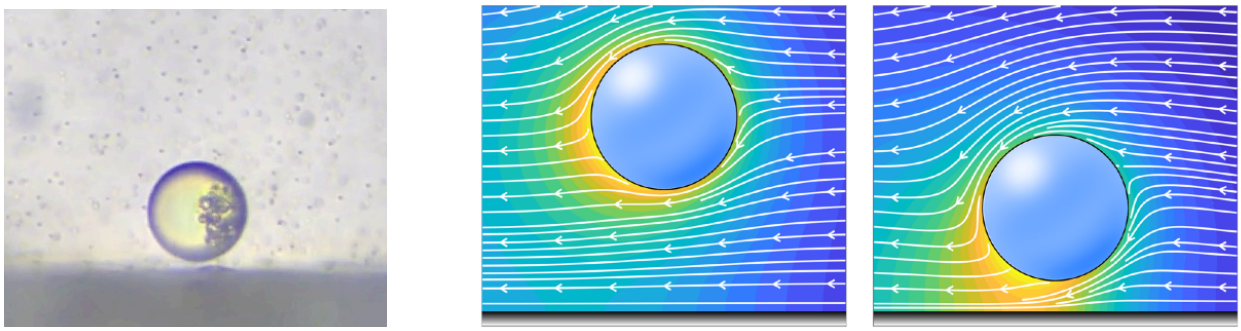

Figure 1. (Left) Side view of a self-propelled chemically-active droplet [4] (Right) Solute distribution and streamlines around a moving droplet for two different buoyancy ratios [3].

References

[1] S. Michelin, *Self-propulsion of chemically-active droplets*, Ann. Rev. Fluid Mech., **55**, 77-101 (2023).
[2] N. Desai & S. Michelin, *Instabilities and self-propulsion of active droplets along a wall*, Phys. Rev. Fluids, **6**, 114103 (2021).
[3] N. Desai & S. Michelin, *Steady state propulsion of isotropic active colloids along a wall*, Phys. Rev. Fluids, **7**, 100501 (2022).
[4] S. I. Cheon, L. B. Capavarde Silva, A. S. Khair and L. Zarzar, *Interfacially-adsorbed particles enhance the selfpropulsion of oil droplets in aqueous surfactant*, Soft Matter, **17**, 6742–6750 (2021).

W141

DROP BEHAVIOR ON HETEROGENEOUS RATCHET–STRUCTURED SUBSTRATE VIBRATED HARMONICALLY IN LATERAL DIRECTION

Rodica Borcia[1], Ion Dan Borcia[1] & Michael Bestehorn[1]
[1] *Institut für Physik, Brandenburgische Technische Universität Cottbus–Senftenberg, Germany*

Abstract Keywords: drop motion, computer simulation, ratchet system

We study numerically the propulsion of a microdroplet with applications for microfluidics and microgravity. The investigation will be done via a phase field model earlier developed for describing static and dynamic contact angles [1, 2, 3]. The density field is nearly constant in every bulk region ($\rho = 1$ in the liquid phase, $\rho \approx 0$ in the vapor phase) and varies continuously from one phase to the other with a rapid but smooth variation across the interface. Complicated explicit boundary conditions along the interface are avoided and capturated implicitly by gradient terms of ρ in the hydrodynamic basic equations. The contact angle θ is controlled through the boundary condition for the density at the solid substrate ρ_S, a free parameter varying between 0 and 1. The liquid drop is placed on a heterogeneous ratchet–structured substrate vibrated harmonically in lateral (x) direction. A heterogeneous ratchet–structured substrate could be experimentally realized through chemical patterning, for example. In our simulation this patterning is obtained by varying ρ_S, resulting thus $\theta(x)$ indicated in Figure 1. Computer simulations are performed and discussed, studying the dependency of the droplet net driven displacement on the excitation parameters (frequency, amplitude).

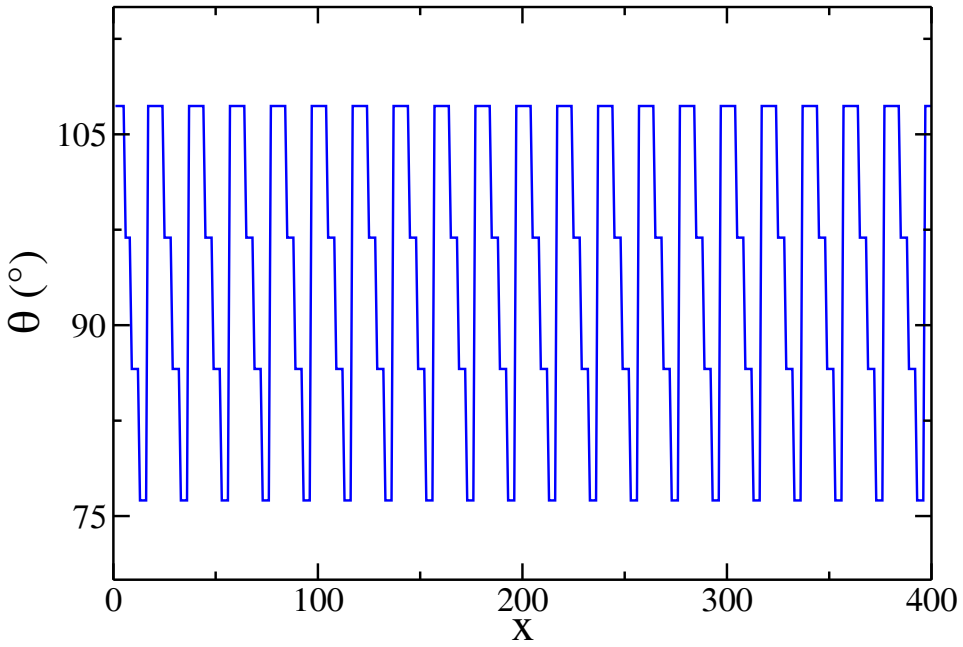

Figure 1. Heterogeneous ratchet–structured substrate realized by varying $\theta(x)$ along the x axis at the bottom boundary.

References

[1] R. Borcia, I.D. Borcia, M. Bestehorn, *Drops on an arbitrarily wetting substrate: A phase field description*, Phys. Rev. E **78**, 066307 (2008).
[2] R. Borcia, I.D. Borcia, M. Bestehorn, *Can vibrations control drop motion?*, Langmuir **30**, 14113–14117 (2014).
[3] R. Borcia, I.D. Borcia, M. Bestehorn, *Dancing drops over vibrating substrates*, Eur. Phys. J. Special Topics **266**, 1297–1306 (2017).

DAY 4 - Thursday, 27 June 2024 Morning Sessions			
09:00	**Keynote 6: Prof Julia Yeomans** ***Chair: Dr Rodrigo Ledesma-Aguilar*** ***Larch Lecture Theatre***		
	Droplets 2 ***Chair: Prof Stephen Wilson*** ***Larch Lecture Theatre***	***Particles & Suspensions 1*** ***Chair: Prof Roberto Zenit*** ***Yew Lecture Theatre***	***Convection 1*** ***Chair: Dr Marilize Everts*** ***Elm Lecture Theatre***
09:45	Th142: Shear-induced depinning of thin droplets on rough substrates *by S Kumar, NV Mhatre*	Th163: Rheology of phoretic suspensions in shear flows *by P Vinze, S Michelin*	Th184: Intermittent turbulence in a Rayleigh-Bénard convection problem by *DM Martínez, H Herrero, F Pla*
10:00	Th143: Impacts of liquid drops: when do gas microfilms prevent merging? *by P Lewin-Jones, D Lockerby, J Sprittles*	Th164: Colloidal deposits from evaporating sessile droplets: Meniscus touchdown and arbitrary contact lines *by N Coombs, M Chubynsky, J Sprittles*	Th185: Well-posedness and stability of slightly compressible Boussinesq's flow in Darcy-Bénard problem *by F Capone, G Arnone*
10:15	Th144: The effect of imbibition on the deposition from an evaporating droplet on a porous substrate *by D Craig, AW Wray, K Sefiane, SK Wilson*	Th165: Electrically and magnetically driven instabilities and microscale patterns *by JVI Timonen*	Th186: Stability of penetrative convective currents in local thermal nonequilibrium *by JA Gianfrani, G Arnone, F Capone*
10:30	Th145: Desiccation of human blood droplets: Joint effect of droplet volume and substrate inclination *by R Bhardwaj, S Chatterjee, B Kumar, A Agrawal*	Th166: Numerical simulations of in-line spheroids settling in a linearly stratified fluid *by A Abdal, L Kahouadji, S Shin, J Chergui, D Juric, CCP Caulfield, OK Matar*	Th187: Analysis of lift coefficient and trailing vortices properties at low Reynolds number with spanwise deformation *by PS García, M Garrido-Martin, E Duran, P Gutierrez-Castillo, C del Pino*
10:45	Th146: Hollow droplet impacting on inclined solid surfaces: A combined experimental and numerical study *by MM Nasiri, M Tembely, C Moreau, A Dolatabadi*	Th167: Temporal evolution of coherent structures formed by low-Stokes number particles in a high aspect ratio liquid bridge *by S Noguchi, I Ueno*	Th188: Computation of bifurcation diagrams in 3D Rayleigh-Bénard configurations involving Bingham fluids *by M Medale, M Keddar, B Draqui*
11:00	**Coffee Break (Alder Lecture Theatre)**		
11:30	Th147: Electrohydrodynamic interactions of droplet pairs *by M McDougall, D Das, SK Wilson*	Th168: Complex morphology on the underside of a Leidenfrost-levitated hydrogel sphere *by VLD Melian, I Lenton, J Binysh, A Souslov, S Waitukaitis*	Th189: Thermal convection due to internal heating in liquid metal battery *by A Hiremath, I Mutabazi, HN Yoshikawa*
11:45	Th148: Dynamics through pitchfork bifurcations of droplets on smooth patterns *by M Pradas, M Ewetola, M Haynes, R Ledesma-Aguilar*	Th169: Instabilities and pattern transitions in co-rotating suspension Taylor-Couette flow *by M Ghosh, M Alam*	Th190: The dry salt lake instability *by C Beaume, MR Threadgold, L Goehring*
12:00	Th149: The evaporation of arrays of non-circular droplets *by A Wray, M Moore*	Th170: Chaotic orbits of multiple immersed ellipsoids *by A Boyd, P Valluri, D Scott, M Sawyer, R Govindarajan*	Th191: Anisotropy effect on the thermal instability for a porous channel with symmetric wall heat fluxes *by M Celli, A Barletta, PV Brãndao, S Lazzari, E Ghedini*
12:15	Th150: Evaporation dynamics of multiple sessile droplets *by J Kilbride, FF Ouali, DJ Fairhurst*	Th171: Particle deposition from a sessile droplet evaporating according to the one-sided model *by HT Sharp, SK Wilson, AW Wray*	Th192: The effect of a non-uniform heating on the axisymmetric Rayleigh-Bénard instability *by L Biancofiore, D Ozev, F Gallaire*
12:30	**Lunch Break (Alder Lecture Theatre)**		

Keynote 6

Active Matter: “evading the decay to equilibrium”

Julia Yeomans

Department of Physics, University of Oxford, UK

Julia Yeomans is Professor of Physics at the University of Oxford. She obtained her MA and DPhil in Physics from Oxford and then spent two years as a post-doc at Cornell University. She returned to the UK, as a Lecturer at the University of Southampton, before joining the Rudolf Peierls Centre for Theoretical Physics. Julia applies techniques from theoretical and computational physics to problems in soft condensed matter and biophysics. Her current research interests include active matter and mechanobiology. She has been awarded the EPJE-de Gennes Lecture Prize and the Sam Edwards prize of the Institute of Physics and she is a Fellow of the Royal Society.

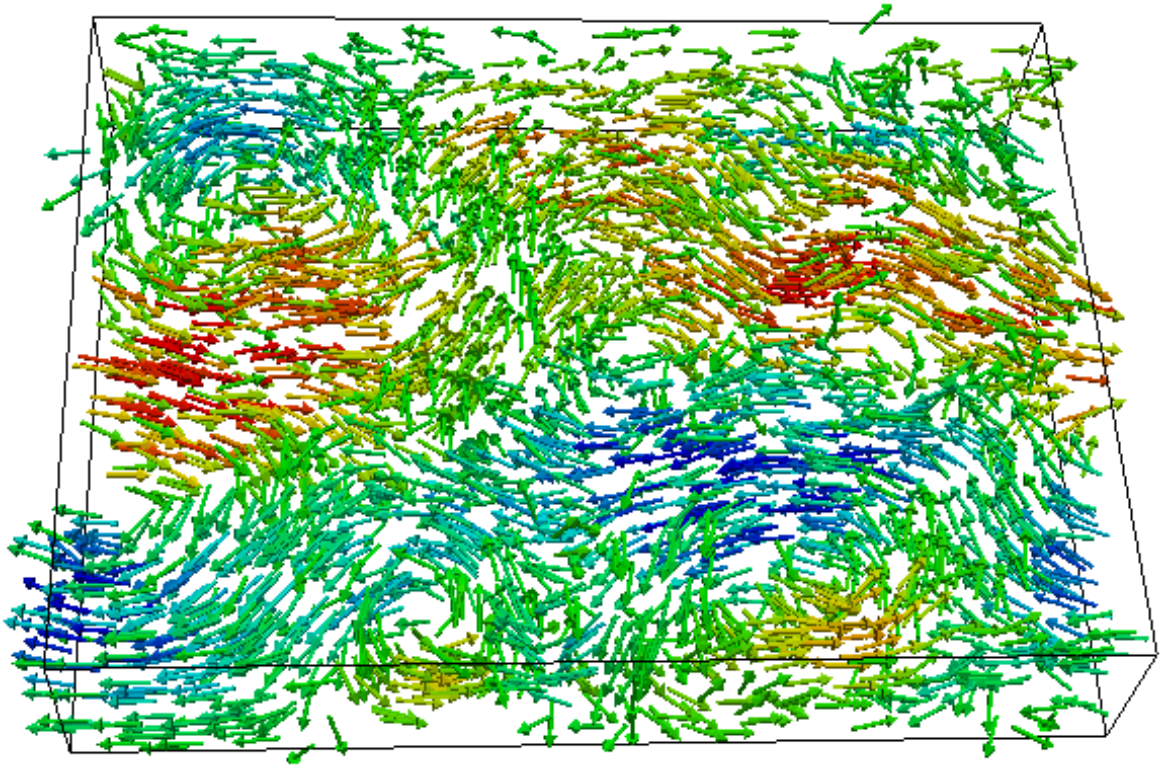

Abstract

Active systems such as bacteria, motor proteins and eukaryotic cells continuously transform chemical energy from their surroundings to mechanical work. Dense active matter shows mesoscale turbulence, the emergence of chaotic flow structures characterised by high vorticity and self-propelled topological defects. The theories of active matter are suggesting new ways of studying collective cell migration and remodelling which are important in early embryogenesis, wound healing, and biofilm formation.

Th142

SHEAR-INDUCED DEPINNING OF THIN DROPLETS ON ROUGH SUBSTRATES

Ninad V. Mhatre[1] & Satish Kumar[1]
[1]*Department of Chemical Engineering and Materials Science, University of Minnesota, Minneapolis, MN 55455, USA*

Keywords: Droplet, Contact line, Depinning, Surface roughness

Abstract

Depinning of liquid droplets on substrates by flow of a surrounding immiscible fluid is central to applications such as crossflow microemulsification, oil recovery, and waste cleanup. Surface roughness, either natural or engineered, can cause droplet pinning, so it is of both fundamental and practical interest to determine the flow strength of the surrounding fluid required for droplet depinning on rough substrates. Here, we develop a lubrication-theory-based model for droplet depinning on a substrate with topographical defects by flow of a surrounding immiscible fluid. The droplet and surrounding fluid are in a rectangular channel, a pressure gradient is imposed to drive flow, and the defects are modeled as Gaussian-shaped bumps. Using a precursor-film/disjoining-pressure approach to capture contact-line motion, a nonlinear evolution equation is derived describing the droplet thickness as a function of distance along the channel and time. Numerical solutions of the evolution equation are used to investigate how the critical pressure gradient for droplet depinning depends on the viscosity ratio, surface wettability, and droplet volume. Simple analytical models are able to account for many of the features observed in the numerical simulations. The influence of defect height is also investigated, and it is found that when the maximum defect slope is larger than the receding contact angle of the droplet, smaller residual droplets are left behind at the defect after the original droplet depins and slides away. The model presented here yields considerably more information than commonly used models based on simple force balances, and provides a framework that can readily be extended to study more complicated situations involving chemical heterogeneity and three-dimensional effects.

Th143

IMPACTS OF LIQUID DROPS: WHEN DO GAS MICROFILMS PREVENT MERGING?

Peter Lewin-Jones[1], Duncan Lockerby[2] & James Sprittles[1]
[1]*Mathematics Institute, University of Warwick, Coventry, CV4 7AL, UK*
[2]*School of Engineering, University of Warwick, Coventry, CV4 7AL, UK*

Abstract Drop Impacts, Thin Gas Films, Non-continuum Effects.

Collisions and impacts of drops are critical to numerous processes, including raindrop formation, inkjet printing, food manufacturing and spray cooling. For drop-drop collisions, increasing the relative speed leads to multiple transitions: from merging to bouncing and then back to merging - transitions which were recently discovered to be sensitive to the drops' radii as well as the ambient gas pressure. The outcome of a drop impacting a liquid bath is even more complex: for a fixed speed, the result can go from merging to bouncing to merging and back to bouncing with increasing bath depth.

To provide new insight into the physical mechanisms involved and as an important predictive tool, we have developed a novel, open-source computational model for both drop-drop and drop-bath events, using the finite element package oomph-lib. This uses a lubrication framework for the gas film and incorporates fully, for the first time, the crucial micro- and nano-scale influences of gas kinetic effects and disjoining pressure.

Our simulations show strong agreement with experiments for the transitions between merging and bouncing, but can also go beyond these regimes to make new experimentally-verifiable predictions. We will show how our model enables us to explore the parameter space and discover the regimes of contact (that are inaccessible to experiments). Finally, we will overview potential extensions to the computational model, including impacts in Leidenfrost conditions and post-contact dynamics.

A review of this topic can be found in Sprittles (2024) [1], and a paper on drop-drop collisions is under review [2].

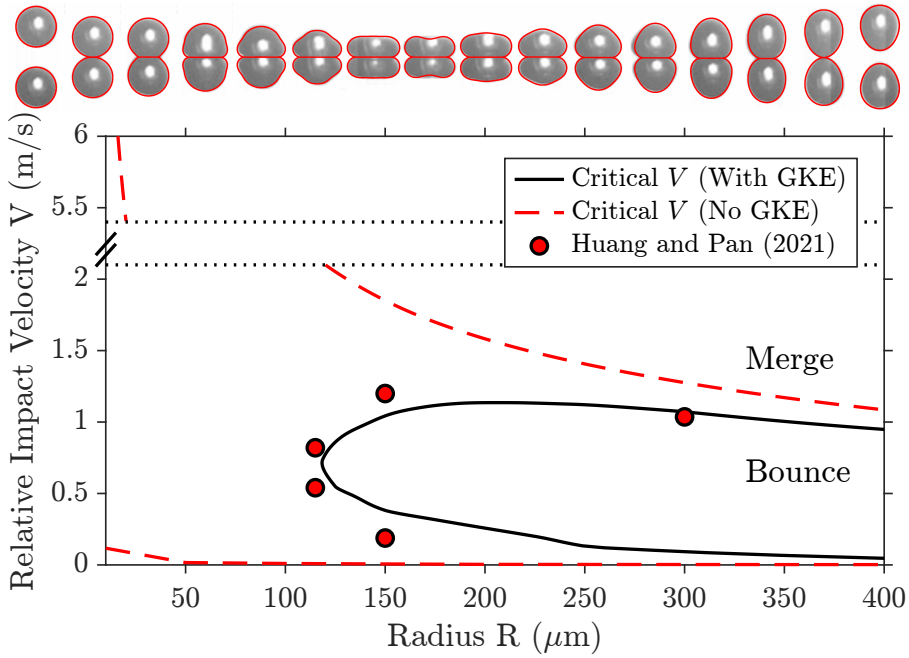

Figure 1. Regime diagram for the head-on collision of tetradecane drops, showing the transitions between bouncing and merging, with comparison to the experiments of Huang and Pan [3]. In red, the results when Gas Kinetic Effects (GKE) are not included, showing the importance of GKE in predicting these transitions. Above: simulation profiles in red, compared to an experiment from Pan et. al. [4].

References

[1] J. E. Sprittles *Gas Microfilms in Droplet Dynamics: When Do Drops Bounce?*, Annu. Rev. Fluid Mech., **56** (2024).
[2] P. Lewin-Jones, D. Lockerby, J. Sprittles *Collision of Liquid Drops: Bounce or Merge?*, Under Review.
[3] K.-L. Huang, K.-L. Pan, *Transitions of bouncing and coalescence in binary droplet collisions*, Journal of Fluid Mechanics, **928**, A7 (2021).
[4] K.-L. Pan, C. K. Law, B. Zhou, *Experimental and mechanistic description of merging and bouncing in head-on binary droplet collision*, Journal of Applied Physics, **103**, 064901 (2008).

Th144

THE EFFECT OF IMBIBITION ON THE DEPOSITION FROM AN EVAPORATING DROPLET ON A POROUS SUBSTRATE

David Craig[1], Alexander W. Wray[1], Khellil Sefiane[2], and Stephen K. Wilson[1]
[1] *Department of Mathematics and Statistics, University of Strathclyde, Livingstone Tower, 26 Richmond Street, Glasgow G1 1XH*
[2] *School of Engineering, Institute for Multiscale Thermofluids, The University of Edinburgh, Edinburgh EH9 3FD*

Keywords: Droplets, Evaporation, Imbibition, Flow, Deposition, Coffee-ring effect.

Abstract The majority of the previous work on the evaporation of sessile droplets has focused on the case in which the substrate is solid (i.e. non-porous). However, in many applications, such as printing onto paper and fabric textiles, the substrate is porous, and the transport of liquid into the substrate may play a significant role in the evolution, and hence the lifetime, of a droplet [1]. We extend the analysis of [2] to consider a droplet evaporating on a porous substrate and develop analytical models, based on lubrication theory, for the evolution of a droplet subject to simultaneous evaporation and imbibition. Specifically, the evolution of a thin droplet situated on an initially dry or an initially flooded porous substrate of varying thickness is analysed. The evaporation from the droplet is driven by the diffusion of liquid molecules into the passive atmosphere. In contrast, the imbibition from the base of the droplet is driven by the pressure difference between the droplet and the porous substrate. We use Darcy's law to model the flow of liquid within the substrate. We analyse the evolution, and hence the lifetime, of such droplets, in a variety of modes, specifically the constant angle, constant radius, stick-slide, and stick-jump modes. While, as expected, imbibition leads to a decrease in the lifetime of the droplet, the dynamics of a droplet undergoing pure imbibition are qualitatively different from those of a droplet undergoing pure evaporation. Furthermore, our results demonstrate that imbibition-driven flow within the droplet is qualitatively different to evaporation-driven flow. A particle-laden droplet evaporating on a solid substrate usually leads to particles being deposited at the edge of a droplet in a coffee-ring pattern [3, 4]. Hence, it is of interest to consider whether a droplet evaporating on a porous substrate leads to the same coffee-ring pattern. Recent experimental work [5] observed that the additional imbibition dynamics lead to an enhancement of the coffee-ring effect. In contrast, [6] observed that the additonal imbibition dynamics lead to suppression of the coffee-ring effect. Motivated by these experimental results, we show that in the limit of a sufficiently small Péclet number the transport rate of particles within the droplet to the contact line is enhanced by the effect of imbibition. Additionally, we show that in the limit of a sufficiently large Péclet number the transport rate of particles within the droplet to the contact line is suppressed by the effect of imbibition. Hence, our findings would suggest that the discrepancy between both sets of experimental results is due to the difference in underlying diffusion and advection mechanicisms responsible for transporting particles to the edge of the droplet.

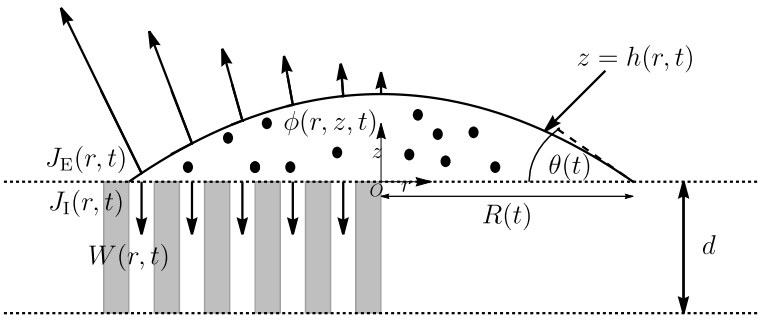

Figure 1. Sketch of a thin particle-laden droplet evaporating on a porous substrate.

References

[1] D. Lohse, *Fundamental Fluid Dynamics Challenges in Inkjet Printing*, Annual Review of Fluid Mechanics, **54**, 349–382 (2022) .
[2] H.-M. D'Ambrosio, S. K. Wilson, A. W. Wray, and B. R. Duffy, *The effect of the spatial variation of the evaporative flux on the deposition from a thin sessile droplet*, Journal of Fluid Mechanics, **970**, A1 (2023) .
[3] R. D. Deegan, O. Bakajin, T. F Dupont, G. Huber, S. R. Nagel, and T. A Witten, *Capillary flow as the cause of ring stains from dried liquid drops*, Nature, **389** 6653, 827–829 (1997).
[4] T. Pham, and S. M. Kumar, , *Imbibition and evaporation of droplets of colloidal suspensions on permeable substrates*, Physical Review Fluids, **4** 3, 034004 (2019) .
[5] R. Dou and B. Derby, *Formation of coffee stains on porous surfaces*, Langmuir, **28** 12, 5331–5338 (2012).
[6] M. Pack, H. Hu, D-O. Kim, X. Yang, and Y. Sun, *Colloidal Drop Deposition on Porous Substrates: Competition among Particle Motion, Evaporation, and Infiltration*, Langmuir, **31** 29, 7953–7961 (2015).

Th145

DESICCATION OF HUMAN BLOOD DROPLETS: JOINT EFFECT OF DROPLET VOLUME AND SUBSTRATE INCLINATION

Rajneesh Bhardwaj[1], Sanghamitro Chatterjee[1], Bibek Kumar[1]& Amit Agrawal[1]
[1]*Department of Mechanical Engineering, Indian Institute of Technology Bombay, Mumbai, India*

Keywords: Blood Stain Pattern, Evaporation, Sessile Droplets, Dried Deposits, Cracks

Abstract: Dried deposit or desiccation patterns of sessile droplets of human blood on solid surfaces is crucial in disease diagnosis in bioengineering and bloodstain pattern analysis (BPA) in forensics [1]. Herein, we study the desiccation patterns with varying droplet volume and inclination angle of the surface. We systematically varied the droplet volume $V_d \in [1-10\mu\text{L}]$ and inclination angle $\alpha \in [1-10\mu\text{L}]$. For $\alpha = 0°$, typical deposits of toroidal geometry in the peripheral region containing cracks in radial and azimuthal directions were seen [2] (first row of figure 1). On the inclined surfaces, the droplet shape is modulated by the combined action of gravity and surface tension forces [3], which yields asymmetric mass deposits in the desiccation patterns along the advancing and receding fronts. A consequence of the asymmetric deposits is the difference in the number and dimensions of crack patterns between the advancing and receding fronts. Typical optical microscopic images depicting the observations are shown in figure 1. The observations were further confirmed by quantification through optical surface profiling. The observations corroborate with a scaling analysis involving the release of mechanical stress that provides the surface energies of the newly created surface in crack formation [4].

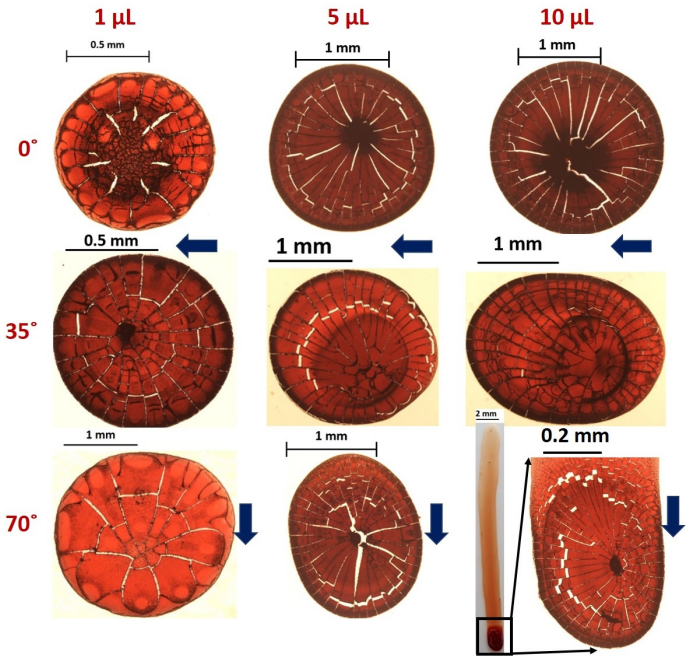

Figure 1. Desiccation patterns for varying blood droplet volumes and inclination angle. The blue arrows indicate the direction of inclination for the respective cases.

References

[1] F. Smith, D. Brutin, *Wetting and spreading of human blood: Recent advances and applications*, Current Opinion in Colloid & Interface Science **36**, 78–83 (2018).
[2] B. Sobac, D. Brutin, *Desiccation of a sessile drop of blood: Cracks, folds formation and delamination*, Colloids and Surfaces A: Physicochemical and Engineering Aspects **448**, 34–44 (2014).
[3] W.C. Extrand, Y. Kumagai, *Liquid drops on an inclined plane: the relation between contact angles, drop shape, and retentive force*, Journal of colloid & interface science **170**, 515–521 (1995).
[4] K. B. Singh, M. S. Tirumkudulu, *Cracking in drying colloidal films*, Physical review letters **98**, 218302 (2007).

Th146

Hollow Droplet Impacting on Inclined Solid Surfaces: a Combined Experimental and Numerical Study

Mohammad Mahdi Nasiri[1], Moussa Tembely[1] , Christian Moreau[1] & Ali Dolatabadi[2]
[1]*Department of Mechanical, Industrial and Aerospace Engineering, Concordia University, Montreal, Canada*
[21]*Department of Mechanical Engineering, University of Toronto, Toronto, Canada*
.

Keywords:
Droplet impact, Hollow droplet flattening, Counter-jet formation, Surface wettability.

Abstract

The study of droplet impact on a solid surface is crucial in understanding natural phenomena and various industrial applications such as raindrop impact on the ground, drip irrigation, spray cooling, spray coating, inkjet printing, and thermally sprayed coatings. In particular, the impact of hollow droplets has been studied experimentally and numerically to understand the dynamics of droplet flattening on different surfaces held at various angles. The study reveals two significant distinctions between the flattening of a hollow droplet and a dense droplet. The first distinction is the formation of a counter-jet following the collision of a hollow droplet perpendicular to the surface. The length of the counter-jet is dependent on the normal component of the droplet velocity vector and liquid viscosity, while only affects its size. The second distinction is the final shape of the flattened droplet, which takes the form of a donut on a hydrophobic surface due to bubble rupture during the spreading droplet surface. The study provides an in-depth insight into the formation of splat and counter jets and highlights the role of surface wettability, liquid properties, and impact velocity on the droplet flattening process. The experiments were conducted on different surfaces, including aluminum, sand-blasted steel, and superhydrophobic surfaces. The numerical simulations further compare pressure contours and velocity vectors for dense and hollow droplets, providing a comprehensive understanding of the post-impact process. Overall, this study contributes to a better understanding of droplet impact dynamics and provides insights into how to control splat properties in various applications.

Th147

ELECTROHYDRODYNAMIC INTERACTIONS OF A PAIR OF LEAKY DIELECTRIC DROPLETS

Michael A. McDougall, Stephen K. Wilson & Debasish Das
Department of Mathematics and Statistics, University of Strathclyde, Glasgow, UK

Keywords: When a leaky dielectric droplet is suspended in another fluid and exposed to a uniform DC electric field, it becomes polarised and electric stresses tangential to the droplet interface drive fluid motion inside and outside the droplet [1]. In the presence of a second droplet, the dynamics of the first droplet are modified due to electrohydrodynamic interactions; most importantly, the droplets start translating due to dielectrophoretic forces and hydrodynamic interactions [2]. A three-dimensional small deformation theory for a pair of identical, widely-separated, leaky dielectric droplets suspended in a weakly conducting fluid medium is presented, valid in the limit of high droplet viscosity and surface tension, such that the drop remains nearly spherical. The theory is constructed in accordance with the Taylor–Melcher leaky dielectric model [3], which retains the effects of transient charge relaxation and convection. This makes the charge transport equation nonlinear and challenging to solve analytically. It gives rise to spontaneous droplet rotation in sufficiently strong fields [4] known as Quincke rotation, corresponding to a pitchfork bifurcation in the steady state angular velocity of the droplets. The flow field around each droplet is governed by the Stokes equations. Interfacial Maxwell stresses arise on the surface of the droplets due to the applied field as well as the polarisation of both droplets. These electric stresses are balanced by capillary stresses and induced hydrodynamic stresses. Further, an analytical expression for the critical electric field strength for Quincke rotation of an isolated spherical droplet is derived. (Electrohydrodynamics, droplets, interactions).

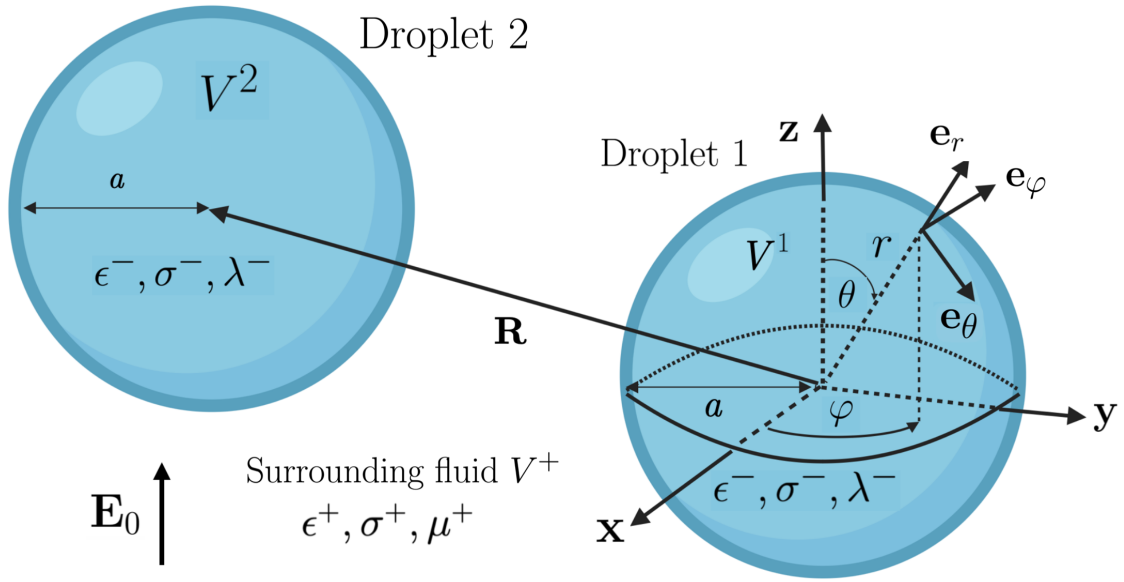

Figure 1. A pair of leaky dielectric droplets suspended in a viscous fluid and exposed to a uniform electric field $\mathbf{E}_0$.

References

[1] G.I. Taylor, *Studies in electrohydrodynamics I. The circulation produced in a drop by an electric field*, Proc. R. Soc. Lond. A **291**, 159–166 (1966).
[2] J.C. Baygents, N.J. Rivette, H. Stone, *Electrohydrodynamic deformation and interaction of drop pairs*, J. Fluid Mech. **368**, 359–375 (1998).
[3] J.R. Melcher, G.I. Taylor, *Electrohydrodynamics: a review of the role of interfacial shear stresses*, Annu. Rev. Fluid Mech. **1**, 111–146 (1969)
[4] D. Das, D. Saintillan, *A three-dimensional small-deformation theory for electrohydrodynamics of dielectric drops*, J. Fluid Mech. **914**, A22 (2021).

Th148

DYNAMICS THROUGH PITCHFORK BIFURCATIONS OF DROPLETS ON SMOOTH PATTERNS

Marc Pradas[1], Michael Ewetola[1], Mathew Haynes[2] & Rodrigo Ledesma-Aguilar[3]
[1]*School of Mathematics and Statistics, The Open University, Milton Keynes, UK*
[2]*Bader College, Queen's University, Hailsham, UK*
[3]*Institute for Multiscale Thermofluids, School of Engineering, University of Edinburgh, UK*

Abstract We quantify the dynamics of a droplet that undergoes a stability change via a pitchfork bifurcation as its volume slowly varies in time because of an external driving mechanism (e.g., evaporation).

Controlling droplet transport and localisation on structured solid surfaces is important for key technologies, such as liquid-repellent surfaces, microchemical reactors, and micro- and nano-fluidic systems. Consequently, considerable effort has been devoted to designing solid surfaces that enhance/inhibit wetting [1], control droplet's contact area [2], and direct droplet's motion [3].

Droplets that are subjected to external, time-dependent variations, such as evaporation and condensation, exhibit complex dynamics that strongly depends on the interaction with the solid surface. Recently, we have shown that the shape and location of a droplet that is slowly evaporating on a smooth wettability pattern undergo changes due to surface instabilities. These arise from a hierarchy of pitchfork bifurcations as the volume $V(t)$ of the droplet decreases [4, 5]. At each bifurcation point, the stability changes so the droplet must change its shape and position $s(t)$ as dictated by the underlying solid pattern [Fig. 1(a)].

Building upon these results, here we use a combination of theory and diffuse-interface simulations to study the dynamics of droplets passing through such bifurcation points, and how it depends on the physical properties of the system (capillary and Weber numbers). We show that at each bifurcation point the droplet exhibits a rapid change in its position that we quantify in terms of its instantaneous velocity. We find that there are two distinctive dynamical regimes: an over-damped regime that is dominated by viscous dissipation and surface tension; and an under-damped regime where inertial effects become important and that is characterised in terms of a decaying oscillatory dynamics [see Fig. 1(b)]. We observe that the under-damped regime can be described in terms of scaling relations between the maximum droplet's speed and capillary number. Our results indicate that the interplay between a phase change and surface wettability can be exploited to control the motion of droplets on patterned solids.

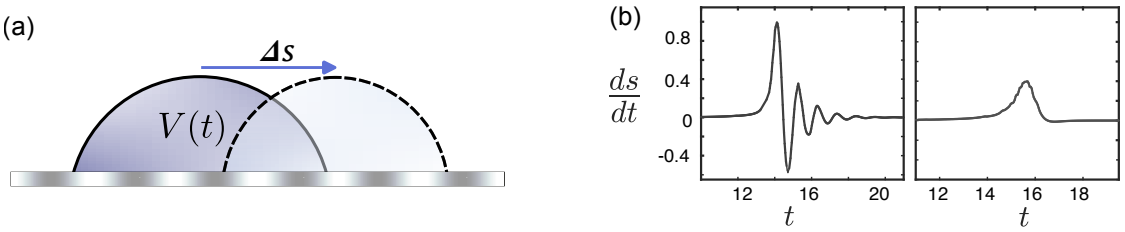

Figure 1. (a) Droplet lateral displacement Δs triggered by a bifurcation point as the volume $V(t)$ decreases in time. (b) Droplet's instantaneous speed, ds/dt, plotted versus time in the under-damped oscillatory state with capillary number $Ca = 0.005$ (left) and in the over-damped state with $Ca = 0.05$ (right).

References

[1] D. Quéré, *Wetting and Roughness*, Annu. Rev. Mater. Res. **38**, 71–99 (2008).
[2] R. Raj, S. Adera, R. Enright & E. N. Wang *High-resolution liquid patterns via three-dimensional droplet shape control*, Nature Commun. **5**, 4975 (2014).
[3] M. S. Sadullah, G. Launay, J. Parle, R. Ledesma-Aguilar, Y. Gizaw, G. McHale, G. G. Wells & H. Kusumaatmaja *Bidirectional motion of droplets on gradient liquid infused surfaces*, Commun. Phys. **3**, 166 (2020).
[4] G. G. Wells, E. Ruiz-Gutierrez, Y. Le Lirzin, A. Nourry, B. V. Orme, M. Pradas, & R. Ledesma-Aguilar *Snap evaporation of droplets on smooth topographies*, Nature Commun. **9**, 1380 (2018).
[5] M. Ewetola, R. Ledesma-Aguilar, & M. Pradas *Control of droplet evaporation on smooth chemical patterns* , Phys. Rev. Fluids **6**, 033904 (2021).

Th149

THE EVAPORATION OF ARRAYS OF NON-CIRCULAR DROPLETS

Alexander Wray[1] & Madeleine Moore[2]
[1]*Department of Mathematics and Statistics, University of Strathclyde, Livingstone Tower, Glasgow, UK*
[2]*Department of Mathematics, School of Natural Sciences, University of Hull, Cottingham Road, Hull, UK*

Keywords: evaporation, droplets, thin films, printing.

Abstract The evaporation of droplets has been a much-studied problem in recent years, finding applications everywhere from the spraying of pesticides on leaves to diagnostic applications of blood drying. Unfortunately, many of the most critical industrial applications, such as the printing of OLED screens, involve arrays of droplets with polygonal footprints in close enough proximity to one another that the evaporative behaviours interfere with one another via the vapour phase. This is in stark contrast to the state of the theoretical literature which has solely focussed on droplets with circular or elliptic footprints, and even then, only for such droplets in isolation.

We discuss recent advancements in this area relaxing both of these constraints, demonstrating how arbitrary arrays of non-circular droplets may be analysed theoretically. We examine a variety of industrially relevant problems, including the evaporative behaviours of rectangular droplets (used for OLED screens), arrays of droplets of different sizes (see Figure 1), and a continuum formulation designed to cope with the extremely large arrays observed in 8K screens ($O(10^8)$ droplets). We also briefly discuss the uses of these solutions in other physical contexts.

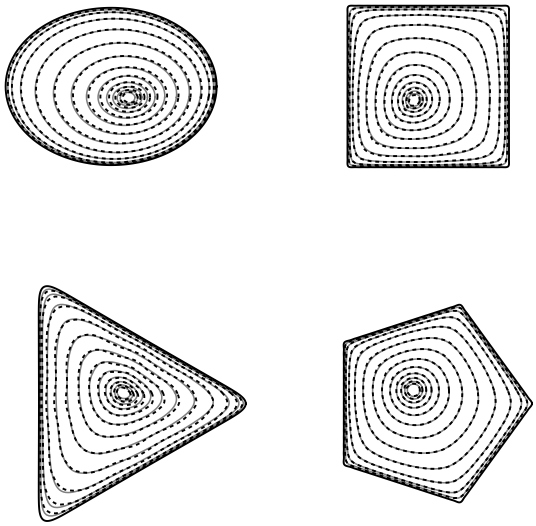

Figure 1. Contours of evaporative flux according to COMSOL (solid lines) and the new asymptotic model (dashed lines)

Th150

EVAPORATION DYNAMICS OF MULTIPLE SESSILE DROPLETS

J.J Kilbride[1], F.F Ouali[1] & D.J Fairhurst[2]
[1]*SOFT Group, School of Science and Technology, Nottingham Trent University, Nottingham, UK.*
[2]*School of Physics and Astronomy, University of Edinburgh, Edinburgh, UK.*

Keywords: Droplets, Evaporation, Diffusion

Abstract
The evaporation of a single droplet on a surface has been well studied. The literature provides successful theoretical predictions of how long a droplet takes to evaporate and even describes the internal flow of the liquid. It is however more common to see droplets appearing in groups, for example, condensing from warm breath on a cold day, on the underside of a coffee cup lid and as raindrops on windows. The evaporation of these droplets have many applications in spray cooling, ink-jet printing and limiting viral transmission. Despite this, there is much less research on multiple droplets and how each droplet influences the evaporation of those surrounding it.

Recent theoretical models describe the reduced evaporation rates of multiple droplets on surfaces caused by the diffusive vapour interactions[1,2]. However, the experimental work required to validate these models has fallen behind due to difficulties dispensing and determining the transient volumes of droplets arranged in arbitrary 2D patterns [3]. We take experimental data from various sessile droplet arrays (see figure 1) to understand these droplet-to-droplet interactions. By using Pattern Distortion [4], a technique which utilises a droplets lens like magnification of a pattern placed beneath, we can extract transient volumes as well as lifetimes. This data is quantitatively compared to the different theoretical models [1,2], evaluating their performance and extending our previous work [4,5].

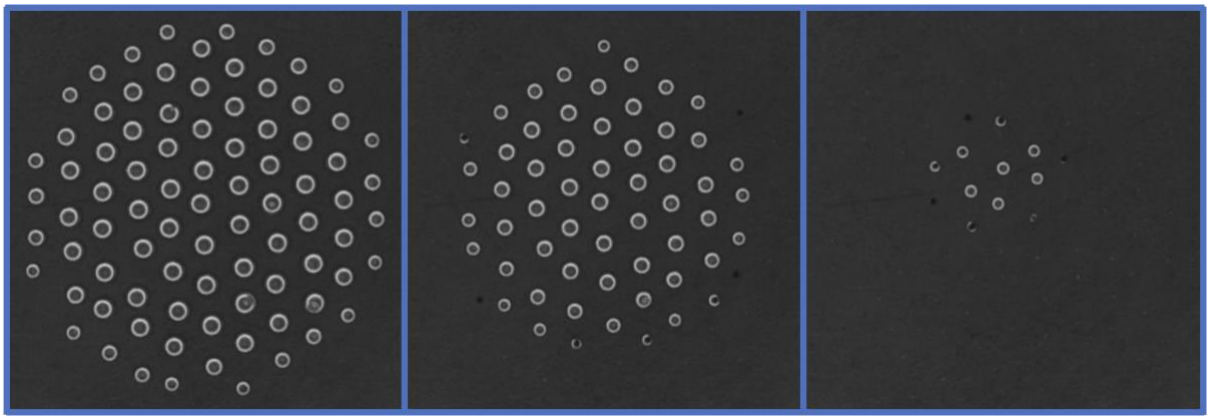

Figure 1. Experimental frames in time (left to right) as an 85 droplet circular array of radius 15mm evaporates.

[1] Wray, A., et al (2020). Competitive evaporation of multiple sessile droplets. Journal of Fluid Mechanics, 884, A45. doi:10.1017/jfm.2019.919
[2] Masoud, H., et al (2021). Evaporation of multiple droplets. Journal of Fluid Mechanics, 927, R4. doi:10.1017/jfm.2021.785
[3] Edwards, A. M., et al (2021). Interferometric measurement of co-operative evaporation in 2D droplet arrays. Applied Physics Letters, 119(15), 151601.
[4] Kilbride, J. J., et al. "Pattern-Distortion Technique: Using Liquid-Lens Magnification to Extract Volumes of Individual Droplets or Bubbles within Evaporating Two-Dimensional Arrays." Physical Review Applied 19.4 (2023): 044030.
[5] Iqtidar, A., et al. (2022) Drying dynamics of sessile-droplet arrays.

Th163

RHEOLOGY OF PHORETIC SUSPENSIONS IN SHEAR FLOWS

Prathmesh Vinze, Sebastien Michelin
LadHyX, CNRS–Ecole Polytechnique, Institut Polytechnique de Paris, 91120 Palaiseau, France

Abstract Active Matter,Collective Behaviour, Complex fluid

Phoretic particles are micron-sized particles which exploit chemical energy present in the environment to self-propel [1]. These particles interact through their chemical and hydrodynamic footprints, which result in passive reorientation and drift of their neighbors. This, along with the presence of boundaries, gives rise to complex collective dynamics [2, 3].
In this work, we use a continuum kinetic model to study numerically the suspensions' self-organisation focusing specifically on the effect of the collective dynamics on the rheology of the suspension. Microswimmers are known to alter the rheological properties through the hydrodynamic stresses they exert on the surrounding fluid.The nature of the microswimmer (puller or pusher) and its geometry determines whether the effective viscosity is reduced or increased. The hydrodynamic signature of chemotactic phoretic particles is more complex and includes both an intrinsic pusher contribution and a puller component controlled by the particle's chemical environment, resulting in more complex effective rheology. The effective viscosity in a Couette flow cell is defined here globally from the measurements of the total force exerted by the fluid and particles on one of the bounding walls. Unsurprisingly, we show that the regime of self-organisation critically affects the rheology of the suspension which we characterize for each self-organisation regime.For example, when chemotactic particles from regular aggregates along each wall, the induced flow consists of vortical flow cells (Fig. 1), whose symmetry is broken by the imposed background shear flow. As a result, the flow induced by the particles can increase/decrease (be specific!) the suspension viscosity. To obtain further insight, a reduced model is proposed which relates the induced flow and the resulting modification in effective viscosity to physical quantities such as particle density, average particle orientation, and the background solute gradient.

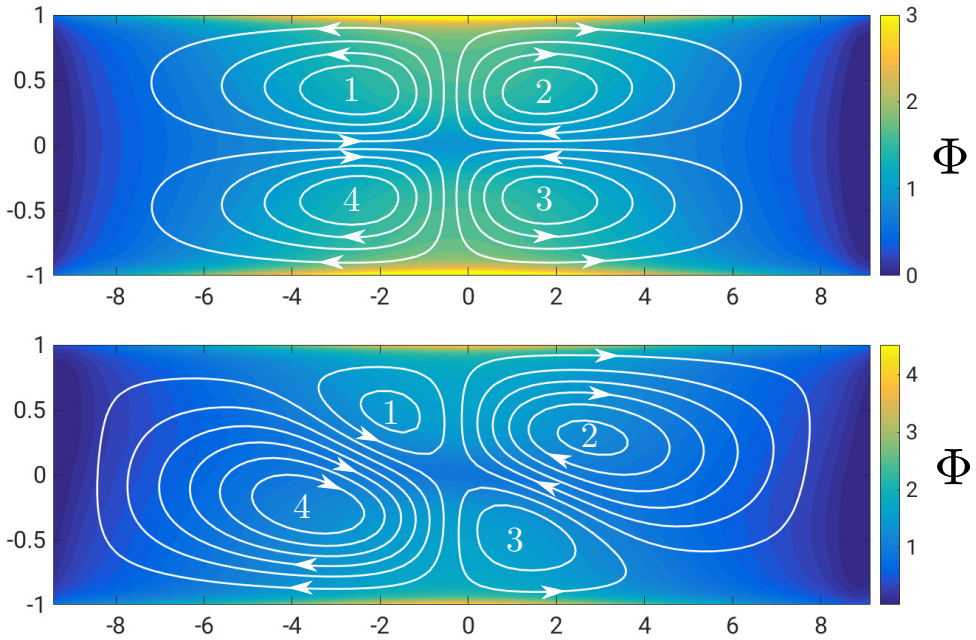

Figure 1. Streamlines (white lines) and particle concentration (color) of the induced flow for 2D steady state in the absence of flow(top) and for weak background shear (bottom).

References

[1] J L Moran and J D Posner *Phoretic self-propulsion*, Annual Review of Fluid Mechanics **49**,511-540, 2017.
[2] T. Traverso and S. Michelin *Hydrochemical interactions in dilute phoretic suspensions: From individual particle properties to collective organization*, Phyiscal Review Fluids, **5**, 104203, 2020.
[3] T Traverso and S Michelin. *Collective dynamics and rheology of confined phoretic suspensions.* Journal of Fluid Mechanics, 943:A21, 2022

Th164

COLLOIDAL DEPOSITS FROM EVAPORATING SESSILE DROPLETS: MENISCUS TOUCHDOWN AND ARBITRARY CONTACT LINES

Nathan Coombs[1], Mykyta Chubynsky[2] & James Sprittles[1]
[1]*Mathematics Institute, University of Warwick, Coventry, UK*
[2]*Research Centre for Fluid and Complex Systems, Coventry University, Coventry, UK*

Abstract We present a computational model for the evaporation of colloidal suspensions. Through our novel approach to modelling particle jamming, our model is capable of making realistic predictions of the morphology of the colloidal deposit once evaporation has completed. Solution via the finite element method allows a straightforward extension to arbitrary contact line shapes, allowing us to explore the dependence of the contact line curvature on the local deposit intensity.

Understanding the physics of colloid deposition in evaporating sessile droplets is important in numerous industrial applications. For example, in the field of inkjet-printed electronics conductive tracks are built up by drop-wise deposition of the printing medium onto a substrate. These drops then coalesce to form a liquid line from which the solvent evaporates to leave a conductive deposit [1]. In such a setting it is desirable that the deposit be spatially uniform [2]; voids or regions with very little deposit will limit the mobility of charge carriers. A practical challenge thus arises in circumventing the *coffee ring effect* (CRE). The CRE refers to accumulation of solute towards the contact line of the droplet and is purely fluid-dynamical in origin: Evaporation-induced capillary flow transports particles towards the contact line where they aggregate and so an enhanced deposit is seen there.

From a modelling perspective, realistic predictions of the deposit's dimensions require the inclusion of jamming: as particles approach a threshold volume fraction ϕ_c (≈ 0.64 for mono-disperse spherical particles), they form an immobile porous solid and so the advection of solute ceases. Here we present a modelling framework that incorporates this behaviour. Through use of the finite element library oomph-lib [3], the model can be easily applied to arbitrary contact line geometries. This makes it an ideal candidate for studying the practically relevant case of inkjet-printed lines. Strong qualitative agreement is found between the model predictions and available experimental data. See below, for example, the case of a triangular contact line geometry.

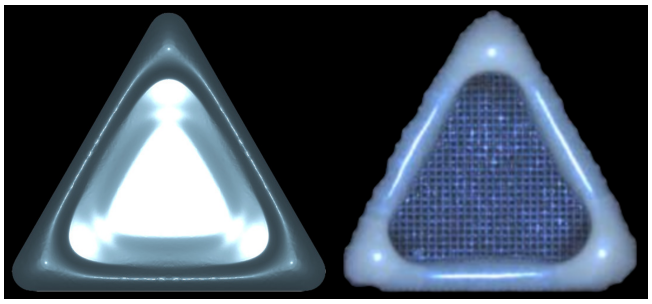

Figure 1. A bird's eye view of dried deposit morphologies. Left: our simulation. Right: adapted from reference [4]

A novel feature of our model is that simulations can be run through the entirety of the drying process, achieved through implicit tracking of jammed particle fronts. This feature is not present in the works of Popov [5] and Kaplan and Mahavedan [6], for example, due to topological changes as the drop surface approaches the substrate at the late stages of evaporation.

In this talk, I will explore the model framework and dynamics in detail. Time permitting, I will also address the *surface capture* phenomenon, which refers to solute adhering to the surface of the drop at higher evaporation rates.

References

[1] D. Lohse, *Fundamental fluid dynamics challenges in inkjet printing*, Annual Review of Fluid Dynamics **54**, 349 (2022).
[2] M. N. Gueye *et al.*, *Progress in understanding structure and transport properties of PEDOT-based materials: A critical review*, Progress in Materials Science **108**, 100616 (2020).
[3] M. Heil, A. Hazel, *oomph-lib - an object-oriented multi-physics finite-element library*, Lect. Notes Comput. Sci. Eng. **53**, 19-49 (2006).
[4] A. He *et al.*, *Tunable coffee-ring effect on a superhydrophobic surface*, Optics Letters **42**, 3936-3939 (2017).
[5] Y. Popov, *Evaporative deposition patterns: Spatial dimensions of the deposit*, Physical Review E, **71** 036313 (2005).
[6] C.N. Kaplan, L. Mahadevan, *Evaporation-driven ring and film deposition from colloidal droplets*, Journal of Fluid Mechanics **781**, R2 (2015).

Th165

ELECTRICALLY AND MAGNETICALLY DRIVEN INSTABILITIES AND MICROSCALE PATTERNS

Jaakko V. I. Timonen[1,2]
[1]*Department of Applied Physics, Aalto University, Espoo, Finland*
[2]*Center of Excellence in Life-Inspired Hybrid Materials, Aalto University, Espoo, Finland*

Keywords: Magnetic fields, electric fields, electrohydrodynamics, ferrofluids, magnetic colloids, oils

Abstract

Application of electric and magnetic fields on liquids and colloidal dispersions is known to lead to various forces, flows, instabilities and, under appropriate conditions, well-defined patterns. I'll start by briefly mentioning our recent efforts related to magnetically driven and controlled instabilities and patterns. This includes observation of the Rosensweig instability (normal-field instability) in a ferrofluidic aqueous two-phase system [1], analogous instability in an electrically driven and maintained gradient of magnetic nanoparticles [2], and magnetically controllable active turbulence in dense bacterial suspensions [3]. In the rest of the presentation, I focus on electrically driven instabilities and pattern formation in a system consisting of two immiscible oils, one conductive and one non-conductive, placed in a Hele-Shaw cell [4]. Therein a static and uniform electric field is capable of driving the oil-oil interface out of the thermodynamic equilibrium, resulting in major restructuring of the interface (Figure 1). The observed structures range from a simple corrugation pattern to rolling filaments, filament networks and bicontinuous lattices. In stronger electric fields, we observe detachment of polygonal, toroidal, and active droplets that form dilute gas-like states at low densities and complex active emulsions at higher densities. I try to rationalize the findings by using the basic theoretical framework of electrohydrodynamics, i.e. electric field driven generation of space charge at the oil-oil interface, leading to Coulomb force that drives the fluid flow.

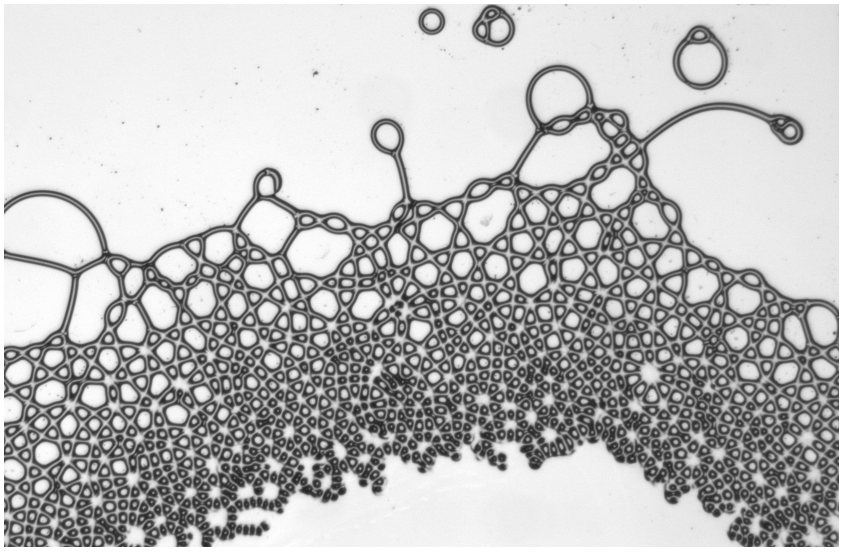

Figure 1. A snapshot of the highly dynamic interface between a conductive liquid (dodecane with docusate, top of the image) and an insulating liquid (perfluoropolyether, bottom of the image) when subjected to an out-of-plane electric field in a Hele-Shaw cell.

References

[1] C. Rigoni, G. Beaune, B. Harnist, F. Sohrabi, J. V. I. Timonen, *Ferrofluidic aqueous two-phase system with ultralow interfacial tension and micro-pattern formation*, Communications Materials **3**, 26 (2022).
[2] T. Cherian, F. Sohrabi, C. Rigoni, O. Ikkala, J. V. I. Timonen, *Electroferrofluids with nonequilibrium voltage-controlled magnetism, diffuse interfaces, and patterns*, Science Advances **7**, eabi8990 (2021).
[3] K. Beppu, J. V. I. Timonen, *Magnetic control of orientational order and intrinsic hydrodynamic instability in bacterial turbulence*, arXiv:2307.05951.
[4] G. Raju, N. Kyriakopoulos, J. V. I. Timonen, *Diversity of non-equilibrium patterns and emergence of activity in confined electrohydrodynamically driven liquids*, Science Advances **7**, eabh1642 (2021).

Th166

NUMERICAL SIMULATIONS OF IN-LINE SPHEROIDS SETTLING IN A LINEARLY STRATIFIED FLUID

Abdullah M. Abdal[1]*, Lyes Kahouadji[1], Seungwon Shin[2], Jalel Chergui[3], Damir Juric[3,4], Colm-Cille P. Caulfield[4] & Omar K. Matar[1]

[1]*Department of Chemical Engineering, Imperial College London, SW7 2AZ, London, United Kingdom*

[2]*Department of Mechanical and System Design Engineering, Hongik Univeristy, Republic of South Korea*

[3]*Université Paris Saclay, Center de la Recherche Scientifique (CNRS), LISN, Orsay, France*

[4]*Department of Applied Mathematics and Theoretical Physics, Centre for Mathematical Sciences, University of Cambridge, Wilberforce Road, Cambridge CB3 0WA, United Kingdom*

Abstract

This study investigates the transport of particles in density-stratified fluids, a prevalent natural phenomenon. In oceans, particles and marine snow descend through fluids with significant density variations due to salinity and temperature gradients. Such heterogeneity in the background fluid affects the settling or rising rates of particles, often leading to accumulation at transitional density layers. Previous research has primarily focused on spherical particles, examining their isolated motion, pairwise interactions, and collective transport in stratified fluids. This work, however, extends the investigation to the interaction between two spheroidal particles settling in-line in a linearly-stratified fluid. This study employs a hybrid front-tracking/level-set technique to perform particle-resolved numerical simulations in a 3D Cartesian domain. The spheroidal particles, released from rest and in-line, are immersed in a quiescent, linearly-stratified fluid within a $12D_p \times 12D_p \times 24D_p$ computational domain, where $D_p = 250$ μm is equivalent spherical particle diameter. The spheroids' shape is determined by their aspect ratio $(Ar = b/a)$; they are modeled using a fictitious domain method, with a no-slip condition on their surfaces. Governed by the Galilei, Froude, and Schmidt numbers, the work considers a particle density of 1141 kg/m^3 and the unperturbed background fluid density profile varies linearly with depth such that $\rho_f(z) = \rho_0 + \gamma z$ where $\mathrm{d}\rho/\mathrm{d}z = \gamma$ and z is the vertical component of the position vector. The Schmidt number is set at 700, representing a salinity-stratified fluid, and the particles are initially oriented perpendicular to the direction of gravity. The results showcase the effects of varying the stratification strength through the Froude number (Fr), varying the particles' aspect ratios (Ar), and varying the initial separation distance between the particles (S_0) on the interaction dynamics between the settling spheroids.

Keywords: Stratified flows, Particle-laden, Sedimentation

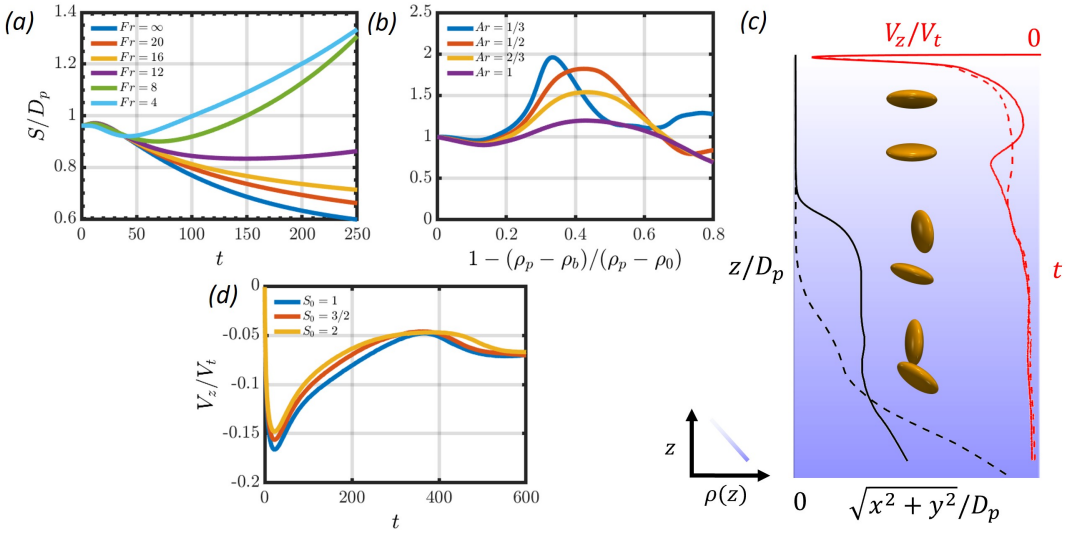

Figure 1. Panel (a) displays how the normalized distance between spheroids' center of mass (S) changes over time for various Froude numbers (Fr) and an aspect ratio (Ar) of 1/3. Panel (b) shows the evolution of S with $Fr = 4$ under different Ar values. Panel (c) is a diagram depicting the settling velocity and particle positions for $Ar = 1/3$ and $Fr = 4$, with solid and dashed lines representing trailing and leading particles, respectively. Panel (d) shows the average settling velocity of the two particles when varying the initial separation distance S_0 with $Ar = 1/3$ and $Fr = 8$.

* Corresponding author. E-mail: abdullah.abdal20@imperial.ac.uk

Th167

TEMPORAL EVOLUTION OF COHERENT STRUCTURES FORMED BY LOW-STOKES NUMBER PARTICLES IN A HIGH ASPECT RATIO LIQUID BRIDGE

Shin Noguchi[1] & Ichiro Ueno[2]

[1] *Division of Mechanical & Aerospace Engineering, School of Science &Technology, Tokyo University of Science, Chiba, Japan*

[2] *Department of Mechanical & Aerospace Engineering, Faculty of Science & Technology, Tokyo University of Science, Chiba, Japan*

Keywords: coherent structure, thermocapillary liquid bridge, low-Stokes number particles

Abstract Our research focal point is the behavior of low-stokes number particles one-dimensional coherent structures, so-called Particle Accumulation Structure (PAS) [1, 2], observed in time-dependent traveling wave type convection in high aspect ratio (Γ = height/radius > 1) thermocapillary liquid bridge (Fig. 1 (i)). In the convective field exhibiting an azimuthal wave number mHTW = 1, two distinct structures have been identified through experiments [3, 4, 5] and numerical simulation [6, 7]: PAS with a spiral structure, characterized by particles orbiting and rising in the central region of the liquid bridge, closed around the z-axis in two loops, and PAS without a spiral structure, which exhibits motion near the free surface of the liquid bridge, closed around the z-axis in one loop. Currently, among the structures predicted with high accuracy through numerical simulation for PAS without a spiral motion, many have yet to be observed experimentally. In this study, intentionally disrupting the convection field where PAS is forming, we tracked particle behavior from the steady flow until PAS was formed again. This allowed us to confirm the existence of a structure that was predicted only in numerical analysis [7] (Fig. 2 (i)) and was present only in the initial stages of PAS formation. Furthermore, we observed that these particles, over time, accumulate into a structure that has already been reported [5, 7] (Fig. 2 (ii)).

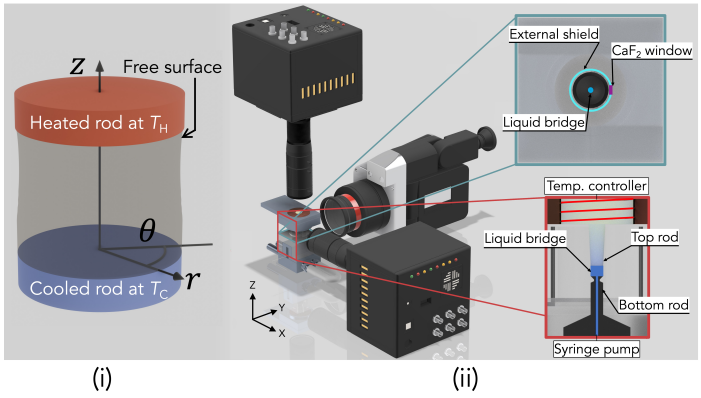

Figure 1. (i) Diagram of half-zone liquid bridge. (ii) Schematic of experimental apparatus.

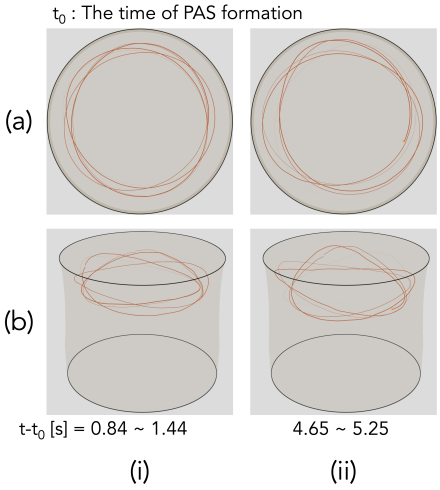

Figure 2. (a), (b) Time series of projected particle trajectories in the rotating frame of reference from the top view and bird view, respectively. Trajectories (i) in the initial stage and (ii) final stage of PAS formation.

References

[1] D. Schwabe, P. Hintz, S. Frank, *New features of thermocapillary convection in floating zones revealed by tracer particle accumulation structures (PAS)*, Microgravity Sci. Technol. **9**, 163–168 (1996).

[2] D. Schwabe, A. Mizev, M. Udhayasankar, S. Tanaka, *Formation of dynamic particle accumulation structures in oscillatory thermocapillary flow in liquid bridges*, Phys. Fluids **18**, (2007).

[3] T. Sakata, S. Terasaki, H. Saito, S. Fujimoto, I. Ueno, T. Yano, K. Nishino, Y. Kamotani, S. Matsumoto, *Coherent structures of $m = 1$ by low-Stokes-number particles suspended in a half-zone liquid bridge of high aspect ratio: Microgravity and terrestrial experiments*, Phys. Rev. Fluids **7**, 014005 (2022).

[4] S. Terasaki, S. Sensui, I. Ueno, *Thermocapillary-driven coherent structures by low-Stokes-number particles and their morphology in high-aspect-ratio liquid bridges*, Int. J. Heat Mass Transf. **203**, 123772 (2023).

[5] S. Noguchi, I. Ueno, *Spatial-temporal behaviors of low-Stokes-number particles forming coherent structures in high-aspect-ratio liquid bridges by thermocapillary effect*, Phys. Rev. Fluids **8**, 114002 (2023).

[6] P. Capobianchi, M. Lappa, *On the influence of gravity on particle accumulation structures in high aspect-ratio liquid bridges*, J. Fluid Mech. **908**, A29 (2021).

[7] I. Barmak, F. Romanò, H. Kuhlmann, *Finite-size coherent particle structures in high-Prandtl-number liquid bridges*, Phys. Rev. Fluids **6**, 084301 (2021).

Th168

COMPLEX MORPHOLOGY ON THE UNDERSIDE OF A LEIDENFROST-LEVITATED HYDROGEL SPHERE

Vicente Luis Diaz-Melian[1], Isaac Lenton[1], Jack Binysh[2], Anton Souslov[3] & Scott Waitukaitis[1]
[1]*Institute of Science and Technology Austria, Klosterneuburg, Austria*
[2] *Faculty of Science, Institute of Physics, University of Amsterdam, Amsterdam, Netherlands*
[3]*TCM Group, Cavendish Laboratory, Cambridge, United Kingdom.*

Abstract Leidenfrost effect, Hydrogels, High-speed interferometric.

When a liquid droplet approaches a hot surface, vaporization can become sufficient to cause the drop to levitate—this is the Leidenfrost effect [1]. Vaporizable soft solids, e.g., hydrogels, can also exhibit levitation [2] or, additionally, a sustained bouncing effect [2]. In case of floating liquids, vapor pressure and surface tension balance create an inversion of curvature on the droplet underbelly. Naively, one might expect that with a levitating soft solid, vapor pressure and elasticity should create a similar equilibrium with a similar curvature inversion. We use high-speed interferometric imaging [4] to measure the 2D height profile underneath a floating hydrogel sphere, and discover that the presence of such curvature inversion depends critically on the approach speed of and total duration in the levitation state. Poking the system from a variety of experimental angles, we find that this curious behavior is due to permanent morphological changes caused by mass loss during vaporization.

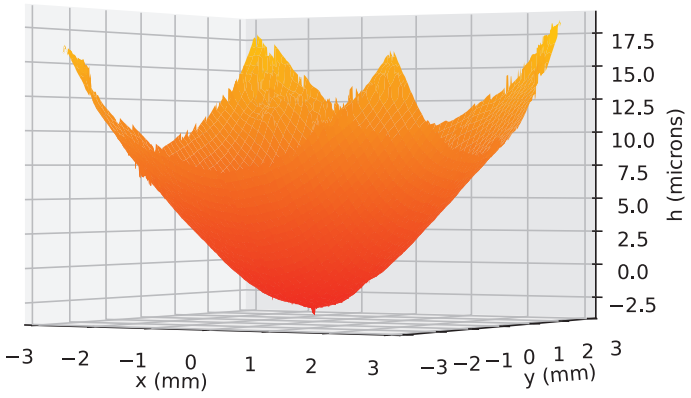

Figure 1. 3D height profile underneath a hydrogel sphere floating on its own vapor layer.

References

[1] A.L. Biance, C. Clanet, D. Quéré *Leidenfrost drops*, Physics of Fluids **15**, 1632-1637 (2003).
[2] S. Waitukaitis, K. Harth, M. van Hecke *From Bouncing to Floating: The Leidenfrost Effect with Hydrogel Spheres* , Phys. Rev. Lett. **121**, 048001 (2012)
[3] S. Waitukaitis, A. Zuiderwijk, A. Souslov, C. Coulais, and M. v. Hecke, *Coupling the Leidenfrost effect and elastic deformations to power sustained bouncing*, Nat. Phys. **13**, 1095–1099 (2017).
[4] J. C. Burton, A.L. Sharpe, R. C. A. v. d. Veen, A. Franco, and S. R. Nagel, *The Geometry of the Vapor Layer Under a Leidenfrost Drop*, Phys. Rev. Lett. **109**, 074301 (2012).

Th169

INSTABILITIES AND PATTERN TRANSITIONS IN CO-ROTATING SUSPENSION TAYLOR-COUETTE FLOW

Manojit Ghosh & Meheboob Alam
Engineering Mechanics Unit, Jawaharlal Nehru Centre For Advanced Scientific Research, Jakkur P.O., Bangalore 560064, India

Abstract Suspensions, Taylor-Couette flow, Instabilities

The Taylor-Couette flow (TCF) of Newtonian fluids exhibits a plethora of flow patterns in the co-rotation regime (i.e. the rotation ratio $\Omega = \omega_i/\omega_o > 0$, where ω_i and ω_o are the angular speed of the inner and outer cylinders, respectively) [1, 2]. Here, we report experimental results on pattern transitions in a neutrally buoyant, non-colloidal suspension confined between two independently rotating, concentric cylinders up to a particle volume fraction of $\phi = 0.3$, extending our recent work on the counter-rotation regime [3]. Our analyses reveal that the pattern transition in dilute suspensions ($\phi \leq 0.05$) is similar to what is known for a Newtonian fluid, i.e., the base state circular Couette flow (CCF) bifurcates into Taylor vortex flow (TVF) which then goes through successive transitions to produce higher-order states as the shear Reynolds number ($Re_s(\phi)$) increases [2]. With increasing particle loading, for $0.1 \leq \phi \leq 0.2$, we find the emergence of non-axisymmetric flow states, namely, the ribbon (RIB) and/or spiral vortex flow (SVF) between CCF and TVF as reported in suspension TCF with a stationary outer cylinder ($\Omega = 0$) [4, 5] and counter-rotating cylinders ($\Omega < 0$) [3]. At a higher particle loading ($\phi = 0.3$), the primary bifurcating state SVF is sustained over a larger range of $Re_s(\phi)$, and for $\Omega \geq 0.1$, only CCF $\leftrightarrow$ SVF transition takes place in the considered range of $Re_s(\phi)$. For $\phi \leq 0.2$, the pattern transitions are found to be hysteretic at all Ω, but the degree of hysteresis decreases with increasing Ω; at $\phi = 0.3$, however, the pattern transition is non-hysteretic for $\Omega \geq 0.5$ and hysteretic for $\Omega \leq 0.3$. It is found that the critical shear Reynolds number for primary bifurcation $Re_s^{c1}(\phi)$ decreases with increasing ϕ and Ω. At $\Omega = 0.05$, the wavy Taylor vortices (WTV), characterized by a single dominant frequency, appear as the bifurcating state of TVF. The effect of particle loading on wavy vortices is found to decrease their normalized propagation frequencies; on the other hand, the normalized rotation frequency of spiral vortices at $\phi = 0.3$ is found to increase with increasing Ω.

References

[1] D. Coles, *Transition in circular Couette flow*, Journal of Fluid Mechanics **21**, 385–425 (1965).
[2] C. D. Andereck, S. S. Liu, & H. L. Swinney, *Flow regimes in a circular Couette system with independently rotating cylinders*, Journal of Fluid Mechanics **164**, 155–183 (1986).
[3] S. P. Singh, M. Ghosh, & M. Alam, *Counter-rotating suspension Taylor–Couette flow: pattern transition, flow multiplicity and the spectral evolution*, Journal of Fluid Mechanics **944**, A18 (2022).
[4] M. V. Majji, S. Banerjee, & J. F. Morris, *Inertial flow transitions of a suspension in Taylor–Couette geometry*, Journal of Fluid Mechanics **835**, 936–969 (2018).
[5] P. Ramesh, S. Bharadwaj, & M. Alam, *Suspension Taylor–Couette flow: co-existence of stationary and travelling waves and the characteristics of Taylor vortices and spirals*, Journal of Fluid Mechanics **870**, 901–940 (2019).

Th170

Chaotic Behaviour of Multiple Immersed Ellipsoids

Andrew Boyd[1,2], Prashant Valluri[1], David Scott[2], Mark Sawyer[2] & Rama Govindarajan[3]
[1]*Institute of Multiscale Thermofluids, School of Engineering, Edinburgh University*
[2]*Edinburgh Parallel Computing Centre,*
[3]*International Centre for Theoretical Sciences, Bangalore, India.*

Keywords:

Abstract

Building on previous work [1] exploring the complex dynamics of a single immersed ellipsoid, we investigate the dynamics of multiple immersed ellipsoids under both inviscid and viscous environments. Earlier, using our in-house fully-coupled 6DoF solid-fluid DNS solver, GISS [2], we showed that a single body can present chaotic motions even under viscous environments under certain conditions due to vortex shedding. Here, we extend Kirchoff's equations to multiple bodies under inviscid conditions, using Lamb (1932) as a starting point. Analytical solutions for added mass and inertia are no longer available for multiple bodies, and so we solve for the potential flow using boundary integral equations (BIE), and resolve for the forces on the bodies by interpolating over the body and integrating. Calculations are carried out in Rust and are parallelised with a high degree of efficiency. Rotational motion is represented using quaternions. Using recurrence quantification and cross-correlation analyses [3], we will present how we can characterise chaos and how the number of solids affects chaos. Results are compared to DNS simulations run on Xcompact3D[4].

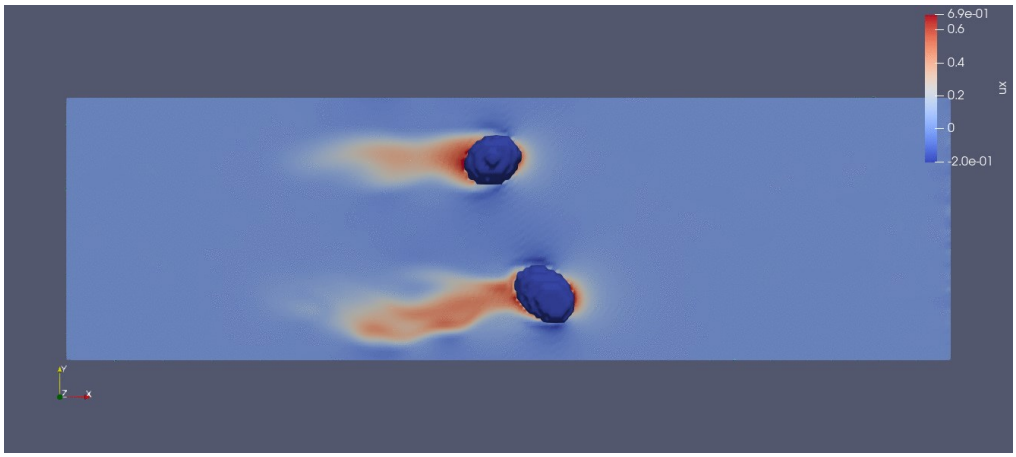

Figure 1. Two ellipsoids in initially stationary flow.

References

[1] Essmann E, Shui P, Popinet S, Zaleski S, Valluri P, Govindarajan R. Chaotic orbits of tumbling ellipsoids. *Journal of Fluid Mechanics*. 2020;903:A10.
[2] E. Essmann et al 2020, https://github.com/eessmann/GISS
[3] N. Marwan et al, Recurrence plots for the analysis of complex systems, *Physics Reports*, **438**, 2007, pages 237-329
[4] https://www.incompact3d.com/

Th171

PARTICLE DEPOSITION FROM A SESSILE DROPLET EVAPORATING ACCORDING TO THE ONE-SIDED MODEL

Henry T. Sharp, Stephen K. Wilson, Alexander W. Wray
Department of Mathematics and Statistics
University of Strathclyde, Livingstone Tower
26 Richmond Street, Glasgow G1 1XH, United Kingdom

Keywords: evaporation, droplet, deposition, non-equilibrium.

Understanding the deposits left behind by evaporating particle-laden sessile droplets and what causes particular deposition patterns to occur is a topic of significant interest due to the applications that rely on particular deposition morphologies. For example, Devineau *et al.* [1] showed that the deposition pattern left by haemoglobin-laden polystyrene droplets can be used to detect mutations responsible for sickle cell anaemia, and Bigdeli & Tsai [2] demonstrated how ring-like deposits from silica-laden water droplets can be used to manufacture photonic crystals. In the case of an evaporating sessile droplet where the surrounding atmosphere is composed entirely of vapour, or where vapour moves very quickly away from the surface of the droplet, the liquid and gas phases can be decoupled, and the influence of the vapour can be neglected when examining the dynamics of the liquid phase [3]. The resulting divergence from thermodynamic equilibrium is what drives evaporation and leads to the so-called “one-sided" model of evaporation [4]. For a pinned evaporating sessile droplet undergoing one-sided evaporation, diverging further from thermodynamic equilibrium leads to less uniform evaporation across the surface of the droplet with the evaporative mass flux increasing as the surface of the droplet steepens. The evaporative mass flux also increases as the height of the droplet decreases. Figure 1 shows that non-uniform evaporation drives capillary flow from the centre of the droplet towards its edge. The effect of the degree of non-equilibrium on the deposition morphology is analysed by considering both asymptotic and numerical solutions to the advection-diffusion equation governing the concentration of suspended particles. In particular, how particles move towards the contact line of the droplet as it evaporates to form a so-called “coffee-ring" deposit [5] will be analysed.

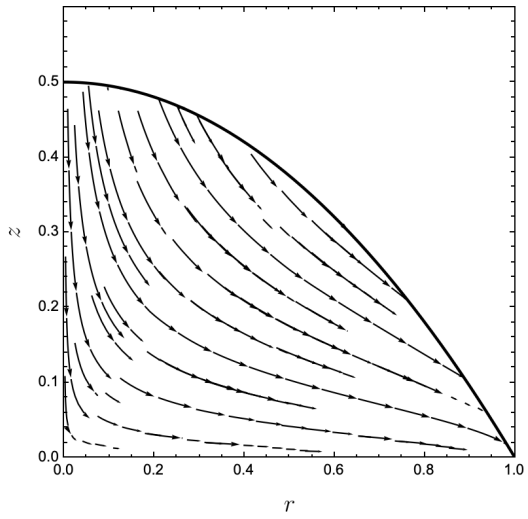

Figure 1. Plot of streamlines representing fluid flow within an axisymmetric sessile droplet undergoing one-sided evaporation.

References

[1] S. Devineau, M. Anyfantakis, L. Marichal, L. Kiger, M. Morel, S. Rudiuk, D. Baigl, *Protein Adsorption and Reorganization on Nanoparticles Probed by the Coffee-Ring Effect: Application to Single Point Mutation Detection*, J. Am. Chem. Soc. **138(26)**, 11623–11632 (2016).
[2] M. B. Bigdeli, P. A. Tsai, *Making Photonic Crystals via Evaporation of Nanoparticle-Laden Droplets on Superhydrophobic Microstructures*, Langmuir **36(17)**, 4835–4841 (2020).
[3] N. Murisic, L. Kondic, *On Evaporation of Sessile Drops with Moving Contact Lines*, J. Fluid Mech. **679**, 219-246 (2011).
[4] M. Knudsen, *Die maximale Verdampfungsgeschwindigkeit des Quecksilbers*, Ann. Phys. **352(13)**, 697–708 (1915).
[5] R. D. Deegan, O. Bakajin, T. F. Dupont, G. Huber, S. R. Nagel, T. A. Witten, *Capillary Flow as the Cause of Ring Stains from Dried Liquid Drops*, Nature **389**, 827–829 (1997).

Th184

Intermittent turbulence in a Rayleigh-Bénard convection problem

January 19, 2024

Darío Martínez Martínez[1], Henar Herrero Sanz[1] & Francisco Pla Martos[1]
[1]Department of Mathematics, University of Castilla-La Mancha, Ciudad Real, Spain

Keywords: Intermittent turbulence, Rayleigh-Bénard convection, spectral method, domain decomposition

Abstract The evolution from a laminar flow to a complete turbulent regime is not sudden. These two regimes keep alternating for Rayleigh numbers between $\mathcal{O}(10^5)$ and $\mathcal{O}(10^6)$. This phenomenon is called intermittent turbulence. It implies that not only turbulent regimes appear from laminar flows, but also laminar regimes can be generated from turbulence. Our goal is to study the intermittent turbulence for a Rayleigh-Bénard convection problem. Starting from a stationary flow with 3 rolls, the evolution of the solutions is calculated for Rayleigh numbers between $2.5 \cdot 10^5$ and $1.8 \cdot 10^6$. On this data, different parameters and statistical measures, as the energy or Nusselt number, are analysed to give a better understanding of what is happening and what characterizes each behaviour. All the solutions have been calculated using a Legendre collocation method with a Schwarz domain decomposition method, as shown in [1] and [2].

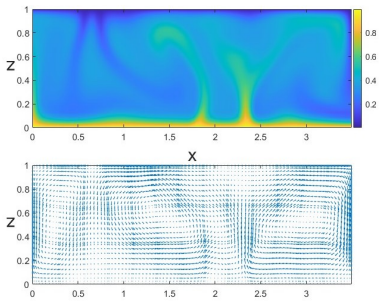

(a) $Ra = 2.6 \cdot 10^5$

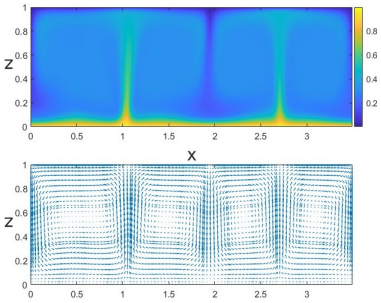

(b) $Ra = 3.8 \cdot 10^5$

References

[1] Martínez, D.; Herrero, H.; and Pla, F. *2D Newton Schwarz Legendre Collocation Method for a Convection Problem*, Mathematics, 10(19), 3718 (2022).

[2] Martínez, D.; Herrero, H.; and Pla, F. *A Schwarz alternating method for an evolution convection problem*, Applied Numerical Mathematics (2023).

Th185

WELL-POSEDNESS AND STABILITY OF SLIGHTLY COMPRESSIBLE BOUSSINESQ'S FLOW IN DARCY–BÉNARD PROBLEM

Giuseppe Arnone[1] & Florinda Capone[1]
[1]*Department of Mathematics and Applications "Renato Caccioppoli", University of Naples "Federico II", Naples, Italy*

Keywords: Porous media, Boussinesq approximation, Well-posedness, Compressibility factor

Abstract

Thermal convection phenomena in Newtonian fluid-saturated horizontal porous layers heated from below, are in essence physically motivated by buoyant force induced from density variations due to the presence of a thermal gradient across the layer. Indeed, in non-isothermal processes variations in temperature generate variations in the fluid's properties. In particular, concerning the fluid density, an analysis including the full effect of this variation is so complicated that some approximations become essential. The vast majority of the studies concerning the stability of basic steady state motions, in clear fluids as well as in fluid-saturated porous media, are addressed under a celebrated hypothesis, known as the Boussinesq, or Oberbeck-Boussinesq (OB) approximation. However, in [1] Müller proved that as long as one assume as incompressible a medium whose constitutive equations do not depend on pressure p but only on temperature T, then only a *constant density function* wouldn't be in contradiction with the Gibbs law. This conclusion is in disagreement with empirical observations, according to which fluids expand when heated, and the theoretical assumptions such as the OB approximation. For this reason the above conclusion was called *Müller paradox*. In order to fix this contradiction, a less restrictive model of incompressibility was proposed by Gouin and Ruggeri [2]. In particular, enforcing essential thermodynamic conditions, namely entropy principle and thermodynamic stability, the class of *extended-quasi-thermal-incompressible fluids* (EQTI) was introduced. For this class of fluids, the following constitutive law for the fluid density ρ is considered:

$$\rho(p,T) = \rho_0[1 - \alpha(T - T_0) + \beta(p - p_0)], \tag{1}$$

where ρ_0 is the reference density in correspondence of a temperature T_0 and pressure p_0, α is the thermal expansion coefficient and β is the compressibility factor.
The objective of the present talk is to show the well-posedness of the mathematical model describing the flow of a EQTI fluid saturating a Darcy porous medium described by the following system

$$\begin{cases} \dfrac{\mu}{K}\mathbf{v} = -\nabla p - \rho_0[1 - \alpha(T - T_0) + \beta(p - p_0)]g\mathbf{k}, \\ \nabla \cdot \mathbf{v} = 0, \\ \rho c_V \left(\dfrac{\partial T}{\partial t} + \mathbf{v} \cdot \nabla T\right) = \chi \Delta T, \end{cases} \tag{2}$$

to which we associated the following isothermal boundary conditions:

$$\begin{aligned} T &= T_L \quad \text{on } z = 0, \\ T &= T_U \quad \text{on } z = d. \end{aligned} \tag{3}$$

References

[1] I. Müller, *Thermodynamics*, Pitman-London, (1985).
[2] H. Gouin, T. Ruggeri, *A consistent thermodynamical model of incompressible media as limit case of quasi-thermal-incompressible materials*,International Journal of Non-Linear Mechanics **47**(6), 688-693 (2012).
[3] G. Arnone, F. Capone, *Existence and uniqueness of slightly compressible Boussinesq's flow in Darcy-Bénard problem*, Preprint ArXiv (2023).

Th186

STABILITY OF PENETRATIVE CONVECTIVE CURRENTS IN LOCAL THERMAL NONEQUILIBRIUM

G. Arnone[1], F. Capone[1] & J. A. Gianfrani[2]
[1]*Department of Mathematics, University of Naples Federico II, Naples, Italy*
[2]*Research Centre for Fluid and Complex Systems, Coventry University, Coventry, United Kingdom*

Abstract Porous media, Penetrative convection, Local thermal nonequilibrium, Stability analysis

The onset of penetrative convection in a layer of water subject to an upward gradient of temperature is a well-known phenomenon due to a density inversion occurring in water density profile for temperatures close to $4\ ^\circ C$. To be precise, for temperature values in the interval $[0, 4]\,^\circ C$, water density exhibits an increasing trend. The opposite happens for temperatures greater than $4\ ^\circ C$ (see Figure 1). This anomalous behaviour was modeled for the first time by Veronis in 1963 [1]. He proposed the following constitutive law for the density ρ_f

$$\rho_f(T^f) = \rho_0 \left[1 - \alpha(T^f - T_0)^2\right], \tag{1}$$

where $T_0 = 4\ ^\circ C$ is the reference temperature, ρ_0 the corresponding reference fluid density and α is the thermal expansion coefficient. As shown in Figure 1, this constitutive law matches the experimental data in the interval of interest.

So far in literature the problem of penetrative convection in porous media has been modeled under the hypothesis of local thermal equilibrium (LTE), by defining a single temperature for both fluid and solid phases. Moreover, the single temperature equation is obtained upon defining a weighted mean thermal conductivity as $k = (1 - \varepsilon)k_s + \varepsilon k_f$. In this respect, the LTE condition may be inadequate in those physical frameworks where either fluid and solid thermal conductivities are very different or the portion of pores is much larger than the solid one. Therefore, a local thermal nonequilibrium (LTNE) assumption needs to be introduced in these frameworks. In such a way, heat exchanges between the two phases are modeled with the employment of two temperature equations.

In this talk we are going to investigate the onset of penetrative convection in a Darcy-Brinkman porous medium in the LTNE regime [2]. We prove the absence of oscillatory motions at the onset of instability, and analyse the interplay between a nonzero heat transfer coefficient (defined in the LTNE regime) and the upper boundary temperature (characterising the onset of penetrative convection). Linear and nonlinear stability analyses of the basic state are performed with the aid of rigorous analytical techniques and numerical schemes. The differential eigenvalue problems arising from these analyses are solved via implementation of numerical methods, such as the Chebyshev-τ method, the shooting method with a Newton routine and the golden search method, to determine stability/instability thresholds.

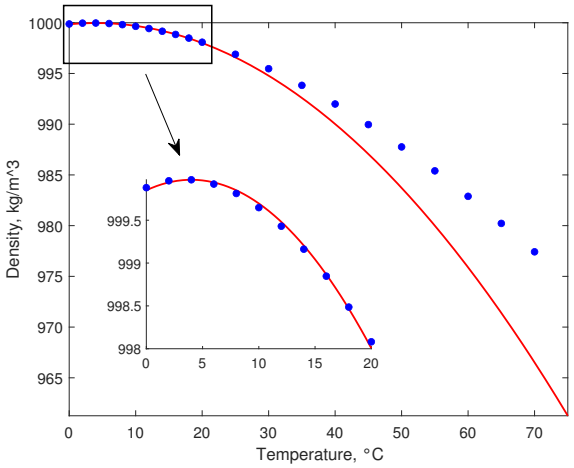

Figure 1. Comparison between experimental values of the water density under isobaric condition and the Veronis' constitutive law (1) where $\alpha = 7.68 \times 10^{-6}\ ^\circ C^{-2}$ and $T_0 = 4^\circ C$.

References

[1] G. Veronis *Penetrative Convection*, Astrophysical Journal **137**, 641–663 (1963).
[2] G. Arnone, F. Capone, J.A. Gianfrani *Stability of penetrative convective currents in local thermal nonequilibrium*, (Submitted) (2024).

Th187

ANALYSIS OF LIFT COEFFICIENT AND TRAILING VORTICES PROPERTIES AT LOW REYNOLDS NUMBER WITH SPANWISE DEFORMATION

Pedro Solis[1], Manuel Garrido-Martin[1], Eduardo Duran[1], Paloma Gutierrez-Castillo & Carlos del Pino[1]
[1]*Fluid Mechanics, University of Málaga, Institute for Mechatronics Engineering & Cyber-Physical Systems (IMECH.UMA), Málaga, Spain*

Abstract We have experimentally studied the effects of spanwise wing deformation on the lift coefficient and wingtip vortices (wingtip vortex, lift coefficient, PIV2D, wing model deformation).

Wing aerodynamic loads lead to significant spanwise deformations at low Reynolds number regimes where Micro air vehicles (MAVs) and unmanned aerial vehicles (UAVs) operate. The flow behaviour at this regime is particularly complex, and it is influenced strongly by a laminar separation bubble (LSB) formed in the suction side of the wing profiles. Thus, any subtle variation of experimental conditions or wing geometry affects wing forces and flow structures.

We have measured the hydrodynamic forces and velocity fields of the trailing vortices generated by three different wing models in a towing water tank at several angles of attack before reaching the stall. We performed all the experiments at a constant chord-based Reynolds number, $Re = 20 \times 10^3$. The models are NACA 0012 rigid wings with semi-aspect (semi-span length to chord) ratio $sAR = 2$ and have an imposed spanwise deformation replicating the experimental data reported by [1]. Specifically, one model is non-deformed (ND), and the other two have a maximum tip deflection of $\delta = 2\%$ (intermediate deformation, ID) and $\delta = 4.5\%$ (large deformation, LD). Our results elucidate that for the smaller angles of attack (e.g. $\alpha = 4°$), spanwise deformation decreases the lift generated by the models, but at higher angles (e.g. $\alpha = 8°$ or $9°$) the deformation increases the lift, see the comparison between ND and LD in Fig. 1.

We also used two-dimensional particle image velocimetry (PIV2D) in a plane perpendicular to the free-stream direction to obtain velocity fields of trailing vortices at different axial distances. The parameters of the theoretical models of Batchelor [2] and Moore & Saffman [3] were computed and used to corroborate that we did not find any variation of the vortex structure with the wingspan deformation. Furthermore, we employed an empirical formula recently proposed by [4] to relate the lift measurements with the circulation of the trailing vortices, computed from PIV measurements, observing a direct relationship between the two.

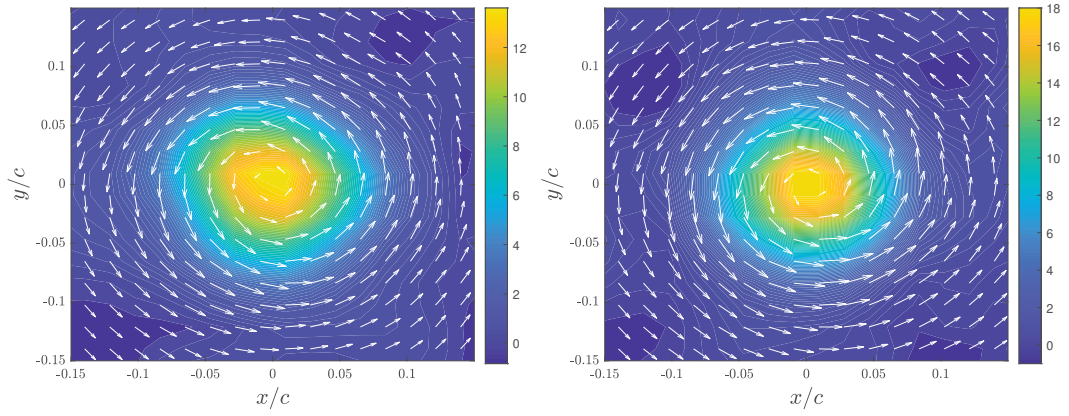

Figure 1. Velocity and vorticity fields around the vortex core at z/c =3, $\alpha = 9°$, and δ = 0% (ND, left) and 4.5% (LD, right) for $Re = 20 \times 10^3$.

References

[1] Farnsworth, J. A., Corbett, S., Seidel, J., and McLaughlin, Thomas E. *Aeroelastic Response of a Finite Span NACA 0018 Wing Part 1: Experimental Measurements*, 53rd AIAA Aerospace Sciences Meeting, 0249 (2015).
[2] Batchelor, G. *Axial flow in trailing line vortices*, Journal of Fluid Mechanics **20(4)**, 645–658 (1964).
[3] Moore, D. W. and Saffman, P. G. *Axial flow in laminar trailing vortices*, Proceedings of the Royal Society of London. A. Mathematical and Physical Sciences **333(1595)**, 491–508 (1973).
[4] Xu, M., Cheng, H., Ji, B., & Peng, X. *Prediction method of tip vortex circulation based on hydrofoil load*, Ocean Engineering **288**, 116176 (2023).

Th188

COMPUTATION OF BIFURCATION DIAGRAMS IN 3D RAYLEIGH-BÉNARD CONFIGURATIONS INVOLVING BINGHAM FLUIDS

Marc Médale[1], Mohamed Keddar[2] & Belkacem Draoui[2]
[1]*Aix Marseille University, CNRS, IUSTI, Marseille, France.*
[2]*UniversityTahriMohammed, Bechar, Algeria.*

Abstract This communication aims at presenting the methodology and related computations done to draw bifurcation diagrams in 3D Rayleigh-Bénard configurations where the working fluid obeys the Bingham model along with the Boussinesq?s approximation. First of all, a continuation method based on the Asymptotic Numerical Method enables to compute branches of steady-state solutions in the parameter space defined by Rayleigh and Bingham numbers. Then, linear stability analyses of the previously computed steady-state solutions is performed. The nature of bifurcation at the onset of convection switches from a pitchfork bifurcation with a Newtonian fluid to a subcritical one for Bingham fluid.

The Rayleigh-Bénard problem (liquid layer heated from below and cooled from above) has been extensively studied with Newtonian fluids. Whatever been the shape of the container and its size (confining aspect ratios), it possesses several specific features: i) a threshold of convection, that corresponds to a critical temperature difference over the liquid depth for the onset of convection that depends on geometrical parameters (shape and size of the container) ; ii) the nature of the bifurcation at threshold is a pitchfork bifurcation; iii) above the threshold of convection, the fluid flow pattern depends on geometrical parameters (shape and size of the container), Rayleigh and Prandtl numbers.

On the other hand when dealing with non-Newtonian fluids, the picture is much less canonical and therefore much less well-known. In particular, two of the key questions to be answered are: i) how does the nature of the bifurcation at onset of convection evolves from Newtonian to non-Newtonian rheology? ii) How far from the onset do the secondary bifurcations arise for a given container geometry? In the present study we address the questions for a visco-plastic (Yield stress) fluid that obeys the Bingham model and contained a parallelepiped box. From a computational point of view, the Bingham model leads to a singular solution once the strain rate gets close to zero. Several regularization techniques can be implemented to mitigate the numerical issue, but the question is how does the chosen numerical trick affect the solution at threshold.

To reach the desired goal, we have developed complementary numerical tools. The first one implements a steady-state continu s along the cor s linear stabilit solved by PE ram in a paral eys the Bingha ation at the ons

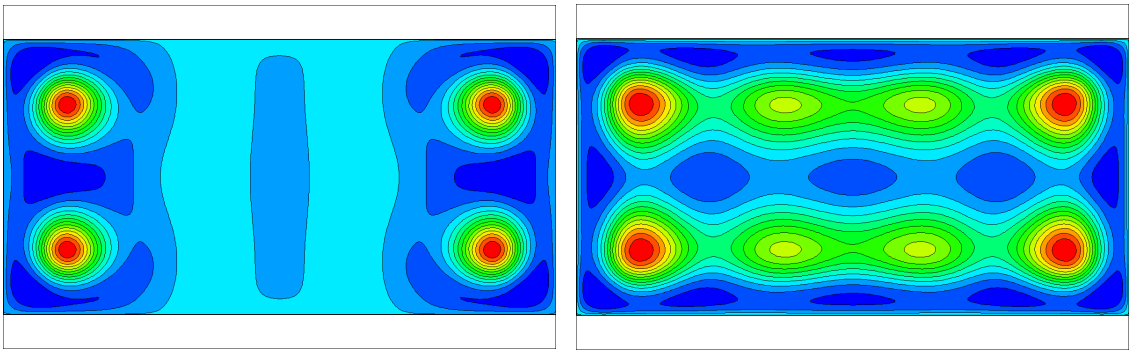

1st bifurcation mode: Ra_{c1}=2671.6 2nd bifurcation mode: Ra_{c2}=3139.1

Figure 1: Bifurcation modes in Rayleigh-Bénard convection inside a parallelepiped box ($\Gamma_w = 4$, $\Gamma_L = 10$), filled with a Bingham fluid ($Bn = 1$ and $Pr = 9$).

16

References

[1] Balay, S. et al. : PETSc users manual. Technical Report ANL-95/11 - Revision 3.20, Argonne National Laboratory, 2023.

Th189

Thermal convection due to internal heating in liquid metal battery

Anupam M. HIREMATH[1], Innocent MUTABAZI[1] & Harunori N. YOSHIKAWA[2]
[1]*Normandie Université, UNIHAVRE, LOMC UMR CNRS 6294, Le Havre, France*
[2]*Université de Côte d'Azur, INPHYNI UMR CNRS 7010, Nice, France.*

Keywords: Internal heating, Thermal convection, Liquid metal batteries

Abstract

The decarbonisation of the energy production has surged development of technics capable of harnessing the renewable energy from sources such as wind, solar, tidal etc., which are fluctuating in time. The integration of produced renewable energy into the global electrical grid distribution requires reliable storage solutions. Liquid metal batteries (LMB) represent one of the promising storage solutions especially for stationary applications [1,2].
A LMB is a 3-layer system of superimposed liquids in stable density stratification. The top and bottom electrodes are made of liquid metals that sandwich a molten salt with relatively lower thermal and electrical conductivity. An electrical current applied across the LMB leads to different multi-physical phenomena such as electro-vortex flow, Tayler instability, internal heating induced thermal convection, thermocapillary convection and etc., Intense research work on these different phenomena in LMB have been engaged recently by different teams [2]. The present work is focused on thermal convection in LMB due to internal heating in the electrolyte arising due to its low thermal and electrical conductivities. We analyse the generation of convective flows in the LMB for two different situations (a) iso-thermal boundary condition when the boundaries of LMB are the same as its environment and (b) Fourier-Robin boundary condition when there is a heat exchange between the battery and its environment.

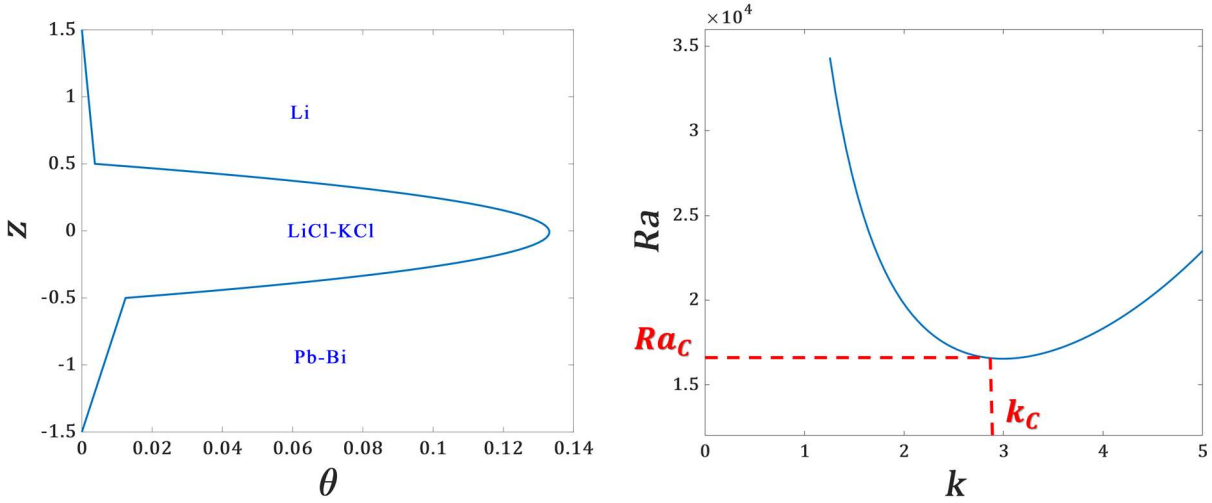

(a) (b)

Figure 1. (a) Temperature profile in the conduction state (b) marginal stability curve for the battery where all the 3 layers have the same thickness ratio [3].

The base state of LMB is conduction state in which the temperature profile is linear in the electrodes and quadratic in the electrolyte. Linear stability analysis has been performed for rectangular shape LMBs to determine the critical parameters for triggering of thermal convection depending on the layer thicknesses and the interface tensions between the electrodes and the electrolyte. The effect of an externally applied magnetic field on the thermal convection in the LMB is analysed both for iso-thermal and Fourier-Robin boundary conditions.

References

[1] S. Wu, X. Zhang, R. Wang & T. Li, *Progress and perspectives of liquid metal batteries*, Energy Storage Materials **57:205-227**, (2023).
[2] D. H. Kelly and T. Weier, *Fluid mechanics of liquid metal batteries*, Applied Mechanics Reviews, **70(2):020801**, (2018).
[3] T. Köllner, T. Boeck and J. Schumacher, *Thermal Rayleigh-Marangoni convection in a three-layer liquid-metal-battery model*, Physical Review E, **95(5):053114**, (2017).

Th190

THE DRY SALT LAKE INSTABILITY

Cédric Beaume[1], Matthew Threadgold[1] & Lucas Goehring[2]
[1]*School of Mathematics, University of Leeds, United Kingdom*
[2]*School of Science and Technology, Nottingham Trent University, United Kingdom*

Abstract We present the fluid instability supporting the formation of salt polygons on the crust of dry salt lakes (porous media convection, dry salt lake, polygons).

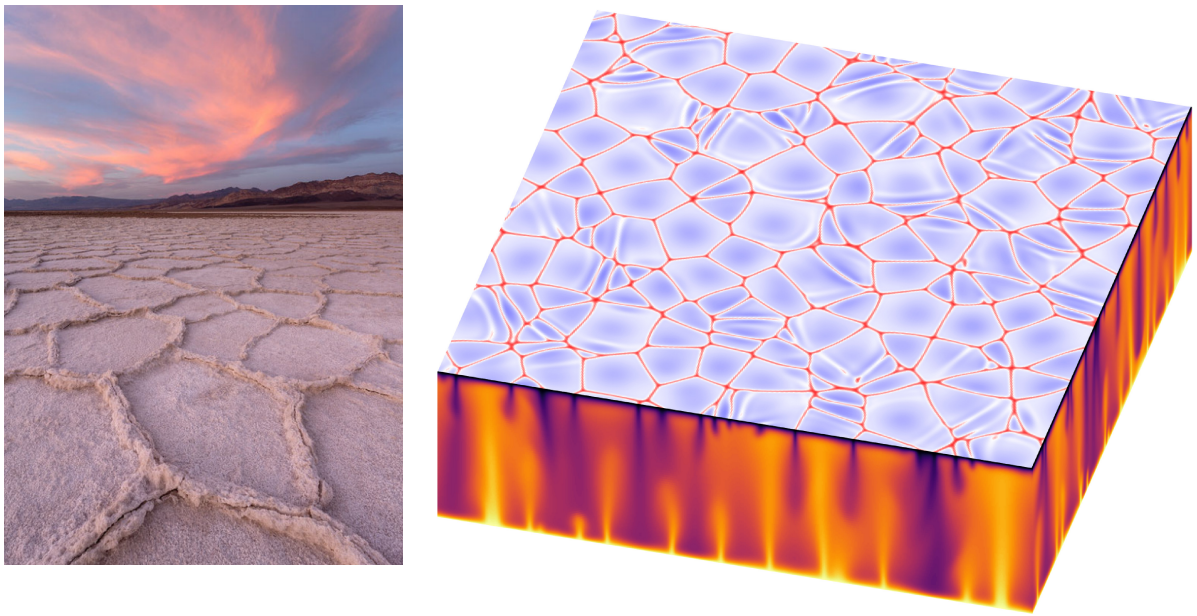

Figure 1. Left: Photograph of the salt crust at Middle Basin in Death Valley [1] (courtesy of Sara Marino). Right: Numerical simulation of the fluid dynamics inside a dry salt lake showing the salinity on the side faces (the darker, the higher) and the vertical salinity flux on the top surface (red: upward to the crust; blue: downward into the lake).

Dry salt lakes are spectacular geological landscapes that occur in arid environments. The strong evaporation and limited rainfall characteristic of these environments (but also, in certain cases, human intervention!) may progressively deplete existing lakes from their water, resulting in the formation of "lakes" whose surface appears dry. Below this dry surface, however, the water table is generally not very deep and evaporation remains a driving mechanism for groundwater flow. The dissolved minerals, or salts, present in the depths of the lake are carried upward by the resulting flow and precipitate to form a salt crust at the surface. Salt lake crusts are known to produce polygonal patterns that typically span 1m and are delimited by salt ridges reaching up to 10cm (see Figure 1, left panel). Remarkably, these patterns present little variation with the location or salt lake considered. Understanding the formation of crust patterns on dry salt lakes is a fascinating problem in itself but it is also key to understand the potential of salt lakes for dust emission and for its control. In this talk, we present a new model for the fluid dynamics that takes place below the surface of dry salt lakes. The lake is modelled using a three-dimensional porous medium subject to a uniform through-flow due to evaporation and forced by the buoyancy generated by the presence of salt: the salt crust at the surface yields a more concentrated, hence denser, fluid in its vicinity. This configuration possesses a simple, spatially homogeneous solution, which is unstable at sufficiently large values of the Rayleigh number, the only parameter in the system. We study the resulting instability numerically and identify the emergence of polygonal patterns in the fluid flow at the surface of the lake [1]. These patterns show great agreement with the crust patterns observed in situ [2] (see Figure 1, right panel).

References

[1] J. Lasser, J. M. Nield, N. Ernst, V. Karius, G. F. S. Wiggs, M. R. Threadgold, C. Beaume, L. Goehring, *Salt Polygons and Porous Media Convection*, Phys. Rev. X **13**, 011025 (2023).
[2] M. R. Threadgold, C. Beaume, S. M. Tobias, L. Goehring, *preprint* (2024).

Th191

ANISOTROPY EFFECT ON THE THERMAL INSTABILITY FOR A POROUS CHANNEL WITH SYMMETRIC WALL HEAT FLUXES

Michele Celli[1], Antonio Barletta[1], Pedro V. Brãndao[1], Stefano Lazzari[2] & Emanuele Ghedini[1]
[1] *Department of Industrial Engineering, Alma Mater Studiorum Università di Bologna, Viale Risorgimento 2, 40136 Bologna, Italy*
[2]*Department of Architecture and Design, University of Genoa, Stradone S. Agostino 37, 16123 Genoa, Italy*

Abstract Linear stability; Porous media; Anisotropy; Thermal convection; Symmetric wall heat fluxes.

The onset of thermal instability in fluid saturated porous layers is the subject of a wide research activity. For this topic, the pioneering papers are those by Horton and Rogers [1] and by Lapwood [2]. They studied the now well–known Horton, Rogers and Lapwood (HRL) or Darcy–Bénard problem: they found the threshold values of the governing parameters for the onset of thermal convection for a porous layer heated from below (the porous medium counterpart of the classical Rayleigh–Bénard problem). For the HRL problem, the basic stationary state whose stability is investigated is still with a purely vertical temperature gradient, as for the Rayleigh–Bénard problem. The governing parameter defining the stability threshold is a modified Rayleigh number based on the permeability of the porous medium (Darcy–Rayleigh number). Prats [3] developed the HRL problem by including a basic horizontal throughflow and found that the net mass flow rate does not influence the threshold value of the Darcy–Rayleigh number for the onset of thermal convection.
For the HRL problem, when symmetric wall heat fluxes are considered, a rest basic stationary state does not exist anymore and a net mass flow rate must be considered to ensure the closure of the energy balance under steady conditions. Together with a prescribed horizontal pressure gradient, the symmetric wall heat flux boundary conditions yield a temperature gradient with both a vertical and a horizontal component. The stability of this configuration has been investigated by Barletta [4]. The latter contribution considered an isotropic porous layer *i.e.* a solid matrix with the same value of permeability in every direction. In the recent years, on the other hand, the rapidly developing area of additive manufacturing techniques allowed the researcher to produce anisotropic porous layers.
The present work aims to investigate how the anisotropy in the porous structure may influence the onset of thermal instability for a porous channel with symmetric wall heat fluxes. For this goal, two different values of the permeability are considered: one holds in the vertical direction and the other one in the horizontal directions. The linear stability of this system is investigated by solving the eigenvalue problem obtained by using the normal modes method. In order to simplify the mathematical procedure, the disturbances are arbitrarily inclined to the direction of the horizontal through flow. This approach allows one to simplify the fully three dimensional problem to a two dimensional problem involving a parameter (*i.e.* the inclination angle). Since the stability problem is two dimensional, a streamfunction–temperature formulation is employed. Both the neutral stability curves and the critical values of the Darcy–Rayleigh number are computed as functions of the inclination angle, of the Péclet number (measuring the strength of the horizontal flow rate) and of the dimensionless parameter describing the anisotropy. The shape of the convective cells arising is also presented.

References

[1] C.W. Horton, F.T. Rogers, *Convection currents in a porous medium*, Journal of Applied Physics **16**, 367–370 (1945).
[2] E.R. Lapwood, *Convection of a fluid in a porous medium*, Mathematical proceedings of the Cambridge philosophical society **44**, 508–521 (1948).
[3] M. Prats, *The effect of horizontal fluid flow on thermally induced convection currents in porous mediums*, Journal of Geophysical Research **71**, 4835–4838 (1966).
[4] A. Barletta, *Thermal instability in a horizontal porous channel with horizontal through flow and symmetric wall heat fluxes*, Transport in Porous Media **92**, 419–437 (2012).

Th192

THE EFFECT OF A NON-UNIFORM HEATING ON THE AXISYMMETRIC RAYLEIGH-BÉNARD INSTABILITY

Dilara Özev[1], François Gallaire[2] & Luca Biancofiore[1,3]
[1]*Department of Mechanical Engineering, Bilkent University, Ankara, Turkey*
[2]*Laboratory of Fluid Mechanics and Instabilities, Ecole Polytechnique Federale de Lausanne, Switzerland*
[3]*Department of Industrial Engineering, Information and Economics, University of L'Aquila, Italy*

Abstract Exploring Rayleigh-Bénard instability with non-uniform heating reveals a critical relationship between the temperature gradient, the system stability and the multiplicity of flow states.

The Rayleigh-Bénard problem investigates gravity-induced convective systems influenced by density variation [1]. The present research explores the instability of a fluid layer with non-uniform heating, specifically with a normally distributed temperature field at the bottom wall, to advance our understanding of fluid thermal behaviour in optically manipulated fluids [2].

The Navier-Stokes equations are coupled with the energy equation using the Boussinesq approximation. A linear stability analysis (LSA) is conducted to examine the stability of the 2D steady-state axisymmetric base flow under small perturbations. Key dimensionless parameters include the Rayleigh number (Ra), reflecting the balance between buoyant and viscous forces, and the Prandtl number (Pr), representing the ratio of momentum diffusivity to thermal diffusivity in the fluid. The top and bottom walls of the infinite cylindrical domain are assumed to be no slip and kept at constant temperatures. The bottom wall temperature is defined as $\theta_b(r) = \frac{2}{\sqrt{\pi}} \frac{\Gamma\left(\sqrt{\frac{1}{2\sigma^2}}\right)}{\mathrm{erf}\left(\Gamma\sqrt{\frac{1}{2\sigma^2}}\right)} e^{-\frac{r^2}{2\sigma^2}}$ where σ is the standard deviation the temperature at the wall and $\Gamma = R/d$ is the aspect ratio, i.e., radius R over height d of the cylindrical domain. FreeFem++ [3] is the software used for solving the equations by using the Finite Elements approach. The critical Rayleigh number Ra_c, i.e. the value of Ra for which we have the onset of instability, for uniform bottom heating (i.e. $\theta_b = 1$), is 1708 [4]. In the present study, the Prandt number is set to $Pr = 1$.

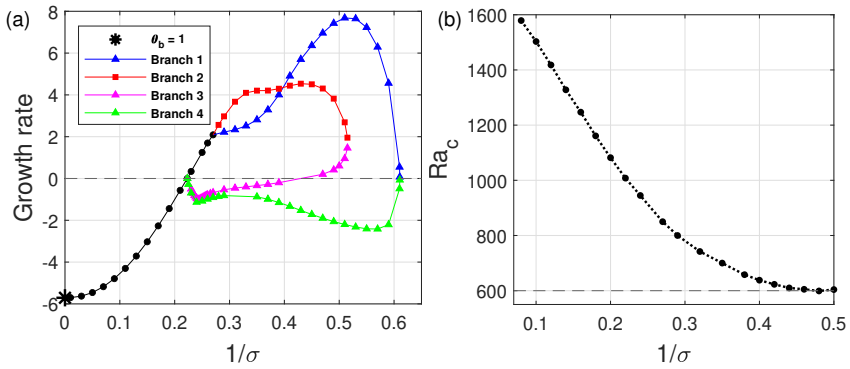

Figure 1. (a) Azimutal wavenumber $m = 0$ mode LSA results for $Ra = 1000$; (b) The critical Rayleigh number Ra_c vs $1/\sigma$.

In Fig. 1(a), we observe the system to become unstable at $1/\sigma > 0.223$ for $Ra = 1000$, which is much lower than the critical Rayleigh number for uniform boundaries. Two bifurcations occur, one at the primary instability point and one at $1/\sigma = 0.27$, resulting in coexisting base flow branches, i.e. flow state multiplicity. Fig. (b) shows that the critical Rayleigh number decreases with $1/\sigma$ before reaching a saturation around $1/\sigma = 0.48$, as large temperature gradients become restricted in a region of insufficient extension.

References

[1] E. L. Koschmieder, *Instabilities in fluid dynamics*, Synergetics, 70–78. (1977).
[2] S. M. Mousavi, I. Kasianiuk, D. Kasianiuk, S. K. Velu, A. Callegari, L. Biancofiore and G. Volpe, *Clustering of janus particles in an optical potential driven by hydrodynamic fluxes, Soft Matter*, **15**(28), 5748–5759 (2019).
[3] P. Meliga, and F. Gallaire, *Control of axisymmetric vortex breakdown in a constricted pipe: Nonlinear steady states and weakly nonlinear asymptotic expansions*, Physics of Fluids, **23**(8), 084102 (2011).
[4] M. Wanschura, H. Kuhlman and H. Rath,*Three-dimensional instability of axisymmetric buoyant convection in cylinders heated from below*, Journal of Fluid Mechanics, **326**, 399-415 (1996).

DAY 4 - Thursday, 27 June 2024 Afternoon Sessions			
	Active Matter ***Chair: Prof Julia Yeomans*** ***Larch Lecture Theatre***	***Particles 2 & Bio Flows*** ***Chair: Prof Halim Kusumaatmaja*** ***Yew Lecture Theatre***	***Convection 2*** ***Chair: Dr Khushboo Pandey*** ***Elm Lecture Theatre***
13:30	Th151: Transport and delivery by active materials in complex flows *by A Mathijssen* ***(WITHDRAWN)***	Th172: Sedimentation of a nematic emulsion *by Y Mimoh, S Michelin*	Th193: Thermoelectric convection in microgravity environment *by I Mutabazi, C Kang, EB Barry, H Yoshikawa*
13:45	Th152: Activity-induced self-constraint of nematic defects and flow structures *by T Shendruk, LC Head, C Doré, K Thijssen, T López-León*	Th173: Liquid-liquid dispersions within milli-scale symmetric confined impinging jets *by C Duan, P Angeli*	Th194: Finite-amplitude solutions & multistability in magnetoconvection *by M McCormack, A Teimurazov, O Shishkina, M Linkmann*
14:00	Th153: Dynamics of artificial microswimmers in soft fluidic confinements *by SS Sontakke, A Kajampady, R Dey*	Th174: Violation of Stokes-Einstein relation in a one-component fluid interacting via MIE potential by *M Priya, S Suvarna*	Th195: Exploring state space pathways leading to spiral defect chaos *by CH Chan, MZ Hossain, SJ Sherwin, Y Hwang*
14:15	Th154: Flow states of two dimensional active gels driven by external shear *by T Powers, W Luo, A Baskaran, RA Pelcovits*	Th175: Oscillations and instabilities in granular surface flows *by A Tripathi, S Patro, Soniya*	Th196: 3D magneto-convective instabilities of liquid metal flow in a rectangular cavity with a coaxial circular cooling pipe *by B Lyu, L Buehler, C Koehly, C Mistrangelo*
14:30	Th155: Active fluid-induced dynamics of passive polymers *by Z Valei, TN Shendruk*	Th176: Competing aggregation and iso-density equilibrium lead to band patterns in density gradients by *A Darras, F Maurer, C Romero, N Lerch, T John, L Kaestner, C Wagner*	Th197: Solutal convection in liquid metal and molten salt batteries *by T Weier, C Duczek, S Landgraf, P Personnettaz, N Weber*
14:45	Th156: Simulating collective bacterial swarming in sparse systems *by F de Tournemire, K Thijssen, G Melaugh, TN Shendruk*	Th177: Red blood cell shape dynamics in time-dependent capillary flow *by C Wagner, SM Recktenwald, K Graessel, FM Maurer, T John, S Gekle*	Th198: Instabilities in a non-isothermal nanofluid layer in a gravity field *by R Gandhi, A Nepomnyashchy, A Oron*
15:00	Th157: Opposing vortices characterize the average flow around 3D free-swimming sperm *by X Ren, P Hernández-Herrera, F Montoya, A Darszon, G Corkidi, H Bloomfield-Gadêlha*	Th178: Impact of hole size on pattern formation in lifted Hele-Shaw cells *by D K Roughton-Reay, P Agrawal, V Barrioz*	Th199: Subcritical and heteroclinic bifurcations in Rayleigh-Bénard convection of shear-thinning fluids confined in Hele-Shaw cell *by OM Najib, PV Brandão, SC Hirata, LS de B Alves*
15:15	**Coffee Break (Alder Lecture Theatre)**		
	Convection 3 ***Chair: Dr Rodrigo Ledesma-Aguilar*** ***Larch Lecture Theatre***		
15:45	Th158: A model of localized convection appearing in Euglena suspensions *by H Yamashita, T Suzumura, T Yamaguchi, NJ Suematsu, M Iima*	Th179: Elastocapillary phenomena inside biological cells *by H Kusumaatmaja, A Brown, X Ma, L Frigerio, R Knorr*	Th200: Nonlinear dynamics of steady oblique rolls in rotating magnetoconvection *by L Sharma, P Pal, M Ghosh*
16:00	Th159: Multiple states and transition to chaos in quasi-static magnetoconvection *by SH Bader, V Kannan, X Zhu*	Th180: CFD analysis of stenosed artery and plaque rupture risk stratification using in-house CFSSI solver by *A Lagwankar, S Morab, J Muralidharan, A Sharma*	Th201: Rayleigh-Benard-Marangoni convection in a binary fluid system *by A Dubey, S Mishra, SV Diwakar, S Amiroudine*
16:15	Th160: Elasto-inertial instabilities and turbulence in Taylor-Couette flows *by T Boulafentis, S Balabani*	Th181: Dynamics of mucus films in ciliated lung airways *by S Hazra, JR Picardo*	Th202: Convection patterns in an annular cavity subjected to a radial temperature gradient *by A Prigent, Z Ntarmouchant, I Mutabazi*
16:30	Th161: The effect of aspect ratio on mixed convective developing laminar flow through rectangular channels *by M Everts, N Harris, KJ Craig*	Th182: Role of asymmetric acinar wall motion on the particle transport in the lung acinus *by P Kumar, P Jutur, A Roy, M Panchagnula*	Th203: Sensitivity analysis of the first instability in a differentially heated square cavity *by J Williams, UA Qadri, HS Thorne*
16:45	Th162: Surface acoustic wave induced flow in porous media by O Manor, G Unoh, J Friend	Th183:	Th204

Th151

TRANSPORT AND DELIVERY BY ACTIVE MATERIALS IN COMPLEX FLOW

Arnold Mathijssen[1]
[1]*Department of Physics and Astronomy, University of Pennsylvania, U.S.A.*

Keywords: Active matter, biological fluid dynamics, emergent phenomena, complex fluids

Abstract

One of the major challenges in transport technology is controlling micromanipulation by active and adaptive materials. Existing delivery technologies often suffer from limited navigation control, low speeds, and proneness to environmental disturbances. Biology often solves these problems by collectively organizing actuation at the microscale. For example, pathogens are removed from our lungs by an active carpet of cilia [1]. Inside these cilia, in turn, microtubules form highways for molecular motors. Here, I will present developments in the microfabrication of "artificial cilia" [2] and "artificial microtubules" [3] operating in complex fluids. We designed amphibious cilia that can transport both liquids and dry objects. These carpets can sort particles by size and by shape using a crowd-surfing effect. We also designed magnetic microtubules, structured microfibers that rapidly guide particles through flow networks such as the cardiovascular system. These works offer unique strategies for robust microscale delivery, but equally shed light on non-equilibrium diffusion [4] and active transport [5] in biological transport processes.

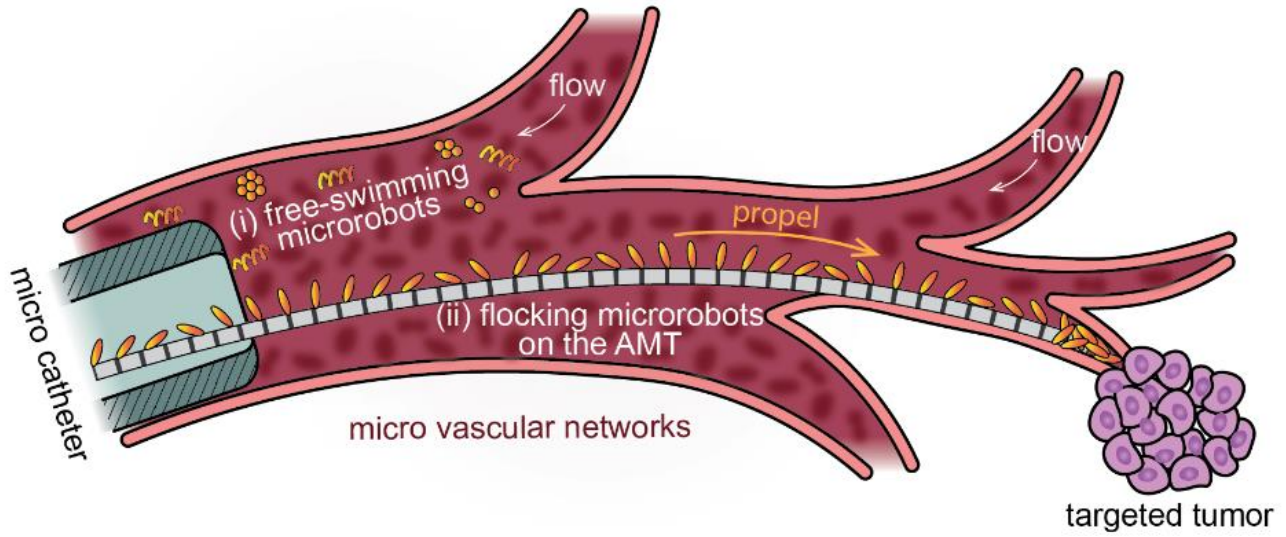

Figure 1. Drug delivery by artificial microtubules (AMT) in microvascular networks [3]. First, a microcatheter (diameter ~0.5 mm) is inserted to its limitation, where it cannot enter into smaller vessels. Then, an AMT (diameter ~0.05 mm) is pushed through the microcatheter and guided magnetically into a microvascular branch to the targeted tumour. Finally, drug capsules are transported along the AMT against the cardiovascular flow to the target. Compared with freely swimming microrobots (i), the transport along AMTs (ii) is faster and more robust due to the magnetic anchoring to the stepping stones, especially in complex flows.

References

[1] G.R. Ramirez-San Juan, A.J.T.M. Mathijssen, M. He, L. Jan, W.F. Marshall, M. Prakash M, *Multi-scale spatial heterogeneity enhances particle clearance in airway ciliary arrays*, Nat. Phys. **16**: 958–964 (2020)
[2] A.F. Demirörs et al., *Amphibious transport of fluids and solids by soft magnetic carpets*, Adv. Sci. 202102510 (2021)
[3] H. Gu, E. Hanedan, Q. Boehler, T.Y. Huang, A.J.T.M. Mathijssen* & B.J. Nelson*, *Artificial microtubules for rapid and collective transport of magnetic microcargos*, Nat. Mach. Intel. **4**: 678–684 (2022) * Joint corresponding authors
[4] F. Guzman-Lastra, H. Löwen, A.J.T.M. Mathijssen, *Active carpets drive non-equilibrium diffusion and enhanced molecular fluxes*, Nat. Commun. **12**: 1906 (2021)
[5] C. Jin, Y. Chen, C.C. Maass, A.J.T.M. Mathijssen, *Collective entrainment and confinement amplifies transport by schooling micro-swimmers*, Phys. Rev. Lett. **127**: 088006 (2021)

Th152

ACTIVITY-INDUCED SELF-CONSTRAINT OF NEMATIC DEFECTS AND FLOW STRUCTURES

L. C. Head[1], C. Doré[2], K. Thijssen[3], T. López-León[2] & T. N. Shendruk[1]
[1]*School of Physics and Astronomy, University of Edinburgh, Edinburgh, United Kingdom*
[2]*Laboratoire Gulliver, UMR CNRS 7083, ESPCI Paris, PSL Research University, Paris, France*
[3]*Niels Bohr Institute, University of Copenhagen, Blegdamsvej 17, Copenhagen, Denmark*

Abstract Active fluids; self-motile topological defects; viscometric structures.

Active nematics exhibit spontaneous flows with complex spatiotemporal structure. In bulk, disorderly dynamics arise due to the coupling between nematic deformations and active flows, and are characterized by steady-state populations of half-integer topological defects. This talk will demonstrate that, despite their disorderly dynamics, there exists a strong self-constraint that arises between the self-propulsion of motile defects and mesoscale flow structures. Through a combination of microtubule/kinesin-based experiments and nematohydrodynamic simulations, we show that self-motile defects are tightly constrained to particular flow structures where vorticity and the strain rate are balanced, called viscometric surfaces. Although this is consistent with models for the flows generated by isolated +1/2 defects that predict the defect resides at an intersection between two crossing viscometric surfaces, experiments and simulations show that +1/2 defects are predominantly found on a single viscometric surface — only fleetingly passing through intersections — and, thus, possess broken-mirror symmetry. Through a series of simple models, we explain that this spontaneous self-constraint arises from an interdependence between viscometric lines and elongated narrow bend walls in the director field. We provide evidence that this result is not limited to bulk turbulence but occurs whenever self-motile defects are present. These results underscore the continual role of bend walls in steady-state dynamics, showing that active nematic defects cannot be viewed as solitary points but are one component of mesoscale nematic structures, which suggests potential new avenues for exploring topological dynamics.

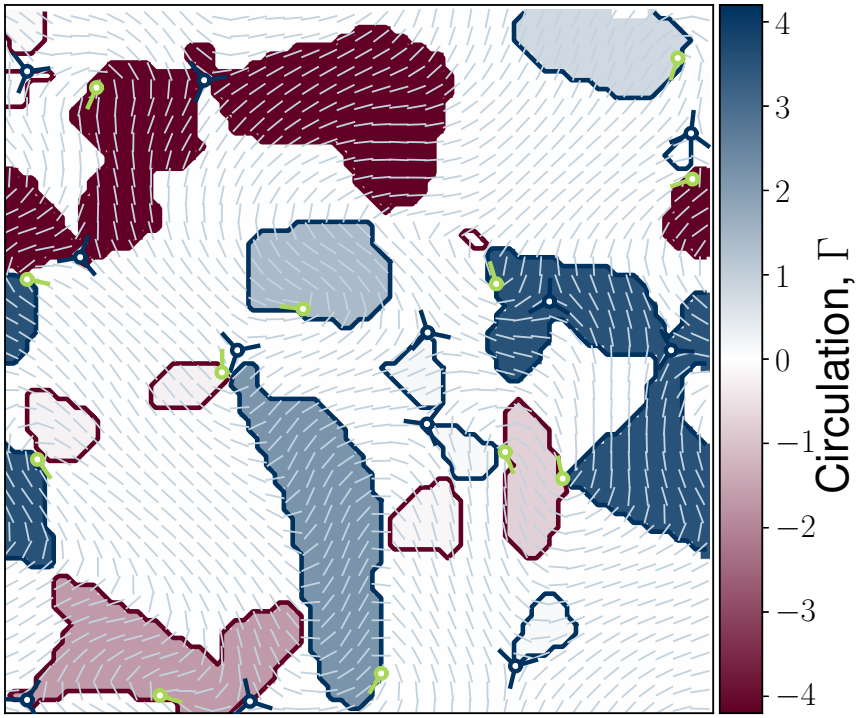

Figure 1. Numerical simulations of active turbulence, in which vorticity dominated flows are coloured according to their circulation (red for clockwise; blue for anti-clockwise). Viscometric lines (solid lines) enclose each vortex. Positive defects (green symbols) in the orientation field (dashed grey lines) are constrained to be found on the viscometric lines, whereas negative defects (blue symbols) are typically found close to viscometric lines but are not constrained to reside immediately on them.

Th153

DYNAMICS OF ARTIFICIAL MICROSWIMMERS IN SOFT FLUIDIC CONFINEMENTS

Smita S. Sontakke[1], Aneesha Kajampady[1] & Ranabir Dey[1]
[1]*Department of Mechanical and Aerospace Engineering, Indian Institute of Technology Hyderabad, India*

Abstract Self-propelled microswimmers, active droplets, soft microconfinements, microhydrodynamics

Biological microswimmers alter their motility in response to external cues like chemical concentration, boundary proximity, and ambient flow. However, the response of self-propelled microswimmers to the stiffness of a confining wall in their vicinity, and their dynamics remain ambiguous. Here, we experimentally investigate the effects of varying stiffness of the micro-confinement walls on the swimming dynamics of self-propelled microswimmers, considering active droplets as a model system [1, 2]. We note significant differences in the swimming dynamics of these droplet microswimmers in a rigid micro-confinement ($E = 360kPa; El \sim O(10^8)$), and in a soft-walled micro-confinement ($E = 35.2kPa; El \sim O(10^7)$) of identical geometry. While for the rigid case the active droplets exhibit steady unidirectional swimming velocity along a confinement wall (Figures 1(a, b)), in case of soft confinements the microswimmer exhibits unsteady swimming dynamics with intermittent deceleration, stopping, and subsequent acceleration (Figure 1(c)). These changes in the self-propulsion velocity are accompanied by sharp re-orientation of the swimming direction (Figure 1(d)). These observations are better seen from the probability distributions shown in Figures 1 (e, f). Figure 1(e) shows that the droplet microswimmer exhibits a broader distribution of $|\vec{u}|$ in the soft microchannel, including intermittent stopping, and a relatively lower mean value compared to rigid case. Figure 1(f) shows the distribution of the reorientation angle ($|\Delta\Psi| = \Psi_2 - \Psi_1$; Figure 1(g)) for the microswimmer in rigid and soft microchannels. $|\Delta\Psi|$ has a wider distribution in the soft microchannel as compared to that in the rigid microchannel. In Figure 1(f), shaded area represents the occurrence of sharp re-orientation event ($|\Delta\Psi| > 9°$) of the microswimmer in the soft microchannel. Interestingly, the microswimmer exhibits autonomous changes in its flow field characteristics over such stopping and acceleration events. We use high-resolution microscopy and micro-PIV analysis to characterize such dynamics. This will aid the understanding of bio-physical response of swimming micro-organisms to mechanical cues from the confinement walls, and conceptualization of active cargo-delivery in soft, complex environment.

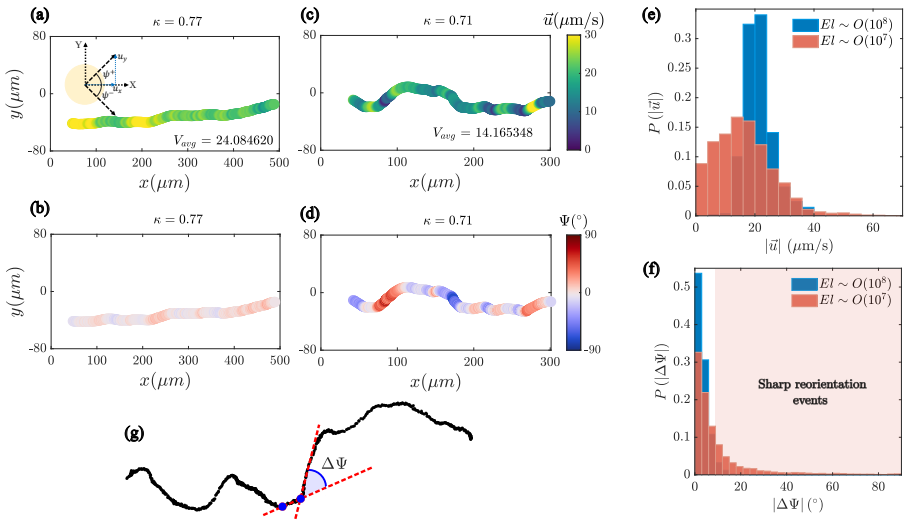

Figure 1. Dynamics of active droplets in rigid and soft microchannels. (a, b) Trajectory of the active droplet color coded with the magnitude of the instantaneous swimming velocity $\vec{u}$ and swimming orientation Ψ in the rigid microchannel (**Click here**), and (c, d) in the soft microchannel (**Click here**). (e, f) Probability distributions of the self-propulsion speed $|\vec{u}|$, and velocity reorientation angle $|\Delta\Psi|$ (illustrated in (g)) for rigid and soft microchannels (for $0.7 < \kappa < 0.8$, κ is the strength of confinement). Note: We use a non-dimensional number known as the elastoviscous number (El), defined as the ratio of elastic to viscous forces, for identifying the confinements of varying elasticity.

References

[1] S. Thutupalli, R. Seemann, S. Herminghaus, *Swarming behavior of simple model squirmers*, New Journal of Physics **13(7)**, 073021 (2011).
[2] S. Michelin, *Self-propulsion of chemically active droplets*, Annual Review of Fluid Mechanics **55**, 77-101 (2023).

Th154

FLOW STATES OF TWO DIMENSIONAL ACTIVE GELS DRIVEN BY EXTERNAL SHEAR

Thomas R. Powers[1234], Wan Luo[1], Aparna Baskaran[5] & Robert A. Pelcovits[34]
[1] *School of Engineering, Brown University, Providence, RI 02912, U.S.A.*
[2] *Center for Fluid Mechanics, Brown University, Providence, RI 02912, U.S.A.*
[3] *Department of Physics, Brown University, Providence, RI 02912, U.S.A.*
[4] *Brown Theoretical Physics Center, Brown University, Providence, RI 02912, U.S.A.*
[5] *Martin Fisher School of Physics, Brandeis University, Waltham, MA 02453 U.S.A.*

Abstract active matter, flow instabilities, liquid crystals.

Using a minimal hydrodynamic model, we theoretically and computationally study the Couette flow of active gels in straight and annular two-dimensional channels subject to an externally imposed shear [1]. The gels are isotropic in the absence of externally- or activity-driven shear, but have nematic order that increases with shear rate. Using the finite element method, we determine the possible flow states for a range of activities and shear rates. Linear stability analysis of an unconfined gel in a straight channel shows that an externally imposed shear flow can stabilize an extensile fluid that would be unstable to spontaneous flow in the absence of the shear flow, and destabilize a contractile fluid that would be stable against spontaneous flow in the absence of shear flow. These results are in rough agreement with the stability boundaries between the base shear flow state and the nonlinear flow states that we find numerically for a confined active gel. For extensile fluids, we find three kinds of nonlinear flow states in the range of parameters we study: unidirectional flows, oscillatory flows, and dancing flows. To highlight the activity-driven spontaneous component of the nonlinear flows, we characterize these states by the average volumetric flow rate and the wall stress. For contractile fluids, we only find the linear shear flow and a nonlinear unidirectional flow in the range of parameters that we studied. For large magnitudes of the activity, the unidirectional contractile flow develops a boundary layer. Our analysis of annular channels shows how curvature of the streamlines in the base flow affects the transitions among flow states.

References

[1] W. Luo, A. Baskaran, R. A, Pelcovits, T. R. Powers, *Flow states of two dimensional active gels driven by external shear*, in press Soft Matter (2023); arXiv:2307.12910.

Th155

Active fluid-induced dynamics of passive polymers

Zahra Valei[1*] and Tyler Shendruk[1]
[1]School of Physics and Astronomy, University of Edinburgh, Edinburgh, UK

Keywords: Active nematic flow, flexible polymer

Anisotropic and rheologically complex materials are ubiquitous in living systems, in which biochemically fuelled activity can give rise to intriguing nonequilibrium effects that act on small solutes, whole organelles, and biomolecular polymers. Of these, passive polymers embedded in active liquid crystalline solvents are particularly interesting because of the interplay between the broken symmetry of the anisotropic medium, nonequilibrium activity and the conformational degrees of freedom of the macromolecules. This work reports the first study of a passive polymer in active nematic flows. We numerically study the conformation and dynamics of individual flexible polymers coupled to the velocity field of 2D extensile active turbulence. For this purpose, we employ a hybrid Multi-Particle Collision Dynamics [1] and Molecular Dynamics [2] simulation. We find the diffusivity of polymers increases with activity up to the onset of turbulence, at which point it saturates. This is due to the competition between active forcing and conformational changes. And it is the characteristic length scale of the fluid that dictates the conformational changes of polymers. While polymers longer than active length scale are stretched, those which are shorter get compressed. This demonstrates how activity represents a pathway by which biological systems can control polymer properties.

References

[1] T. Kozhukhov and T. Shendruk, Science Advances, 8(34), 2022.
[2] Slater et al., Electrophoresis, 30(5), (2009).

* Correspondence : z.valei@sms.ed.ac.uk

Th156

SIMULATING COLLECTIVE BACTERIAL SWARMING IN SPARSE SYSTEMS

François de Tournemire[1], Kristian Thijssen[2], Gavin Melaugh[1] & Tyler N. Shendruk[1]
[1]*School of Physics and Astronomy, University of Edinburgh, UK*
[2]*Niels Bohr Institute, Copenhagen, DK*

Abstract Bacterial swarming, Multi-Particle Collision Dynamics, Multipole expansion

Collective swarming of bacterial swimmers is a complex behaviour, often-seen in experiments. It consists of organisms moving rapidly while creating flow structures, such as vortices or jets, on a scale much larger than individual cells. While computational models have been successful at modelling dilute suspensions of swimming bacteria [1], they have struggled to reproduce the complexity of swarming. In particular, swarming is known to occur in sparser systems than predicted by current models, due to a near-field interaction between flagella and cell bodies. To tackle this complexity, we introduce a new minimal model to efficiently simulate bacteria, in which cell bodies are treated as dumbbells subject to a propulsive force and flagellar bundles are modelled as phantom forces applied directly to the surrounding fluid. The fluid is modelled using Multi-Particle Collision Dynamics (MPCD)[2], a coarse-grained simulation technique that solves the fluctuating Navier-Stokes equations. We validate this new 'Active Dumbbell' model with a multipole expansion [3] and single swimmer simulations. We demonstrate that this numerical approach allows for swarming to occur at a sparser packing fraction than predicted for suspensions of swimmers. Our results are in line with experiments [4], and the relatively low computational costs of this approach will allow future studies to probe more complex systems than previously considered, such as swarming in the vicinity of large obstacles or in porous media.

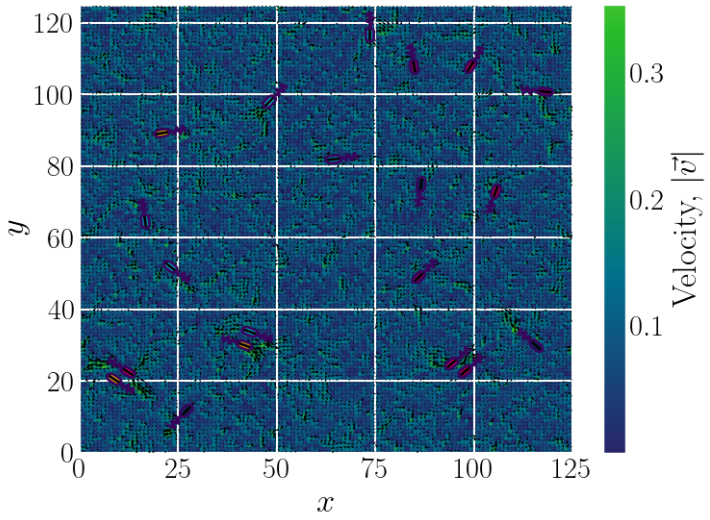

Figure 1. Simulation snapshot of Active Dumbbells in a Multi-Particle Collision Dynamics fluid.

References

[1] V. Škultety, C. Nardini, J. Stenhammar, D. Marenduzzo, and A. Morozov, *Swimming supresses correlations in dilute suspensions of pusher microorganisms*, Physical Review X **10**, 031059 (2020)
[2] M. P. Howard, A. Nikoubashman, and J. C. Palmer, *Modeling hydrodynamic interactions in soft materials with Multi-Particle Collision Dynamics*, Current Opinion in Chemical Engineering **23** (2019)
[3] J. Yeomans, D. O. Pushkin, and H. Shum, *An introduction to the hydrodynamics of swimming microorganisms*, The European Physical Journal Special Topics **223** (2014)
[4] A. Be'er and G. Ariel, *A statistical physics view of swarming bacteria*, Movement Ecology **7** (2019)

Th157

Opposing vortices characterize the average flow around 3D free-swimming sperm

Xiaomeng Ren[1], Paul Hernández-Herrera[2], Fernando Montoya[2], Alberto Darszon[3], Gabriel Corkidi[2], & Hermes Bloomfield-Gadêlha[1*]

[1]*Department of Engineering Mathematics, University of Bristol, BS8 1UB Bristol, UK.*

[2]*Laboratorio de Imágenes y Visión por Computadora, Departamento de Ingeniería Celular y Biocatálisis, Universidad Nacional Autónoma de México, Cuernavaca, Mexico.*

[3]*Departamento de Genética del Desarrollo y Fisiología Molecular, Instituto de Biotecnología, Universidad Nacional Autónoma de México, Cuernavaca, Mexico.*

Keywords: fluid flow; sperm; experiment; simulation.

Abstract

Experimental sperm free swimming driven by a 3D waveform is reconstructed and the surrounding 3D hydrodynamics is investigated numerically. Swimming in proximity to a boundary exhibits minimal impacts on the free sperm movements, yet considerable influence on the fluid flow. As the boundary distance increases, the average flow field comoving with the sperm during the global cycles of the 3D sperm trajectory gradually turns organized and reveals opposing vortices distributed along the sperm body. The vortices proximal to the head swirl in a counterclockwise direction, same as the head spinning direction when viewed from head to tail, whilst the vortices near the flagellar distal tip are in a clockwise direction. Such flow pattern can also be produced by 3D virtual sperm models despite with distinct waveforms, implying the opposed vortices a generic phenomenon and potentially providing new insights into studies on flows around 3D free sperm.

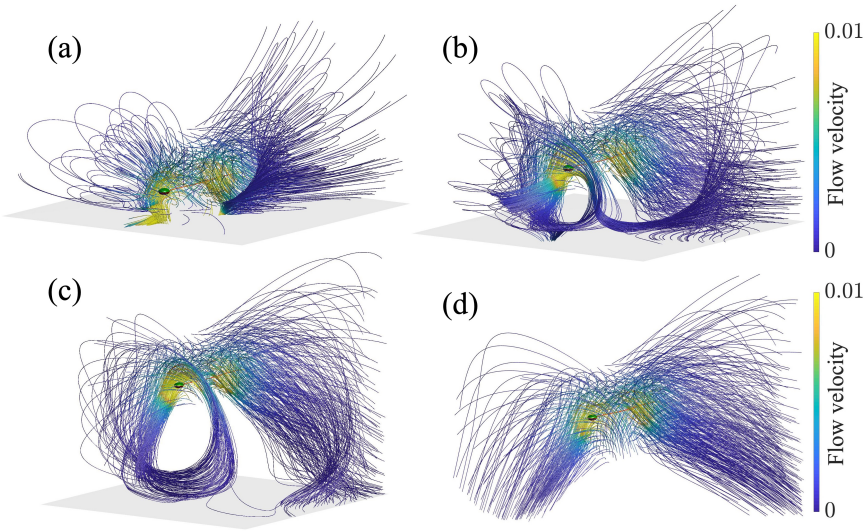

Figure 1. Time-averaged fluid flow around the experimental sperm, with different boundary conditions.

Th158

A MODEL OF LOCALIZED CONVECTION APPEARING IN *EUGLENA* SUSPENSIONS

Hiroshi Yamashita[1], Takuya Suzumura[1], Takayuki Yamaguchi[2], Nobuhiko J. Suematsu[3,4] & Makoto Iima[1]
[1]*Graduate School of Integrated Sciences for Life, Hiroshima University, Hiroshima, Japan*
[2]*Data Science and AI Innovation Research Promotion Center, Shiga University, Shiga, Japan*
[3]*Graduate School of Advanced Mathematical Sciences, Meiji University, Tokyo, Japan*
[4]*Meiji Institute for Advanced Study of Mathematical Sciences (MIMS), Meiji University, Tokyo, Japan*

Keywords: Bioconvection, Model, Localized structure, Numerical simulation

Abstract

When a strong light is shone from below onto a suspension of *Euglena*, a photosynthetic microorganism, convection occurs. It is due to the motility of the microorganism and hydrodynamic instability. *Euglena* exhibits negative phototaxis, whereby individuals move away from strong light. Therefore, when a suspension of *Euglena* is strongly illuminated from below, individuals of *Euglena* move towards the top layer of the suspension. The local mass density of the suspension becomes higher near the top layer, and downward flows occur due to Rayleigh–Taylor instability. Convective flows in the suspension are maintained by the balance between the upward swimming of the microorganisms and the downward flows. This convection is a type of phenomenon known as bioconvection.

Previous experimental studies have shown that localized structures appear in *Euglena* bioconvection [1, 2, 3]. For instance, when convection is observed under uniform illumination with a special initial cell density distribution prepared under temporally changing illumination, a single convective cell forms in a wide container, and its structure is maintained [3]. It has been suggested that the reason convective cells can become localized in a suspension is due to the self-shading effect [1]. The effect refers to the phenomenon where the light intensity becomes lower in high-cell-density areas due to the shadows cast by microorganisms. Thus, *Euglena* exposed to strong light tend to move towards these high-cell-density regions, thereby maintaining a convective flow locally.

The present study aims to understand the characteristics of localized convection appearing in *Euglena* bioconvection. We considered a model for negative phototaxis and the self-shading effect and conducted numerical simulations of bioconvection that included this model. We defined the flux of cells $\boldsymbol{J}$ as follows:

$$\boldsymbol{J} = n\boldsymbol{u} - D\nabla n + n\boldsymbol{W}, \quad \boldsymbol{W} = W_d f \boldsymbol{q},$$

where n represents cell density, $\boldsymbol{u}$ represents fluid velocity, and $\boldsymbol{W}$ represents average swimming velocity of cells. We calculated the light intensity field $I(n)$ following Lambert–Beer's law and assumed that the swimming direction $\boldsymbol{q}$ is given by $-\nabla I/|\nabla I|$. This implies that cells move towards darker (denser) regions. f represents phototactic susceptibility, and we simply assumed that $f(I) = I$. W_d represents the swimming speed of cells and is constant.

We considered the situation where a strong light is shone from below onto a suspension of *Euglena* in a two-dimensional rectangular enclosure. The incompressible Navier–Stokes equations, under the Boussinesq approximation, and the equation for cell conservation were numerically calculated using the spectral collocation method. Figure 1 shows a representative result from our calculations. It was found that a single convective cell can maintain its structure within a rectangular enclosure. For comparison, we also performed calculations for two additional models: gravitaxis ($\boldsymbol{W} = W_d \boldsymbol{e}_y$) and negative phototaxis only ($\boldsymbol{W} = W_d f \boldsymbol{e}_y$), where $\boldsymbol{e}_y$ represents a vertical unit vector. Our calculations demonstrated that the self-shading effect facilitates the maintenance of convective flows.

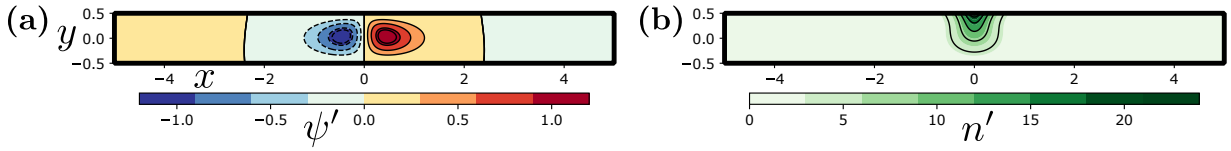

Figure 1. A heat map and contours of non-dimensional stream function (a) and local cell density divided by average cell density (b) for $\mathrm{Sc} = 7.7$, $\mathrm{Pe} = 3.8$, $\mathrm{Ra} = 58$, $\alpha = 0.041$. α: non-dimensional absorption coefficient of light.

References

[1] N. J. Suematsu, A. Awazu, S. Izumi, S. Noda, S. Nakata, H. Nishimori, *Localized bioconvection of Euglena caused by phototaxis in the lateral direction*, Journal of the Physical Society of Japan, **80**, 064003 (2011).

[2] E. Shoji, H. Nishimori, A. Awazu, S. Izumi, and M. Iima, *Localized bioconvection patterns and their initial state dependency in Euglena gracilis suspensions in an annular container*, Journal of the Physical Society of Japan, **83**, 043001 (2014).

[3] H. Yamashita, T. Kamikubo, K. Muku, N. J. Suematsu, S. Izumi, and M. Iima, *Emergence of a Euglena bioconvection spot controlled by non-uniform light*, Frontiers in Ecology and Evolution, **11**, 1132956 (2023).

Th159

MULTIPLE STATES AND TRANSITION TO CHAOS IN QUASI-STATIC MAGNETOCONVECTION

Shujaut H. Bader[1], Veeraraghavan Kannan[1] & Xiaojue Zhu[1]

[1]*Max Planck Institute for Solar System Research, 37077, Göttingen, Germany*

Abstract quasi-static magnetoconvection, bifurcation, chaos, transition, multiple states.

In this work, the emergence of the multiple states in two-dimensional quasi-static magnetoconvection in the presence of a strong vertical magnetic field, is explored. Top and bottom plates are free-slip, isothermal and the lateral boundaries are periodic. The imposed magnetic field, characterized by the Chandrasekhar number (Q), is anti-parallel to the gravity, and the Prandtl number (Pr) is set to unity. Different initial roll-states, prescribed by a Fourier basis, lead to different final, statistically stationary states, characterized by a different number of stable rolls and a different set of global transport properties. An attempt is made to quantify the lower and upper bounds on the aspect ratio of the allowable roll states.

Furthermore, the behaviour of the system to initial conditions is also observed to be vital for the transition pathway to chaos. At a fixed Q, upon increasing the Rayleigh number (Ra), a specific set of initial conditions different from a Fourier basis is observed to lead to an atypical bifurcation sequence: steady state $\rightarrow$ periodic $\rightarrow$ quasi-periodic $\rightarrow$ *steady state*, finally leading to chaos after yet another intermediary periodic state. Consistent with the similar observations for non-magnetic RBC [1], this atypical behavior of the transition from quasi-periodic to *steady* state is accompanied by a significant change in the length scale of the flow. From the solution of the full set of nonlinear governing equations, the present study provides the first instance of the numerical evidence in support of the inverse bifurcation in 2D Boussinesq magnetoconvection.

References

1. Mukutmoni, D. and Yang, K. T., *Thermal convection in small enclosures: an atypical bifurcation sequence*, International Journal of Heat and Mass Transfer **38**, 113–126 (1995).

Th160

ELASTO-INERTIAL INSTABILITIES AND TURBULENCE IN TAYLOR-COUETTE FLOWS

Theofilos Boulafentis[1] & Stavroula Balabani[1]
[1]*FLUME, Department of Mechanical Engineering, University College London (UCL), London WC1E 7JE, UK*

Abstract Viscoelastic instabilities, Elasto-Inertial Turbulence, Particle Image Velocimetry

Elasto-Inertial Turbulence (EIT), a chaotic flow state known to be the result of viscoelasticity combined with non-negligible inertia, has been reported in the literature for different geometries, ranging from channel [1] and jet [2] flows to Taylor-Couette [3]. In all cases, it has been associated with the modification of the dominant coherent structures by elasticity. Particularly in Taylor-Couette flow, comprising two concentric cylinders with the inner one rotating, it is connected to the appearance of solitary pairs of vortices and mechanisms such as Merging and Splitting Transition and Disorder Oscillations. However, most of the phenomena are highly dependent on the polymer solutions elasticity. None of the existing works provide velocity data to elucidate the role of elasticity on the coherent structures and the timescales of the flow.

In this work, we characterise the flow fields in both the meridional and azimuthal plane using Particle Image Velocimetry (PIV) for TC flows of polymer solutions with varied elasticity ($El = 0 - 0.52$) at a fixed Reynolds number ($Re = 120$). We analyse the modification of the Newtonian, stable Taylor-Vortex flow for increasing elasticity at both planes. Our findings suggest that the initial destabilisation in the meridional plane for El up to 0.19, is reversed at higher values of El, where the velocity fluctuations seem to decrease. On the other hand, the flow systematically destabilises in the azimuthal plane for all El values. This suggests a progressive transition towards a flow state with a highly $2 - D$ character as suggested by [4] in EIT.

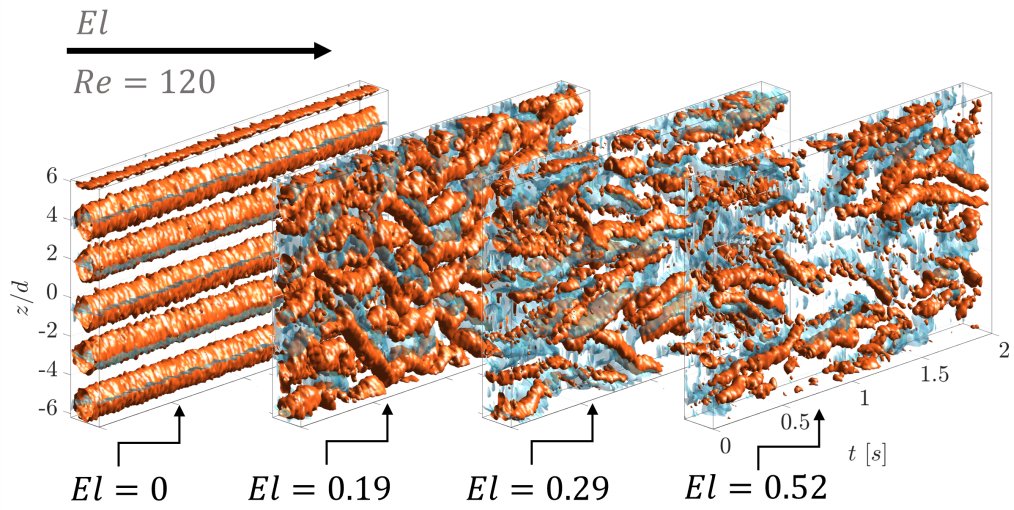

Figure 1. Spatio-temporal evolution of vortex structures for fluids of different elasticity (El) in the meridional plane of Taylor-Couette cell. Initially, the flow is destabilised due to the polymers up to $El = 0.19$, followed by annihilation of the vortical structures for increased El.

References

[1] Choueiri GH, Lopez JM, Varshney A, Sankar S, Hof B. Experimental observation of the origin and structure of elastoinertial turbulence. Proc. Natl. Acad. Sci.;118(45):1–5 (2021).
[2] Yamani S, Raj Y, Zaki TA, McKinley GH, Bischofberger I. Spatiotemporal signatures of elastoinertial turbulence in viscoelastic planar jets. Phys. Rev. Fluids;8(6):064610 (2023).
[3] Song J, Lin F, Liu N, Lu X-Y, Khomami B. Direct numerical simulation of inertio-elastic turbulent Taylor–Couette flow. J Fluid. Mech.;926:A37 (2021).
[4] Dubief Y, Terrapon VE, Hof B. Elasto-Inertial Turbulence. Annu. Rev. Fluid. Mech.55(1):675–705 (2023).

Th161

THE EFFECT OF ASPECT RATIO ON MIXED CONVECTIVE DEVELOPING LAMINAR FLOW THROUGH RECTANGULAR CHANNELS

Marilize Everts[1], Nikha Harris[2] & Ken Craig[2]
[1]*Department of Mechanical Engineering, University College London, London, United Kingdom*
[2]*Department of Mechanical and Aeronautical Engineering, University of Pretoria, Pretoria, South Africa*

Keywords:Laminar flow, developing flow, constant heat flux, rectangular channels, mixed convection

Abstract

In industrial heat exchanger applications where space is limited, compact heat exchangers such as printed circuit heat exchanger (PCHE) using non-circular cross sections are commonly employed. Due to the length-to-diameter ratio of the channels, the developing region cannot necessarily be ignored. Engineers need to know when the flow is developing or fully developed since it determines whether the heat transfer coefficients are dependent (developing flow) or independent (fully developed flow) of the axial position. The research of Everts and Meyer [1,2] closed the gap for developing mixed convective flow through circular tubes heated at a uniform heat flux. They showed the importance of accounting for mixed convection, which raises the question of whether the same will apply to non-circular geometries and what the effect of changing the aspect ratio would be on the Nusselt numbers and the entrance lengths. Shah and London [3] investigated laminar heat transfer in rectangular channels with different aspect ratios, but recommended that more research be done in the developing region. The purpose of this study was to numerically investiagate the effect of aspect ratio on the heat transfer characteristics through non-circular channels heated at a constant heat flux using Ansys Fluent. Special attention was given to flow patterns, thermal entrance length, circulation strength and heat transfer effectiveness. A circular tube and three rectangular channels, all sharing the same length of 9.5 m and hydraulic diameter of 11.5 mm but different aspect ratios (½, 1, and 2), were investigated for Reynolds numbers of 1 800 and 1 000 and heat inputs of 300 W and 1 000 W. It was found that heat transfer was enhanced by mixed convection when decreasing the aspect ratio. As indicated in Figure 1, vortex pairs formed due to cross-sectional temperature and density variations. Furthermore, for higher aspect ratios, a secondaryvortex pair formed which assisted in heat transfer enhancement. Overall, it was found that the heat transfer characteristics were different from those in circular tubes and that mixed convective flow through rectangular channels are significantly affected by aspect ratio, Reynolds number, and heat input. It was also found that a single-channel model can be used to predict a multi-channel counter flow PCHE problem as long as the total heat input is similar for a channel. This valuable finding can reduce simulation costs and time during heat exchanger design.

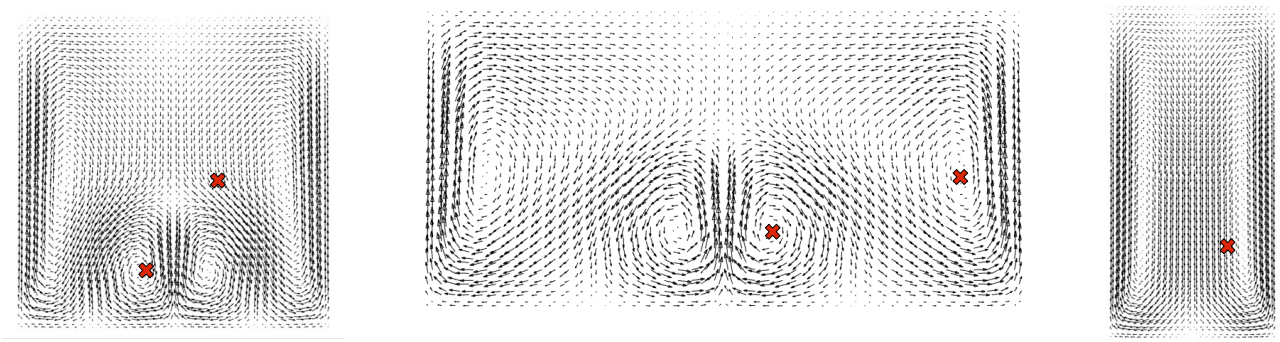

Figure 1. Cross-sectional flow patterns at z/D = 420 for rectangular channels with aspect ratios of (a) 1, (b) 2 and (c) 1/2 at *Re* = 1 800 and *Q* = 1 000 W. Due to symmetry, the vortex core location is indicated by a red 'x' on the right side.

References

[1] Everts, M. and J.P. Meyer, *Laminar hydrodynamic and thermal entrance lengths for simultaneously hydrodynamically and thermally developing forced and mixed convective flows in horizontal tubes.* Experimental Thermal and Fluid Science, **118**., (2020)
[2] Everts, M. and J.P. Meyer, *Flow regime maps for smooth horizontal tubes at a constant heat flux.* International Journal of Heat and Mass Transfer, **117**: p. 1274-1290, (2018)
[3] Shah, R.K. and A.L. London, *Laminar flow forced convection in ducts : a source book for compact heat exchanger analytical data*. Advances in heat transfer : Supplement ; 1, New York: Academic Press, (1978).

Th162

SURFACE ACOUSTIC WAVE INDUCED FLOW IN POROUS MEDIA

Gideon Onuh[1], James Friend[2], and Ofer Manor[1]
[1] *Department of Chemical Engineering, Technion - Israel Institute of Technology, Haifa, Israel*
[2] *Department of Mechanical and Aerospace Engineering, University of California San Diego, CA, USA*

Abstract porous media, surface acoustic wave, acoustic flow
We use theory and experiment to study the steady acoustic flow—acoustic streaming—to appear in a model porous medium—a strip of LFIA paper of well defined porosity and pore size—in contact with a MHz-frequency surface acoustic wave (SAW). We give new insights to previous findings of acoustic contributions to mass transport in porous media in geological (Elkhoury et al. 2006; Hamida & Babadagli 2008) and unit operation (Poesio et al. 2002; Yao et al. 2012) length scales as well as in smaller length scales of submicron- and nano-channels on lab on a chip platforms (Miansari & Friend, 2016; Guttenberg et al., 2004; Xu, 2018; Connacher et al., 2018; Ang et al., 2017; Martinez et al., 2010; Ho et al., 2011; Parolo & Merko ci, 2013).

Our theory [1] details the integral transport of mass through cylindrical pores of arbitrary azimuth compared to the acoustic path. See illustration in Fig 1. Where the acoustic impedance of the solid medium deviate from the liquid therein, the acoustic forcing introduces both flow through the bulk of pores and boundary layer flow near the pore surfaces. However, where the acoustic impedance of the solid and liquid therein are the same, mass transport is solely a product of bulk flow through pores. In this case, the acoustic forcing contribution to flow is similar to the one of the pressure forcing term in the classic Darcy equation for flow through porous media.

In experiment, we excite MHz-frequency surface acoustic wave (SAW) in contact with wet LFIA paper. The SAW leak ultrasonic waves that translate through the paper porous structure, introducing Reynolds stress therein and flow. We show unidirectional flow in a water infused paper strip along the path of the SAW, which we generate in an underlying acoustic actuator. The flow velocity increases monotonically with acoustic power and is in agreement with theory.

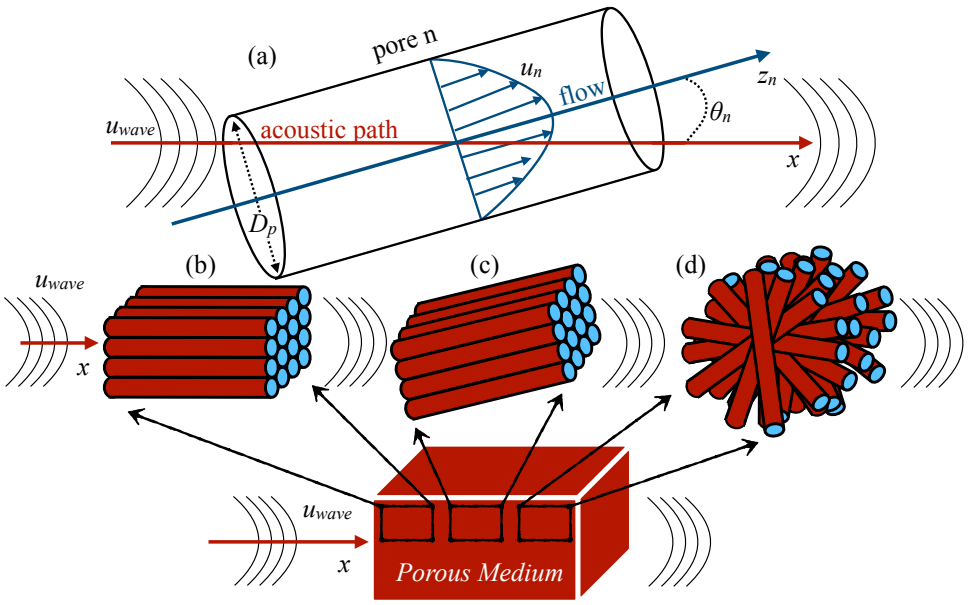

Figure 1. An illustration of a porous media that is comprised of an array of cylindrical pores, where (a) pore number n, of diameter D_p, is oriented so that its axial axis, z_n, and its axial flow component, u_n, are at an angle, θ_n, with respect to the path of the acoustic wave, x; the pores in the solid medium may be (b) aligned along the path of the acoustic wave (c) aligned along a path different to the acoustic wave, and (d) randomly aligned, among other options. [1]

References

[1] O. Manor, *Acoustic flow in porous media*, J. Fluid Mech., **920**, A11 (2021)

Th172

SEDIMENTATION OF A NEMATIC DROPLET

Yassine Mimoh[1] & Sébastien Michelin[1]
[1]*LadHyX, CNRS - Ecole Polytechnique, Institut Polytechnique de Paris, 91120 Palaiseau, France*

Abstract Key words: Liquid crystals, Fluid Elasticity, Droplet sedimentation

The local molecular polarization of liquid crystals provides them with distinctive optical, mechanical, and magnetic properties that have been a focal point of research and technological advancement over the past decade from LCDs to cutting-edge engineering tools. In a liquid crystal, molecules adopt locally a preferred orientation, a director, which resists deformation thus introducing some internal elasticity. Molecular interactions further impose preferred orientation at confining surfaces. The nematic ordering of such an anisotropic liquid phase results from the interplay of these anchoring constraints with the liquid's internal elasticity, external fields and hydrodynamics, and can lead to singular points known as topological defects.

While their control by electromagnetic fields or transport within liquid crystal phases have been the focus of intense research, there is relatively little understanding yet of the motion and flow of confined liquid crystals, such as nematic droplets. Recent experiments on chemically-active swimming droplets (Figure 1) however brought some new interests to understand such intriguing systems.

To obtain some insight on the interplay of nematic ordering and hydrodynamics within confined environment, we analyse here the sedimentation properties of a nematic droplet with preferred radial anchoring resulting in a central topological defect. We compare its sedimentation velocity to that of a pure liquid droplet with similar viscosity to ascertain the competition between perpendicular-to-the-surface anchoring, elasticity and hydrodynamics. Employing the Leslie-Ericksen viscosity and elastic distortions model, we also investigate limiting behaviors pertaining to minimal viscoelastic coupling. Notably, we analyze the elastic aspect of the sedimentation by employing a director vector field description, circumventing the need for the analytically taxing order parameter tensor field description.

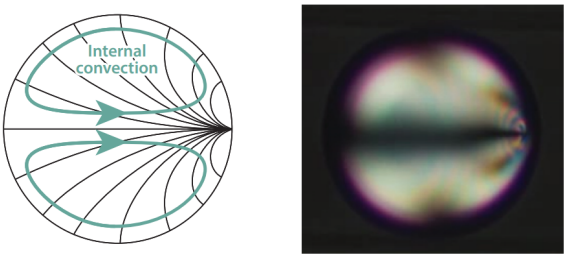

Figure 1. Self-propelling nematic droplet (moving from left to right). Schematic on the left; black lines denote the local orientation of the nematic director. Appearance between crossed polarizers on the right [1].

References

[1] Maas et al., *Ann. Rev. Cond. Matter Phys, (2016).*

Th173

Liquid-liquid dispersions within milli-scale symmetric confined impinging jets

Cong Duan[1], Panagiota Angeli[1*]
[1]*Department of Chemical Engineering, University College London, London, UK*
*p.angeli@ucl.ac.uk

Keywords: Emulsions; Small channels; Droplets; Confined Impinging Jets; Computational Fluid Dynamics

Abstract

This work presents the emulsification process of two immiscible liquids and the flow of droplets in symmetric confined impinging jets (CIJs) with two opposing outlets. A combined approach consisting of experiments based on high-speed imaging and computational fluid dynamics simulations is employed to study these complex phenomena. CIJs find numerous applications such as rapid precipitation, crystallization, and flash synthesis[1]. They are particularly favoured as they enhance mass transfer and lead to process intensification [2]. The fundamental working principle of CIJs entails the convergence of two streams of high-velocity liquids from opposite directions in a micro- or milli-scale contactor, leading to rapid mixing or emulsification of the liquids. However, the hydrodynamics at the impinging zone and the corresponding emulsion specifications, especially when the impinging jets are symmetrically configured, are still not well explored.
In this work, the flow pattern map in the downstream tubing from the impinging jets area is developed as the flow rate and dispersed phase fraction change. The instantaneous evolution of the fluid streams at the impinging zone is not directly accessible with imaging; thus, CFD simulations were used to determine the mechanism of droplet formation at the impinging zone and to study the drop size distributions in the downstream tubing. Three pairs of fluids with different viscosity ratios and interfacial tensions have been evaluated for their emulsification performance. Experimentally, the droplet size distribution was measured for both oil-in-water (O/W) and water-in-oil (W/O) emulsions using high speed imaging. The results show that drop size distributions are significantly influenced by the *Weber* and the *Reynolds* numbers of the liquid mixture. The specific interfacial area and the Sauter diameter were obtained at different operating conditions. Compared with asymmetric CIJs with only one outlet, it is found that the emulsions with symmetric CIJs have smaller droplet sizes and larger specific interfacial area at higher energy dissipation rates compared to the asymmetric ones, which makes symmetric CIJs preferred for high-throughput manufacturing and extractions. A CFD approach which utilises a model transition from Volume of Fluid to Discrete Phase Model was employed to study the mechanism of droplet formation from the continuous films. Following this approach, it is not necessary to use a very fine mesh to resolve the dispersed drops. The predicted drop sizes were found to agree well the experimental measurements.

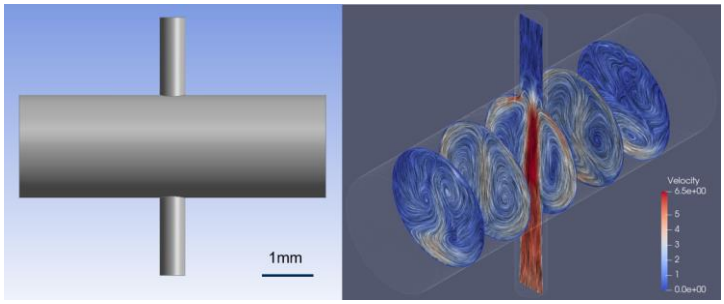

Figure 1. Schematic diagram of symmetric confined imping jets and a contour of velocity field within it.

References

[1] S.W. Siddiqui, W.A.F. Wan Mohamad, M.F. Mohd. Rozi, I.T. Norton, Continuous, High-Throughput Flash-Synthesis of Submicron Food Emulsions Using a Confined Impinging Jet Mixer: Effect of in Situ Turbulence, Sonication, and Small Surfactants, Industrial & Engineering Chemistry Research 56(44) (2017) 12833-12847. https://doi.org/10.1021/acs.iecr.7b02124.
[2] D. Tsaoulidis, P. Angeli, Liquid-liquid dispersions in intensified impinging-jets cells, Chemical Engineering Science 171 (2017) 149-159. https://doi.org/https://doi.org/10.1016/j.ces.2017.05.016.

Th174

VIOLATION OF STOKES-EINSTEIN RELATION IN A ONE-COMPONENT FLUID INTERACTING VIA MIE POTENTIAL

Saumya Suvarna, & Madhu Priya
Department of Physics, Birla Institute of Technology Mesra, Ranchi, Jharkhand, INDIA

Abstract
We investigate the role of the range of interparticle interaction on the structure and dynamics of a system of particles interacting via a Mie $(2n, n)$ potential using molecular dynamics simulations. The radial distribution function in the vicinity of the liquid-solid transition indicates a decrease in the local structural order with an increase in the range of interaction potential, while the six-fold orientational order remains almost invariant to it. We explore the dynamics of the system by computing mean-squared displacement and the self-intermediate scattering function, and further use the data to analyze the temperature dependence of the self-diffusion coefficient and the alpha-relaxation time for different interaction potentials. A temperature-dependent crossover is observed in the diffusion coefficient and the alpha-relaxation time when the range of interparticle interaction is varied. The validity of the Stokes-Einstein relation can be explored in terms of the Stokes-Einstein parameter, which is defined as the product of the diffusion coefficient, the alpha-relaxation time, and inverse temperature [1, 2]. Thus, we further investigate the Stokes-Einstein relation for the system interacting with different forms of Mie potentials and observe a deviation from it as the system approaches the liquid-solid transition temperature. The temperature dependence of the Stokes-Einstein parameter has been shown in Figure 1. The violation of the Stokes-Einstein relation also exhibits a temperature-dependent crossover as the range of interaction is varied.
Key Words: Liquid-Solid phase transition, Diffusion coefficient, Stokes-Einstein relation

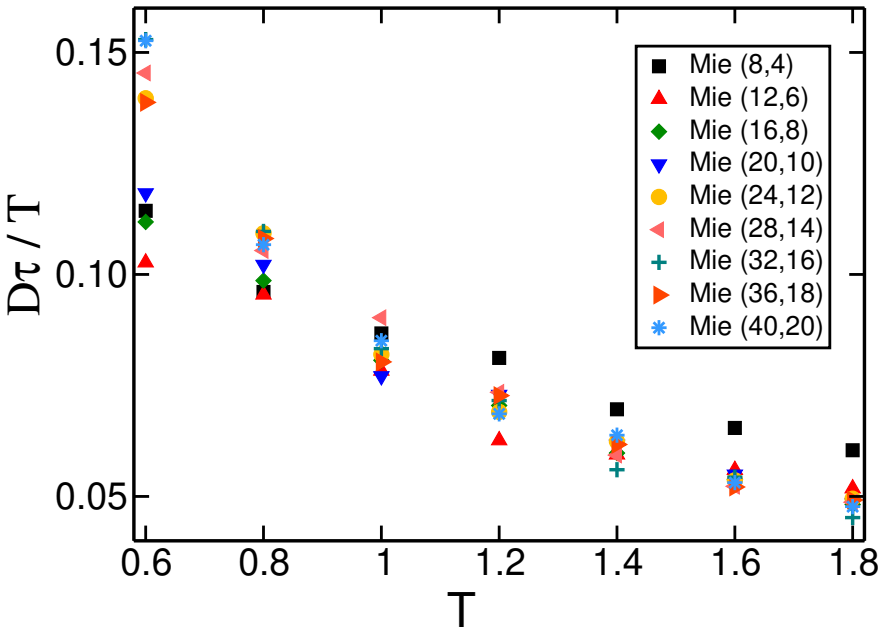

Figure 1. The Stokes-Einstein parameter $D\tau/T$ as a function of temperature T.

References

[1] Z. Shi, P. G. Debenedetti, and F. H. Stillinger, J. Chem. Phys. **138**, 12A526 (2013).
[2] B. P. Bhowmik, R. Das, and S. Karmakar, Journal of Statistical Mechanics: Theory and Experiment **2016**, 074003 (2016).

Th175

OSCILLATIONS AND INSTABILITIES IN GRANULAR SURFACE FLOWS

Satyabrata Patro[1], Soniya[2] & Anurag Tripathi[2]
[1] *R& D Division, Tata Steel Ltd., Tata Nagar, India*
[2] *Department of Chemical Engineering, Indian Institute of Technology Kanpur, Kanpur, India*

Keywords: Oscillations, Instabilities, Granular Flow, Granular Mixtures

Abstract

Granular surface flows are a common occurrence in industrial and geophysical situations. Given the frictional and inelastic nature of contacting grains comprising these systems, the energy supplied to such systems gets dissipated very quickly. In case of free surface flows under gravity, the balance of work done by gravity and energy dissipation leads to a range of inclination angles over which a steady flow is typically observed. In this work, we consider the case of free surface granular flows over an inclined surface under the influence of gravity using Discrete Element Method simulations. Two-dimensional simulation of flowing disks as well as three-dimensional simulations of spherical particles are performed at different inclination angles. While a steady fully developed flow regime is observable at lower inclination angles, we observe oscillatory flow regime at higher inclinations. These oscillatory flows are characterized by a significant slip at the base despite the roughness and bumpiness of the base. The centre of mass of the layer as well as the kinetic energy of the layer shows periodic oscillations. Despite the oscillatory nature of the flow, a recently proposed inertial number based rheological description accounting for the presence of the significant normal stress difference appears to be able to predict the steady [1] as well as transient [2] flow properties of the flow accurately. The simulations are also performed for granular mixtures differing in size/density. In the case of mixtures of grains differing in density, instabilities in the flow are observed in binary as well ternary mixtures. However, such instabilities are not observed in case of mixtures differing in size. Implications of these observations in the continuum modelling of granular mixtures will be discussed in detail.

References

[1] Satybrata Patro, Mahesh Prasad, Ayushi Tripathi, Puneet Kumar and Anurag Tripathi, *Rheology of two-dimensional granular chute flows at high inertial numbers*, Phys. Fluids, **33**, 113321 (2021).
[2] Satyabrata Patro, Anurag Tripathi, Sumit Kumar, and Anubhav Majumdar, *Unsteady granular chute flows at high inertial numbers,* Phys. Rev. Fluids **8**, 124303 (2023).

Th176

COMPETING AGGREGATION AND ISO-DENSITY EQUILIBRIUM LEAD TO BAND PATTERNS IN DENSITY GRADIENTS

Felix Maurer[1], Camila Romero[1], Nikolas Lerch[1], Thomas John[1], Lars Kaestner[1,2], Christian Wagner[1,3] & Alexis Darras[1]

[1]*Experimental Physics, Saarland University, 66123 Saarbruecken, Germany*

[2]*Theoretical Medicine and Biosciences, Saarland University, 66424 Homburg, Germany*

[3]*Physics and Materials Science Research Unit, University of Luxembourg, Luxembourg City, Luxembourg*

Abstract pattern formation, density separation, cell aggregation, red blood cells/erythrocytes

Centrifugation of erythrocytes (aka Red Blood Cells, RBCs) in self-forming percoll gradient is a protocol often used as a way to sort RBCs by age. However, a pattern formation of discrete bands is systematically observed along the continuous density gradient. Although early studies mentioned that aggregation between cells might modify their spatial distribution [1], it is debated whether a population with continuous density distribution can form discrete bands. Here, we develop a continuous equation, considering the aggregation of cells with a continuous density distribution, which describes the macroscopic evolution of RBCs concentration in a density gradient. Using numerical resolutions, we demonstrate that the competition between iso-density distribution and aggregation is sufficient to create band patterns. Our model reproduces qualitatively the temporal evolution observed in the conventional experimental protocol, but also predicts several types of bifurcation-like behaviors for the steady-state patterns in constant gradients, when the volume fraction and aggregation energy of the cells are varied. We developed an experimental protocol where a constant density gradient is formed and where the results of the model match the observed patterns. The competition between aggregation and iso-density distribution is therefore a novel physical mechanism leading to a new and rich pattern formation system..

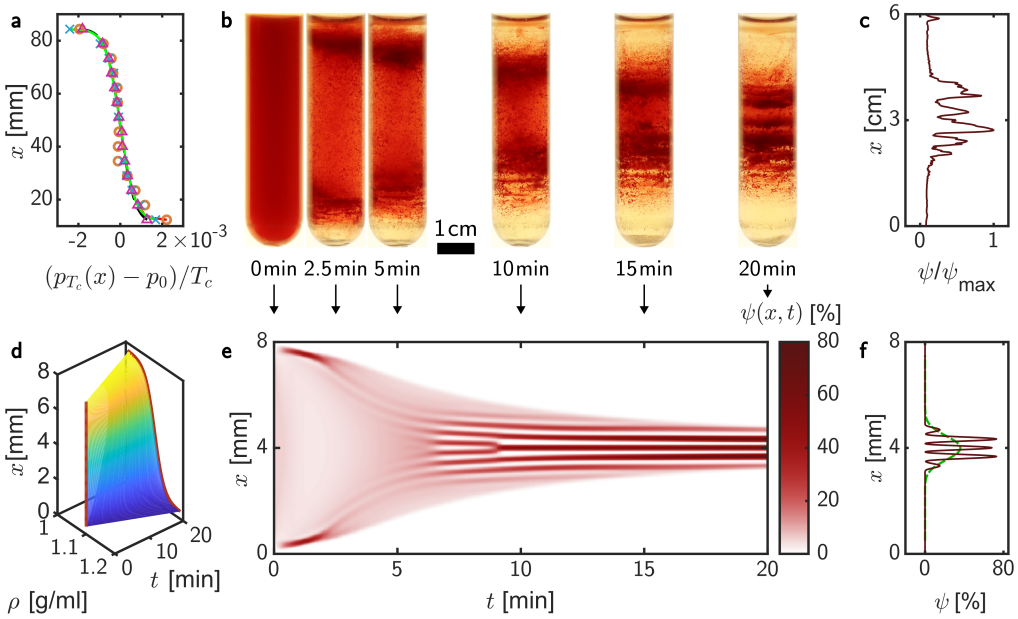

Figure 1. Lab protocol for RBC fractionation in a self-forming gradient and simulation. **a** Collapse of sigmoidal density gradients after subtraction of the average density and division by centrifugation duration T_c. **b** photographs from the separation protocol after different T_c. **c** end state of the experiment showing distinct bands. $\psi(x)$ was obtained from image profiles. **d** Gradient function adapted from regression to measurements. **d** simulation of a similar system for comparison. The system size is smaller due to numerical limitations. **e** end state of the simulation, red, and end state without interaction, green.

References

[1] F. Maurer, *et al.*, *Continuous Percoll Gradient Centrifugation of Erythrocytes—Explanation of Cellular Bands and Compromised Age Separation*, Cells **11**(8), 1296 (2022).

Th177

RED BLOOD CELL SHAPE DYNAMICS IN TIME-DEPENDENT CAPILLARY FLOW

Steffen M. Recktenwald[1], Katharina Graessel[2], Felix M. Maurer[1], Thomas John[1], Stephan Gekle[2] & Christian Wagner[1]
[1]*Department of Experimental Physics, Saarland University, Saarbruecken, Germany*
[2]*Department of Physics, University of Bayreuth, Bayreuth, Germany*

Keywords: red blood cells, microfluidics, numerical simulations, shape transitions, unsteady flow

Abstract

Blood is mainly comprised of red blood cells (RBCs) that determine the unique flow properties of blood in the circulatory system. Their high deformability allows them to squeeze through vessels much smaller than their equilibrium size. In microfluidic flows with channel dimensions similar to their size, RBCs exhibit characteristic shapes, such as croissants and slippers, depending on their confinement, velocity, and internal cell properties [1,2]. Although RBCs have been studied under steady flow conditions, knowledge about their flow behavior and shape transitions in unsteady flows remains vague.

In this study, we perform microfluidic experiments and numerical simulations to examine single-cell RBC flow under time-dependent flow conditions [3]. We use a high-precision pressure device to generate an unsteady driving of the flow in the microchannels. Additionally, we employ a customized feedback-control mechanism between the camera and the motorized microscope stage to track and follow single RBCs along the channel flow direction in a co-moving frame. Applying an increasing pressure ramp, we find that the transition from the croissant to the slipper shape is faster than the opposite shape transition at a decreasing pressure ramp (Fig. 1). Further, we observe that slipper-shaped RBCs oscillate laterally while traveling through the microchannel. The frequency of these oscillations increases with the cell velocity and viscosity of the surrounding fluid. Supported by our numerical simulations, our study reveals how the time scale of single RBC dynamics couples with the internal cell properties, such as the cytosol viscosity and membrane elasticity.

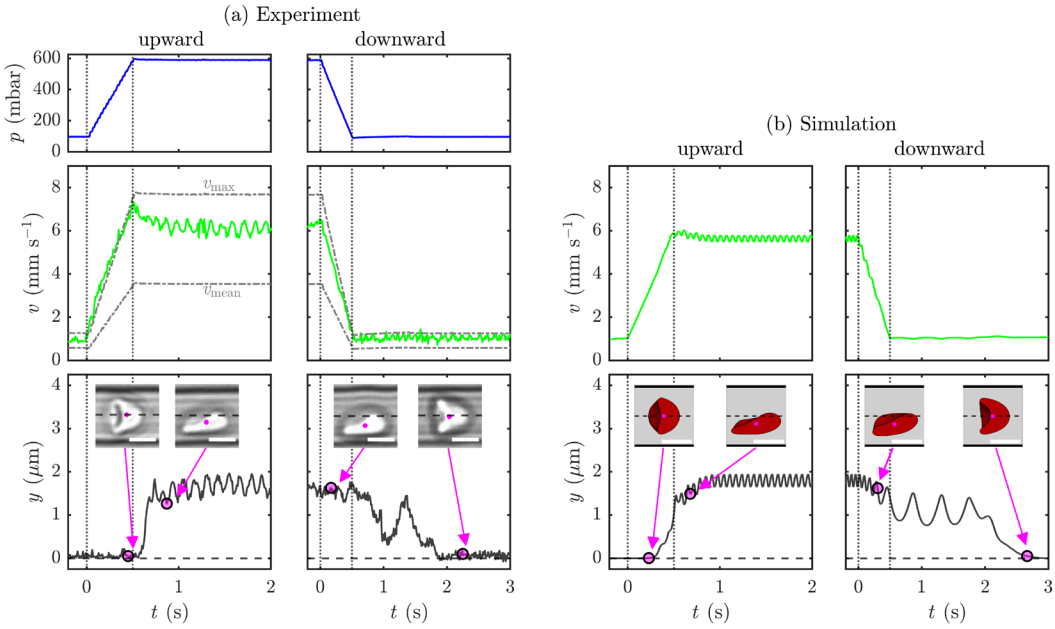

Figure 1. Dynamics of single RBCs in time-dependent flows for (a) an experiment and (b) a simulation. The left and right columns in (a) and (b) correspond to upward and downward ramps, respectively. In (a), the top panels show the applied pressure drop signal over time. The middle panels in (a) show the cell velocity as a green line. The gray dashed-dotted lines correspond to analytical solutions of the maximum and mean velocity inside the channel. Vertical dotted lines indicate the start and end of the ramps. The bottom panels in (a) and (b) show the y-coordinate of the cell's center of mass. The inset images (scale bars, 5 μm) show the cells at the start and end points of the shape transitions, highlighted by the magenta markers.

References

[1] G. Tomaiuolo, S. Guido, *Start-up shape dynamics of red blood cells in microcapillary flow*, Microvasc. Res. **82**, 35-41 (2011).
[2] M. Nouaman, *et al.*, *Effect of Cell Age and Membrane Rigidity on Red Blood Cell Shape in Capillary Flow*, Cells. **12**, 1529 (2023).
[3] S.M. Recktenwald, *et al.*, *Red blood cell shape transitions and dynamics in time-dependent capillary flows*, Biophys. J. **121**, 23–36 (2022).

Th178

IMPACT OF HOLE SIZE ON PATTERN FORMATION IN LIFTED HELE-SHAW CELLS

David Roughton-Reay, Vincent Barrioz and Prashant Agrawal

Department of Mathematics, Physics and Electrical Engineering, Northumbria University, Ellison Building, Newcastle upon Tyne, NE1 8ST, United Kingdom

Keywords:

Hele-Shaw cells, Saffman-Taylor instability, liquid-air interface, multiscale features, charge transport.

Abstract

A Hele-Shaw cell consists of a liquid sandwiched between two parallel plates at a fixed separation distance. When one plate is lifted from the other, a pressure differential is created which forces ambient air into the liquid. As the liquid recedes, a Saffman-Taylor instability develops at the liquid-air interface, which evolves into long fingers, leaving a branched liquid pattern behind [1]. Control over the branching pattern can be achieved by strategically introducing asymmetry in one of the plates and controlling air entry points, for example, through the addition of holes [2]. By controlling the path of air in this Hele-Shaw cell, the pattern formed by the liquid can be controlled [2].

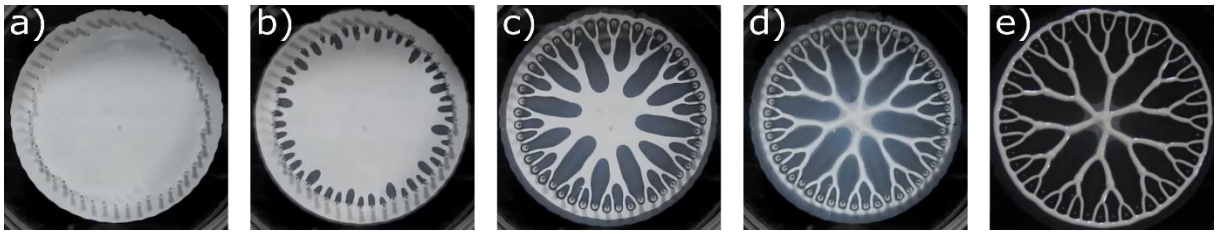

Figure 1. A time-sequence of pattern formation in a lifted Hele-Shaw cell, where holes at the perimeter of the spread radius control the formation of air fingers. a) A liquid is squeezed between two plates. b) One plate is lifted while the other remains stationary to allow air to preferentially displace the liquid through the holes. c) Air displacing the liquid towards its centre, leaving branches in its wake. d) Final stages of plate separation, where the displaced liquid is confined into multiscale branches. e) Final pattern produced showing multiple generations of branches [2].

In this work, the effect of single holes (varying in size) on pattern formation is investigated experimentally. A hole is drilled in the centre of one of the plates, which introduces another liquid-air interface that initiates air fingers from the centre to the outer liquid-air interface. The two air fingers create a ring of liquid at a radial distance between the outer liquid-air interface and the central hole. The height, width and inner radii of the ring is characterised for different hole sizes, separation distances and lift speeds.

By understanding the effect of hole sizes on pattern formation, strategies can be developed to precisely control the air finger formation, producing controlled multiscale features. Such methods could be used to mimic leaf venation patterns, utilizing their efficient nutrient transport properties for applications in charge, heat and mass transport while providing an aesthetic benefit.

References

[1] P. Saffman and F. Sir G. Taylor, *The penetration of a fluid into a porous medium or hele-shaw cell containing a more viscous liquid*, 20, (1958).

[2] T. u. Islam and P. S. Gandhi, *Viscous fingering in multiport hele shaw cell for controlled shaping of fluids*, Scientific Reports, 7, 9, (2017).

Th179

ELASTOCAPILLARY PHENOMENA INSIDE BIOLOGICAL CELLS

Halim Kusumaatmaja[1,2], Alexander Brown[2], Xiaotian Ma[1,2], Lorenzo Frigerio[3] & Roland Knorr[4]
[1]*Institute for Multiscale Thermofluids, University of Edinburgh, Edinburgh, UK*
[2]*Department of Physics, Durham University, Durham, UK*
[3]*School of Life Sciences, University of Warwick, Coventry, UK*
[4]*Institute of Biology, Humboldt University of Berlin, Berlin, Germany*

Keywords: Droplet, Interfacial Phenomena, Wetting, Biomolecular Condensates, Lipid Membranes

Abstract

Biomolecular condensates are liquid droplets comprising of proteins and RNAs that are formed via cellular phase separation processes, and they are increasingly recognised to play major roles in cellular organisation [1,2]. Here, we show how the interactions between biomolecular condensates and lipid membranes inside biological cells can lead to elastocapillary phenomena important for cellular functions. We will highlight two phenomena which we have studied using a combination of theoretical modelling, live-cell observations, and in vitro experimental model systems. First, during seed development of the plant Arabidopsis thaliana, micrometer-sized condensate droplets form within the vacuolar lumen and wet the tonoplast membrane (Figure 1(a)) [3]. Distinct tonoplast shape changes and instabilities arise in response to membrane wetting by condensate droplets. Conditions of low membrane spontaneous curvature and moderate wettability favour droplet-induced membrane budding, whereas high membrane spontaneous curvature and strong wettability promote membrane nanotubes that sit at the condensate interface. Second, recent observations on the mitochondria of HeLa cells show that condensate droplets can form capillary bridges between two opposing lipid membranes. Interestingly, the interplay between the condensate surface tension and membrane elasticity leads to several distinct morphologies, which we term bridging, enclosing and zipping (Figure 1(b)). We hypothesise that the zipping morphology may play a crucial biological role for bringing two membranes into close contacts.

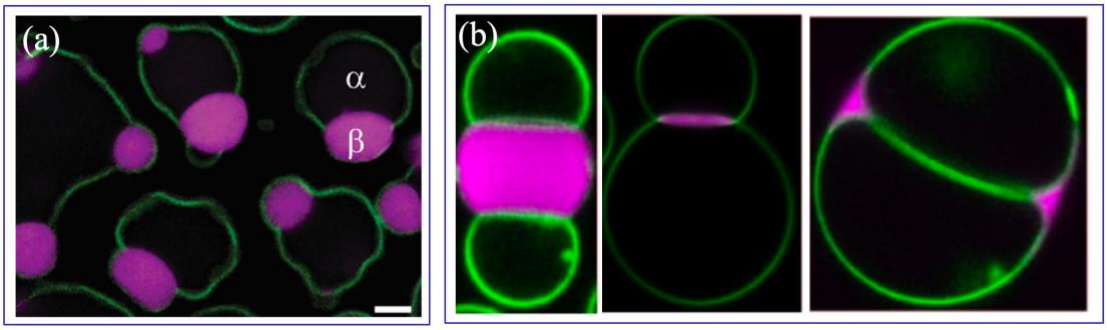

Figure 1. (a) Condensate droplets wetting on tonoplast membranes of plant vacuoles. (b) Condensate droplets form capillary bridges between two lipid membrane vesicles, leading to several distinct morphologies.

References

[1] Y. Shin, C. P. Brangwynne, *Liquid phase condensation in cell physiology and disease*, Science **357**, eaaf4382 (2017).
[2] H. Kusumaatmaja, A. I. May, R. L. Knorr, *Intracellular Wetting Mediates Contact between Liquid Compartments and Membrane-Bound Organelles*, J. Cell Biol. **220**, e202103175 (2021).
[3] H. Kusumaatmaja, A. I. May, M. Feeney, J. F. McKenna, N. Mizushima, L. Frigerio, R. L. Knorr, *Wetting of Phase-Separated Droplets on Vacuole Membranes Leads to A Competition between Tonoplast Budding and Nanotube Formation*, PNAS **118**, e2024109118 (2021)

Th180

CFD Analysis of Stenosed Artery and Plaque Rupture Risk Stratification using In-House CFfSI Solver

A. Lagwankar[1], S. Morab[1], J. Muralidharan[1] and A. Sharma[1]
Corresponding author: atharva.lagwankar@iitb.ac.in
[1]*Department of Mechanical Engineering, Indian Institute of Technology Bombay*

Keywords: CFD, FSI, Hemodynamics, Stenosis, Plaque Rupture Risk Stratification

Abstract

An arterial stenosis is the narrowing of an artery, usually caused by the build-up of fats, cholesterol and other substances in and on the artery walls, known as atherosclerosis. Over 20% of ischemic strokes are thrombotic in nature [2], stemming from blood clots generated over the ruptured plaque. Timely diagnosis of stenosis can be critical in this regard. This study explores a novel approach to diagnose arterial stenosis by correlating external acoustic patterns (arterial bruits) [3] with computational simulations using an in-house Finite Volume Method-based Computational Fluid-Structure Interaction (CFfSI) solver [4]. Traditional diagnostic methods, such as ultrasound or MRI, can be time-consuming and invasive. By simulating blood flow in stenosed arteries and assessing plaque rupture risk through Von-Mises Stress and Wall Shear Stress calculations, the study aims to establish a correlation between computed critical conditions [1] and external acoustic signals. This correlation could provide a non-invasive and timely means of diagnosing arterial stenosis and assessing plaque rupture risk during various physical activities [5]. A comprehensive study and risk stratification will be obtained for a range of degrees of stenosis and blood flow rates.

The Figure 1. shown below demonstrates the magnitude response of the Integrated Pressure Force Rate (IPFR) for blood flow in a flexible stenosed artery with 50% blockage and normal blood flow rates [5]. The blood is assumed to be a Newtonian and homogenous fluid, a valid assumption as seen in past studies [3]. The cut-off frequency (~88 Hz here) obtained can be comprehended by physicians and help in timely diagnosis of arterial stenosis. Hence, a stratified plaque rupture risk for a range of degrees of stenosis and blood flow rates is imperative in early non-invasive diagnosis.

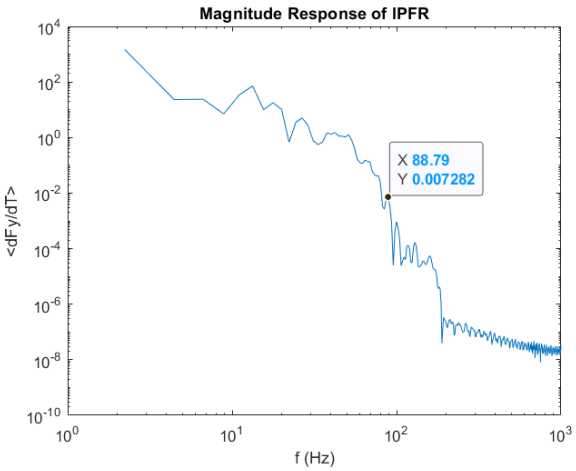

Figure 1. Magnitude Response of the Integrated Pressure Force Rate (IPFR)

References

[1] Li, Z. Y., Taviani, V., Tang, T., Sadat, U., Young, V., Patterson, A., Graves, M., & Gillard, J. H. (2009). The mechanical triggers of plaque rupture: shear stress vs pressure gradient. The British journal of radiology, 82 Spec No 1, S39–S45. https://doi.org/10.1259/bjr/15036781
[2] Pu, L., Wang, L., Zhang, R., Zhao, T., Jiang, Y., & Han, L. (2023). Projected Global Trends in Ischemic Stroke Incidence, Deaths and Disability-Adjusted Life Years From 2020 to 2030. Stroke, 54(5), 1330-1339. doi:10.1161/STROKEAHA.122.040073
[3] Seo, J.H., Mittal, R. (2012) A coupled flow-acoustic computational study of bruits from a modeled stenosed artery. Med Biol Eng Comput 50, 1025–1035. https://doi.org/10.1007/s11517-012-0917-5
[4] S Morab, A Sharma, J Murallidharan, (2023) Fully Finite Volume Method on a Curvilinear Grid-Based Arbitrary Lagrangian Eulerian Approach for Computational Fluid flexible-Structure Interaction
[5] Yang, S., Wang, Q., Shi, W. et al. Numerical study of biomechanical characteristics of plaque rupture at stenosed carotid bifurcation: a stenosis mechanical property-specific guide for blood pressure control in daily activities. Acta Mech. Sin. 35, 1279–1289 (2019). https://doi.org/10.1007/s10409-019-00883-w

Th181

DYNAMICS OF MUCUS FILMS IN CILIATED LUNG AIRWAYS

Swarnaditya Hazra[1] & Jason R. Picardo[1]
[1]*Department of Chemical Engineering, Indian Institute of Technology Bombay, Mumbai, India*

Abstract Cilia-driven transport can prevent airway blockage by mucus plugs, despite the Rayleigh-Plateau instability, but within limits (interfacial instability, thin films, reduced-order modelling).

The healthy functioning of mucus-bearing airways (inset of Fig. 1a) is potentially compromised by the capillary-driven Rayleigh-Plateau instability that prevents the annular mucus film from staying uniform and instead causes it to form bulging lobes. If the lobes grow too large, then they can form a liquid bridge that blocks the flow of air. Several studies have analysed airway blockage [1] and shown how liquid-bridge formation is affected by airflow [2], viscoelasticity and surfactants [3]. Here we investigate how blockage is altered by the presence of cilia. In particular, we consider a finite airway (as opposed to an infinite periodic domain) with a constant input of mucus and an outlet boundary condition that allows cilia to evacuate the mucus. Can a dynamically-stable film be maintained? And if so, how is this stability affected by the cilia beat-rate, the mucus volume fraction, and other system properties?

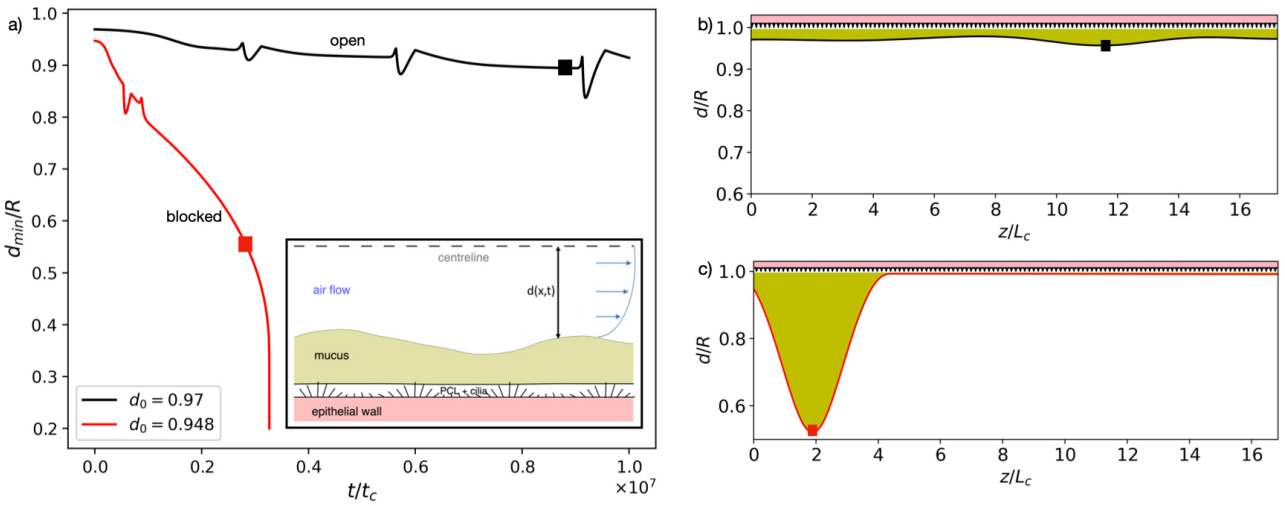

Figure 1. (a) The inset shows a schematic of the ciliated airway with its mucus film, and the main panel traces the evolution of the minimum distance of the mucus from the centreline, $d_{\min}$, which approaches zero in a blockage scenario. Here, the mucus input rates is set so as to produce a base state with a uniform $d = d_0$. The red line corresponds to a slightly larger flow rate than the black line; snapshots of the respective interface profiles are shown in panels (b) and (c).

To answer these questions, we use the second-order WRIBL (Weighted-Residual Integral Boundary Layer) thin-film model for the coupled flow of mucus and air [2] and incorporate the effect of cilia via a coarse-grained boundary condition [4, 5] at the bottom of the mucus layer. This open-domain system admits a steady flat-film base state in which the constant input of mucus is balanced by cilia-induced transport and evacuation. Infinitesimal perturbations destabilize this state, however, and produce growing and translating lobes. Our results show that if the input (or secretion) rate of mucus is low, then the cilia is able to evacuate the lobes and keep the airway open (see Fig. 1a, black line). There is a critical input rate, however, beyond which this is no longer possible—strong capillary forces cause all incoming mucus to stay trapped in an ever growing lobe, near the inlet, that ultimately blocks the airway (see Fig. 1a, red line). Importantly, the critical volume fraction for blockage is less than that predicted by equilibrium calculations for a closed domain without cilia [6]; we calculate this critical volume and examine its dependence on the properties of the cilia and mucus.

References

[1] Levy R., Hill D.B., Forest M.G., Grotberg J.B., *Integr. Comp. Biol.* **54**:985–1000, 2014.
[2] Dietze G.F., Quil C.R., *J. Fluid Mech*, **762**:68–109, 2015.
[3] Halpern D., Hideki F., Grotberg J.B., *Phys. Fluids*, **22.1** :011901, 2010.
[4] Vasquez P. A., Jin Y., Palmer E., Hill D., Forest M.G., *PLoS Comput. Bio*, **12.8**:e1004872, 2016.
[5] Choudhury A., Filoche M., Ribe N.M., Grenier N., Dietze G. F. *J. Fluid Mech.*, **971**:A33, 2023.
[6] Everett D.H., Haynes J.M., *J. Colloid Interface Sci.* **38.1**:125–137, 1972.

Th182

ROLE OF ASYMMETRIC ACINAR WALL MOTION ON THE PARTICLE TRANSPORT IN THE LUNG ACINUS

Prabhash Kumar, Prahallada Jutur, Anubhab Roy & Mahesh Panchagnula
Department of Applied Mechanics, Indian Institute of Technology Madras, Chennai, India

Abstract In this study, we report an experimental and numerical investigation to study the role of asymmetry in the acinar wall's expansion-contraction on particle transport in lung acinus. The experimental setup consists of a T-section; two arms connect to two independent programmable stepper motors, which drive the syringe-piston system to rhythmically infuse and withdraw the fluid to mimic the inhalation and exhalation processes, and the third arm is left open to the atmosphere. The dye pattern injected at the T-junction is stretched, folded and regularly returns to the initial state at symmetric piston motion ($\phi = 0^\circ$). In this case, the phased-locked images (images taken at intervals of one oscillation) are almost identical for all Sr, indicating no mixing (Sr is nondimensional oscillation frequency). However, the differential piston velocity arises at even a small non-zero ϕ, which exhibits an additional clockwise rotation in the flow field, breaking the flow periodicity. For lower ϕ values, say $\phi = 10^\circ$, we observe the buckling in the dye, which folds on each other in a nice regular fashion with increasing the number of cycles N and a structure is formed with various layers of dye lamina stacked on top of each other, having a finite gap between them at the end of 50 cycles. However, on increasing ϕ to 70°, the structure becomes significantly complex, which comprises an irregular and buckled set of layers that merge into each other and the structure at $N = 50$ is well-mixed on the scale of the image, as shown in Figure 1. At some optimum ϕ, we observe the appearance of space-filling features in layers of dye on increasing N, which breaks both periodicity and regularity. Once periodicity breaks at certain non-zero ϕ, even decreasing Sr adds more and more irregularities in the deformation. We formally quantify these distinctions by calculating the line length of the dye from the data from the tracer particle simulation and compute the finite time Lyapunov exponent (FTLE) fields [1, 2] to visualise the coherent structures. The increase in line length is exponential for $70^\circ \leq \phi \leq 150^\circ$ at $Sr = 0.5$, indicating the onset of chaos and the span of ϕ for exponential growth increasing on reducing Sr, implying that at $Sr = 0.25$, the exponential growth occurs for $30^\circ \leq \phi \leq 170^\circ$. We indicate the region of chaotic and nonchaotic behaviour of particle motion in Figure 2 (a) by visually inspecting the experimental data and calculating the Lyapunov exponents from the simulation data. The particle motion at the two extreme ends of the ϕ axis ($\phi = 0^\circ$ and $\phi = 180^\circ$) is always nonchaotic and periodic irrespective of Sr. We find Chaotic behaviour as we move down on the Sr axis. The span of chaotic behaviour on the ϕ axis increases on reducing Sr and is constrained by the extreme points. We calculate the quantity $\Delta L/L\Delta N$ from the line length to represent exponential and nonexponential growth, which scale as N^{-1} for the nonexponential case, which appears as a straight line on the log-log plot as shown in the in Figure 2 (b). In this case, the intercept of the ordinate axis gives information on the exponent of power-law growth. For the exponential growth, $\Delta L/L\Delta N$ attain a constant value equal to the Lyapunov exponent, as shown in Figure 2 (c).

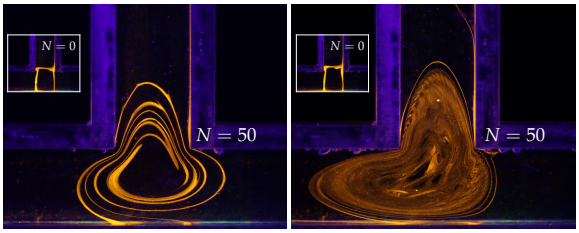

Figure 1: The Poincaré maps of experiential images at $N = 50$. The left panel corresponds to $\phi = 10^\circ$ and $Sr = 0.5$, and the right one corresponds to $\phi = 70^\circ$ and $Sr = 0.5$. The left insets in each panel show the corresponding initial dye configuration.

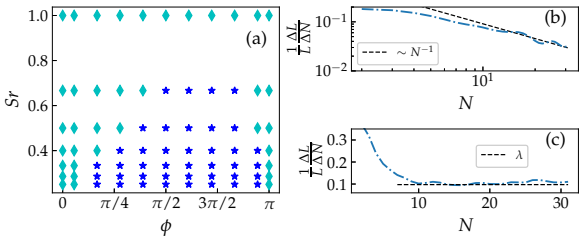

Figure 2: (a) The regime plot of Sr Vs ϕ indicates the regions of nonchaotic and chaotic advection of tracers. Here, the symbol represents the nonchaotic aperiodic advection and $*$ indicates the chaotic advection. Figures (b) and (c) plot $\frac{1}{N}\frac{\Delta L}{\Delta N}$ as a function of N for a non-chaotic case ($\phi = 10^\circ$, $Sr = 0.5$) and chaotic case ($\phi = 70^\circ$, $Sr = 0.5$), respectively. λ is the Lyapunov exponent of the corresponding chaotic case.

References

[1] Shawn C Shadden, Francois Lekien, and Jerrold E Marsden. Definition and properties of lagrangian coherent structures from finite-time lyapunov exponents in two-dimensional aperiodic flows. *Physica D: Nonlinear Phenomena*, 212(3-4):271–304, 2005.

[2] George Haller. Lagrangian coherent structures. *Annual review of fluid mechanics*, 47:137–162, 2015.

Th193

Thermoelectric convection in microgravity environment

Innocent Mutabazi[1], Changwoo Kang[2], Elhadj B. Barry[1] & Harunori Yoshikawa[3]
[1]*LOMC, UMR 6294, CNRS-Université Le Havre, Normandie Université, Le Havre, France*
[2]*Department of Mechanical Engineering, Jenobuk National University, Jeonju, Republic of Korea*
[3] *Institut de Physique de Nice, UMR 7210, Université de Côte d'Azur, Nice, France*

Keywords:thermoelectric conection, microgravity, electric gravity, Nusselt number

Abstract

We investigate the conditions of triggerring thermal convection in a dielectric liquid subject to a temperature gradient and a high-frequency electric field. The temperature gradient generates an inhomogeneity in the liquid permittivity. The gradient of the permittivity coupled to the electric field yields a dielectrophoretic force [1] whose non-conservative part plays the role of a buoyancy force associated with an electric gravity $\vec{g}_e$ [2]. The magnitude of the electric gravity is proportional to the square of the effective electric tension.
This electric buoyancy can be used to generate natural convection in microgravity environment such as the International Space Station (ISS) where the effective gravity is of the order of 10^{-6}g [3]. It can also be used for heat exchange in small-size systems such as microfluidic circuits where the natural convection would require large temperature gradients which may damage the circuits. We will show that both in parallelepipedic and cylindrical annular cavities, above a critical value of the applieed effective electric tension, thermoelectric convective structures are generated and their dynamics becomes complex as the electric tension is increased. The heat transfer coeffcient is evaluated and it is shown that for fixed temperature gradient, there is a significant increase of the Nusselt number (Nu), within the limitations imposed by the breakdown potential of the dielectric liquids. These DNS studies are complementary to experiments performed either in parabolic flight experiments on board of zero-g airbus or on Sounding Rocket [5].

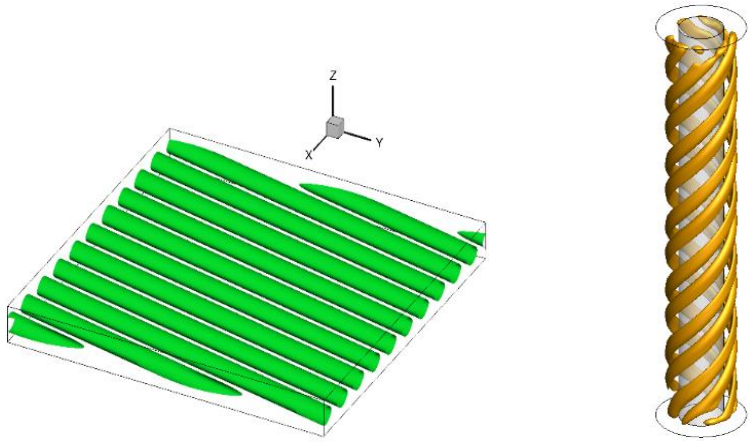

a) b)

Figure : Thermoelectric convective structures under microgravity : a) in parallepipedic, b) in a cylindrical annulus

Acknowledgements

The present work is supported by the French Spatial Agency (CNES) and the French-Korean bilateral exchange program STAR.

References

[1] L.L. Landau & E.M. Lifshitz, *Electrodynamics of Continuous Media*, Pergamon Press (1989)
[2] I. Mutabazi *et al*., *Fluid. Dyn. Res*. **48**, 061413 (2006).
[3] B. Futterer *et al*., *J. Fluid Mech*. **735**, 647-683 (2013).
[4] C. Kang & I. Mutabazi, *J. Fluid. Mech*. **908**, A26 (2021)
[5] A. Meyer, A. Meier, V. Motuz &C. Egbers, *J.Fluid Mech.* **972**, A26 (2023).

Th194

FINITE-AMPLITUDE SOLUTIONS & MULTISTABILITY IN MAGNETOCONVECTION

Matthew McCormack[1], Andrei Teimurazov[2], Olga Shishkina[2] & Moritz Linkmann[1]
[1]*School of Mathematics and Maxwell Institute for Mathematical Sciences, University of Edinburgh, Edinburgh, UK*
[2]*Max Planck Institute for Dynamics and Self-Organization, Göttingen, Germany*

Keywords: magnetoconvection, multistability, subcritical transition

Abstract
In magnetoconvection subjected to a fixed vertical magnetic field with impenetrable, insulating boundaries, the motionless conducting state becomes linearly unstable at a critical value of the dimensionless temperature difference given by the Rayleigh number Ra. This linear instability has been thought to be connected to solutions at higher supercriticalities. In this talk, we will present recent direct numerical simulation results which suggest that many previously observed solutions (numerical and experimental) of magnetoconvection [1–5] exist on a solution branch which is disconnected from the branch stemming from the bifurcation point of the linear instability, and possesses a different kind of symmetry. This disconnected upper branch solution extends beneath the stability threshold of the linear stability theory, meaning that stable finite-amplitude subcritical convective solutions can be obtained in this system. Furthermore, we will show that solutions on this upper branch can display hysteretic behaviour by varying Ra or the magnetic field strength Ha, leading to the formation of multiple attracting solutions (a middle and upper branch) for fixed Ra and Ha, distinguished by their kinetic energy and by large-scale structure formation. This bistability persists to high Ra, an example of which is shown below in Figure 1, highlighting the difference in the mean flow of the two solutions.

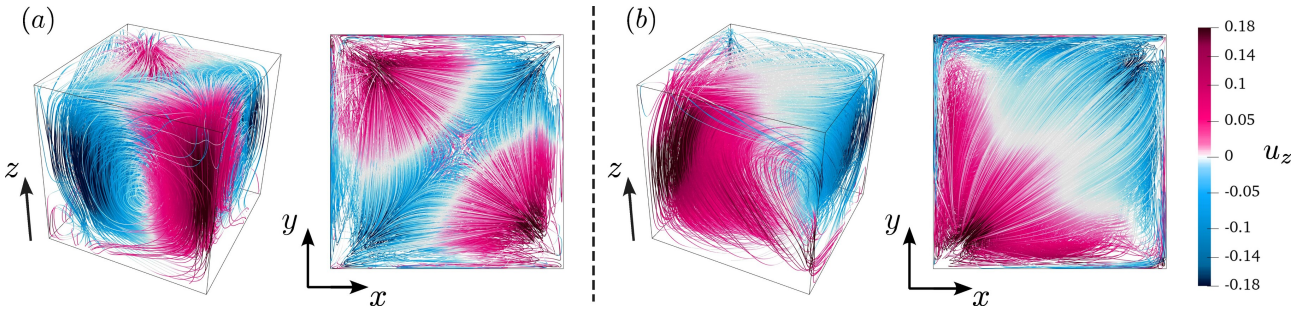

Figure 1. Mean flow of two different attracting solutions at $Ha = 500, Ra = 1 \times 10^9$. (a) middle branch solution with cellular pattern, (b) upper branch solution with large-scale roll pattern. Streamlines are coloured by the veritcal velocity u_z.

References

[1] W. Liu, D. Krasnov, and J. Schumacher. Wall modes in magnetoconvection at high Hartmann numbers. *J. Fluid Mech.*, 849:R21–R212, 8 2018.

[2] T. Zürner, F. Schindler, T. Vogt, S. Eckert, and J. Schumacher. Flow regimes of Rayleigh–Bénard convection in a vertical magnetic field. *J. Fluid Mech.*, 894:A21, 2020.

[3] R. Akhmedagaev, O. Zikanov, D. Krasnov, and J. Schumacher. Turbulent Rayleigh–Bénard convection in a strong vertical magnetic field. *J. Fluid Mech.*, 895:R4, 2020.

[4] Y. Xu, S. Horn, and J. M. Aurnou. Transition from wall modes to multimodality in liquid gallium magnetoconvection. *Phys. Rev. Fluids*, 8:103503, 2023.

[5] M. McCormack, A. Teimurazov, O. Shishkina, and M. Linkmann. Wall mode dynamics and transition to chaos in magnetoconvection with a vertical magnetic field. *J. Fluid Mech.*, 975:R2, 2023.

Th195

EXPLORING STATE SPACE PATHWAYS LEADING TO SPIRAL DEFECT CHAOS

Chi Hin Chan[1], Mohammad Z. Hossain[1,2], Spencer J. Sherwin [1] & Yongyun Hwang[1]
[1]*Department of Aeronautics, Imperial College London, United Kingdom.*
[2]*Department of Mechanical and Materials Engineering, University of Western Ontario, Canada.*

Abstract Rayleigh-Bénard convection, linear stability, pattern formation

The intrinsic bistable system between a chaotic state (spiral defect chaos - SDC, fig. 1a), and stationary states (ideal straight rolls - ISRs, fig. 1b) of Rayleigh-Bénard convection in a large extended domain ($\Gamma \geq 40$, where Γ is the aspect ratio of the domain) is well established. [1, 2].

In this study, we aim to isolate the localised features of SDC via a minimal domain, and identify the state-space pathways leading to SDC. By reducing the computational domain systematically, we have identified various stable states referred to as elementary states. Remarkably, these elementary states are statistically and visually similar to SDC. Next, we performed numerical experiments along the unstable manifolds of ISRs outside of the boundaries of the Busse balloon to identify the state-space structure. Near the Busse balloon, a network of heteroclinic orbits connecting unstable ISRs and stable ISRs were identified. On the other hand, integrating along some unstable manifolds of ISRs far from the Busse balloon led to a transient chaotic state before settling into an elementary state. An additional numerical experiment along the same unstable manifold in an extended domain led to a prolonged chaotic state. This suggests that the unstable ISRs sit on the state-space boundary between stable ISRs and SDC, providing a state-space pathway to SDC in an extended domain.

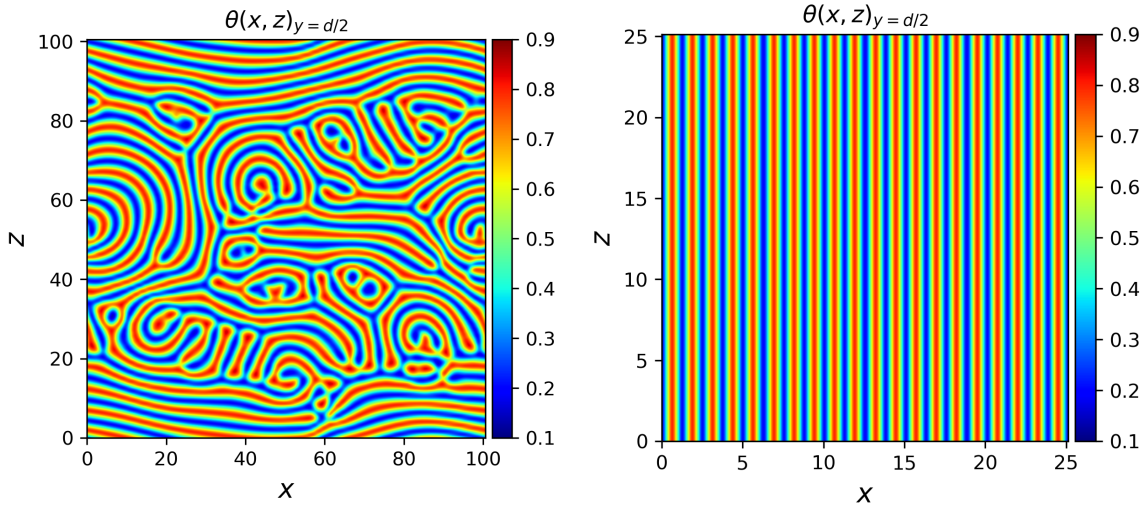

(a) Spiral defect chaos (SDC)

(b) Ideal Straight Rolls (ISRs)

Figure 1: Bistable system between SDC (a) and ISRs (b) in Rayleigh-Bénard convection at $Ra = 2900$.

References

[1] Bodenschatz E, Pesch W, Ahlers G, *Recent developments in Rayleigh-Bénard convection*, Annual Review of Fluid Mechanics **32**(1), 709-778 (2000).

[2] Cakmur RV, Egolf DA, Plapp BB, Bodenschatz E, *Bistability and competition of spatiotemporal chaotic and fixed point attractors in Rayleigh-Bénard convection*, Physical Review Letters **79**(10), 1853 (1997).

Th196

3D magneto-convective instabilities of liquid metal flow in a rectangular cavity with a coaxial circular cooling pipe

B. Lyu, L. Bühler, C. Koehly, C. Mistrangelo
Karlsruhe Institute of Technology, Postfach 3640, 76021 Karlsruhe, Germany

Keywords: Magnetohydrodynamics (MHD), liquid metal breeder blankets, magneto-convection, volumetric heating

Abstract

A water-cooled lead-lithium breeding blanket has been selected as one of the test blanket modules for the International Thermonuclear Experimental Reactor (ITER). In this blanket concept, the heat released by neutron collisions is removed by water-cooled pipes immersed in the liquid eutectic lead-lithium alloy (PbLi) that serves as breeder material and heat transfer medium. Temperature gradients that develop in the liquid metal drive a buoyant motion while Lorentz-forces caused by flow-induced currents oppose the flow. A general understanding of these complex 3D magnetohydrodynamic (MHD) phenomena is essential to assess the feasibility of liquid metal blankets. Therefore, it is proposed to study the convective MHD flow in a generic model geometry featuring a long rectangular cavity with a coaxial circular cooling pipe maintained at constant temperature with imposed volumetric heating in the fluid. The magneto-convective flow is characterized mainly by a balance between the driving buoyant force, quantified in terms of the nondimensional Grashof number *Gr*, and the braking Lorentz force expressed by the Hartmann number *Ha*.

Previous numerical simulations [1] with assumed fully established conditions along the axial direction revealed a magneto-convective motion in transverse planes where a cold plume “falls down” below the cooling pipe (Fig. 1a). It has been shown that such flows could become unstable at sufficiently high Grashof numbers. With increasing magnetic field, the present 3D study finds a bifurcation and transition from the formerly 2D state towards complex 3D flow patterns with convection rolls aligned preferentially with the transverse horizontal magnetic field (Fig. 1b and 1c). The competition between buoyancy forces promoting the convection and electromagnetic forces suppressing the flow becomes evident by the variation of the heat flux in terms of the Nusselt number *Nu* as a function of *Gr* and *Ha*.

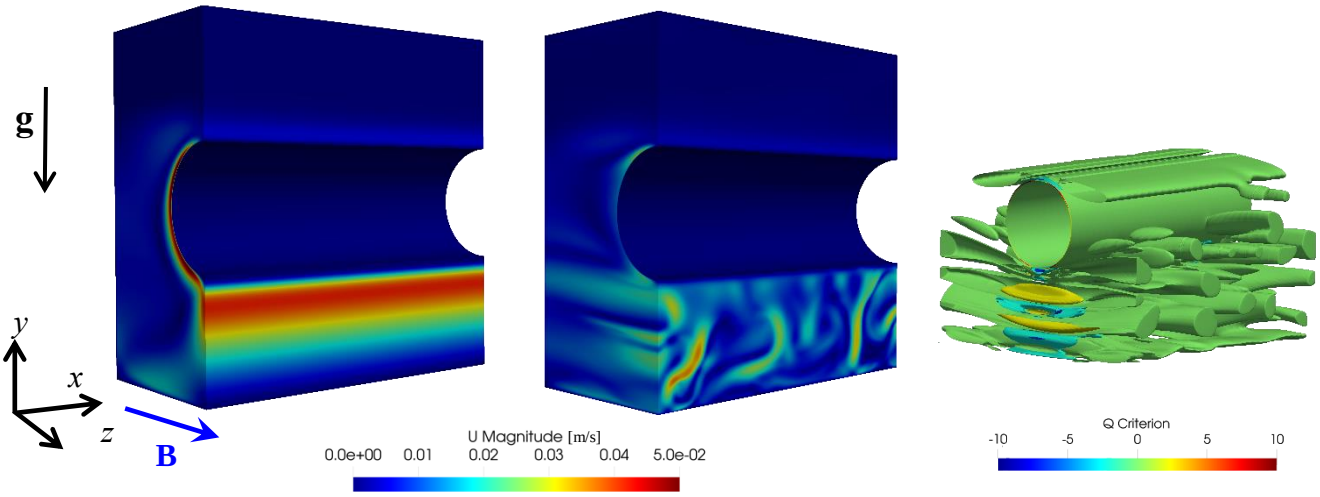

a) *Ha* = 200, *Gr* = 3.2×10^9 b): *Ha* = 500, *Gr* = 3.2×10^9 c): *Ha* = 500, *Gr* = 3.2×10^9

Figure 1: Velocity field in the cavity. a) *Ha* = 200, the convective flow remains uniform in the axial direction. b) *Ha* = 500, instability occurs with convection rolls preferentially aligned with magnetic field lines. c): Visualization of vortices by isosurfaces of Q criterion.

References

[1] C. Mistrangelo, L. Bühler and C. Koehly, "Considerations on magneto-convective flows in model geometries relevant for fusion applications," in Proceedings of the 11th International PAMIR Conference - Fundamental and Applied MHD, July 01 - 05, 2019, Reims, France, 2019, pp. 7-11.

Th197

SOLUTAL CONVECTION IN LIQUID METAL AND MOLTEN SALT BATTERIES

Tom Weier[1], Carolina Duczek[1], Steffen Landgraf[1], Paolo Personnettaz[1,2,3] & Norbert Weber[1]
[1]*Institute of Fluid Dynamics, Helmholtz-Zentrum Dresden-Rossendorf, Dresden, Germany*
[2]*Institut des Sciences de la Terre, Université Grenoble Alpes, Grenoble, France*
[3]*Centre National d'Etudes Spatiales, Paris, France*

Abstract Solutal convection in the electrolyte of molten salt and the cathode of liquid metal batteries is discussed (convection, onset).

Liquid metal (LMB) [1], e.g. Li-Bi, and molten salt (MSB), e.g. Na-$ZnCl_2$, batteries consist of two layers of liquid metals interspaced by one (LMBs) or two (MSBs) fused salt layers in stable density stratification. This conceptually very simple and self-assembling structure has the advantage to allow for an easy scale-up at the cell level. While mass transport in most modern battery systems is typically dominated by diffusion and migration in micrometer-scale liquid layers and solids, convection - with the exception of redox-flow batteries - rarely plays a role. This is in stark contrast to LMBs and MSBs where - mediated by the fully liquid interior - fluid flow can be driven by various mechanisms and might affect cell performance and operational safety [2]. Electric currents and heat and mass transfer are tightly coupled with the cells' electrochemistry.

The contribution at hand concentrates on the role of solutal convection that is responsible for markedly different mass transport overpotentials during charge and discharge of LMBs [3]. In the discharged state, the positive electrode consists of a Li(Bi) alloy. When charging the cell, low density Li is removed from the top of the positive electrode. This increases locally the density of the alloy and Li-depleted fluid starts to sink down in plumes. Rapidly, solutal convection drives a flow in the whole cathode and intensely mixes the remaining alloy, see Fig. 1. The initial stage of the process is the diffusion controlled buildup of a layer of high density fluid that becomes unstable akin to a Rayleigh-Taylor instability [4]. Scaling laws for the onset time and the Péclet as well as the Sherwood number in dependence of the Rayleigh number will be discussed [5].

In MSBs solutal convection occurs in the molten salt layers. During charge, stratification in the anolyte becomes unstable, during discharge it is the catholyte where motion sets in first. In the other cell area, stable stratification builds up so that penetrative convection can be observed in both periods.

Acknowledgments
This project has received funding from the European Union's Horizon 2020 research and innovation programme under grant agreement No 963599.

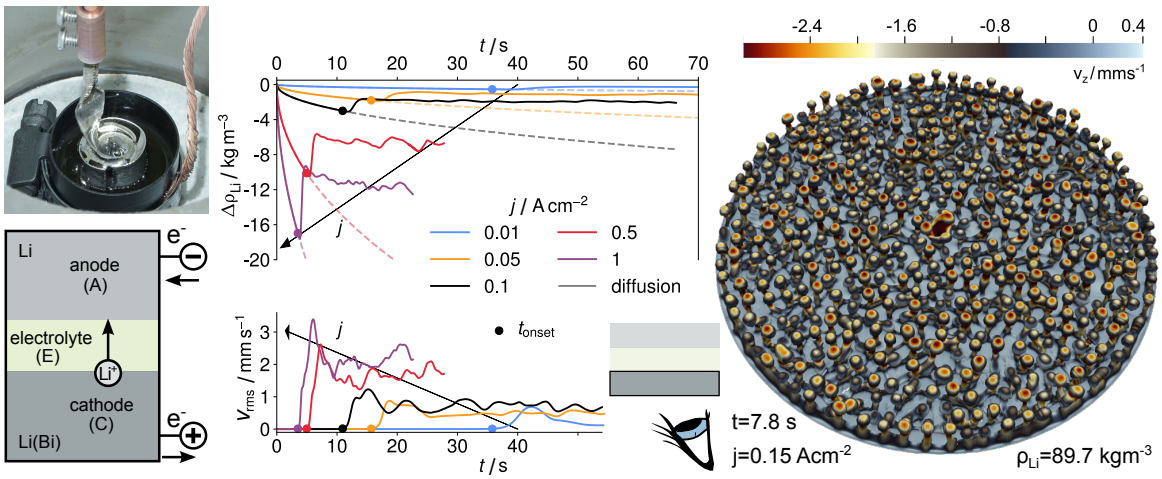

Figure 1. A Li-Bi liquid metal battery during charge: Li mass concentration difference ($\Delta\rho_{\mathrm{Li}}$) between the top and the bulk of the cathode and rms-velocity (v_{rms}) in the cathode vs. time for different current densities (middle). Li-mass-concentration iso-surface colored by the vertical velocity component v_z shortly after the onset of solutal convection (right, seen from below).

References

[1] H. Kim, D. Boysen, J. Newhouse, B. Spatocco, B. Chung, P. Burke, D. Bradwell, K. Jiang, A. Tomaszowska, K. Wang, W. Wei, L. Ortiz, S. Barriga, S. Poizeau, and D. Sadoway, *Liquid metal batteries: Past, present, and future*, Chem. Rev. **113**, 2075–2099 (2013).
[2] D. H. Kelley and T. Weier, *Fluid mechanics of liquid metal batteries*, Applied Mechanics Reviews **70**(2), 020801 (2018).
[3] P. Personnettaz, S. Landgraf, M. Nimtz, N. Weber, and T. Weier, *Mass transport induced asymmetry in charge/discharge behavior of liquid metal batteries*, Electrochemistry Communications **105**, 106496 (2019).
[4] P. Personnettaz, T. S. Klopper, N. Weber, and T. Weier, *Layer coupling between solutal and thermal convection in liquid metal batteries*, International Journal of Heat and Mass Transfer **188**, 122555 (2022).
[5] P. Personnettaz, *Simulations of mass transport in liquid metal electrodes*, PhD, Technische Universität Dresden, Dresden (2022).

Th198

INSTABILITIES IN A NON-ISOTHERMAL NANOFLUID LAYER IN A GRAVITY FIELD

R. Gandhi[1], A. Nepomnyashchy[1] & A. Oron[2]
[1]*Department of Mathematics, Technion – Israel Institute of Technology, Haifa 3200003, Israel.*
[2]*Department of Mechanical Engineering, Technion – Israel Institute of Technology, Haifa 3200003, Israel.*

Keywords: Nanofluid, Instability, Heat and Mass Transfer, Soret Effect

Abstract

We investigate the Marangoni instability driven by the surface-tension gradient at the deformable interface of a nanofluid layer subjected to a prescribed heat flux at the solid substrate in the gravity field. The thermophysical properties of the nanofluid, e.g., density, viscosity, thermal conductivity, heat capacity are assumed to depend on the bulk particle concentration. We also assume the presence of the Soret effect with the thermodiffusion coefficient proportional to the bulk particle concentration. Figure 1 presents a set of neutral curves in the case of a monotonic pure solutocapillary instability for different Biot numbers, when the layer is cooled at the substrate. Here, we observe that the neutral curves are non-monotonic with respect to the wave number k. We also find a significant stabilizing contribution of thermocapillarity on the onset of the solutocapillary instability. Furthermore, we find the emergence of a purely thermocapillary oscillatory instability in the case of the nanofluid layer heated from below. This result underlines the competition between thermocapillary and gravity effects in the system considered here. Moreover, we emphasize that the Soret effect leads to the emergence of the unstable density stratification when the system is heated at the substrate and the nanoparticles are heavier than the base fluid. The system displays the onset of the solutal buoyancy instability for sufficiently large values of the modified Galileo number.

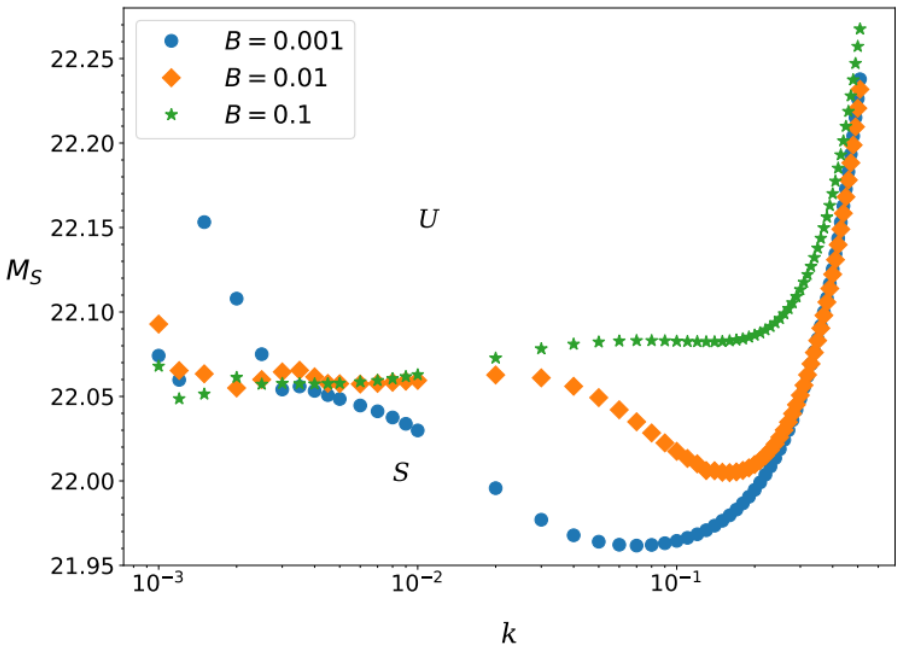

Figure 1. Pure solutocapillary monotonic instability boundaries in terms of the solutal Marangoni number M_S vs the wave number k in the case of cooling at the substrate for various Biot numbers B. S and U stand for stable and unstable domains, respectively.

This work is supported by the Grant from the European Union's Horizon 2020 research and innovation program under the Marie Skłodowska-Curie grant agreement number 955612 (NanoPaInt).

Th199

SUBCRITICAL AND HETEROCLINIC BIFURCATIONS IN RAYLEIGH-BÉNARD CONVECTION OF SHEAR-THINNING FLUIDS CONFINED IN HELE-SHAW CELL

M. N. Ouarzazi[1], P .V. Brandão[2], S. C. Hirata[1] & L.S. de B. Alves[3]

[1]*Unité de Mécanique de Lille, Joseph Boussinesq, EA 7512, Université de Lille, Bd. Paul Langevin, 59655 Villeneuve d'Ascq Cedex, France*

[2]*Department of Industrial Engineering, Alma Mater Studiorum Università di Bologna, Viale Risorgimento 2, Bologna 40136, Italy*

[3]*Departamento de Engenharia Mecânica, Universidade Federal Fluminense, Rua Passo da Pátria 156, Bloco E, Sala 216, SÃčo Domingos, Niterói, RJ 24210-240, Brazil*

Abstract We derive a mathematical model for convection of shear-thinning fluids in Hele-Shaw cell and performed a weakly nonlinear stability analysis (key words: shear-thinning fluids, convection, Hele-Shaw, bifurcation).

In a laterally infinitely extended horizontal layer, Bouteraa et al. [1] performed a weakly nonlinear stability analysis for convection of shear-thinning fluids. The rheological behaviour of the fluid viscosity was assumed to obey to carreau model:

$$\frac{\mu - \mu_\infty}{\mu_0 - \mu_\infty} = (1 + (\lambda^2 \dot{\gamma}_{ij}\dot{\gamma}_{ij})^{\frac{n-1}{2}} \tag{1}$$

where $\dot{\gamma}_{ij}$ is the dimensionless shear rate, the constant μ_∞ is the infinite shear rate viscosity, λ is a dimensionless characteristic time of the fluid and $n < 1$ is the shear-thinning index. These authors found that for weakly shear-thinning fluids, the bifurcation is supercritical while when the shear-thinning character is large enough, the bifurcation becomes subcritical, pointing out the destabilizing effect of the nonlinearities arising from the Carreau rheological model. The same conclusion was drawn by Brandão and Ouarzazi [2] who considered convection of shear-thinning fluids in porous media. The objective of the present contribution is twofold. At first, we use the lubrification approximation to derive a set of governing equations describing convection of shear-thinning fluids in a narrow channel, i.e. Hele-Shaw cell. In a second time, by employing weakly nonlinear theory we derived the following quintic Ginzburg-Landau equation with nonlinear amplitude gradients that describes the spatio-temporal evolution of the amplitude of convection rolls in the unstable regime,

$$\frac{\partial A}{\partial t} = \frac{R_a - Ra_c}{2} A + \delta\, A\,|A|^2 - \gamma\, A\,|A|^4 + \beta\, \frac{\partial^2 A}{\partial x} + ib\,\overline{A}\frac{\partial A}{\partial x} + ic\,A\frac{\partial \overline{A}}{\partial x} \tag{2}$$

The coefficients b, c, β, δ and γ depend on the rheological parameters λ and n and on the lateral aspect ratio of the chanel. Comparing the results with those obtained in [1] for a laterally infinitely extended horizontal layer shows that the transition to subcritical bifurcation is precipitated in a narrow channel. Moreover, we found that decreasing the shear-thinning index n (see 1) or increasing the characteristic time time λ expand the hysteresis cycle induced by the subcritical bifurcation. The effect of the nonlinear amplitude gradients on the spatial heteroclinic bifurcation is also highlighted.

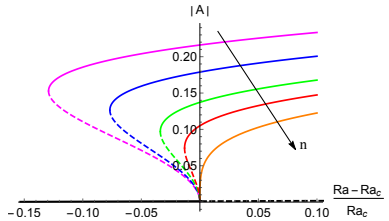

Figure 1. Amplitude of convection versus the relative distance to criticality. The arrow indicates increasing index n from $n = 0.5$ to the case of Newtonian fluid $n = 1$.

References

[1] M. Bouteraa, C. Nouar, E. Plaut, C. Métivier, A., Kalck, *Weakly nonlinear analysis of Rayleigh-Bénard convection in shear-thinning fluids: nature of the bifurcation and pattern selection*, J. Fluid Mech. **767**, 696-734 (2015).

[2] P. V. Brandão, M. N. Ouarzazi, *DarcyâĂŞCarreau model and nonlinear natural convection for pseudoplastic and dilatant fluids in porous media*, Trans. Porous Media **136**, 521-539 (2021).

Th200

NONLINEAR DYNAMICS OF STEADY OBLIQUE ROLLS IN ROTATING MAGNETOCONVECTION

Lekha Sharma[1*], Pinaki Pal[1] & Manojit Ghosh[2]
[1]*Department of Mathematics, National Institute of Technology, Durgapur 713209, India*
[2]*Engineering Mechanics Unit, Jawaharlal Nehru Centre For Advanced Scientific Research, Jakkur P.O., Bangalore 560064, India*

Abstract Rotating magnetoconvection, Rayleigh-Bénard convection, Pattern transitions.

The interplay of rotation, magnetic field, and convective motion of fluids is often encountered in various geophysical and astrophysical applications [1, 2]. But, due to the presence of inherent nonlinearities, complex geometries, and insufficient knowledge, the dynamics of these systems is not well understood. In simplified planar geometry, when both rotation and magnetic field are comparable and nonparallel, it is found that the convective motion emerges in the form of an oblique roll whose nonlinear structure is known for an inviscid fluid only. Here, we report the nonlinear dynamics of steady oblique roll that appears in a rotating hydromagnetic system for a viscous fluid. For this purpose, we consider plane layer Rayleigh-Bénard geometry with horizontal magnetic field and vertical rotation, and solve the governing equations numerically by varying the control parameters, namely, the Taylor number (Ta), the Chandrasekhar number (Q), the Rayleigh number (Ra), and the Prandtl number (Pr) in a widespread parameter space. Based on our numerical results, we identify two structurally distinct oblique rolls at the onset of convection viz. positive oblique roll (SOR^{+}) and negative oblique roll (SOR^{-}) that lie at angles $\pm\gamma$ with the magnetic field. The appearance of two different oblique rolls is found to divide the parameter space into three regions where SOR^{+}, SOR^{-}, and double-roll (both SOR^{+} and SOR^{-}) emerge as the primary bifurcating states. Depending on Pr, we find that for weak and moderate magnetic field, the SOR^{+} shows up at the onset when Ta is relatively low; at moderate and high Ta, we notice double-roll and SOR^{-}, respectively. In contrast, a stronger magnetic field is found to eliminate SOR^{+} from the system and either double-roll or SOR^{-} is observed in that case. As the Rayleigh number increases, the SOR^{-} is found to go through successive bifurcations and a plethora of flow patterns in the form of secondary and higher order states emerges in the system. On the contrary, for all Ta, Q, and Pr, the SOR^{+}, when appears at the onset does not go through any bifurcation and remains stable in the entire range of the Rayleigh number considered in this study. The Nusselt number in this case is found to follow a well-defined scaling law which is independent of both Ta and Q. Finally, we uncover the effect of Pr on the oblique roll instability at the onset of convection. We find that at low Pr, the onset of convection can be subcritical depending on Ta and Q; finite amplitude steady oblique roll persists there. However, as either of Ta, Q, and Pr increases, the subcritical convection is found to inhibit and supercritical convection takes place in the system.

References

[1] I. A. Eltayeb, *Hydromagnetic convection in a rapidly rotating fluid layer*. Proc. R. Soc. Lond. A **326** (1565), 229–254 (1972).
[2] P. H. Roberts, C. A. Jones, *The onset of magnetoconvection at large Prandtl number in a rotating layer I. Finite magnetic diffusion*, Geophys. Astrophys. Fluid Dyn. **92** (3-4), 289–325 (2000).
[3] L. Sharma, P. Pal, M. Ghosh, *Nonlinear dynamics of steady oblique rolls in rotating magnetoconvection*, J. Fluid Mech. **In Revision** (2022).

*Present address: Department of Physics, Indian Institute of Technology, Kanpur 208016, India

Th201

RAYLEIGH-BÉNARD-MARANGONI CONVECTION IN A BINARY FLUID SYSTEM

Anubhav Dubey[1], Saumyakanta Mishra[2], S.V. Diwakar[2] & S. Amiroudine[1]
[1] Université de Bordeaux, I2M, UMR CNRS 5295, Talence F-33400, France
[2] Engineering Mechanics Unit, Jawaharlal Nehru Centre for Advanced Scientific Research, Bangalore, 560064, India

Keywords: Binary fluids, Phase field method, Linear stability analysis

Abstract

Multiphase flows have been a vibrant area of research owing to its ubiquitous nature ranging from natural phenomenon to industrial processes. The specific two-phase flow problem investigated through current work is Rayleigh-Bénard-Marangoni convection in a binary fluid system. We specifically focus on FC-72 and Silicone oil pair. Binary fluids pose a unique property of having varied degrees of miscibility in each other depending on system temperature. The two fluids are completely miscible above a particular temperature called the upper critical solution temperature (UCST) and have been modeled recently using the diffuse interface approach [1]. The degree of closeness with respect to UCST (θ_c) is characterized by a parameter r, where $r = f(\frac{\theta-\theta_c}{\theta_c})$. This parameter allows the system to transition continuously from the immiscible regime ($r = 1$) to miscible regime ($r \leq 0$) when included in the formulation of free energy functional of the phase field approach. Due to the presence of an interface in a two-layer system and the propensity of onset of convection in individual layers, the convective flow could manifest in numerous ways [2]. A spectral [3] collocation-based linear phase field model is deployed to study the onset characteristics of such convection. For Rayleigh-Bénard convection, as depicted through Fig.1, the critical Rayleigh number (and the growth rate) was found to be a function of interface location in the domain and the parameter r. The peak magnitude of Rayleigh number was found to decrease as we approached the UCST. The bottom and the top dragging modes were demarcated. In case of Rayleigh-Bénard-Marangoni convection, the surface tension was found to play either a stabilizing role or destabilizing role depending upon the position of the interface.

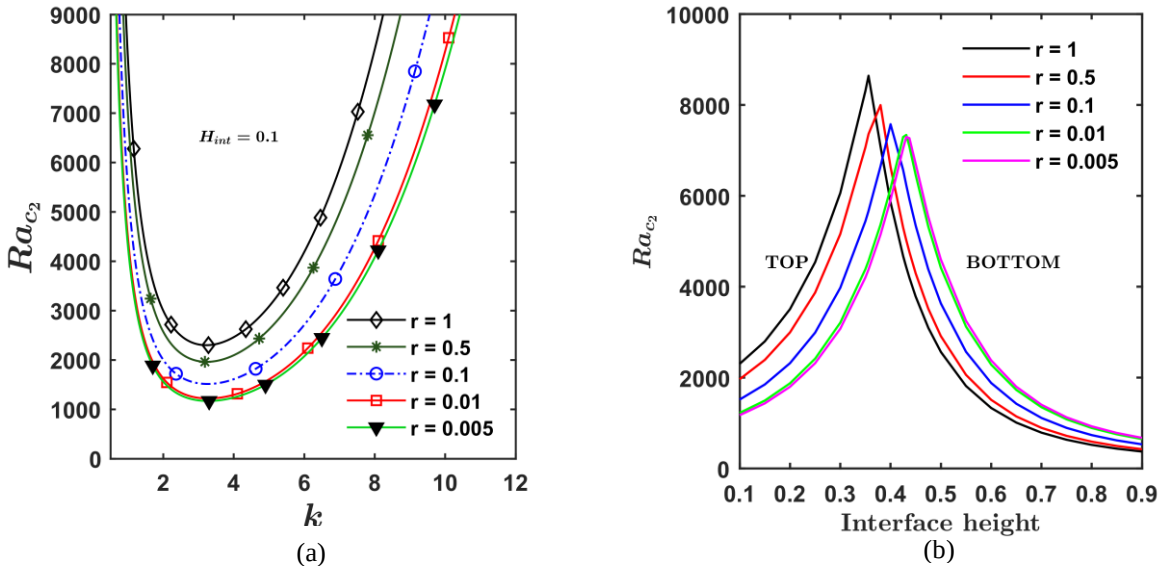

(a) (b)

Fig1. (a) Variation of critical Rayleigh number with wavenumber for interface located at $h1 = 0.1$ for varying r, (b) Variation of critical Rayleigh number with interface height for varying r.

References

[1] M. Bestehorn, D. Sharma, R. Borcia, and S. Amiroudine, *Faraday instability of binary miscible/immiscible fluids with phase field approach*, Phys. Rev. Fluids, 6, p. 064002 (2021).

[2] D. Johnson and R. Narayanan, *Geometric effects on convective coupling and interfacial structures in bilayer convection*, Physical Review E, **54(4)**, 3102-3104 (1997).

[3] S.V. Diwakar, S. Tiwari, S.K. Das and T. Sundararajan, *Stability and resonant wave interactions of confined two-layer Rayleigh-Bénard systems*, J. Fluid Mech., 754, pp. 415-55 (2014).

Th202

CONVECTION PATTERNS IN AN ANNULAR CAVITY SUBJECTED TO A RADIAL TEMPERATURE GRADIENT

Arnaud Prigent[1], Ziad Ntarmouchant[1] & Innocent Mutabazi[1]
[1]*LOMC, Le Havre University Normandy – CNRS, Le Havre, France*

Keywords: annular cavity, natural convection, pattern

Abstract

Several studies have been devoted to the investigation of the flow regimes occurring in deferentially heated cavities [1-10]. Two main heat transfer regimes have been identified (conduction and convection) [1,10]. Between concentric vertical cylinders, in the Taylor-Couette configuration, the nature of the heat transfer regime is determined by a criterion involving Ra, the radius ratio η and the aspect ratio Γ. Here we present investigations of the flow obtained in the thermal turbulent Taylor-Couette facility (THETACO) designed for the study of the turbulence generated by differential rotation and radial temperature gradient [11]. The gap width of the system is 2 cm and its radius ratio $\eta = 0.869$. Its height is 97.5 cm and $\Gamma = 48.75$. In the present study the cylinders were stationary and the working fluid was water with $Pr \simeq 7$. The temperature of the outer and inner cylinders were set in order to obtain a temperature gradient $0.5 < T < 20$°C and a Rayleigh number ranging from $5.2.10^4$ to $3.3.10^6$. Following the work of Lopez et al [10], for our system, the value of the transition between the conductive and the convective regimes is $Ra^* = 2.08.10^4$. Therefore, our study is performed in the convective regime. As soon as a radial temperature gradient is imposed in the annular cavity, a large convection cell appears with the fluid moving upwards near the inner hot cylinder and downwards near the outer cold cylinder. However, no pattern is observed for $Ra < 1.6 \cdot 10^5$. For $1.6 \cdot 10^5 < Ra < 3.3 \cdot 10^6$, propagating waves are observed in the vicinity of both cylinders. These waves propagate downwards near the outer cold cylinder and upwards near the inner hot cylinder. Whatever the value of the Rayleigh number is $Ra > 1.6 \cdot 10^5$, propagating waves are always present in the system. We present visualizations, temperature and velocity fields for the different patterns observed in this context.

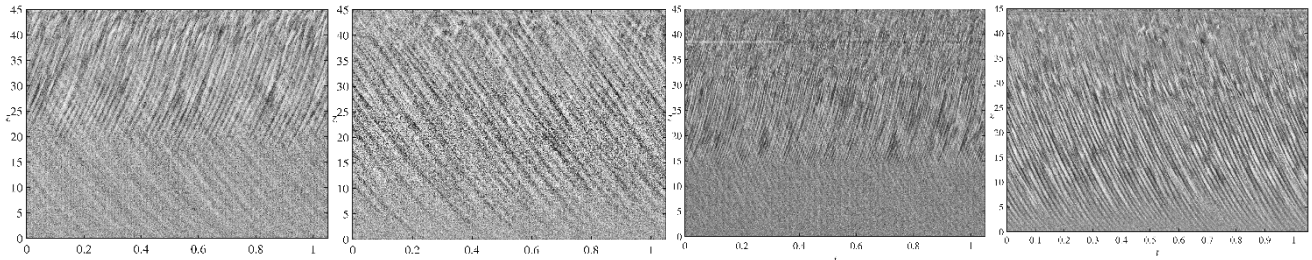

Figure 1. Space-time diagrams of the pattern observed near the inner (a,c) and outer (b,d) cylinder walls for $Ra = 3.2 \cdot 10^5$ (a,b) and $Ra = 3.3 \cdot 10^6$ (c,d).

References

[1] Thomas R.W. and de Vahl Davis G. Natural convection in annular and rectangular cavities a numerical study. 4th International Heat Transfer Conference (Paris), Elsevier, New York, 1970.
[2] Choi I. G. and Korpela S. A. Stability of a conduction regime of natural convection in a tall vertical annulus. J. Fluid Mech. 99: 725, 1980.
[3] McFadden G. B., Coriell S. R., Boisvert R. F., and Glicksman M. E. Asymmetric instabilities in buoyancy-driven flow in a tall vertical annulus," Phys. Fluids 27:1359, 1984.
[5] Weidman P. D. and Mehrdadtehranfar G., Instability of natural convection in a tall vertical annulus. Phys. Fluids 28: 776, 1985.
[6] Le Quéré P. and Pécheux J. Numerical simulations of multiple flow transitions in axisymmetric annulus convection. J. Fluid Mech. 206:517, 1989.
[7] Pécheux J., Le Quéré P., and Abcha F. Curvature effects on axisymmetric instability of conduction regime in a tall air-filled annulus. Phys. Fluids 6: 3247, 1994.
[9] Bahloul A., Mutabazi I., and Ambari A. Codimension 2 points in the flow inside a cylindrical annulus with a radial temperature gradient. Eur. Phys. J. A 9: 253, 2000.
[10] Lopez J.M., Marques F., and Avila M. Conductive and convective heat transfer in fluid flows between differentially heated and rotating cylinders. Int. J. Heat Mass Transfer 90:959-967, 2015.
[11] Singh H. et al. A large thermal turbulent Taylor-Couette (THETACO) facility for investigati²on of turbulence induced by simultaneous action of rotation and radial temperature gradient. Rev. Sci. Instrum. 90:115112, 2019.

Th203

SENSITIVITY ANALYSIS OF THE FIRST INSTABILITY IN A DIFFERENTIALLY HEATED SQUARE CAVITY

Josh Williams[1], Ubaid Ali Qadri[1] & H. Sue Thorne[1]
[1]*The Hartree Centre, STFC Daresbury Laboratory, Warrington WA4 4AD, UK*

Keywords:

Abstract

A differentially heated cavity represents a simple proxy of some of the physics present in a tokamak fusion reactor. Identifying the onset of instabilities and developing passive/active control strategies is crucial to ensure the success of the nuclear fusion process. In this study, we consider the linear stability of a differentially-heated square cavity with a heated left wall and cold right wall under the Boussinesq approximation. We consider two possibilities for the top and bottom walls – firstly, where both top and bottom walls are conducting, and secondly, where both top and bottom walls are perfectly adiabatic or insulating. Previous studies [1,2] have shown that for a Prandtl number representative of air (Pr=0.71), simulations with conducting boundaries have a critical Rayleigh number two orders of magnitude smaller than for simulations with insulating boundaries. In this study, we investigate this in more detail using adjoint-based sensitivity analysis.

We use direct numerical simulation using a spectral-element method to obtain steady base flows for the two cases near their respective bifurcation points. We obtain the linear direct and adjoint global eigenmodes using matrix-free time-stepping of the linearised and adjoint governing equations. We combine these eigenmodes to identify the regions responsible for driving the instability in each of the cases [3]. We then formulate and solve a constrained optimization problem to understand the sensitivity of the linear instability to changes in the hot wall temperature [4]. These results guide us in understanding the significant difference in the instability mechanism responsible for the primary bifurcation in the two cases.

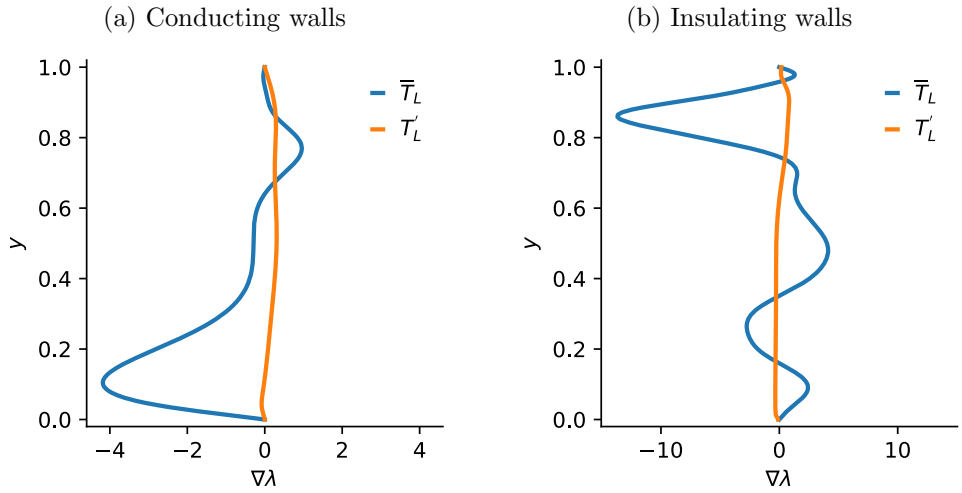

Figure 1. Sensitivity of the linear growth rate to steady changes (blue) and harmonic forcing (orange) of the hot wall temperature for the case with (a) conducting walls (left) and (b) insulating walls (right).

References

[1] P. Le Quere, M. Behnia. *From onset of unsteadiness to chaos in a differentially heated square cavity,* Journal of Fluid Mechanics, 359, 81-107 (1998).
[2] S. Xin, P. Le Quere. *Linear stability analyses of natural convection flows in a differentially heated square cavity with conducting horizontal walls.* Physics of Fluids, 13(9) (2001)
[3] F. Giannetti, P. Luchini. *Structural sensitivity of the first instability of the cylinder wake.* Journal of Fluid Mechanics, 581, 167-197 (2007).
[4] P. Meliga, D. Sipp. J.-M. Chomaz. *Open-loop control of compressible afterbody flows using adjoint methods*. Physics of Fluids, 22(5) (2010)

DAY 5 - Friday, 28 June 2024 (Open Colloquia) Larch Lecture Theatre	
09:00	**Tea and Coffee**
09:15	**OC001: Dr Daphne Lemasquerier:** *Fluid Dynamics of the Outer Solar System: from Gas Giants to Icy Satellites* ***Chair: Dr Rachel Schwind (Larch Lecture Theatre)***
10:15	**OC002: Prof David Quéré:** *Bouncing Droplets* ***Chair: Prof Halim Kusumaatmaja (Larch Lecture Theatre)***
11:15	**Coffee Break**
11:45	**OC003: Prof KR Sreenivasan:** *Changes in outlook on turbulent wall flows over the past forty years* ***Chair: Prof Alexander Morozov (Larch Lecture Theatre)***
12:45	**Closing and Lunch (own arrangements)**
13:45	**Lab Tours (see below)**

DAY 5 - Friday, 28 June 2024 Lab Tours	
13:45	Start from Nucleus Entrance (PhD students will take you around)
13:50	**Wetting, Interfacial Science and Engineering Laboratory**, *Process Lab, Sanderson Building*
14:10	**Chemical Engineering Labs**, *Sanderson Building*
14:40	**Two Phase Flows and Heat Transfer Laboratory**, *Fleeming Jenkin Building*
15:00	**Small Research Facility for Multiphase Flows at High Pressure and Temperature**, *Fleeming Jenkin Building*
15:20	**FloWave Ocean Energy Research Facility**, *Max Born Crescent*
15:45	Return back to Nucleus Entrance

Open Colloquium – OC001

Fluid Dynamics of the Outer Solar System: from Gas Giants to Icy Satellites

Daphné Lemasquerier

Mathematics and Statistics, University of St. Andrews, UK

Daphné Lemasquerier first studied Physics and Chemistry of the Earth and other planets at ENS Lyon, France. She took an interest in geophysical fluid dynamics during an internship at Spinlab (UCLA, Los Angeles), where she studied experimentally libration-driven flows in planetary cores and subsurface oceans. She complemented her formation in Planetary sciences by a master in Fluid Mechanics and Nonlinear Physics at Aix-Marseille Université (France), before receiving a fellowship from ENS Lyon for a PhD at IRPHE laboratory (Marseille, France). She modelled experimentally, numerically and theoretically Jupiter's dynamics, including zonal jets, vortices and zonostrophic turbulence. She received her PhD in Engineering, Mechanics and Physics of Fluids in October 2021. For this work, she received the Andreas Acrivos Dissertation Award of the American Physical Society, the Turcotte Award of the American Geophysical Union and the L'Oréal-UNESCO "For Women In Science" award. From January to August 2022, she held a post-doctoral position at the University of Texas at Austin and worked on modelling the circulation in subsurface oceans of icy satellites of Jupiter and Saturn. Since September 2022, she is a Lecturer in Fluid Dynamics in the School of Mathematics and Statistics at the University of St Andrews (United Kingdom).

Abstract

The Jovian system is witnessing a major interdisciplinary scientific interest due to new observations from NASA's Juno mission, and upcoming observations by NASA's Europa Clipper and ESA's JUICE missions. In this talk, I propose to review some aspects and challenges of the fluid dynamics involved in the interiors of Jupiter and its icy satellites. In the first part of the talk, I will focus on subsurface oceans of icy moons which are responsible for coupling the deep mantle to the observed ice crust via material and heat exchanges. I will discuss how direct numerical simulations of turbulent rotating convection in spherical shells can help us to better constrain the mean circulation taking place in subsurface oceans. I will discuss in particular the effect of tidal heating within the silicate mantle, which is laterally heterogeneous. In the second part of the talk, I will focus on the complex, multiscale dynamics that takes place in the atmosphere and liquid hydrogen of Jupiter. Jupiter's atmosphere exhibits strong large-scale east-west winds called zonal jets, which self-organize from the underlying turbulent flow. Based on experimental observations and analytical modelling, I will discuss the emergence and nonlinear equilibration of zonal jets and emphasize the role of Rossby waves in exchanging momentum with the zonal flow, as well as the feedback of the zonal flow on the waves.

Open Colloquium – OC002

Bouncing Droplets

David Quéré

ESPCI Paris and École Polytechnique, France

David Quéré obtained a Ph.D. from Université Pierre et Marie Curie, Paris – after one year in the French Navy (where he scrutinised the radioactive cloud of Chernobyl). He became since a research director at CNRS and a Professor at École Polytechnique (Departments of Physics and Mechanics). He is engaged in experimental research in Soft Matter Physics and Fluid Mechanics, with a strong interest in interfacial hydrodynamics (drops, films, bubbles, coating, wicking) as well as in aerodynamics, morphogenesis and biomimetics, all topics on which he coworked with about 35 PhD students. He received the 2014 Silver Medal of CNRS and the 2021 APS Prize in Fluid Dynamics, and he became a Distinguished Professor at ESPCI in 2016.

Abstract

We discuss a few situations where drops impacting a solid bounce on it, which defines what we can call 'repellency'. The discussion includes the role of the solid, the nature of the liquid and the parameters that characterize the rebounds.

Open Colloquium – OC003

Changes in outlook on turbulent wall flows over the past forty years

Katepalli R Sreenivasan

Tandon School of Engineering, Department of Physics & Courant Institute of Mathematics, NYU, USA

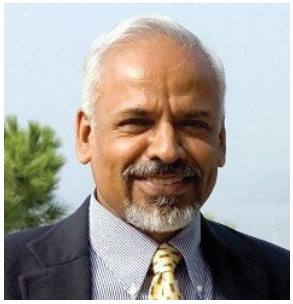

Katepali R Sreenivasan (Sreeni) is a professor at New York University, where he is the University Professor and Eugene Kleiner Chair for Innovation, Professor in the Physics Department, Courant Institute of Mathematical Sciences, and Tandon School of Engineering, and directs the Center for Space Science at the NYU Abu Dhabi campus. He is a fluid dynamicist with a broad range of interests, and expertise spanning experiment, theory and simulations. He has an enormous range of experience in scientific leadership and has served the scientific community, especially the APS, in various capacities. Sreeni obtained his Ph.D. from the Indian Institute of Science (IISc) and did post doctoral work in Australia and the USA. He was Horald W. Cheel professor at Yale where he worked for 22 years. He then took up the position of director, Institute of Physical Sciences and Technology at the University of Maryland. He was the director of Abdus Salam ICTP during 2003-09. His memberships include: US National Academy of Sciences; US National Academy of Engineering; American Academy of Arts and Sciences; Indian Academy of Sciences; Indian National Science Academy; and African Academy of Sciences. His honours include the Guggenheim Fellowship; Otto Laporte Award, American Physical Society; Distinguished Alumnus Award, IISc; International Panetti-Ferrari Prize and Gold Medal, Torino Academy of Sciences; and National Order of Scienctific Merit, Brazil.

Abstract

Recent research on turbulent pipe and channel flows, as well as boundary layers, has called into question a number of ideas that had been taken as central and final some forty years ago. We summarize these ideas and discuss their applicability; we will ask and answer the question of whether we have advanced our understanding.